Influence of urbanization on organic matter and trace metals dynamics in mangrove forests

Sarah Louise Robin

UNIVERSITÉ DE LA NOUVELLE-CALÉDONIE

ÉCOLE DOCTORALE DU PACIFIQUE

Institut de Sciences Exactes et Appliquées

Doctorat

Chimie

Institut de Sciences Exactes et Appliquées

Présentée et soutenue par

Sarah ROBIN

Influence de l'urbanisation sur la dynamique de la matière organique et des éléments traces métalliques dans les mangroves

Soutenue le 8 décembre 2023

Sous la direction de

Pr. Cyril MARCHAND, Université de la Nouvelle-Calédonie

Pr. Andrea ALFARO, Université technologique d'Auckland

JURY :

M. Christian SANDERS	Professeur, Coffs Harbour	Rapporteur
Mme. Joanne OAKES	Professeure adjointe, Lismore	Rapporteur
Mme. Peggy GUNKEL-GRILLON	Professeure, Nouméa	Examinateur
M. Pascal PAGAND	Maître de conférences, Nouméa	Examinateur
M. Cyril MARCHAND	Professeur, Nouméa	Directeur de thèse
Mme. Andrea ALFARO	Professeure, Auckland	Directeur de thèse

"Sometimes the future changes quickly and completely, and we're left with only the choice of what to do next. We can choose to be afraid of it, to stand there trembling, not moving, assuming the worst that can happen, or we can step forward into the unknown and assume it will be brilliant."

Cristina Young

Remerciements

Remerciements aux membres du jury

J'aimerais exprimer ma sincère gratitude envers les membres de mon jury pour avoir accepté de participer en tant que membres de mon jury de thèse et d'évaluer le contenu de mon travail.

Remerciements aux partenaires financiers

Un grand merci s'adresse au CRESICA pour les opportunités d'échanges scientifiques ainsi que le soutien financier accordé à ma thèse. Je suis également reconnaissante envers la Banque de la Nouvelle-Calédonie, la Secal et le groupe Vinci, représenté par Cegelec et Fibrelec, pour leurs contributions. Je tiens à exprimer ma profonde gratitude à la ville de Dumbéa et à son maire, Georges Naturel, pour le regroupement de partenaires et la confiance qu'ils m'ont témoignée dans la réalisation de ce projet.

Remerciements

Je tiens tout d'abord à exprimer ma sincère gratitude envers Mme Catherine Ris pour son accueil chaleureux au sein de l'UNC. Mes remerciements s'adressent également aux membres administratifs qui ont fait preuve d'accessibilité et d'amabilité : Laurence Dépont, Sylvian Raffart-Artigues, Soane, Losa et Théophile.

Je souhaite remercier Yves Letourneur et Jean-Marc Boyer, tous deux directeurs de l'EDP pendant ma thèse, pour leur disponibilité et leur écoute précieuse.

Je tiens à exprimer ma reconnaissance envers la tribu de Téouta à Ouvéa, qui nous a réservé un accueil chaleureux lors des missions sur place. Cette expérience s'est révélée enrichissante à la fois sur le plan scientifique et humain.

Mes remerciements vont également à mes partenaires scientifiques qui m'ont accompagnée dans mes analyses et mes rédactions : Andrew Swales, Claude Le Milbeau, Stéphane Mengant et François Baudin. Un remerciement spécial à Paul Coulerie et Ines Le Mao pour leur précieuse aide concernant l'utilisation de l'UPLC, ainsi que pour les debriefs essentiels "Koh-Lanta" durant ma thèse. Je remercie également l’équipe du LAMA, particulièrement Léocadie, Anne et Vincent pour mes analyses au sein de leur laboratoire. J'adresse mes vifs remerciements à Estelle Vidal pour ses précieux conseils en matière de diffusion et de vulgarisation de mes travaux.

J'exprime ma profonde reconnaissance envers Peggy Gunkel-Grillon pour m'avoir accueilli au sein du laboratoire ISEA. Je tiens à remercier chaleureusement tous mes collègues chercheurs pour leur accueil et leur volonté constante de m'apporter leur aide, notamment Michael Meyer, Linda Guentas, Nazha Selmaoui-Folcher, Christine Laporte-Magonie, Bruno Fogliani, Valérie Burtet-Sarramegna et Nicolas Lebouvier.

Je tiens à adresser une mention spéciale à Maximilien Mathian, alias Max la D, pour les innombrables moments de rire partagés. Les souvenirs de nos aventures à Ouvéa resteront à jamais gravés dans ma mémoire. Tes conseils et ta bonne humeur ont été une source d'énergie pendant ces trois années. Je tiens également à remercier France Pattier tout particulièrement. Tu as été un véritable pilier sur lequel je pouvais compter, tant sur le plan scientifique qu'humain. Mon immense gratitude à vous deux.

Je remercie chaleureusement toute l'équipe technique, autant pour votre soutien technique que pour votre bonne humeur. Merci Olivia Barthélémy et Aurélie Monin pour l'aide lors de mes nombreuses sessions au MEB. Merci Sarah Gigante, Valérie Medevielle, Monika Le Mestre et Isabelle Desriaux pour toutes mes manipulations au sein du laboratoire et en dehors. Vous avez activement participé au bon déroulement de cette thèse et à mon bien être au sein du laboratoire, bien que vous soyez toutes sur la pente descendante … Merci également à Sylvie Russet, Thomas Quiniou et Gauthier Hallet.

Une mention spéciale revient à Kapé le S, mon compagnon d'aventure, sans qui cette thèse n'aurait pas eu la même saveur. Merci pour les éclats de rire, les terrains vreuuuumants et les aventures mémorables à Ouvéa. Merci aussi de m'avoir aidé à garder la ligne en volant tous mes goûters !

Un remerciement tout particulier à Pierre Sanlis, mon stagiaire pendant 5 mois. Je te suis extrêmement reconnaissante pour ton travail accompli pour ma thèse et pour la personne exceptionnelle que tu as été, un véritable compagnon d'aventure. Merci également pour ne pas avoir porté plainte pour maltraitance (tu as quand même évité la lepto, on est bon).

Je tiens à dédier mes remerciements à mes collègues de galère et de potins : Leyla, Julie, Noreen, Grégoire, Romane, Naïna, Marie, Pauline, Rodrigue et Vincent. Merci pour l'atmosphère agréable dans notre open space, votre soutien à chaque étape, votre aide précieuse sur mes projets lorsque mes compétences en design étaient limitées, et bien sûr, merci d'avoir activement contribué à la vie de la "chaise des H". Une dédicace à Leyla ma sœur de Nouméa à Bogota. Plein de love pour toi.

Il est évident que je remercie mes directeurs de thèse. Andrea Alfaro pour ses précieux conseils, son expérience, et sa disponibilité. Cyril Marchand, je sais que parfois vous en

avez marre de moi mais je vous prépare à ce qui vous attends avec la relève « Lion et Rat ». Et puis sinon on s'encroûte vite, quelque part je vous aide à rester jeune et éveillé. Sérieusement je vous serais toujours reconnaissante. Vous m'avez tellement apporté au cours de ces 4 années. C'était un peu par hasard que nos chemins se sont croisés mais ce n'est pas un hasard qui a fait que nous sommes là aujourd'hui. Vous m'avez très vite cernée, très vite comprise, et très vite apportée ce dont j'avais besoin : de la confiance et de la stimulation intellectuelle. Vous avez cru en moi dès le début et m'avez portée jusqu'à aujourd'hui. Bien que cette thèse soit mon travail et porte mon nom, c'est avec votre plume que j'ai pu l'amener à bout. J'espère vous avoir fait rayonner et vous avoir fait honneur (même si des fois j'ai menti).

Pour conclure, je tiens à exprimer ma profonde gratitude envers mes proches pour leur soutien inconditionnel au quotidien. Prescillia, qui m'a en quelque sorte inspirée, tu es clairement à l'origine de cette merveilleuse aventure. Valérie et Abel, toujours présents pour m'apporter leur soutien et me rappeler à quel point vous êtes fiers de moi. Mes grands-parents, qui ne comprennent pas tout mais sont mes plus grands fans. Mes amis, si chers à mon cœur : Clément, tes mots "si tu ne fais pas de thèse, c'est du gâchis" résonnent encore en moi. Marie, Sacha, Lucas, Célia, Marine P, Marine L, Cheyenne, Sophie, Lisa, toujours excités à l'idée de me voir en 4 par 3 rue Benebig. Un grand merci à Axel, pour ton amour, tes rires, ton accompagnement dans les défis, et surtout pour me rendre meilleure.

Merci à Little, Gun et Itunes pour le soutien émotionnel essentiel lors de mes longues sessions devant l'ordinateur à la maison. Alex et Marie, vous faites partie de ceux qui croient en moi depuis les premiers jours. Même si vous êtes les brouillons, vous avez placé la barre haute, et donc, je ressens l'obligation de me surpasser pour être meilleure que vous. Vous ne me facilitez pas la tâche, cependant j'ai un avantage, le poids de mon nez ne me freine pas. Un grand merci d'être toujours présents les fat quiches. Par conséquent, si je remercie les jumeaux, j'adresse également mes remerciements aux deux âmes charitables qui ont accepté de nous libérer d'eux, Charlène et Edouard. Votre courage est admirable. S'il vous plaît, restez encore un peu, ils sont devenus bien plus agréables depuis votre arrivée.

Pipou, je m'excuse pour toutes les rides que je t'ai faites apparaître. Tu as toujours affirmé que tu investissais en moi lorsque je te sollicitais pour des millions afin de faire ma belle à des milliers de kilomètres, j'espère que tu trouves à présent cet investissement rentable. Ma présence ici aujourd'hui serait impensable sans ton soutien, financier certes, mais pas que. On n'a beau se le dire tous les jours… moi plus. Mimou, mon rayon de soleil, ce ne

sont pas des rides que je t'ai causées, mais plutôt des maux de ventre, je pense. Quand je suis venue te voir à 15 ans pour te demander de partir loin de vous, alors que je vous aimais plus que tout au monde, je n'arrive pas à imaginer la douleur que cela a dû représenter pour toi de me laisser partir. Merci de m'avoir fait confiance, d'avoir été à mes côtés à chaque étape, chaque moment difficile, chaque appel. Toi et Pipou êtes les personnes les plus importantes à mes yeux (après Little, bien sûr).

Avant-propos

Ce manuscrit de thèse synthétise trois années de travail sur les contaminants et la matière organique dans la mangrove de Nouvelle-Calédonie. Cette thèse a été réalisée au sein de l'Institut de Sciences Exactes et Appliquées (ISEA, EA7484) de l'Université de la Nouvelle-Calédonie (UNC). Cette thèse a été financé par une bourse de l'Ecole Doctorale du Pacifique (EDP) rattachée à l'UNC. Les partenaires financiers sont la Banque de Nouvelle-Calédonie, Cegelec, le Consortium de la Recherche et de l'Enseignement Supérieur et de l'Innovation en nouvelle-Calédonie (CRESICA), le Fonds Pacifique, Fibrelec et la SECAL.

Ce travail a pour objectif d'étudier l'influence de l'urbanisation sur la dynamique des éléments traces métalliques et de la matière organique dans la mangrove. Cette recherche a été menée le long de la côte Ouest de la Nouvelle-Calédonie. Deux mangroves localisées en aval d'un bassin versant d'origine volcano-sédimentaire ont été sélectionnées comme zones d'étude ainsi qu'une mangrove en aval d'un bassin versant latéritique. Des campagnes d'échantillonnage et d'expérimentation ont été menées aux deux saisons, en mai 2021, décembre 2021 et mai 2022.

Cette thèse se compose d'une introduction en français qui expose l'état actuel des connaissances sur la mangrove et sur les thèmes abordés. Elle met en avant la problématique à l'origine de cette thèse, les objectifs poursuivis dans ce travail, la méthodologie suivie pour atteindre ces objectifs et la structure globale du manuscrit. Les objectifs et la structure du manuscrit sont également rédigés en anglais. Le manuscrit est constitué de cinq chapitres en anglais, les chapitres III et IV étant eux-mêmes subdivisés en deux et trois parties distinctes. La majorité de ces chapitres constitue un article, soit publié, soumis, ou en cours de préparation pour des revues scientifiques. Les 4 premiers chapitres débutent par une introduction en français, visant à établir des liens entre les différents chapitres et à synthétiser leurs contenus respectifs. Le dernier chapitre reprend les résultats donnés dans les chapitres précédents pour discuter de leurs liens et proposer une conclusion. Ce chapitre conclusion contient également une liste de perspectives qui découlent des découvertes effectuées dans ce travail de recherche. En annexe se trouvent deux articles de journal qui ont été publiés au cours de la réalisation de cette thèse. Le premier article est une revue sur les hydrocarbures aromatiques polycycliques (HAP) dans la mangrove. La dynamique des HAP dans les mangroves était à l'origine un sujet de cette thèse, mais notre étude a révélé l'absence de HAP dans les sols et les végétaux des forêts étudiées. Les HAP ne sont donc pas discutés dans ce manuscrit. La

seconde annexe est une communication courte sur le H_2S dans une mangrove urbaine en Nouvelle-Calédonie, dont je suis co-auteure.

Forword

This manuscript synthesizes three years of work on contaminants and organic matter in the mangrove forests of New Caledonia. This thesis was conducted at the Institute of Exact and Applied Sciences (ISEA, EA7484) of the University of New Caledonia (UNC). The funding for this thesis was provided by a scholarship from the Pacific Doctoral School (EDP) associated with UNC. Other financial partners include the Bank of New Caledonia, Cegelec, the Consortium for Research and Higher Education and Innovation in New Caledonia (CRESICA), the Pacific Fund, Fibrelec, and SECAL.

The objective of this work is to study the influence of urbanization on the dynamics of trace metals and organic matter in mangrove forests. This research was carried out along the West coast of New Caledonia. Two mangrove forests located downstream of a volcano-sedimentary watershed were selected as study areas as well as a mangrove forest developing downstream from lateritic soils. Sampling and experimentation campaigns were conducted during two seasons, in May 2021, December 2021, and May 2022.

This thesis consists of an introductory section in French that presents the current state of knowledge about mangrove ecosystems and the topics addressed in this thesis. It highlights the issue that led to this thesis, the objectives pursued in this work, the methodology followed to achieve these objectives, and the overall structure of the manuscript. The objectives and the structure of the manuscript are also written in English. The manuscript consists of five chapters in English, with Chapters III and IV further subdivided into two and three distinct sections. The majority of these chapters constitute articles, either published, submitted, or in preparation for scientific journals. The first four chapters begin with an introduction in French, aiming to establish connections between the different chapters and synthesize their respective contents. The final chapter revisits the results discussed in the preceding chapters to examine their relationships and provide a conclusion. This concluding chapter also contains a list of perspectives that stem from the findings of this research. In the appendices, there are two journal articles that were published during the course of this thesis. The first article is a review of polycyclic aromatic hydrocarbons (PAH) in mangrove forests. The dynamics of PAH in mangrove forests was originally a subject of this thesis, but our study revealed the absence of PAH in the soils and vegetation of the studied forests. Therefore, PAH are not discussed in this manuscript. The second appendix is a short communication on H_2S in an urban mangrove forest in New Caledonia, of which I am a co-author.

Table of Contents

Liste des abréviations

ACP = Analyse en Composantes Principales

Ad/Al = Acid over Aldehyde ratio

ARN = Acides RiboNucléiques

ATP = Adenosine TriphosPhate

BCF = BioConcentration Factor

BCR = Bureau Communautaire de Référence

BSTFA = BiS(triméthylsilyl)TriFluoroAcetamide

C/N = mass ratio of Carbon/Nitrogen

C/V = Cinnamyl phenols over Vanillyl phenols ratio

CO = Carbone Organique

COT = Carbone Organique Total

DCB = Dithionite Citrate Bicarbonate solution

DNA = DeoxyriboNucleic Acid

DRX = Diffractomètre à Rayon X

EDX = Energy Dispersive X-ray

EEC = Extreme Effect Concentration

ERL = Effect Range Low

ERM = Effect Range Median

ERO = Espèces Réactives de l'Oxygène

ETM = Elément Trace Métallique

FID = Flame Ionization Detector

GC = Gas Chromatography

HCD = Higher energy Collision Dissociation

HI = Hydrogen Index

HMW = High Molecular Weight

ICP-OES = Inductively Coupled Plasma – Optical Emission Spectroscopy

IPE = International Plant-analytical Exchange

IRD = Institut de Recherche et Développement

ISE = International Soil-analytical Exchange

Kow = octanol-water coefficient

LMW = Low Molecular Weight

MEB = Microscope Electronique à Balayage

MEC = Median Effect Concentration

MO = Matière Organique

MOD = Matière Organique Dissoute

MPS = Matière Particulaire en Suspension

MS = Mass Spectrometry

NC = New Caledonia

NOAA = National Oceanic and Atmospheric Administration

OI = Oxygen Index

OM = Organic Matter

P/V = P-hydroxyl phenols over Vanillyl phenols ratio

P/(V+S) = P-hydroxyl phenols over sum of Vanillyl and Syringyl phenols

PAH = Polycyclic Aromatic Hydrocarbon

PBDE = PolyBromoDiphenyl Ether

PCA = Principal Component Analysis

PEL = Probable Effect Level

ROL = Radial Oxygen Loss

S/V = Syringyl phenols over Vanillyl phenols ratio

SD = Standard Deviation

SEM = Scanning Electron Microscopy

SRM = Selected Reaction Monitoring

TEC = Threshold Effect Concentration

TEL = Threshold Effect Level

TF = Translocation Factor

TFA = TriFluoroacetic Acid

TM = Trace Metal

TOC = Total Organic Carbon

TpS2 = Temperature of the Peak S2

UPLC = Ultra Performance Liquid Chromatography

w/v = Weight/Volume

XRD = X-Ray Diffraction

ZAC = Zone d’Aménagement Concerté

Liste des Tableaux

Liste des Figures

INTRODUCTION

1. Etat de l’art

1.1. Généralités sur l’écosystème de mangrove

1.1.1. Définition et intérêts

La mangrove est un écosystème intertidal qui se développe le long des côtes tropicales et subtropicales entre 30°N et 30°S (Lugo and Snedaker, 1974) ; les facteurs hydrodynamiques agissent donc sur la structure et les fonctions des mangroves (Massel et al., 1999). Les forêts de mangrove représentent 0.5% de la surface des forêts mondiales (Donato et al., 2011), affichent une structure relativement simple et sont moins riches en espèces que les forêts tropicales classiques (Alongi, 2002). Elles sont principalement composées d’espèces végétales uniques à l’écosystème de la mangrove, mais il est également possible de trouver d’autres espèces végétales présentes dans les marées salées ou les forêts humides (Lugo and Snedaker, 1974). Les espèces végétales se développent en groupes de végétation uniforme depuis le front de mer jusqu'à la limite intérieure de l'écosystème, qui est uniquement inondée par les marées les plus hautes (Fromard et al., 2018).

La mangrove fournit de nombreux services écosystémiques évalués à 1.6 milliard de dollars US par an (Costanza et al., 1998), en raison de sa position, de son système racinaire dense et de la faible teneur en oxygène de son sol (Lee et al., 2014). Tout d'abord, la mangrove limite l'érosion des côtes en atténuant l'impact des vagues et des tempêtes sur le littoral (Massel et al., 1999; McIvor et al., 2012; Spalding et al., 2014). Elle sert également de nurserie à de nombreuses espèces de poissons, de crustacés et d'oiseaux grâce à sa production élevée de matière organique (MO) et à son système racinaire qui réduit la prédation (Laegdsgaard and Johnson, 1995; Thollot, 1996). Il est estimé qu’environ 80% des poissons pêchés pour la consommation personnelle ou le commerce dépendent directement ou indirectement de la mangrove (Ellison, 2008). Une étude récente estime que 1 m² de mangrove peut produire jusqu’à 70 individus consommables par an (Leal and Spalding, 2022). Pour l’Homme, la mangrove est également une ressource en bois d’excellente qualité qui peut être utilisé aussi bien pour des constructions que pour la production de charbon (Fromard et al., 2018). D’autres ressources provenant des palétuviers sont utilisées par certaines populations comme teinture, latex, ou médicaments (Fromard et al., 2018). La mangrove agit aussi comme un filtre pour l'eau, les particules et les contaminants potentiels en provenance de la terre (Harbison, 1986; Furukawa et al., 1997; MacKenzie et al., 2016), tout en étant une source essentielle de nutriments pour les écosystèmes adjacents grâce à sa production de MO

(Lee, 1995; Dittmar et al., 2006; Sippo et al., 2017; Ray et al., 2018). Enfin, la mangrove agit comme un piège à CO_2 grâce à sa biomasse et à sa capacité de stockage de carbone dans le sol (Kristensen et al., 2008; Alongi, 2014; Murdiyarso et al., 2015). Le taux d'assimilation moyen du CO_2 par les feuilles de palétuviers est quasiment deux fois supérieur à celui des arbres de forêts tropicales humides (Fromard et al., 2018). C'est pourquoi actuellement, 42% des mangroves mondiales sont des aires protégées reconnues par l'Union Internationale pour la Conservation de la Nature (IUCN) (Leal and Spalding, 2022).

1.1.2. Distribution géographique

Les forêts de mangrove couvrent les littoraux de 105 pays (Hamilton and Casey, 2016), pour une superficie estimée à 147 359 km² (*Figure 1-1*) (Leal and Spalding, 2022). La région avec le plus de richesse spécifique est l'Indo-Pacifique (Alongi, 2002). La taille des palétuviers au sein des mangroves est en corrélation avec la latitude. Près de l'équateur, on peut trouver des forêts de mangrove atteignant la même taille que les forêts tropicales humides (Clough, 1992). À l'échelle mondiale, la distribution des écosystèmes de mangrove est limitée par la température, avec une moyenne de 20 °C pendant les mois les plus frais (Duke et al., 1998). À l'échelle régionale, la structure et la superficie des mangroves sont déterminées par des facteurs tels que les cours d'eau, les vagues, les marées et les précipitations (Alongi, 2002). L'actuelle répartition de la mangrove ainsi que la dispersion de ses espèces végétales sont le produit de son histoire évolutive, de ses méthodes et voies de dispersion, et des extinctions d'espèces qui ont pu survenir depuis le début du Tertiaire, époque à laquelle sont associés les plus anciens fossiles de palétuviers identifiés (Fromard et al., 2018).

Ainsi, la mangrove mondiale se divise en deux vastes domaines biogéographiques, se distinguant par la variété et le nombre d'espèces qui les caractérisent : un domaine oriental couvrant de l'Indo-Malaisie à l'Australie jusqu'à la côte Est africaine, et un domaine occidental comprenant les littoraux atlantiques, leurs îles associées et la côte pacifique américaine. Du côté oriental, la mangrove abrite plus de 60 espèces, tandis que l'occident ne compte qu'une douzaine d'espèces. Aucune espèce n'est partagée entre ces deux domaines, du fait que l'immensité de l'océan Pacifique d'un côté et les eaux froides du sud de l'Afrique de l'autre, entravent la libre dispersion des propagules (graines germées) (Fromard et al., 2018). L'Indonésie possède la plus grande superficie de mangrove au monde, représentant environ 28% de la totalité des mangroves de la planète (Hamilton and Casey, 2016). Les quatre pays ayant la plus grande superficie de mangrove se partagent 50% de l'ensemble des mangroves mondiales. Après

l'Indonésie, ces pays sont le Brésil (9%), la Malaisie (6%) et la Papouasie-Nouvelle-Guinée (5%). Les 20 pays possédant la plus grande superficie de forêts de mangrove englobent plus de 85% de l'ensemble des mangroves (Hamilton and Casey, 2016).

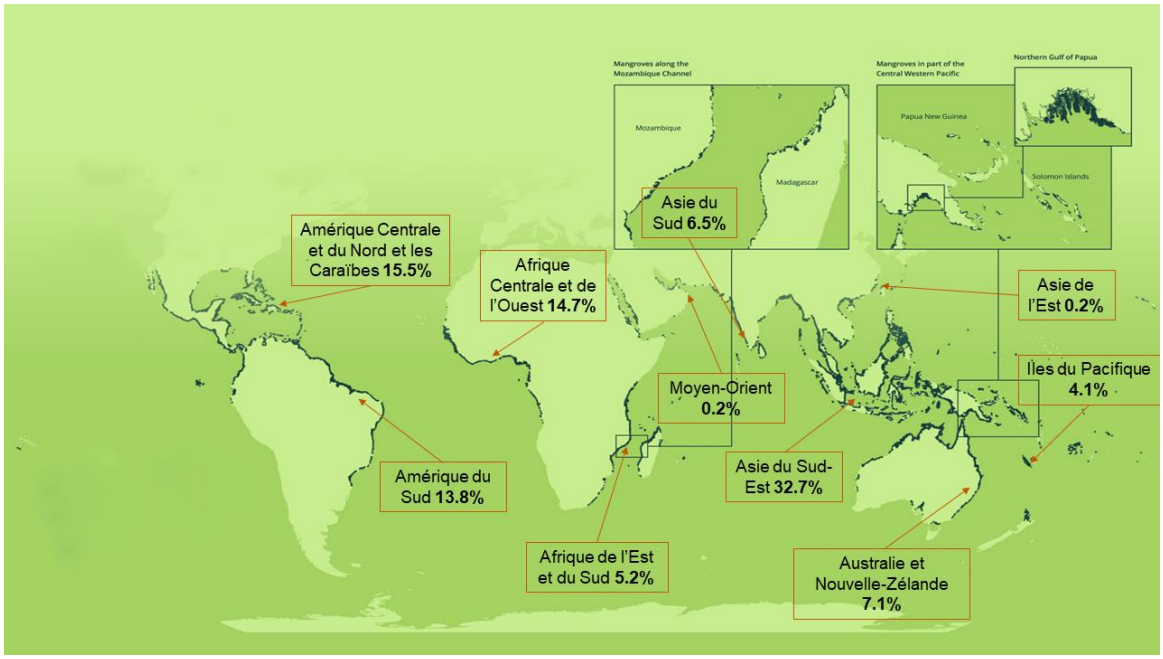

Figure 1-1. Forêts de mangrove dans le monde en 2020 et pourcentage de surface par région (modifiée de Leal and Spalding, 2022).

1.1.3. Les espèces

1.1.3.1. Les palétuviers

Les palétuviers sont des halophytes de type C3 (Kathiresan and Bingham, 2001), capables de pousser sur des sols présentant une salinité allant jusqu'à 100 g L^{-1} (Ball, 1998), avec une tolérance qui s'accroît avec l'âge. Sur des sols à forte salinité, les palétuviers consacrent davantage d'énergie au maintien des concentrations ioniques et à l'équilibre hydrique qu'à leur croissance. Cependant, dans des conditions non-salines, les palétuviers ne rivalisent pas efficacement avec les plantes des marais d'eau douce (Barik et al., 2018).

Dans le monde, on répertorie 9 ordres, 20 familles, 27 genres et 69 espèces de palétuviers (Spalding et al., 1997). Une seule famille appartient à la division des fougères (Polypodiophyta), les autres étant des angiospermes de la division Magnoliophyta (Kathiresan and Bingham, 2001). Le genre de palétuvier le plus répandu est *Rhizophora*, qui compte 8 espèces. Les genres *Laguncularia* (11 espèces), *Avicennia* (9 espèces), *Bruguiera* (6 espèces), *Sonneratia* (5 espèces), *Ceriops* (2 espèces), *Lumnitzera* (2 espèces), *Kandelia* (1 espèce) et *Nypa* (1 espèce) sont également fréquemment présents (Kathiresan and Bingham, 2001).

Les espèces se développent en bandes monospécifiques en fonction de l'élévation et de la salinité du sol, entre autres facteurs (Bunt, 1996; Ball, 1998). Cette zonation peut également être influencée par la physiologie de l'espèce, telle que les concentrations de tannins et de polyphénols (Wang et al., 2014a). Les palétuviers peuvent croître sur différents types de sols, ce qui entraîne une variation considérable de la structure des forêts de mangrove en termes d'espèces à l'échelle mondiale, régionale et locale (Hossain and Nuruddin, 2016). Au sein d'une même espèce, des variations physiologiques peuvent être observées en raison des réponses phénotypiques à l'environnement local (Kathiresan and Bingham, 2001). Il existe cinq types de structures de mangrove en fonction de la géomorphologie du terrain et des apports en eau (*Figure 1-2*).

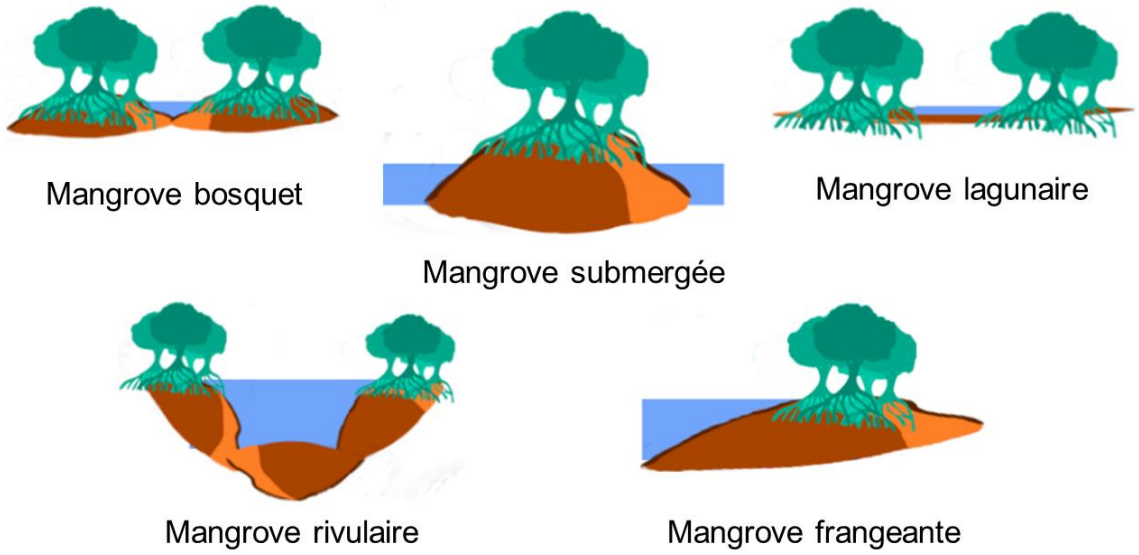

Figure 1-2. Types de structures des mangroves.

1.1.3.2. La macrofaune et la méiofaune

La densité racinaire des forêts de mangrove et l'abondance de nutriments offrent un habitat protégé adéquat pour de nombreuses espèces pendant une partie ou la totalité de leur cycle de vie (Nagelkerken et al., 2008). Entre le sol et l'eau, un grand nombre de crustacés et de poissons trouvent refuge, certains d'entre eux pouvant ensuite migrer vers les eaux plus profondes. Les Périophtalmes constituent une exception parmi les poissons, car ils résident exclusivement dans les mangroves, que ce soit à marée haute ou à marée basse (*Figure 1-3*). Les mollusques, quant-à-eux, sont fixés aux racines et aux troncs de palétuviers. Une multitude de petits animaux (copépodes, nématodes, insectes, etc.) réside également dans la vase ce qui attire une variété considérable d'oiseaux qui viennent se nourrir de ces animaux. En Australie, on a recensé jusqu'à 186 espèces d'oiseaux au sein d'une seule forêt de mangrove (Noske, 1996), et une dizaine d'entre elles se trouvent exclusivement dans les mangroves (Nagelkerken et al., 2008). Au niveau

du sol et dans la canopée, on trouve de nombreuses espèces de reptiles et même de mammifères. Des reptiles tels que les geckos, les caïmans et les pythons peuvent être observés dans les forêts de mangrove du monde, où ils pondent, vivent, ou se nourrissent de poissons et de crustacés (Macintosh and Ashton, 2002).

Figure 1-3. Deux individus de Périophtalme dans la mangrove d'Apogoti.

1.1.3.3. Les microorganismes

L'abondance en carbone et en autres nutriments au sein des écosystèmes de mangrove favorise la présence d'un grand nombre de communautés microbiennes (Thatoi et al., 2013). Ces communautés microbiennes jouent un rôle essentiel dans le cycle des nutriments tels que le carbone, l'azote, le soufre et le phosphore (Alongi et al., 1993). Parmi les composants microbiens, les protozoaires (2%) et les algues (7%) représentent la plus petite fraction de la biomasse microbienne dans les sols des mangroves tropicales, tandis que les bactéries et les champignons représentent 91% de l'ensemble (Alongi, 1988). On retrouve de nombreux types de champignons dans les sols de mangrove, tels que les actinomycètes, les cellulolytiques, les pectinolytiques et les ligninolytiques (Kathiresan and Bingham, 2001). En ce qui concerne les bactéries, les groupes les plus courants sont les sulfato-réductrices, les fixatrices d'azote, les solubilisatrices du phosphate et les méthanogéniques (Sahoo and Dhal, 2009). La répartition, la dynamique et l'abondance de ces microorganismes sont régulées par une variété de facteurs environnementaux physiques (salinité, température, etc.), chimiques (pH, carbone, etc.) et biologiques (brouteurs) (Fromard et al., 2018).

1.1.4. Les pressions subies par la mangrove

Les forêts de mangrove sont exposées à différentes pressions environnementales et anthropiques. Toutes formes de stress peuvent rendre les palétuviers plus vulnérables aux maladies et aux parasites (Alongi, 2002), et peuvent entraîner l'accumulation d'espèces réactives de l'oxygène (ERO) (Wang et al., 2014a). Ainsi, les palétuviers ont développé des systèmes antioxydants efficaces par la production d'enzymes afin de contrer les effets négatifs des ERO (Ghosh et al., 2021; Wang et al., 2014a). Toutefois, la mangrove se caractérise également par sa forte résilience. Elle peut rapidement recoloniser un espace, après avoir été détruite, à condition que les conditions d'habitat, notamment hydro-sédimentaires, le permettent toujours (Fromard et al., 2018).

1.1.4.1. Les pressions naturelles

La position intertidale des mangroves induit un stress dû à l'instabilité du substrat, à la submersion et à la salinité du sol. Les palétuviers ont ainsi développé des caractéristiques uniques, telles que le développement d'une biomasse souterraine importante et la mise en place d'un système racinaire latéral pour accroître leur stabilité (Youssef and Saenger, 1996; Nizam et al., 2022). Les palétuviers n'ont pas besoin du sel marin pour leur métabolisme, mais ils se sont adaptés pour lutter contre celui-ci. En réponse au stress salin, la viviparité permet aux palétuviers d'éliminer l'excès de sel pendant la phase de germination (Nizam et al., 2022). Le sel peut également être excrété par les glandes excrétrices de sels présentes sur les feuilles de certaines espèces (*Avicennia*, *Acanthus*, *Aegiceras*), ainsi que lors de la chute des feuilles sénescentes (Kathiresan and Bingham, 2001). Certaines espèces peuvent également piéger les excès de sodium et de chlore au sein de vacuoles pour limiter leur toxicité. D'autres palétuviers tels que les *Rhizophora*, *Bruguiera* et *Ceriops* éliminent l'excès de sel par l'ultrafiltration au niveau de la membrane des cellules racinaires (Nizam et al., 2022).

La submersion du sol expose les palétuviers à de longues périodes sans oxygène, à l'accumulation de phytotoxines solubles, au manque de nutriments essentiels et à la prolifération de microorganismes parasites anaérobiques (Youssef and Saenger, 1996). Le développement de diverses racines aériennes chez les palétuviers constitue un mécanisme efficace pour pallier le manque d'oxygène dans le sol en captant de l'oxygène de l'atmosphère pour le diffuser dans les tissus souterrains (Scholander et al., 1955). Différentes espèces de palétuviers présentent des structures racinaires aériennes distinctes, telles que les pneumatophores chez *Avicennia marina*, les racines contreforts chez *Heritiera littoralis*, les racines coudées chez *Bruguiera gymnorrhiza* et les racines échasses chez *Rhizophora stylosa* (*Figure 1-4*) (Youssef and Saenger, 1996). A la surface

de ces racines, se trouvent des pores ou des lenticelles qui assurent à la plante la continuité d'échange de l'oxygène même lorsque la marée haute la submerge. Chaque système racinaire est adapté pour faciliter un transfert d'oxygène interne efficace en fonction de la durée d'immersion de l'espèce (Pi et al., 2009). Ce transport d'oxygène dans les racines souterraines favorise également l'oxydation de phytotoxines telles que le Fe^{2+} ou le H_2S, les rendant inoffensifs (Armstrong and Armstrong, 1988).

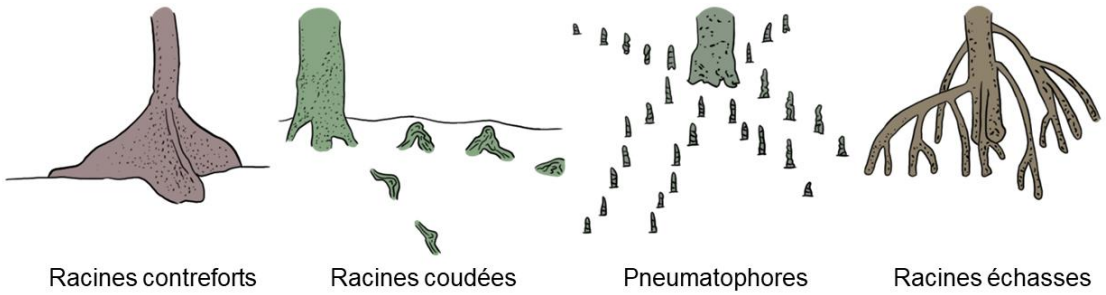

Figure 1-4. Types de racines (modifiée de Tyler Gantuangco, CCEF).

En plus des conditions environnementales stressantes dans lesquelles elles se développent, les mangroves doivent s'adapter aux conséquences du changement climatique. Le réchauffement climatique entraîne une augmentation des températures moyennes dans la plupart des régions du monde, ce qui conduit à une expansion latitudinale des forêts de mangrove (Nizam et al., 2022). De plus, le changement climatique provoque une élévation du niveau des océans, impactant les mangroves en tant qu'écosystèmes côtiers. La mangrove est un écosystème dynamique qui a survécu aux fluctuations du niveau des océans au cours des derniers millénaires (Alongi, 2015). Cette résilience est rendue possible grâce à l'accrétion verticale ou à la migration horizontale (MacKenzie et al., 2016). Actuellement, l'accrétion des forêts de mangrove, due au taux élevé de sédimentation, peut potentiellement compenser la montée des eaux dans certaines régions (Field, 1995). Cependant, cette accrétion peut être perturbée et la migration vers les terres peut être limitée par la présence d'infrastructures anthropiques (Woodroffe et al., 2016).

1.1.4.2. Les pressions anthropiques

1.1.4.2.1. La déforestation

La déforestation des forêts de mangrove a été très importante au XX^{e} siècle, avec une perte d'environ 35% de leur surface mondiale entre 1980 et 1990 (Valiela et al., 2001), à un rythme moyen de 1% de perte de surface par an (FAO, 2007), pouvant atteindre jusqu'à 8% dans certaines régions (Miththapala, 2008). Cette perte est principalement due à l'aquaculture de crevettes, qui représente plus d'un tiers des pertes de surface de mangrove (Thomas et al., 2017). Les autres causes de déforestation comprennent

l'utilisation du bois, l'aquaculture de poissons et l'utilisation d'herbicides (Valiela et al., 2001). La déforestation de cet écosystème riche en carbone contribue à environ 10% des émissions mondiales de carbone dues à la déforestation (Donato et al., 2011), et une émission supplémentaire de 2 391 Tg de CO_2 est estimée d'ici la fin du siècle (Adame et al., 2021). Au début du XXI^{e} siècle, la perte de surface des mangroves a considérablement diminué, avec une moyenne de 0.16% à 0.39% par an à l'échelle mondiale. Cependant, la région d'Asie du Sud-Est demeure préoccupante, abritant plus de la moitié des forêts de mangrove et affichant le taux de perte le plus élevé dû à la déforestation (3.58% à 8.08%) (Hamilton and Casey, 2016). Entre 2010 et 2020, la diminution de la surface de mangrove est estimée à une moyenne de 0.04% par an à l'échelle globale (Leal and Spalding, 2022). La déforestation des mangroves prive les côtes de nombreux services, notamment la protection du littoral et le stockage des contaminants (Bastakoti et al., 2019b).

1.1.4.2.2. Les apports anthropiques

Étant situées au point le plus bas des bassins versants, les mangroves reçoivent les apports de ces derniers. Ces apports peuvent contenir des contaminants naturels, provenant du lessivage des sols, tels que les métaux présents dans la croûte terrestre. Les activités minières et agricoles peuvent aggraver ce lessivage, contribuant ainsi à la contamination de l'écosystème en aval (Marchand et al., 2012; Johnston et al., 2016). De plus, les activités humaines génèrent également des rejets de contaminants (pesticides, hydrocarbures, antibiotiques, plastiques, etc.) par voie aquatique ou atmosphérique, qui atteignent les sols et la biomasse des mangroves (Lewis et al., 2011; van Bijsterveldt et al., 2021). Les mangroves sont également vulnérables aux contaminants apportés par les marées, tels que les hydrocarbures issus des marées noires, ainsi que par les plastiques flottants qui se retrouvent piégés dans les racines des palétuviers (Hensel et al., 2014; Cordova et al., 2021). L'apport de nutriments provenant des effluents de crevetticulture, d'origine domestique ou agricole, entraîne une augmentation de la productivité et de la croissance des palétuviers, mais les rend également plus vulnérables aux stress environnementaux (Lovelock et al., 2009). Un excès de nutriments peut altérer les propriétés physico-chimiques du sol, réduisant ainsi la capacité de piégeage de certains éléments (Marchand et al., 2011b; Suárez-Abelenda et al., 2014).

1.1.4.2.3. L'urbanisation

Les mangroves urbaines se développent dans ou à proximité des villes. Il existe trois catégories de mangroves urbaines : 1) celles qui colonisent naturellement l'espace, après le développement urbain, 2) celles qui ont été restaurées après le développement urbain et 3) celles qui sont les vestiges d'une mangrove plus grande datant d'avant le

développement urbain. En moyenne, environ un tiers de la population mondiale vit à proximité du littoral, un chiffre qui augmente pour les pays tropicaux (CIESIN, 2012). Cela engendre rapidement un conflit d'espace entre les mangroves et le développement des infrastructures urbaines. Plusieurs menaces pèsent donc sur les mangroves urbaines, la déforestation étant la pression la plus directe (Tuholske et al., 2017). L'aménagement anthropique du littoral peut également générer de nouveaux effluents susceptibles de modifier les conditions physico-chimiques du système (Torres et al., 2019), agissant comme source de nutriments ou de contaminants (Cavalcante et al., 2009; Bastakoti et al., 2019a). Ces rejets urbains peuvent provoquer des modifications physiologiques chez certaines espèces (Pi et al., 2010) et altérer les communautés microbiennes du sol (Torres et al., 2019; Fiard et al., 2022). Les mangroves urbaines peuvent également faire face à des modifications des apports hydrologiques terrestres ou marins, entraînant un déséquilibre de l'écosystème. L'urbanisation du littoral entrave la migration intérieure des mangroves, un processus naturel d'adaptation à la montée du niveau de la mer. Le développement d'infrastructures anthropiques à proximité des forêts de mangrove a également des effets écologiques sur le long-terme en inhibant le flux de gènes des palétuviers (Nizam et al., 2022). Ce phénomène limite la diversité génétique des palétuviers ce qui peut entrainer des pertes de résilience des mangroves.

1.2. La matière organique dans la mangrove

1.2.1. Quelques chiffres

La mangrove est un écosystème à carbone bleu, car il s'agit d'un écosystème côtier qui possède une forte capacité de stockage de carbone dans sa biomasse et son sol. Les écosystèmes à carbone bleu ne représentent que 0.2% de la surface des océans, mais ils contribuent à la séquestration en carbone de plus de 50% des sédiments marins (Mcleod et al., 2011). Les mangroves font partie des forêts tropicales les plus riches en carbone de la planète, avec une estimation de 1 023 Mg de carbone par hectare (Donato et al., 2011). En termes de carbone organique (CO), les mangroves représentent 17% du CO tropical marin, avec en moyenne 739 Mg de CO par hectare, comparé à 317 Mg pour les marais salants et 315 Mg pour les forêts tropicales (Alongi, 2020). C'est dans son sol que la mangrove stocke plus des trois quarts de son CO, le reste étant réparti entre la biomasse hors-sol et la biomasse souterraine (Alongi, 2020). La répartition du stock de carbone par région est en grande partie déterminée par les précipitations annuelles, les régions tropicales humides ayant des stocks plus élevés que les régions tropicales sèches (Sanders et al., 2016). Les taux de séquestration du carbone dans le sol varient entre 1 et 1 722 g de CO par m² et par an, avec une moyenne de 180 g, ce qui est considérablement

supérieur aux taux observés pour les forêts tropicales (62.5 g m^{-2} a^{-1}) ou les récifs coralliens (5.69 g m^{-2} a^{-1}) (Alongi, 2020). Les conditions souvent anoxiques du sol limitent la minéralisation du CO, favorisant ainsi son stockage à long terme dans les sols de mangrove (Kristensen et al., 2008). De plus, le système racinaire dense des palétuviers contribue à piéger la MO particulaire, ce qui augmente le stock de carbone dans le sol (Kristensen et al., 2008). Le stock carboné associé à la biomasse dépend des parties aériennes et souterraines des palétuviers. La majorité de la biomasse est aérienne (environ 60%) car le réseau racinaire sous-terrain se développe rarement en profondeur du fait de l'abondance d'eau en surface (Fromard et al., 2018).

1.2.2. La litière végétale

Les forêts de mangroves présentent d'importants stocks de carbone en raison de la forte productivité de cet écosystème, estimée à 11 Mg de carbone par hectare et par an (Alongi, 2014). La productivité est généralement évaluée à partir des taux de production de la litière végétale annuelle (Twilley, 1988), mais cela ne représente que 25% de la production nette totale (Kristensen et al., 2008). La litière est composée de feuilles, branches, fruits et fleurs et sa production varie en fonction de la latitude. Aux latitudes les plus hautes, la production de litière annuelle est estimée à 4.5 t de matière sèche par hectare contre 10 t au niveau de l'équateur (Fromard et al., 2018). La litière végétale joue un rôle essentiel dans la chaîne trophique de la forêt de mangrove et des écosystèmes adjacents. La décomposition de la litière contribue activement aux flux d'énergie et de matière dans la mangrove et constitue une source d'énergie pour la productivité côtière (Lugo and Snedaker, 1974; Twilley et al., 1986). La MO provenant de la litière végétale peut être consommée directement sur le sol de mangrove par la faune et les microorganismes autochtones. Cette MO peut également être dissoute pendant la décomposition, ou exportée par les marées sous forme de débris, de MO dissoute ou de matière inorganique dissoute (Kristensen et al., 2017; Ray et al., 2018; Taillardat et al., 2018; Kida et al., 2019b). L'origine et le taux de la dégradation de la MO peut, entre autres, être déterminés à partir de sa composition moléculaire. Au cours de cette thèse, deux types de molécules organiques ont été étudiés : la lignine et les glucides neutres.

1.2.3. La lignine

Les parois cellulaires des plantes vasculaires sont composées de cellulose, d'hémicellulose et de lignine. La lignine représente généralement entre 16% et 30% de la biomasse totale des plantes et agit comme un liant pour les composés fibreux (Zhang et al., 2014). La lignine est la plus grande source de composés aromatiques sur la planète. Elle n'a pas de structure prédéfinie; sa structure se forme lorsque des unités

monomériques se lient de manière aléatoire en fonction des conditions environnementales et des concentrations de ces unités (Letourneau and Volmer, 2021). La lignification est associée au développement du système vasculaire des plantes, fournissant une résistance à la biodégradation et aux stress environnementaux (Argyropoulos and Ben Menachem, 1997). Associée à l'hémicellulose, la lignine confère une rigidité aux plantes en combinant trois précurseurs phénylpropanoïques : l'unité p-hydroxyphényle (0 groupe méthoxyle), l'unité guaiacyl (1 groupe méthoxyle) et l'unité syringyl (2 groupes méthoxyle) (Reid, 1995). La lignine joue également un rôle crucial dans le transport interne de l'eau, des métabolites et des nutriments au sein de la plante (Lebo, 2002). Les plantes primitives telles que les algues et les champignons ne possèdent pas de lignine dans leur système (Argyropoulos and Ben Menachem, 1997). L'oxydation de la lignine produit une série de phénols simples, caractéristiques de la source et du taux de dégradation de la MO (*Figure 1-5*) (Hedges and Ertel, 1982). Les gymnospermes présentent des signatures ligniniques différentes de celles des angiospermes, et les tissus durs présentent des signatures distinctes de celles des tissus mous (Hedges and Mann, 1979).

En raison de sa structure aromatique, de sa rigidité et de l'hétérogénéité de ses liaisons intramoléculaires, la lignine est peu accessible à la dégradation par les microorganismes, ce qui en fait une composante de la MO réfractaire (Reid, 1995). Ce sont principalement des champignons spécialisés, appelés champignons lignivores, qui sont capables de dégrader la lignine (Zabel and Morrell, 2020). Les trois modes de dégradation de la lignine sont les suivants : 1) oxydation du noyau aromatique, 2) oxydation des liaisons entre les carbones alpha et bêta, et 3) clivage des liaisons éther (Chen and Chang, 1985). Les proportions individuelles des dérivés phénoliques fournissent des informations sur les mécanismes de dégradation. L'oxydation des chaînes latérales est un mécanisme de dégradation caractérisé par une augmentation des rapports acide/aldéhyde. La perte de groupements méthoxyle se traduit par une diminution des rapports entre les composés de l'unité syringique et ceux de l'unité vanillique (Benner et al., 1990).

Dans le sol de mangrove, la lignine représente moins de 10% du carbone organique total (COT), mais son taux de dégradation est généralement inférieur à celui du CO (Dittmar and Lara, 2001; Marchand et al., 2005; Lallier-Vergès et al., 2008). Les quelques études réalisées sur la lignine dans le sol de mangrove montrent que sa dégradation est influencée par les conditions redox. Étant donné que le sol de mangrove est principalement anoxique, le mécanisme principal de dégradation de la lignine est le clivage du noyau aromatique (Marchand et al., 2005; Lallier-Vergès et al., 2008).

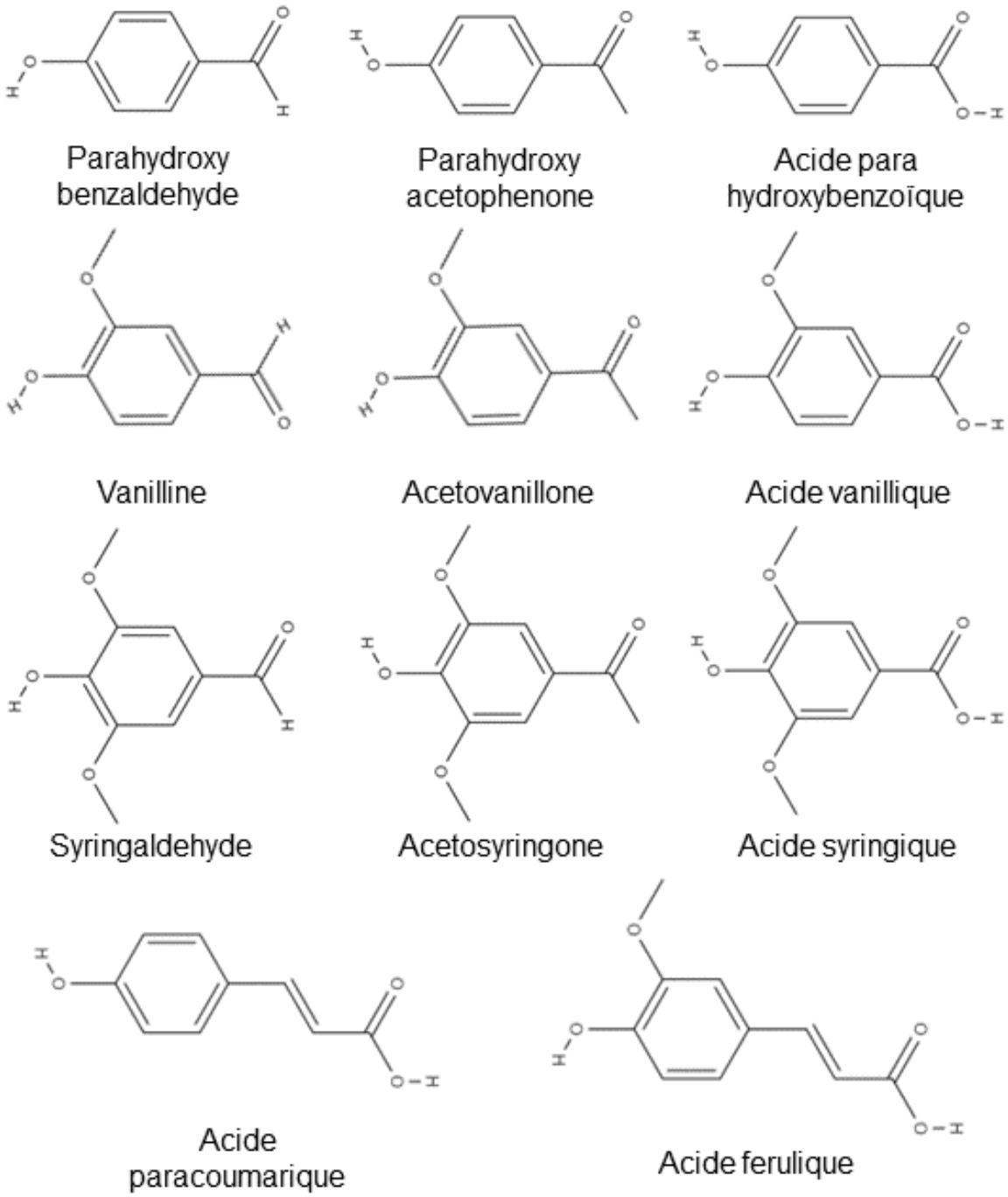

Figure 1-5. Les dérivés phénoliques de la lignine étudiés dans cette thèse.

1.2.4. Les glucides neutres

Les glucides sont l'une des principales classes de biomolécules produites par les organismes vivants, ayant des fonctions structurelles et de stockage. Ils représentent entre 20% et 40% de la masse des phytoplanctons, 40% de la masse des bactéries et plus de 75% de la masse des plantes vasculaires (Moers et al., 1993). Les glucides sont des molécules organiques composées de carbone, d'oxygène et d'hydrogène, constituées

d'unités monomériques appelées saccharides. Il existe des monosaccharides (1 unité), des disaccharides (2 unités), des oligosaccharides (entre 3 et 10 unités) et des polysaccharides (>10 unités). Les polysaccharides les plus courants sont la cellulose, l'hémicellulose et la pectine (Cowie and Hedges, 1984a). Les monosaccharides, également appelés "sucres", sont la forme la plus simple de glucides et peuvent se combiner pour former des molécules plus complexes. L'hydrolyse des polysaccharides naturels en leurs composantes de sucres neutres (*Figure 1-6*) permet de distinguer leur origine (marine vs terrigène ou microbienne vs végétale), ainsi que différents types de tissus végétaux (Cowie and Hedges, 1984b). Par exemple, le ribose est un composé de l'ARN et est proportionnellement beaucoup plus présent chez les microorganismes que dans les tissus des plantes vasculaires. Le fucose est un sucre de stockage très présent chez les bactéries et le phytoplancton, mais se trouve en quantités beaucoup plus faibles chez les plantes (Barker and Somers, 1970). Les concentrations de xylose et de mannose peuvent permettre de distinguer entre la MO provenant des angiospermes et celle provenant des gymnospermes, car ces dernièrs sont moins riches en xylose mais plus riches en mannose. Enfin, les tissus foliaires contiennent généralement plus de pectine et donc ont des concentrations plus élevées en arabinose et en galactose que les tissus ligneux (Aspinall, 1970). Lors de l'étude des glucides neutres dans un environnement, deux processus s'opposent : la perte de sucres par lessivage ou dégradation par les microorganismes qui décomposent la MO, et la production de sucres par ces mêmes microorganismes. Contrairement à la lignine, les glucides sont une excellente source d'énergie et de carbone pour de vastes groupes microbiens (Gunina and Kuzyakov, 2015). Leur dégradation dans le sol de mangrove est donc favorisée, même dans des conditions anoxiques (Moers et al., 1990; Marchand et al., 2005; Lallier-Vergès et al., 2008).

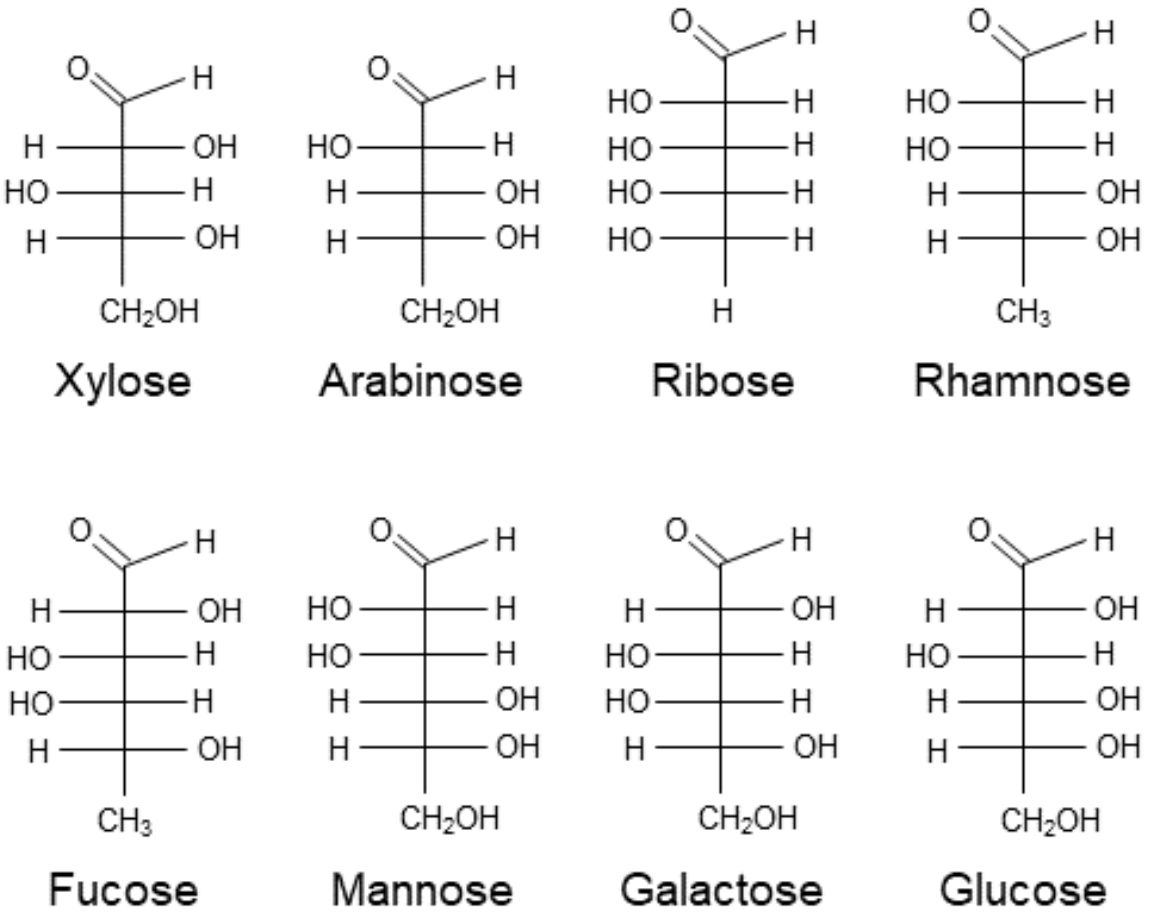

Figure 1-6. Les glucides neutres étudiés dans cette thèse.

1.3. Les éléments traces métalliques dans la mangrove

1.3.1. Généralités sur les éléments traces métalliques

Les métaux sont des éléments naturels partageant des caractéristiques physiques communes, telles qu'une densité élevée, une conductivité électrique et thermique, une ductilité et une malléabilité (Tremel-Schaub and Feix, 2005). Les éléments dits « traces » sont définis par une concentration moyenne dans la croûte terrestre inférieure à 1‰, et dans les organismes inférieure à 0.1‰ (Turekian and Wedepohl, 1961; Tremel-Schaub and Feix, 2005). Certains métaux, comme l'Al, le Fe et le Mn, sont considérés comme des éléments traces dans les organismes mais non dans la croûte terrestre (Tremel-Schaub and Feix, 2005). Certains éléments traces métalliques (ETM) sont essentiels aux organismes vivants, participant aux fonctions biologiques et chimiques de l'organisme (Appenroth, 2010). Cependant, ces ETM, bien qu'essentiels, peuvent devenir toxiques au-delà d'une certaine concentration, dépendant de l'élément, de sa forme et de l'organisme. D'autres ETM sont strictement considérés comme contaminants, car non essentiels aux organismes. C'est le cas du Br et du Cd dans les plantes, ainsi que du Cd, du Hg, du Pb et du Tl chez les humains (Appenroth, 2010).

La concentration des ETM est constante à l'échelle mondiale. Cependant, localement, les concentrations peuvent varier en raison de processus naturels ou anthropiques. Les sources naturelles d'ETM incluent les éruptions volcaniques, les incendies de forêt, le lessivage des roches et les poussières désertiques (Nagajyoti et al., 2010). Les ETM provenant d'activités humaines sont généralement plus biodisponibles que ceux provenant de sources naturelles, ce qui en fait une plus grande menace pour l'environnement et la santé (Tremel-Schaub and Feix, 2005). Les ETM d'origine anthropique peuvent découler des rejets industriels, des fertilisants, des routes et des stations d'épuration, entre autres (Nagajyoti et al., 2010).

1.3.2. Les éléments traces métalliques dans le sol de la mangrove

La dynamique des ETM dans la mangrove a été largement étudiée à travers le monde. Plusieurs facteurs font de la mangrove un piège à ETM : son taux élevé de sédimentation, sa richesse en MO et la réactivité biogéochimique du substrat (Harbison, 1986). Une fois piégés, ces ETM peuvent être remobilisés par des événements météorologiques (tempêtes), des changements des conditions physico-chimiques (salinité, pH) ou même par des activités humaines (dragage). Les ETM associés aux particules sédimentaires terrestres peuvent s'accumuler dans la mangrove lors du dépôt de ces particules. Le taux élevé de sédimentation limite le temps de contact à la surface du sol, qui serait plus propice au lessivage et à l'exportation. La richesse en MO des forêts de mangrove offre un substrat pour l'absorption ou l'adsorption des ETM. En effet, la MO peut former des complexes avec les ETM, et ainsi le cycle de la MO influence la distribution et la biodisponibilité des ETM (Zhou et al., 2010; Nath et al., 2013). Plusieurs études ont établi une corrélation entre le COT et les concentrations en ETM dans le sol de la mangrove (Ray et al., 2006; Mukherjee et al., 2009; Marchand et al., 2011a; Lei et al., 2019). Par exemple, les glucides neutres offrent une large surface et des groupements hydroxyles et carboxyles pour l'adsorption des ETM (Duan et al., 2020), tandis que la lignine, composé réfractaire, offre de nombreux sites pour la formation de complexes métalliques (Thakur et al., 2014). Les ETM sont également piégés dans le sol de la mangrove en association avec les sulfures (Clark et al., 1998; Kehrig et al., 2003). Le soufre est abondant dans les mangroves sous forme de sulfate grâce aux marées. Les sulfures (H_2S, HS^-) se forment à partir du SO_4^{2-} par l'action des bactéries sulfato-réductrices, catalysant la sulfato-réduction microbienne (Crémière et al., 2017). Les sulfures peuvent être ré-oxydés chimiquement ou biologiquement par les bactéries sulfato-oxydantes en sulfates ou en acide sulfurique (SamKamaleson and Gonsalves, 2019). En présence de fer labile, les sulfures réduisent le Fe^{3+} en Fe^{2+} pour précipiter sous forme de pyrite (FeS_2) (Jian et al., 2017). Les ETM sont majoritairement chalcophiles et

donc piégés lors de la précipitation des sulfures minéraux au cours de la diagenèse (Huerta-Diaz and Morse, 1992; Morse and Luther, 1999). La mobilité et la biodisponibilité des ETM dépendent également de nombreux paramètres environnementaux tels que la salinité (Jayachandran et al., 2018), les conditions rédox (Froelich et al., 1979; Clark et al., 1998), l'activité microbienne (Lei et al., 2019) et le pH.

1.3.3. Transfert des éléments traces métalliques vers les palétuviers

Les plantes sont capables d'assimiler les ETM sous forme soluble uniquement (Tremel-Schaub and Feix, 2005). Ces ETM peuvent être piégés au niveau de l'épiderme des racines ou absorbés dans les cellules racinaires, puis transférés vers les organes supérieurs. Les ions métalliques sont mobilisés par des transporteurs membranaires spécifiques à chaque ion ou par des transporteurs d'autres cations, comme c'est le cas du Cd, qui est non essentiel et utilise les transporteurs du Fe, du Mn ou du Zn (Tremel-Schaub and Feix, 2005). La biodisponibilité de chaque ETM dépend de plusieurs paramètres du sol, tels que les caractéristiques physico-chimiques et la capacité d'échange cationique. La biodisponibilité des ETM augmente lorsque le pH du sol diminue, car les ions H^+ entrent en compétition avec les ions métalliques pour les sites d'adsorption des colloïdes à charges négatives (Tremel-Schaub and Feix, 2005). En revanche, une salinité plus élevée dans le sol diminue la biodisponibilité des ETM, car les complexes ETM-Cl formés dans le sol sont difficilement absorbables par les plantes (Cheng et al., 2014). La température du sol a également un impact sur la biodisponibilité des ETM, car une température plus élevée peut altérer la structure de la membrane plasmique, facilitant ainsi la mobilité des ETM dans les racines (Thakur et al., 2016).

Sur les palétuviers, les ETM peuvent diminuer l'activité photosynthétique, la croissance, et même engendrer la mort (MacFarlane and Burchett, 2002; MacFarlane, 2003; Naidoo et al., 2014). Cependant, les palétuviers sont tolérants aux stress métalliques et développent divers mécanismes d'adaptation. En cas de forte concentration d'ETM dans le sol, les palétuviers augmentent leur production d'enzymes antioxydantes (Ghosh et al., 2021) telles que la proline, stabilisant ainsi la structure cellulaire, et la production de PCs-SH, un ligand se liant aux ETM (Huang and Wang, 2010). Certaines espèces épaississent l'exoderme de leurs racines par lignification, réduisant ainsi le passage des ETM vers les organes internes de la plante (Cheng et al., 2012, 2014). Les excrétions au niveau des feuilles par les glandes excrétrices de sel permettent également l'élimination d'ETM en excès du système (Naidoo et al., 2014). Une autre stratégie d'exclusion des ETM consiste en la formation d'une plaque d'oxyde de fer à la surface des racines ou des pneumatophores. Cette plaque se forme par l'oxydation du Fe^{2+} présent

dans le sol par l'apport d'oxygène diffusé par la plante vers la rhizosphère. Cette plaque d'oxyde de fer a principalement été observée chez les palétuviers du genre *Avicennia* (Machado et al., 2005). Plusieurs études ont mis en évidence la réduction de l'absorption des ETM par la plante grâce à la plaque de fer au niveau des racines (Machado et al., 2005; Pi et al., 2011), ainsi que le rôle de réservoir de cette couche dans l'immobilisation des métaux indésirables tels que le Ni et le Cr (Pi et al., 2011; Chowdhury et al., 2017).

1.4. La mangrove en Nouvelle-Calédonie

1.4.1. La Nouvelle-Calédonie

La Nouvelle-Calédonie est un territoire français situé dans le Pacifique Sud, entre les latitudes 19°S et 24°S. Il s'agit d'un archipel couvrant une superficie de 18 350 km² de terres, tandis que sa zone économique exclusive s'étend sur 1 360 000 km². La plus grande île de l'archipel est la Grande Terre, mesurant environ 400 km de long sur 50 km de large en moyenne. Elle est entourée à l'est par les Îles Loyauté, au nord par l'archipel des Bélep et au sud par l'Île des Pins. La Grande Terre est bordée par le plus grand lagon du monde, inscrit au patrimoine mondial de l'UNESCO depuis 2008, avec une barrière de corail s'étendant sur 1 500 km (Maurizot et al., 2020a). D'un point de vue géologique, la Nouvelle-Calédonie est unique dans le Pacifique Sud en tant que partie préservée de la marge Est du supercontinent Gondwana (Cluzel et al., 2001).

L'une des unités géologiques dominantes en Nouvelle-Calédonie est la Nappe Péridotite, un manteau ultramafique contenant des ressources minérales importantes en Ni, Co, Cr et Fe. Cette nappe s'étend sur plus de 8 000 km², représentant 30 à 40% de la surface de la Grande Terre (Maurizot et al., 2020b). D'autres roches d'origine volcano-sédimentaire, principalement des quartz et plagioclases, datant d'avant l'obduction éocène couvrent une surface similaire. Le reste du territoire est partagé entre des roches volcaniques, principalement des basaltes, et des roches métamorphiques (Nicholson et al., 2011).

Le climat en Nouvelle-Calédonie est tropical, voire semi-aride sur la côte Ouest de la Grande Terre, influencé par les phénomènes El Niño et La Niña. Les Alizés, des vents de Sud-Est, prédominent la majeure partie de l'année. Deux saisons principales alternent avec deux intersaisons. La saison chaude s'étend de mi-novembre à mi-avril, tandis que la saison fraîche se déroule de mi-mai à mi-septembre. Les perturbations tropicales, telles que les cyclones et les dépressions, se forment généralement pendant la saison chaude. Les précipitations annuelles moyennes sont d'environ 1 350 mm et les températures

annuelles moyennes atteignent 23.3 °C. Les températures maximales enregistrées sont de 39 °C et les minimales de 5 °C (Maitrepierre, 2012).

1.4.2. La distribution géographique de la mangrove

La mangrove recouvre plus de 35 000 hectares en Nouvelle-Calédonie, représentant 80% du littoral de la côte Ouest de la Grande Terre (*Figure 1-7*). Le relief abrupt de la côte Est limite la présence de mangroves. L'activité économique dominante de ce territoire est l'exploitation minière et industrielle du nickel (Trescases, 1975; Maurizot et al., 2020b). Étant donné qu'un tiers du territoire est composé de sols ultrabasiques, la mangrove se développe principalement en tant que zone de transition entre le lagon et les déversements fluviaux riches en ETM, tels que le Fe, le Cr et le Ni, provenant des sols ultrabasiques et des mines de nickel à ciel ouvert en amont (Bird et al., 1984; Fernandez et al., 2006). La mangrove se développe également sur l'île d'Ouvéa, l'une des trois Îles Loyauté, qui se caractérise par un sol carbonaté.

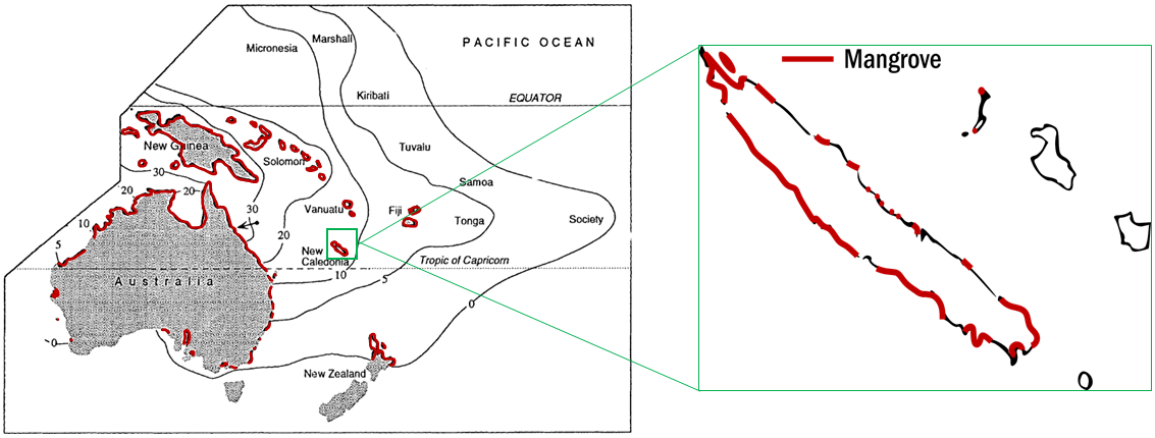

Figure 1-7. Distribution de la mangrove dans le Pacifique et en Nouvelle-Calédonie (modifiée de Duke et al., 1998).

1.4.3. Les espèces floristiques

Au cours d'une campagne d'identification en 2006, 24 espèces de palétuviers appartenant à 15 genres et 13 familles ont été recensées dans les mangroves de Nouvelle-Calédonie. Parmi ces espèces, 4 espèces hybrides sont communes des mangroves calédoniennes et 3 appartiennent au genre *Rhizophora*. La répartition géographique des palétuviers en Nouvelle-Calédonie semble être liée au climat, et quatre groupes d'espèces ont été identifiés : généralistes, nordiques, préférant l'humidité et spécialistes des milieux arides. Le nombre d'espèces par région augmente avec les précipitations jusqu'à un seuil annuelle (2 000 - 2 500 mm), au-delà duquel il diminue avec l'augmentation des précipitations. Les espèces dominantes sont *Acanthus ilicifolius*,

Avicennia marina, *Bruguiera gymnorhiza*, *Excoecaria agallocha*, *Rhizophora samoensis* et *Rhizophora stylosa* (Duke, 2007).

La végétation caractéristique des mangroves calédoniennes de la côte Ouest est organisée en plusieurs strates. Le "tanne," principalement composé de *Salicornia*, occupe la topographie la plus élevée et se développe sur des sols présentant une salinité comprise entre 60 et 100 g L^{-1}. En dessous se trouve *Avicennia marina*, couvrant plus de 15% de la surface totale des mangroves en Nouvelle-Calédonie. Cette espèce préfère les zones de salinité situées entre 35 et 70 g L^{-1}. Les pneumatophores, petites racines à géotropisme négatif, permettent à *A. marina* de distribuer l'oxygène de l'atmosphère dans sa rhizosphère. Le développement de *A. marina* reculé par rapport à la mer induit une faible croissance de cette espèce qui dépasse rarement le stade de buisson (Leopold et al., 2016). Les palétuviers du genre *Rhizophora*, en particulier l'espèce *Rhizophora stylosa*, représentent plus de 50% de la superficie des mangroves calédoniennes et se trouvent le plus près de la mer, dans des zones où la salinité varie entre 5 et 40 g L^{-1} (Marchand, 2007). Les racines échasses des *Rhizophora* stabilisent les arbres dans les substrats vaseux. La reproduction des *Rhizophora* se fait par le biais de longues propagules qui s'enfoncent dans le sol ou se dispersent avec les marées à maturité. Ces espèces prospèrent dans des conditions de salinité similaires à celles de l'eau de mer (Parida and Jha, 2010).

1.4.4. Les services écosystémiques

La mangrove joue un rôle crucial en Nouvelle-Calédonie pour la préservation et la protection du lagon. En retenant les sédiments et les contaminants, elle protège les écosystèmes fragiles tels que les récifs coralliens contre l'étouffement et la pollution. De plus, les populations calédoniennes dépendent directement ou indirectement de la mangrove pour leur subsistance. La pêche aux crabes et aux coquillages dans les mangroves fait partie intégrante du patrimoine culturel de la population locale. En 2010, environ 60% des apports en protéines des Calédoniens provenaient des poissons du lagon (Gontard and de Coudenhove, 2010). Les espèces de poissons d'intérêt économique que l'on trouve dans les mangroves de Nouvelle-Calédonie représentent 60% de la diversité spécifique totale, principalement à un stade juvénile (Thollot, 1996). Enfin, la mangrove peut revêtir une dimension sacrée, comme en témoigne la grande mangrove de Hnimëk, au nord d'Ouvéa, qui abrite selon la tribu de Téouta des esprits et des ancêtres.

1.4.5. Les études scientifiques

Ces dernières années, la mangrove de Nouvelle-Calédonie a suscité un intérêt scientifique croissant, avec de multiples projets de recherche menés à ce sujet. Certaines de ces études se sont penchées sur le carbone sous forme gazeuse, en examinant notamment les variations des émissions de CO_2 et de CH_4 du sol vers l'atmosphère (Leopold et al., 2013, 2016; Jacotot et al., 2019). Le stockage de carbone et le taux de CO dans le sol ont également été mesurés (Jacotot et al., 2018). La dynamique du carbone et d'autres éléments a été étudiée sur plusieurs sites, tant dans le sol (Deborde et al., 2015; Bourgeois et al., 2019b) que dans l'eau (Leopold et al., 2017). Marchand et al. (2011a) ont exploré le lien entre la MO du sol et la dynamique des ETM. Ces ETM ont fait l'objet d'une attention particulière, notamment en aval des roches ultramafiques. Leurs cycles dans les mangroves (Noël et al., 2014, 2015) ainsi que leurs concentrations dans le sol (Marchand et al., 2012; Bourgeois et al., 2020) et les plantes ont été étudiés (Marchand et al., 2016; Bourgeois et al., 2020). Étant donné que l'aquaculture exerce une pression anthropique majeure sur les mangroves dans le monde, plusieurs études ont évalué les effets des effluents des fermes de crevettes sur les taux d'ETM (Marchand et al., 2011b; Bourgeois et al., 2020), sur la MO du sol (Aschenbroich et al., 2015) et les propriétés biogéochimiques des sols (Molnar et al., 2014), ainsi que sur la dynamique de l'azote et la qualité de l'eau (Molnar et al., 2013).

2. Problématique

La Nouvelle-Calédonie est un archipel peuplé de 270 000 habitants au 1er janvier 2022, ce qui représente une augmentation de plus de 200% depuis 1965 (Isee, 2023). La densité de population est relativement faible, avec une moyenne de 16 habitants par km². Cette densité est inférieure à celle des pays possédant les plus vastes étendues de mangrove au monde, tels que l'Indonésie (134 hab km^{-2}), le Brésil (23 hab km^{-2}) et la Malaisie (98 hab km^{-2}) (Nations Unies, 2022). Cependant, environ trois quarts de la population de la Nouvelle-Calédonie est concentrée dans la Province Sud, et plus de 67% de la population réside dans les quatre principales villes, toutes situées au Sud-Ouest de la Grande Terre. Nouméa, qui abrite 35% de la population, est la capitale, suivie de Dumbéa (13%), Mont-Dore (10%) et Païta (9%), formant ainsi le Grand Nouméa (*Figure 2-1*). Le pourcentage de la population urbaine par rapport à la population totale est passé de 37% en 1960 à 72% en 2021 (Nations Unies, 2022).

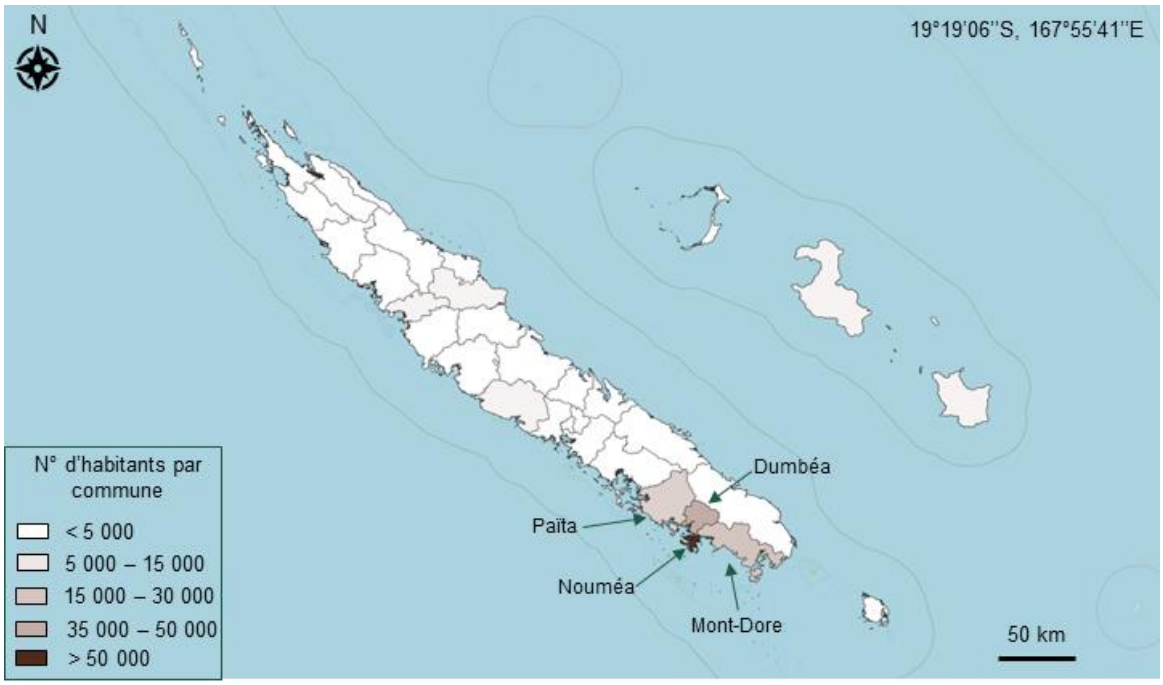

Figure 2-1. Distribution de la population de Nouvelle-Calédonie par commune.

Pour la première fois dans l'histoire, la population de Nouméa est en train de diminuer au profit des villes du Grand Nouméa. En conséquence, des projets d'urbanisme et de développement sont en train de voir le jour dans ces villes où la population ne cesse de croître. Notamment à Dumbéa, deux zones d'aménagement concerté (ZAC) sont toujours en cours d'aménagement depuis 2007. La ZAC de Dumbéa-sur-Mer, qui s'étend sur 500 hectares, la plus grande ZAC de France, et la ZAC Panda de 250 hectares (Ruiz et al., 2020). Ces ZAC se développent en bordure du littoral, à proximité des forêts de mangrove (*Figure 2-2*). Avant le début des travaux des deux ZAC, cette zone était

composée uniquement de deux quartiers principalement résidentiels : Koutio, âgé de plus de 50 ans, et Pointe à la Dorade, érigé au début des années 2000. Nouméa était également une ville dont le littoral était recouvert de forêts de mangrove, avant son urbanisation massive après la Seconde Guerre mondiale. En quelques années, environ 380 hectares de mangrove ont été abattus en raison d'endiguements et de remblaiements à Nouméa. Aujourd'hui, des plans sont en cours pour replanter de la mangrove le long du littoral de la capitale, suite à la prise de conscience des bienfaits de cet écosystème par les collectivités. Forte de l'expérience de Nouméa, la ville de Dumbéa nécessite des mesures préventives et des études scientifiques approfondies afin de mener à bien son expansion tout en limitant l'impact sur les mangroves de son littoral.

Figure 2-2. Carte de Dumbéa avec les deux ZAC, le quartier de Koutio et la localisation des mangroves (fond satellite de Google Earth).

L'étude des mangroves en Nouvelle-Calédonie s'est principalement concentrée jusqu'à présent sur les impacts des activités minières et de l'aquaculture. Les mangroves urbaines ont suscité peu d'intérêt, alors qu'à l'échelle mondiale, les recherches se multiplient, mettant en évidence à la fois leurs valeurs et leurs vulnérabilités (Cavalcante et al., 2009; Alemu I et al., 2021; Reyes et al., 2022). C'est dans ce contexte que cette thèse a vu le jour. Dumbéa a été choisie comme ville pour cette étude car elle est bordée de mangrove. D'une part, elle est composée de vieux quartiers urbains pouvant avoir un impact sur les mangroves depuis des décennies, et d'autre part, elle est en cours d'expansion urbaine, ce qui peut être étudié. Avec un bassin versant d'origine volcano-sédimentaire principalement composé de quartz et plagioclase, l'influence des sols latéritiques riches en ETM est limitée. De plus, les mangroves de Dumbéa sont principalement constituées de deux espèces de palétuviers prédominantes en Nouvelle-Calédonie : *Avicennia marina* et *Rhizophora stylosa*. Une mangrove a été choisie comme

site "urbain" car elle est influencée par les eaux pluviales qui s'écoulent depuis plus de 50 ans dans Koutio et se déversent directement dans cette mangrove. Les arbres *R. stylosa*, qui se développent sur des sols moins salés que ceux d'*A. marina*, se trouvent à la sortie de cette eau urbaine. De ce fait, les arbres sont également beaucoup plus grands que la moyenne pour la même espèce dans les mangroves semi-arides non influencées par l'urbanisation (*Figure 2-3*).

L'urbanisation a des conséquences significatives sur les écosystèmes littoraux, en particulier sur la mangrove. Les flux de matières provenant de la terre ferme vers la mangrove (particulaires ou dissous) peuvent évoluer au fil du temps, entraînant des déséquilibres marqués dans l'écosystème (Branoff, 2017). Comme tout écosystème soumis à des pressions anthropiques, la mangrove doit faire face à diverses formes de pollution. Parmi celles-ci figure la pollution métallique, résultant par exemple des revêtements routiers, des déchets tels que les batteries ou encore des canalisations (Marx and McGowan, 2010). Ces contaminants sont transportés jusqu'à la mangrove par diverses voies (atmosphérique, ruissellement…) et ils peuvent être emprisonnés, accumulés ou transférés vers les écosystèmes voisins, comme les baies, les herbiers ou les lagons (Lacerda et al., 1988; Fernandez et al., 2006; Sadat-Noori and Glamore, 2019). Les ETM ont le potentiel d'être toxiques pour l'homme et l'environnement en fonction de leurs concentrations et de leurs formes (biodisponibilité, état d'oxydation, etc.).

Figure 2-3. Grands palétuviers de l'espèce *R. stylosa* se développant à l'entrée d'eau urbaine provenant de Koutio.

Le taux élevé de sédimentation, la richesse en MO et la réactivité biogéochimique du substrat sont trois facteurs qui confèrent à la mangrove le potentiel d'être une zone d'accumulation des ETM. Au sein des sols, la MO présente une capacité d'adsorption

notable pour divers contaminants (Harbison, 1986). Plus précisément, les monomères issus de la lignine possèdent de nombreux sites actifs qui leur permettent de retenir les ETM (absorption, adsorption, séquestration) (Ge and Li, 2018), de même que les glucides naturels dont les groupements peuvent former des complexes avec des cations métalliques (Angyal, 1989; Alekseev et al., 1998). Plus de 90 % de la MO exportée de la mangrove vers la mer se trouve sous forme dissoute (MOD). La disponibilité de cette MOD peut découler de mécanismes qui influencent également la biodisponibilité des ETM sous forme dissoute, facilitant ainsi le transport de ces contaminants vers le lagon (Ray et al., 2018).

3. Objectifs

Afin de répondre à la problématique exposée ci-dessus, cette thèse a défini des objectifs sous forme de questions scientifiques. Les objectifs sont les suivants :

1. Évaluer l'impact de l'urbanisation sur la nature et les concentrations d'éléments traces métalliques dans les sols de mangrove.

- Quelles sont les sources (anthropiques ou naturelles) d'ETM et comment sont-elles réparties verticalement dans les sols de mangrove ?
- Comment l'espèce dominante (*Avicennia marina* et *Rhizophora stylosa*) et sa position dans la mangrove influencent-elles cette répartition verticale ?
- Comment l'urbanisation affecte-t-elle cette distribution et les concentrations mesurées ?
- Les concentrations d'ETM dépassent-elles les seuils environnementaux dans les mangroves étudiées, et comment se comparent-elles avec d'autres mangroves dans le monde ?

2. Analyser l'impact de l'urbanisation sur la bioaccumulation et le transfert des éléments traces métalliques du sol vers les tissus de palétuviers.

- Quelles sont les concentrations d'ETM dans les feuilles et les racines des palétuviers, et où sont-ils localisés ?
- Quels sont les facteurs de bioconcentration et de translocation propres à chaque espèce et chaque ETM ?
- Comment les caractéristiques spécifiques d'*Avicennia marina* et de *Rhizophora stylosa* influent-elles sur ces facteurs ?
- Comment l'urbanisation influence-t-elle les concentrations d'ETM et les facteurs de bioaccumulation pour chaque tissu ?

3. Identifier les mécanismes d'adaptation des palétuviers face au stress métallique.

- Quel est le rôle de la plaque d'oxyde de fer à la surface des pneumatophores face au stress métallique ?
- L'urbanisation impacte-t-elle la formation de la plaque d'oxyde de fer ?
- Comment l'urbanisation affecte-t-elle la capacité de la plaque d'oxyde de fer à retenir les ETM ?
- Quelles sont les réponses physiologiques visibles aux stress métalliques chez les deux espèces ?

4. Examiner l'effet de l'urbanisation sur la qualité de la matière organique des deux espèces de palétuviers.

- Quelles sont les compositions isotopique et moléculaire des racines, des feuilles fraîches et des feuilles sénescentes d'*Avicennia marina* et de *Rhizophora stylosa* ?
- Les différences entre les deux espèces sont-elles d'ordre physiologique ou environnemental ?
- Comment l'urbanisation affecte-t-elle ces paramètres décrivant les tissus des deux espèces ?

5. Caractériser la dynamique de la matière organique et des éléments traces métalliques au sein de la litière pendant sa décomposition et évaluer l'impact de l'urbanisation sur cette dynamique.

- Quelle est la vitesse de décomposition de la litière végétale dans le sol de mangrove ?
- L'urbanisation affecte-t-elle la vitesse de décomposition de la litière végétale ?
- Comment évoluent les paramètres de la litière végétale (^{13}C, ^{15}N, C/N, composition moléculaire, etc.) au cours de la décomposition ?
- Quel est le rôle de la litière végétale dans le cycle des nutriments et des ETM dans la mangrove ?

6. Caractériser l'origine de la matière organique dans le sol et les processus de décomposition/préservation dans le sol d'une mangrove semi-aride.

- Quelle est la contribution de la MO autochtone dans le sol d'une mangrove semi-aride typique de la côte Ouest de la Nouvelle-Calédonie sans rivière ?
- Quels sont les processus de décomposition de la MO dans les sols de mangrove en fonction des conditions oxydo-réductrices ?
- Quelles molécules de la MO sont labiles et lesquelles sont réfractaires ?
- Quelle est l'origine de la MO en profondeur (mangrove actuelle ou ancienne) et quelle est sa signature chimique ?

7. Évaluer l'impact de l'urbanisation sur la qualité et la quantité de la matière organique dans les sols de mangrove.

- Quelle est la contribution de la MO autochtone dans les sols de mangrove urbaine, et quel est son taux de minéralisation ?

- Comment l'espèce dominante (*Avicennia marina* et *Rhizophora stylosa*) et sa position dans la mangrove influencent-elles l'origine et le taux de minéralisation de la MO ?
- Comment l'urbanisation influence-t-elle l'origine et le taux de minéralisation de la MO dans le sol de mangrove ?

8. Étudier les facteurs influençant la dynamique des éléments traces métalliques dans les sols de mangrove.

- Comment la nature du sol de mangrove (texture et minéralogie) influence-t-elle la dynamique des ETM ?
- Comment les paramètres physico-chimiques influencent-ils la dynamique des ETM ?
- Quel est l'impact des sources de MO et de la composition moléculaire de la MO (lignine et sucres neutres) sur la dynamique des ETM ?

3’. Objectives

To address the issue outlined above, this thesis has defined objectives in the form of scientific questions. The objectives are as follows:

1. Evaluate the impact of urbanization on the identity and concentrations of trace metals in mangrove soils.

- What are the sources (anthropogenic or natural) of TM, and how are they vertically distributed in mangrove soils?
- How do the dominant mangrove species (*Avicennia marina* and *Rhizophora stylosa*) and their positions in the forest influence this vertical distribution?
- How does urbanization affect this distribution and the measured concentrations?
- Do TM concentrations exceed environmental thresholds in the studied mangrove forests, and how do they compare with other mangrove forests worldwide?

2. Analyze the impact of urbanization on the bioaccumulation and transfer of trace metals from soil to mangrove tissue.

- What are the concentrations of TM in mangrove leaves and roots, and where are they located within the root?
- What are the bioconcentration and translocation factors specific to each species and each TM?
- How do the specific characteristics of *Avicennia marina* and *Rhizophora stylosa* influence these factors?
- How does urbanization influence TM concentrations and bioaccumulation factors in each tissue?

3. Identify the adaptation mechanisms of mangroves to metal stress.

- What is the role of the iron plaque on pneumatophores in responding to metal stress?
- Does urbanization impact the formation of the iron plaque?
- How does urbanization affect the ability of the iron plaque to retain TM?
- What are the observable physiological responses to metal stress in both species?

4. Examine the effect of urbanization on the quality of organic matter in the two mangrove species.

- What are the isotopic and molecular compositions of roots, fresh leaves, and senescent leaves of *Avicennia marina* and *Rhizophora stylosa*?

- Are the differences between the two species physiological or environmental?
- How does urbanization affect these parameters, describing the tissues of both species?

5. Characterize the dynamics of organic matter and trace metals within litter during decomposition and assess the impact of urbanization on these dynamics.

- What is the decomposition rate of leaf litter in mangrove soil?
- Does urbanization affect the decomposition rate of leaf litter?
- How do litter parameters ($\delta^{13}C$, $\delta^{15}N$, C/N, molecular composition, etc.) change during decomposition?
- What is the role of leaf litter in the nutrient and TM cycling in this ecosystem?

6. Characterize the origin of organic matter in the soil and the decomposition/preservation processes in the soil of a semi-arid mangrove.

- What is the contribution of autochthonous OM in the soil of a typical semi-arid mangrove forest on the West coast of New Caledonia without rivers?
- What are the decomposition processes of OM in mangrove soils?
- Which OM molecules are labile, and which are refractory?
- What is the origin of deep-seated OM (current or ancient mangrove) and what is its chemical signature?

7. Evaluate the impact of urbanization on the quality and quantity of organic matter in mangrove soils.

- What is the contribution of autochthonous OM in urban mangrove soils, and what is its mineralization rate?
- How do the dominant mangrove species (*Avicennia marina* and *Rhizophora stylosa*) and their positions in the intertidal zone influence the origin and mineralization rate of OM?
- How does urbanization influence the origin and mineralization rate of OM in mangrove soil?

8. Study the factors influencing the dynamics of trace metals in mangrove soils.

- How does the nature of mangrove soil (texture and mineralogy) influence the dynamics of TM?
- How do physicochemical parameters influence the dynamics of TM?
- What is the impact of OM sources and the molecular composition of OM (lignin and neutral carbohydrates) on the dynamics of TM?

4. Méthodologie

4.1. Sites d’étude

Pour évaluer l'influence de l'urbanisation sur une mangrove, il est nécessaire d'avoir une référence en termes de structure et pour chaque paramètre. Nous avons choisi trois sites d'étude (*Figure 4-1*). Les deux premiers sites sont : une forêt de mangrove sous l'influence de l'urbanisation et une forêt de mangrove de contrôle, les plus similaires possibles en termes de bassin versant et d'espèces, notamment pour pouvoir limiter au maximum l'influence d'autres facteurs que l'urbanisation. Il était important de sélectionner une mangrove urbaine dont l'influence de l'urbanisation était connue et datée. De plus, les roches ultramafiques étant abondantes en Nouvelle-Calédonie, de même que les activités minières, il était essentiel de sélectionner des forêts qui n'étaient pas influencées par ces roches ni par les apports provenant des rivières. Pour avoir un point de références sur l’effet de ces roches sur les sols de mangrove, le troisième site d’étude sélectionné est une forêt de mangrove en aval d’un bassin versant ultrabasique. Le choix des sites d'étude s'est également basé sur la facilité d'accès au site et la distance par rapport au laboratoire.

Les sites d'étude urbain et contrôle sont situés sur le littoral de la ville de Dumbéa, une ville en pleine expansion urbaine, et à proximité de Nouméa (*Figure 4-1*). Tout d'abord, la mangrove "urbaine" a été identifiée, comme mentionné dans la problématique. Il s'agit de la mangrove située à côté du Médipôle, en aval de Koutio, qui reçoit depuis plus de 50 ans les eaux pluviales du quartier situé en amont. Cette forêt est composée des deux espèces de palétuviers dominantes sur la côte Ouest de la Nouvelle-Calédonie, à savoir *A. marina* et *R. stylosa*, et son bassin versant est de type volcano-sédimentaire. Ensuite, la mangrove de contrôle a été sélectionnée, à moins de 2 km au nord de la mangrove urbaine, dans la baie d'Apogoti. Cette mangrove, située au fond de la baie, est également constituée d'*A. marina* et de *R. stylosa*, et partage le même bassin versant géologique. Des habitations récentes ont été construites aux alentours de la mangrove de contrôle, sans pour autant être à l'origine d'effluents urbains. La troisième mangrove est située à l’embouchure de la rivière de Dumbéa, à Nakutakoin, et reçoit des sédiments ultrabasiques provenant de son bassin versant par la rivière. Notamment, en amont de cette rivière se trouve une ancienne mine de nickel à ciel ouvert (*Figure 4-1*). Cette troisième mangrove est également constituée des deux espèces *A. marina* et *R. stylosa*. Ces mangroves sont relativement faciles d'accès et ne sont pas soumises aux lois coutumières.

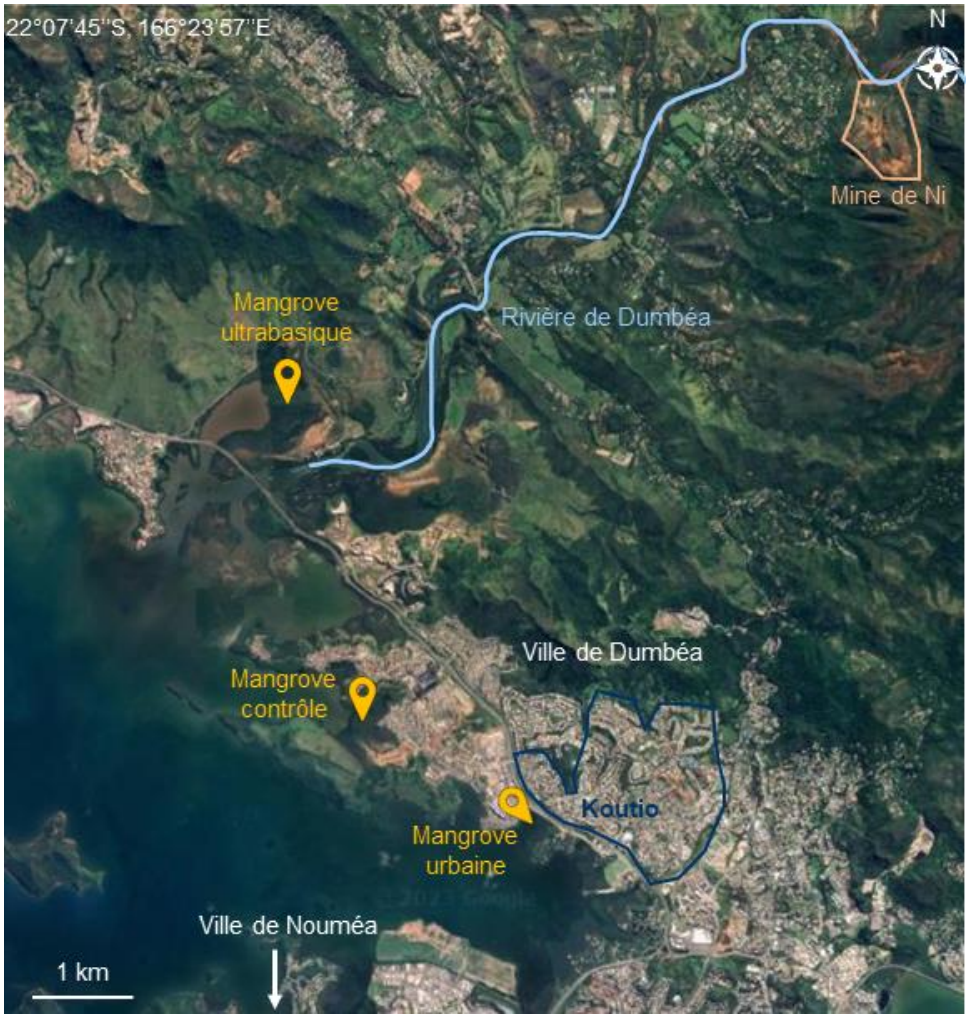

Figure 4-1. Carte de localisation des trois mangroves d'étude (fond satellite de Google Earth).

4.2. Echantillonnage

L'échantillonnage a été réalisé en deux phases sur les sites urbain et contrôle : la première en 1ère année de thèse en 2021 et la seconde en 2ème année de thèse en 2022. En amont de cette thèse, un échantillonnage et traitement des échantillons similaire à la 1ère phase a été réalisé sur le site ultrabasique en 2020. En Nouvelle-Calédonie, il y a deux saisons distinctes au cours de l'année. Par conséquent, dans un premier temps, nous avons cherché à étudier l'influence des saisons sur les différents paramètres d'étude. Cependant, cette thèse s'est déroulée sur une période de trois années au cours de laquelle un phénomène La Niña a eu lieu, modifiant la pluviométrie et la température des saisons. De plus, une étude comparative entre la saison sèche et la saison humide a tout de même été réalisée en 1ère année, mais aucune différence significative n'a été observée en termes de conditions physico-chimiques, de concentrations en ETM ou encore de granulométrie. Par conséquent, aucune mention de la comparaison des saisons n'est faite par la suite dans ce manuscrit.

4.2.1. 1ère phase : caractérisation des sols

La première phase d'échantillonnage s'est déroulée en mai 2021 sur les deux sites d'étude principaux, le site urbain et le site contrôle. Cette première phase consistait à prélever tous les échantillons nécessaires pour déterminer les concentrations en ETM dans les différentes matrices, les compositions moléculaires, ainsi que les caractéristiques du substrat (physico-chimie, granulométrie, etc.).

Pour le sol, nous avons prélevé trois carottes à l'aide d'un carottier en acier inoxydable au milieu des stands monospécifiques, avec environ 30 mètres de distance entre chacune d'elles. Ces carottes ont ensuite été sectionnées en six segments : 0-5 cm, 5-10 cm, 10-15 cm, 15-20 cm, 20-30 cm et 30-40 cm. Nous avons choisi une profondeur totale de 40 cm, car au site urbain, cela correspondait au substrat rocheux. Le choix de six segments, en commençant par des intervalles de 5 cm, puis de 10 cm, était motivé par notre volonté de limiter le nombre d'échantillons tout en garantissant leur représentativité. Nous savions que, avec la profondeur, les caractéristiques du sol ont tendance à changer de moins en moins, tandis qu'à proximité de la surface, d'importantes variations peuvent être observées à seulement 5 cm d'intervalle. Ainsi, 18 échantillons de sol ont été prélevés par espèce et par site, ce qui totalise 72 échantillons pour l'ensemble de la thèse. Ces échantillons de sol ont été placés dans des sacs en plastique hermétiques jusqu'à leur arrivée au laboratoire. Ils ont ensuite été immédiatement congelés, puis soumis à un processus de lyophilisation pendant une période allant de 24 à 72 h. Environ un tiers de chaque échantillon de sol séché a été conservé tel quel, tandis que les deux tiers restants ont été broyés à l'aide d'un broyeur à billes. Tous les échantillons ont été stockés à l'abri de l'humidité et de la lumière.

Les eaux interstitielles ont été prélevées à partir des sections de carottes dont il a été discuté dans le paragraphe précédent. Ainsi, il y a également un total de 72 échantillons d'eaux interstitielles. Chaque échantillon d'eau interstitielle a été obtenu en insérant un RHIZON® dans la section de sol encore fraîche. Une seringue de 20 mL a été connectée au RHIZON® et mise sous dépression à l'aide d'une cale en bois. Cette dépression dans la seringue a permis à l'eau du sol de traverser la membrane du RHIZON® et de s'écouler dans la seringue. Après quelques heures, lorsque les seringues étaient remplies, les eaux ont été filtrées à 45 µm. Environ un tiers de chaque échantillon a été transféré dans un tube en plastique et congelé, tandis que les deux tiers restants ont été transvasés dans un second tube, puis acidifiés avec du HNO_3 à raison d'environ une goutte pour 5 mL (pH< 2), avant d'être stockés à 4 °C. L'acidification des échantillons

d'eaux interstitielles est nécessaire pour prévenir la précipitation de certains composés ou le développement microbien.

Nous avons également souhaité étudier certains tissus de palétuviers. Par souci éthique, il était nécessaire de prélever des tissus en quantités suffisantes sans risquer d'impact négatif sur les palétuviers. Nous avons donc choisi de nous focaliser en premier lieu sur les feuilles, car elles constituent un organe supérieur facile à échantillonner et représentent une grande partie de la litière végétale. Autour de chaque carotte de sol prélevée, un échantillon de feuilles a été collecté. Un échantillon est constitué d'une vingtaine de feuilles provenant de 5 arbres différents se développant dans un périmètre de 2 mètres autour de la carotte. Ainsi, pour chaque site et chaque espèce, nous disposons de 3 échantillons de feuilles destinés à des analyses chimiques. En plus de ces 3 échantillons, un échantillon de feuilles supplémentaire a été prélevé pour chaque espèce et chaque site en vue d'analyses microscopiques. En tout, 16 échantillons de feuilles ont été collectés. Les échantillons foliaires destinés aux analyses chimiques ont été soigneusement lavés à l'eau ultrapure et brossés pour éliminer toute éventuelle contamination superficielle. Les feuilles ont ensuite été congelées, puis séchées au lyophilisateur pendant 24 heures, et enfin broyées au broyeur à lame jusqu'à obtenir une granulométrie inférieure à 1 mm. Ces échantillons sont également conservés au sec et à l'abri de la lumière. Quant aux échantillons destinés à la microscopie, six sections de feuilles ont été découpées au scalpel (*Figure 4-2A & B*). La moitié de ces sections ont été placées dans une étuve à 40 °C pour un séchage immédiat, tandis que l'autre moitié a été soumise à un processus de fixation : trempage dans une solution de 2.5 % de glutaraldéhyde pendant 24 heures dans l'obscurité, suivi d'un triple rinçage à l'aide d'un tampon phosphate 0.1 M à pH 7.4, puis d'une déshydratation de 20 minutes dans de l'éthanol à 60 %, 20 minutes à 70 %, 20 minutes à 85 %, 20 minutes à 90 %, et enfin 1 heure dans de l'éthanol à 96 %. Les sections fixées ont ensuite été placées dans une étuve à 40 °C pour le séchage. La fixation au glutaraldéhyde vise à stabiliser la structure de l'échantillon frais avant le séchage, en vue d'une observation optimale au microscope. Seule la moitié des sections a été fixée afin de garantir la disponibilité d'échantillons non traités pour la microscopie si la fixation ne fournissait pas de résultats satisfaisants. Les échantillons séchés en vue de la microscopie sont conservés à l'abri de la lumière dans un dessiccateur.

Les racines sont le deuxième type de tissu de palétuvier étudié. Les racines sont le premier tissu en contact avec le sol et jouent donc un rôle crucial dans l'absorption et le transfert de l'eau, des nutriments et des contaminants du sol de mangrove vers les palétuviers.

Chez *A. marina*, ce sont les pneumatophores qui ont été collectés dans un rayon de 2 mètres autour de chaque carotte. La collecte de pneumatophore est moins destructrice que la collecte de racines principales. Pour chaque carotte, deux pneumatophores ont été prélevés en les coupant à leur base à l'aide d'un sécateur, en notant soigneusement la partie immergée du sol par rapport à la partie émergée du sol, ce qui donne un total de 12 pneumatophores pour cette thèse. Une fois arrivés au laboratoire, les pneumatophores ont été soigneusement lavés à l'eau ultrapure et à l'aide d'une brosse. Parmi les deux pneumatophores prélevés pour chaque carotte, l'un était destiné aux analyses chimiques et l'autre à l'analyse par microscopie électronique. Pour les pneumatophores destinés aux analyses chimiques, la partie immergée a été divisée en six sections à l'aide d'une scie circulaire en acier inoxydable (*Figure 4-2C*). De manière aléatoire, parmi ces six sections, trois ont été immédiatement placées dans une étuve à 40 °C pour le séchage, tandis que les trois autres ont été traitées au DCB (dithionite-citrate-bicarbonate) afin de retirer la plaque d'oxyde de fer présente à la surface des pneumatophores. L'un des objectifs de cette thèse était en effet d'étudier le rôle de la plaque d'oxyde de fer se développant à la surface des pneumatophores dans la réponse au stress métallique. Le traitement au DCB permet de retirer cette plaque d'oxyde de fer de la surface du pneumatophore. L'analyse chimique de la solution de DCB ainsi que du pneumatophore traité permet de déterminer la concentration de la plaque d'oxyde de fer ainsi que les concentrations en ETM immobilisés dans cette plaque. Les sections traitées ont été immergées dans une solution de DCB pendant 3 heures, rincées à l'eau ultrapure, puis séchées dans une étuve à 40 °C. Les échantillons secs ont ensuite été broyés à l'aide d'un broyeur à lame et conservés au sec et à l'abri de la lumière. Les solutions de DCB ont été stockées à 4 °C. Les pneumatophores restants, destinés aux analyses microscopiques, ont également été sectionnés à l'aide d'une scie circulaire en tranches d'environ 0.5 cm de hauteur (*Figure 4-2D*) dans la partie immergée du pneumatophore. Certaines de ces sections ont été traitées au DCB, d'autres ont été fixées comme les feuilles, tandis que le reste n'ont pas subi de traitement. Toutes les sections ont été séchées dans une étuve à 40 °C et conservées dans un dessiccateur.

En ce qui concerne les racines de *R. stylosa*, ce sont les parties immergées du sol des racines échasses qui ont été collectées à l'aide d'une scie et d'un sécateur. De manière similaire aux pneumatophores, deux racines par carotte ont été récoltées (une pour les analyses chimiques et une pour la microscopie), ce qui totalise 12 racines. Le traitement subi par les racines est identique à celui des pneumatophores, à l'exception du traitement au DCB.

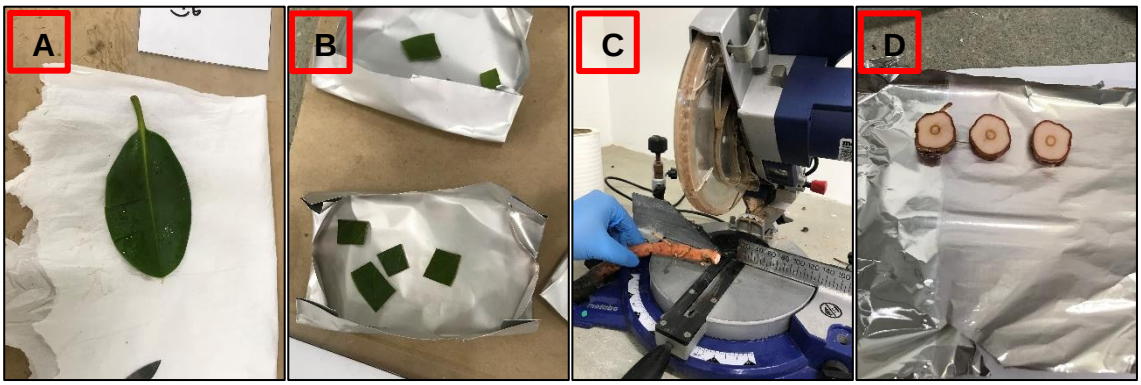

Figure 4-2. Photos de traitement des échantillons de végétaux au laboratoire avec (A) feuille de *R. stylosa* fraiche, (B) sections de la feuille A pour analyse MEB, (C) découpe d'une racine de *R. stylosa* avec scie circulaire et (D) sections de pneumatophores d'*A. marina* pour analyse MEB.

4.2.2. 2ème phase : décomposition de la litière

En mars 2022, a débuté la deuxième phase de l'expérience, qui portait sur l'étude de la décomposition de la litière végétale. Pour ce faire, au début du mois de mars, des échantillons de feuilles sénescentes ont été récoltés sur le site contrôle. Ces échantillons ont été prélevés uniquement sur le site contrôle afin d'éliminer l'effet de la "composition initiale des feuilles" parmi les facteurs pouvant influencer les différences de dégradation entre les sites.

Pour chaque espèce, dans la même zone que lors de la première phase, environ 600 feuilles jaunissantes sur le point de tomber ont été récoltées à partir de plusieurs arbres. Ces feuilles sénescentes ont été soigneusement rincées à l'eau ultrapure, puis étalées sur des supports propres à l'air libre pour les faire sécher. Le lendemain, des triplicats aléatoires d'échantillons ont été sélectionné pour chaque site et chaque espèce, composé d'environ 200 g de feuilles, correspondant aux échantillons à l'instant initial "feuilles sénescentes". Ces échantillons ont été congelés, lyophilisés, puis broyés à une granulométrie inférieure à 1 mm à l'aide d'un broyeur à lame. Le reste des feuilles sénescentes a été placé dans des sacs en nylon à pores de 2 mm, communément appelés "litterbags". Ces sacs ont été remplis avec environ 6 g de feuilles pour *A. marina* et 15 g pour *R. stylosa*. En tout, 90 sacs par espèce ont été remplis et refermés.

Ces sacs ont été répartis dans les deux mangroves d'étude. Pour chaque site et chaque espèce, trois arbres ont été marqués à l'aide de rubalise, à environ 30 mètres les uns des autres, dans chaque stand monospécifique. Cela correspondait approximativement aux mêmes zones que celles où les triplicats des carottes avaient été prélevés lors de la première phase de l'étude. À la surface du sol, 15 sacs en nylon de la même espèce ont été attachés au tronc principal de chacun de ces arbres. Cela signifie

qu'il y avait 3 sacs par arbre, soit 9 sacs par stand monospécifique, 18 sacs par site, et un total de 36 sacs pour chaque jour de récupération. Ces sacs ont été récupérés après 7 jours, 14 jours, 28 jours, 56 jours et 72 jours passés dans la mangrove. La deuxième phase d'échantillonnage s'est donc terminée à la fin du mois de mai 2022. L'expérience a été arrêtée après 72 jours car lors de la récolte au 56ème jour, il est apparu qu'il restait déjà peu de matière pour réaliser les analyses, et attendre les 90 jours initialement prévus pourrait compromettre les analyses du dernier prélèvement. Une fois les sacs ramenés au laboratoire, ils ont été ouverts, les feuilles ont été lavées, puis congelées, lyophilisées et broyées pour les analyses ultérieures.

4.3. Méthodes d'analyse

4.3.1. Paramètres physico-chimiques

4.3.1.1. Température

La température des échantillons de sol a été obtenue sur le site au moment du prélèvement et à l'abri du soleil. La température a été mesurée à l'aide d'une sonde pH en verre (SENTIX - Xylem Analytics) qui est également connectée à un pH-mètre (pH3110 - WTW). La précision de la mesure est de ±0.05 °C.

4.3.1.2. pH

Le pH est la mesure de l'acidité ou de l'alcalinité, quantifiée sur l'échelle du pH, qui signifie "potentiel hydrogène". Il représente la concentration d'ions H^+. L'échelle varie de 0 (très acide) à 14 (très alcalin). La mesure du pH du sol a été effectuée à l'aide d'une électrode pH en verre (SENTIX - Xylem Analytics) connectée à un pH-mètre (pH3110 – WTW). Cette électrode mesure la différence de potentiel générée par les ions H^+ du sol qui interagissent avec la membrane en verre. Cette différence de potentiel est ensuite convertie en valeur de pH. Une calibration de l'appareil et de l'électrode a été préalablement réalisée à une température similaire à celle des échantillons mesurés, qui était proche de la température ambiante avec trois standards à 4.01, 7.00 et 10.00 de pH. La précision de la mesure est de ±0.005.

4.3.1.3. Potentiel redox

Le potentiel redox du sol est une mesure de sa capacité à subir une réaction d'oxydation ou de réduction. Le capteur redox fonctionne en mesurant la différence de potentiel électrique entre une électrode de travail, où ont lieu les réactions d'oxydoréduction, et une électrode de référence ayant un potentiel connu et stable. Le potentiel redox a été mesuré à l'aide d'une électrode en platine et d'une électrode en argent/chlorure d'argent (SENTIX - Xylem Analytics). Les mesures de redox ont été

réalisées sur le terrain au moment du prélèvement en connectant l'électrode au voltmètre (pH3110 – WTW) pour obtenir les valeurs en mV. Étant donné que tous les chercheurs n'utilisent pas les mêmes électrodes de référence, les valeurs redox sont converties en valeurs "Eh", c'est-à-dire le potentiel de différence si l'électrode de référence est une électrode H^+/H_2. Pour obtenir cette valeur à partir d'une électrode Ag/AgCl, il suffit d'ajouter +202 mV à la valeur lue sur le pH-mètre à 25 °C. La précision de mesure est de ±0.1 mV.

4.3.1.4. Salinité

La salinité du sol a été mesurée à partir des échantillons d'eaux interstitielles avant acidification à l'aide d'un réfractomètre (ATC). Un réfractomètre est un capteur qui permet de mesurer la salinité d'un échantillon d'eau en déterminant la réfraction de la lumière (déviation) lorsqu'elle traverse l'échantillon. Plus la teneur en sel de l'eau est élevée, plus la lumière est déviée. Le réfractomètre est équipé d'une échelle permettant de lire directement la salinité en mg L^{-1}. La précision de la mesure est de ±1 mg L^{-1}.

4.3.1.5. Teneur en eau

La teneur en eau des échantillons de sol de mangrove a été calculée à partir du poids des échantillons avant et après séchage en suivant l'équation suivante :

$$SWC = \frac{masse\ humide - masse\ sèche}{masse\ humide} * 100 \quad (4.1)$$

Avec SWC (pour Soil Water Content) pour la teneur en eau en %, masse humide pour la masse de l'échantillon de sol avant séchage en g et masse sèche pour la masse de l'échantillon de sol après lyophilisation en g.

4.3.1.6. Masse volumique

La masse volumique des échantillons de sol a également été calculée à partir de la masse sèche de chaque échantillon et de la dimension du carottier cylindrique en suivant l'équation suivante :

$$Masse\ volumique = \frac{masse\ sèche}{rayon^2 * section * \pi} \quad (4.2)$$

Avec la masse volumique en g cm^{-3}, masse sèche pour la masse de l'échantillon après lyophilisation en g, rayon pour la taille du rayon du carottier en cm (4 cm ici) et section pour la taille de la section de sol pesée en cm (5 ou 10 cm ici).

4.3.2. Granulométrie

La granulométrie du sol a été mesurée à l'aide d'un granulomètre laser (Malvern Mastersizer hydro 2000S AWA2001) au laboratoire de l'ISEA. Le fonctionnement d'un granulomètre laser repose sur le passage d'un faisceau laser à travers un échantillon de

particules dispersées, suivi de l'analyse des motifs de lumière diffusée pour déterminer la distribution de la taille des particules. La granulométrie de chaque échantillon a été obtenue après traitement de la MO avec un mélange d'eau oxygénée et d'acide acétique. Le taux élevé de MO dans le sol de mangrove peut biaiser les résultats granulométriques. Par conséquent, la MO des échantillons bruts (non-broyés) a été préalablement minéralisée en chauffant l'échantillon avec une solution de H_2O_2 : acide acétique dans un rapport de 5:1 (v/v). Pour éviter d'endommager l'appareil, de l'eau distillée a été ajoutée à la suspension de sol afin de neutraliser la solution. Le Mastersizer génère ensuite une courbe de distribution de taille des particules, qui illustre l'abondance relative des particules dans différentes plages de taille. Les proportions en argile, limon et sable ont été obtenues en additionnant les abondances des particules <0.002 mm, entre 0.002 et 0.05 mm, et entre 0.05 et 2 mm, respectivement.

4.3.3. Minéralogie

La minéralogie des bassins versants des sites d'études est bien connue, et ces données peuvent être consultées dans la littérature. Cependant, la minéralogie des mangroves peut varier en fonction de l'abondance des apports terrestres, éoliens et marins, ainsi que de la formation *in situ* de nouveaux minéraux non présents dans le bassin versant. Pour obtenir la minéralogie des sites d'études, des échantillons ont été séchés et broyés à une taille inférieure à 0.5 mm, puis analysés à l'aide d'un diffractomètre à rayons X (DRX) (PANalytical – Aeris XRD) au laboratoire de l'ISEA. Le diffractomètre à rayons X génère des rayons X à l'aide d'un tube à rayons X. Les rayons X produits par le tube sont dirigés vers l'échantillon que l'on souhaite analyser. Les rayons X interagissent avec les atomes du sol et sont diffractés en raison de la disposition ordonnée des atomes dans la structure cristalline. Les rayons X sont réfléchis à des angles spécifiques en fonction de la distance interplanaire des plans cristallins et de la longueur d'onde des rayons X incident. Un détecteur de rayons X est placé de l'autre côté de l'échantillon pour mesurer l'intensité des rayons X diffractés à différents angles de diffraction. Les données de diffraction obtenues sont ensuite utilisées pour créer un diagramme de diffraction des rayons X, appelé un diffractogramme. Ce diffractogramme représente l'intensité des rayons X diffractés en fonction de l'angle de diffraction. Chaque minéral a un pattern de diffraction propre ce qui permet d'identifier tous les minéraux présents dans un échantillon de sol.

4.3.4. Eléments majeurs et éléments traces métalliques

La quantification des éléments majeurs (Ca, K, Na, Mg, P) et des ETM (Al, As, Cd, Co, Cr, Cu, Fe, Mn, Ni, Pb, Ti, Zn) a été effectuée par spectroscopie d'émission optique de plasma à couplage inductif (ICP-OES) au laboratoire LAMA de l'IRD à Nouméa.

Pour commencer, l'extraction des éléments à quantifier a été réalisée sur les échantillons de sol et de végétaux préalablement séchés et broyés. Cette extraction a été effectuée au laboratoire de l'ISEA par digestion micro-ondes à l'aide d'un appareil Ethos Easy (Milestone). Le principe de la digestion par micro-ondes repose sur l'utilisation d'ondes électromagnétiques de haute fréquence, appelées micro-ondes, pour chauffer rapidement et de manière homogène l'échantillon, accélérant ainsi la digestion chimique. Cette méthode offre l'avantage d'une digestion rapide, reproductible et efficace. L'extraction totale des éléments présents dans la biota a été réalisée en utilisant un mélange HNO_3 : H_2O_2 dans un rapport de 5:1 (v/v), tandis que celle des éléments dans le sol a été effectuée avec un mélange HNO_3 : HCl : HF dans un rapport de 5:1:1 (v/v/v). De plus, une extraction séquentielle des échantillons de sol a été réalisée en suivant le processus du Bureau Communautaire de Référence (BCR) afin d'obtenir les concentrations en éléments dans chacune des fractions du sol (section II.3.3.3). Les échantillons d'eaux interstitielles et les solutions DCB ont pu être analysés par ICP-OES sans extraction préalable. Cependant, des dilutions à l'eau ultrapure ont dû être réalisées pour éviter de saturer l'instrument en sel.

L'ICP-OES utilise une source plasma inductivement couplée comme source d'énergie. Cette source génère un plasma en utilisant un gaz inerte et en l'ionisant à l'aide d'une bobine d'induction électromagnétique. L'échantillon liquide est introduit dans l'instrument et est acheminé dans la source plasma. Lorsqu'il entre en contact avec le plasma chaud, les atomes de l'échantillon sont ionisés. Les ions formés sont portés à des niveaux d'énergie élevés. Lorsqu'ils retournent à leurs niveaux d'énergie de base, ils émettent de l'énergie sous forme de lumière visible et ultraviolette. La lumière émise est dispersée par un système de spectromètre. Ce spectromètre décompose la lumière en ses composantes spectrales en fonction de leurs longueurs d'onde. Un détecteur mesure l'intensité de la lumière à différentes longueurs d'onde. Chaque élément chimique émet une lumière à des longueurs d'onde spécifiques lorsque ses ions retournent à leurs niveaux d'énergie de base. Les intensités lumineuses mesurées sont comparées à celles des standards connus pour chaque élément, ce qui permet de déterminer la concentration de chaque élément présent dans l'échantillon. Les concentrations des éléments dans

l'échantillon sont calculées en utilisant les intensités lumineuses mesurées et les courbes d'étalonnage établies à partir des standards.

Afin de garantir la qualité des résultats, des contrôles de qualité ont été mis en place. Ces contrôles consistent à utiliser régulièrement des solutions préparées séparément de la gamme d'étalons, avec des concentrations connues pour chacun des éléments à quantifier (quality control). Cette démarche vise à vérifier qu'il n'y a pas de déviation des résultats lors de l'utilisation de l'instrument. De plus, des échantillons certifiés (CRM) de végétaux et de sols ont également été soumis à la digestion et à l'analyse par ICP-OES. Ces échantillons certifiés sont achetés et contiennent des concentrations connues et certifiées en certains éléments. En les traitant de la même manière que nos échantillons, nous pouvons vérifier que l'extraction et la quantification sont correctement réalisées. À partir des concentrations obtenues pour les CRM, un score z peut être calculé pour chaque élément. Ce score indique si les résultats sont fiables ou non. Un score supérieur à 3 ou inférieur à -3 indique que les résultats obtenus sont trop éloignés de la réalité pour être considérés comme valides.

4.3.5. Distribution des éléments dans les tissus de palétuviers et caractéristiques des phases minérales

Le microscope électronique à balayage (MEB) (JEOL JSM-IT 300 LV) et sa sonde de spectrométrie par sélection d'énergie (EDS) (Oxford x max 80T) de la plateforme P2M de l'UNC ont eu plusieurs utilisations au cours de cette thèse. Le MEB est un instrument de microscopie qui permet d'obtenir des images détaillées de la surface d'échantillons à l'échelle micrométrique en utilisant un faisceau d'électrons. Le MEB émet un faisceau d'électrons focalisé dont l'énergie est choisie entre 1 et 30 keV, ici 15 keV principalement. Les électrons pénètrent dans l'échantillon et y perdent de l'énergie. Les électrons émis par l'échantillon (électrons rétrodiffusés ou électrons secondaires) sont utilisés pour former l'image alors que les rayons X émis par l'échantillon sont utilisés pour réaliser l'analyse chimique. Les différents types de signaux fournissent des informations sur la topographie, la composition chimique et la structure cristalline de la surface de l'échantillon. La sonde EDX permet de déterminer la composition élémentaire d'un échantillon. Les rayons X caractéristiques émis par l'échantillon sont collectés par la sonde EDS. Cette sonde est équipée d'un détecteur qui peut mesurer l'énergie des rayons X. Les énergies de ces rayons sont propres à chaque élément chimique. La sonde EDS peut également être utilisée pour cartographier la distribution des éléments à l'intérieur de l'échantillon. Les échantillons non-conducteurs d'électrons (ex. les végétaux) doivent préalablement être métallisés avec une couche de carbone ou de platine pour pouvoir les observer au MEB.

Le MEB couplé à l'EDS a d'abord été utilisé pour localiser les ETM au sein des feuilles et des racines. Par exemple, nous avons examiné si les ETM détectés par l'EDS étaient principalement localisés dans le cœur de la racine ou dans l'épiderme (*Figure 4-3A*). De même, nous avons vérifié si les glandes excrétrices de sel sur les feuilles d'*A. marina* sécrétaient également des ETM (*Figure 4-3B*). Ensuite, les échantillons de sols secs et non broyés ont été observés au MEB afin d'obtenir des informations plus détaillées sur leur structure et leur contenu. Nous avons notamment examiné la forme des pyrites néoformées (octaédriques ou framboïdales) présentes dans les sols de mangrove (*Figure 4-3C*). Principalement, l'image été obtenue à partir du détecteur des électrons secondaires (SED). Toutefois, afin de trouver plus rapidement certains objets telle que la pyrite dans le sol, le détecteur des électrons rétrodiffusés (BED-C) a également été utilisé. Pour des images plus nettes, la distance entre le détecteur et la surface de l'échantillon (Working Distance) été fixée à 10 mm et l'échantillon placée dans le microscope en mode vide élevé (High-Vac). Tous les échantillons, même les sols, ont été métallisée avec du platine à 35 mA pendant 100 s pour avoir une couche d'environ 10 nm.

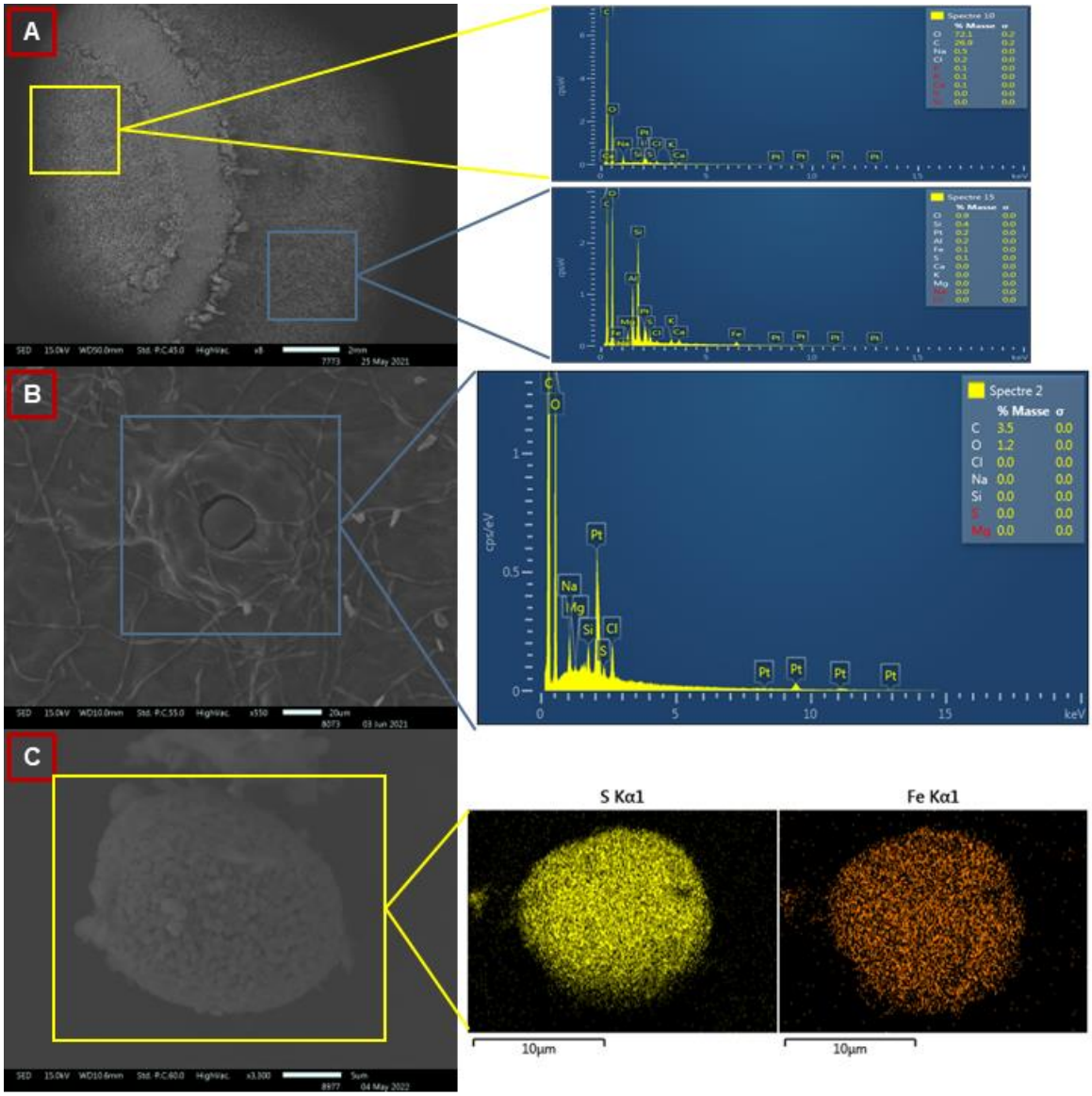

Figure 4-3. Images MEB et spectres ou cartographie EDS (A) d'une racine de *R. stylosa* en coupe transversale, (B) d'une glande excrétrice de sel d'une feuille de *A. marina* et (C) d'une pyrite framboïdale dans le sol.

4.3.6. Isotopes stables

Le traçage des sources de la MO a été réalisé notamment grâce aux signatures en isotopes stables du carbone et de l'azote. Cette technique est couramment utilisée pour identifier et tracer la MO au sein de la chaîne trophique ou dans un environnement donné. Dans la mangrove, ces isotopes stables peuvent être utilisés pour différencier la MO terrestre ou marine, la MO autochtone ou allochtone, ainsi que la MO microbienne ou végétale, par exemple. Des processus biogéochimiques peuvent également être déterminés à partir des ratios isotopiques. Les concentrations totales en C et en N, ainsi que les rapports $^{13}C/^{12}C$ ($\delta^{13}C$) et $^{15}N/^{14}N$ ($\delta^{15}N$), ont été obtenus pour les échantillons de

sol et de biota au laboratoire LAMA de l'IRD de Nouméa, à l'aide d'un spectromètre de masse à rapport isotopique (Sercon Integra 2).

Avant passage dans l'instrument, les échantillons doivent être décarbonatés pour obtenir le C et les isotopes de C appartenant uniquement au CO. Les échantillons très riches en CO et ne contenant que des taux très faibles de carbonates, n'ont pas eu à subir de décarbonatation au préalable. Pour l'utilisation de l'analyseur isotopique, l'échantillon est vaporisé, et les gaz ou les ions résultants sont acheminés vers le spectromètre de masse. Les atomes ou molécules sont ionisés et l'instrument sépare les ions en fonction de leur rapport masse sur charge (m/z). Les ions séparés sont détectés à l'intérieur du spectromètre de masse en fonction de leur m/z. La mesure de l'intensité des ions à différents m/z permet de déterminer la composition isotopique de l'échantillon. Une fois l'analyse terminée, le spectromètre de masse fournit un rapport isotopique, c'est-à-dire la proportion relative des isotopes présents dans l'échantillon.

4.3.7. Rock-Eval

La pyrolyse Rock-Eval est une technique d'analyse principalement utilisée en géologie pétrolière. Elle permet d'évaluer les propriétés géochimiques des échantillons de roches sédimentaires en déterminant la composition organique des roches, leur potentiel pétrolier, leur maturité thermique et d'autres informations importantes. Ici, c'est la pyrolyse Rock-Eval 7S de la plateforme GEORG de Sorbonne Université qui a été utilisée à partir d'une méthode adaptée aux sols et sédiments récents (Baudin et al., 2015). L'échantillon de sol est placé dans un four sous atmosphère anaérobie. La température du four est augmentée progressivement dans une plage allant de 300 à 650 °C (ou plus) au cours d'un cycle de chauffage. À mesure que la température augmente, les composés organiques présents dans la roche commencent à se décomposer et à libérer des gaz et des composés organiques volatils. Ces composés incluent le méthane, le dioxyde de carbone, l'eau, et d'autres composés organiques légers. Les gaz et les composés organiques sont collectés et analysés. La quantité de gaz libéré et les caractéristiques des composés organiques volatils permettent de tirer des conclusions sur la quantité et la qualité de la MO contenue dans la roche, ainsi que sur sa maturité thermique (Behar et al., 2001; Disnar et al., 2003).

Les résultats de la pyrolyse Rock-Eval 7S sur les végétaux et les sols ont révélés plusieurs informations. Cette technique, donne notamment les concentrations en hydrocarbures libres (pic S1) volatilisés à 200 °C. Ensuite, le chauffage avec une rampe conduit à la vaporisation des produits issus du craquage thermique de la MO jusqu'à 650 °C. La concentration de ces produits est donné par le pic S2. Les effluents d'hydrocarbures

continuellement détectés par un détecteur à ionisation de flamme (FID) sont exprimés en mg par g d'échantillon, tandis que le CO et le CO_2 sont mesurés par une cellule infrarouge et correspondent au pic S3. À la fin de l'étape de pyrolyse, les échantillons sont automatiquement transférés dans un four d'oxydation, où ils sont soumis à une isotherme à 300 °C, puis à une rampe jusqu'à 850 °C. Les signaux totaux de CO et CO_2 sont exprimés en mg par g d'échantillon. Tous ces thermogrammes permettent le calcul du carbone organique total (TOC) en ajoutant le carbone de pyrolyse et le carbone résiduel détecté pendant la phase d'oxydation. Les indices d'hydrogène (HI) et d'oxygène (OI) sont calculés avec les équations S2/TOC*100 et S3/TOC*100, respectivement, et approximent le rapport atomique H/C et O/C de la MO. HI et OI donnent des informations sur le taux d'hydrogénation et d'oxygénation de la MO du sol, indiquant sont taux de dégradation. Le TpS2 est la température du four de pyrolyse au rendement maximal du pic S2, et est généralement utilisée comme paramètre de maturité de la MO. Plus le TpS2 est élevé, moins la MO est thermolabile et donc est plus mature. Le Rock-Eval 7S a également la particularité de quantifier le soufre total, le soufre organique et les quantités de soufre inorganique dans les échantillons.

4.3.8. Lignine

Un des objectifs de cette thèse était d'identifier l'existence ou l'absence de corrélation entre les ETM et le type de MO dans les végétaux et le sol de mangrove. Pour caractériser la MO, il a été nécessaire de choisir les molécules d'intérêt qui permettent à la fois d'identifier les sources de la MO, les processus de dégradation ou de préservation, et qui peuvent former des complexes avec les ETM. Notre choix s'est d'abord porté sur la lignine. La lignine est un composé majeur des plantes vasculaires, donc abondant. De plus, elle est spécifique aux plantes vasculaires, ce qui nous permet d'exclure les multiples origines possibles de la MO, telles que les phytoplanctons ou les bactéries. La lignine suscite un intérêt en chimie des matériaux en tant que polymère robuste et abondant, plus écologique que ce qui est disponible sur le marché (Thakur et al., 2014). La lignine est également étudiée pour son pouvoir d'absorption de contaminants tels que les hydrocarbures aromatiques polycycliques et les ETM dans les sols et les eaux pollués (Zhang et al., 2014; Ge and Li, 2018; Khan et al., 2020).

Étant donné que la lignine est un polymère complexe, ce sont les dérivés de la lignine qui sont analysés et quantifiés. Les ratios entre les monomères fournissent des informations sur la structure de la lignine dans l'échantillon, sa labilité, ainsi que les mécanismes de dégradation qu'elle subit. Pour obtenir ces monomères, les échantillons doivent être oxydés, généralement avec du CuO, et hydrolysés, ce qui produit des

composés phénoliques tels que les acides, les aldéhydes et les cétones. Plusieurs instruments d'analyse peuvent être utilisés pour quantifier les dérivés de la lignine, tels que la chromatographie gazeuse, la résonance nucléaire ou encore la spectroscopie infrarouge (Letourneau and Volmer, 2021). Ici, les dérivés de la lignine ont été analysés par chromatographie liquide ultra performante (UPLC) (Vanquish Flex system – Thermo Fischer Scientific) couplée à la spectrométrie de masse (MS) (Orbitrap Exploris 120 – Thermo Fischer Scientific) au laboratoire de l'ISEA en partenariat avec la start-up NCBioressources.

Le couplage entre l'UPLC et la MS permet une séparation efficace des composés dans la colonne UPLC, suivie d'une détection précise et sélective des ions dans la MS. Les informations de rétention obtenues par l'UPLC et les données de spectrométrie de masse sont combinées pour identifier les composés présents dans l'échantillon de manière plus fiable. L'échantillon est injecté dans une colonne de chromatographie, généralement remplie de petites particules poreuses appelées supports stationnaires. Ces particules permettent la séparation des composés en fonction de leurs interactions chimiques avec la phase stationnaire (dans notre cas une colonne Hypersil GOLD 1.9 µm, 50 x 2.1 mm de Thermo Fisher Scientific). Un solvant mobile, appelé phase mobile (dans notre cas un mélange d'eau ultra pure, de méthanol et d'acide formique à 0.1%), est pompé à travers la colonne. Les composés se séparent en fonction de leur affinité respective envers la phase stationnaire et la phase mobile, entraînant leur élution à des vitesses différentes, ce qui permet leur séparation. Après avoir quitté la colonne UPLC, les composés sont introduits dans le spectromètre de masse. Les ions sont générés à partir des composés par des techniques telle que l'ionisation électrospray. Les onze molécules dérivées de la lignine (*Figure 1-5*) ont été recherchées spécifiquement. Deux méthodes d'analyses ont été utilisées. La méthode Full MS ddMS² permet de détecter tous les ions présents dans l'échantillon. La méthode SRM (Selected Reaction Monitoring) permet de détecter seulement les molécules sélectionnées. Les molécules sont identifiées à partir de leurs ions précurseurs et leurs ions produits. L'identification des composés a été réalisée simultanément avec l'aide de la littérature, des bases de données spectrales et de nos expériences par analyses de standards. La quantification de chaque monomère de lignine est réalisée à partir d'une gamme étalon (0.1 – 8 mg L^{-1}).

4.3.9. Glucides neutres

Le second type de molécule à l'étude est les glucides neutres. Tout d'abord, les glucides constituent une source importante de CO dans les écosystèmes et contribuent donc au cycle du C. Comprendre comment les glucides neutres sont produits, transformés

et dégradés dans l'environnement est essentiel pour comprendre la dynamique du carbone. De plus, les glucides neutres jouent un rôle dans divers processus biologiques et écologiques. Ils servent de source d'énergie pour les microorganismes, soutiennent la croissance microbienne et influencent le cycle des nutriments. Étudier leur rôle dans le fonctionnement des écosystèmes peut nous aider à comprendre comment les écosystèmes réagissent aux changements environnementaux tel que l'urbanisation. Aussi, l'analyse des glucides peut aider à identifier leurs sources dans l'environnement. Par exemple, certains types de glucides peuvent provenir de plantes terrestres, d'algues ou de communautés microbiennes.

L'analyse des glucides neutres dans des matrices environnementales se fait principalement par chromatographie gazeuse (GC) et spectrométrie de masse (MS) après dérivation. Pour des raisons de temps, de moyens et de compétences, les analyses des glucides neutres ont été réalisées au laboratoire de l'Institut des Sciences de la Terre d'Orléans (ISTO) à l'aide d'une GC Trace 1300 (Thermo Fisher Scientific) couplée à une MS ISQ7000 (Thermo Fisher Scientific).

Dans un premier temps, les glucides neutres ont été extraits des échantillons de sol et de végétaux par hydrolyse, puis dérivés. La dérivation est nécessaire car les glucides neutres ne sont pas suffisamment volatils sous leur forme native. La dérivation peut augmenter la volatilité de ces composés, les rendant ainsi plus adaptés à la phase de GC pour leur analyse sur cet appareil. En effet, le principe de la GC est, tout comme pour l'UPLC, de séparer les molécules d'un échantillon, mais cette fois-ci sous forme gazeuse. La dérivation a été réalisée avec un agent dérivant, le BSTFA, dans de la pyridine. Un échantillon contenant les composés à analyser est injecté dans le système de chromatographie gazeuse. L'injection peut se faire sous forme liquide. Contrairement à l'UPLC, la phase mobile est un gaz inerte, ici de l'hélium. Ce gaz transporte l'échantillon à travers une colonne chromatographique (ici Restek Rxi-5Sil d'envergure 60 m x 0.25 mm, 0.25 µm de diamètre avec 5 m de pré-colonne) remplie de matériau stationnaire. La phase stationnaire est spécialement sélectionnée pour avoir une affinité différentielle avec les composés à analyser en fonction de leurs propriétés chimiques, telles que leur poids moléculaire, leur polarité et leur volatilité. Lorsque l'échantillon est injecté dans la colonne, les différents composés interagissent avec la phase stationnaire de manière spécifique. Les composés se séparent en fonction de leur affinité relative pour la phase stationnaire et la phase mobile. Les composés plus volatils ou ayant une plus grande affinité pour la phase mobile se déplacent plus rapidement à travers la colonne, tandis que les composés moins volatils ou ayant une plus grande affinité pour la phase stationnaire se déplacent plus lentement. Les composés séparés sortent de la colonne un par un et passent devant

un détecteur. Le détecteur mesure l'abondance de chaque composé en fonction du temps. Cela génère un chromatogramme, qui est un graphique montrant les pics correspondant à chaque composé et leur intensité relative. Les pics du chromatogramme sont comparés à des données de référence pour identifier les composés présents dans l'échantillon. La surface des pics est utilisée pour quantifier la concentration des composés. Après la sortie du détecteur GC, les composés sont introduits dans le spectromètre de masse. Le principe est évoqué dans la section 4.3.8.

4.3.10. Analyses statistiques

Des analyses statistiques ont été réalisées à l'aide du logiciel R pour répondre à deux objectifs principaux : 1) comparer des variables entre un ou plusieurs groupes et 2) définir les corrélations entre plusieurs paramètres dans un même environnement.

Pour atteindre le premier objectif, des tests comparatifs ont été effectués afin de détecter d'éventuelles différences significatives entre un ou plusieurs paramètres selon différents critères tels que les sites, les espèces, les tissus ou les profondeurs. Étant donné qu'il y avait au maximum 36 valeurs par paramètre, nous avons opté pour des tests non paramétriques.

Lorsqu'il s'agissait de comparer seulement deux groupes indépendants, comme dans le cas d'une comparaison entre les deux espèces (*A. marina* et *R. stylosa*) nous avons utilisé le test de Mann-Whitney. Le principe de ce test consiste à comparer les distributions de deux échantillons indépendants pour déterminer s'il existe une différence significative entre eux. Pour ce faire, les observations des variables d'intérêt ont été classées de manière ascendante, en les regroupant pour les deux groupes. Un rang a été attribué à chaque observation, le rang le plus bas étant attribué à la plus petite valeur, et les rangs ont été attribués en fonction de la taille des valeurs. Ensuite, nous avons calculé la somme des rangs pour chaque groupe et comparé ces sommes pour obtenir une valeur "p" comprise entre 0 et 1. Nous avons adopté les règles statistiques conventionnelles, considérant une différence significative lorsque $p < 0.05$.

Lorsqu'il s'agissait de comparer des variables avec plus de deux groupes indépendants, tels que différentes sections de profondeur (soit 6 sections), nous avons utilisé le test de Kruskal-Wallis. Le test de Kruskal-Wallis permet de déterminer si trois groupes indépendants ou plus ont des moyennes significativement différentes pour une variable dépendante mesurée sur une échelle ordinale ou nominale. Toutes les données de tous les groupes ont été combinées et classées en ordre croissant. Ensuite, la statistique de test a été calculée à partir des rangs attribués aux observations, prenant en compte les écarts entre les rangs moyens des groupes et la taille des échantillons. La

valeur de "p" a été calculée et utilisée pour déterminer si les différences étaient significatives, tout comme dans le test de Mann-Whitney. Si p< 0.05, nous avons ensuite effectué un test de Wilcoxon pour identifier entre quels groupes indépendants la différence était significative. Par exemple, si p< 0.05 pour la profondeur, le test de Wilcoxon nous indiquait si la différence d'une variable telle que la salinité du sol était significative entre chaque section ou seulement entre les sections 0-5 cm et 30-40 cm.

Pour atteindre le second objectif, deux outils statistiques ont été utilisés : l'analyse en composantes principales (ACP) et la matrice de corrélation. Ces méthodes ont été appliquées à plusieurs variables du sol, notamment la salinité, le TOC et la teneur en sucres neutres. Ces analyses ont été menées à la fois sur l'ensemble des données du sol (comprenant les deux sites et les deux espèces), ainsi que sur les données spécifiques au site urbain ou au site de contrôle, et de même pour les deux espèces. Étant donné que les conditions du sol peuvent varier de manière significative entre les espèces et les sites, les corrélations entre les paramètres peuvent également différer considérablement, voire être opposées. Avant d'utiliser ces outils, les données été normalisées en les centrant (en soustrayant la moyenne) et en les mettant à l'échelle (en divisant par l'écart type) pour que toutes les variables aient la même échelle.

4.3.10.1. Matrice de corrélation

La matrice de corrélation est une représentation tabulaire des coefficients de corrélation entre différentes variables d'un ensemble de données. Elle est utilisée pour examiner les relations linéaires entre les variables et évaluer la force et la direction de ces relations. Pour chaque paire de variables, nous avons calculé le coefficient de corrélation de Pearson. Ce coefficient mesure la force et la direction de la relation linéaire entre les deux variables. Il varie de -1 à 1, où -1 indique une corrélation négative parfaite (une variable augmente lorsque l'autre diminue), 1 indique une corrélation positive parfaite (les deux variables augmentent ensemble), et 0 indique l'absence de corrélation linéaire. La matrice où chaque élément représente le coefficient de corrélation entre deux variables est générée. La matrice est carrée, et la diagonale (éléments où les variables sont les mêmes) contient des 1, car une variable est parfaitement corrélée avec elle-même (*Figure 4-4*).

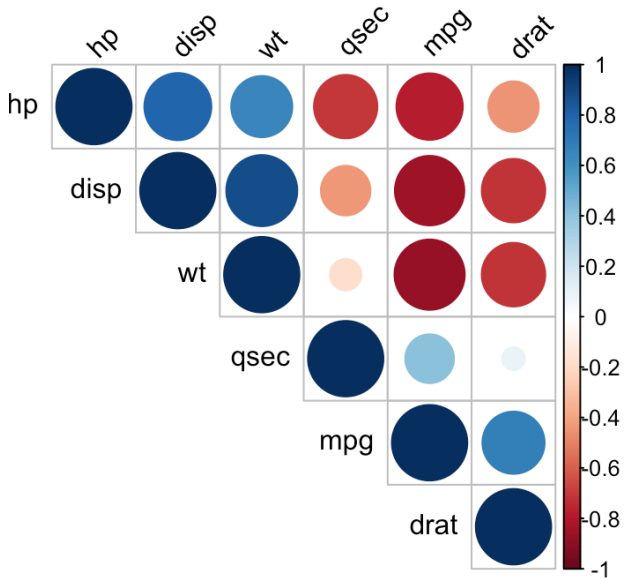

Figure 4-4. Exemple de matrice de corrélation.

4.3.10.2. Analyse en composantes principales

L'ACP est une technique d'analyse des données qui vise à réduire la dimensionnalité des données tout en préservant autant d'informations que possible. Le principe de base de l'ACP consiste à transformer un ensemble de variables initiales (qui peuvent être corrélées les unes aux autres) en un nouvel ensemble de variables non corrélées appelées "composantes principales". Ces composantes principales sont ordonnées en fonction de leur variabilité, de sorte que la première composante principale capture la plus grande part de la variabilité des données, la deuxième composante principale capture la deuxième plus grande part de variabilité, et ainsi de suite. Dans un premier temps la matrice de covariance ou de corrélation est calculée, puis les composantes principales sont calculées à partir de la matrice de covariance ou de corrélation. La première composante principale est une combinaison linéaire des variables initiales qui maximise la variance. Les composantes suivantes sont calculées de manière itérative de manière à être non corrélées aux composantes précédentes tout en maximisant la variance. Les composantes principales sont ordonnées en fonction de leur variabilité décroissante. La première composante principale explique la plus grande partie de la variabilité des données, la deuxième explique la deuxième plus grande partie, et ainsi de suite. Les composantes principales peuvent être interprétées pour comprendre comment les variables initiales contribuent à la variabilité des données. Les variables qui ont des coefficients élevés dans une composante principale sont celles qui ont le plus d'influence sur cette composante. Pour une meilleure visualisation et interprétation des données, toutes les ACP ont été représentée en seulement 2 dimensions, c'est-à-dire en conservant que les deux premières composantes principales (*Figure 4-5*).

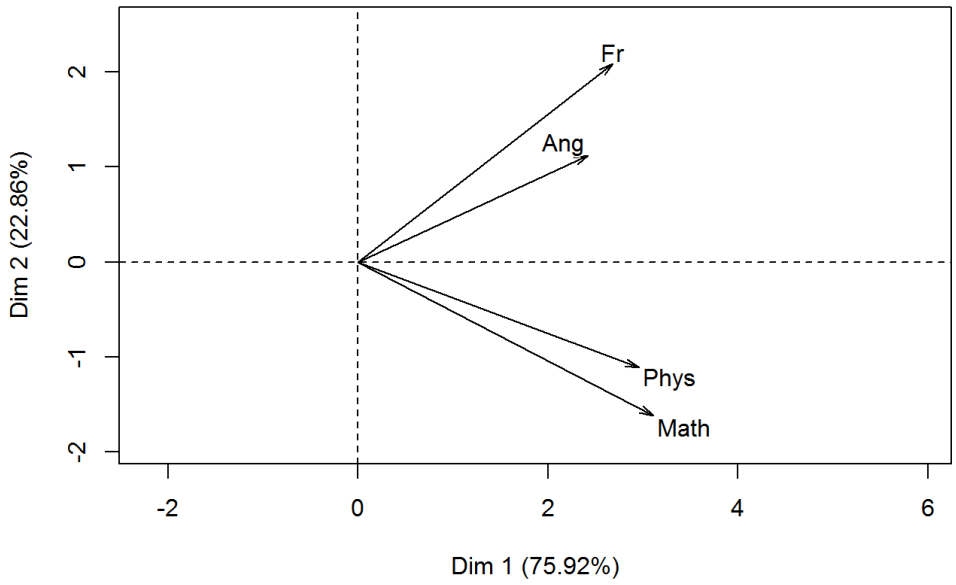

Figure 4-5. Exemple de représentation d'une analyse en composantes principales à deux dimensions.

Dans l'exemple d'ACP ci-dessus, on observe que les variables Fr et Ang sont positivement corrélées entre elles et les variables Phys et Math également. La dimension 1 est la première composante principale qui explique 75.92% des variables et la dimension 2 la seconde composante principale qui explique 22.86% des variables. Les deux premières composantes principales expliquent donc 98.78% des variables.

5. Déroulement du manuscrit

Ce manuscrit est composé de cinq chapitres qui visent à répondre aux questions scientifiques précédemment soulevées. Les chapitres sont les suivants :

Le **chapitre I** examine l'influence du bassin versant sur la dynamique des ETM dans les sols de mangrove et leur transfert vers les racines des palétuviers. Il aborde également l'impact de l'espèce de palétuvier sur la bioaccumulation des ETM. Ce chapitre a été publié sous forme d'article en 2021 dans la revue *Science of the Total Environment*.

Le **chapitre II** met en évidence l'impact de l'urbanisation sur la dynamique des ETM dans les sols de mangrove, ainsi que sur la bioaccumulation de ces éléments par les palétuviers. Il étudie différents paramètres du sol susceptibles d'influencer la mobilité des ETM, en comparant une mangrove urbaine à une mangrove contrôle partageant le même bassin versant géologique. Ce chapitre a été publié sous forme d'article en 2022 dans la revue *Frontiers in Environmental Science*.

Le **chapitre III** examine la dégradation de la litière végétale au sein du sol de mangrove et l'impact de l'urbanisation sur ce processus. Dans sa première partie, ce chapitre étudie la vitesse de dégradation et l'évolution de la composition isotopique et moléculaire de la litière pendant une période de 72 jours. La partie A de ce chapitre a été soumis sous forme d'article à la revue *Geochimica et Cosmochimica Acta*. Dans la seconde partie, ce chapitre analyse l'évolution des éléments majeurs et des ETM au sein de la litière au cours de sa dégradation. La partie B de ce chapitre est prête pour soumission à la revue *Chemosphere*.

Le **chapitre IV** se concentre sur la MO dans les sols de mangrove. Dans la première partie, ce chapitre examine la MO de la mangrove contrôle, représentative de la côte Ouest de la Nouvelle-Calédonie, en utilisant une approche moléculaire et isotopique. Ce chapitre explore les sources de MO ainsi que les processus de préservation et de dégradation dans le sol. La partie A de ce chapitre est prête pour soumission à la revue *Geochimica et Cosmochimica Acta*. Dans la seconde partie, ce chapitre caractérise une couche enfouie riche en MO (à 40 cm de profondeur) en utilisant une approche isotopique et moléculaire. La partie B est une short communication qui a été soumise à la revue *Science of the Total Environment*. Enfin, la dernière partie de ce chapitre, partie C, évalue l'influence des effluents urbains sur les sources et processus de dégradation de la MO dans le sol de la mangrove urbaine, toujours par approche isotopique et moléculaire.

Le **chapitre V** est le chapitre discussion et conclusion de la thèse. Ce chapitre synthétise les résultats développés dans les précédents chapitres pour chacun des huit objectifs.

Des analyses statistiques sont développées pour déterminer les facteurs contrôlant la distribution des ETM dans les sols de mangrove. Une courte conclusion générale de la thèse est également donnée ainsi que des perspectives.

5’. Manuscript structure

This manuscript consists of five chapters aimed at addressing the scientific questions previously raised. The chapters are as follows:

Chapter I examines the influence of the watershed on the dynamics of TM in mangrove soils and their transfer to mangrove root systems. It also explores the impact of the mangrove species on TM bioaccumulation. This chapter was published as an article in 2021 in the journal *Science of the Total Environment*.

Chapter II highlights the impact of urbanization on the dynamics of TM in mangrove soils and their bioaccumulation by mangroves. It investigates various soil parameters that may influence TM mobility by comparing an urban mangrove forest to a control mangrove forest sharing the same geological watershed. This chapter was published as an article in 2022 in the journal *Frontiers in Environmental Science*.

Chapter III examines the decomposition of leaf litter within mangrove soil and the impact of urbanization on this process. In its first part, this chapter studies the degradation rate and changes in the isotopic and molecular composition of litter over a period of 72 days. Part A of this chapter has been submitted as an article to the journal *Geochimica et Cosmochimica Acta*. In the second part, this chapter analyzes the changes in major elements and TM within the litter during its decomposition. Part B of this chapter is ready for submission to the journal *Chemosphere*.

Chapter IV focuses on OM in mangrove soils. In the first part, this chapter examines OM in the control mangrove forest, representative of the West coast of New Caledonia, using a molecular and isotopic approach. It explores OM sources as well as preservation and degradation processes in the soil. Part A of this chapter is ready for submission to the journal *Geochimica et Cosmochimica Acta*. In the second part, this chapter characterizes a buried layer rich in OM (at a depth of 40 cm) using an isotopic and molecular approach. Part B is a short communication that has been submitted to the journal *Science of the Total Environment*. Finally, the last part of this chapter, Part C, evaluates the influence of urban effluents on OM sources and degradation processes in the soil of the urban forest, again using an isotopic and molecular approach. This last part is also ready for submission.

Chapter V is the discussion and conclusion chapter of the thesis. This chapter synthesizes the results developed in the previous chapters for each of the eight objectives. Statistical analyzes are conducted to determine the factors controlling the distribution of TM in mangrove soils. A brief overall conclusion for the thesis is also provided with perspectives.

I. Chapter I: Influences of species and watersheds inputs on trace metal accumulation in mangrove roots

Robin, S.L., Marchand, C., Ham, B., Pattier, F., Laporte-Magoni, C., Serres, A., 2021. Influences of species and watersheds inputs on trace metal accumulation in mangrove roots. *Science of The Total Environment* 787, 147438. https://doi.org/10.1016/j.scitotenv.2021.147438

Présentation :

L'activité économique principale en Nouvelle-Calédonie est l'exploitation minière axée sur le nickel (Kowasch, 2018). L'archipel se classe au troisième rang mondial pour la production de minerai de nickel en raison de l'abondance de sols ultrabasiques riches en Ni, ainsi qu'en Fe, Mn, Co et Cr (Maurizot et al., 2020b). À l'heure actuelle, il existe trois usines de traitement métallurgique et vingt et une mines exploitées sur l'île, alors qu'auparavant, pendant près de 100 ans, une seule usine et quatre mines étaient en activité (Kowasch, 2018). Les mangroves qui se développent en aval des mines à ciel ouvert se trouvent en première ligne pour capturer les ETM entraînés par le lessivage et l'érosion renforcée par l'activité anthropique des sols ultrabasiques (Baltzer, 1981). Les concentrations en Co, Cr, Fe et Ni dans les sols des mangroves sont nettement plus élevées en Nouvelle-Calédonie que dans le reste du monde (*Figure I-1*). Même si toutes les mangroves de Nouvelle-Calédonie ne sont pas situées en aval de roches ultrabasiques, le fond métallique ambiant des sols en Nouvelle-Calédonie dépasse la moyenne mondiale pour certains métaux, ce qui signifie que leurs concentrations dans les sols des mangroves peuvent également être supérieures (Beliaeff et al., 2011).

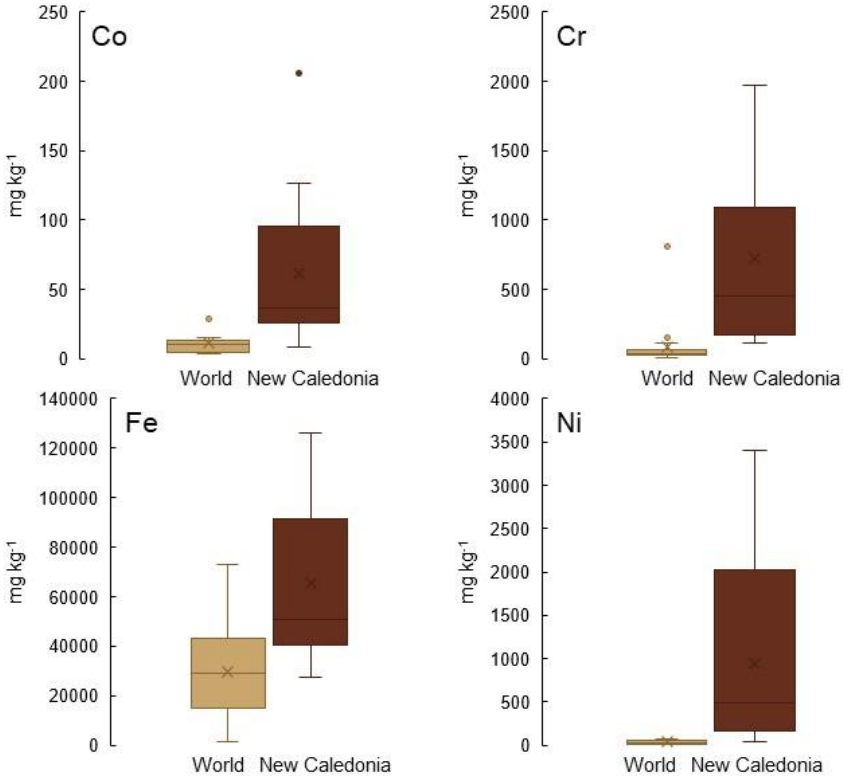

Figure I-1. Concentrations de Co, Cr, Fe et Ni mesurées dans les sols de mangrove dans le monde et en Nouvelle-Calédonie en mg kg^{-1}.

L'objectif principal de ce chapitre est de déterminer l'influence de la géologie du bassin versant sur le transfert des ETM dans les systèmes racinaires des deux espèces

de palétuviers dominantes en Nouvelle-Calédonie, à savoir *Avicennia marina* et *Rhizophora stylosa*. La première mangrove se développe en aval d'un bassin versant ultrabasique, tandis que la deuxième mangrove, que nous considérons comme notre mangrove contrôle pour les prochains chapitres, se développe en aval d'un bassin versant volcano-sédimentaire. Les concentrations en ETM ont été mesurées dans le sol, les eaux interstitielles et les racines des deux espèces et des deux sites grâce à la spectroscopie d'émission optique à plasma induit (ICP-OES). Une analyse des sols a été effectuée sur des carottes d'une profondeur de 30 cm, permettant l'acquisition des paramètres physico-chimiques et l'identification de la nature minéralogique du substrat. Cette étude met en évidence l'influence du bassin versant sur les conditions redox et les concentrations en ETM dans le sol de la mangrove. La majorité des ETM sont présents en concentrations significativement plus élevées dans le sol de la mangrove en aval du bassin versant ultrabasique. Cependant, aucune différence significative n'a été observée pour les concentrations en ETM dans les racines. On peut donc en conclure que le transfert vers les racines est principalement influencé dans ce cas par les mécanismes physiologiques propres aux palétuviers. Il est également à noter que le transfert des ETM est plus élevé chez *A. marina* que chez *R. stylosa* sur les deux sites. Enfin, l'analyse de la plaque d'oxyde de fer à la surface des pneumatophores d'*A. marina* indique que sa formation est influencée par la concentration de fer dans le sol, bien que la capacité de piégeage des ETM dans cette plaque ne présente pas de différence entre les deux sites.

Ce chapitre permet d'approfondir notre compréhension du transfert des ETM du sol vers les racines des palétuviers dans notre mangrove contrôle, ce qui facilitera ensuite une meilleure comparaison avec notre mangrove urbaine. Nos résultats soulignent particulièrement l'impact des sols ultrabasiques sur la mangrove contrôle, même en aval de sols volcano-sédimentaires, en raison d'événements tels que les cyclones. Par ailleurs, tant l'activité minière que l'urbanisation constituent des sources d'ETM. Ainsi, il sera possible de déterminer ultérieurement si l'urbanisation et l'activité minière exercent la même influence sur la distribution des ETM dans le sol de la mangrove et leur transfert dans les tissus des palétuviers. Ces résultats nous permettront également de confirmer ou d'infirmer les hypothèses formulées dans le chapitre II, notamment en ce qui concerne l'influence de la concentration en fer dans le sol de mangrove sur la formation de la plaque d'oxyde de fer à la surface des pneumatophores et le rôle de cette plaque dans la protection contre le stress métallique.

Influences of species and watersheds inputs on trace metal accumulation in mangrove roots

Sarah Louise ROBIN, Cyril MARCHAND, Brian HAM, France PATTIER, Christine LAPORTE-MAGONI, Arnaud SERRES

Published in Science of the Total Environment

I.1. Abstract

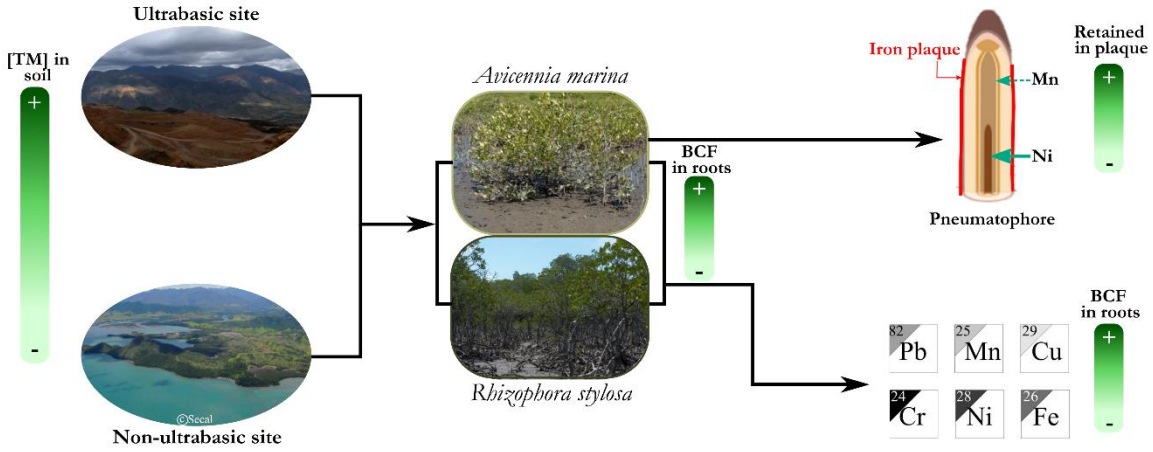

Mangrove forest is a key ecosystem between land and sea, and provides many services such as trapping sediments and contaminants. These contaminants include trace metals (TM) that can accumulate in mangrove soil and biota. This paper innovates by the comparative study of the effects of watershed inputs on TM distribution in mangrove soil, on root bioconcentration factors of two mangrove species (*Avicennia marina* and *Rhizophora stylosa*), and on Fe plaque formation and immobilization of these TM. Two mangrove forests in New Caledonia were chosen as study sites. One mangrove is located downstream from ultramafic rocks and a Ni mine (ultrabasic site), whereas the second mangrove ends a volcano-sedimentary watershed (non-ultrabasic site). TM concentrations (Co, Cr, Cu, Fe, Hg, Mn, Ni, Pb, Zn) were measured in soil, porewaters, and roots of both species via ICP-OES or Hg analyzer. Analyzed TM were significantly more concentrated in soils at the ultrabasic site with Fe, Cr, and Ni the most abundant. Iron, Mn, and Ni were the most concentrated in the roots with mean values of 9 651, 192, and 133 mg kg^{-1} respectively. However, the bioconcentration factors (BCF) of Fe (0.16) and Ni (0.11) were low due to a lack of ions in the dissolved phase and potential uptake regulation. The uptake of TM by mangrove trees was influenced by concentrations in soil, but more importantly by their potential bioavailability and the physiological characteristics of each species. TM concentrations and BCF were lower for *R. stylosa* probably due to a less permeable root system. *A. marina* limits TM absorption through Fe plaque formation

on its pneumatophores with a capacity to retain TM up to 94 % for Mn. Mean Fe plaque formation is potentially correlated to Fe concentration in soil. Eventually, framboids of pyrite were observed within root tissues in the epidermis of the pneumatophores of *A. marina*.

Keywords: coastal wetlands, element cycling, ultrabasic, bioconcentration, iron plaque, New Caledonia

I.2. Introduction

Mangrove forest is an intertidal ecosystem developing along subtropical and tropical coastlines. Even though mangrove accounts for less than 0.5% of the world's forest surface area, it is a remarkable sink for atmospheric CO_2 and plays a crucial role in the flow of energy, nutrients, and in the carbon cycle (Kristensen et al., 2008; Donato et al., 2011). Mangroves provide physical protection to the coastline against storms and wave action and act as a buffer between the land and the sea by accumulating sediments and associated contaminants (Massel et al., 1999; McIvor et al., 2012; Lee et al., 2014). Nevertheless, this ecosystem is particularly endangered, notably due to urbanization and the release of anthropogenic effluents, with some countries using mangroves as filters. In the 80s and the 90s, about 35% of mangrove forest area was lost (Valiela et al., 2001; Alongi, 2002; Duke et al., 2007). In a few emerging countries, the estimation reached up to 8% per year (Polidoro et al., 2010). Between 2000 and 2012, the annual loss rates decreased significantly in some regions, ranging from 0.16% to 0.39%, which demonstrates global awareness on the significance of the conservation of mangroves (Hamilton and Casey, 2016).

Trace metals (TM) are metallic elements naturally present in limited concentrations in the environment due to their occurrence in the Earth's crust (Turekian and Wedepohl, 1961). However, anthropogenic activities have considerably increased their concentrations in many ecosystems (Shtiza et al., 2005; Cao et al., 2018). As TM are not biologically or chemically degraded, they can accumulate in the environment or be transported over long distances (Marx and McGowan, 2010; Chowdhury et al., 2017). They can be transferred to mangrove forests via atmospheric routes (wind, rain) or aquatic routes (rivers, sea) (Marx and McGowan, 2010). Mangrove soils are mainly characterized by low oxygen levels (anoxic conditions) and high sulfur and organic matter (OM) contents (Holmer et al., 1994; Dittmar et al., 2006). Strong biogeochemical activity, OM richness, and high sedimentation rate are three factors that make mangrove ecosystems a sink for contaminants (Harbison, 1986; Wu et al., 2014; Cennerazzo, 2017). TM are quickly immobilized in soil by precipitation with pyrite (FeS_2) or by adsorption onto OM for example

(Marchand et al., 2011a; Chakraborty et al., 2016; Cennerazzo, 2017). The dynamics of TM within mangrove soil are well studied worldwide, with their partitioning mainly impacted by physico-chemical parameters (redox potential, pH) and bonding phases (carbonates, OM, sulfides, oxides, etc.) (Jayachandran et al., 2018; Duan et al., 2020; Huang et al., 2020a).

Mangrove flora is adapted to the habitat specificities such as poor O_2 availability and high salinity (Duke et al., 1998; Kathiresan and Bingham, 2001). Metal stress is another challenge for mangrove species since TM can inhibit development processes and reduce photosynthetic activity (Prasad et al., 2006; Nagajyoti et al., 2010). Many authors studied the mechanisms of mangrove plants against metal stress (Zheng et al., 1997; Cheng et al., 2014; Nath et al., 2014). Multiple studies showed that essential metals (i.e., Cu and Zn) are regulated, with their transfer to shoots limited (Machado et al., 2005; MacFarlane et al., 2007). In contrast, non-essential metals (i.e., Cr and Pb) are excluded from the root system or accumulated on the surface of the roots, and are not transferred to the highest organs (MacFarlane and Burchett, 2000; Chowdhury et al., 2017).

In some mangrove species such as the *Avicennia*, the formation of an iron plaque was observed at the surface of their root system (Machado et al., 2005; Pi et al., 2010; Lin et al., 2018). This plaque results from the precipitation of Fe (III) via the oxidation of free Fe (II) from the diffusion of O_2 by the plant in its rhizosphere (Taylor and Crowder, 1983; Williams et al., 2014). Studies have also exposed the role of bacteria at the root surface for biological oxidation of Fe^{2+} into Fe plaque, but to a lesser extent (Maisch et al., 2019). This Fe plaque helps prevent the absorption of excessive TM and other pollutants by the mangrove through the root system (Otte et al., 1989; Pi et al., 2011; Yamaguchi et al., 2014). Iron plaque can only be formed under waterlogged conditions since Fe^{2+} must be soluble, brought to the surface by transpiration pull, oxidized automatically by O_2 diffusion, and precipitated (St-Cyr et al., 1993). The formation of the Fe plaque is driven by many abiotic and biotic factors (Mendelssohn et al., 1995). Higher Fe^{2+} solubility leading to higher Fe plaque formation is observed at lower pH and redox potential. However, pH is higher in the rhizosphere of more efficient O_2-diffusing species that also lead to higher Fe plaque formation (Tripathi et al., 2014). There is still a debate on how the Fe fraction in the soil influences Fe plaque formation. St-Cyr and Crowder (1988) showed positive correlation between Fe plaque formation and the Fe fraction bound to carbonates while other studies exposed a positive correlation with the exchangeable fraction only (Tripathi et al., 2014). Consequently, it is difficult to predict the magnitude of Fe plaque formation at a specific site due to the number of factors involved but it has been extensively

confirmed that Fe^{2+} availability and O_2 diffusion capacity of the species are the two predominant factors affecting Fe plaque development (Tripathi et al., 2014).

In New Caledonia (NC), some mangrove forests develop between ultramafic soils, including Ni mining sites, and the largest lagoon in the world. Massive exploitation of ultramafic laterites intensifies erosion and favors TM transfer towards rivers and the lagoon, as laterites display high concentrations of some TM (Bird et al., 1984; Fernandez et al., 2006). Multiple studies have been conducted on the dynamic of TM in New Caledonian mangroves with different stress factors (Marchand et al., 2012; Noël et al., 2014; Bourgeois et al., 2019b). It has been shown that the distribution and partitioning of TM is partially affected by the initial concentrations and speciation of TM from the effluent. Iron, Ni, and Cr, characteristic metals of the ultramafic rocks, have been found in concentrations much higher than world average in mangroves soil downstream from those rocks, and those elements are mostly detected in oxide or oxy/hydroxide forms (Marchand et al., 2012; Noël et al., 2015). The mobility and bioavailability of these TM are mostly influenced by the vegetation (Marchand, 2008), the OM content (Marchand et al., 2011a), and the redox conditions (Bourgeois et al., 2019b), which will affect the biogeochemical processes that take place in the soil and will consequently impact the speciation of the TM. The two predominant species of the archipelago are *Rhizophora stylosa* seaward and *Avicennia marina* landward (Marchand et al., 2007). The root systems of these two species are broadly different with distinct particularities. *R. stylosa* has extensive aerial stilt support roots (Kathiresan and Bingham, 2001) while *A. marina* possesses pneumatophores (roots growing upward) equipped with lenticels that allow the passive diffusion of oxygen (Purnobasuki et al., 2017). To our knowledge, only one study looked at the bioaccumulation of TM from soil to roots and shoots of mangroves in NC and was not interested in the functions of the Fe plaque in TM absorption (Marchand et al., 2016). Globally, the processes of TM exchange at the soil-vegetation interface are understudied worldwide, especially *in situ*.

In the context of mangroves developing downstream from lateritic soils enriched in TM, our main objective was to assess the influence of watershed inputs on the accumulation of TM in the root systems of the two main mangrove species developing along the semi-arid coastline of New Caledonia. In addition, we were interested in the influence of elemental inputs and soil redox conditions on the formation of Fe plaque at the root surface of *A. marina*. Eventually, a potential relationship between Fe plaque concentrations and the amount of TM retained within the plaque was investigated. To achieve those objectives, concentrations of TM in the rhizosphere and root system of the two species as well as in the Fe plaque of *A. marina* were quantified by Optical Emission

Spectrometry by Inductive Current Plasma (ICP-OES), and the roots were analyzed by Scanning Electron Microscopy (SEM). Two study sites, one ultrabasic and one non-ultrabasic, were chosen to evaluate the impact of TM-rich watersheds on TM distribution in mangroves downstream. We hypothesize that due to the capacity of *A. marina* to diffuse O_2 to its rhizosphere, thanks to a more permeable root system, the root bioconcentration of TM is higher in this species than in *R. stylosa*. We also expect that the accumulation of TM is not subject to a threshold and therefore, TM are found in higher concentrations in the roots when it is also the case in the soil.

I.3. Material & methods

I.3.1. Study sites

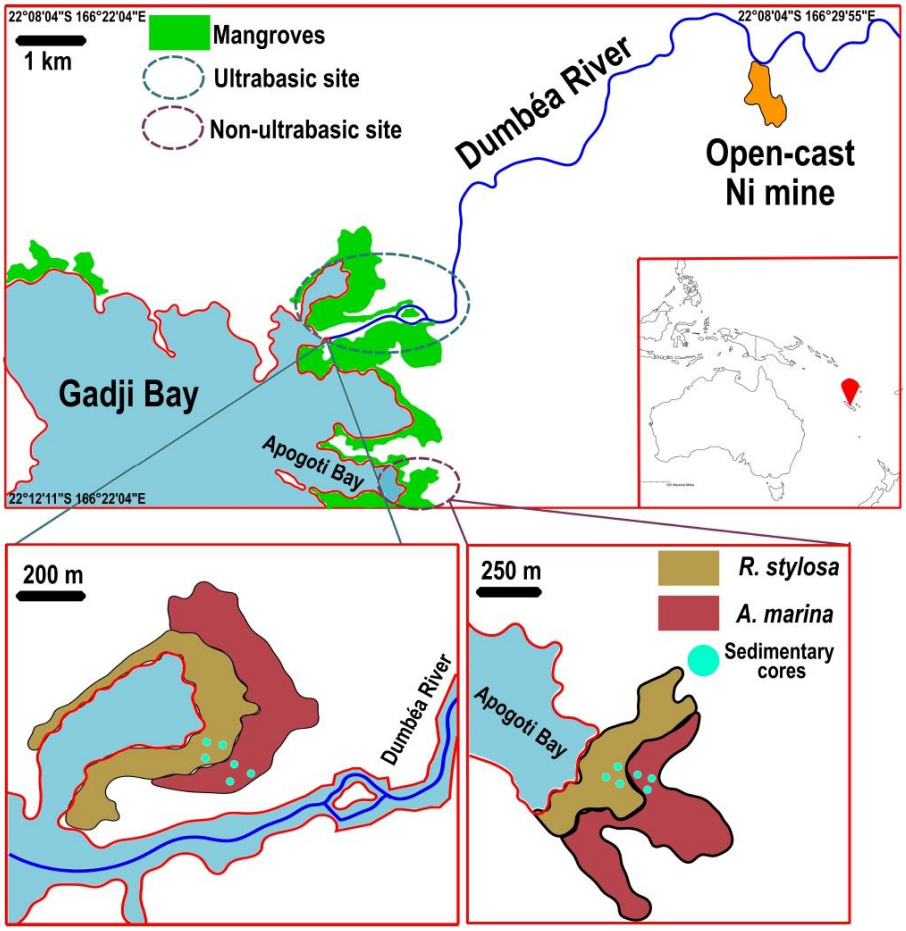

Figure I-2. Map of the two ultrabasic and non-ultrabasic sites with the Dumbea River and the old open-cast nickel mine. Stands of *A. marina* and *R. stylosa* are displayed at the ultrabasic and non-ultrabasic sites with the collected soil cores.

New Caledonia is a French archipelago, located in the South Pacific Ocean, 1 500 km away from the East coast of Australia and enclosed by the largest lagoon in the world, registered at UNESCO since 2008 (UNESCO, 2020). The main island is about 500 km long and 50 km wide between 20°S and 23°S. Mangrove forest represents more than 35

000 hectares and 80% of the western coast of the main island is covered by this ecosystem (Marchand et al., 2007). The western coastline is subject to a semi-arid climate and to semidiurnal tidal cycle (Douillet et al., 2001). The intertidal zone of NC is the habitat of more than 20 mangrove species. Floristic diversity of mangrove forests is divided into monospecific stands depending on multiple factors such as frequency of tidal immersion and porewater salinity (Duke et al., 1998). On the West coast of the main island, three distinct monospecific stands are observed depending on the elevation. On the seashore, *Rhizophora* spp. cover 50% of mangrove area with porewater salinity ranging from 5 to 40 g L^{-1}. *A. marina* covers >15% of mangrove area and develops higher in the intertidal zone with salinity between 35 and 70 g L^{-1}. Eventually, salt-flat is the highest topographical stand of vegetation composed mainly of *Salicornia*, and flourishes on soil with salinity ranging from 60 to 100 g L^{-1} (Marchand et al., 2007, 2016).

On the main island, ultramafic soil represents a third of the territory with alteration profiles particularly rich in Ni (Dalvi et al., 2004; Nicholson et al., 2011). Open-cast Ni mines are exploited all along the central mountain chain. Ultramafic soils, including those open-cast mines, are eroded during rainfall events, and part of it flows into nearby rivers. Two study sites were therefore chosen. The first one for lateritic inputs from its watershed and another one for the absence of known lateritic inputs.

The first study site is a mangrove located at the mouth of the Dumbea River (22°172.797'S, 166°429.493'E), in the Gadji Bay (*Figure I-2*). 9 km upstream the river is an old Ni open-cast mine (22˚143.293'S, 166˚491.718'E) (*Figure I-2*) exploited from the 19th to mid-20th century but deserted since then (Marchand et al., 2012). The first site is named "ultrabasic site" thereafter. The second site is a mangrove located in the Apogoti bay, 3.5 km south of the mouth of the Dumbea River (22°202.072'S, 166°439.939'E) (*Figure I-2*). It is named thereafter "non-ultrabasic site" since it is a volcano-sedimentary soil mainly made of quartz and plagioclase and its watershed does not include the Dumbea River or ultramafic soils (Service de la Géologie de Nouvelle-Calédonie, 2016). The hydrography of the Gadji Bay is rather south to north and therefore the effluent from the Dumbea River does not flow into the Apogoti Bay (Douillet et al., 2001). At both sites, the monospecific stands identified are homogeneous in terms of tree density and height.

I.3.2. Sampling & processing

Samples were collected in June 2020, during the short dry season. On both sites, stands of *A. marina* and *R. stylosa* stands were identified (*Figure I-2*). For each species, triplicates of 30 cm long soil cores were collected with an Eijkelkamp gouge auger about 20 m apart from each other (*Figure I-2*). Soil cores were cut along depth with a wooden

knife into 5 sections of 6 cm each. This sampling strategy was chosen because we are studying the transfer of TM to the root system that develops in the 30 first centimeters and smaller steps in sections probably would not give further information (Kathiresan and Bingham, 2001). The pH and redox potential (Eh) were immediately measured using a pH meter (pH3110 – WTW). A glass electrode (SENTIX – Xylem Analytics) was used to measure the pH, calibrated with standards prior to measurements, while a combined Pt and Ag/AgCl electrode (SENTIX – Xylem Analytics) was used to measure the Eh, calibrated with standards prior to measurements. The soil sections were then placed into tightly closed plastic bags. To extract porewater from the soil, a rhizon (Rhizon SMS – 10 cm, OD 2.5 mm – Rhizosphere) was inserted into each soil section and a 12 mL syringe was connected. The syringe was kept fully pulled with an adapted wooden block. The plastic bags with the soil and the attached syringes were immediately placed into a cooler (~4 °C) until processed at the laboratory less than 6 h after sampling. Within the same area where the soil cores were collected, coarse roots of *R. stylosa* were chopped with a saw with a segment out of the soil and a segment immersed in the soil. For *A. marina*, pneumatophores were gently torn from the main roots. All biotic samples were immediately placed into plastic bags and kept in a cooler (~4 °C) until processed at the laboratory less than 6 h after sampling.

Upon arrival at the laboratory, the porewaters were collected and salinity was measured using a refractometer (ATC). Porewater samples were filtered at 0.45 µm and 2 drops of 70% HNO_3 were added before storage at 4 °C. The soil samples were tightly closed and kept in the freezer at -20 °C. Triplicate pneumatophores from both sites were kept fresh for Fe plaque extraction (see I.3.3.2) but the rest of the biotic samples were also placed in the freezer. Frozen soil samples were lyophilized for 72 h (FreeZone - LABCONCO) before sieving at 2 mm and then ground with a ball mill (FRITSCH). The frozen roots and pneumatophores were washed with distilled water. Transversal sections were obtained using a proxxon (Dremmel 3000, SpeedClic SC544) and dried in a heat chamber at 40 °C until reaching constant mass. One dried section per root and per pneumatophore were kept intact in a desiccator for scanning electron microscopy (SEM). The other dried sections were ground using a cutting mill (POLYMIX – px-mfc90d) for TM analysis.

I.3.3. Analyzes

I.3.3.1. Reagents

All reagents were analytical grade or better. Sodium bicarbonate and ammonium fluoride were obtained from Sigma Aldrich. Tri-sodium citrate dihydrate was obtained from

AnalaR NORMAPUR, VWR. Sodium dithionite was obtained from Panreac. Concentrated nitric acid (70%) was obtained from Ajax Finechem. Multi-element (Ca, Co, Cr, Cu, Fe, K, Mg, Mn, Ni, Na, Zn) standard solution for ICP (1 000 mg L^{-1} in HNO_3 2%) was obtained from CPAChem and Pb standard solution for ICP (1 000 mg L^{-1} in HNO_3 2%) from Perkin-Elmer. Certified reference materials (ISE 1729 sample ID 910 “Clay Soil” and IPE 1804 sample ID 198 “Banana”) were obtained from the Wageningen Evaluating Programmes for Analytical Laboratories.

I.3.3.2. Iron plaque extraction

Triplicate fresh pneumatophores for both sites were washed with distilled water and immerged sections were obtained using a proxxon. In order to extract the Fe plaque from the root surface, a treatment with a solution of dithionite-citrate-bicarbonate (DCB) established by Taylor and Crowder (1983) and modified by Lin et al. (2018) was used. Briefly, 0.5 g of pneumatophore was immersed in 20 mL of the DCB solution (0.03 M $Na_3C_6H_5O_7 \cdot 2H_2O$, 0.125 M $NaHCO_3$, and 0.144 M $Na_2S_2O_4$ in MilliQ water) for 3 h at room temperature. Samples were then rinsed with MilliQ water to obtain 25 mL of final volume. The extract was filtered at 0.45 µm and kept at 4 °C until analysis. Treated samples were dried in a heat chamber at 40 °C until constant mass, then ground using a cutting mill.

I.3.3.3. Trace metal extraction

Acid extraction elaborated by Bourgeois et al. (2019) was used to extract TM from soil and biota. Briefly, 100 mg of dried sample were weighed in a 15 mL polypropylene tube and 1 mL of 10% FNH_4:HNO_3 concentrated (w/v) for the soil samples and 1% FNH_4:HNO_3 concentrated (w/v) for biotic samples was added. Sample was vortexed and left at room temperature overnight. The sample was then heated in a sand bath for 6 h at 100 °C. Once cooled down, the volume was adjusted to 10 mL with MilliQ water and the sample was vortexed. After centrifugation at 3 000 rpm for 5 min, the supernatant was transferred to a new tube and kept at 4 °C until analysis. For quality control, certified materials (ISE sample ID 910 and IPE sample ID 198) were also extracted and analyzed.

I.3.3.4. Trace metal analysis

TM concentrations (Co, Cr, Cu, Fe, Hg, Mn, Ni, Pb, and Zn) in soil extracts, biotic extracts (roots of *R. stylosa*, treated pneumatophores, and untreated pneumatophores of *A. marina*), DCB solutions, and porewaters were obtained via ICP-OES (Varian 730-ES) at the chemistry laboratory LAMA of the French Research Institute for Sustainable Development in New Caledonia (IRD) except for Hg, which was measured using a Hg analyzer (Brooks rand, Merx) at IRD for soil and biotic samples. Concentrations were obtained using a calibration curve previously prepared with the right matrices from a stock

solution of TM at 1 000 mg L^{-1}. Certified reference materials were used to calculate a z-score for each TM. In the soil, for Co, Cr, Fe, Mn, Ni, and Zn, |z-score| < 2. Results are therefore validated. For Cu and Pb, 2 < |z-score| < 3. Results can be exploited but questionable. In biotic extracts, the z-score's absolute value is inferior to 2 for all TM except for Co that has a score between 2 and 3 (*Supplementary Table I-1*). Due to matrix interferences, Cu and Pb were not measured in the DCB extracts.

I.3.3.5. Total organic carbon

The percentage of total organic carbon (TOC) in the soil was obtained via a TOC analyzer (TOC-LCPH-SSM500A – Shimadzu Corporation).

I.3.3.6. Scanning electron microscopy

Semi-quantitative analysis of dried transversal sections of roots and pneumatophores was performed by Scanning Electron Microscopy (SEM) using a JEOL JSM-IT 300 LV apparatus coupled with an Energy Dispersive Spectroscopy (EDX) Oxford x max 80T device at the Electronic Microscopy Platform (P2M) at the University of New Caledonia. Before analysis, because of the electric insulator nature of the samples, they were coated with a 4 nm Pt layer using a Leica EM ac600 vacuum evaporator to avoid electron accumulation on the surface. Coated biotic sections and dried ground soil samples were then glued to aluminum stubs with conductive carbon tape before observation.

I.3.3.7. Mineralogical analysis

Mineralogical composition of soil samples was determined by X-ray powder diffraction (XRD) (PANalytical – AERIS XRD Diffractometer) with a Co source at the ISEA laboratory. A rock sample originating from the watershed of the non-ultrabasic site and sampled nearby the mangrove site was also analyzed by XRD. Scans were taken between 5 and 80 °2θ with a generator power of 600 W. Spectra were treated and analyzed with the High Score software.

I.3.4. Data analyzes

I.3.4.1. Iron plaque calculations

Iron plaque concentration was calculated using the following equation (Lin et al., 2018):

$$[\text{Fe plaque}] = \frac{0.1591 \times m_{Fe\ in\ DCB}\ (\text{mg})}{m_{dried\ root}\ (\text{kg})} \quad \text{(I-1)}$$

with m the mass. To obtain the mass percentages of TM retained in the Fe plaque, the following equation was used:

$$\%_{TM\ in\ Fe\ plaque} = \frac{m_{TM\ in\ DCB}\ (\text{mg})}{m_{TM\ in\ DCB}\ (\text{mg}) + m_{TM\ in\ treated\ root}\ (\text{mg})} \times 100 \qquad \text{(I-2)}$$

I.3.4.2. Bioconcentration factor

The bioconcentration factor (BCF) was calculated by dividing the concentration of TM in roots by the concentration of TM in the soil in the section between 6 and 12 cm deep that corresponds to the depth at which roots were collected. The collection of roots between 6 and 12 cm validates our sampling strategy of 30 cm soil cores.

I.3.4.3. Statistical analysis

Statistical analyzes were performed on R studio software (version 1.2.5001). First, normality was checked with a Shapiro Wilk test. For comparison between species or study sites (two samples), parameters following a normal law were statistically verified with a Student's t-test with equal or unequal variances depending on F-test scores. For parameters not following a normality curve, the Mann-Whitney test was performed. All other statistical analyzes with more than two samples were verified with one-way ANOVA analysis followed by a Tukey's HSD test for parameters following a normal curve. Other parameters were tested with a Kruskal-Wallis test followed by a Wilcoxon test. All tests were performed with a 95% confidence interval and $n \geq 3$.

I.4. Results

I.4.1. Soil description

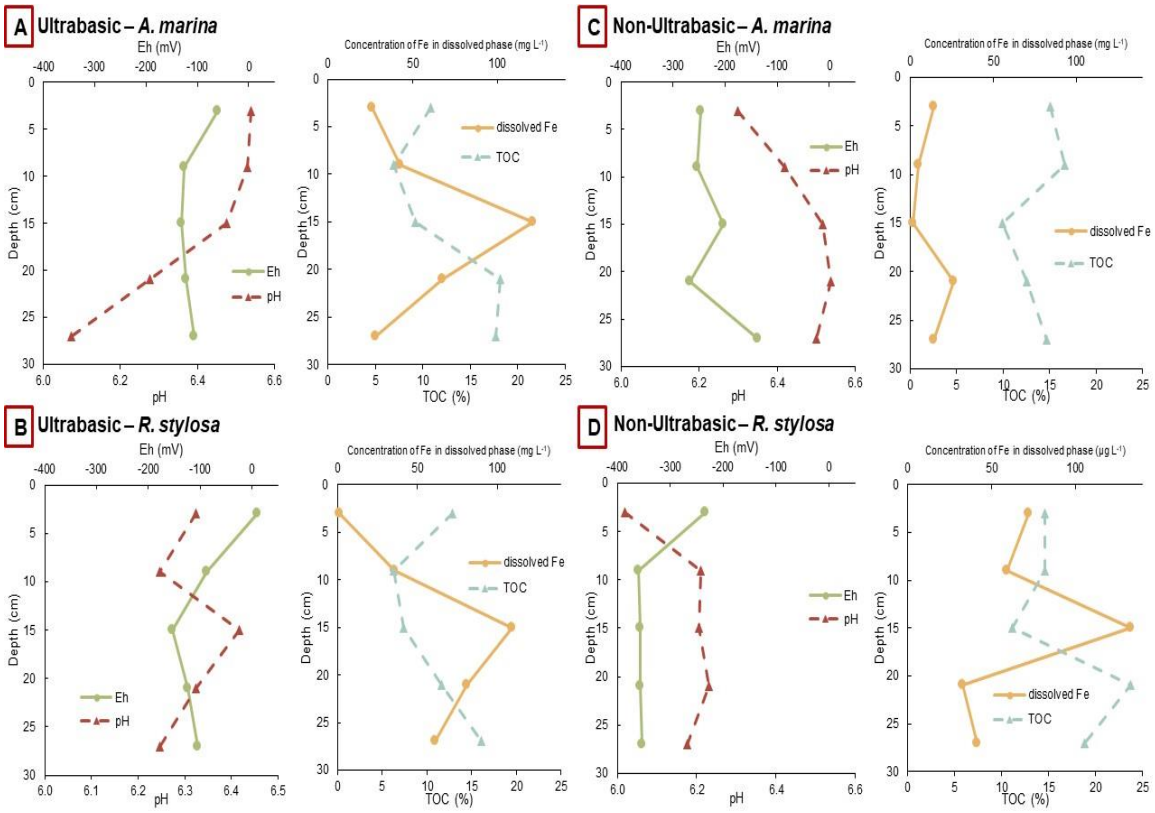

Figure I-3. Depth profile of mean pH, Eh (mV), TOC (%) (n=3) and dissolved Fe (mg L^{-1} except for (D) (µg L^{-1}) (n=2) at the ultrabasic and non-ultrabasic sites under *A. marina* and *R. stylosa*.

Percentages of TOC, pH, and Eh of the soil as well as concentrations of Fe in the dissolved phase (porewater) are presented for both species at both sites as a function of depth in *Figure I-3*. Eh values along soil cores are significantly more negative at the non-ultrabasic site (p-value < 0.001) with an average value of -277 mV, whereas at the ultrabasic site the average value is -100 mV. The pH of the soil at both sites is slightly acidic (6 – 6.6). The soil is significantly more acidic under *R. stylosa* (p-value < 0.001) with an average of 6.2 against 6.4 under *A. marina*. Even though there is no significant difference in pH overall between sites, pH is significantly lower at the non-ultrabasic site under *R. stylosa* compared to the ultrabasic site (p-value < 0.001). Negative correlations are obtained between Eh and pH for cores under *R. stylosa* only (-0.59 and -0.97) (*Supplementary Table I-2*).

The amount of TOC in the soil is larger at the non-ultrabasic site compared to the ultrabasic site with values ranging from 9.95 to 23.70%, with a mean value of 15.17%, and ranging from 6.91 to 18.20%, with a mean value of 11.71%, respectively. TOC is correlated

negatively with pH for soil cores under *A. marina* (-0.73 and -0.71) (*Supplementary Table I-2*).

Concentrations of dissolved Fe are much higher at the ultrabasic site with an average value of 64 mg L^{-1}, and with a large increase of dissolved Fe at a depth of 15 cm followed by a significant decrease (*Figure I-3A & B*). Concentration of dissolved Fe along the vertical gradient is positively correlated to the pH (0.66) and negatively correlated to the Eh (-0.91) under *R. stylosa* at the ultrabasic site (*Supplementary Table I-2*).

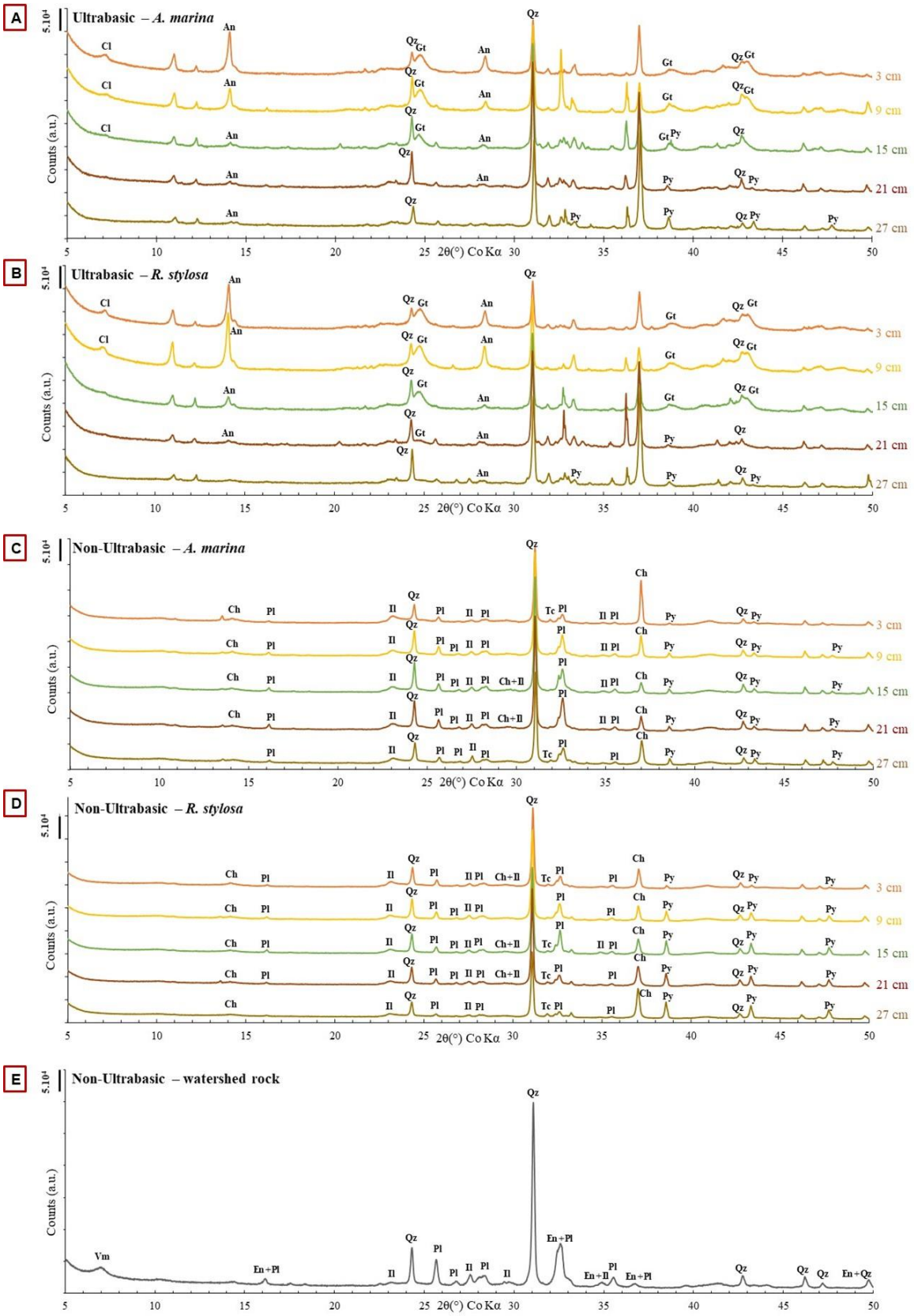

Figure I-4. XRD spectra of soil at the ultrabasic site beneath (A) *A. marina* and (B) *R. stylosa* and at the non-ultrabasic sites beneath (C) *A. marina* and (D) *R. stylosa* and (E) XRD spectra of rocks nearby the non-ultrabasic site with mineralogical phases labeled: An – Antigorite, Ch – Chlorite, Cl – Clinochlore, En – Enstatite, Gt – Goethite, Il – Illite, Pl – Plagioclase, Py – Pyrite, Qz – Quartz, Tc – Talc, and Vm – Vermiculite.

For both mangrove sites and in the watershed rock of the non-ultrabasic site, the main identified mineralogical phase was quartz (SiO_2) (*Figure I-4*). Plagioclase ($NaAlSi_3O_8$ / $CaAl_2Si_2O_8$) and illite ($KAl_4Si_2O_{12}$) were identified for the non-ultrabasic site and the watershed rock of this site (*Figure I-4C-E*). For this rock sample, vermiculite ($(Mg,Ca)_{0,7}(Mg,Fe,Al)_6(Al,Si)_8O_{22}(OH)_4$) and enstatite $(Mg,Fe)SiO_3$, two Fe-bearing phases, were named (*Figure I-4E*) while talc ($Mg_3Si_4O_{10}(OH)_2$) and chlorite ($(Fe,Mg,Al)_6(Si,Al)_4O_{10}(OH)_8$) were identified in the mangrove soil of the non-ultrabasic site (*Figure I-4C & D*). The neoformed pyrite crystals (FeS_2) were detected at both mangrove sites (*Figure I-4A-D*). For the ultrabasic site, three Fe-bearing mineralogical phases were identified: the oxyhydroxide goethite (α-FeOOH) and the phyllosilicates antigorite ($(Mg,Fe)_3Si_2O_5(OH)_4$) and clinochlore ($(Mg,Fe)_5Al(Si_3Al)O_{10}(OH)_8$).

For the non-ultrabasic site, all identified mineralogical phases are present along the cores (*Figure I-4C & D*). However, for the ultrabasic site, goethite and clinochlore are mainly detected close to the surface and tend to vanish as depth increases. Pyrite is present in the sections lacking those two Fe-bearing phases (*Figure I-4A & B*).

I.4.2. Trace metal distribution in soil

Table I-1. Influence of sites on trace metal concentrations (mean ± SD) in soil between 6 and 12 cm deep (n=3 except Hg n=1), which corresponds to the depth at which root sections were taken, and influence of species on trace metal concentrations (mean ± SD) in roots (n=3 except Hg n=2) in mg kg^{-1} except for Hg in µg kg^{-1}.

						mg kg^{-1}					µg kg^{-1}
Sample	**Site**	**Species**	Co***	Cr***	Cu***	Fe***	Mn***	Ni***	Pb***	Zn***	Hg
Soil	Ultrabasic	*A. marina*	99±50	2 087 ±218	65±5	176 358 ±3 268	492±103	2 706 ±1 237	19±1	78±21	66
		R. stylosa	162±7	2 501 ±38	73±3	177 623 ±3 130	815 ±49	4 291 ±258	20±1	110±9	60
		Average	131±48	2 294 ±259	69±6	176 991 ±3 261	654±181	3 499 ±1 194	20±1	94±23	63±3
	Non-Ultrabasic	*A. marina*	41±2	483 ±39	20±2	39 628 ±3 141	117±8	682 ±63	13±1	66±6	48
		R. stylosa	32±6	435 ±28	18±3	38 029 ±6 502	97±7	438 ±28	8±1	46±3	43
		Average	37±6	460 ±42	19±2	38 828 ±5 169	107±2	560 ±132	11±2	56±11	46±3
	Species	**Site**	Co	Cr†	Cu††	Fe††	Mn	Ni	Pb††	Zn††	Hg
Roots	*A. marina*	Ultrabasic	19±4	76±32	15±2	15 624 ±9 639	377±240	173 ±43	34±17	20±3	8±2
		Non-Ultrabasic	11±2	88±17	23±1	17 125 ±6 358	226±46	155 ±31	39±10	39±8	7±2
		Average	15±5	82±26	19±5	16 375 ±8 200	301±188	164 ±39	37±14	30±12	7±2
	R. stylosa	Ultrabasic	15±8	33±4	5±0	2 486 ±306	76±13	165 ±82	7±1	6±4	5±2
		Non-Ultrabasic	3±1	23±5	4±1	3 370 ±1 081	88±31	40±9	12±3	7±5	4±1
		Average	9±8	28±7	4±1	2 928 ±909	82±24	102 ±85	9±3	5±3	5±2

*** p< 0.001 for soil between sites

† p< 0.05, ††p< 0.01 for roots between species

For each soil core, all TM except for Pb and Zn are significantly more concentrated in the soil at the ultrabasic site (*Supplementary Table I-3*). As shown in the supplementary materials (*Supplementary Table I-4*), no significant differences in TM concentrations in porewaters between species have been detected.

Sections of roots and pneumatophores were collected between 6 and 12 cm deep and the concentrations of TM in the soil for this section are presented in *Table I-1*. In the soil between 6 and 12 cm deep, all TM are significantly more concentrated at the ultrabasic site. Iron, Ni, and Cr are the three most concentrated TM in the soil at both sites with mean concentrations of 176 991 mg kg^{-1}, 3 499 mg kg^{-1}, and 2 294 mg kg^{-1}, respectively, at the ultrabasic site, and 38 828 mg kg^{-1}, 560 mg kg^{-1}, and 460 mg kg^{-1}, respectively, at the non-ultrabasic site. Under both species and at both sites, Hg is the least concentrated TM with a mean values of 0.063 mg kg^{-1} at the ultrabasic site and to 0.046 mg kg^{-1} at the non-ultrabasic site followed by Pb with mean values of 20 mg kg^{-1} at the ultrabasic site and 11 mg kg^{-1} at the non-ultrabasic site.

I.4.3. Bioaccumulation of trace metals from soil to roots

Iron is the most concentrated TM in the roots of both species (16 375 mg kg^{-1} for *A. marina* and 2 928 mg kg^{-1} for *R. stylosa*) with Mn (301 mg kg^{-1} for *A. marina* and 82 mg kg^{-1} for *R. stylosa*) and Ni (164 mg kg^{-1} for *A. marina* and 102 mg kg^{-1} for *R. stylosa*) the 2nd and 3rd most concentrated TM (*Table I-1*). However, Fe and Ni, as well as Co, Cr, and Hg have low BCF (0.16, 0.11, 0.16, 0.07, and 0.11, respectively) (*Figure I-5A*). Manganese, Cu, and Zn have higher BCF (0.93, 0.42, 0.26), and Pb is the TM with the highest BCF (1.60) (*Figure I-5A*).

The ratio of TM concentrations in porewaters over concentrations in soil samples (dissolved/solid ratio) are low for Fe (0.14), Ni (0.27), and Cr (0.08), while high for Mn (3.34), Cu (1.86), and Zn (3.03) (*Figure I-5B*). The dissolved/solid ratio of Co is high (2.81) while that of Pb is low (0.40) (*Figure I-5B*).

Chromium, Cu, Fe, Pb, and Zn are significantly more concentrated in the pneumatophores of *A. marina* than in the roots of *R. stylosa* (*Table I-1*). Cobalt, Hg, Ni, and Mn are also more concentrated in pneumatophores but not significantly (p-value > 0.05) (*Table I-1*). The BCF of *A. marina* is always greater than that of *R. stylosa* (*Figure 1-5A*), which is not always the case regarding TM dissolved/solid ratios (*Figure 1-5B*).

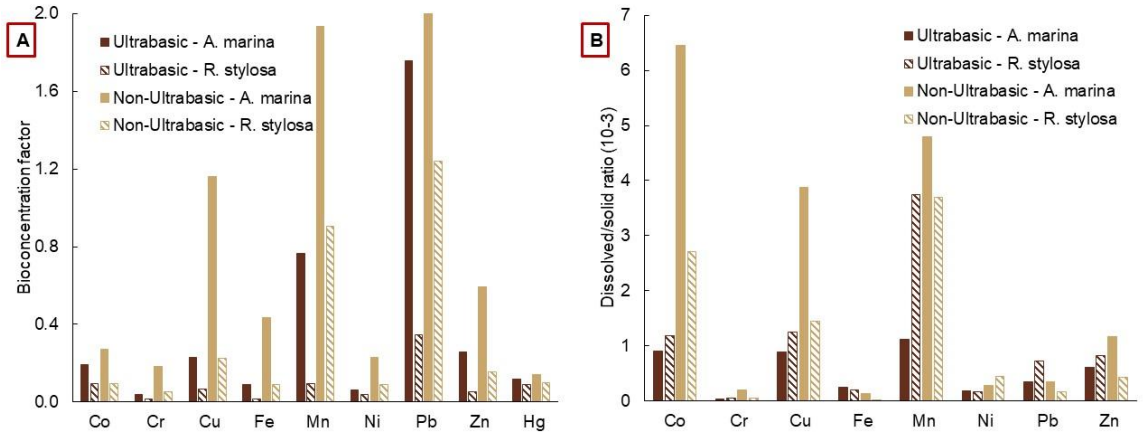

Figure I-5. (A) Bioconcentration factors of trace metals in the pneumatophores of *A. marina* and roots of *R. stylosa* at the ultrabasic and non-ultrabasic sites and (B) ratio of the dissolved/solid fractions (µg L^{-1}/mg kg^{-1}) of trace metals except Hg in the soil.

I.4.4. Iron plaque & associated immobilized trace metals

Variabilities are high but the concentration of the Fe plaque at the surface of the pneumatophores of *A. marina* is higher at the ultrabasic site (4 132 mg kg^{-1}) compared to the non-ultrabasic site (1 863 mg kg^{-1}) (*Figure I-6A*). However, the percentages of TM retained in the plaque is not site-dependent with slight differences between the ultrabasic site and the non-ultrabasic site (*Figure I-6B*). Mass percentages of TM contained in the Fe plaque vary between 47% and 94% (*Figure I-6B*). Nickel is the TM the least immobilized by the Fe plaque with mean mass concentration of 51% while Co and Mn are the most immobilized with mean values of 85% and 92%, respectively (*Figure I-6B*).

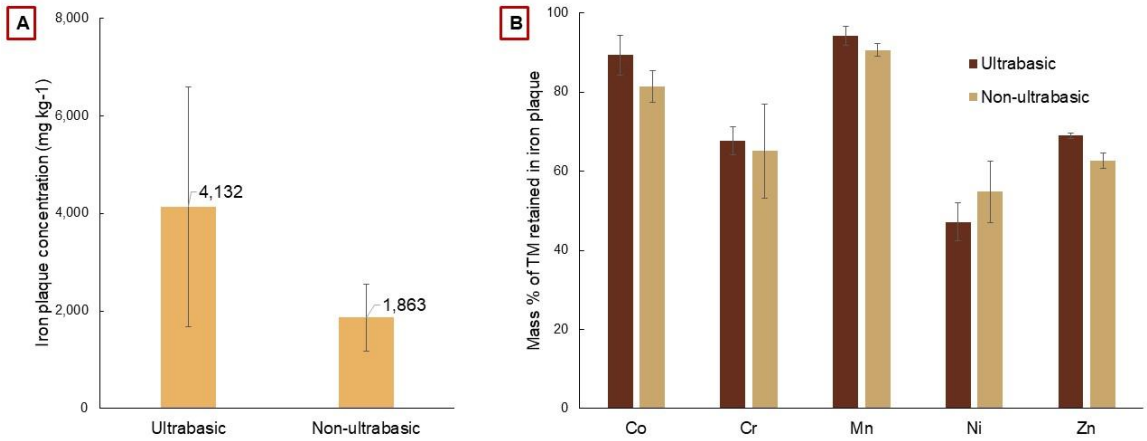

Figure I-6. (A) Mean concentrations and standard deviations of iron plaque extracted from pneumatophores of *A. marina* at the ultrabasic and non-ultrabasic sites (n=3). (B) Mean percentages and standard deviations of trace metals retained in the iron plaque (n=3), calculated from the concentrations obtained from the DCB extracts and the DCB-treated pneumatophores.

I.4.5. Scanning electron microscopy – energy dispersive X-ray spectroscopy

Roots of *R. stylosa* and pneumatophores of *A. marina* were analyzed by SEM. *Figure I-7* shows a cross section of a pneumatophore of *A. marina*, cut into two images, which allows scanning of the root from the vascular bundle to the epidermis. EDX elemental spectra associated to the four different parts of the root are also displayed. From all roots observed, Fe is the only TM that has been detected by the EDX apparatus on biotic samples, and seem to be localized in the epidermis. The vascular bundle, inner, and outer cortical cells seem to be free of TM according to SEM-EDX analysis. Interestingly, aggregates of framboidal pyrite like those seen in the soil were observed in the epidermis of some pneumatophores of *A. marina* (*Figure I-8A*) and were identified via elemental mapping using EDX (*Figure I-8B*).

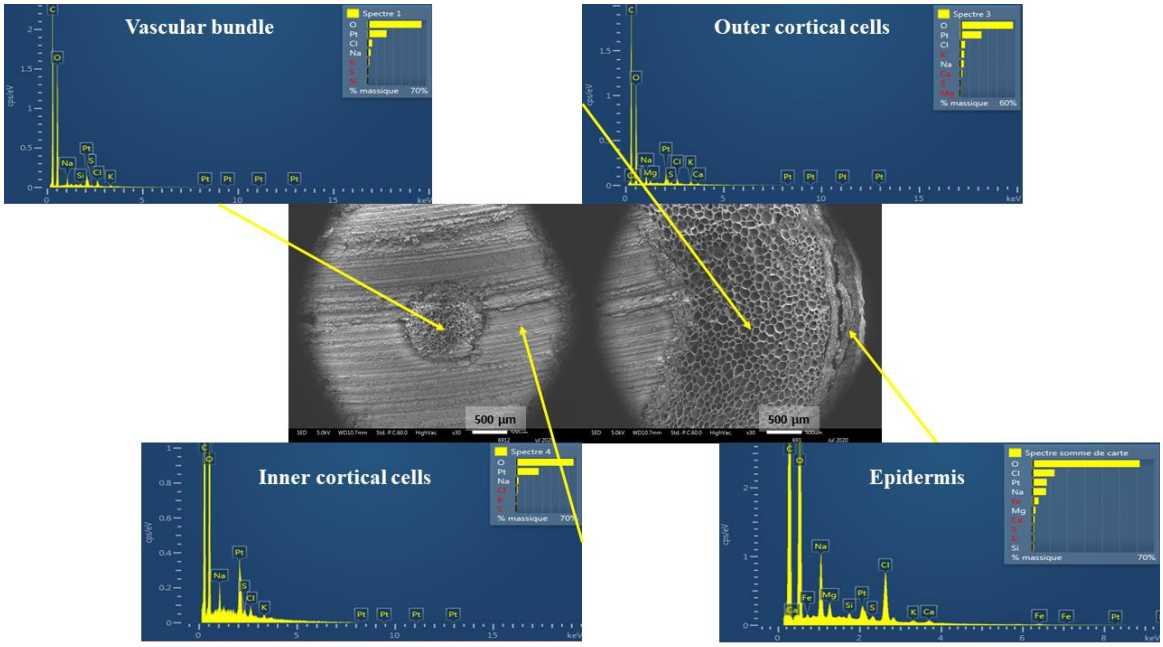

Figure I-7. SEM images of a cross-section of a pneumatophore from *A. marina* and elemental spectra obtained by EDX for the different section areas indicated by the respective arrows.

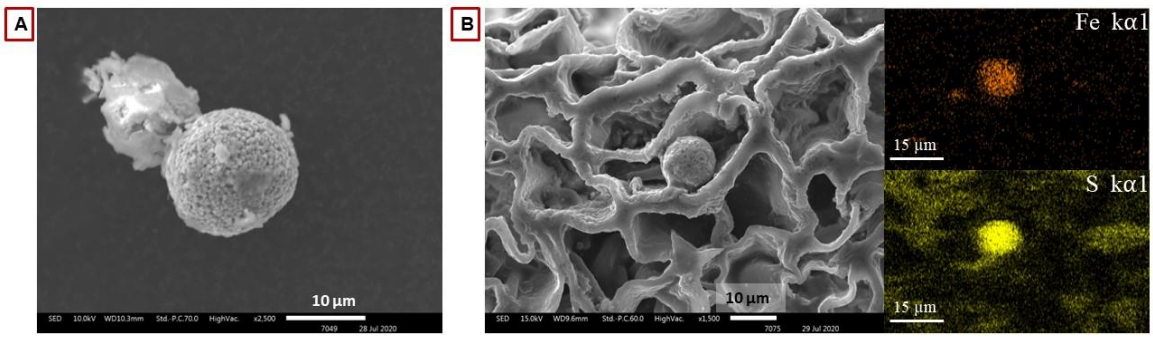

Figure I-8. SEM images of framboidal pyrite (A) in a soil sample and (B) in a cross-section of the pneumatophore epidermis from *A. marina*; elemental EDX maps for Fe and S are shown.

I.5. Discussion

I.5.1. Influence of watersheds inputs on mangrove soil conditions

At the non-ultrabasic site, the highly negative Eh values associated with the low Fe concentrations in the dissolved phase indicate that the soil is anoxic. The presence of pyrite under both species but not in the watershed rock implies that sulfate reduction processes occur in the soil. Conversely, at the ultrabasic site, less negative Eh values and higher concentrations of dissolved Fe in the upper soil layers (*Figure I-3A & B*) suggest suboxic conditions, which most probably result from continuous goethite inputs from upstream lateritic soils allowing Fe reduction. The latter process and goethite dissolution led to the release of Fe in porewaters, which can be further precipitated as pyrite during sulfate-reduction processes in the deeper anoxic layers (Marchand et al., 2006; Kristensen et al., 2017).

Larger organic carbon accumulation was measured at the non-ultrabasic site. Considering that mangrove characteristics (zonation, tree density, height) were similar between the two sites, we suggest that different mineralization processes and rates may explain this trend. In fact, the suboxic conditions that prevail at the ultrabasic site due to the presence of a large amount of goethite may result in more efficient decay processes than the anoxic non-ultrabasic site.

At both sites, pH is significantly more acidic under *R. stylosa* than under *A. marina* (*Figure I-3*). In mangrove soil, OM mineralization and sulfide oxidation are the two main processes that result in H^+ release and thus in soil acidification (Clark et al., 1998). *R. stylosa* is closer to the shore and more influenced by daily tidal fluctuations. Inputs of electron acceptors is greater for OM mineralization or sulfide oxidation under this species leading to a more acidic soil (Bourgeois et al., 2019b). The pH is not significantly different between sites under *A. marina* and is significantly more acidic at the non-ultrabasic site under *R. stylosa* even though we suggest mineralization rates are slower at this latter site (*Figure I-3*). The soil anoxia at the non-ultrabasic site may indicate a greater amount of reduced sulfide in its soil compared to the suboxic ultrabasic-site. This leads to more oxidation reactions of sulfides under *R. stylosa*, which contributes to the soil acidification (Noël et al., 2014).

The geology of the watershed affects the mineralogy of mangrove soil and thus the conditions (TOC, Eh, pH…) as well as the elemental composition. Chemical interactions between different ligands in the soil and TM determine the speciation they take in the

system. Those forms control the mobility, the bioavailability, and the toxicity of these TM (Chakraborty et al., 2016).

I.5.2. Concentrations of trace metals in soil driven by watersheds inputs

At the ultrabasic site, the higher mean concentrations of the analyzed TM in the soil can be explained by the difference in the geology of the watersheds (*Table I-1*). The ultrabasic-site's watershed is composed mostly of laterites rich in goethite and other phases that contain TM such as antigorite (*Figure I-4A & B*) (Baltzer, 1981; Vithanage et al., 2019). Furthermore, the erosion and leaching of the old Ni mine located upstream of the Dumbea River contributes to the input of Ni and other TM such as Co, Cr, and Mn (Fandeur et al., 2009; Metian et al., 2013; Gwenzi, 2020). At the non-ultrabasic site, the volcano-sedimentary soil, mainly composed of quartz and plagioclase (*Figure I-4C & D*), contributes less importantly to analyzed TM inputs to the mangrove soil. Nevertheless, two Fe-bearing phases were identified in the watershed rock: vermiculite and enstatite (*Figure I-4E*). Enstatite was previously identified in the Dumbea watershed and can also be a Ni-bearing phase (Trescases, 1975; Baltzer, 1981). In the conditions that prevail in our study sites, medium to high rainfall (866 mm) and slightly acidic soil with daily basic sea water influx, enstatite is not stable (Oelkers and Schott, 2001; Halder and Walther, 2011). The alteration products of enstatite are talc and chlorite, which were observed in the mangrove soils (*Figure I-4C & D*), with the latter potentially bearing Fe and Ni as well (Trescases, 1975). Illite can also potentially contribute to Fe input or storage (Xie et al., 2020) explaining the high concentrations in the soil in these TM.

TM concentrations in the soil of the ultrabasic site are close to those measured by Marchand et al. (2016) on the same site in 2012 with Fe, Ni, and Cr the three most concentrated in descending order. Iron and Ni concentrations in soil are much higher than world average. Here, Fe represents as high as 18% in mass of the soil, whereas average values in mangroves vary between 0.02 and 6% with a mean value around 1-2% (Alagarsamy, 2006; Chatterjee et al., 2007; Kruitwagen et al., 2008). In the present study, Ni values as high as 4 000 mg kg^{-1} were measured (*Table I-1*) downstream from the Dumbea River while a literature review exposed maximum values of Ni in mangroves soil of 200 mg kg^{-1} (Bayen, 2012). Even though the concentrations of TM in the soil at the non-ultrabasic are lower than those of the ultrabasic site, relatively high values of Fe and Ni were still measured when compared to world average: 680 mg kg^{-1} for Ni and 4% in mass of the soil for Fe (*Table I-1*).This can be explained by the high background noise of TM in New-Caledonian soils and marine sediments, mainly Fe, Ni, Cr, and Mn (Beliaeff et al., 2011). Natural or anthropogenic-driven erosion of nearby soils in addition to wild and man-

made effluents driven by the currents contribute to TM accumulation in the soil of the non-ultrabasic site. This mangrove is located in an urbanized area and models of current show possible inputs from urban discharge as well as an influence from a containment site located 2.5 km south-east of the studied mangrove (Douillet, 2001).

TM concentrations in the soil are therefore dependent on the watershed inputs with the leaching of laterized soil the major factor causing the ultrabasic site to be richer in TM than the other site. We hypothesize that the bioaccumulation of TM in the roots of both studied mangrove species is partly dependent on other factors than TM concentrations in the soil such as the nature of the TM (essential or non-essential).

I.5.3. Bioaccumulation factors differ between trace metals and are independent of the watershed inputs

Iron and Ni concentrations in mangrove roots at both sites are relatively high (*Table I-1*). Iron concentrations obtained in tissues for the ultrabasic site are as high as values reported in Marchand et al. (2016) in the same mangrove, at around 10 000 mg kg^{-1}. Measured Fe concentrations at both sites are much higher than those measured in roots of mangroves in India, which had a maximum value of 938 mg kg^{-1} (Chowdhury et al., 2015). We measured Ni mean values of 164 mg kg^{-1} in the pneumatophores of *A. marina*, which is greater than the maximum values reported in literature of 100 mg kg^{-1} (Lewis et al., 2011; Bayen, 2012). However, the BCF of these two TM are low (*Figure I-5A*) with the dissolved fractions minor in comparison to the solid fractions in the soil (*Figure I-5B*). Chowdhury et al., (2017) estimated that 95% of Fe present in soil of mangrove forests is not bioavailable for the biota since most of it is associated to sulfides. Therefore, even though Fe and Ni are essential metals, their absorption by the plant may be limited due to a lack of ions in the dissolved phase, which is also the case for the non-essential metal Cr that is usually one of the least bioavailable TM in the soil as it was observed here (*Figure I-5*) (Zhu et al., 2015). In the previous study done at the ultrabasic site, Fe and Ni were the most concentrated TM in roots and leaves of *A. marina* and *R. stylosa* but with low bioconcentration and translocation factors as well, partly due to biological barriers that were not explored in the study (Marchand et al., 2016). The high concentrations measured in the roots, especially Fe and Ni, despite low BCF, are explained by the very high concentrations of those TM in the soil at both sites as exposed previously in the discussion.

A low BCF was also calculated for Co at both sites but with a high dissolved/solid ratio in soil (*Figure I-5A*), confirming the observation made by Marchand et al. (2016) at the ultrabasic site. A higher dissolved fraction potentially indicates more ions in the bioavailable form. This result indicates that the uptake of Co by mangroves must be regulated at the biological level rather than at the physico-chemical level. Cobalt is an

essential metal since it is a component of many enzymes and co-enzymes and particularly contributes to plant growth and CO_2 assimilation (Nagajyoti et al., 2010; Reece et al., 2014). However, some publications acknowledge Co as a non-essential metal for mangroves (Nath et al., 2014; Bourgeois et al., 2019a). It is therefore possible that only small quantities of Co are required by the plant, and for the rest of it, mangroves regulate Co uptake through biological mechanisms such as regulation at the root surface with the epidermis acting as a barrier (MacFarlane et al., 2007).

The non-essential metal Pb, weakly present in the dissolved phase compared to the solid phase in the soil (*Figure I-5B*), is highly bioaccumulated in the root systems at both sites (*Figure I-5A*). The maximum value of 39 mg kg^{-1} is still much less than the alarming values obtained in roots of the same species worldwide reaching up to more than 200 mg kg^{-1} (MacFarlane et al., 2007; Lewis et al., 2011; Bayen, 2012). Lead is usually easily mobilized in the soil (Zhu et al., 2015; Yan et al., 2017), and has a high chelation affinity with roots cell walls (associated to carbohydrates) (Turner and Marshall, 1972; Verkleij and Schat, 1990). In *A. marina*, it was observed that Pb is largely accumulated as immobile, bound to cell walls, and sequestered in the roots mainly in the epidermal layers (MacFarlane and Burchett, 2000, 2002). This implies that even though not much Pb is present in the dissolved phase, the plant absorbs a large proportion of it. For *A. marina*, BCF values greater than 1 were also described for Pb in literature (Nath et al., 2014).

Regarding the essential metals Cu, Mn, and Zn, their uptakes by mangroves may not be regulated. Relatively high concentrations of those TM in the dissolved phase compared to the solid phase (*Figure I-5B*) imply that they are potentially more bioavailable and therefore are better absorbed by the roots of both species (high to moderate BCF) (*Figure I-5A*). The BCF values obtained for Mn in *A. marina* are close to those exposed in literature at both sites (Nath et al., 2014; Yadav et al., 2015). Marchand et al. (2016) also exposed a greater mobility and bioavailability of Zn and Cu compared to Fe and Ni at the ultrabasic site. Copper is important in ATP synthesis and plays an essential role in the respiratory electron transport chain (Demirevska-Kepova et al., 2004). Zinc is the second most abundant TM in plants after Fe and the only metal present in the 6 enzymes classes (Broadley et al., 2007). Copper and Zn also have a high chelation affinity with the cell walls of mangroves root with Cu preferentially chelated with amino acids and Zn with organic acids (Verkleij and Schat, 1990; MacFarlane et al., 2007).

High values of some TM in roots, particularly Fe and Ni, are therefore due to high concentrations of TM in the soil at both sites. TM are not similarly bioconcentrated in the roots, with Pb the most transferred from soil to roots and Cr the least. The BCF of TM is

not site-dependent indicating that the watershed inputs do not influence the uptake of TM by the plants. TM mobility and biological and/or physiological factors do affect TM transfer from soil to roots.

I.5.4. Trace metal bioaccumulation in roots is species-dependent

In this study, results evidenced the greater TM uptake in roots of *A. marina* compared to *R. stylosa* (*Table I-1*). One explanation is that roots of *R. stylosa* are weakly permeable due to a thickening mechanism and exodermis cell lignification facing metal stress that act as a physical barrier to TM uptake (Cheng et al., 2012, 2014). *A. marina,* with more permeable pneumatophores, is more subject to TM absorption through the root system. We focused on pneumatophores rather than on main roots. One hypothesis is that TM are accumulated in pneumatophores as a mechanism to limit metal stress in the central root system (MacFarlane et al., 2007). Since *A. marina* diffuses oxygen in its rhizosphere, oxidation of reduced TM can occur, which mobilizes the TM that become bioavailable for direct absorption by the plant (Thakur et al., 2016). MacFarlane et al. (2007) showed a trend in higher root BCF for species that are less frequently inundated, which results in less anoxic soil (i.e. *Kandelia* spp.) and species with pneumatophores (i.e. *Avicennia* spp.). The difference in BCF between the two species can also result from different metabolisms and therefore different physiological needs (Yan et al., 2017). Also, *A. marina* is able to excrete some TM in excess through the salt glands on its leaves as it was observed for Cu and Zn (Naidoo et al., 2014). In the review of MacFarlane et al. (2007) on TM accumulation in mangroves, high variability of Cu, Pb, and Zn for each species were displayed but the mean BCF of reviewed literature confirm the higher capacity of *A. marina* to absorb TM through its roots. The *Rhizophora* genus has already been characterized in the literature as a low TM-accumulating species (Peters et al., 1997). Consequently, there are differences in TM bioconcentration between species due to factors expressed above and different mechanisms are used by species in order to limit metal stress such as the formation of Fe plaque, which is the case for *A. marina*.

I.5.5. Role of the iron plaque against metal stress

The mean concentration of Fe plaque is two times higher on the pneumatophores of *A. marina* at the ultrabasic site compared to the non-ultrabasic site (*Figure I-6A*). The variability can be explained by the fact that the Fe plaque was extracted from multiple pneumatophores in the same area. The age, length, and tree belonging can influence Fe plaque formation capacity. Higher mean Fe plaque formation is consistent with the higher concentrations of Fe obtained in the solid and dissolved phases of the soil at the ultrabasic site. More Fe in the soil, if in reduced form, enable more reactions between Fe^{2+} and O_2 to

form the plaque. Multiple studies showed positive relationship between Fe plaque concentration on roots surface and reduced Fe in the soil (Christensen and Wigand, 1998; Pi et al., 2010, 2011). Pi et al. (2011) even showed that Fe plaque formation does not reach a threshold of Fe concentration in the soil since plaque formation occurs until the mangrove's death. Sequential extractions are though required in order to get the proportion of Fe in the reduced form to confirm what was presented in literature.

Iron plaque formation is extensive on the pneumatophores at both sites since more than 40% of Fe extracted from the pneumatophores come from the Fe plaque. Available Fe^{2+} ions are phytotoxic for mangroves as they can cause DNA damage and a reduction of photosynthesis (Nagajyoti et al., 2010). Through radial oxygen loss (ROL) via pneumatophores, the formation of Fe plaque is an efficient mechanism to reduce Fe^{2+} concentrations and uptake through the root system (Youssef and Saenger, 1996). The measured iron plaque concentrations suggest that ROL is significant enough to ensure important Fe^{2+} oxidation in a mangrove with large concentrations of dissolved Fe.

Cobalt, Cr, Mn, Ni and Zn are retained in significant quantities in the Fe plaque at both sites (> 47%) (*Figure I-6B*). Iron oxides and hydroxides have a strong TM adsorption capacity due to their large specific surface area (> 200 $m^2\ g^{-1}$) (Lin et al., 2018). Several authors reported the significant role of Fe plaque against metal stress, mainly by trapping TM (Taylor and Crowder, 1983; Machado et al., 2005; Pi et al., 2011; Tripathi et al., 2014). The calculated percentages of TM immobilized in the plaque of *A. marina* are consistent with previous studies and show the significance of the Fe plaque against metal stress for this species (Machado et al., 2005; Pi et al., 2011; Lin et al., 2018). For example in Brazil, more than 60% of immobilization on the surface of an *Avicennia* species, and between 25 and 60%, was observed for Mn and Zn, respectively (Fonseca, 1994). In a study concerning the role of Fe plaque on three mangroves species (*Bruguiera gymnorrhiza*, *Excoecaria agallocha*, and *Acanthus ilicifolius)*, authors described a mean immobilization of TM in the following order: Mn > Ni > Zn > Cr (Pi et al., 2011). These results are slightly different from what we observed here since Ni is the least trapped TM but not significantly compared to Zn and Cr (*Figure I-6B*). However, in this previous study by Pi et al. (2011), TM immobilization order was species-dependent as multiple studies exposed previously (Tripathi et al., 2014). In addition, the experiment was set up in a laboratory in controlled conditions that are not always representative of *in situ* conditions, which has an influence on TM speciation.

More Fe plaque was measured on pneumatophores at the ultrabasic site; however, no significant difference between sites in percentages of TM retained in the plaque was observed (*Figure I-6B*). Two groups of TM can be identified from this observation; one

composed of Co, Mn, and Ni, and the other one of Cr and Zn. Larger concentrations of Co, Mn, and Ni are retained in the plaque at the ultrabasic site, where there is more of these TM in the soil compared to the non-ultrabasic site. There are also larger concentrations of these TM in the DCB-treated pneumatophores (pneumatophores without Fe plaque). In this case, a greater volume of Fe plaque equals a greater volume of TM immobilized; however, in terms of percentage of immobilization (capacity of the plaque to immobilize TM), it is equivalent at both sites. This scenario is consistent with previous findings that show a positive correlation between Fe plaque concentrations and TM immobilization (Pi et al., 2011; Tripathi et al., 2014). For Cr and Zn, the concentrations of TM in the treated pneumatophores and in the DCB extract (Fe plaque), are similar between both sites. Therefore, there is no positive relationship between Fe plaque concentration and TM immobilization. This observation may indicate a threshold of concentration of TM that can be retained in the plaque. Some studies highlighted the ability of the Fe plaque of the rice species *Oryza sativa* to trap TM such as Cr and Cd from the environment without affecting uptake and translocation of the TM (Liu et al., 2008; Hu et al., 2014). In the present study, this means that Fe plaque concentration does not impact the amount of Cr and Zn that will be bioaccumulated in the pneumatophores. Fe plaque has never been previously studied in New Caledonian mangroves and further research must be conducted to confirm or disprove the results obtained.

I.5.6. Iron and pyrite accumulation within roots epidermis

Iron plaque formation is an efficient mechanism for *A. marina* to limit metal stress by trapping TM and limiting their uptake by the roots as discussed earlier. Nevertheless, a fraction of TM passes through this physical barrier and can accumulate in the roots or be transferred to other plant organs. The amount of TM in the roots depends on the TM considered, its concentration in the soil, its mobility, the redox conditions and the mangrove species. Using SEM-EDX analysis, we looked for possible zones of accumulation of TM in the roots of both species. Fe was the only TM observed in roots of mangroves (*Figure I-7*). Iron is the most concentrated TM in roots with mean values between 2 486 and 17 125 mg kg^{-1}, which is between 15 and more than 1 500 times greater than the other TM (except Hg) (*Table I-1*). The detection limit of the apparatus must restrain the observation of TM other than Fe.

Iron has only been detected in the epidermis of the roots of both *A. marina* and *R. stylosa* (*Figure I-7*). The epidermis is a barrier against physical damage and pathogens. The epidermis limits water loss and is the first line for water and nutrient absorption by the roots (De Granville, 1974; Reece et al., 2014). Iron is preferentially accumulated in the root

system limiting transport to higher organs, which is why it will be more concentrated on, or in, the epidermis rather than in the cortex or vascular cylinder (Machado et al., 2005). Free Fe is highly toxic for plants and is therefore rarely observed on its own in tissues. Iron, mostly in its reduced form Fe^{2+}, is bound to chelators and chaperones or present as Fe sequestering proteins such as ferritin and frataxin. Iron is essential for the synthesis of Fe-S clusters, fundamental in the structure of Fe-S proteins such as ferredoxins that intervene in electron transfer in many metabolic reactions (Morrissey and Guerinot, 2009). With the EDX elemental maps of mangroves roots, we observed clusters of Fe linked to S in the epidermis of the pneumatophores of *A. marina* (*Figure I-8B*). However, the clusters were identified as framboidal pyrite. The sphere of FeS_2 visible in *Figure I-8B* seems attached to the cell walls. A hypothesis is that pyrite formed within the root from organic sulfur. Plants naturally fix sulfides in multiple forms (carbonates, amino acids, esters, polysaccharides, etc.) that can then produce H_2S and will precipitate within the vascular tissues if Fe is present (Vallentyne, 1963; Altschuler et al., 1983). A suggested scenario is that pyrite formation within the pneumatophores of *A. marina* is a mechanism to limit Fe, and other chalcophile TM, transfer to higher organs. Pyrite crystals, framboidal and in lines, were previously observed in vascular channels of roots of *Spartina alterniflora*, a salt-marsh cordgrass of the East coast of the United States (Giblin, 1988). Framboids were also identified in the root vascular tissues of mangroves in the Everglades in Florida (Altschuler et al., 1983). The explanation mentioned by Altschuler *et al*. (1983) and Giblin (1988) is that in-root pyrite formation happens when the main source of sulfide within the soil is organic sulfide, which is not the case in intertidal ecosystems. To our knowledge, observation of pyrite crystals within vascular tissues has never been reported in mangroves. Further research must be conducted on the occurrence of those FeS_2 crystals and on its drivers, soil properties, seasons, and species.

I.6. Conclusion

Despite their geographical proximity, two mangroves located on the semi-arid West coast of New Caledonia differ greatly in the properties of their soil and in the distribution of TM due to distinct watersheds. Mangrove soil located downstream of an old Ni mine, the ultrabasic site, was characterized by TM concentrations higher than world average due to the laterized soil leached and eroded upstream. In addition, inputs of Fe oxy/hydroxide allows a good renewal of electron acceptors, and consequently, soil was characterized by suboxic conditions, which influences TM dynamics. The nature of the watershed should therefore be taken into account when studying geochemical processes and TM dynamics in mangroves. If significant differences were observed in TM concentrations in the soil of the two mangroves, TM concentrations in the roots did not seem influenced by the

watershed inputs, but rather by the species. We suggest that TM uptake by those two mangroves were mainly driven by plant metabolisms and species-related biochemical mechanisms. Iron and Ni were of the most concentrated TM in the roots of both species but showed low BCF possibly due to the lack of ions in the dissolved phase and the excessively large concentrations in the soil leading to potential uptake regulation by the plants. Uptake of TM by *A. marina* was greater than that of *R. stylosa* potentially due to a more permeable root system. Eventually, Fe plaque formation on pneumatophores of *A. marina* may be correlated to Fe concentration in the soil. Iron plaque plays an important role in limiting TM uptake by the plant up to 94% for Mn. Pyrite crystals were observed for the first time via SEM-EDX in the epidermis of pneumatophores of *A. marina.* We hypothesize that those framboids limit TM uptake by the plant via TM immobilization the same way as in mangroves soil. The acute investigation of pyrite crystals in root epidermis is considered for perspectives. Eventually, studies on TM species and locations within mangroves' organs should be further explored.

I.7. Acknowledgments

The authors acknowledge Kapeliele Gututauava and Franck Bouilleret for their technical help on site. Sarah Gigante and Valérie Medevielle are acknowledged for their technical support at the lab. The authors are grateful to Valérie Sarramegna for the knowledgeful discussions. Aurélie Monnin and Olivia Barthélémy are acknowledged for the technical assistance during SEM observations. The authors thank Leocadie Jamet and Monika Lemestre for Hg analysis and ICP-OES measurements, respectively. Lastly, the authors are grateful to the two anonymous reviewers who helped improve the manuscript with their constructive comments and suggestions.

I.8. Supplementary materials

Supplementary Table I-1. Quality control of ICP-OES measurements for trace metals in soil and biota.

CRM type	Element	Detection limit (mg kg^{-1})	Certified NDA mean value (mg kg^{-1})	Certified NDA standard deviation	Measured value (mg kg^{-1})	z-score
Soil	Co	0.124	18.79	3.20	18.53	-0.08
	Cr	0.375	126.3	8.3	124.8	-0.18
	Cu	0.174	37.32	2.79	45.65	2.98
	Fe	0.920	55 140	1 460	54 840	-0.21
	Mn	0.196	474.8	26.2	450.3	-0.94
	Ni	0.330	53.45	4.04	51.33	-0.53
	Pb	0.744	78.72	4.01	68.70	-2.50
	Zn	0.327	235.0	18.2	214.0	-1.15
Biota	Co	0.124	0.270	0.047	0.150	-2.53
	Cr	0.375	1.63	0.28	1.15	-1.74
	Cu	0.174	3.58	0.73	3.31	-0.37
	Fe	0.920	678.5	84.6	555.3	-1.46
	Mn	0.196	481.4	42.1	474.1	-0.17
	Ni	0.330	1.06	0.24	0.95	-0.44
	Pb	0.744	1.08	0.15	1.21	0.88
	Zn	0.327	0.027	0.004	0.024	-0.74

Supplementary Table I-2. Correlation matrix for physico-chemical parameters, TOC (%) and concentrations of dissolved Fe in the soil cores at the ultrabasic and non-ultrabasic sites beneath *A. marina* and *R. stylosa*.

	Ultrabasic						Non-Ultrabasic					
	A. marina			*R. stylosa*			*A. marina*			*R. stylosa*		
	pH	Eh	TOC	pH	Eh	TOC	pH	Eh	TOC	pH	Eh	TOC
Eh	0.40			-0.59			0.15			-0.97		
TOC	-0.73	-0.13		0.07	0.25		-0.71	0.18		-0.41	0.25	
Dissolved Fe	-0.06	-0.47	0.07	0.66	-0.91	-0.22	-0.03	-0.47	-0.17	-0.18	0.08	-0.30

Supplementary Table I-3. Trace metal concentrations in soil in mg kg^{-1} except for Hg in µg kg^{-1} at the ultrabasic and non-ultrabasic sites beneath *A. marina* and *R. stylosa*.

Site	Species	Depth (cm)	Sample	Co	Cr	Cu	Fe	Mn	Ni	Pb	Zn	Hg
Ultrabasic	*A. marina*	0 - 6	1	220	2 026	72	177 800	594	4 814	19	106	55
			2	107	2 106	80	177 800	579	2 993	19	93	
			3	118	2 081	51	177 104	601	3 428	16	92	
		6 - 12	1	162	2 223	72	175 728	601	4 172	19	99	66
			2	40	1 780	60	180 639	353	1 146	20	49	
			3	95	2 259	63	172 710	521	2 801	18	86	
		12 - 18	1	113	2 358	57	173 040	505	2 966	14	82	83
			2	63	1 687	31	93 492	174	848	11	27	
			3	38	1 960	40	142 396	288	775	12	38	
		18 - 24	1	106	1 535	28	46 373	141	1 184	6	26	65
			2	186	1 723	30	66 878	265	1 801	8	37	
			3	43	1 560	19	35 757	135	709	5	25	
		24 – 30	1	246	1 542	36	74 708	266	2 302	10	46	47
			2	237	1 455	35	93 299	429	2 361	10	52	
			3	122	1 520	19	36 679	161	1 286	6	24	
	R. stylosa	0 - 6	1	192	2 011	61	178 150	793	4 105	18	115	68
			2	153	2 044	65	181 545	1059	3 884	19	94	
			3	216	2 195	62	175 388	1082	4 201	19	111	
		6 - 12	1	171	2 472	75	178 677	758	4 435	21	123	60
			2	163	2 555	69	173 372	878	4 509	19	104	
			3	153	2 476	75	180 819	810	3 929	21	102	
		12 - 18	1	116	2 658	56	178 854	531	2 841	15	88	89
			2	60	2 091	62	181 000	499	1 871	18	59	
			3	30	1 529	47	179 920	337	768	15	32	
		18 - 24	1	29	1 750	23	47 065	150	533	6	26	73
			2	32	1 448	26	94 492	223	564	11	20	
			3	26	1 380	14	44 509	166	366	6	18	
		24 – 30	1	38	1 722	19	29 897	161	498	3	30	59
			2	28	1 715	16	42 253	242	444	6	62	
			3	41	1 541	15	26 652	181	391	5	18	
Non - Ultrabasic	*A. marina*	0 - 6	1	31	365	24	36 937	143	413	12	66	72
			2	28	396	25	39 501	158	429	12	68	
			3	29	379	23	38 491	147	428	12	67	
		6 - 12	1	38	428	18	35 523	109	601	11	58	48
			2	44	511	19	40 208	114	756	13	68	
			3	41	512	22	43 152	127	689	14	72	
		12 - 18	1	36	395	24	51 276	124	461	13	57	41
			2	35	474	21	42 965	117	563	13	60	
			3	35	460	24	55 811	117	418	12	58	
		18 - 24	1	33	381	25	59 894	127	329	13	57	41
			2	42	441	24	56 364	131	465	12	60	
			3	30	393	26	51 488	107	312	11	45	
		24 – 30	1	29	360	24	49 647	116	287	12	55	56
			2	39	496	22	54 483	141	450	12	65	
			3	33	284	32	48 029	99	385	10	50	
	R. stylosa	0 - 6	1	25	421	22	30 274	118	374	10	52	74
			2	30	404	20	30 847	109	385	10	46	
			3	34	548	24	41 777	161	623	13	65	
		6 - 12	1	38	407	20	42 180	96	466	10	49	43
			2	35	426	19	43 060	107	447	10	41	
			3	24	473	14	28 847	89	400	9	46	
		12 - 18	1	36	417	23	54 478	117	465	12	49	46
			2	33	419	20	46 188	112	358	9	38	
			3	35	445	19	42 042	94	405	11	50	
		18 - 24	1	32	355	26	53 499	118	352	11	40	64
			2	41	312	28	88 813	137	578	10	38	
			3	34	342	26	55 868	109	406	11	41	
		24 – 30	1	39	276	26	63 137	114	461	11	42	55
			2	35	224	27	88 813	134	574	10	29	
			3	39	275	26	52 359	99	499	11	41	

Supplementary Table I-4. Trace metal concentrations in porewaters in µg L^{-1} at the ultrabasic and non-ultrabasic sites beneath *A. marina* and *R. stylosa*. X are under detection limits.

Site	Species	Depth (cm)	Sample	Co	Cr	Cu	Fe	Mn	Ni	Pb	Zn
Ultrabasic	*A. marina*	0 - 6	1	103	112	95	34 288	447	485	8	91
			2	42	67	36	17 325	551	110	6	28
		6 - 12	1	128	96	76	43 656	622	715	14	65
			2	50	49	40	41 549	473	274	X	30
		12-18	1	79	114	72	61 821	646	486	6	56
			2	0	104	85	179 827	1 006	453	26	37
		18-24	1	73	115	65	37 985	663	213	14	47
			2	43	133	67	96 732	876	193	X	39
		24-30	1	64	72	46	16 232	803	205	4	34
			2	65	107	58	40 067	1 042	177	8	41
	R. stylosa	0 - 6	1	203	135	122	2 742	2 203	468	X	137
			2	195	27	26	30	1 146	305	X	22
		6 - 12	1	293	193	170	37 753	3 547	913	19	175
			2	90	31	13	34 234	2 570	482	10	6
		12-18	1	120	179	110	97 777	2 790	397	22	108
			2	21	69	22	120 911	3 407	258	18	5
		18-24	1	118	177	105	55 039	2 517	214	30	102
			2	88	71	39	106 570	3 412	210	8	15
		24-30	1	114	148	89	41 927	2 601	174	9	108
			2	31	66	26	80 923	3 258	160	12	11
Non - Ultrabasic	*A. marina*	0 - 6	1	128	90	86	19 808	607	110	6	90
			2	20	5	13	9 010	274	58	X	2
		6 - 12	1	439	173	148	9 837	757	191	X	148
			2	88	14	5	20	364	190	9	6
		12-18	1	531	164	144	3 651	692	201	1	148
			2	69	10	8	250	363	29	1	4
		18-24	1	137	78	76	4 912	713	78	17	81
			2	10	1	14	8 157	471	17	X	X
		24-30	1	78	44	51	26 540	649	50	X	56
			2	32	4	8	1 583	475	60	6	X
	R. stylosa	0 - 6	1	60	23	17	144	214	59	X	30
			2	20	2	X	X	413	37	11	X
		6 - 12	1	120	44	40	118	257	140	X	39
			2	55	4	11	X	462	249	3	X
		12-18	1	58	22	21	266	235	121	10	17
			2	71	7	3	X	376	146	X	X
		18-24	1	184	44	35	66	263	67	6	43
			2	31	1	4	X	412	164	3	X
		24-30	1	37	12	2	83	228	18	X	10
			2	94	6	5	X	372	131	5	X

II. Chapter II: Distribution and bioaccumulation of trace metals in urban semi-arid mangrove ecosystems

Robin, S.L., Marchand, C., Mathian, M., Baudin, F., Alfaro, A.C., 2022. Distribution and bioaccumulation of trace metals in urban semi-arid mangrove ecosystems. *Frontiers in Environmental Science* 17. https://doi.org/10.3389/fenvs.2022.1054554

Présentation :

Dans ce deuxième chapitre, l'étude de la distribution des ETM dans le sol de mangrove et de leur transfert dans les tissus des palétuviers est poursuivie. Cependant, l'attention se porte cette fois sur l'influence de l'urbanisation, un contexte peu exploré en Nouvelle-Calédonie. L'impact de l'urbanisation sur la répartition des ETM est examiné en comparant deux mangroves situées en aval d'un bassin versant volcano-sédimentaire à Dumbéa, toutes deux abritant les deux espèces de palétuviers dominantes, à savoir *Avicennia marina* et *Rhizophora stylosa*. La mangrove dite "urbaine" est influencée par les eaux pluviales provenant du quartier de Koutio depuis plus de 50 ans, se déversant directement dans cette mangrove.

Ce chapitre apporte de nouvelles perspectives sur l'impact des eaux pluviales urbaines sur les mangroves. En comparant une mangrove urbaine à une mangrove contrôle partageant le même bassin versant géologique, cette étude révèle comment le flux continu des eaux urbaines altère les propriétés physico-chimiques naturelles du sol, perturbant ainsi la biodisponibilité des ETM. L'apport constant des eaux urbaines régule la salinité et le pH du sol, créant des conditions suboxiques qui influencent la distribution des ETM. Dans le sol de la mangrove impactée par l'urbanisation, les concentrations de la plupart des ETM sont plus faibles. Ce phénomène peut être expliqué par la salinité du sol, le taux de MO ou encore la réduction du lessivage des sols en amont due à la bétonisation. En revanche, les ETM associés à l'urbanisation (Cu, Pb, Ti, Zn) présentent des concentrations supérieures dans le sol de la mangrove urbaine, potentiellement en raison de l'apport provenant de ces eaux urbaines. Cette étude démontre également que les ETM sont significativement davantage transférés vers les racines au sein de la mangrove urbaine, augmentant ainsi les chances d'intégration dans la chaîne alimentaire. Les eaux urbaines restreignent la formation de complexes entre les ETM et les sels, ainsi que le piégeage des ETM par la pyrite dans le sol, ce qui augmente la biodisponibilité des ETM. Cette plus grande biodisponibilité conduit à des facteurs de bioconcentration racinaire élevés pour les deux espèces. Cependant, les concentrations en ETM dans les feuilles restent cohérentes entre les deux mangroves étudiées, et les facteurs de translocation ne diffèrent pas entre les sites, suggérant une régulation du transfert des ETM vers les feuilles par les palétuviers. Contrairement au chapitre I, la formation de plaque d'oxyde de fer ne semble pas être corrélée aux concentrations en fer dans le sol, mais pourrait être liée au stress environnemental subi par l'espèce.

Distribution and bioaccumulation of trace metals in urban semi-arid mangrove ecosystems

Sarah Louise ROBIN, Cyril MARCHAND, Maximilien MATHIAN, François BAUDIN, Andrea C. ALFARO

Published in Frontiers in Environmental Science

II.1. Abstract

Mangrove ecosystems are known to act as filters for contaminants between land and sea. In New Caledonia, urbanization has increased along the coastline during the last decades. However, the impact of urbanization on contaminant cycling in mangrove forests has remained unexplored. In this study, we investigated trace metal (TM) dynamics in an urban mangrove soil and their transfer to mangrove tissues for the two dominant mangrove species in New Caledonia: *Avicennia marina* and *Rhizophora stylosa*. The results suggest that decades of urban rainwater runoff from an upper neighborhood induced large variations of mangrove soil physico-chemical properties compared to a control mangrove site sharing the same geological watershed. The urban mangrove site had a neutral pH and low salinity in the upper soil, while the control mangrove site presented acidic pH and a salinity ranging from 24 to 62 g L^{-1}. Most TM were significantly less concentrated in the urban mangrove soil varying from 1.3±0.3 µg g^{-1} at the urban site and 1.9±0.5 µg g^{-1} at the control site for Cd, to 30±8 mg g^{-1} and 49±11 mg g^{-1} for Fe at the urban and control site, respectively. However, higher root bioconcentration factors were measured for As, Cd, Co, Cr, Fe, Mn, Ni, and Pb in the urban mangrove soil (1.7±0.9, 0.14±0.06, 0.23±0.13, 0.042±0.026, 0.088±0.057, 0.47±0.39, 0.21±0.12, and 0.25±0.09, respectively) compared to the control mangrove soil (0.11±0.03, 0.041±0.016, 0.045±0.021, 0.010±0.004, 0.013±0.007, 0.094±0.030, 0.022±0.011, and 0.12±0.03, respectively). The bioavailability of TM in the urban mangrove soil may be favored by suboxic conditions associated to less Cl-TM complexes and pyrite-TM complexes in the soil. Only Cu, Pb, Ti, and Zn, usually associated with urbanization, were more concentrated in the urban mangrove soil with mean concentrations of 27±4, 17±2, 4 571±492, and 62±12 µg g^{-1} at the urban site, respectively, and 21±4, 10±3, 2 834±541, and 57±12 µg g^{-1} at the control site, respectively. No significant difference in translocation factors was measured between the two sites, evidencing a regulation of TM translocation to the upper tissues by mangrove trees.

Keywords: mangrove forests, trace metals, urbanization, bioaccumulation, anthropogenic pressure, *Avicennia marina*, *Rhizophora stylosa*

II.2. Introduction

Mangrove forests are tidal ecosystems developing in tropical, subtropical, and some temperate areas (Thomas et al., 2017). These ecosystems provide many ecosystem services, such as the function of buffers for sediments and contaminants between diverse watersheds and the adjacent aquatic ecosystems (e.g. lagoon, estuaries, sea) (Lee et al., 2014). Mangrove forests cover littoral areas of more than 100 countries. Out of the 20 countries with the most mangrove surface areas, 17 are referred to as developing countries, according to the International Monetary Fund (International Monetary Fund, 2022), and a third of their population lives on the coast (Center for International Earth Science Information Network, 2012). There is inevitably competition for space between mangrove ecosystems and economic and urban development.

Accordingly, mangrove forests are endangered ecosystems despite awareness of their benefits. Economic and urban development have resulted in high mangrove deforestation rates with about 35% of mangrove surface area lost between the 80s and the 90s (Valiela et al., 2001; Alongi, 2002). In addition to direct mangrove forest destruction, urbanization can also impact mangrove forests through the input of anthropogenic effluents, and specifically rainwater runoff enriched with trace metals (TM). These effluents can contaminate and stress mangrove ecosystems, but also change hydrological and geochemical conditions, creating a disequilibrium in coastal areas (Cavalcante et al., 2009; Lewis et al., 2011; Kristensen et al., 2017; Alemu I et al., 2021).

TM are one of the many types of pollutants in mangrove forests and mainly originate from anthropogenic activities. TM are naturally occurring elements in the Earth's crust (<1 000 mg kg^{-1}) and are therefore present in the environment (Turekian and Wedepohl, 1961; Thornton, 2012). Anthropogenic activities such as industrial, mine, agricultural, and housing development activities increase their concentrations in the environment (Bayen, 2012). TM are of great concern because even though most of them are micronutrients, which can be used by a range of organisms, they can have significant negative impacts beyond specific thresholds (e.g., toxicity). For instance, TM can inhibit developmental processes and decrease photosynthetic activity of plants (Bayen, 2012). In contrast to organic pollutants, TM cannot be biologically or chemically degraded and can therefore be transported over long distances or accumulate in the environment (Prasad et al., 2006), adsorbed on organic complexes and reactive mineral surfaces, or trapped within mineral structures (Brown and Parks, 2001).

Mangrove ecosystems act as reservoirs for TM due to their high sedimentation rate, high organic matter (OM) content, and high biogeochemical reactivity (Harbison,

1986). TM dynamics in mangrove soil are generally well documented and depend on many factors, with the main ones being bonding phases and physico-chemical parameters (Jayachandran et al., 2018; Duan et al., 2020; Huang et al., 2020a). For example, the modification of redox conditions can limit or favor the precipitation of pyrite (FeS_2), which can trap TM, supporting TM immobility in the mangrove soil (Noël et al., 2015; Chakraborty et al., 2016). Also, the amount of OM in the soil and the quality of the OM can influence TM accumulation and bioavailability in mangrove soils. TM can form complexes with the OM, and the capacity of formation is dependent on the nature of the OM with a preference of TM for mature OM with high lignin content (Marchand et al., 2005; Kristensen et al., 2008; Thakur et al., 2014, 2016; Ge and Li, 2018; Duan et al., 2020). TM can also be exported to mangrove trees or outside the mangrove forest in the dissolved phase with litterfall or tidal flushing and tidal pumping (Silva et al., 1998; Ferreira et al., 2007; Holloway et al., 2016, 2018). In urban contexts, previous studies have measured moderate to highly TM contaminated mangrove soils due to urban inputs (Marx and McGowan, 2010; Singh et al., 2010; Bastakoti et al., 2019a).

Mangrove plants are considered resistant to metal stress, partly due to the production of antioxidants limiting reactive oxygen species (MacFarlane and Burchett, 2002). However, some direct effects of TM on mangrove trees were reported, including growth inhibition, increased peroxidase activity, and death (MacFarlane and Burchett, 2001, 2002; Cheng et al., 2014; Naidoo et al., 2014). The transfer of TM from mangrove soils to mangrove trees depends on the bioavailability of the TM in the soil as plants can only assimilate TM in the soluble form (Tremel-Schaub and Feix, 2005). Soil factors such as redox potential, pH, and cationic exchange capacity drive TM bioavailability in mangrove soils, and therefore transfer to mangrove trees (Batty, 2000; Fritioff et al., 2005; Marchand et al., 2016; Bourgeois et al., 2020; Huang et al., 2020b; Robin et al., 2021). TM transfer to mangrove plants differs greatly between TM, tissues, and species since it depends on metabolic requirements (He et al., 2014; Marchand et al., 2016; Rezaei et al., 2021; Robin et al., 2021). Mangrove species have developed mechanisms to prevent metal stress. Some species, such as *Avicennia* spp., have pneumatophores (aerial roots exhibiting negative geotropism), which allow for gas exchange between the atmosphere and the rhizosphere, notably O_2 (Purnobasuki et al., 2017). The O_2 can oxidize labile Fe(II) available in the rhizosphere to form an iron (III) plaque at the root surface (Taylor and Crowder, 1983). Studies have shown that this iron plaque can trap TM and therefore prevent their transfer to the plant tissues (Pi et al., 2011; Yamaguchi et al., 2014; Robin et al., 2021). Other species, such as *Rhizophora* spp., rely on the thickness of their roots and lignification processes to limit TM absorption within their tissues (Cheng et al., 2012, 2014).

In New Caledonia, mangrove ecosystems account for about 80% of the West coast of the main island and 15% of its East coast (Marchand et al., 2007). While the human population density is low (17 inhabitants per km²) (Insee, 2020), and the island is relatively pristine, anthropogenic activities still threaten these ecosystems to various degrees. Due to the lateritic nature of one third of the soil on the island (e.g., rich in oxides and TM) (Tardy and Roquin, 1992), most studies were interested in the impact of mining activities, that increase erosional processes, and lateritic sediments inputs on mangrove forests (Marchand et al., 2012, 2016; Bourgeois et al., 2020; Robin et al., 2021). Few studies have also considered the impact of aquaculture and its discharge (Marchand et al., 2011b). However, the impact of urbanization on TM inputs and distribution in mangrove forests remains unexplored and is of critical importance. The understanding of the impact of urbanization in a pristine island is necessary to manage future urban development and limit the threat of TM contamination. In addition, the Caledonian population rely on mangrove forests and their resources for personal and economic use. Studies worldwide have already shown the potential threat of urbanization as a source of TM contamination in mangrove forests (Ray et al., 2006; He et al., 2014; Celis-Hernandez et al., 2020).

Our main objectives were to assess TM dynamics in mangrove soils receiving urban rainwater runoff for more than 50 years, as well as their bioaccumulation in tissues of two main mangrove species, *Avicennia marina* and *Rhizophora stylosa*. To this end, we collected soil, porewater, roots, and leaves in an urban and a control mangrove forest. The control site had the same geological watershed as the urban site, but was not exposed to urban runoff. Our hypotheses are i) that trace metals are in higher concentrations at the urban site due to a greater input of these contaminants within the mangrove forest with the urban rainwater runoff, ii) that their physico-chemical conditions also differ because of a more waterlogged soil at the urban site, and iii) that their bioaccumulation in mangrove tissues at the urban mangrove site will differ from natural mangrove forests such as the control mangrove site due to those differences in physico-chemical conditions. To evaluate these hypotheses, sequential extractions were performed on soil samples and bioconcentration factors (BCF) were determined for the roots and the leaves of the two mangrove species.

II.3. Material & methods

II.3.1. Study sites

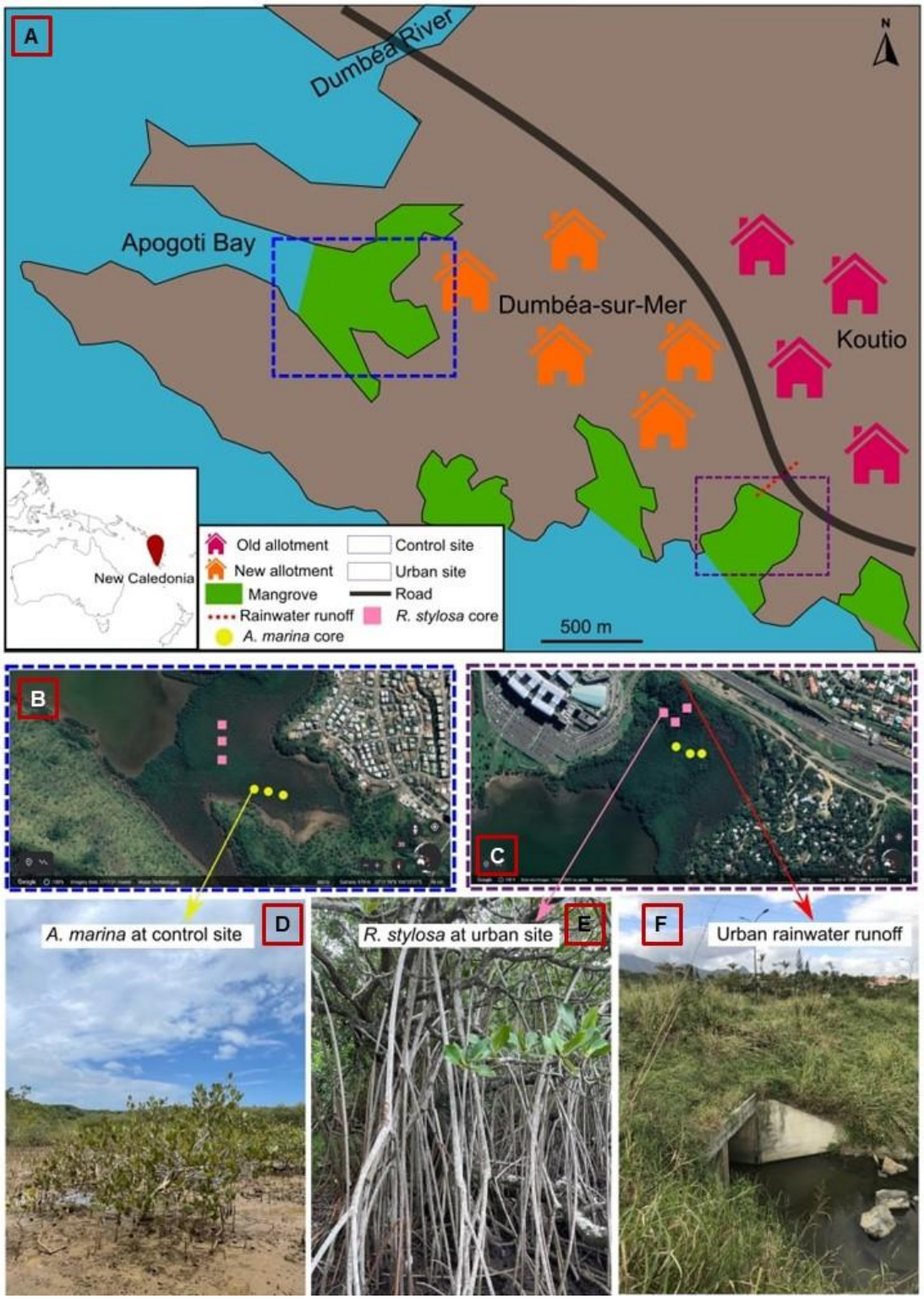

Figure II-1. (A) Map of the urban and control sites with (B) triplicate soil cores taken under *A. marina* and *R. stylosa* at the control site (C) and urban site, and pictures of (D) *A. marina* at the control site, (E) *R. stylosa* at the urban site, and (F) the entrance of the urban rainwater in the urban site.

New Caledonia is a French archipelago located between 20°S and 23°S in the South Pacific. Mangrove forests cover more than 35 000 hectares of the archipelago (Marchand et al., 2007). The climate of the western coast of the main island is semi-arid with semi-diurnal tidal cycles (Douillet et al., 2001). In New Caledonia, mangrove species develop in monospecific stands along gradients depending on soil geochemical parameters, such as salinity and topography (Marchand et al., 2011b; Deborde et al., 2015). More than 20 mangrove species are found in New Caledonia, but two are dominant. *Rhizophora* spp. represent 50% of mangrove area and grow along the sealine in soils with porewater salinity ranging from 5 to 40 g L^{-1}. *Avicennia marina* represents more than 15% of the mangrove area and grows in areas of higher elevation with porewater salinity between 35 and 70 g L^{-1} (Marchand et al., 2007, 2016).

The archipelago is composed of 33 towns and is characterized by a very low human population density. 57% of the population lives in the 4 main cities, all located in the southwest coast of the main island (Insee, 2020). This population aggregation generates substantial urban activities. Dumbea, the second most populated city, has increased its population by 33% in the past 10 years, leading to an outbreak of anthropogenic activities and urban development (Insee, 2020), while the littoral area of this city is almost completely covered by mangrove forests.

Two mangrove sites containing both dominant mangrove species were chosen as study sites in the littoral zone of Dumbea to investigate the impact of urbanization (*Figure II-1*). Both sites have the same geological watershed, characterized by a Cretaceous sedimentary formation (sandstone and limestone) that often host volcano-clastic fragments (Service de la Géologie de Nouvelle-Calédonie, 2016), and are only 2 km apart. The first mangrove site is the undisturbed “control” mangrove site located in the Apogoti Bay (22°12’08”S, 166°26’20”E). The site is adjacent to a recent housing lot, still under construction, without any direct anthropogenic inputs. The wastewater discharges and rainwater effluents are not released in this control mangrove site. The second mangrove site is the “urban” mangrove site (22°12’39”S, 166°27’19”E) and is characterized by an input of rainwater runoff streaming from the upper allotments for more than 50 years. The upper allotments have few petrol stations and are mainly residential with a population of about 10 000 inhabitants. This urban freshwater is therefore potentially charged in contaminants. At the urban site, the *R. stylosa* trees are about 8 to 10 m tall, which is much higher than those at the control site and other typical mangrove stands in New Caledonia, which are usually about 2 m tall. Also, in contrast to the control site, the species zonation at the urban site is unusual, with *R. stylosa* trees developing further away from the sealine

where *A. marina* trees usually develop and where the runoff enters the mangrove ecosystem.

II.3.2. Sampling & processing

II.3.2.1. Sampling

Samples were collected in May 2021, at the end of the rainy season, characterized by a La Niña phenomena. In both sites and at each mangrove stand (*A. marina* and *R. stylosa*), triplicate soil cores (40 cm long) were collected with an Eijkelkamp gouge auger about 30 m apart from one another. The 40 cm depth allowed for differential analysis with an above and below portion of the root system. Soil cores were cut along the depth with a wooden knife into 6 sections (0-5 cm, 5-10 cm, 10-15 cm, 15-20 cm, 20-30 cm, and 30-40 cm). The pH and redox potential were immediately measured using a pH meter (pH3110 – WTW). A glass electrode (SENTIX – Xylem Analytics) was inserted in the middle of the soil section to measure the pH, calibrated with standards prior to measurements, while a combined Pt and Ag/AgCl electrode (SENTIX – Xylem Analytics) was inserted in the soil to measure the redox, calibrated with standards prior to measurements. Eh values correspond to the redox values obtained on site + 202 mV to adjust to a H electrode. The soil sections were placed into tightly closed plastic bags. To extract porewater from soil samples, rhizon samplers (Rhizon SMS – 10 cm, diameter 2.5 mm – Rhizosphere) were inserted into the soil sections. Each rhizon was connected to a 20 mL syringe. The plastic bags with the soil and the attached syringes were immediately placed into a cooler (~4 °C) until processed at the laboratory, less than 6 h after collection. Within the same area where the soil cores were collected, coarse roots of *R. stylosa* were extracted with a stainless-steel saw. For *A. marina*, pneumatophores were gently torn from the main roots. Leaf samples were also collected from both tree species. One leaf sample corresponds to 20 leaves collected from 5 different trees. All biotic samples were immediately placed into plastic bags and kept in a cooler (~4 °C) until processed at the laboratory, less than 6 h after sampling.

II.3.2.2. Processing

Upon arrival at the laboratory, salinity was measured in the porewater samples using a refractometer (ATC). Porewater samples were filtered at 0.45 µm and 2 drops of H_2SO_4 were added before storage at 4 °C. The soil samples were tightly closed and kept in the freezer at -20 °C. The biotic samples (roots and leaves) were thoroughly washed with MilliQ water and dried in a heat chamber at 40 °C until reaching constant mass.

Frozen soil samples were lyophilized 72 h (FreeZone - LABCONCO) before sieving at 2 mm. Half of each sample was ground with a ball mill (FRITSCH) and the other half

kept unground for scanning electron microscopy (SEM). Biotic samples for TM analysis were ground using a cutting mill (POLYMIX – px-mfc90d) after drying. Dried samples were kept at room temperature, in the dark, and away from humidity.

II.3.2.3. Iron plaque extraction

In order to extract the iron plaque from the root surface, a treatment with a solution of dithionite-citrate-bicarbonate (DCB) established by Taylor and Crowder (1983) and modified by Lin et al. (2018) was used. Briefly, pneumatophores were immersed in 40 mL of the DCB solution (13% w/v $Na_3C_6H_5O_7 \cdot 2H_2O$, 16% w/v $NaHCO_3$, and 37% w/v $Na_2S_2O_4$ in MilliQ water) for 3 h at room temperature. Samples were then rinsed with MilliQ water to obtain 50 mL of final volume. The extract was filtered at 0.45 µm and kept at 4 °C. Treated samples were dried in a heat chamber at 40 °C until reaching constant mass.

II.3.3. Analyzes

II.3.3.1. Total element extraction in soil samples

Total elements were extracted from soil samples by multiwave digestion. Samples between 5 and 20 cm, where the root system is mainly located, were used for BCF calculations. Briefly, 100 mg of sample was weighed in the vessel. 5 mL of 70% HNO_3, 1 mL of 32% HCl, and 1 mL of 70% HF were added. Digestion was performed on an Ethos Easy – Milestone apparatus starting with a 25 min heating step from room temperature to 220 °C followed by a 15 min plateau and a 20 min cooldown step. The extract was transferred to a Teflon tube and heated at 180 °C on a heating plate to get rid of HF. After complete evaporation, 1 mL of HCl was added for dissolution of resistant particles. The extract was then transferred to a polypropylene tube, the volume was adjusted to 10 mL with MilliQ water and placed at 4 °C until analysis. For quality control, certified material (MESS-3 Marine sediments) was also extracted and analyzed (*Supplementary Table II-1*).

II.3.3.2. Trace metal extraction in biota

Trace metals were extracted from biotic samples by multiwave digestion. Briefly, 500 mg of sample was weighed in the Teflon vessel. 5 mL of 70% HNO_3 and 1 mL of 30% H_2O_2 were added. The digestion program started with a 10 min heating step from room temperature to 160 °C, then 15 min step to 210 °C, followed by a 10 min plateau and a 20 min cooldown step. The extract was transferred to a polypropylene tube, the volume was adjusted to 15 mL with MilliQ water and placed at 4 °C until analysis. For quality control, certified material (IPE sample ID 949) was also extracted and analyzed (*Supplementary Table II-2*).

II.3.3.3. Soil sequential extractions

The Community Bureau of Reference sequential extractions were used for elemental analysis in soil samples (Rauret et al., 1999). Briefly, 500 mg of sample was weighed in a centrifuge tube. For the exchangeable fraction, 20 mL of 0.11 M acetic acid (pH 5) was added, and the sample was placed on a horizontal shaker for 16 h. The sample was centrifuged at 3 000 rpm for 20 min, and the supernatant was filtered at 0.45 µm and transferred to another tube. Water was added to the sample for washing, and after 20 min centrifugation at 3 000 rpm the water was discarded. For the reducible fraction, 20 mL of 0.5 M hydroxylamine hydrochloride (pH 2) was added to the sample. After 16 h of shaking, the extract was filtered and transferred to a tube. After the washing step, 5 mL of 8.8 M H_2O_2 was added to the sample to extract the oxidizable fraction. The sample sat for 1 h partially opened, and then placed in a diethylene glycol bath fully opened for 1 h at 85 °C. After 1 h, 5 mL of 8.8 M H_2O_2 were added and heated until completely dried. A total of 25 mL of 1 M ammonium acetate was then added to the sample, which was shaken for 16 h. After transfer of the supernatant to a tube and washing, the sample was dried at 80 °C in a heat chamber. A dried residue of 400 mg was weighed in a vessel for total microwave digestion of the residual fraction (II.3.3.1. Total element extraction in soil samples).

II.3.3.4. Elemental analysis

Elemental concentrations in soil extracts, biotic extracts (leaves, roots of *R. stylosa*, and pneumatophores of *A. marina*), DCB solutions, and porewater were obtained via ICP-OES (Varian 730-ES) at the chemistry laboratory LAMA of the French Research Institute for Sustainable Development in New Caledonia. Concentrations were obtained using a calibration curve previously prepared with the right matrices from a stock solution of elements at 100 mg L^{-1}. Certified reference materials were used to calculate a z-score for each element when available (*Supplementary Table II-1 & Supplementary Table II-2*). The |z-scores| range from 0.30 and 3.00 for the soil samples and 0.17 and 2.33 for the biotic samples.

II.3.3.5. Mineralogical analysis

The mineralogical composition of each soil sample was determined by X-Ray Diffraction (XRD), using a PANalytical - AERIS XRD Diffractometer equipped with a Co source at the ISEA laboratory. XRD patterns were recorded between 5 and 80 °2θ, with steps of 0.01, an acquisition time of 480 ms $step^{-1}$, and using a generator power of 600 W. Diffractograms were treated and analyzed with the High Score software. XRD peaks were identified based on the Crystallography Open Database (COD_may22_2019).

II.3.3.6. Scanning electron microscopy

The petrography of bulk soil samples was performed by SEM using a JEOL JSM-IT 300 LV apparatus coupled with an energy dispersive spectroscopy Oxford x max 80T device. The measurements were performed at a working distance of 10 mm and an energy of 15 kV.

II.3.4. Data analyzes

II.3.4.1. Bioconcentration factors and translocation factors

The root and leaf BCF were calculated by dividing the concentration of TM in the tissue by the total mean concentration of TM in the soil between 5 and 20 cm, which corresponds to the depth sections where roots and pneumatophores were collected. The translocation factor (TF) was calculated by dividing the concentration of TM in leaves by the TM concentration in the roots of the same sample.

II.3.4.2. Iron plaque concentration calculation

The iron plaque concentration was calculated following this equation:

$$Iron\ plaque\ (mg\ kg^{-1}) = \frac{m_{Fe\ in\ DCB}\ (mg) * 0.1591}{m_{dried\ pneumatophore}\ (kg)} \quad \text{(II-1)}$$

where m is the mass and 0.1591 is the correction due to the fact that the iron plaque has the formula FeOOH but only Fe is measured in the DCB solution.

II.3.4.3. Statistical analysis

Statistical analyzes were performed using R studio software (version 1.2.5001). For comparison between species or study sites the Mann-Whitney test was performed. All other statistical analyzes with more than two variables were tested with a Kruskal-Wallis test followed by a Wilcoxon test. All tests were performed with a 95% confidence interval and n ≥ 3. Kendall correlation analysis was performed to obtain correlation matrices.

II.4. Results

II.4.1. Physico-chemical parameters

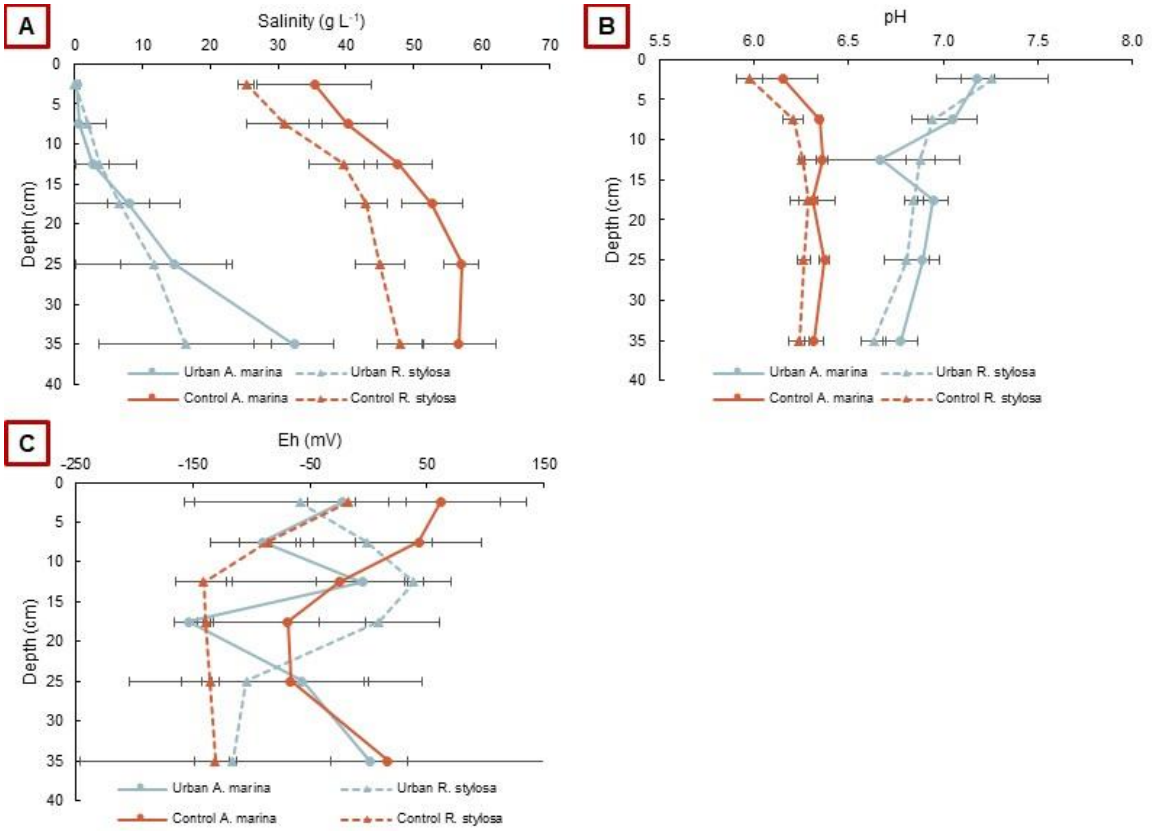

Figure II-2. Mean values for (A) salinity in g L^{-1}, (B) pH, and (C) Eh in mV along the soil cores of the urban and control sites under both mangrove species (*A. marina and R. stylosa*) with error bars corresponding to standard deviation of triplicates.

Soil porewater salinity was significantly ($p< 0.001$) lower at the urban site compared to the control site. Soil porewater salinity at the urban site ranged between 0 g L^{-1} and 39 g L^{-1}. At the control site, salinity ranged between 25 and 62 g L^{-1}. Along the soil core of the control site, salinity under *A. marina* (mean = 48 g L^{-1}) was significantly ($p< 0.05$) higher than under *R. stylosa* (mean = 39 g L^{-1}). For both sites and both species, salinity was significantly ($p< 0.05$) lower close to the surface (*Figure II-2A*).

The urban site was significantly ($p< 0.001$) less acidic with a mean pH value of 6.9, compared with the control site, which had a mean pH value of 6.3. At the control site, the pH along the soil core was significantly ($p< 0.01$) more acidic beneath *R. stylosa*. At the urban site, the pH was significantly ($p< 0.05$) more basic at the surface than in depth (*Figure II-2B*).

Eh values varied between -214 and 134 mV, and variability among triplicates was high. The Eh of the soil at the control site under *R. stylosa* (mean = -108 mV) was

significantly more negative than the soil of the control site under *A. marina* (mean = -7 mV, p< 0.01), and the urban site under *R. stylosa* (mean = -39 mV, p< 0.05) (*Figure II-2C*).

II.4.2. Mineralogy

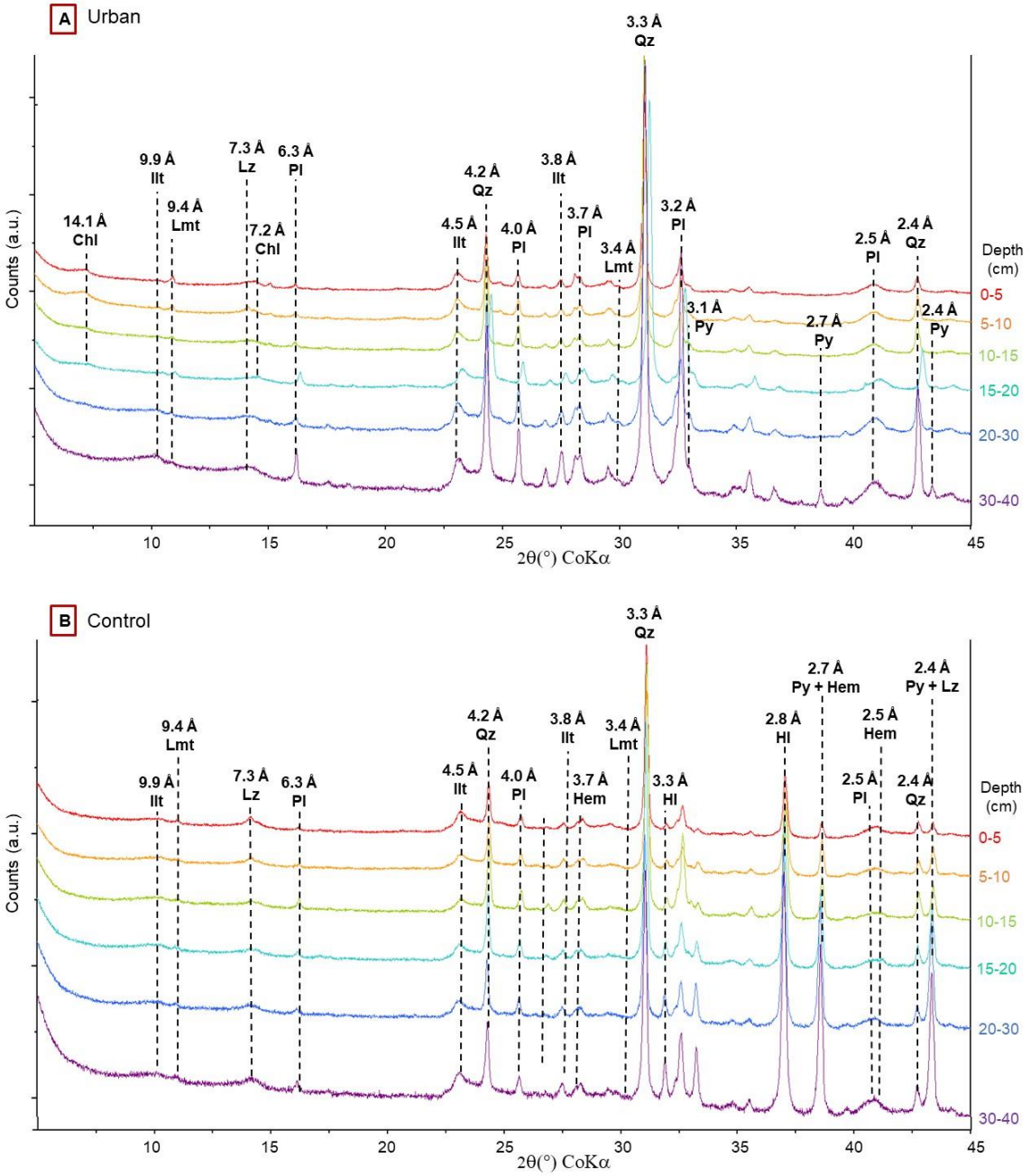

Figure II-3. XRD diffractograms of the (A) urban site and (B) control site along soil core with depth and characteristic peaks labelled in d-spacing (Å). Chl–Chlorite, Hl–Halite, Hem–Hematite, Ilt–Illite, Lmt–Laumontite, Lz–Lizardite, Pl–Plagioclase, Py–Pyrite, Qz–Quartz.

Both sites develop downstream of the same geological watershed characterized by a rock basement made of sandstones and limestones rich in quartz (SiO_2). Quartz is the main species present in both mangrove soils. Several minerals from the mangrove

soils seem to be also inherited from this substrate in both sites such as illite ($KAl_2Si_4O_{12}$), laumontite ($Ca[AlSi_2O_6]_2$), lizardite ($Mg_3Si_2O_5(OH)_4$) and plagioclase ($Na/Ca[AlSi_3O_8]$), and likely albite (*Figure II-3*). Pyrite (FeS_2) was detected at both sites, from the surface to the bottom of the sample soil core at the control site, and only observed at 10 cm and below at the urban site. At the urban site, chlorite ($(Fe,Mg,Al)_6(Si,Al)_4O_{10}(OH)_8$) was observed above 20 cm (*Figure II-3A*). At the control site only, hematite (Fe_2O_3) was also determined (*Figure II-3B*).

II.4.3. Total elemental concentrations in soil

Table II-1. Mean ± SD elemental total concentrations in soil (mg kg^{-1}) for the urban and control site under *A. marina* and *R. stylosa* with significant differences displayed and Effect Range Low (ERL) and Effect Range Median (ERM) of TM in marine sediments from NOAA.

Site	**Urban**		**Control**			
Species	*A. marina*	*R. stylosa*	*A. marina*	*R. stylosa*	ERL	ERM
As***	1.7±1.1	1.4±0.6	8.8±3.4	10±5	8.2	70
Cd***	1.4±0.4	1.1±0.3	1.9±0.3	2.0±0.7	1.2	9.6
Co***	8.9±3.1	8.2±1.4	36±6	37±1		
Cr***	121±60	108±37	797±23	775±115	81	370
Cu***	28±4	25±4	22±3	20±5	34	270
Fe***	32 795±9 640	27 596±5 895	47 611±7 362	50 280±16 463		
K*	10 100±1 032	7 697±189	12 320±634	8 819±152		
Mg***	1 146±513	1 782±867	10 730±927	11 437±1 319		
Mn	125±3	148±27	127±10	125±20		
Na***	8 865±983	10 748±1 503	31 855±1 085	38 872±2 148		
Ni***	37±5	39±8	563±59	498±60	20.9	51.6
Pb***	18±1	17±2	13±0	7.9±0.3	46.7	218
Ti***	4 741±486	4 403±534	3 316±101	2 353±157		
Zn	61±6	63±18	68±2	46±2	150	410

*p< 0.05, ***p< 0.001 between sites

Most elements in the soil had concentrations significantly higher at the control site compared to the urban site (*Table II-1*). Only, Cu, Pb, Ti beneath both mangrove species, and Mn and Zn beneath *R. stylosa*, were found in significantly higher concentrations in the urban mangrove soil compared with the control site. Under both mangrove species, Fe was the most concentrated measured element in the soil, with mean values of 30 g kg^{-1} at the urban site and 49 g kg^{-1} at the control site. The most concentrated TM after Fe at the urban site were Ti and Mn (4.6 and 0.1 g kg^{-1}, respectively), and Ti and Cr at the control site (2.8 and 0.8 g kg^{-1}, respectively). The least concentrated TM at both sites were As and

Cd, with mean values of 1.5 and 1.3 mg kg^{-1} at the urban site, and 9.4 and 1.9 mg kg^{-1} at the control site, respectively.

II.4.4. Elemental soil fractions distribution

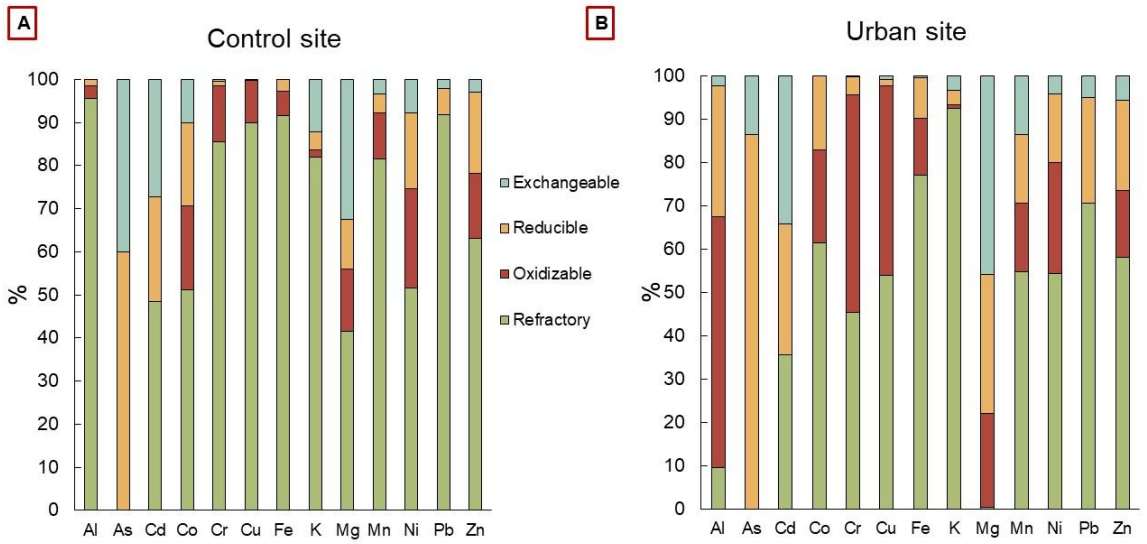

Figure II-4. Mean percentage composition of elements in each fraction (exchangeable, reducible, oxidizable, refractory) obtained by sequential extractions of the entire soil cores in triplicates at the (A) control site and (B) urban site.

At the control site, all TM, except for As, were predominantly measured in the refractory fraction of the soil, representing 41% for Mg and 96% for Al (*Figure II-4A*). At the urban site, Cd and Mg were primarily determined in the exchangeable fraction of the soil with 34% and 46%, respectively; As in the reducible fraction (86%), and Al and Cr in the oxidizable fraction of the soil with 58% and 50%, respectively (*Figure II-4B*). In the exchangeable fraction of the soil, Al, Cu, Fe, and Mn were significantly ($p < 0.05$) more concentrated at the urban site. The same elements and Pb were significantly ($p < 0.01$) more concentrated in the reducible fraction at the urban site. Cu was significantly ($p < 0.001$) more concentrated in the oxidizable fraction at the urban site (*Supplementary Table II-3*). All elements except for As and K were significantly ($p < 0.05$) less concentrated in the refractory fraction of the urban site compared to the control site (*Supplementary Table II-3*).

II.4.5. Trace metals in biota

Fe was the most concentrated TM in the roots of both species and at both sites with mean concentrations reaching up to 5.1 g kg^{-1} followed by Al with mean values up to 4.1 g kg^{-1}. The least concentrated TM in the roots was Cd with mean values up to 0.2 mg kg^{-1}. Al, Cd, Mn, and Ti were significantly more concentrated in the roots collected at the urban site compared to those collected at the control site (*Table II-2*). At the urban site,

Cd, Mn, Ni, and Pb concentrations in the roots were positively correlated to their concentrations in the exchangeable fraction of the soil with r = 0.73, 0.58, 0.47, and 0.47, respectively.

No significant difference was observed between sites for TM concentrations in the leaves, except for Ni, which had higher concentrations at the control site compared with the urban site. Mn and Fe were the most concentrated TM in the leaves with mean concentrations up to 321 and 122 mg kg^{-1}, respectively. Cd, Co, and Pb were the least concentrated in the leaves. At both sites, Mn was more concentrated in the leaves than in the roots. At the control site, Zn was more concentrated in the leaves than in the roots of both species, and As and Cu only for *A. marina* (*Table II-2*).

Table II-2. Mean ± SD trace metal concentrations in roots and leaves in mg kg^{-1} at the urban and control site for *A. marina* and *R. stylosa*.

	Roots				**Leaves**			
	Urban		**Control**		**Urban**		**Control**	
	A. marina	*R. stylosa*	*A. marina*	*R. stylosa*	*A. marina*	*R. stylosa*	*A. marina*	*R. stylosa*
Al*	1 933±1 514	4 079±2 215	824±181	312±153	6.2±1.2	29±10	13±1	31±44
As	3.1±1.5	1.9±0.5	2.4±2.2	0.9±0.3	1.0±0.4	0.5±0.1	3.3±1.5	0.5±0.1
Cd*	0.2±0.1	0.2±0.1	0.1±0.04	0.03±0.03	0.08±0.04	0.03±0.02	0.04±0.01	0
Co	2.8±1.4	1.3±0.7	2.2±0.4	1.0±0.6	0.2±0.03	0.2±0.1	0.2±0.02	0.09±0.05
Cr	3.3±1.6	27±36	11±1	5.3±2.3	0.4±0.1	0.3±0.1	0.05±0.01	0.5±0.3
Cu	6.1±3.0	3.8±1.3	7.0±0.7	2.9±1.9	8.6±0.7	4.6±0.6	14±6	2.6±0.7
Fe	2 355±1 668	2 943±2 035	5 143±7414	403±222	42±2	67±16	122±24	45±51
Mn*	23±3	115±62	11±2	27±25	66±7	321±130	33±9	99±9
Ni°°	7.4±1.9	8.7±8.4	14±5	8.5±5.2	1.4±0.1	2.1±1.1	4.3±0.3	3.7±0.6
Pb	4.1±1.7	4.5±1.5	1.5±0.1	0.6±0.6	0	0.2±0.2	0.2±0.3	0.6±0.2
Ti*	45±30	72±23	37±9	12±6	1.6±0.5	2.0±0.5	2.6±0.7	1.6±2.0
Zn	22±13	12±3	16±9	2.4±0.9	14±1	6.5±1.4	18±3	3.5±2.1

* $p < 0.05$, ** $p < 0.01$ between sites in roots

°° $p < 0.01$ between sites in leaves

II.4.6. Bioconcentration factors and translocation factors

Mean root BCF ranged between 0.008 and 1.7. All TM, except Cu, Ti, and Zn, had significantly higher root BCF at the urban site. This site displayed the highest root BCF for As and Mn with 1.7 and 0.5, respectively. At the control site, Cu and Zn were the most proportionally transferred to the roots with root BCF of 0.23 and 0.14, respectively. Cr and Ti had the lowest root BCF with 0.042 and 0.013 at the urban site, and 0.010 and 0.008 at the control site, respectively (*Figure II-5A*).

Some elements (Cd, Co, Cr, Ni) showed higher leaf BCF at the urban site. The most transferred TM from soil to leaves was Mn with leaf BCF of 1.34 at the urban site and 0.53

at the control site. The least transferred TM were Cr, Fe, and Ti with leaf BCF of 0.003, 0.002, and under detection limit at the urban site, and 0.0005, 0.002, and 0.001 at the control site, respectively (*Figure II-5B*).

A greater proportion of As, Al, and Zn was significantly transferred from roots to leaves at the control site compared to the urban site (*Figure II-5C*). Mn was once again the most transferred with TF values of 2.9 and 4.5 at the urban and control sites, respectively, and Al the least with 0.008 at the urban site and 0.51 at the control site.

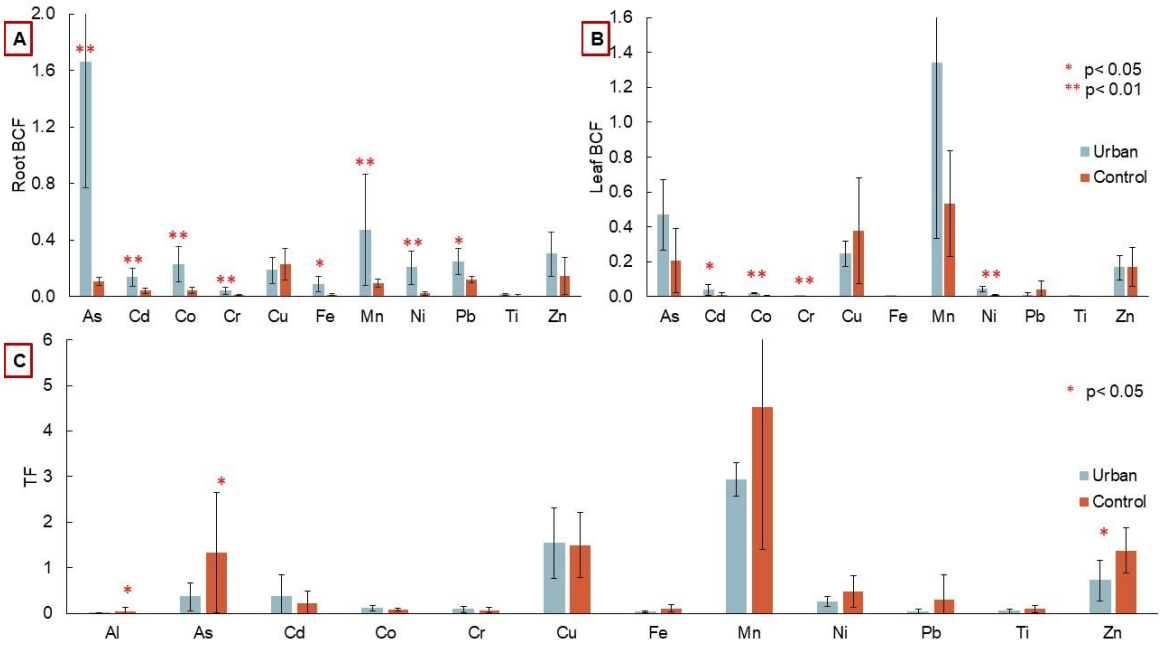

Figure II-5. Mean (A) root bioconcentration factors (root BCF), (B) leaf bioconcentration factors (leaf BCF), and (C) translocation factors (TF) with error bars corresponding to standard deviation of triplicates for both species (*A. marina* and *R. stylosa*) at the urban and control sites, with significant differences displayed.

II.4.7. Iron plaque

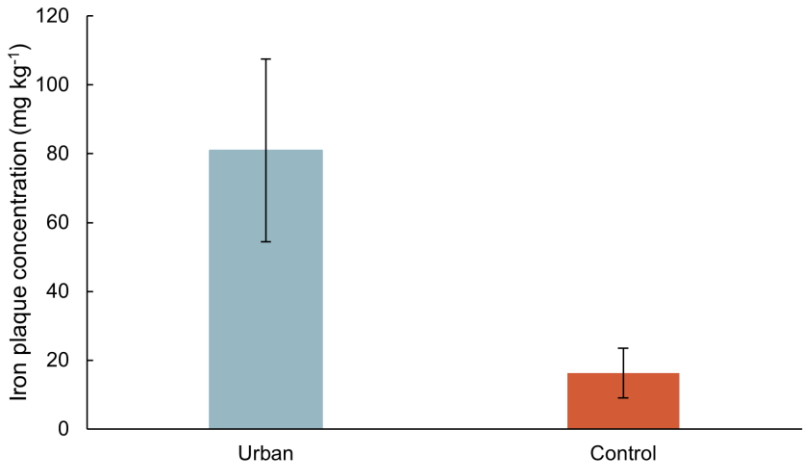

Figure II-6. Mean iron plaque concentrations on *A. marina* pneumatophores' surfaces (mg kg^{-1}) at both sites with error bars.

The iron plaque concentration at the surface of the pneumatophores of *A. marina* at the urban site is significantly higher than at the control site with mean values of 81 mg kg^{-1} and 16 mg kg^{-1}, respectively (*Figure II-6*).

II.5. Discussion

II.5.1. Soil characteristics of the mangrove forests

Mangrove species zonation at the control site is typical of semi-arid mangrove forests, with *Rhizophora* spp. trees developing on the seaside of the mangrove ecosystem, and *A. marina* developing on the landside at higher elevation. Being less frequently inundated, the soil in *A. marina* stand at the control site is more subjected to evaporation, explaining why porewater salinity was higher beneath the *A. marina* stand (Deborde et al., 2015). These differences in soil porewater salinity between mangrove species were not observed at the urban site. The inputs of urban rainwater runoff during decades, with a salinity of almost zero, disrupt the typical mangrove forests zonation. In fact, at the urban site, *Rhizophora* spp. trees develop also in the landside of the urban mangrove forest where the urban rainwater runoff enters the site. In addition, mangrove trees at the urban site, especially *R. stylosa* trees, are visually much taller than in most mangrove forests in New Caledonia, including the control site. The lower soil porewater salinity can explain this observation as mangrove trees spend less energy to adapt to highly saline conditions and have therefore more energy to spend to growth (Clough, 1984). At both sites, porewater salinity increased with depth, which may result from dilution with rain in the upper layer and salts percolation down the cores (Marchand et al., 2004; Bourgeois et al., 2020).

Beneath *R. stylosa* at the control site, Eh values were low (<100 mv), dissolved Fe concentrations were close to zero (*Supplementary Figure II-1*), and pyrite was observed all along the core, even in the top soil, suggesting that sulfate-reduction was the dominant decay process as early as the first upper centimeters. Conversely at the urban mangrove site, Eh values were less negative, dissolved Fe concentrations reached up to 4 164 µg L^{-1} (*Supplementary Figure II-1*) and pyrite was observed only at depth. Consequently, under *R. stylosa*, conditions were less anoxic at the urban mangrove site and other decay processes, like iron respiration, may dominate in the upper soil.

Despite suboxic conditions in the upper soil, pH values were less acidic than at the control site, and almost basic for some layers. Usually, in mangrove ecosystems, OM decomposition, along with pyrite oxidation, which can both be enhanced in suboxic conditions, induces a soil acidification (Marchand et al., 2004; Kristensen et al., 2008, 2017; Noël et al., 2014). However, in this specific urban mangrove ecosystem, the main

pH driver is the amount of rainwater from the urban runoff, as the rainwater collected had a pH higher than 7.

Regarding *A. marina*, it is known that oxic to suboxic conditions usually prevail in the upper soil due to its root system, capable of diffusing O_2 in its rhizosphere (Purnobasuki and Suzuki, 2005; Kristensen et al., 2017). At the control site, Eh values under *A. marina* varied between 61 and -69 mV, and large concentrations of dissolved Fe were measured (3 000 – 13 000 µg L^{-1}) (*Supplementary Figure II-1*), confirming suboxic conditions. Surprisingly, at the urban site, despite similar redox values, dissolved Fe concentrations were low (114 – 760 µg L^{-1}) (*Supplementary Figure II-1*). This result may either indicate different OM decay processes or export of dissolved elements from the mangrove soil. However, the absence of pyrite in the upper layer indicates that sulfate-reducing process is limited.

The disturbed mangrove forest zonation, the very low porewater salinity, and the high pH values measured at the urban site are clear indicators of the impact of the urban rainwater runoff on the mangrove forest. TM dynamics in the environment being dependent on these parameters, the partitioning and bioaccumulation of TM in soil and mangrove tissues must be evaluated in the urban and control mangrove sites.

II.5.2. Trace metal concentrations in mangrove soils

The two mangrove sites studied have a Cretaceous sedimentary watershed, dominated by sandstone and limestone (Service de la Géologie de Nouvelle-Calédonie, 2016), and are therefore less subjected to high concentrations of TM compared to mangrove forests located downstream of lateritic soils (Noël et al., 2014). In both the urban and the control mangrove sites, lower soil concentrations of Co, Cr, Fe, Mn, and Ni (characteristic of New Caledonia's lateritic soils) were measured compared to mangrove forests developing downstream of mining activities in New Caledonia (Bourgeois et al., 2020; Robin et al., 2021). For instance, Cr and Ni concentrations measured in a mangrove site downstream from a lateritic watershed were 17 times and 89 times greater than the mean concentrations at the urban site (*Supplementary Table II-3*) (Robin et al., 2021). However, the studied mangrove sites were still characterized by higher concentrations of Cd, Cr, Fe, and Ni than many mangrove soils in the world such as in Australia, in New Zealand, Mexico, China, or in the Sundarbans (*Supplementary Table II-3*) (Chaudhuri et al., 2014; Chowdhury et al., 2015; Bastakoti et al., 2019a; Deng et al., 2019; Celis-Hernandez et al., 2020). Cr and Ni soil concentrations at the control site were much higher than the effect range median (ERM), which corresponds to the level of contamination of marine sediments, where biological toxicity effects are generally observed according to

the National Oceanic and Atmospheric Administration (NOAA) (*Table II-1*) (Buchman, 1999).

Regarding some TM (As, Cu, Pb, Zn) often associated with urbanization and of major public health concern according to the World Health Organization (Vracko et al., 2007), their concentrations were lower than the effect range low (ERL) (*Table II-1*), a value below which biological toxicity effects are scarcely observed (Buchman, 1999). For instance, As, Cu, Pb, and Zn soil concentrations were up to 10 times lower than in the other mangrove forests of the world such as in China (He et al., 2014; Deng et al., 2019), in Tanzania (Kruitwagen et al., 2008), in Mexico (Celis-Hernandez et al., 2020), or in India (Ray et al., 2006), where extensive urbanization and industrial activities occur (*Supplementary Table II-3*).

The high TM background of New Caledonia must therefore affect both sites, even though they have a sedimentary rocks-dominated watershed (Fernandez et al., 2006; Beliaeff et al., 2011; Maurizot et al., 2020a), but the concentrations are well under those measured in mangrove forests directly affected by upstream lateritic soils. In addition, TM associated with urbanization and industrial activities do not reach hazardous concentrations, and are lower than in other urbanized world mangrove forests (Ray et al., 2006; Kruitwagen et al., 2008; He et al., 2014; Cao et al., 2018), implying that a large part of New Caledonia has not reached an alarming state for urban mangrove forest TM contamination.

The two studied sites share the same geological watershed, but the urban site has been influenced by an urban rainwater runoff for decades. It has been observed and mathematically modelled that urbanization leads to an increase in watershed erosion during the construction process, but can then inhibit sediment transport from the upper watershed to the coastal area (Randhir, 2003; O'Driscoll et al., 2010). Therefore, soil erosion and TM transport into the urban mangrove stands from the volcano-sedimentary watershed may be limited, explaining lower concentrations of the majority of TM in the urban mangrove soils. Conversely, at the control site, the presence of hematite, which is generally absent from the New Caledonia volcano-sedimentary watershed (Maurizot et al., 2020a), indicates possible inputs from an adjacent watershed composed of lateritic soils (Service de la Géologie de Nouvelle-Calédonie, 2016; Robin et al., 2021). Even though the currents do not directly flow from the lateritic watershed to the control mangrove site (Douillet, 2001), the intense rainfall events that occurred during the rainy season impacted by a La Niña phenomena, or punctual cataclysmic events such as cyclones, may have induced larger inputs of minerals from the adjacent watershed in this control mangrove

soil. For the elements significantly more concentrated at the urban site (Cu, Pb, Ti, Zn), they are typical of urban anthropogenic activities. In the environmental monitoring of the construction of the Dumbea-sur-Mer allotment, the urban mangrove site showed higher Cu and Zn concentrations than all other monitored mangrove sites in Dumbea (Ruiz et al., 2020). Cu, Pb, Ti, and Zn are used in many urban items in buildings and transportation. For instance, particles from car brakes increase the amount of Cu in environments close to highways, which is the case for our urban mangrove site (Davis et al., 2001). Cu, Pb, Ti, and Zn are also used in building sidings (e.g., bricks, painted walls), roofs, and tire wear (Davis et al., 2001; Neal et al., 2011; Panagos et al., 2018). These TM can therefore be in higher concentrations in the urban mangrove soils due to greater inputs from the rainwater runoff.

As detailed in the previous section, mangrove soil at the urban site is characterized by suboxic conditions in the upper layer, and anoxic ones at depth. These suboxic conditions in the upper layer result in high TM concentrations in the dissolved phase. In fact, Cr and Fe were significantly more concentrated in the porewater of the urban site beneath *R. stylosa* stand (*Supplementary Figure II-1*). Noël et al. (2014) suggested that tidal fluctuations may be a major cause for continuous Fe reduction-oxidation cycles in mangrove soils, which could significantly affect the Fe mass balance with the export of dissolved Fe from stands closest to the sea. Deborde *et al.* (2015) suggested that the loss of some elements towards the seaside may be related to sulfur oxidation and to more intense tidal flushing of dissolved elements. In the present study, redox conditions induced the presence of high concentrations of dissolved TM, which can be easily exported towards adjacent ecosystems or being subject to plant uptake. These observations could explain in part why concentrations of most TM are lower in the urban mangrove soils compared to the control site.

II.5.3. Trace metal transfer to mangrove roots

In the mangrove sites studied, root concentrations of Co, Cr, Cu, Fe, Ni, Pb, and Zn were lower than in roots collected downstream of highly eroded lateritic soil in New Caledonia (Marchand et al., 2016; Bourgeois et al., 2020; Robin et al., 2021). In fact, Fe and Ni mean root concentrations were 8 and 150 times greater in mangrove plants collected downstream from a Ni mine (Bourgeois et al., 2020). However, root concentrations of As, Cr, Fe, and Ni were between 8 and 30 times greater in the present study than in the poorly urbanized mangrove forest of the Sundarbans (Chowdhury et al., 2015), which can be attributed to the high TM background of New Caledonia. Nonetheless, Cu, Pb, and Ti, which are usually associated with urbanization, were 20 to 40 times more

concentrated in the roots of mangrove trees collected in the Sydney harbor, where there is extensive boat traffic that can cause greater discharge of those TM in the environment (Chaudhuri et al., 2014).

In the urban mangrove site, despite lower TM concentrations in the soil, concentrations of some TM in the roots were higher than at the control site, suggesting different TM uptake mechanisms by the mangrove trees between sites, and/or distinct TM bioavailability in the soil. Al, Cd, Mn, and Ti were between 2 and 5 times more concentrated in the roots collected at the urban site. In addition, root BCF were significantly higher at the urban site, up to 20 times for some TM, with values similar or higher to what is observed in mangrove stands developing downstream of highly eroded lateritic soils in New Caledonia (Marchand et al., 2016; Bourgeois et al., 2020).

TM in the exchangeable fraction of the soil are supposedly more bioavailable for plant uptake (Marchand et al., 2016; Bourgeois et al., 2020). Here, in the exchangeable fraction, Al, Cu, Fe, and Mn were significantly more concentrated at the urban site compared to the control site (*Supplementary Table II-3*) explaining higher root BCF at the urban site. In addition, there was a positive correlation between concentrations in the roots and concentrations in the exchangeable fractions of the soil for Cd, Mn, Ni, and Pb in the urban site. This relationship was not observed at the control site possibly because of sulfate-reducing processes and the presence of salt. As soon as TM enters the dissolved phase, they can be trapped immediately either by pyrite (Noël et al., 2017) or salt (Cheng et al., 2014). XRD analysis showed that pyrite was present all along the core at the control site, but only at depth in the urban mangrove site, which has suboxic conditions in top soils. In addition, Ni associated with framboidal pyrite has been observed on SEM at the surface of the control site (*Supplementary Figure II-2*), but not at the urban site. Consequently, mangrove roots at the urban site have more access to TM such as Ni and Cd that are not trapped within pyrite crystals. In addition, soil porewater salinity was significantly lower at the urban site due to the input of urban rainwater. It has been reported that soil salinity affects TM uptake by mangrove roots as Cl-TM complexes can form, which makes it more difficult to absorb by the plant (Cheng et al., 2014). Li et al. (2018) observed high negative correlations between the concentrations of Cd in the roots of a mangrove species and its content of Na and Cl. The urban mangrove soil may form less Cl-TM complexes, favoring TM uptake by mangrove roots. TM bioavailability in the soil seems therefore to be the main factor influencing the transfer to mangrove roots, as previously suggested (Ray et al., 2006; Chaudhuri et al., 2014; Nguyen et al., 2019). A combined analysis with leaf BCF and TF helps identify the role and the biological mechanisms of mangrove trees facing TM bioavailability.

II.5.4. Trace metal transfer to mangrove leaves

There was no difference in TM concentrations in leaves between the urban and the control mangrove sites, except for Ni, which was more concentrated in the leaves at the control site. Concentrations in leaves of Cr, Pb, and Zn, TM with potentially an urban origin, were at least 5 times lower than what is reported in the literature for a large urban area in Futian, China (He et al., 2014). Regarding TM that mainly originate from lateritic soils in New Caledonia, Co, Fe, and Ni, their concentrations in the leaves of the urban mangrove site were 10 to 50 times lower than in leaves collected downstream of an open-cast Ni mine in New Caledonia (Marchand et al., 2016). Therefore, the studied mangrove sites do not seem affected in terms of TM accumulation in the leaves compared to other stressed mangrove forests.

With lower TM total concentrations in the soil, and similar concentrations in the leaves, the urban mangrove trees have higher leaf BCF for Cd, Co, Cr, and Ni. The leaf BCF of Co and Ni were actually greater at the urban site compared to the values obtained in a mangrove forest developing near a large urban area in China (He et al., 2014) and compared to a mangrove forest downstream from a big city in Vietnam (Nguyen et al., 2019). Ni leaf BCF were also higher than downstream of a Ni mine in New Caledonia (Bourgeois et al., 2020). The results suggest that transfer of elements in the leaves, other than macronutrients, are rather negatively correlated to soil concentrations, either because TM are not bioavailable in the soil for plant uptake, or because of biological mechanisms, immobilizing TM in the root system. For example, chelation of TM cations with the roots cell walls can inhibit TM transfer to the vascular bundle, and thus to other organs (MacFarlane et al., 2007). Arbuscular mycorrhizal fungi in symbiosis with mangrove trees in the root system (D'Souza, 2016) can also help prevent TM transfer to the higher organs (Garg and Chandel, 2011; Hassan et al., 2013). For *A. marina*, the formation of an iron plaque at the surface of the roots and pneumatophore can help retain extensive amounts of some TM (Pi et al., 2011; Robin et al., 2021). The results show that there is significantly more iron plaque formation at the surface of the pneumatophores at the urban site. This mechanism limits the uptake of TM in the roots of the urban mangrove trees, and therefore protects the higher tissues from metal stress.

The measured TF for most TM were similar to those measured in other mangrove forests around the globe, such as in China (Zhou et al., 2011; Huang et al., 2020b), in Hong Kong (Eric, 2003), and in Iran (Rezaei et al., 2021). However, TF were lower in our studied mangrove sites by up to two order of magnitudes, compared to the TF values obtained in the Sundarbans (Ray et al., 2021). The concentrations of Al, Cd, Co, Fe, Pb,

and Zn measured in the leaves by Ray et al. (2021) were similar or higher than the concentrations measured in this study, while TM concentrations in the roots were much lower than those measured herein. This result indicates transfer regulation of TM from roots to leaves. Ray et al. (2021) suggested that excess nutrients or toxic elements can be excluded from the plant via litterfall, but the lower TF measured in our study sites suggests that this is not the primary strategy adopted by the mangrove trees in the urban context studied. With similar concentrations in the roots at the urban site, and comparable concentrations in the leaves, TF of most TM were similar at the urban and control sites implying that, even in an urban context, mangrove trees limit the transfer of potentially toxic TM to the higher organs where vital processes occur such as photosynthesis.

Our results show that the urban rainwater runoff increases the bioavailability of TM in the urban mangrove soil compared to the control site by modifying TM bearing phases and soil physico-chemical parameters. Consequently, urbanization, via the inputs of urban effluents in the mangrove forest, is a factor able to affect root uptake. However, its influence on TM transfer from roots to shoots seems to be limited. TM soil concentrations and bearing phases influence primarily the root BCF, while mangrove species biology and physiology regulate TF and accumulation in the leaves.

II.6. Conclusion

This study provides new insights on the influence of urban rainwater runoff on mangrove forests. The comparison between an urban mangrove forest and a control mangrove forest sharing the same geological watershed demonstrates that the almost continuous runoff of urban rainwater modified the natural physico-chemical properties of the mangrove soil and disrupt TM dynamics. The basic freshwater urban runoff controlled mangrove soil porewater salinity and pH, and induced suboxic conditions influencing TM distribution. Most total TM soil concentrations were lower in the mangrove soil influenced by urbanization due potentially to, on the one hand, watershed urbanization that reduced TM inputs, and on the other hand, to more TM bioavailability resulting from the suboxic conditions. Only Cu, Pb, Ti, and Zn presented higher concentrations in the urban mangrove soils; these TM are known to derive from urban activities and inputs can be attributed to the urban rainwater runoff. The urban rainwater runoff limits salt-TM complexes or pyrite-TM trapping in soil, which can lead to the lower TM bioavailability. The higher bioavailability resulted in higher root bioconcentration factors for both mangrove species, *A. marina* and *R. stylosa*. However, TM concentrations in leaves are similar between the two studied mangrove forests and translocation factors do not differ between sites suggesting a regulation of the transfer of TM to the leaves by the mangrove trees. In

order to improve the understanding of the effects of the urban runoff on the mangrove ecosystem, further analysis should be performed on the nature of the OM in the soil and on TM exports to adjacent coastal waters. A monitoring of various parameters of the urban rainwater runoff should also be done periodically over a year to assess the nature of the inputs in the urban mangrove site.

II.7. Acknowledgments

The authors acknowledge Kapeliele Gututauava for technical help on site. Aurélie Monin and Olivia Barthélémy are acknowledged for the technical assistance during SEM observations. The authors thank Leocadie Jamet and Monika Lemestre for ICP-OES measurements.

II.8. Supplementary materials

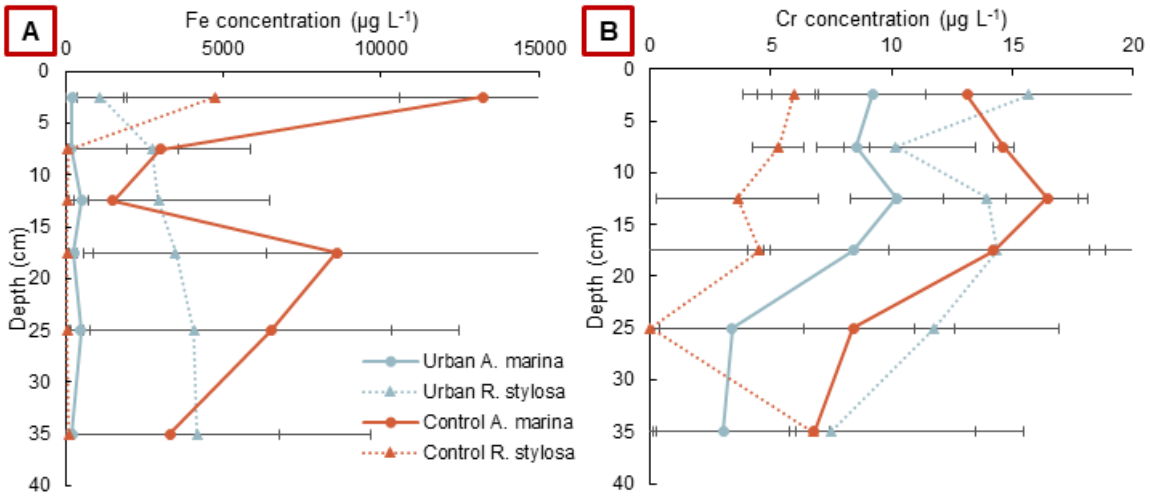

Supplementary Figure II-1. (A) Iron and (B) Chromium concentrations in porewater with depth (µg L^{-1}) at the urban and control sites beneath *A. marina* and *R. stylosa*.

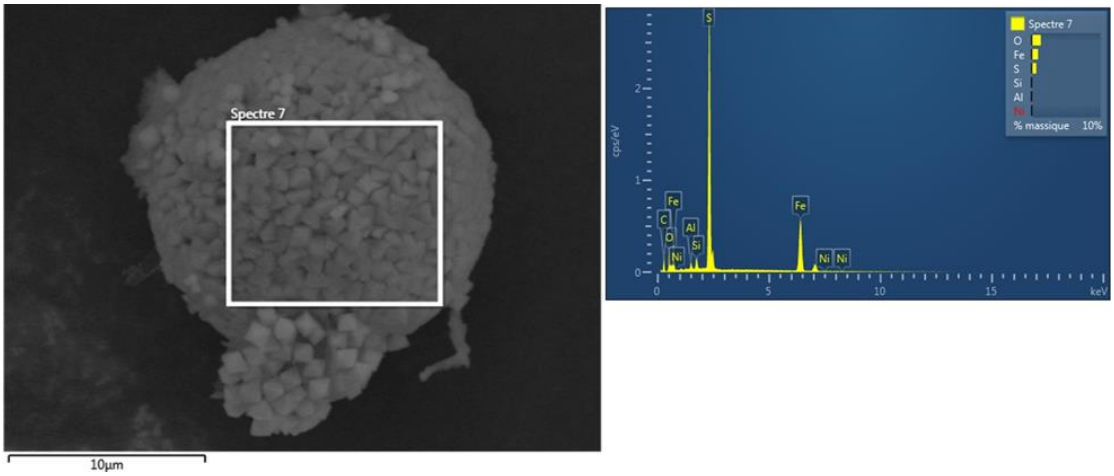

Supplementary Figure II-2. Scanning electron microscopy image of framboidal pyrite from the control site top soil (between 0 and 5 cm deep). Electron dispersive X-ray spectrum demonstrated that this type of pyrites hosted Ni within its structure as observed by Noël et al. (2015).

Supplementary Table II-1. Quality control of total soil inductive coupled plasma measurements using a certified reference material MESS3 – Marine sediments, with z-score or percentage depending on the availability of standard deviation values and detection limits.

Element	Standard mean value (mg g^{-1})	Standard deviation value (mg g^{-1})	Measured value (mg g^{-1})	z-score	%	Detection limit (mg kg^{-1})
Cd	0.00024	0.00001	0.00020	- 3.0		0.0001
Co	0.0144	0.002	0.0154	0.5		0.031
Cr	0.105	0.004	0.098	- 1.8		0.042
Cu	0.0339	0.0016	0.0387	3.0		0.037
Fe	43.4	1.1	43.7	0.3		0.182
K	26		23		88.5	0.188
Mg	16		11		66.8	0.068
Mn	0.324	0.012	0.332	0.7		0.031
Na	16		13		81.6	0.17
Ni	0.0469	0.0022	0.0429	- 1.8		0.059
Pb	0.0211	0.0007	0.0206	- 0.7		0.0001
Ti	4.4	0.6	3.6	- 1.3		0.029
Zn	0.159	0.008	0.146	- 1.6		0.04

Supplementary Table II-2. Quality control of biota inductive coupled plasma measurements using the certified reference material IPE Sample ID 949, with z-score and detection limits.

Element	Standard mean value (mg g^{-1})	Standard deviation value (mg g^{-1})	Measured value (mg g^{-1})	z-score	Detection limit (mg kg^{-1})
Cd	0.00041	0.00004	0.00040	- 0.2	0.00003
Co	0.00010	0.00002	0.00053	0.19	0.0093
Cr	0.00051	0.00010	0.00015	2.33	0.0126
Cu	0.00667	0.00058	0.00601	- 1.13	0.0111
Fe	0.2001	0.0225	0.2048	0.17	0.0546
Mn	0.01972	0.00184	0.01738	- 1.27	0.0093
Ni	0.00042	0.000006	0.00041	- 1.54	0.0177
Pb	0.00086	0.00014	0.00099	0.91	0.00003
Zn	0.104	0.008	0.102	-0.29	0.012

Supplementary Table II-3. Comparative table of trace metal concentrations in mangrove soils worldwide.

TM	Location	Impact	Value range (mg kg^{-1})	Reference
Al	New Caledonia	None	40 – 49 504	(Bourgeois et al., 2020)
		Mining activity	1 513 – 60 416	
		Aquaculture	24 262 – 52 157	
	Tanzania	Urbanization	15 557	(Kruitwagen et al., 2008)
	Australia	Acid sulfate soil	26 414 – 71 612	(Nath et al., 2013)
As	Australia	Urbanization	0.5 - 35	(Chaudhuri et al., 2014)
	Sundarban	None	3.2 – 4.4	(Chowdhury et al., 2015)
	China	Urbanization	161	(He et al., 2014)
	Australia	Acid sulfate soil	4.1 – 17	(Nath et al., 2013)
Cd	New Zealand	Urbanization	0.03 – 0.3	(Bastakoti et al., 2019a)
	China	Mining activity	0.5 – 11	(Cao et al., 2018)
	Australia	Urbanization	0 – 3.5	(Chaudhuri et al., 2014)
	Sundarban	None	0.2 – 0.22	(Chowdhury et al., 2015)
	China	Urbanization	0.1 – 0.9	(Deng et al., 2019)
	China	Urbanization	1.9	(He et al., 2014)
	Tanzania	Urbanization	6.3	(Kruitwagen et al., 2008)
	Australia	Acid sulfate soil	0.3 – 1.2	(Nath et al., 2013)
	India	Urbanization	6.0 – 17	(Ray et al., 2006)
Co	New Zealand	Urbanization	2.4 – 5.7	(Bastakoti et al., 2019a)
	New Caledonia	None	12 – 40	(Bourgeois et al., 2020)
		Mining activity	95 – 217	
		Aquaculture	61 – 81	
	Mexico	Urbanization	4.0 - 22	(Celis-Hernandez et al., 2020)
	Australia	Urbanization	0.2 – 23	(Chaudhuri et al., 2014)
	Sundarban	None	6.8 – 8.6	(Chowdhury et al., 2015)
	Tanzania	Urbanization	7.7	(Kruitwagen et al., 2008)
	New Caledonia	Mining activity	123 – 130	(Marchand et al., 2016)
	Australia	Acid sulfate soil	7.7 – 28	(Nath et al., 2013)
	India	Urbanization	21 – 44	(Ray et al., 2006)
	New Caledonia	Mining activity	26 – 246	(Robin et al., 2021)
		None	24 – 44	
Cr	New Zealand	Urbanization	15 – 53	(Bastakoti et al., 2019a)
	New Caledonia	None	105 – 212	(Bourgeois et al., 2020)
		Mining activity	538 – 1 740	

		Aquaculture	274 – 520	
	Mexico	Urbanization	57 - 289	(Celis-Hernandez et al., 2020)
	Australia	Urbanization	1.3 – 199	(Chaudhuri et al., 2014)
	Sundarban	None	28 – 29	(Chowdhury et al., 2015)
	China	Urbanization	89	(He et al., 2014)
	Tanzania	Urbanization	805	(Kruitwagen et al., 2008)
	Australia	Acid sulfate soil	22 – 49	(Nath et al., 2013)
	India	Urbanization	1.5 – 2.7	(Ray et al., 2006)
	New Caledonia	Mining activity	1 380 – 2 658	(Robin et al., 2021)
		None	224 – 548	
Cu	New Zealand	Urbanization	7.3 – 27	(Bastakoti et al., 2019a)
	New Caledonia	None	15 – 32	(Bourgeois et al., 2020)
		Mining activity	2.0 – 31	
		Aquaculture	19 – 48	
	China	Mining activity	19 - 172	(Cao et al., 2018)
	Mexico	Urbanization	3.0 – 311	(Celis-Hernandez et al., 2020)
	Australia	Urbanization	1.0 – 206	(Chaudhuri et al., 2014)
	Sundarban	None	35 – 42	(Chowdhury et al., 2015)
	China	Urbanization	24 – 42	(Deng et al., 2019)
	China	Urbanization	91	(He et al., 2014)
	Tanzania	Urbanization	512	(Kruitwagen et al., 2008)
	New Caledonia	Mining activity	8.9 – 17	(Marchand et al., 2016)
	Australia	Acid sulfate soil	18 – 48	(Nath et al., 2013)
	India	Urbanization	34 – 58	(Ray et al., 2006)
	New Caledonia	Mining activity	14 – 80	(Robin et al., 2021)
		None	14 – 32	
Fe	New Zealand	Urbanization	20 969 – 26 683	(Bastakoti et al., 2019a)
	New Caledonia	None	24 010 – 52 730	(Bourgeois et al., 2020)
		Mining activity	61 760 – 118 200	
		Aquaculture	55 660 – 79 150	
	Sundarban	None	2 865 – 3 019	(Chowdhury et al., 2015)
	Tanzania	Urbanization	19 278	(Kruitwagen et al., 2008)
	New Caledonia	Mining activity	99 993 – 119 635	(Marchand et al., 2016)
	Australia	Acid sulfate soil	48 972 – 146 713	(Nath et al., 2013)
	India	Urbanization	4 461 – 4 697	(Ray et al., 2006)
	New Caledonia	Mining activity	26 652 – 180 639	(Robin et al., 2021)
		None	28 847 – 88 813	
Mn	New Zealand	Urbanization	139 – 343	(Bastakoti et al., 2019a)
	New Caledonia	None	101 – 429	(Bourgeois et al., 2020)
		Mining activity	309 – 1 031	
		Aquaculture	253 – 532	
	Sundarban	None	646 – 648	(Chowdhury et al., 2015)
	New Caledonia	Mining activity	370 – 609	(Marchand et al., 2016)
	Australia	Acid sulfate soil	52 – 158	(Nath et al., 2013)
	India	Urbanization	429 – 3 253	(Ray et al., 2006)
	New Caledonia	Mining activity	135 – 1 082	(Robin et al., 2021)
		None	89 – 161	
Ni	New Caledonia	None	44 – 298	(Bourgeois et al., 2020)
		Mining activity	1 456 – 3 997	
		Aquaculture	237 – 924	
	Mexico	Urbanization	15 – 96	(Celis-Hernandez et al., 2020)
	Australia	Urbanization	0.7 – 48	(Chaudhuri et al., 2014)

	Sundarban	None	34	(Chowdhury et al., 2015)
	China	Urbanization	15 – 27	(Deng et al., 2019)
	China	Urbanization	45	(He et al., 2014)
	Tanzania	Urbanization	32	(Kruitwagen et al., 2008)
	New Caledonia	Mining activity	2 134 – 2 546	(Marchand et al., 2016)
	Australia	Acid sulfate soil	21 – 79	(Nath et al., 2013)
	India	Urbanization	7.5 – 52	(Ray et al., 2006)
	New Caledonia	Mining activity	366 – 4 814	(Robin et al., 2021)
		None	287 – 756	
Pb	New Zealand	Urbanization	8.0 – 31	(Bastakoti et al., 2019a)
	China	Mining activity	47 – 2 024	(Cao et al., 2018)
	Mexico	Urbanization	3.0 – 111	(Celis-Hernandez et al., 2020)
	Australia	Urbanization	4.9 – 534	(Chaudhuri et al., 2014)
	Sundarban	None	12 – 20	(Chowdhury et al., 2015)
	China	Urbanization	42 – 108	(Deng et al., 2019)
	China	Urbanization	75	(He et al., 2014)
	Tanzania	Urbanization	83	(Kruitwagen et al., 2008)
	Australia	Acid sulfate soil	12 – 46	(Nath et al., 2013)
	India	Urbanization	16 – 95	(Ray et al., 2006)
	New Caledonia	Mining activity	3.0 – 21	(Robin et al., 2021)
		None	9.0 – 14	
Zn	New Zealand	Urbanization	39 – 138	(Bastakoti et al., 2019a)
	New Caledonia	None	25 – 56	(Bourgeois et al., 2020)
		Mining activity	60 – 87	
		Aquaculture	48 – 68	
	China	Mining activity	108 – 2 823	(Cao et al., 2018)
	Mexico	Urbanization	12 – 794	(Celis-Hernandez et al., 2020)
	Australia	Urbanization	9.3 – 668	(Chaudhuri et al., 2014)
	Sundarban	None	32 – 36	(Chowdhury et al., 2015)
	China	Urbanization	72 – 199	(Deng et al., 2019)
	China	Urbanization	305	(He et al., 2014)
	Tanzania	Urbanization	356	(Kruitwagen et al., 2008)
	New Caledonia	Mining activity	38 – 56	(Marchand et al., 2016)
	Australia	Acid sulfate soil	45 – 439	(Nath et al., 2013)
	New Caledonia	Mining activity	18 – 123	(Robin et al., 2021)
		None	29 – 72	

Supplementary Table II-4. Minimum, maximum, average, and standard deviation values for elements in the 4 fractions of the soil obtained via sequential extractions (Exc – Exchangeable, Red – Reducible, Oxi – Oxidizable, Ref – Refractory) in µg g^{-1}.

			Al				As			
Site	Species		Exc	Red	Oxi	Ref	Exc	Red	Oxi	Ref
Urban	*A. marina*	Min	26	618	725	162	0	0	0.0	0.0
		Max	155	1 506	2 791	551	6	20	0.0	0.0
		Mean	67	1 123	1 851	333	1	13	0.0	0.0
		Stdev	35	265	663	118	2	5	0.0	0.0
	R. stylosa	Min	18	530	1 163	63	0	0	0.0	0.0
		Max	357	1 575	4 154	922	10	23	0.0	0.0
		Mean	103	1 038	2 278	350	3	13	0.0	0.0
		Stdev	106	323	1 014	216	3	6	0.0	0.0
Control	*A. marina*	Min	19	673	1 551	51 824	0	0	0.0	0.0
		Max	156	1 254	2 378	113 491	19	27	0.0	0.0
		Mean	59	920	1 865	74 997	8	15	0.0	0.0
		Stdev	41	138	245	17 785	7	6	0.0	0.0
	R. stylosa	Min	17	679	1 640	30 152	0	0	0.0	0.0
		Max	152	1 272	2 389	68 632	20	24	0.0	0.0
		Mean	48	917	1 930	50 768	6	5	0.0	0.0
		Stdev	42	180	230	9 122	7	9	0.0	0.0

			Cd				Co			
Site	Species		Exc	Red	Oxi	Ref	Exc	Red	Oxi	Ref
Urban	*A. marina*	Min	0.00	0.00	0.0	0.41	0	0.5	0.5	4.7
		Max	0.83	0.72	0.0	0.60	0	2.9	2.6	8.0
		Mean	0.46	0.37	0.0	0.48	0	1.4	1.7	6.1
		Stdev	0.22	0.24	0.0	0.04	0	0.6	0.6	0.8
	R. stylosa	Min	0.00	0.00	0.0	0.30	0	1.1	0.9	1.0
		Max	0.67	0.75	0.0	0.55	0	3.1	4.9	9.1
		Mean	0.40	0.40	0.0	0.42	0	1.7	2.2	5.0
		Stdev	0.21	0.24	0.0	0.08	0	0.6	1.0	2.4
Control	*A. marina*	Min	0.00	0.00	0.0	0.56	0	1.0	3.6	12.7
		Max	0.81	0.72	0.0	0.90	12	10.9	14.1	20.8
		Mean	0.49	0.27	0.0	0.68	4	7.0	8.5	15.6
		Stdev	0.26	0.30	0.0	0.10	3	2.8	2.8	1.7
	R. stylosa	Min	0.13	0.00	0.0	0.34	0	1.8	3.8	8.8
		Max	0.62	0.77	0.0	2.02	10	14.3	8.2	37.9
		Mean	0.45	0.56	0.0	0.98	3	6.7	5.5	20.9
		Stdev	0.14	0.18	0.0	0.47	3	3.0	1.2	7.7

			Cr				Cu			
Site	Species		Exc	Red	Oxi	Ref	Exc	Red	Oxi	Ref
Urban	*A. marina*	Min	0.00	0.9	5	16	0.02	0.00	1.12	4
		Max	0.90	4.9	105	59	0.32	1.05	7.74	16
		Mean	0.28	3.3	37	35	0.10	0.39	5.13	8
		Stdev	0.33	1.2	31	15	0.07	0.33	2.25	3
	R. stylosa	Min	0.00	0.2	3	5	0.04	0.00	2.87	3
		Max	0.62	6.9	73	64	0.32	0.52	15.78	15
		Mean	0.19	2.8	35	31	0.16	0.05	7.44	7
		Stdev	0.22	1.9	23	20	0.08	0.13	3.60	3
Control	*A. marina*	Min	0.30	5.5	50	276	0.00	0.00	0.52	7
		Max	5.42	15.9	118	647	0.16	0.00	4.90	17
		Mean	2.38	9.1	86	413	0.05	0.00	2.22	13
		Stdev	1.53	2.7	22	93	0.05	0.00	1.32	3
	R. stylosa	Min	0.67	4.3	49	347	0.00	0.00	0.00	6
		Max	5.91	10.8	109	1 363	0.08	0.00	2.55	18
		Mean	2.52	6.3	80	681	0.01	0.00	0.62	13
		Stdev	1.75	2.4	21	362	0.02	0.00	0.72	3

			Fe				K			
Site	Species		Exc	Red	Oxi	Ref	Exc	Red	Oxi	Ref
Urban	*A. marina*	Min	44	1 193	1 327	16 905	56	401	95	10 457
		Max	418	3 209	3 537	29 729	836	765	149	17 605
		Mean	157	2 113	2 634	22 279	538	557	121	12 883
		Stdev	103	629	634	3 630	205	126	20	1 954
	R. stylosa	Min	26	861	1 835	8 757	50	149	45	2 952
		Max	194	6 275	9 222	26 820	590	429	125	14 062
		Mean	91	2 719	3 972	17 149	296	291	83	9 948
		Stdev	51	1 361	2 186	5 326	134	78	23	2 457
Control	*A. marina*	Min	10	426	2 425	32 508	23	83	148	9 699
		Max	40	2 673	4 814	79 811	2 825	865	387	24 639
		Mean	22	1 533	3 638	47 748	1 774	701	231	14 655
		Stdev	10	743	666	12 493	823	184	55	3 863
	R. stylosa	Min	8	904	2 145	16 135	74	360	149	4 799
		Max	27	2 665	6 785	108 942	2 207	718	357	12 623
		Mean	16	1 549	3 123	58 619	1 767	525	246	9 049
		Stdev	6	550	1 071	27 924	465	100	53	1 903

			Mg				Mn			
Site	Species		Exc	Red	Oxi	Ref	Exc	Red	Oxi	Ref
Urban	*A. marina*	Min	537	286	201	3	7	7	8	75
		Max	2 000	1 211	823	14	74	62	27	103
		Mean	1 165	824	531	9	18	19	18	90
		Stdev	468	294	176	3	18	14	6	7
	R. stylosa	Min	596	393	189	3	11	12	9	34
		Max	3 166	1 717	1 645	25	75	90	103	136
		Mean	1 469	1 013	712	11	25	31	32	83
		Stdev	657	391	438	6	18	22	23	24
Control	*A. marina*	Min	2 404	1 135	928	1 184	3	3	12	83
		Max	8 121	2 330	4 313	13 169	10	10	25	163
		Mean	4 052	1 525	2 195	6 998	5	7	18	118
		Stdev	1 564	317	885	3 472	2	2	4	17
	R. stylosa	Min	3 355	1 155	987	493	5	5	14	47
		Max	6 160	2 086	3 083	7 684	16	21	27	345
		Mean	4 724	1 602	1 734	4 221	7	8	19	159
		Stdev	871	245	736	2 275	3	4	4	80

			Ni				Pb			
Site	Species		Exc	Red	Oxi	Ref	Exc	Red	Oxi	Ref
Urban	*A. marina*	Min	0.6	2	0.9	7	0.31	6	0.0	26
		Max	3.7	8	39.2	34	4.47	14	0.0	49
		Mean	2.0	6	9.8	22	2.02	10	0.0	34
		Stdev	1.0	2	8.0	8	1.06	3	0.0	6
	R. stylosa	Min	0.3	4	1.6	5	0.06	6	0.0	10
		Max	3.5	16	34.5	58	3.83	14	0.0	39
		Mean	1.4	7	10.9	22	2.04	10	0.0	24
		Stdev	0.8	3	8.7	14	1.12	2	0.0	8
Control	*A. marina*	Min	3.4	19	78.6	150	0.37	5	0.0	47
		Max	135.5	196	217.3	333	4.18	9	0.0	96
		Mean	45.4	93	138.4	246	2.16	6	0.0	66
		Stdev	34.4	44	41.6	55	1.24	2	0.0	14
	R. stylosa	Min	12.7	39	56.9	136	0.00	2	0.0	20
		Max	91.1	184	173.0	597	4.03	6	0.0	222
		Mean	37.9	96	108.6	309	1.82	4	0.0	99
		Stdev	22.3	39	37.4	128	1.21	1	0.0	58

			Zn			
Site	Species		Exc	Red	Oxi	Ref
Urban	*A. marina*	Min	1.1	2	3	32
		Max	6.6	22	16	52

		Mean	2.8	9	8	43
		Stdev	1.7	6	4	6
	R. stylosa	Min	1.2	4	3	17
		Max	22.3	83	40	55
		Mean	4.7	19	12	34
		Stdev	5.4	23	10	10
Control	*A. marina*	Min	0.8	4	8	31
		Max	4.6	21	18	67
		Mean	2.5	15	12	47
		Stdev	0.9	4	3	9
	R. stylosa	Min	0.8	6	6	22
		Max	3.9	18	12	64
		Mean	1.7	12	10	43
		Stdev	0.8	3	2	10

III. Chapter III: Influence of urban runoff on litterfall composition dynamics during degradation in mangrove forest

Robin, S.L., Le Milbeau, C., Gututauava, K., Marchand, C., submitted. Influence of species and stand position on the evolution of isotopic and molecular signatures of leaf litter during degradation in urban mangrove forest. *Geochimica et Cosmochimica Acta*.

Robin, S.L., Marchand, C., Gututauava, K. Alfaro, A.C., in prep. Urban runoff influence on major element and trace metal dynamics during leaf litter decomposition in semi-arid mangrove. *Chemosphere*.

Présentation :

Les chapitres précédents se sont concentrés sur la répartition des ETM dans les sols et leur accumulation dans les palétuviers, en relation avec plusieurs paramètres du substrat. Une fois transférés dans les feuilles, les ETM peuvent être libérés à nouveau dans le sol et transférés vers le lagon par le biais de la production de litière végétale (Silva et al., 1998; Vinh et al., 2020). Ce chapitre aborde l'étude de la dégradation de la litière végétale et de l'évolution de sa composition au fil du temps. La litière végétale constitue une source de MO et potentiellement de contaminants pour les sols de mangrove (Wafar et al., 1997; Li and Ye, 2014; Duan et al., 2021). Elle peut également être consommée directement sur le sol ou être emportée par la marée vers les écosystèmes adjacents (Robertson, 1986). L'analyse de la litière végétale est donc essentielle pour comprendre le cycle de la MO et des ETM dans les mangroves.

Les feuilles constituent la majeure partie de la litière végétale des palétuviers (Twilley et al., 1986). Pour ce chapitre, la méthode du "litterbag" est utilisée. Des feuilles jaunes en phase de sénescence, sur le point de tomber de l'arbre, sont récoltées, lavées, séchées et pesées (*Figure III-1A*). Ensuite, ces feuilles sont placées dans des sacs en nylon dotés de trous inférieurs à 2 mm de diamètre pour éviter l'attaque de la macro et méiofaune. Les sacs en nylon refermés sont positionnés à la surface du sol dans la mangrove, accrochés à une racine (*Figure III-1B*). Après 7, 14, 28, 56 et 72 jours, les sacs et leur contenu sont récupérés, lavés, séchés et pesés (*Figure III-2*). Par la suite, les échantillons sont broyés en vue de multiples analyses.

Figure III-1. (A) Feuilles sénescentes récoltées sur l'arbre et (B) sacs en nylon avec feuilles mis en place sur site pour l'expérience.

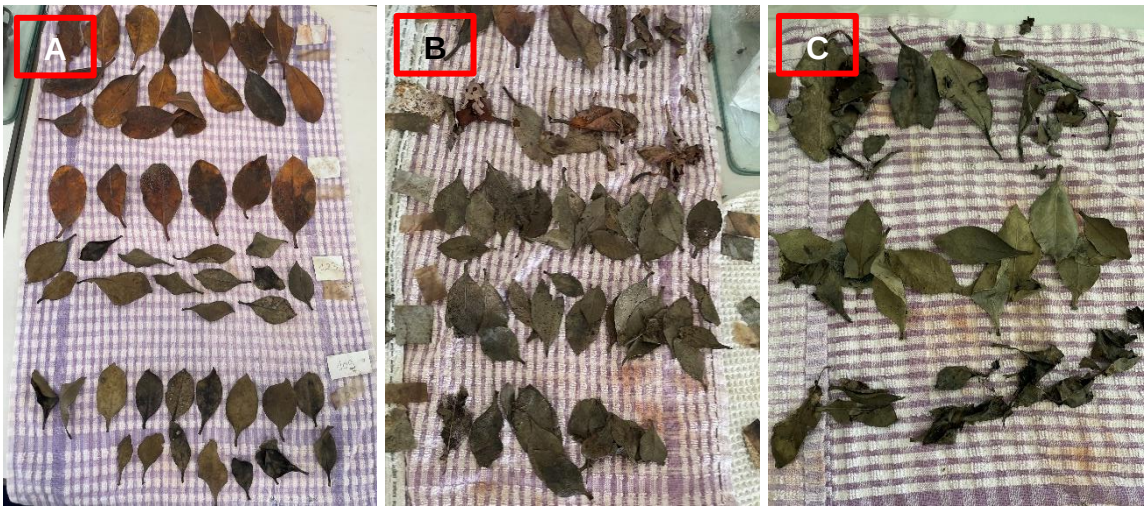

Figure III-2. Feuilles dégradées sorties des sacs en nylon après (A) 7 jours, (B) 28 jours et (C) 56 jours.

Dans la partie A de ce chapitre, le taux de décomposition de la litière est mesuré en fonction du site (influence de l'urbanisation) et de l'espèce (influence de la position et de la composition initiale). Cette étude examine les changements dans la qualité de la MO de la litière lors de sa décomposition. Les résultats révèlent des différences dans la composition des feuilles fraîches et sénescents d'*A. marina* et de *R. stylosa*, notamment en ce qui concerne le carbone, l'azote, les isotopes stables et la composition moléculaire. Ces variations sont principalement attribuables aux caractéristiques physiologiques des espèces et aux conditions environnementales dans lesquelles elles se développent, incluant la salinité du sol. Les taux de décomposition de la litière sont plus rapides pour *R. stylosa*, probablement en raison de sa position dans la zone intertidale. De plus, la composition initiale de la litière joue un rôle dans la qualité de la MO lors de la décomposition, influençant des facteurs tels que le rapport C/N, la teneur en lignine et en sucres neutres. La décomposition de la litière est également plus rapide pour les deux espèces dans la mangrove urbaine, phénomène attribué à l'apport d'eaux urbaines. Ces eaux favorisent le développement de communautés microbiennes à la surface du sol, ce qui impacte la décomposition de la litière. Cette étude constitue la première investigation des changements moléculaires survenant dans la litière au cours de la décomposition au sein d'une mangrove. Les résultats mettent en évidence que certains sucres neutres et phénols dérivés de la lignine présentent des schémas évolutifs distincts lors de la dégradation, influencés par l'espèce de palétuvier et le type de mangrove. Cependant, certaines molécules ne sont pas impactées par ces paramètres. Ces conclusions sont essentielles pour approfondir notre compréhension de l'évolution de la MO dans les sols de mangroves, y compris ses sources et ses processus diagenétiques.

Dans la partie B de ce chapitre, l'objectif est d'examiner l'évolution des éléments majeurs (Na, K, Mg, Ca, P) et des ETM dans la litière au cours de sa décomposition, et d'évaluer l'influence de l'urbanisation sur cette évolution. Les résultats démontrent que le flux presque continu des eaux urbaines favorise la lixiviation de certains éléments majeurs. Cependant, ce flux n'altère pas l'ordre de labilité des éléments majeurs. Les variations des concentrations en Ca et en P dépendent de l'espèce et sont régulées par la position de l'espèce dans la mangrove. Les concentrations en ETM augmentent généralement pendant la décomposition de la litière, indiquant un transfert du sol vers la litière plutôt que l'inverse. L'As et le Mn présentent des tendances différentes par rapport aux autres ETM, en raison de leurs capacités de complexation et de leurs états d'oxydation. De manière similaire aux éléments majeurs, l'enrichissement en ETM pendant la décomposition semble être influencé par le flux urbain qui augmente la biodisponibilité des ETM. La composition initiale de la litière, et donc les caractéristiques physiologiques des espèces, régissent la capacité d'absorption des ETM pendant la décomposition.

A. Chapter III.A: Influence of species and stand position on isotopic and molecular composition of leaf litter during degradation in urban mangrove forest

Sarah Louise ROBIN, Claude LE MILBEAU, Kapeliele GUTUTAUAVA, Cyril MARCHAND

Submitted to Geochimica et Cosmochimica Acta

III.A.1. Abstract

Understanding the diagenetic processes of organic matter (OM) within mangrove forests is essential to grasp ecosystem dynamics and exchanges with adjacent ecosystems. This study investigated the influence of urban runoff on leaf litter degradation in a New Caledonian mangrove forest, subjected to urban rainwater for over 50 years. Focusing on *Avicennia marina* and *Rhizophora stylosa*, our objectives were to determine factors affecting leaf litter degradation, assess urban runoff effects on decay rates and element concentrations, and understand OM changes at the molecular level. Litterbags containing senescent leaves placed on the mangrove floor were collected after 7, 14, 28, 56, and 72 days. C and N along with their stable isotopes were evaluated during decomposition as well as lignin and neutral carbohydrates contents. The experiment in control and urban mangrove forests revealed unexpected findings, challenging conventional notions of decay rates. Despite lower initial N content, *R. stylosa* exhibited faster degradation, emphasizing the critical role of species position within the mangrove forest regarding tidal immersion. Urban runoff, submerging the urban site, intensified leaf litter degradation, influencing both mass loss and molecular changes in OM. This research exposed the global implications of urban runoff, indicating accelerated leaf litter degradation in mangrove forests, potentially disrupting C sequestration dynamics and threatening ecosystem services. The study underscored the need to consider not only direct environmental impacts but also cascading effects on biodiversity and vital ecosystem functions.

Keywords: mangrove, litterbag, stable isotopes, lignin, neutral carbohydrates

III.A.2. Introduction

Mangrove forests are coastal ecosystems established in tropical and sub-tropical areas around the world, with some species present in temperate regions (e.g. Auckland,

NZ). These forests have a very large organic carbon (OC) stock, much larger than any marine and terrestrial ecosystems within the same latitudes (Alongi, 2014). Most of this OC is stored in the soil, but about 15% is in the aboveground biomass (Alongi, 2020). 31% of the total net primary production of mangrove forests comes from the production of litter (Bouillon et al., 2008). Once this biomass turns into litter, it becomes a crucial part of the trophic chain of the mangrove forest and adjacent ecosystems. Litterfall degradation actively contributes to the energy and material flow in the forest and is considered an energy source for coastal productivity (Lugo and Snedaker, 1974; Twilley et al., 1986). The litterfall organic matter (OM) can be consumed in the forest floor by autochthonous fauna and microorganisms, dissolved during decomposition, and exported to adjacent ecosystems at ebb tide as debris, dissolved OM, or dissolved inorganic matter, which also has a key role in the trophic chain (Fleming and Lin, 1990; Rezende et al., 1990; Wafar et al., 1997; Kristensen et al., 2017; Kida et al., 2019b).

Mangrove leaves account for the major part of the litterfall (Twilley et al., 1986; Day et al., 1987), varying between 40 and 90% (Mackey and Smail, 1996). Fruits, flowers, and the woody tissues account for the remaining litterfall. Therefore, most studies on litterfall degradation focused on leaf litter, using the litterbag experiment for comparison with literature (Nordhaus et al., 2017; Yang et al., 2018; Vinh et al., 2020). Leaf litter degradation occurs in three main stages: 1) the initial leaching of soluble compounds, 2) the colonization by microorganisms (i.e., fungi, bacteria, and protozoa) and decomposition via litter breakdown (Fell et al., 1975; Cundell et al., 1979; Fell and Master, 1980), and 3) the slow refractory phase where the least labile molecules are consumed (Valiela et al., 1984; Wilson et al., 1986; Tam et al., 1990). The rate of degradation of the leaf litter depends on multiple parameters, with varying significance depending on the context. The initial chemical composition of the leaves, especially C/N ratio, tannin, and lignin content, is one of the key parameters influencing the decay rates (Robertson, 1988; Tam et al., 1990; Mfilinge et al., 2002; Vinh et al., 2020). The leaf-consuming fauna and microbial communities of the forest floor also impact degradation rates (Fell and Master, 1980; Robertson, 1986; Imgraben and Dittmann, 2008). Many abiotic factors can influence litterfall degradation such as particle size of the forest soils, redox conditions, temperature, available oxygen, and the degree and frequency of tidal inundation (Lugo and Snedaker, 1974; Steinke and Ward, 1987; Chale, 1993; Vinh et al., 2020).

Leaf litter degradation in mangrove forests is a source of nutrients; therefore, the change in element contents such as C, N, macronutrients, and neutral carbohydrates during degradation is of interest. The capacity of elements to be mobilised from degrading litter depends on the concentrations of these elements in the soil and incoming water, as

well as on their role for litter feeders and whether they form complexes with leachable or refractory compounds (Mfilinge et al., 2002; Hossain et al., 2014; Gautam et al., 2016; Nordhaus et al., 2017). Neutral carbohydrates and organic N-rich compounds are easily degraded from the plant material, while lignin-rich litter resists decay (Fell et al., 1975; Cundell et al., 1979; Twilley et al., 1986; Chale, 1993). The depletion of elements during leaf litter degradation indicates leaching to the surroundings, or breakdown and consumption by microorganisms (Fell and Master, 1980; Fourqurean and Schrlau, 2003; Gautam et al., 2016; Nordhaus et al., 2017). The enrichment of elements and macronutrients in leaf litter during the degradation process is attributed to the production of these elements from microorganisms during decomposition such as the polysaccharides exudates from bacteria (Fell et al., 1975; Robertson, 1988; Mfilinge et al., 2002; Yang et al., 2018), or inputs from the water column (Rice and Windom, 1982; Lacerda et al., 1988; Tam et al., 1990; Vinh et al., 2020). The study of these various elements and molecular compounds such as neutral carbohydrates and lignin give essential information on the litterfall degradation and preservations processes, which directly affect the soil OM and exported OM quality.

One of the major worldwide threats to mangrove ecosystems is the urbanization of the littoral zone. Almost half of the world's mangrove forests are located in only 4 countries: Indonesia (28.4%), Brazil (9.4%), Malaysia (5.8%), and Papua New Guinea (5.1%) (Hamilton and Casey, 2016). On average, a third of the population of these countries lives on the coastline (CIESIN, 2012). Consequently, there is competition for space between mangrove ecosystems and economic and urban development. Urbanization can inhibit mangrove landward migration, prevent the water flow into the mangrove forest, and be a source of urban water runoffs, which may contain contaminants (Friess et al., 2019). The inputs of urban runoff can modify the immersion conditions of the mangrove trees, change the physico-chemical parameters of the mangrove soil such as pH, redox conditions, and salinity, and be a source of dissolved nutrients, OM, and multiple contaminants (Cavalcante et al., 2009; Bastakoti et al., 2019a; Fiard et al., 2022; Robin et al., 2022). Therefore, urban runoff in mangrove forests may influence the decay rates of the litterfall on the soil surface as well as the quality of this litterfall during degradation. To our knowledge, only one study looked at the effect of anthropogenic sewage on mangrove litterfall degradation and concluded that the discharge had no effect on the degradation processes (Tam et al., 1998). It is therefore essential to collect data and gain knowledge on which mangrove characteristic changes driven by the urbanization of the coasts influence the litterfall degradation processes.

New Caledonia is a French archipelago located in the South Pacific Ocean between 20°S and 23°S. Semi-arid mangrove forests cover 80% of the West coast of the main island, which has semi-diurnal tidal cycles (Douillet, 2001). 24 mangrove species develop mainly in monospecific stands, but two are dominant, *Rhizophora* spp., which are present on the seaward side of the forests and represent more than 50% of mangrove plants, and *Avicennia marina*, which are established at higher elevation and on saltier soil, representing about 15% of mangrove plants in the archipelago (Deborde et al., 2015). The population density in New Caledonia is low (16 people per km²), but 60% of the population is concentrated in the capital and the four cities nearby, that are all located on the littoral zone where mangrove forests develop (Insee, 2020). Urbanization in New Caledonia has caused the destruction of mangrove forests, but only few studies have been conducted on the influence of urbanization on mangrove forests dynamics (Robin et al., 2022).

The study of change in element concentrations during litterfall degradation in a mangrove forest is crucial to understand the OM diagenetic and preservation processes within the forest and exchanges with adjacent ecosystems. The aim of this paper is to evaluate leaf litter degradation dynamics in an urban semi-arid mangrove forest (New Caledonia), receiving urban rainwater for more than 50 years. The objectives of this study are 1) to determine factors influencing the differences in leaf litter degradation between mangrove species (i.e., initial composition of the leaves or position of the stand in the mangrove forest), 2) to assess the effects of urban rainwater runoff on leaf litter decay rates and leaf litter changes in element concentrations, and 3) to understand OM litterfall changes with degradation at the molecular level (neutral carbohydrates and lignin content). We hypothesize that the main factors affecting leaf litter decay rates are the urban rainwater runoff and the stands position in the intertidal zone as higher stands immersion times enhance leaching. We also hypothesize that the change in composition of leaf litter during degradation will be mainly influenced by the initial composition of the litter and the redox conditions. To this aim, a litterbag experiment has been undertaken for 72 days in a control and an urban mangrove forest for the two main mangrove species present in New Caledonia, *Avicennia marina* and *Rhizophora stylosa*. Decay rates have been calculated from the mass loss, while total C, total N, and their stable isotopes have been determined for each sample, as well as their neutral carbohydrates and lignin contents.

III.A.3. Material & methods

III.A.3.1. Study sites

One of the main cities of New Caledonia, Dumbea, has seen its population increase by 33% this last decade resulting in the development of urban infrastructures in the littoral

zone (Insee, 2020). Two mangrove forests in Dumbea have been chosen as study sites in order to compare forests that share a common geological unit as the source of their watersheds and the same vegetation type. The first site is the control mangrove forest (22°12'08"S, 166°26'20"E), located in the Apogoti Bay. Even though housing lots have developed recently around the mangrove, no direct anthropogenic inputs are discharged in the mangrove forest. The second site is the urban mangrove forest (22°12'39"S, 166°27'19"E). Urban rainwater runoff from the upper allotment (mainly housing lots for 10 000 inhabitants) flows into the mangrove forest and has done so for more than 50 years (*Figure III.A-1*). At both sites, the two main mangrove species observed, developing in monospecific stands, are *R. stylosa* and *A. marina*. Visible impacts of urban runoff in the urban mangrove forest are the position of *R. stylosa* stand landward of *A. marina* at the entrance of the runoff, with much higher *R. stylosa* trees (about 8-10 m high compared to 2 m high at the control site).

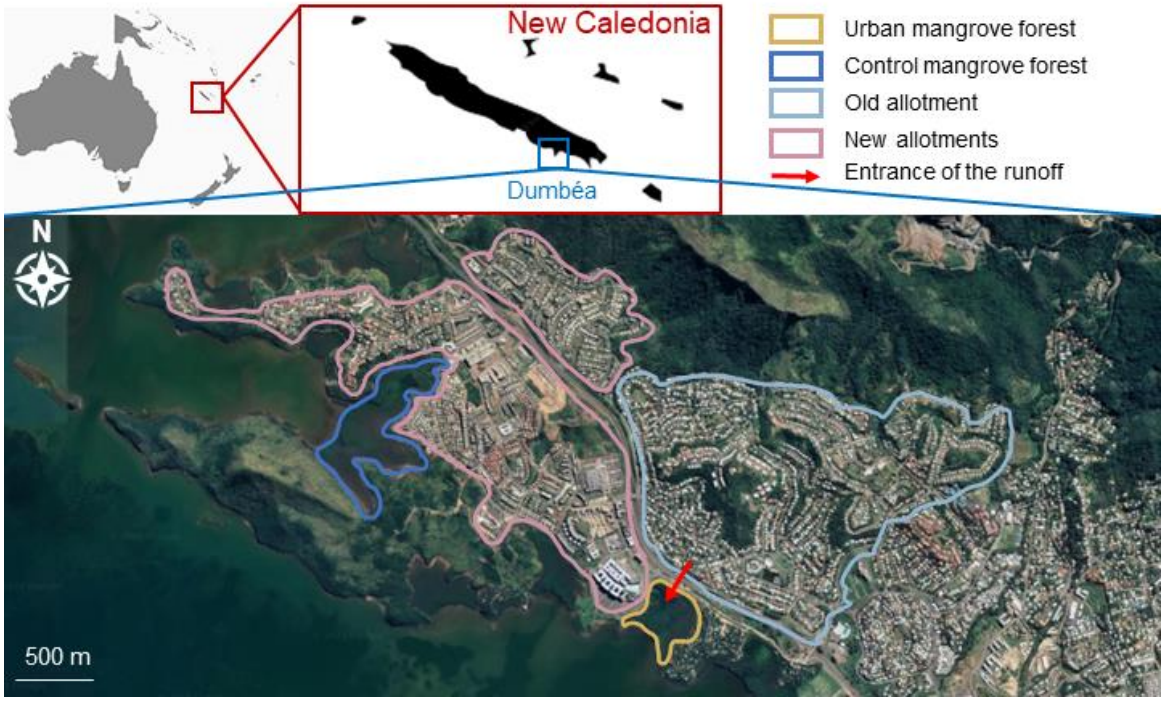

Figure III.A-1. Control mangrove forest and urban mangrove forest in Dumbea city in New Caledonia with delimitation of the new allotments and the old allotment and the entrance of the urban rainwater runoff (satellite image from Google Earth).

III.A.3.2. Sampling & processing

Yellow senescent leaves about to fall on *A. marina* and *R. stylosa* trees were collected at the control site. To limit factors other than the urban runoff, potentially affecting leaf litter degradation such as the senescent leaves initial composition, it was chosen to use the same senescent leaves samples at both sites. This is why senescent leaves were only collected at the control site. Fresh green leaves were also collected from the trees in

triplicates, but at both sites, to determine whether the composition of the leaves change significantly between the fresh and senescing stage. One sample of fresh leaves correspond to 30 leaves picked from 5 different adjacent trees. The leaves were carefully washed and air-dried for 24h at the laboratory. Three random samples of about 50 g of whole senescent leaves per species were frozen, freeze-dried, and ground with a cutting mill, corresponding to the samples at t0 “senescent leaves”. Samples of about 6 g of dried *A. marina* whole leaves and 15 g of dried *R. stylosa* whole leaves were prepared and precisely weighed. Each samples were placed into individual nylon litterbags (2 mm mesh size) for the litterbag experiment. The 2 mm mesh size allowed for soil contact enabling bacterial activity while limiting the physical actions of large detritivores such as crabs. A total of 90 bags were attached to the roots of the corresponding tree species, on the surface of the soil, and in three different spots within the same species stand in both the control and urban mangrove sites. Triplicates of litterbags were collected at the three spots, for each species, after 7, 14, 28, 56, and 72 days (a total of 36 bags per day of collection). The experiment was stopped after 72 days because the degradation was already very advanced, and samples further degraded would be too hard to analyse properly. The litterbags were immediately opened at the laboratory, the leaves were carefully washed and air-dried for 24h prior to weighing. Samples were then frozen, freeze-dried, and ground with a cutting mill. Fresh green leaves were also collected immediately from the trees at both sites in triplicates, washed, freeze-dried, and ground.

III.A.3.3. Mass loss and half-life

The percentage mass loss or percentage mass remaining after 7, 14, 28, 56, and 72 days of degradation were obtained with the initial mass (±0.001 g) of the air-dried leaves prior to placing in the litterbags and the mass of the same air-dried leaves after collection (±0.001 g) in the mangrove site. For comparison with literature, single exponential trends were plotted for each species:

$$W_t = W_0 e^{-kt} \qquad \text{(III.A-1)}$$

with W_t the mean mass remaining in g, W_0 the initial mass in g, k the exponential factor, and t the time in days. The half-lives ($t_{1/2}$) in days were obtained with the following equation and the uncertainties calculated with R from the decay rates and their standard deviations:

$$t_{1/2} = \ln(2)/k \qquad \text{(III.A-2)}$$

III.A.3.4. Carbon, nitrogen, and stable isotopes analysis

Total C, total N, and their stable isotopes were measured on an isotope ratio mass spectrometer Sercon Intergra 2 at the LAMA laboratory of the Institute of Research and

Development of New Caledonia. About 30 mg of samples were weighed in tin cups and folded into tightly closed spheres. The samples were transported in a combustion column with helium gas where they were heated at 1 000 °C and oxidized with Cu and Cr oxides, while silver wool trapped sulphur and halogens. The samples were then transferred to the reduction column at 600 °C where the Cu interacts with excess oxygen so that the NOx is reduced to N_2. The water in the samples was trapped with $Mg(ClO_4)_2$ and N_2 and CO_2 of the samples were separated by gas chromatography. The separated molecules were quantified by mass spectrometry in positive ESI mode. The mass spectrometer measures the relative abundances of isotopes in the sample gas. For carbon, it measures the ratio of ^{13}C to ^{12}C (expressed as $\delta^{13}C$), while for nitrogen, it measures the ratio of ^{15}N to ^{14}N (expressed as $\delta^{15}N$). To calculate the δ values, the measured isotopic ratio is compared to a known standard. The standard used is the Vienna Pee Dee Belemnite (VPDB) standard for C, and the atmospheric nitrogen standard for N. For quality control, duplicate of samples were passed through the spectrometer (1 every 10 samples) (*Supplementary Table III.A-1*).

III.A.3.5. Neutral carbohydrates

Neutral carbohydrates were analysed at the Earth Sciences Institute of Orleans (ISTO). About 50 mg of samples were hydrolysed 4h at 105 °C in pyrex tubes with 5 mL of 4M of trifluoroacetic acid (TFA). After cooling in an ice bath, 500 µL of internal standard (2-deoxyglucose at 8 mg L^{-1}) were added and the sample was centrifuged for 30 min at 5 600 rpm. The extract was evaporated, and the dried samples were kept frozen. Prior to analysis, neutral carbohydrates were derivatized with the addition of 500 µL of ethoxy ammonium chloride solution in pyridine (40 mg mL^{-1}) heated for 1h at 70 °C. 250 µL of BSTFA were added and the sample was once again heated at 70 °C for 1h. After evaporation, the residue was dissolved in 2 mL of heptane, and the solution passed through a 45 µm filter prior to injection in the GC-MS. The GC is a Trace 1 300 (Thermo Scientific) coupled to a MS ISQ7000 (Thermo Scientific). The GC is equipped with at Restek Rxi-5Sil MS column (60 m x 0.25 mm, 0.25 µm diameter) with 5 m of pre-column. Helium gas is used as vector and the analysis is carried out at constant 1 mL min^{-1} flow rate. The injector was heated at 280 °C and the transfer line at 300 °C. 1 µL of sample was injected in splitless mode and passed through the column with a temperature program (*Supplementary Table III.A-2*). For the MS analysis the source was heated at 240 °C and the ions obtained via electronic impact (70 eV). The spectra were obtained between 50 and 750 Da with a scan time of 0.4 s $scan^{-1}$. Quality control consisted of duplicate technical samples (≤11% standard deviation) and measurement of the internal standard (*Supplementary Table III.A-3*).

III.A.3.6. Lignin-derived phenols

200 mg of samples were hydrolysed for 3 h at 170 °C in 8 mL of 2N NaOH with 100 mg of $Fe(NH_4)_2(SO_4)_2$ under N_2. After cooling, the extract was collected once the sample was centrifuged at 3 000 rpm for 10 min. The extract was acidified at pH 1 with HCl and lignin-derived phenols were extracted twice with 3 mL of anhydrous diethyl ether. After complete evaporation, lignin-derived phenols were diluted in 1 mL of 50:50 methanol:H_2O, filtered at 45 µm and analysed via UPLC-MS. Chromatographic separation was achieved using a Vanquish Flex system (Thermo Fisher Scientific, France) consisting of a binary pump, an autosampler and a heated column compartment. Samples were separated on a Hypersil GOLD column (1.9 µm particle size), 50 x 2.1 mm (Thermo Scientific). For elution, a binary gradient program was used (Table S4), the mobile phase was a mixture of ultrapure water containing 0.1% of formic acid (Carlo Erba) (eluent A) and methanol OPTIMA LC/MS (Fischer) with 0.1% of formic acid (eluent B). The flow rate was set to 0.5 mL min^{-1} and injection (2 µL) was made automatically by the autosampler. UV detection was carried out at 280 nm. MS detection was performed using an Orbitrap Exploris 120 (Thermo Fisher Scientific, France) and operated with the heated electrospray ionization source in negative ion mode with a vaporizer temperature of 300 °C. Scan modes were both full MS – $ddMS^2$ and SRM. The full MS mode had a resolution of 30 000 and a scan range of 50 – 250 m/z with HCD Collision energies specified for each molecule. The SRM mode had a resolution of 120 000 at 20% HCD collision energy. The full UPLC-MS optimized parameters are displayed in *Supplementary Table III.A-4*. The quantification was performed with an external calibration curve (*Supplementary Table III.A-5*) and laboratory reference materials spiked with the analytes. For quality control, a blank solution was passed at the beginning and end of every series in the same conditions as the samples and values were all below detection limits (*Supplementary Table III.A-6*). A quality control solution (QC) consisting of a point of the calibration curve was passed every 10 samples in the same conditions as the samples and the values obtained were all below 15% difference with the expected value (*Supplementary Table III.A-6*).

III.A.3.7. Statistical analyzes

Statistical analyzes were performed using R studio software (version 1.2.5001). For comparison between species or study sites the Mann-Whitney test was performed. All other statistical analyzes with more than two variables were tested with a Kruskal-Wallis test followed by a Wilcoxon test. All tests were performed with a 95% confidence interval and $n \geq 3$. Kendall correlation analysis was performed to obtain correlation matrices.

III.A.4. Results

III.A.4.1. Sources characteristics

All measured variables for the fresh and senescent leaves of *A. marina* and *R. stylosa* at both sites are displayed in *Table III.A-1*. The fresh leaves of both species have significantly higher $\delta^{15}N$ values ($p< 0.01$) and lower $\delta^{13}C$ values ($p< 0.05$) at the urban site (5.8‰ and -27.7‰, and 2.6‰ and -30.7‰, for *A. marina* and *R. stylosa*, respectively) than those collected at the control site (1.1‰ and -25.8‰, and -1.3‰ and -27.5‰, for *A. marina* and *R. stylosa*, respectively). At the control site, fresh leaves are more enriched in ^{13}C than senescent leaves for both species, but for *R. stylosa* they are less enriched in ^{15}N (-1.3‰ vs -0.2‰). Both fresh and senescent leaves of *A. marina* have significantly higher N contents ($p< 0.01$), $\delta^{13}C$ ($p< 0.05$), and $\delta^{15}N$ values ($p< 0.05$) than *R. stylosa* but lower C/N ratios ($p< 0.01$) (39 for *A. marina* and 166 for *R. stylosa*).

Table III.A-1. Fresh and senescent leaves characteristics (mean value ±SD).

Species	***A. marina***			***R. stylosa***		
Site	**Control**		**Urban**	**Control**		**Urban**
Leaf	**Fresh**	**Senescent**	**Fresh**	**Fresh**	**Senescent**	**Fresh**
C (g kg^{-1})	404±22	441±3	416±23	407±23	374±3	422±24
N (g kg^{-1})	19±2	11±1	24±2	7.6±1.5	2.3±0.4	15±2
C/N	21±4	39±2	17±3	54±14	166±30	28±5
$\delta^{13}C$ (‰vsVPDB)	-25.8±0.3	-27.7±0.0	-27.7±0.7	-27.5±0.1	-28.3±0.3	-30.7±1.0
$\delta^{15}N$ (‰vsAir)	1.1±0.6	0.9±0.7	5.8±1.7	-1.3±0.5	-0.2±0.2	2.6±0.1
Σ11 phenols (mg g^{-1})	4.1±1.2	43±11	5.0±1.3	1.3±0.3	6.6±2.2	1.4±0.5
p-hydroxyl (mg g^{-1})	0.62±0.10	0.27±0.03	0.56±0.11	0.21±0.02	0.15±0.00	0.14±0.04
Vanillyl (mg g^{-1})	2.0±0.6	33±10	2.0±0.4	0.56±0.27	0.90±0.17	0.58±0.16
Syringyl (mg g^{-1})	0.33±0.07	0.22±0.00	0.26±0.04	0.22±0.02	0.14±0.06	0.20±0.04
Cinnamyl (mg g^{-1})	1.1±0.1	9.2±1.1	2.1±0.9	0.34±0.06	5.4±2.3	0.48±0.24
P/V	0.31	0.01	0.28	0.38	0.17	0.24
S/V	0.17	0.01	0.13	0.39	0.16	0.34
P/(V+S)	0.27	0.01	0.25	0.27	0.14	0.18
$(Ad/Al)_p$	0.2	2.57	0.2	0.3	4.58	0.3
$(Ad/Al)_v$	0.8	10.98	3.3	1.1	20.88	2.1
$(Ad/Al)_s$	1.2	2.99	1	3.2	1.36	1.7
Neutral carbohydrates (mg g^{-1})	384	452±52	322	228	499±14	304
Xylose (mg g^{-1})	128	122±23	61	49	104±7	66
Arabinose (mg g^{-1})	97	90±14	62	62	131±6	102
Ribose (mg g^{-1})	1.9	1.0±0.1	1.6	0.48	0.76±0.07	1.4
Rhamnose (mg g^{-1})	41	52±6	29	27	58±1	37
Fucose (mg g^{-1})	1.4	1.9±0.5	0.71	3.8	8.0±0.2	4.5
Mannose (mg g^{-1})	10	11±2	5.1	4.1	11±1	5.6
Galactose (mg g^{-1})	38	42±6	28	34	69±3	61
Glucose (mg g^{-1})	66	133±1	135	48	118±3	27

11 phenols = p-hydroxybenzoic acid, p-hydroxybenzaldehyde, p-hydroxyacetophenone, vanillic acid, vanillin, acetovanillone, syringic acid, syringaldehyde, acetosyringone, coumaric acid, and ferulic acid; p-hydroxyl = p-hydroxybenzoic acid, p-hydroxybenzaldehyde, and p-hydroxyacetophenone; vanillyl = vanillic acid, vanillin, and acetovanillone; syringyl = syringic acid, syringaldehyde, and acetosyringone; cinnamyl = coumaric acid and ferulic acid; P/V = ratio of p-

hydroxyl over vanillyl; S/V = ratio of syringyl over vanillyl; P/(V+S) = ratio of p-hydroxyl over the sum of vanillyl and syringyl; (Ad/Al) = acid/aldehyde.

In *Table III.A-1* it is shown that the total lignin contents (Σ11 phenols) of the fresh and senescent leaves of *A. marina* are significantly higher than those of *R. stylosa* ($p < 0.05$), which is also the case for the 4 phenol groups (p-hydroxyl or P, vanillyl or V, syringyl or S, and cinnamyl or C). The senescent leaves at the control site have significantly higher total lignin concentrations than the fresh leaves ($p < 0.01$) by a factor of 10 for *A. marina* and a factor of 6 for *R. stylosa* due to higher vanillyl and cinnamyl contents. Therefore, the ratios P/(V+S), P/V, and S/V are much lower in the senescent leaves than in the fresh leaves for both species. The acid over aldehyde ratios (Ad/Al) in senescent leaves are also much higher than in the fresh leaves (*Table III.A-1*).

Fresh leaves of *A. marina* are more enriched in neutral carbohydrates than *R. stylosa* but the leaves of *R. stylosa* have higher concentrations of hexoses (mannose and galactose) and deoxy sugars (fucose and rhamnose), especially fucose and galactose than *A. marina* (*Table III.A-1*). Total carbohydrates content is significantly higher in the senescent leaves than the fresh leaves at the control site ($p < 0.05$) (*Table III.A-1*). Neutral carbohydrates represent 45.2% and 49.9% of the total mass for the senescent leaves of *A. marina* and *R. stylosa*, respectively (*Table III.A-1*). Xylose, arabinose, and glucose are the most concentrated neutral carbohydrates measured representing up to 33%, 34%, and 42 % of the total neutral carbohydrates, respectively. Ribose and fucose are the least concentrated neutral carbohydrates measured in both fresh and senescent leaves with values as low as 0.48 mg g^{-1}, and 0.71 mg g^{-1}, respectively (*Table III.A-1*).

III.A.4.2. Decay rates

The decay rates of *A. marina* and *R. stylosa* leaf litter degradation at both sites are displayed in *Figure III.A-2*. The calculated half-lives are 43±9 days and 36±3 days for *A. marina* and *R. stylosa* at the control site, respectively, and 33±4 days and 28±2 days at the urban site, respectively. At both sites, in the first 7 days, *A. marina* leaves lost 41% of their initial mass and *R. stylosa* leaves lost 61% of their initial mass. After 72 days, on average, 26% and 19% of the initial mass of *A. marina* leaves remained at the control and urban sites, respectively, while 17% and 11% were remaining for *R. stylosa,* respectively.

Leaf litter mass loss is significantly more important after 56 and 72 days at the urban site than at the control site ($p < 0.01$). Through the entire degradation experiment, the leaf litter mass loss of *R. stylosa* is more important than that of *A. marina* ($p < 0.001$).

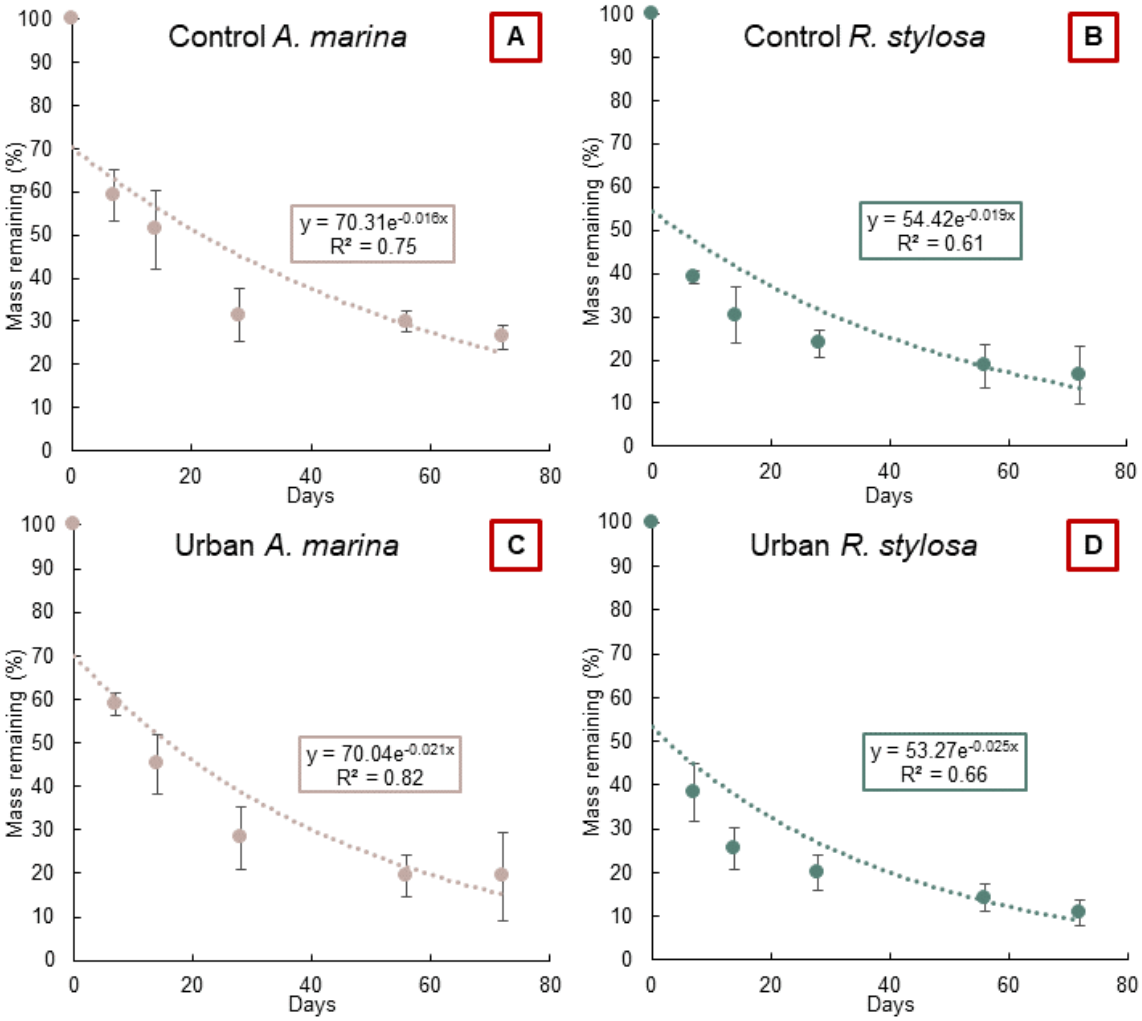

Figure III.A-2. Decay rates of leaf litter degradation represented by the mean mass remaining of the leaf litter in the litterbags during degradation at the control site for (A) *A. marina* and (B) *R. stylosa* and at the urban site for (C) *A. marina* and (D) *R. stylosa*. The error bars represent the standard deviations.

III.A.4.3. Carbon and nitrogen content, and respective stable isotope composition

The C and N content generally increased at both sites over time and for both species. At the control site, the C content for both species and N content for *A. marina* increased the first 28 days, and after 56 days. The N content of *R. stylosa* continuously increased during the 72 days of degradation. At the urban site, the *R. stylosa* litterfall constantly increased in N and C contents. C and N contents increased for *A. marina* until day 56 and 28, respectively, prior to a loss (*Figure III.A-3A & B*). The C/N ratios for *A. marina* were stable the whole 72 days of degradation, while *R. stylosa* C/N ratios continuously decreased with time (*Figure III.A-3C*).

The stable isotope ratios showed an initial enrichment for 7 days for $\delta^{15}N$ and 14 days for $\delta^{13}C$ at both sites and for both species. Overall, after 72 days of degradation, the $\delta^{15}N$ of the litterfall significantly decreased compared to the initial values ($p< 0.05$)except

for *A. marina* at the urban site where it increased (*Figure III.A-3D*). The $\delta^{13}C$ values significantly decreased for *R. stylosa* ($p < 0.001$) while they were similar for *A. marina* at both sites after 72 days of degradation (*Figure III.A-3E*).

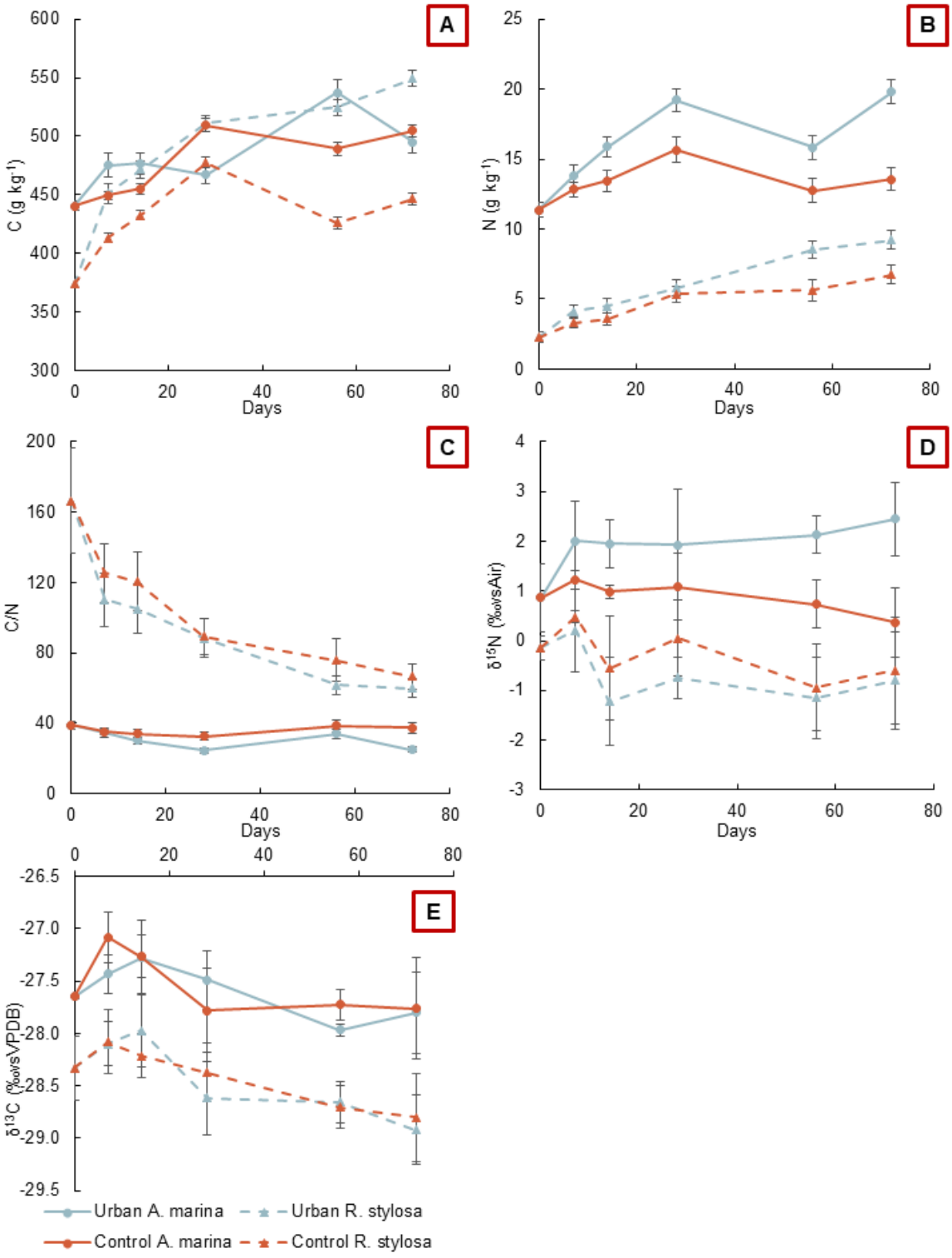

Figure III.A-3. Mean values (±SD) of (A) C in g kg^{-1}, (B) N in g kg^{-1}, (C) C/N ratio, (D) $\delta^{15}N$ (‰vsAir) and (E) $\delta^{13}C$ (‰vsVPDB) during leaf litter degradation for *A. marina* and *R. stylosa* at the control and urban sites.

III.A.4.4. Molecular analyzes

III.A.4.4.1. Neutral carbohydrates

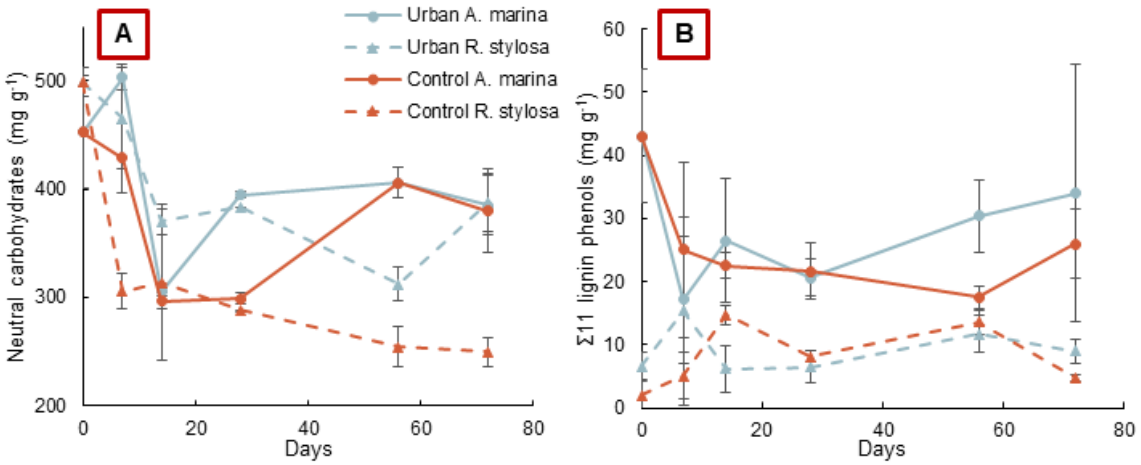

Figure III.A-4. (A) Mean (±SD) total neutral carbohydrate content in mg g^{-1} in leaf litter with degradation at the control and urban sites and for *A. marina* and *R. stylosa* and (B) mean (±SD) sum of the 11 lignin-derived phenols in mg g^{-1}.

After 72 days of litterfall degradation, total neutral carbohydrates content decreased from 452 to 380 mg g^{-1} (-16%) and to 385 mg g^{-1} (-15%) for *A. marina* at the control and urban sites, respectively, and from 498 to 250 mg g^{-1} (-50%) and to 388 mg g^{-1} (-22%) for *R. stylosa* at the control and urban sites, respectively (*Figure III.A-4A*). The most labile neutral carbohydrates after 72 days of degradation were arabinose, rhamnose, galactose, and glucose with loss ranges of 23% to 80%, 2% to 76%, 31% to 50%, and 33% to 53%, respectively (*Table III.A-2*). Xylose, ribose, fucose, and mannose all increased their concentrations in the leaf litter after 72 days of degradation for most stands reaching up to 152 mg g^{-1}, 1.2 mg g^{-1}, 10 mg g^{-1}, and 16 mg g^{-1}, respectively (*Table III.A-2*).

For *A. marina*, the concentrations of pentoses (xylose + arabinose) and deoxy sugars (rhamnose + fucose) in the senescent leaves (212 and 54 mg g^{-1}, respectively) are similar to the concentrations in the 72 days-degraded leaves. For *R. stylosa*, the concentrations in the degraded leaves are lower by 9% to 67% than the senescent leaves (235 mg g^{-1} of pentoses and 66 mg g^{-1} of deoxy sugars). After 72 days of degradation, the concentrations of hexoses (mannose + galactose) significantly decreased ($p < 0.001$) for the four stands by a range of 20% to 39% (*Table III.A-2*).

Table III.A-2. Mean neutral carbohydrate concentrations (±SD) in mg g^{-1} in leaf litter with degradation at the control and urban sites for both *A. marina* and *R. stylosa*.

Control *A. marina*	**senescent**	**7 days**	**14 days**	**28 days**	**56 days**	**72 days**
Xylose	122±23	127±11	97±2	122±1	167±1	152±0
Arabinose	90±14	85±4	57±5	55±1	76±3	70±6
Ribose	1.0±0.1	1.0±0.3	0.71±0.01	0.52±0.20	0.94±0.02	0.83±0.22
Rhamnose	52±6	52±5	37±2	36±1	47±1	45±5
Fucose	1.9±0.5	2.0±0.5	1.7±0.0	1.8±0.1	2.3±0.5	2.5±0.9
Mannose	11±2	18±3	11±0	9.3±2.2	14±5	15±8
Galactose	42±6	41±3	21±2	16±2	24±5	25±9
Glucose	133±1	103±5	70±0	58±0	74±3	71±9
Control *R. stylosa*	**senescent**	**7 days**	**14 days**	**28 days**	**56 days**	**72 days**
Xylose	104±7	73±1	83±17	85±12	86±4	78±5
Arabinose	131±6	76±2	73±10	63±4	50±3	46±2
Ribose	0.76±0.07	0.39±0.07	0.46±0.05	0.48±0.06	0.40±0.02	0.41±0.05
Rhamnose	58±0	33±1	33±6	25±4	15±2	14±1
Fucose	8.0±0.2	6.0±0.7	6.3±1.5	6.9±0.2	7.5±0.3	8.0±0.9
Mannose	11±0	8.6±0.4	8.3±3.5	11±0	11±2	14±4
Galactose	69±3	48±2	47±11	42±2	34±5	34±6
Glucose	117±3	61±11	62±22	56±2	50±10	55±9
Urban *A. marina*	**senescent**	**7 days**	**14 days**	**28 days**	**56 days**	**72 days**
Xylose	122±23	150±6	108±10	134±4	157±14	145±22
Arabinose	90±14	100±2	59±4	67±5	76±9	72±9
Ribose	1.0±0.1	1.3±0.3	1.0±0.0	1.5±0.0	1.2±0.1	1.2±0.1
Rhamnose	52±6	64±5	38±1	52±0	50±14	50±0
Fucose	1.9±0.5	2.8±0.8	1.5±0.0	2.6±0.5	2.2±0.1	2.1±0.0
Mannose	11±2	20±5	11±2	21±3	16±1	13±1
Galactose	42±6	47±9	21±1	30±1	26±2	22±1
Glucose	133±1	118±2	67±6	87±4	79±21	80±3
Urban *R. stylosa*	**senescent**	**7 days**	**14 days**	**28 days**	**56 days**	**72 days**
Xylose	104±7	113±11	96±3	127±4	111±10	135±6
Arabinose	131±6	115±9	83±10	71±17	58±13	78±10
Ribose	0.76±0.07	0.75±0.03	0.70±0.07	1.1±0.0	0.96±0.21	1.2±0.4
Rhamnose	58±0	51±8	36±0	21±15	19±2	21±4
Fucose	8.0±0.2	9.3±0.3	10±0	14±3	7.5±1.0	10±1
Mannose	11±0	13±1	12±1	33±29	15±3	16±3
Galactose	69±3	72±8	55±0	66±14	38±4	47±3
Glucose	117±3	91±10	76±1	30±40	64±8	79±9

III.A.4.4.2. Lignin-derived phenols

During the whole decay process, the sum of the lignin-derived phenols is significantly larger in the *A. marina* litter than in *R. stylosa* litter ($p < 0.01$), whatever the site (*Figure III.A-4B*). This is also the case for the four phenol groups (*Table III.A-3*). After 7

days of degradation, the lignin content increased for *R. stylosa* but decreased for *A. marina*. The total lignin content after 72 days of degradation also increased for *R. stylosa* and decreased for *A. marina* compared to the lignin content in the senescent leaves (*Figure III.A-4B*). This is only the case for the vanillyl phenols, while after 72 days of degradation the syringyl phenols increased all between 71% and 231% (*Table III.A-3*). In contrast to the total lignin content, the ratios p-hydroxyl/vanillyl (P/V), syringyl/vanillyl (S/V), and cinnamyl/vanillyl (C/V) increased after 7 and 72 days of degradation for *A. marina,* but decreased for *R. stylosa,* and followed similar patterns with degradation at the two sites (*Table III.A-3*). In the first days of degradation, there was a decrease in the p-hydroxybenzoic acid/p-hydroxybenzaldehyde ratio ($(Ad/Al)_p$) at both sites and a decrease in the vanillic acid/vanillin ratio ($(Ad/Al)_v$) at the urban site only. After 72 days of degradation, the three acid/aldehyde ratios (Ad/Al) decreased at both sites and for both species (*Table III.A-3*).

Table III.A-3. Lignin-derived phenols parameters in leaf litter with degradation at the control and urban sites for both *A. marina* and *R. stylosa* (mean values ± SD).

Control *A. marina*	**senescent**	**7 days**	**14 days**	**28 days**	**56 days**	**72 days**
p-hydroxyl (mg g^{-1})	0.27±0.03	0.15±0.03	0.20±0.02	0.22±0.04	0.26±0.07	0.26±0.04
Vanillyl (mg g^{-1})	33±10	18±14	15±2	10 ±2	4.4±0.9	14±3
Syringyl (mg g^{-1})	0.22±0.001	0.14±0.05	0.31±0.21	0.42±0.10	0.47±0.26	0.50±0.05
Cinnamyl (mg g^{-1})	9.2±1.1	6.8±0.7	6.8±0.5	11±2	12±2	12±2
P/(V+S)	0.029	0.022	0.028	0.020	0.021	0.022
P/V	0.008	0.008	0.013	0.021	0.058	0.019
S/V	0.007	0.008	0.021	0.041	0.106	0.037
C/V	0.27	0.38	0.45	1.00	2.68	0.86
(Ad/Al)p	2.57	2.01	1.50	0.54	0.49	0.52
(Ad/Al)v	10.98	11.62	5.57	0.89	0.70	1.10
$(Ad/Al)_s$	2.99	2.53	0.52	0.39	0.45	0.47
Control *R. stylosa*	**senescent**	**7 days**	**14 days**	**28 days**	**56 days**	**72 days**
p-hydroxyl (mg g^{-1})	0.15±0.001	0.12±0.02	0.13±0.01	0.11±0.004	0.14±0.01	0.13±0.004
Vanillyl (mg g^{-1})	0.90±0.17	5.7±4.1	2.6±1.5	2.2±0.9	3.3±1.2	3.4±0.4
Syringyl (mg g^{-1})	0.14±0.06	0.12±0.01	0.14±0.03	0.16±0.04	0.20±0.03	0.24±0.02
Cinnamyl (mg g^{-1})	5.4±2.3	4.2±0.5	3.8±0.3	3.0±0.3	4.7±0.9	4.9±0.7
P/(V+S)	0.026	0.027	0.034	0.033	0.029	0.025
P/V	0.160	0.021	0.051	0.048	0.042	0.039
S/V	0.152	0.021	0.054	0.073	0.061	0.073
C/V	5.99	0.75	1.45	1.36	1.42	1.45
(Ad/Al)p	4.58	3.71	2.32	2.38	1.82	1.78
(Ad/Al)v	20.88	19.53	34.32	26.32	19.50	13.59
$(Ad/Al)_s$	1.36	1.08	1.12	1.38	1.40	1.10

Urban *A. marina*	senescent	7 days	14 days	28 days	56 days	72 days
p-hydroxyl (mg g^{-1})	0.27±0.03	0.23±0.005	0.23±0.08	0.21±0.02	0.28±0.03	0.30±0.16
Vanillyl (mg g^{-1})	33±10	7.5±6.0	15±9	11±5	16±6	23±16
Syringyl (mg g^{-1})	0.22±0.001	0.39±0.01	0.68±0.22	0.53±0.19	0.61±0.15	0.73±0.35
Cinnamyl (mg g^{-1})	9.2±1.1	9.1±4.1	10±4	9.1±2.1	14±1	9.7±4.4
P/(V+S)	0.029	0.024	0.021	0.021	0.020	0.029
P/V	0.008	0.030	0.015	0.019	0.017	0.013
S/V	0.007	0.051	0.045	0.049	0.038	0.031
C/V	0.27	1.21	0.68	0.85	0.85	0.42
(Ad/Al)p	2.57	0.56	1.00	0.66	0.86	0.61
(Ad/Al)v	10.98	2.58	3.21	1.83	4.09	2.46
$(Ad/Al)_s$	2.99	0.48	0.43	0.62	0.64	0.60
Urban *R. stylosa*	**senescent**	**7 days**	**14 days**	**28 days**	**56 days**	**72 days**
p-hydroxyl (mg g^{-1})	0.15±0.001	0.20±0.05	0.12±0.02	0.17±0.03	0.23±0.07	0.18±0.07
Vanillyl (mg g^{-1})	0.90±0.17	11±15	3.5±3.2	2.6±0.9	6.8±3.5	2.6±1.2
Syringyl (mg g^{-1})	0.14±0.06	0.17±0.02	0.12±0.09	0.22±0.17	0.11±0.03	0.23±0.08
Cinnamyl (mg g^{-1})	5.4±2.3	3.8±0.6	2.4±0.3	3.5±1.6	4.6±1.6	6.0±1.7
P/(V+S)	0.026	0.051	0.049	0.045	0.050	0.029
P/V	0.160	0.018	0.035	0.064	0.034	0.071
S/V	0.152	0.015	0.036	0.085	0.017	0.091
C/V	5.99	0.34	0.69	1.34	0.67	2.34
(Ad/Al)p	4.58	1.86	1.90	1.37	1.60	1.49
(Ad/Al)v	20.88	6.25	10.69	4.63	2.55	6.25
$(Ad/Al)_s$	1.36	2.31	1.36	1.47	1.09	0.56

P = p-hydroxyl, V = Vanillyl, S = Syringyl, C = cinnamyl, Ad/Al = ratio acid over aldehyde.

III.A.5. Discussion

III.A.5.1. Variability of organic matter quality of the fresh and senescent leaves of *A. marina* and *R. stylosa*

Our investigation into the OM quality of leaves from *A. marina* and *R. stylosa* in urban and control sites presented findings that connect with broader scientific contexts. Fresh leaves from the urban site revealed high N and $\delta^{15}N$ values, aligning with expectations given the anthropogenic influence in urban runoff. This is consistent with previous studies indicating elevated $\delta^{15}N$ values in urban environments (Rumolo et al., 2011). Our study expanded upon this understanding by demonstrating the species-specific nature of ^{15}N discrimination during N uptake, evident in the greater $\delta^{15}N$ values observed in *A. marina* compared to *R. stylosa*, which was previously observed for the same genus in the literature (Herbon and Nordhaus, 2013; Regina Hershey et al., 2021).

The isotopic values, particularly $\delta^{13}C$ mean values of fresh leaves, provided valuable insights into the adaptive responses of mangrove trees. Coastal plants, including mangrove trees, often exhibit enhanced water-use efficiency under salinity stress. Our

findings, showing lower $\delta^{13}C$ values in the urban site and in *R. stylosa*, contributed to the understanding of these adaptive mechanisms (Medina and Francisco, 1997). Plants have a decarboxylating enzyme that discriminates $^{13}CO_2$ when assimilating atmospheric CO_2 (O'Leary, 1981). The salinity of the soil and the position of the mangrove stand in the mangrove forest may impact the mangrove species efficiency to assimilate CO_2 or discriminate $^{13}CO_2$ (Farquhar et al., 1982; Lin and Sternberg, 1992). In New Caledonia, *A. marina* grows on saltier soil than *R. stylosa* (26 and 37 psu, respectively at the control site) (Robin et al., 2022) and therefore, has less $^{13}CO_2$ discrimination and higher $\delta^{13}C$ values. Moreover, the upper soil at the urban site had a salinity of 0 psu for the first 10 cm (Robin et al., 2022), which may explain the lower values measured.

As we explore the changes from fresh to senescent leaves at the control site we observed a decline in N content, $\delta^{13}C$ values, and a notable rise in C/N ratios, especially in *R. stylosa* (up to 150%). These senescence-related shifts are connected with biochemical changes before leaf falling, linking to established knowledge in mangrove ecology (Garten and Taylor, 1992; Rao et al., 1994; Nordhaus et al., 2011). Prior to leaf falling, the mangrove trees can relocate the N from the leaves to other tissues of the plant to limit N loss explaining the decline in N content. A general decrease in C content during senescing can be expected due to the loss of photosynthetic activity, but the relative increase in carbohydrates as a signal for senescing may induce the increase in C content in some mangrove species as observed in this study for *A. marina* (Wingler et al., 2006).

Examining lignin-derived phenols and neutral carbohydrates content, our study contextualized findings within the existing literature on mangrove leaf composition and degradation dynamics (Marchand et al., 2005; Lallier-Vergès et al., 2008; Bala Krishna Prasad and Ramanathan, 2009). Higher lignin and neutral carbohydrate content in the fresh leaves of *A. marina* compared to *R. stylosa* agree with previous studies (Dittmar and Lara, 2001). However, the higher proportions of hexoses and deoxy sugars in the leaves of *R. stylosa*, especially fucose and galactose, underscored the need for a comprehensive insight of initial leaf compositions. The production or loss of neutral carbohydrates and lignin-derived phenols during senescence contribute to our knowledge of the intricate senescence process in mangrove leaves (Benner et al., 1990; Opsahl and Benner, 1995, 1999).

III.A.5.2. Factors influencing leaf litter degradation between mangrove species

The leaf litter of *R. stylosa* was degraded more rapidly on the soil surface than the leaf litter of *A. marina* at both sites; a trend opposite to conventional findings where species with higher initial N content, and consequently lower C/N ratios, typically undergo faster

degradation (Mfilinge et al., 2002; Yang et al., 2018; Vinh et al., 2020). Notably, *A. marina*, initially possessed five times more N in its senescent leaves than *R. stylosa*. The higher N content in plant material is known to attract leaf-degrading organisms due to the nutritional value of N compounds (Wafar et al., 1997; Nordhaus et al., 2011). We propose that the species' position within the mangrove forest is a crucial determinant of litterfall decay rates. Generally, species the most submerged experience faster degradation rates (Twilley et al., 1986; Steinke and Ward, 1987; Silva et al., 1998; Bosire et al., 2005). The physical impact of tides facilitates plant material breakdown (Vinh et al., 2020), and submersion by seawater or runoff promotes microbial development and leaching of soluble compounds from litterfall (Robertson, 1988; Tam et al., 1990; Ashton et al., 1999). In the mangrove forests of New Caledonia, *R. stylosa* is found on the seaward side of the mangrove forest, while *A. marina* is present at higher elevations with higher soil salinity (Deborde et al., 2015). However, in the urban mangrove forest, continuous runoff from urban rainwater altered soil physico-chemical parameters, particularly pH and salinity (0 psu in the upper 10 cm) (Robin et al., 2022). Consequently, *R. stylosa* trees are established on the landside and at the entrance of the runoff in the mangrove, providing a subtidal context unique to the urban site. Therefore, submersion of the *R. stylosa* stand by seawater at the control site and submersion by the urban runoff at the urban site may contribute to enhance litterfall degradation for *R. stylosa*, by favoring leaching and microbial development on the leaf litter compared to *A. marina* (Robertson, 1988; Molnar et al., 2014).

Despite the unexpected degradation trend observed in the leaf litter of *R. stylosa* compared to *A. marina*, further insights into the isotopic dynamics shed light on unique microbial processes driving the decomposition of litterfall of *R. stylosa*. The statistically significant decrease in $\delta^{15}N$ values with leaf litter degradation was only observed for *R. stylosa*. Bacteria dominating decomposition processes have low $\delta^{15}N$ values as bacteria favour the immobilization of ^{15}N-depleted nitrate (Bragazza et al., 2010; Nordhaus et al., 2011). The enhanced microbial development beneath the *R. stylosa* stands at both sites due to their position compared to the water sources can ultimately lead to the lowering of degrading leaf litter $\delta^{15}N$ values (Leopold et al., 2013; Molnar et al., 2014).

Expanding on what we learned from the microbial processes, a closer look at how the composition of leaf litter changes as it breaks down revealed clear differences between the two mangrove species. Leaf litter composition changes during degradation, specifically the N content, C/N ratio, and isotopic values ($\delta^{13}C$ and $\delta^{15}N$), were investigated. Degradation of the leaf litter of *R. stylosa* resulted in a decrease in the C/N ratio not observed for the leaf litter of *A. marina*. This decrease was linked to the degradation of hydrolysable components, particularly neutral sugars, rather than refractory N-rich

components like lignin (Chale, 1993; Yang et al., 2018). Indeed, the neutral carbohydrate content of the leaf litter of *R. stylosa* decreased during degradation, while the lignin content increased. Therefore, bulk leaf decayed more rapidly than lignin, as reported in the literature for anaerobic and sulphate reducing environments (Benner et al., 1984, 1991; Dittmar and Lara, 2001). Conversely, the lignin content decreased in the leaf litter of *A. marina*. The upper soil beneath *A. marina* was less reducing than *R. stylosa* (Robin et al., 2022), which can favour lignin degradation (Benner et al., 1991; Opsahl and Benner, 1995). *A. marina* also had a higher percentage of lignin content in its senescent leaves than *R. stylosa*, suggesting that the initial molecular composition of the leaves influenced the lability of the molecules during degradation. This phenomenon, where the concentrations of the molecules in senescent leaves influence their decays, aligns with findings in terrestrial plants (Talbot et al., 2012).

III.A.5.3. Urban runoff effects on leaf litter degradation

Urban runoff and associated modified conditions at the urban site seemed to affect leaf litter degradation rates as the mass loss was faster in the urban mangrove forest compared to the control mangrove forest. One explanation may be that urban rainwater runoff, almost constantly flooding the forest floor, enhanced the early leaching process of the leaf litter. Faster mass loss was previously reported in subtidal stands compared to intertidal stands (Robertson et al., 1992). However, after 7 days of degradation, the leaf litter mass loss was similar at the urban and the control sites. Statistical differences in mass loss between sites were obtained after 56 days of leaf litter degradation, indicating that the second phase of degradation, that is litter breakdown by microorganisms, may be favoured at the urban site. We suggest that the urban runoff favours microbial development on the soil surface, enhancing leaf litter degradation by giving a more stable, nutritious, and humid environment for microbial development (Robertson, 1988; Leopold et al., 2013; Molnar et al., 2014).

The influence of urban runoff on leaf litter degradation was also evident in the larger increase in N content during degradation at the urban site than the control site. Urban rainwater runoff may have acted as an additional source of N to the forest floor and litter (Tam et al., 1998). Nitrogen can also be produced by microorganisms during leaf litter degradation (Tam et al., 1990; Mfilinge et al., 2002). The higher degradation rates associated with the higher enrichment of fucose and ribose at the urban site, characteristic of microbial production (Cowie and Hedges, 1984a), indicated stronger microbial activity on the soil surface at the urban site.

The modified soil conditions created by the submerging urban runoff may also have influenced molecular degradation processes of the leaf litter. Rhamnose and glucose were less labile during leaf litter degradation at the urban site than at the control site after 72 days of degradation. With a lower soil surface salinity (Robin et al., 2022), the urban mangrove forest was a less suitable environment for the secretion of some enzymes such as cellulases, which enhance cellulose and hemicellulose hydrolysis (Arfi et al., 2013; Ivaldi et al., 2021). Also, the more anoxic environment of the urban forest's upper soil (Robin et al., 2022) limited the hydrolysis of neutral carbohydrates including rhamnose and glucose. The more reducing conditions may also have favoured lignin conservation over bulk OC during the early phase of degradation (Benner et al., 1984, 1991), explaining the higher relative lignin enrichment in the leaf litter of *R. stylosa* at the urban site than at the control site after 7 days of degradation. In contrast, for *A. marina*, the urban rainwater runoff favoured the leaching of lignin molecules, especially vanillyl phenols, leading to a larger relative loss of lignin during degradation.

III.A.5.4. Leaf litter molecular changes

The molecular-level changes of OM during leaf litter degradation revealed species-specific and site-dependent influences on the stability of some molecules. Trends were observed in neutral carbohydrates and lignin-derived phenols during degradation, suggesting a potential end for compositional uniformity (Opsahl and Benner, 1999). The hypothesis of compositional uniformity suggests that the most abundant sugars would be more labile than the least abundant in order to end up with a uniform composition of neutral carbohydrates in the most degraded leaves (Opsahl and Benner, 1999). In this study, the hypothesis is valid with the most abundant sugars glucose, arabinose, galactose, and rhamnose being the most labile, and the least abundant sugars fucose, ribose, and mannose being the most refractory ones. Xylose is an exception to the compositional uniformity hypothesis as it is one of the most abundant neutral carbohydrate but increased in concentration during leaf litter degradation. We suggest that xylose may be associated to more refractory components of the litter such as lignin, which enhanced protection from enzymatic degradation (Opsahl and Benner, 1999), as suggested by the correlation between xylose and p-hydroxyl phenols (r = 0.61) and cinnamyl phenols (r = 0.50) (*Supplementary Table III.A-7*).

The order of lability of the 11 lignin-derived phenols differed between mangrove species and sites but observations agreed with previous work. In the literature, syringyl phenols were classified as the most stable phenols and ferulic acid the least (Benner et al., 1990). In the present study, ferulic acid decreased relatively in the leaf litter at the four

stands after 72 days of degradation, while total syringyl phenols relatively increased. The hypothesis of compositional uniformity may also work here as for both species, the most abundant phenol group in the senescent leaves was also the most labile during degradation; that is vanillyl phenols for *A. marina* and cinnamyl phenols for *R. stylosa.*

III.A.5.5. Limitations of the experiment and models

The litterbag experiment was conducted using senescent leaves from the control site only for both species. This design of experiment aimed to evaluate the changes in leaf litter mass and composition over 72 days of degradation with a focus on the influence of urban runoff on these changes. The choice of having the same senescent leaves at both sites enabled to limit the factors potentially affecting these changes other than runoff such as initial senescent leaves composition. The influence of initial composition was evaluated between species but not between sites. This experiment design was therefore not a limitation regarding the general processes investigated in this study. However, it is not possible from this experiment to quantify the elements or molecules released, stored, or gained by the leaf litter at the urban site. Furthermore, the experiment ended after 72 days of degradation as the mass remaining was the lower limit to conduct all the analyses. A longer experiment could have given further information relative to the refractory degradation stage.

In this study, single exponential models were plotted on the mass loss of the leaf litter with degradation. Single exponential models were used to calculate the half-lives of the litter and are frequently used in similar works using the litterbag experiment (Flores-Verdugo et al., 1987; Ashton et al., 1999; Bosire et al., 2005; Nordhaus et al., 2017; Vinh et al., 2020). However, double exponential models seemed more suitable for the degradation rate in this study as shown by the regression coefficients (R^2) of the exponential regression lines (*Supplementary Figure III.A-1*), as previously suggested in the literature (Wider and Lang, 1982). Two phases of degradation stood out in the double exponential model with a first stage from 0 to 14 days for *R. stylosa* or to 28 days for *A. marina*, and a second to 72 days (*Supplementary Figure III.A-1*). The double exponential model indicated that the mass loss of the leaf litter was faster for the four stands during the first days of degradation as soluble compounds were leached. Still, the use of the single exponential model is preferential as comparison with literature is possible and the differences between species and sites were noticeable as much as with the double exponential model.

III.A.6. Conclusion

In this study, the changes in mangrove leaf litter OM quality during degradation was analysed in relation to mangrove species (*A. marina* and *R. stylosa*) and to mangrove forests (urban and control) with an attention to the influence of urban runoff. Our findings challenged conventions, showing faster degradation of the leaf litter of *R. stylosa* despite lower initial N content than the leaf litter of *A. marina*. This result emphasized the crucial role of species position within the mangrove forest, where coastal proximity and submersion dictate degradation rates.

The urban runoff submerging the soil of the urban mangrove forest amplified leaf litter degradation, attributed to enhanced leaching and microbial activity, though further experiments must be undertaken to better understand the processes. The modified urban site conditions not only influenced mass loss but also reshaped the molecular changes of OM during leaf litter degradation. This impact on neutral carbohydrates and lignin-derived phenols underscored the intricate interplay between environmental factors and OM stability in mangrove ecosystems.

The stability of carbohydrates and lignin-derived phenols varied between species and sites, emphasizing the need to consider both species physiology and environmental conditions in understanding molecular OM dynamics during litterfall degradation. Information on the molecular changes of the leaf litter is essential to understand the molecular changes of the OM in mangrove soils (sources and diagenetic processes). The information obtained in this study may also be important to understand the dynamics of other elements during litterfall degradation such as major elements and trace metals as their cycles depend on the litterfall decay rates and the formation of complexes with OM molecules.

This research underscored the global implications of urban runoff on mangrove ecosystems. The study revealed that urban runoff significantly accelerates the degradation of leaf litter in mangrove forests, potentially altering C cycling dynamics. The faster mass loss and increased microbial activity in the urban mangrove forest suggested a potential reduction in C sequestration capacity, which is critical for mitigating climate change. Moreover, the study highlighted the need to consider not only the direct environmental impacts of urbanization but also the cascading effects on ecosystem services. Mangroves are not only C sinks but also serve as habitats for diverse marine life, support fisheries, and act as buffers against coastal erosion. The accelerated degradation of leaf litter due to urban runoff poses a potential threat to these ecosystem services, with far-reaching consequences for both local and global biodiversity.

III.A.7. Acknowledgments

The authors acknowledge Ines Le Mao from NC Bioressources for UPLC-MS optimization and analyzes and Anne Desnues from IRD for the isotopic analyzes. The authors also acknowledge Pierre Sanlis for the help on the field work. This work was supported by the CRESICA and Banque de la Nouvelle-Calédonie, Cegelec, SECAL, and Fibrelec via the University of New Caledonia Foundation.

III.A.8. Supplementary materials

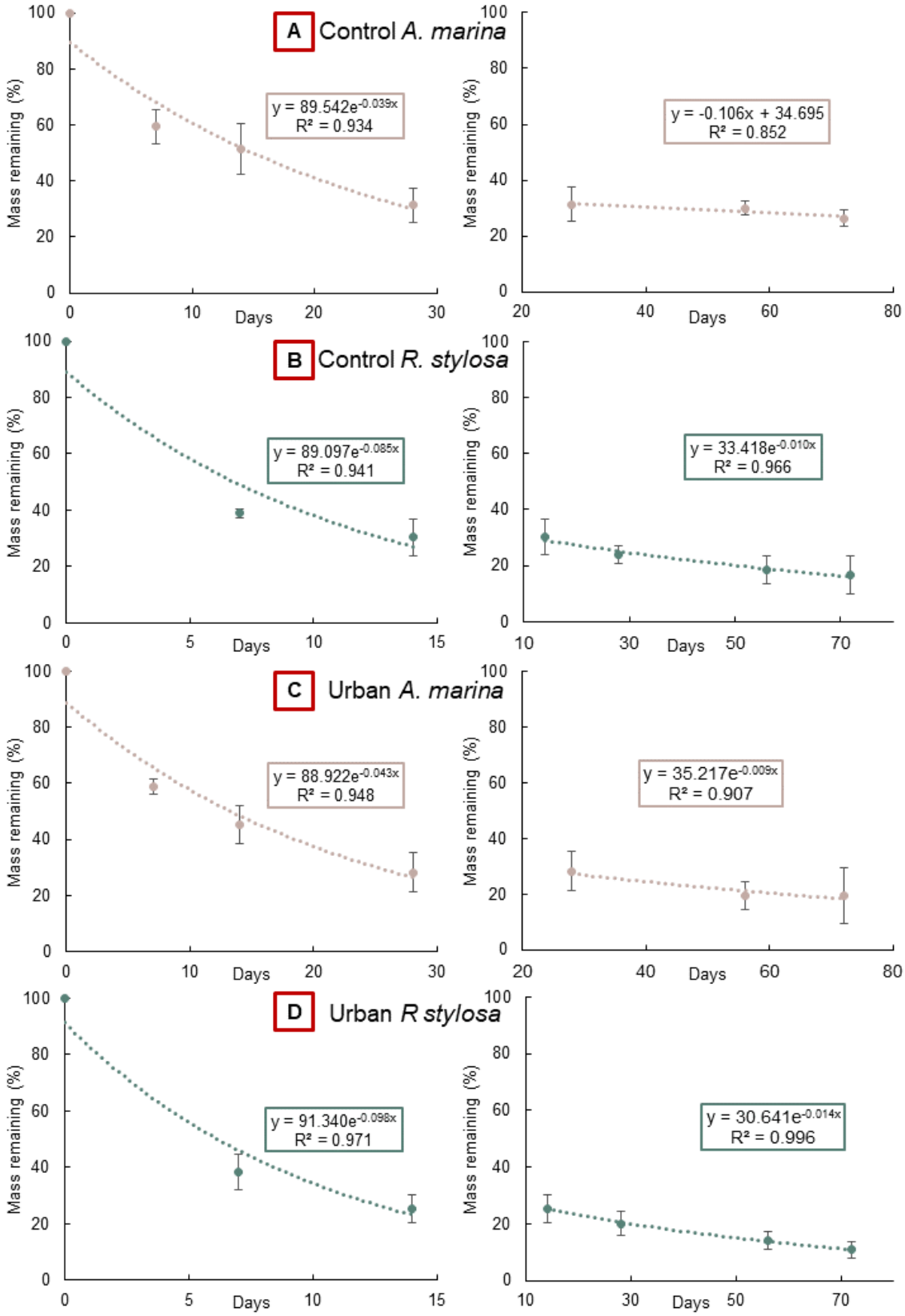

Supplementary Figure III.A-1. Double exponential mass loss decay rates at the control site for (A) *A. marina* and (B) *R. stylosa* and at the urban site for (C) *A. marina* and (D) *R. stylosa*.

Supplementary Table III.A-1. Quality control of the duplicate samples on an isotope ratio mass spectrometer Sercon Intergra 2.

Sample	ΔC (g kg^{-1})	ΔN (g kg^{-1})	$\Delta\delta^{13}C$ (‰vsVPDB)	$\Delta\delta^{15}N$ (‰vsAir)
Control *A. marina* t0 1	3.69	0.56	0.03	0.25
Control *A. marina* t72 2	3.87	0.69	0.24	0.19
Control *R. stylosa* t0 3	3.04	0.34	0.31	0.23
Control *R. stylosa* t7 1	2.73	0.26	0.12	0.11
Control *R. stylosa* t56 2	4.02	0.61	0.08	0.12
Urban *A. marina* t14 2	10.12	0.81	0.41	0.31
Urban *A. marina* t28 2	3.36	0.64	0.28	0.24
Urban *R. stylosa* t14 2	3.71	0.40	0.29	0.32
Urban *R. stylosa* t28 3	4.88	0.57	0.14	0.30
Urban *R. stylosa* t72 2	4.68	0.62	0.15	0.04

Supplementary Table III.A-2. GC-MS temperature program for neutral carbohydrates analysis.

Temperature (°C)	Gradient (°C min^{-1})	Time (min)
50	0	3.0
150	30	3.2
230	1.5	53.2
310	30	2.4
310	0	5.0

Supplementary Table III.A-3. Percentage precision and accuracy of neutral carbohydrate measurements.

Neutral carbohydrates	Precision (2σ) on standard	Relative standard deviation on standard	Precision on duplicate samples
Xylose	12%	3%	3%
Arabinose	12%	5%	2%
Ribose	11%	5%	11%
Rhamnose	12%	4%	2%
Fucose	10%	3%	2%
Mannose	10%	8%	1%
Galactose	8%	6%	8%
Glucose	9%	5%	2%

Supplementary Table III.A-4. UPLC-MS parameters for lignin-derived phenols analysis.

Chromatography			
		Peak Detection	Genesis
	Gradient	Min	%B
		0	5
		0.5	20
		3	50
		3.5	50
		3.6	95
		4.5	95
		4.6	5
		6	STOP
	Ion source	Spray voltage	Static
		Negative ion	2 800 V
		Gas method	Static
		Sheath gas	50 Arb
		Aux gas	10 Arb
		Sweep gas	0 Arb
		Ion transfer tube temperature	320 °C
		Vaporizer temperature	300 °C
Mass spectrometry			
	Global settings	Expected LC peak width	6 s
		Mild trapping	False
		Internal mass calibration	EASY-IC
		Mode	Scan-to-Scan
Full Scan	*Full Scan*	Orbitrap resolution	60 000
		Scan range	50-250 m/z
		RF lens	70%
		AGC target	Standard
		Maximum injection time	100 ms
		Microscans	1
		Data type	Profile
		Polarity	Negative
	Dynamic exclusion	Exclude after n times	1
		Exclusion duration	2.5
		Mass tolerance	ppm
		Low	5
		High	5
		Exclude isotopes	True
	Mass list		
	Compound	*m/z*	*HCD Collision energy*
	Vanillin	151.0401	20%
	Vanillic acid	167.0350	20%
	p-Hydroxybenzaldehyde	121.0295	70%
	p-Hydroxyacetophenone	135.0452	60%
	p-Hydroxybenzoic acid	137.0244	20%
	Coumaric acid	163.0401	20%
	Acetovanillone	165.0557	20%
	Syringaldehyde	181.0506	20%
	Syringic acid	197.0455	30%
		Mass tolerance	ppm
		Low	3
		High	3

		Number of dependent scans	3
	ddMS²	Isolation window	1.5 m/z
		Collision energy type	Normalized
		HCD Collision energy	20%
		Orbitrap resolution	30 000
		Scan range	50-250 m/z
		Maximum injection time	60 ms
		Microscans	1
SRM	*SRM*	Multiplex ion	False
		Q1 offset	Off
		HCD Collision energy	20%
		Orbitrap resolution	120 000
		RF Lens	70%
		AGC target	Standard
		Microscans	1
		Data type	Profile
		Polarity	Negative

	List		
Compound	*Precursor (m/z)*	*Product (m/z)*	*RT (min)*
p-Hydroxybenzaldehyde	121.0295	92.026	2.11
p-Hydroxyacetophenone	135.0452	120.017	2.42
p-Hydroxybenzoic acid	137.0244	93.034	1.80
Vanillin	151.0401	136.066	2.40
Coumaric acid	163.0401	119.050	3.10
Acetovanillone	165.0557	150.032	2.67
Vanillic acid	167.0350	152.011	2.62
Syringaldehyde	181.0506	166.027	2.56
Syringic acid	197.0455	121.029	2.83
Acetosyringone	195.0663	152.997	1.98
Ferulic acid	193.0506	178.027	2.86

Supplementary Table III.A-5. Lignin-derived phenols calibration curves.

Compound	**Regression line**	**R^2**	**Lower detection limit (mg L^{-1})**	**Upper detection limit (mg L^{-1})**
p-Hydroxybenzaldehyde	y = 6.15E5x – 3.13E6	0.9993	0.1	8
p-Hydroxyacetophenone	y = 2.87E5x + 1.85E3	0.9975	0.1	8
p-Hydroxybenzoic acid	y = 4.26E6x – 6.43E5	0.9952	0.1	8
Vanillin	y = 1.38E6x – 3.63E5	0.9989	0.1	8
Coumaric acid	y = 1.73E6x – 6.11E5	0.9971	1	80
Acetovanillone	y = 6.60E3x + 566	0.9983	1	80
Vanillic acid	y = 5.68E4x – 2.45E5	0.9998	1	80
Syringaldehyde	y = 9.40E5x – 2.60E6	0.9984	0.3	24
Syringic acid	y = 2.55E4x – 1.05E5	0.9998	0.3	24
Acetosyringone	y = 2.87E5x + 1.85E3	0.9975	0.1	8
Ferulic acid	y = 4.26E6x – 6.43E5	0.9952	0.1	8

Supplementary Table III.A-6. Concentrations in the 11 lignin-derived phenols in the blank and quality control (QC) solutions obtained in mg L^{-1} with the expected value for the QC.

	Blank		Expected QC	QC							
PAL	0.047	0.060	2	1.924	2.264	2.194	1.909	1.846	1.850	1.820	1.946
PON	0.059	0.055	2	2.145	1.752	1.881	2.221	2.123	2.266	2.191	1.853
PAD	0.001	0.006	2	2.225	2.185	2.111	1.875	1.784	2.243	2.211	2.276
VAL	0.091	0.099	2	2.232	2.093	1.876	2.161	1.801	1.826	2.052	2.047
VON	0.068	0.050	20	19.408	18.885	21.197	19.415	19.786	19.796	20.951	20.972
VAD	0.135	0.297	20	19.944	20.668	19.320	21.149	20.719	19.380	19.131	21.205
SAL	0.045	0.077	6	5.880	6.195	6.525	6.706	5.201	5.105	6.811	6.858
SON	0.029	0.027	2	2.057	2.210	2.077	2.052	1.744	1.705	2.193	2.255
SAD	0.068	0.161	6	5.338	5.394	6.278	6.167	6.677	6.150	5.324	6.702
CAD	0.008	0.099	20	19.904	21.262	21.207	19.030	21.277	18.780	18.850	21.158
FAD	0.023	0.095	2	2.045	2.033	1.905	1.883	2.122	1.900	1.823	1.889

Supplementary Table III.A-7. Correlation matrix between the concentrations in neutral carbohydrates in the leaf litter during degradation and the concentrations in the four phenolic groups for the four studied stands.

	p-hydroxyl	Vanillyl	Syringyl	Cinnamyl
Xylose	0.61	0.26	0.44	0.5
Arabinose	0.05	0.03	-0.2	-0.02
Ribose	0.5	0.29	0.35	0.34
Rhamnose	0.28	0.27	0.11	0.2
Fucose	-0.36	-0.58	-0.34	-0.47
Mannose	0.18	0.04	0.16	0.14
Galactose	-0.3	-0.34	-0.45	-0.47
Glucose	0.28	0.31	0.01	0.24

B. Chapter III.B: Urban runoff influence on major element and trace metal dynamics during leaf litter decomposition in semi-arid mangrove

Sarah Louise ROBIN, Cyril MARCHAND, Kapeliele GUTUTAUAVA, Andrea C. ALFARO

To be submitted to Chemosphere

III.B.1. Abstract

Litterfall decomposition in mangrove forests actively contributes to energy and material flow to and from the forest. As organic matter in mangrove forests can trap various contaminants, such as trace metals (TM), it is essential to investigate the dynamics of these contaminants along with litterfall decomposition. This study examined the evolution of major elements and TM during leaf litter decomposition in two semi-arid mangrove forests—control and urban—located along New Caledonia's West coast. A litterbag experiment was carried out for 72 days at both sites for the two main mangrove species (*Rhizophora stylosa* and *Avicennia marina*) present in New Caledonia. The results indicated that the leaching and enrichment of major elements and TM (Al, As, Co, Cr, Cu, Fe, Mn, Ni, Pb, Ti, and Zn) during decomposition were influenced by initial leaf composition, forest position, salt tolerance mechanisms, and metabolism. K and Mg showed the fastest leaching, while Na content decreased significantly during decomposition, especially in the urban forest. The TM concentrations in leaf litter generally increased during decomposition, with variations depending on the element, species, and forest location. Urbanization, by enhancing TM bioavailability in mangrove soil, favored TM enrichment in the leaf litter during decomposition. Some TM showed specific trends, such as Mn, which is less concentrated in the leaves after 72 days of decomposition. We suggest that the oxidative state of Mn controls its evolution in the decomposing litterfall. The study underscored the complex interplay of factors that influence major elements and TM dynamics during leaf litter decomposition in mangrove ecosystems. The findings contribute to a deeper understanding of the impact of urbanization on nutrient cycling and TM accumulation in these vital coastal ecosystems. This research emphasized the need for further investigation into the intricate relationships between environmental factors, decomposition processes, and the fate of elements and contaminants in mangrove forests.

Keywords: mangrove, urbanization, trace metals, litterfall, decomposition

III.B.2. Introduction

The mangrove ecosystem develops within the intertidal zone of tropical and subtropical regions down to temperate regions in the South (Alongi, 2002). Despite constituting less than 0.5% of the global forest surface, mangrove forests emerge as valuable carbon-sequestering ecosystems, playing an important role in the carbon cycle, energy dynamics, and nutrient flows (Lee et al., 2014). Mangrove forests also serve as filters and buffers between the terrestrial watershed and the adjacent aquatic ecosystems (i.e., bay, lagoon). Three factors contribute to the distinctiveness of mangrove forests—namely, their rapid sedimentation rate, rich organic matter (OM) content, and the biogeochemical reactivity of the substrate. These factors establish mangrove forests as potential areas for the accumulation of contaminants, including trace metals (TM) (Harbison, 1986; Bouillon et al., 2008; Kristensen et al., 2008, 2017; Alongi, 2014; Marchand, 2017).

TM, as natural elements, typically manifest in the environment at minimal concentrations. While some TM serve as micronutrients crucial for diverse life forms, their excess absorption can lead to toxicity (MacFarlane and Burchett, 2000). Other metals, such as Pb and Hg, lack specific functions in most organisms and therefore show toxicity at low concentrations. TM can inhibit plant development processes and reduce photosynthetic activity (Prasad et al., 2006). Elevated TM concentrations in the environment raise concerns due to their potential accumulation and long-range transport (Bayen, 2012).

In mangrove forests, studies have shown the adaptability of mangrove plants to metal-induced stress (MacFarlane and Burchett, 2000, 2002; Cheng et al., 2014; Naidoo et al., 2014). Essential TM, like Zn or Cu, are regulated with limited transfer from the roots to the leaves, or the excess being evacuated through the salt glands of the leaves, as observed for *Avicennia marina* (MacFarlane and Burchett, 2000; Naidoo et al., 2014). Conversely, non-essential metals tend to be excluded or gathered at the root surface to limit their transfer to higher plant tissues (MacFarlane and Burchett, 2000; Robin et al., 2021). Plants can assimilate TM only in the soluble form and if the chemical form is absorbable (Tremel-Schaub and Feix, 2005). Therefore, metal stress in mangrove forests is controlled by various factors affecting TM solubility and mobility in the soil.

OM exhibits high adsorption capabilities for various organic and inorganic contaminants, including TM (Ram and Verloo, 1985; Chakraborty et al., 2015; Ge and Li, 2018; Robin and Marchand, 2022). One component of mangrove OM is lignin, a robust co-polymer integrated in the secondary cell walls of vascular plants, which offers structural

support as well as limited water loss from the roots (Thakur et al., 2014). Lignin's diverse active sites function as traps, enabling the absorption, adsorption, and sequestration of TM (Thakur et al., 2014). In mangrove sediments, carbon derived from lignin primarily comes from the litter of mangrove trees (Kristensen et al., 2008). This litter production constitutes 31% of the overall net primary production within mangrove forests (Bouillon et al., 2008). Litterfall decomposition actively participates in the energy and material flow in the forest and constitutes an energy source for coastal productivity (Lugo and Snedaker, 1974; Twilley et al., 1986). Litterfall OM can be consumed by autochthonous fauna and microorganisms on the forest floor, dissolve during decomposition, and subsequently be conveyed to adjacent ecosystems during ebb tides, either as debris or dissolved organic/inorganic carbon (Ray et al., 2018; Taillardat et al., 2018; Kida et al., 2019b). Mangrove leaves comprise the predominant fraction of litterfall (Twilley et al., 1986; Day et al., 1987), ranging between 40% and 90% (Mackey and Smail, 1996). Consequently, most investigations into litterfall decomposition center on leaf litter, employing the litterbag experiment methodology (Nordhaus et al., 2017; Yang et al., 2018; Vinh et al., 2020).

New Caledonia is one of the top 4 Pacific territories with the most mangrove forests (Hamilton and Casey, 2016), as mangroves cover 80% of the West coast of the main island. The mangrove forests of this region, characterized by a semi-arid climate and a semidiurnal tidal pattern (Douillet, 2001), showcase simple biodiversity structures. Species monospecific stands prevail, shaped by topography and soil salinity (Baltzer, 1981; Marchand et al., 2011a). *Rhizophora* spp., developing seaside, constitute over half of the mangrove flora, while *Avicennia marina*, developing at higher elevations and saltier soils, represent around 15% of the archipelago's mangrove vegetation (Deborde et al., 2015).

Although the human population density is low in New Caledonia, the population living in urban areas has significantly increased this last decade, resulting in the development of urban infrastructures along the littoral zone, where mangrove forests develop (Insee, 2020). A recent study looked into the influence of coastal urbanization on these mangroves (Robin et al., 2022) and found that part of the mangrove forest, receiving urban runoff for >50 years, was constantly submerged by runoff water, leading to the development of *R. stylosa* trees far taller than is typical for such semi-arid mangrove forests. Robin et al., (2022) showed that the runoff controls the physico-chemical parameters of the mangrove soil, reducing soil salinity and elevating pH levels. Furthermore, urban TM concentrations in the soil exceed those present in a “control” mangrove forest, implying greater TM mobility (Robin et al., 2022). A litterbag experiment conducted in the same mangrove forest revealed that the urban runoff favors leaf litter

decay on the mangrove floor by promoting microbial development on the soil surface (Robin et al., submitted).

This study aimed to assess major element and TM evolution in leaf litter decomposition, examining the influence of urbanization. While major elements and TM dynamics during litterfall decay have been explored in various studies (Rice and Windom, 1982; Van Der Valk and Attiwill, 1984; Steinke and Ward, 1987; Tam et al., 1990; Chale, 1993; Silva et al., 1998; Zawislanski et al., 2001; Ramos e Silva et al., 2006; Hossain et al., 2014; Vinh et al., 2020), no investigation has looked into the effect of urbanization on such processes nor in semi-arid mangrove settings. In this study, two semi-arid mangrove forests—control and urban—along New Caledonia's West coast, were selected. Both forests share a common geological unit as the source of their watersheds, yet the urban forest has received urban rainwater runoff for over five decades. Employing a 72-day litterbag experiment, conducted on the main mangrove species (*Rhizophora stylosa* and *Avicennia marina*), we hypothesize the early leaching of K, Mg, Na, Ca, and P during litterfall decomposition, with site-dependent decay. Additionally, we hypothesize an enrichment of all TM in the decomposing litterfall.

III.B.3. Material & methods

III.B.3.1. Study sites

The city of Dumbea in New Caledonia has had a population increase of 33% this last decade, resulting in the development of urban infrastructure on the littoral zone (Insee, 2020). Two mangrove forests in Dumbea were selected as study sites (*Figure III.B-1*). These sites had the same volcano-sedimentary watershed and are dominated by the same two mangrove species (*R. stylosa and A. marina*). One site was located in the Apogoti Bay (22°12’08”S, 166°26’20”E). This site has no direct anthropogenic inputs (limited housing density) into the mangrove forest, and it was selected as a control mangrove forest. Another site is the urban mangrove forest (22°12’39”S, 166°27’19”E) exposed to rainwater runoff from the upper allotment (mainly housing lots for 10 000 inhabitants), which has been flowing into the mangrove forest for more than 50 years. At the control site, the two species develop in monospecific stands similar to most mangrove forests of the West coast, that is, *A. marina* landward and *R. stylosa* seaward. At the urban site, another *R. stylosa* stand develops more landward than the *A. marina* stand, at the entrance of the runoff, and its soil is always flooded with the urban rainwater.

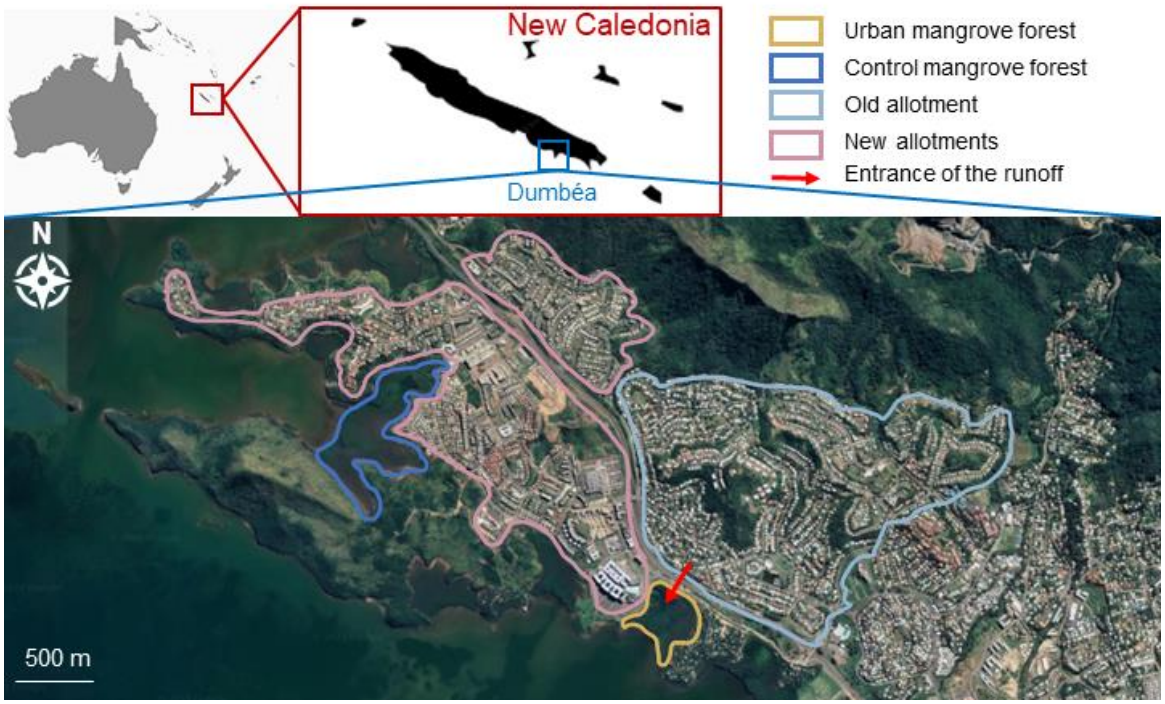

Figure III.B-1. Control mangrove forest and urban mangrove forest in Dumbea city in New Caledonia with delimitation of the new and old allotments, and a red arrow to show the entrance and flow direction of the urban rainwater runoff (satellite image from Google Earth).

III.B.3.2. Litterbag experiment

Yellow senescent leaves about to fall from *A. marina* and *R. stylosa* trees were collected at the control site. The leaves were carefully washed and air-dried at the laboratory until constant mass. Three random leaf samples of 200 g per species were frozen, freeze-dried, and ground with a cutting mill, corresponding to the samples at t0 “senescent leaves”. In order to investigate the influence of urbanization on the evolution of major elements and TM, we decided to use the senescent leaves collected from the same trees, that is at the control site, in both mangrove forests, to limit the effect of initial composition of the leaves on our results. We were able to do so as previous analyzes showed no significant differences in TM contents in the leaves between the control and urban sites (Robin et al., 2022). A total of 90 samples of about 6 g of dried *A. marina* leaves and 90 samples of 15 g of dried *R. stylosa* leaves were weighed to the nearest 0.1 g and placed into nylon litterbags (2 mm mesh size). In each mangrove forest and for each species, three trees about 30 m apart were selected. A total of 15 bags of the corresponding species were attached to the roots of each of these three trees, at the soil surface. Triplicate litterbags were collected at each of these three trees (9 litterbags), for each species, and for each site after 7, 14, 28, 56, and 72 days. The litterbags were immediately opened at the laboratory; the leaves were carefully washed and air-dried until

constant mass prior to weighing. Samples were then frozen, freeze-dried, and ground with a cutting mill. For initial comparison, fresh green leaves were also collected at both sites and for both species in triplicate, washed, freeze-dried, and ground.

III.B.3.3. Major elements and trace metal quantification

The elements were measured in the dried ground leaves by ICP-OES after multiwave extraction. Briefly, 200 mg of each fresh, senescent, and degraded sample was weighed in a Teflon vessel. A volume of 5 ml of 70% HNO_3 and 1 ml of 30% H_2O_2 were added to the vessel. The digestion program started with a 10 min heating step from room temperature to 160 °C, then 15 min step to 210 °C, followed by a 10 min plateau and a 20 min cooldown step. The result of the extraction was transferred to a polypropylene tube. The volume was adjusted to 13 ml with MilliQ water and placed at 4 °C until ICP-OES (Varian 730-ES) analysis at the chemistry laboratory LAMA of the French Research Institute for Sustainable Development in New Caledonia. For quality control, certified material (IPE sample ID 949) was also extracted and analyzed (*Supplementary Table III.B-1*). Concentrations of major elements and TM were obtained using a calibration curve prepared from a stock solution of the measured elements at 100 mg L^{-1}.

III.B.3.4. Porewater sampling & processing

Sampling and processing of porewaters was previously published (Robin et al., 2022). Briefly, in both sites and at each mangrove stand (*A. marina* and *R. stylosa*), triplicate soil cores were collected with an Eijkelkamp gouge auger. Soil cores were cut along the depth into six sections (0–5 cm, 5–10 cm, 10–15 cm, 15–20 cm, 20–30 cm, and 30–40 cm). To extract porewater from soil samples, rhizon samplers (Rhizon SMS—10 cm, diameter 2.5 mm–Rhizosphere) were inserted into the soil sections. Each rhizon was connected to a 20 ml syringe. Upon arrival at the laboratory, porewater samples were filtered at 0.45 µm and two drops of H_2SO_4 were added before storage at 4 °C. Elements concentrations in the porewater samples were obtained via ICP-OES (Varian 730-ES) analysis at the chemistry laboratory LAMA.

III.B.3.5. Data analyzes

III.B.3.5.1. Major elements

To plot the changes in major elements concentrations in the litterfall with degradation, the measured elements' concentrations in µg g^{-1} of dry sample were converted to percentages relative to t0. The values were calculated as follows:

$$\text{Element concentration at } t_n\ (\%) = ([\text{element}]_n * 100) / [\text{element}]_0 \qquad \text{(III.B-1)}$$

with $[element]_n$ the concentration of the element at t_n in µg g^{-1} and $[element]_0$ the concentration of the element at t_0 in µg g^{-1}. For comparison with literature, single exponential trends were plotted when possible:

$$W_t = W_0 e^{-kt} \quad \text{(III.B-2)}$$

with W_t the element content percentage at t, W_0 the initial element content percentage (100 %), k the exponential factor, and t the time in days. The half-lives ($t_{1/2}$) in days were obtained with the following equation:

$$t_{1/2} = \ln(2) / k \quad \text{(III.B-3)}$$

III.B.3.5.2. Trace metals

To plot the changes in TM concentrations in the litterfall with degradation the measured TM maximum concentration in µg g^{-1} was set at 1.00 and the other values were calculated as follows:

$$\text{TM concentration at } t_n = [TM]_n / [TM]_{max} \quad \text{(III.B-4)}$$

with $[TM]_n$ the concentration of the TM at t_n in µg g^{-1} and $[TM]_{max}$ the maximum concentration of the TM between t0 and t72 in µg g^{-1}.

III.B.4. Results

III.B.4.1. Characterization of the fresh and senescent leaves

Prior to comparing the evolution of major elements and TM in the litterfall during decomposition, it is necessary to look at the physiological differences in the leaves between species and between fresh and senescent leaves. The concentrations of the measured elements in fresh and senescent leaves of *A. marina* and *R. stylosa* are displayed in *Table III.B-1*. In all samples and of all TM, Co had the lowest concentration varying from 0.02 to 0.18 µg g^{-1}, while Mn and Fe had the highest concentrations with values up to 238 µg g^{-1} for Fe and 321 µg g^{-1} for Mn.

At the control site, Al, Cr, Mn, and Pb had concentrations between 2 and 10 times higher in the fresh leaves of *R. stylosa* than *A. marina*, while it was the opposite for the other TM. For the senescent leaves, Mn and Ni were the only TM with higher concentrations in the *R. stylosa* trees. Regarding the major elements, P and K had concentrations 5 and 3 times higher in the senescent leaves of *A. marina*, respectively, while Na and Ca had concentrations 2 and 14 times higher in the senescent leaves of *R. stylosa*, respectively.

Table III.B-1. Element mean concentrations (±SD) in the fresh and senescent leaves of *A. marina* and *R. stylosa* at the urban and control sites.

Species	***A. marina***			***R. stylosa***		
Site	**Control**		**Urban**	**Control**		**Urban**
Leaves	**Fresh**	**Senescent**	**Fresh**	**Fresh**	**Senescent**	**Fresh**
Major elements (mg g^{-1})						
Na	NA	17±1	NA	NA	33±1	NA
Mg	NA	12±1	NA	NA	13±1	NA
P	0.93±0.05	1.0±0.1	NA	0.66±0.01	0.21±0.02	NA
K	NA	14±1	NA	NA	5.6±0.5	NA
Ca	NA	1.0±0.2	NA	NA	14±1	NA
Trace metals (µg g^{-1})						
Al	13±1	39±10	6.2±1.2	31±44	9.0±0.01	29±10
As	3.3±1.5	4.1±0.1	0.98±0.44	0.49±0.12	0.30±0.17	0.49±0.14
Co	0.15±0.02	0.09±0.04	0.18±0.03	0.09±0.05	0.02±0.01	0.15±0.04
Cr	0.05±0.01	0.43±0.16	0.38±0.04	0.50±0.31	0.51±0.19	0.34±0.13
Cu	14±6	4.4±0.7	8.6±0.7	2.6±0.7	0.60±0.12	4.6±0.6
Fe	122±24	238±25	42±2	47±51	32±1	67±16
Mn	33±9	34±1	66±7	99±10	157±10	321±130
Ni	4.3±0.3	0.14±0.24	1.4±0.1	3.7±0.6	1.9±0.7	2.1±1.1
Pb	0.15±0.25	0.10±0.01	0	0.57±0.20	0.08±0.01	0.24±0.21
Ti	2.6±0.7	1.7±0.1	1.6±0.5	1.6±2.1	0.46±0.02	2.0±0.50
Zn	18±3	9.2±0.8	14±1	3.5±2.1	1.2±0.1	6.5±1.4

For both mangrove species, at the control site where the senescent leaves were collected, Co, Cu, Ni, Pb, Ti, and Zn were measured between 1.5 and 31 times in higher concentrations in the fresh leaves than the senescent leaves. Al, As, and Fe were measured in higher concentrations in the fresh leaves than the senescence leaves of *R. stylosa,* but it was the opposite for *A. marina*.

Between sites, only Mn was measured in significantly higher concentrations in the leaves of the urban mangrove forest for both species compared to the control mangrove forest. For *A. marina*, it was also the case for Cr, and for *R. stylosa* it was the case for Co, Cu, Fe, and Zn. Conversely, Ni and Pb had higher concentrations in the leaves collected at the control site for both species.

III.B.4.2. Evolution of major elements during leaf litter decomposition

For all stands, K was the fastest released major element from the litterfall during decomposition with a loss between 65% and 87% of initial K content in the first 7 days of

decomposition (*Figure III.B-2A*). K content was rather stable for the rest of the decomposing experiment. Similarly, the loss of Mg was also high in the first 14 days of decomposition, between 50% and 60% (*Figure III.B-2B*).

At the urban site, Na showed single exponential decay, with calculated half-lives of 53 days for *A. marina* and 24 days for *R. stylosa*. After 72 days of decomposition, only 2% of the initial Na content was left in the litterfall of *R. stylosa* and 10% in that of *A. marina*. However, at the control site, Na fluctuated in the litterfall of both species with maximum enrichment after 14 days of decomposition and maximum loss after 28 days of decomposition (*Figure III.B-2C*).

For *R. stylosa*, compared to the initial content in the senescent leaves, P increased by 72% at the control site and by 408% at the urban site. The litterfall of *A. marina* at the urban site had a stable P content, while that of the control site slowly decreased with increasing decomposition (*Figure III.B-2D*). Ca also showed different trends between species. For *R. stylosa*, about 65% of initial Ca content was lost in the litterfall after 72 days of decomposition at both sites. In the litterfall of *A. marina*, Ca content compared to t0 increased by 130% in the first 14 days of decomposition (*Figure III.B-2E*).

The half-lives of K were in order: control *R. stylosa* (13 d) > urban *A. marina* (12 d) > urban *R. stylosa* (9 d) > control *A. marina* (7 d). The half-lives of Mg were in order: urban *A. marina* (24 d) > control *A. marina* (19 d) > control *R. stylosa* (16 d) > urban *R. stylosa* (14 d). For Na, only at the urban site did the element follow an exponential trend and was lost at a higher rate for *R. stylosa* ($t_{1/2}$ of 24 d) than *A. marina* ($t_{1/2}$ of 53 d). In addition, only the litterfall of *R. stylosa* exponentially lost Ca with decomposition, with half-lives of 43 days at the urban site and 30 days at the control site. Finally, P had a half-life of 99 days in the litterfall of *A. marina* at the control site.

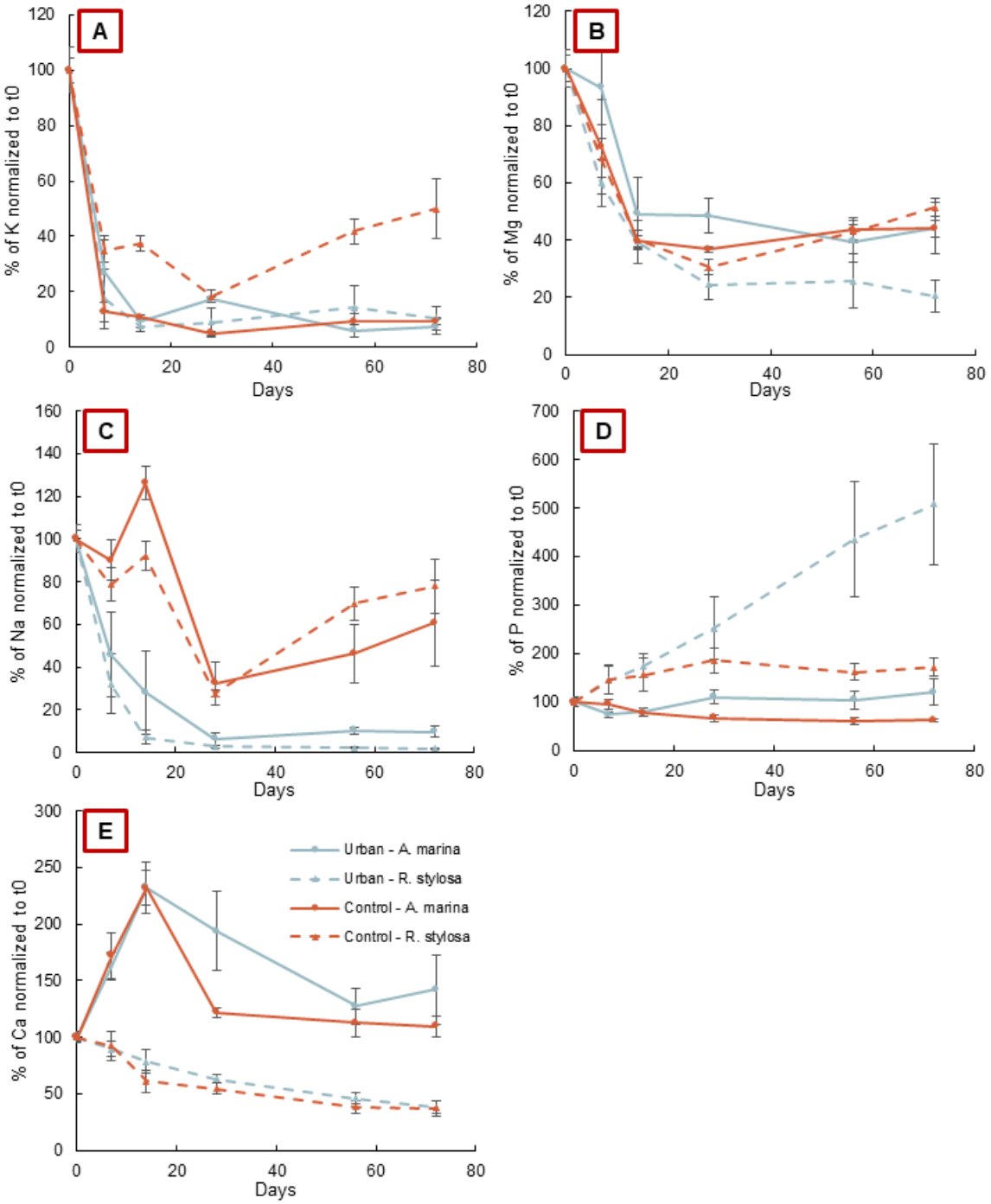

Figure III.B-2. Mean percentage (SD as error bars) of (A) potassium, (B) magnesium, (C) sodium, (D) phosphorous, and (E) calcium in the leaf litter with decomposition relative to t0 at the urban and control sites for *A. marina* and *R. stylosa*.

III.B.4.3. Evolution of trace metals during leaf litter decomposition

The sum of concentrations of TM in the leaf litter continuously increased with decomposition at the control site with concentrations 32 times and 48 times higher for *A. marina* and *R. stylosa,* respectively, after 72 days (*Figure III.B-3A & B*). At the urban site, the sum of TM increased prior to a decreasing phase after 28 days for *A. marina* and 56 days for *R. stylosa*. After 72 days of decomposition the sum of TM was 43 times higher

than in the senescent leaves for *A. marina* and 27 times higher for *R. stylosa* (*Figure III.B-3C & D*).

Regardless of site, most TM had significantly higher concentrations in the leaf litter after 72 days of decomposition, relative to the initial concentrations in the senescent leaves. The exceptions were As for *A. marina* and Mn for *R. stylosa* at both sites. Distinct trends were noticed for most TM with litterfall decomposition: 1) increase in concentrations up to 72 days, observed at the control site, 2) increase in concentrations up to 56 days, observed for *A. marina* at the control site and *R. stylosa* at the urban site, and 3) increase in concentrations up to 28 days, for the litterfall of *A. marina* at the urban site (*Figure III.B-3*). Mn for both species and in both mangrove forests, and As for the litterfall of *A. marina,* differed from the other TM with a decreasing phase in the first days of the experiment. For *A. marina* at the urban site, Cu and Zn also showed a decreasing phase in the first days of the experiment (*Figure III.B-3C*).

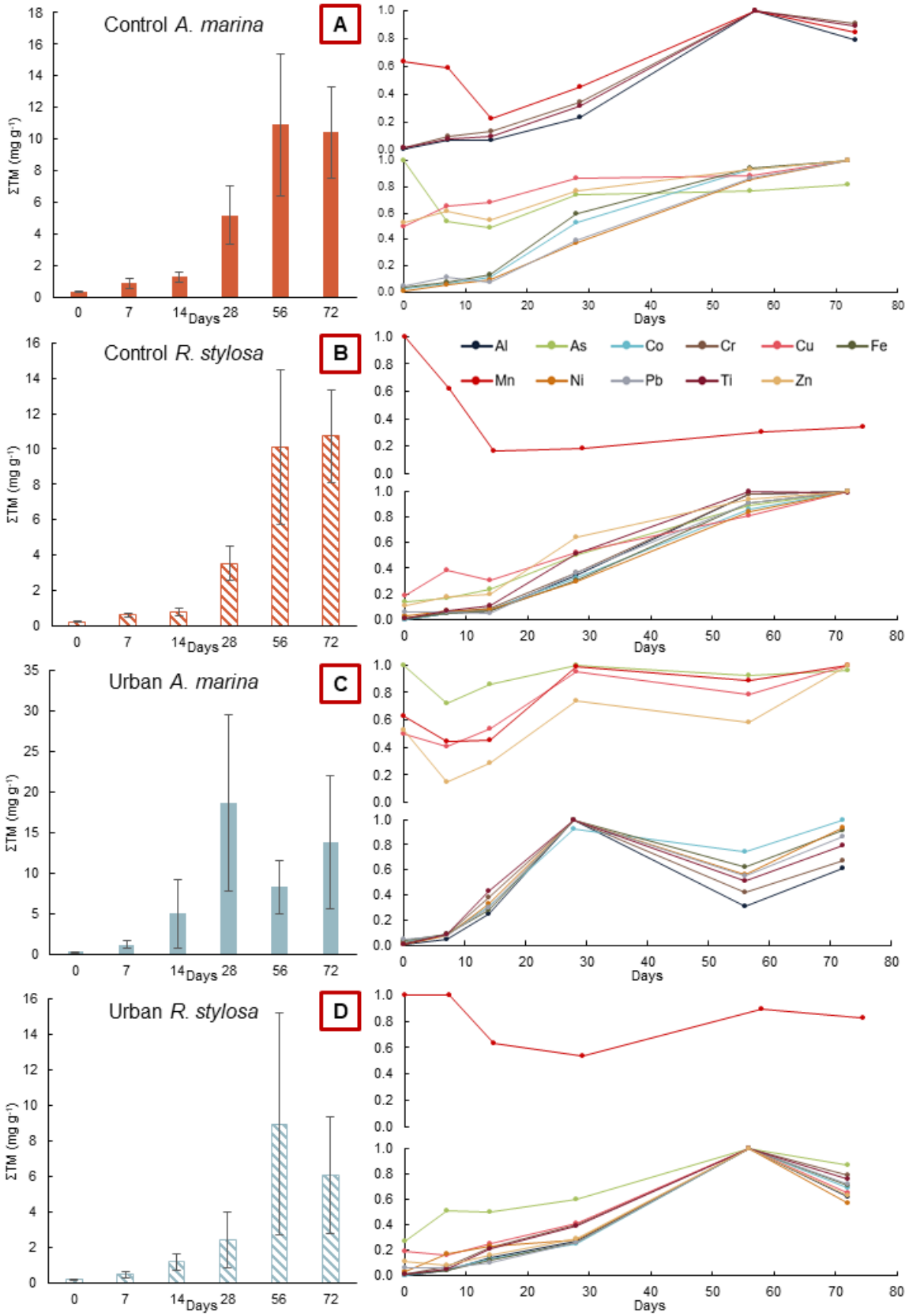

Figure III.B-3. Mean sum of the measured trace metals in mg g^{-1} (SD as error bars) in the litterfall during decomposition and concentrations of the individuals trace metals in the litterfall during decomposition normalized to the highest concentration for each trace metal at the control site for (A) *A. marina* and (B) *R. stylosa* and at the urban site for (C) *A. marina* and (D) *R. stylosa*.

III.B.5. Discussion

III.B.5.1. Initial composition of mangrove leaves differed between species and sites

In the current study, leaf TM concentrations were compared between two sites. Higher concentrations of As, Cr, Fe, and Ni were found in leaves at the control site, likely due to elevated TM levels in the soil. A previous study reported greater soil concentrations for these TM at the control site due to conditions enabling TM storage in soils (Robin et al., 2022). Conversely, Cu and Mn were more concentrated in fresh leaves from the urban site in the present study. Earlier research on the same mangrove area showed significantly higher Cu and Mn in the urban site's soil fractions as they are brought to the forest via the urban runoff (Robin et al., 2022). Furthermore, Co, Cr, and Fe were measured in higher levels in fresh leaves of one or both species at the urban site in the present study. Previous findings demonstrated that leaf bioconcentration factors for these TM were notably higher in the urban site, indicating greater TM transfer from soil to leaves, likely due to salt-TM complexes and pyrite-TM interactions limiting mobility in the control site's soil (Robin et al., 2022). The results suggest that the urban runoff is a factor controlling mangroves leaves' TM concentrations, but other environmental factors may also largely contribute to TM dynamics.

Differences in major element concentrations were observed in senescent leaves between species. In this study, *A. marina* had higher P and K concentrations compared to *R. stylosa*, while *R. stylosa* had elevated Na and Ca concentrations, as previously observed in other mangrove forests (Clough, 1984; Steinke and Ward, 1987; Tam et al., 1990; Alongi, 2021). High *R. stylosa*'s Na and Ca concentrations may be due to the proximity of the stand to the sea as suggested in another study on mangrove leaves chemical composition (Ahmed et al., 2010). The K^+ and Na^+ balance differences between the salt excluder (*R. stylosa*) and salt secretor (*A. marina*) species likely explain the K concentration variation (Parida and Jha, 2010; Ray et al., 2021). Lower P levels in *R. stylosa*'s senescent leaves may be attributed to P redistribution within fresh tissues to limit losses during litterfall, which also accounts for higher P values in fresh leaves (Kathiresan and Bingham, 2001). The higher P concentrations in the leaves of *A. marina* may result from enhanced P transfer facilitated by its microbial community on the forest floor rich in phosphatase-producing bacteria, as indicated in prior research (Abhijith et al., 2018).

Regarding differences in fresh and senescent leaves, three factors play a role including the species position in the forest, salt tolerance mechanisms, and metabolism. The subsequent discussion assesses the impact of these factors on major element content evolution during leaf litter decomposition.

III.B.5.2. Evolution of major elements during leaf litter decomposition

III.B.5.2.1. An expected order of lability for the major elements

For both species and sites, K showed the fastest leaching among major elements. Literature shows K concentration drops rapidly initially due to leaching, then stabilizes during mangrove litter decomposition (Steinke and Ward, 1987; Tam et al., 1990; Chale, 1993; Hossain et al., 2014; Vinh et al., 2020). K^+ is highly mobile, lacking structural roles in plants, making it more labile than other cations (Steinke and Ward, 1987; Bonanomi et al., 2010). Similarly, Mg concentration quickly decreases during initial leaching before stabilizing, consistent with literature findings in multiple environments (Bonanomi et al., 2010; Gautam et al., 2016; Vinh et al., 2020). Partial Mg leaching in early decomposition may be due to the absence of complex organic binding, as suggested in the literature (Van Der Valk and Attiwill, 1984). The major element lability sequence in this study follows K > Mg > Ca > P, aligning with previous litterbag experiments (Bonanomi et al., 2010; Gautam et al., 2016). This confirms consistent major element lability in litterfall for both species. Hence, we suggest that the urban runoff has no impact on the major element lability order in litterfall.

III.B.5.2.2. Major elements evolution influenced by the urban runoff

In the urban forest, K and Mg decayed faster under *R. stylosa* than *A. marina*. *R. stylosa*'s floor stays submerged by ongoing runoff, potentially enhancing leaching. The change in Na concentrations during the decomposition of the leaf litter was site-specific, potentially associated with the forest structure or soil physico-chemical parameters. At the urban site, the rate of Na loss exceeded the rate of mass loss (Robin et al., submitted), with a half-life of 24 days for *R. stylosa*, similar to that obtained in a tropical mangrove forest in Vietnam during the rainy season, suggesting that the runoff affects Na loss comparable to high pluviometry (Vinh et al., 2020). In the present study, the release of Na to the surroundings was greater in the first days of decomposition suggesting that loss is due to leaching. Water-soluble Na in leaves may encourage leaching, and the low salinity of the urban runoff (0 g L^{-1}) (Robin et al., 2022) might promote this process in flooded *R. stylosa* areas. The high salinity at the control site (35 g L^{-1}) and higher Na content, possibly contributes to increasing Na levels during litter decomposition. Finally, P enrichment was significantly greater at the urban site, reaching 400% after 72 days, implying urban runoff may be a source of P (garden fertilizers and pet waste).

The urban runoff therefore enhances K, Mg, and Na leaching during litter decomposition due to its low salinity and its continuous flow through the mangrove forest,

especially for *R. stylosa*. The runoff also seems to influence major element dynamics during leaf litter decomposition as it can be a source of elements such as P.

III.B.5.2.3. Major elements evolution may be influenced by the species position

Ca concentration in *R. stylosa* leaf litter linearly declined at both sites, while *A. marina* showed an increase over the 14 first days of decomposition before loss. Initial Ca content was 4.5 times higher in *R. stylosa* than *A. marina*, possibly making its Ca more leachable. Stand immersion may have influenced Ca evolution as well, aligning with results from a river-influenced mangrove in Vietnam (Vinh et al., 2020). In the study in Vietnam, greater loss occurred in more flooded areas like the *R. stylosa* stands of the current study, submerged by tides or runoff. Ca complexation with refractory compounds may explain the initial increase in Ca content in the leaf litter of *A. marina*.

In the present study, the P concentration in the leaf litter of *A. marina* remained stable, but the concentration in the litter of *R. stylosa* increased relative to senescent leaves at both sites. Literature typically shows mangrove litter P decrease initially due to leaching (Steinke and Ward, 1987; Tam et al., 1990; Mfilinge et al., 2002; Sánchez-Andrés et al., 2010; Hossain et al., 2014; Vinh et al., 2020), then microbial use (Chale, 1993). P rise during decomposition can result from complexation of P with refractory molecules (Vinh et al., 2020) or floor-to-litter transfer via bacteria or fungi (Lindahl et al., 2007). We suggest that the increase in P content in the litter of *R. stylosa* might be due to water column P input, and therefore be dependent on the stand position in the forest. Initial leaf composition may also contribute to the evolution of P; *R. stylosa* had 5 times less P in senescent leaves than *A. marina*, potentially offering more P capture sites.

In summary, Ca and P evolution during decomposition are species-specific. Hydroperiod-driven Ca loss and P enrichment depend on species' forest positions. Initial litter composition also influence trends based on species. In this study, major elements showed evolution variations depending on the element, the mangrove forest, and the mangrove species. Next, we will discuss if those parameters also influence TM evolution during leaf litter decomposition.

III.B.5.3. Evolution of trace metals during leaf litter decomposition

III.B.5.3.1. An expected trace metal enrichment during leaf litter decomposition

All TM, except As and Mn, exhibited higher concentrations in the leaf litter after 72 days of decomposition compared to senescent leaves, aligning with literature expectations (Rice and Windom, 1982; Ramos e Silva et al., 2006; Vinh et al., 2020). The enrichment of TM during decomposition relates to their exchange from forest soil or water column to

leaf litter on the soil surface (Silva et al., 1998). Microbial immobilization through TM uptake by microbial biomass or TM complex formation with microbial-produced extracellular material can also enhance TM accumulation in leaf litter (Rice and Windom, 1982). Additionally, a previous study on the same samples showed the positive evolution of N in decomposing litterfall (Robin et al., submitted), which likely leads to TM accumulation due to complex formation with N-rich compounds like proteins (Rice and Windom, 1982). Still, initial leaching phases were observed for some TM (As, Cu, Mn, Zn).

III.B.5.3.2. Initial leaching of trace metals controlled by their states and concentrations in porewaters

As, Cu, Mn, and Zn displayed initial leaching upon litterfall decomposition. Leaching of As was observed only for *A. marina* litter, possibly indicating molecular binding. In a prior study using the same samples as the present study, it was observed that the leaf litter of *A. marina* initially contained more lignin than that of *R. stylosa*. However, within the first seven days of decomposition, a significant reduction in lignin content was observed for *A. marina* (Robin et al., submitted). Therefore, we suggest that As may form complexes with lignin molecules. Urban site Cu and Zn also showed leaching before enrichment in the litterfall of *A. marina*, a pattern observed in previous mangrove litterbag experiments (Ramos e Silva et al., 2006; Vinh et al., 2020). Cu and Zn concentrations in upper soil porewaters (0-5 cm) were notably lower beneath *A. marina* at the urban site (*Supplementary Figure III.B-1*), suggesting favorable exchange from litterfall in early decomposition.

Mn alone exhibited relative concentration decrease in the first weeks for both species and sites, which was also observed during a litterbag experiment in a Vietnamese mangrove forest (Vinh et al., 2020). Mn is expected to be more leachable than other TM such as Fe and Zn as it is less able to bound with refractory molecules (Silva et al., 1998). Mn's soluble form in leaves (Mn^{2+}) (Joardar Mukhopadhyay and Sharma, 1991), easily solubilized during decomposition, may not oxidize to immobilized Mn^{4+} due to mangrove floor anoxia (Vinh et al., 2020).

Loss of TM from litterfall appears element-dependent, influenced by oxidation state, molecular interactions, and porewater concentrations. Results of the present study also show differences in TM enrichment between stands and is discussed next.

III.B.5.3.3. Differences between stands due to trace metal bioavailability and species absorption capacity

While most TM concentrations were generally higher in decomposed litterfall than senescent leaves, diverse evolutions were observed. At the urban site, peak TM concentrations relative to bulk leaf litter occurred at 28 days for *A. marina* and 56 days for

R. stylosa. In contrast, at the control site, these peaks were reached at 56 or 72 days for *A. marina* and 72 days for *R. stylosa*. A recent study on the same sites has indicated higher TM bioavailability in the urban soils compared to the control soils (Robin et al., 2022). The higher bioavailability was linked to a greater proportion of TM in the refractory soil fraction at the control site (Robin et al., 2022). Elevated root and leaf bioconcentration factors for most TM were significantly higher at the urban site, potentially leading to enhanced TM transfer from mangrove soil to litterfall (Marchand et al., 2016).

In absolute concentrations (µg g^{-1}), peak TM concentrations in *A. marina* litterfall at the urban site surpassed those in the other three areas (*Supplementary Table III.B-2*). This suggests that maximum TM concentrations were attained earlier during litter decomposition of *A. marina*, possibly due to the leaf litter reaching its absorption limit. Additionally, absolute TM concentrations showed the litterfall of *A. marina* had higher levels than the litter of *R. stylosa* in the initial decomposition days at both sites. However, after 56 days at the urban site and 72 days at the control site, leaf litter of *R. stylosa* exhibited higher total TM concentrations and the majority of individual TM concentrations (*Supplementary Table III.B-2*). Tidal flooding at the control site and consistent urban rainwater flow at the urban site favor redox reactions on the floor of *R. stylosa* stands, increasing biogeochemical reactivity that influences TM precipitation-dissolution cycles (Noël et al., 2014), potentially facilitating TM export or transfer to litterfall on the soil surface. Prior work by Marchand et al., (2016) indicated decreasing TM stocks in mangrove soil closer to the shoreline. We suggest that the stand immersion influences TM accumulation in mangrove litter.

III.B.6. Conclusion

The comparison between an urban mangrove forest and a control mangrove forest highlighted that continuous urban rainwater runoff enhances leaching of specific major elements (K, Mg, Na) during litterfall decomposition and could serve as a P source. However, this runoff did not alter major element lability order and is not the sole influencer of element dynamics in litter decomposition. Ca and P evolution exhibited species-specific patterns tied to stand position, hydroperiod, and potentially initial litter composition. TM primarily increased during litterfall decomposition, implying a transfer from forest floor to litterfall. As and Mn diverged due to complexation and oxidation state differences. Like major elements, urban runoff appeared to impact TM enrichment, boosting TM bioavailability for forest floor-to-litter transfer. Initial litter composition and species physiology shaped TM absorption capacity during decomposition. Future research could assess leaf litter's contribution to exported TM and nutrients in adjacent ecosystems as

the results obtained here suggest that the urban site may contribute more than the control site to the export of potentially toxic TM but also nutrients.

III.B.7. Acknowledgements

The authors acknowledge Monika Le Mestre for ICP-OES analysis. The authors also acknowledge Pierre Sanlis for the help with the field work. This work was supported by the CRESICA and Banque de la Nouvelle-Calédonie, Cegelec, SECAL, and Fibrelec via the University of New Caledonia Foundation.

III.B.8. Supplementary materials

Supplementary Table III.B-1. Quality control of biota inductive coupled plasma measurements using the certified reference material IPE Sample ID 949, with z-score and detection limits.

Element	Standard mean value (mg g^{-1})	Standard deviation value (mg g^{-1})	Measured value (mg g^{-1})	z-score	Detection limit (mg kg^{-1})
Cd	0.00041	0.00004	0.00040	- 0.20	0.00003
Co	0.00010	0.00002	0.00053	0.19	0.0093
Cr	0.00051	0.00010	0.00015	2.33	0.0126
Cu	0.00667	0.00058	0.00601	- 1.13	0.0111
Fe	0.2001	0.0225	0.2048	0.17	0.0546
Mn	0.01972	0.00184	0.01738	- 1.27	0.0093
Ni	0.00042	0.000006	0.00041	- 1.54	0.0177
Pb	0.00086	0.00014	0.00099	0.91	0.00003
Zn	0.104	0.008	0.102	-0.29	0.012

Supplementary Table III.B-2. Trace metal mean (±SD) concentrations in the litter during decomposition in μg g^{-1} of dry weight.

Control *A. marina*											
Days	Al	As	Co	Cr	Cu	Fe	Mn	Ni	Pb	Ti	Zn
7	282 ±193	2.2±0.6	0.3±0.1	2.6±1.3	5.7±0.8	505 ±153	32±2	3.5±1.5	0.2±0.1	10±6	11±2
14	306 ±106	2.0±0.5	0.4±0.1	3.8±1.1	6.0±1.0	909 ±307	12±1	6.3±1.6	0.1±0.1	12±6	9.5±1.9
28	1004 ±489	3.0±0.8	1.9±0.5	9.5±2.6	7.6±1.3	4032 ±1788	24±4	25±4	0.6±0.2	40±19	13±4
56	4283 ±2746	3.2±0.8	3.4±0.6	28±10	7.7±1.7	6340 ±1914	54±21	57±8	1.3±0.5	125±59	16±4
72	3402 ±1683	3.3±0.3	3.7±0.5	25±7	8.8±1.7	6734 ±1331	46±13	66±8	1.5±0.3	112±45	17±2
Control *R. stylosa*											
Days	Al	As	Co	Cr	Cu	Fe	Mn	Ni	Pb	Ti	Zn
7	225 ±54	0.4±0.2	0.2±0.0	2.4±0.4	1.2±0.7	257 ±50	97±17	4.7±0.7	0.1±0.1	8.0±3.0	1.9±0.3
14	334 ±110	0.5±0.3	0.3±0.1	3.6±1.4	1.0±0.2	378 ±100	26±9	5.5±2.1	0.1±0.1	13±4	2.1±0.3
28	1627 ±482	1.1±0.3	1.3±0.2	15±4	1.7±0.3	1740 ±446	29±9	20±4	0.5±0.2	63±22	6.8±4.5
56	4556 ±2321	2.0±0.9	3.4±1.3	41±19	2.5±0.8	5248 ±2048	48±20	56±22	1.2±0.5	124±41	10±3
72	4649 ±1302	2.3±0.6	4.0±0.9	42±15	3.1±0.4	5761 ±1609	53±19	68±19	1.3±0.3	123±23	11±2
Urban *A. marina*											
Days	Al	As	Co	Cr	Cu	Fe	Mn	Ni	Pb	Ti	Zn
7	484 ±286	2.4±0.7	0.3±0.1	2.7±1.3	6.5±0.7	652 ±163	49±5	1.4±0.9	0.2±0.2	18±11	15±4
14	2627 ±2548	2.8±0.3	1.0±0.5	11±8	8.6±1.4	2167 ±1540	51±21	6.4±4.5	0.9±0.6	89±64	28±11
28	10473 ±6608	3.3±0.5	2.9±1.3	30±17	15±4.1	7701 ±4075	109±38	20±10	2.9±1.7	207±108	73±29
56	3199 ±1803	3.0±0.5	2.3±1.0	13±5	13±3	4807 ±1666	98±32	11±5	1.6±0.5	105±35	57±33
72	6404 ±5312	3.1±0.3	3.2±1.4	20±12	16±4	7025 ±2763	111±46	18±9	2.5±1.3	164±71	98±60
Urban *R. stylosa*											
Days	Al	As	Co	Cr	Cu	Fe	Mn	Ni	Pb	Ti	Zn
7	153 ±77	0.6±0.2	0.1±0.1	0.9±0.4	1.0±0.3	221 ±83	102±11	2.1±0.8	0.1±0.1	6.0±3.0	4.0±2.4
14	501 ±247	0.6±0.2	0.3±0.1	3.0±1.3	1.5±0.3	608 ±213	65±17	2.8±1.1	0.1±0.1	25±12	7.7±4.1
28	1000 ±774	0.8±0.2	0.6±0.3	5.4±3.0	2.5±0.9	1287 ±772	54±14	3.4±2.4	0.3±0.3	46±33	14±10
56	3683 ±3116	1.3±0.6	2.3±1.4	13±7	6.2±3.3	4982 ±3134	90±36	12±8	1.3±0.9	118±70	47±37
72	2302 ±1722	1.1±0.4	1.6±0.6	10±4	4.1±1.4	3529 ±1787	84±51	6.8±3.1	0.9±0.5	90±50	30±11

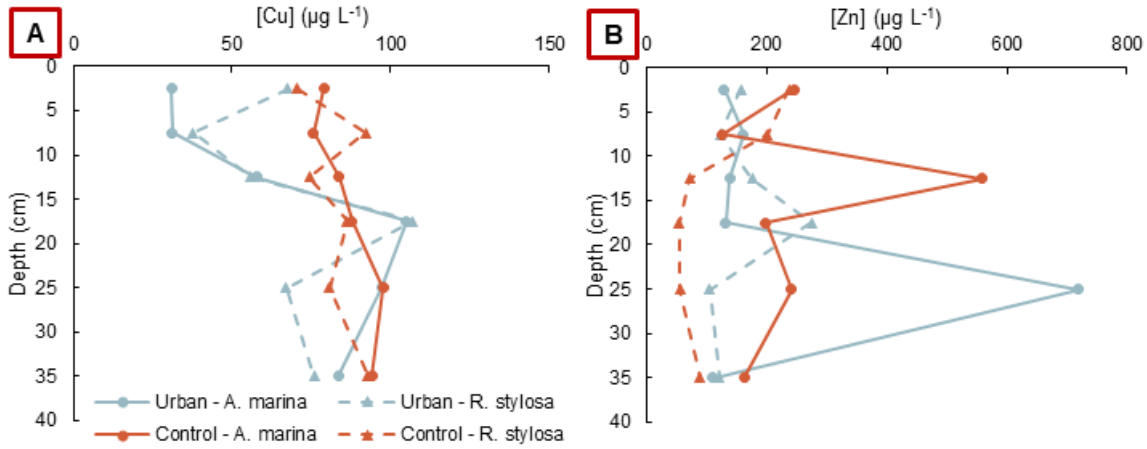

Supplementary Figure III.B-1. (A) Copper and (B) zinc concentrations in porewaters in µg L^{-1} at at the urban and control sites beneath *A. marina* and *R. stylosa*.

IV. Chapter IV: Organic matter dynamics in mangrove soils: Insights on preservation and diagenetic processes

Robin, S.L., Baudin, F., Le Milbeau, C., Alfaro, A.C., Marchand, C., in prep. Sources and decay processes of organic matter in mangrove soils in semi-arid climate. *Geochimica et Cosmochimica Acta*.

Robin, S.L., Baudin, F., Le Milbeau, C., Marchand, C., submitted. Millennial-aged organic matter sequestration and preservation in anoxic and sulfidic mangrove soils: insights from isotopic and molecular analyses*. Science of the Total Environment*.

Robin, S.L., Baudin, F., Le Milbeau, C., Alfaro, A.C., Marchand, C., in prep. Influences of urban runoff on mangrove organic matter sources and transformation. *Geoderma*.

Présentation :

Le chapitre III aborde une composante de la MO dans les mangroves, à savoir la litière végétale. Cette litière peut se dégrader au sein de la mangrove, s'intégrant ainsi dans le pool de MO du sol. Les autres composantes de la MO du sol sont soit autochtones, provenant de la décomposition de la faune, des invertébrés benthiques ou du microphytobenthos qui se développe à la surface du sol, soit allochtones, venant soit de la mer avec les marées (phytoplancton, algues), soit du bassin versant avec les pluies ou les rivières (débris végétaux terrestres). Plusieurs études ont été menées pour déterminer l'origine de la MO présente dans les sols de mangrove à travers le monde, principalement en utilisant des outils isotopiques (Dittmar et al., 2001; Bouillon and Dahdouh-Guebas, 2003; Bala Krishna Prasad and Ramanathan, 2009; Aschenbroich et al., 2015). Ces études comparent notamment les contributions des MO autochtones et allochtones dans le pool de MO du sol en fonction de la géomorphologie, du climat et des espèces présentes. Une fois intégrée dans le sol, la MO peut être partiellement ou entièrement lessivée ou décomposée par les communautés microbiennes (bactéries, champignons, archées) ou être préservée et enfouie pendant plusieurs milliers d'années (Kristensen et al., 2008). Les processus de décomposition et de préservation de la MO dans les sols de mangrove ont également été largement étudiés en utilisant différents types de facteurs (Lacerda et al., 1995; Alongi et al., 2000; Jennerjahn and Ittekkot, 2002; Gonneea et al., 2004; Ezcurra et al., 2016; Kida et al., 2019a). L'étude des processus diagenétiques dans les sols de mangrove est complexe car les paramètres utilisés peuvent fournir des informations sur l'origine de la MO et/ou son taux de décomposition. Il est donc nécessaire d'effectuer ces analyses avec un maximum de proxys possibles.

Le chapitre IV vise à étudier l'origine et les processus de diagenèse et de préservation de la MO. Bien que de nombreuses études aient été menées à ce sujet, très peu ont examiné les mangroves semi-arides, sachant que le climat est un facteur pouvant influencer de nombreux paramètres liés à la dynamique de la MO tels que la pluviométrie et la production primaire des palétuviers. De plus, ce chapitre utilise une combinaison de proxys rarement répertoriée dans la littérature, ce qui permet une analyse robuste du système : les isotopes stables, les paramètres Rock-Eval et les analyses moléculaires de lignine et de sucres neutres.

La dynamique de la MO est intéressante à étudier dans cette mangrove contrôle également car une couche enfouie datant d'environ 4 000 ans a été détectée. En effet, certaines mangroves de la côte Ouest de la Nouvelle-Calédonie semblent contenir une couche enfouie riche en MO, comprenant notamment des racines préservées de l'espèce

Rhizophora (*Figure IV-1*) (Marchand et al., 2011b, 2011a, 2012; Deborde et al., 2015; Jacotot et al., 2018). Cette couche résulte d'une préservation significative de la MO pendant une période de stabilité du niveau de la mer. Vers environ 4 500 ans cal BP, le niveau de la mer sur la côte Ouest de la Nouvelle-Calédonie était environ 1.1 m plus élevé qu'aujourd'hui et est resté stable pendant 3 700 ans. Vers environ 2 800 ans cal BP, le niveau de la mer a commencé à baisser, entraînant une migration des espèces de palétuviers (Mitrovica and Peltier, 1991; Yamano et al., 2014; Nunn and Carson, 2015). L'espèce *Rhizophora* s'est déplacée avec la mer vers des zones topographiques plus basses, tandis que *A. marina* et le tanne ont colonisé l'espace autrefois occupé par *Rhizophora*.

Figure IV-1. Couche enfouie riche en matière organique avec indication (flèche) de tissus d'une racine de *R. stylosa* préservée dans cette couche.

Dans la partie A de ce chapitre, l'objectif est de déterminer les origines de la MO dans le sol et les mécanismes de dégradation liés aux conditions de rédox. Aussi, divers indicateurs sont utilisés pour déterminer les molécules labiles et réfractaire dans le sol. Les analyses isotopiques et moléculaires (lignine et sucres) indiquent que la MO du sol est principalement d'origine autochtone (débris de palétuviers). Pour le sol sous *A. marina*, les principaux contributeurs à la MO sont les débris de litière et les racines d'*A. marina*, ainsi que le microphytobenthos se développant à la surface du sol. La litière d'*A. marina* semble avoir subis des processus de dégradation importants avant incorporation dans le sol. En revanche, sous *R. stylosa*, les principales sources de MO sont les racines de *R. stylosa* et les débris de litière d'*A. marina*, probablement apportés par les marées. La MO dérivée d'*A. marina* et de *R. stylosa* présente des caractéristiques distinctes en raison de leurs positions respectives au sein de la forêt de mangrove et de leurs compositions chimiques uniques. Après intégration dans le sol, la dégradation de la MO se produit sous les deux espèces, caractérisée par une déshydrogénation ; cependant, la présence de conditions anoxiques limite l'oxygénation de la MO pendant la diagenèse.

L'environnement anoxique plus prononcé sous *R. stylosa* restreint la décomposition de la MO par rapport à *A. marina*, dont la MO du sol est principalement composée de composés matures. Les observations sur la lignine totale et les sucres neutres révèlent un comportement généralement labile dans le sol de mangrove. L'ordre de labilité des groupes phénoliques reflète celui de la litière développé dans le chapitre III. Les mécanismes de dégradation de la lignine dans le sol de mangrove englobent le clivage de cycle, la perte de -OCH_3 et, de manière surprenante, l'oxydation de la chaîne latérale dans le sol anoxique sous *R. stylosa*. Les comportements distincts des sucres neutres individuels en fonction de la profondeur et entre les sols indiquent une dégradation sélective, potentiellement influencée par des caractéristiques réfractaires ou par les communautés microbiennes.

La partie B de ce chapitre se concentre sur une couche enfouie riche en MO présente dans les sols de mangroves de la côte Ouest de Nouvelle-Calédonie, résultant d'une longue période de stabilité du niveau de la mer durant l'Holocène. Cette partie vise à caractériser isotopiquement et moléculairement cette couche enrichie en MO, tout en identifiant les processus de décomposition et de préservation dans ces conditions anoxiques et sulfureuses. Les rapports isotopiques stables indiquent que les racines de *R. stylosa* sont principalement à l'origine de la MO présente dans cette couche. Les mécanismes de dégradation comprennent la déshydrogénation et la perte de sucres neutres majeurs, tandis que les processus de préservation impliquant l'arabinose, la vanilline et le p-hydroxyacétophénone contribuent à la stabilisation de la MO. La présence de matériel racinaire bien préservé associé à la pyrite constitue une preuve tangible des interactions entre la MO et les minéraux, renforçant la préservation dans des environnements anoxiques et sulfureux. Grâce à la datation au radiocarbone, la couche enrichie en MO est replacée dans le contexte historique d'une période caractérisée par des niveaux de mer stables, il y a environ 4 000 ans, soulignant l'impact profond de la stabilité prolongée sur l'accumulation de MO.

La partie C de ce chapitre se penche sur les effets des eaux de ruissellement urbain sur les sources et les processus de la MO au sein de la mangrove urbaine. L'étude a englobé une analyse approfondie de plusieurs paramètres, notamment les isotopes stables, la pyrolyse Rock-Eval, et des analyses moléculaires telles que la lignine et les glucides neutres. Les résultats de cette étude ont révélé que le pool de MO du sol était principalement composé de MO autochtone, similaire à ce qui a été observé sur le site contrôle. La décomposition précoce de la litière d'*A. marina* avant intégration dans le sol a pour conséquence une MO moins labile, résultant en une augmentation relative de la lignine et des sucres dans le sol. Cependant, dans le cas de *R. stylosa*, le pool de MO du

sol était également influencé par les eaux de ruissellement urbain, agissant comme une source de ^{15}N et favorisant le développement microbien en surface du sol. Cette différence dans les valeurs de $\delta^{15}N$ entre les sites pourrait être attribuée à l'apport des eaux de pluie urbaines, potentiellement porteuses de niveaux élevés de ^{15}N. De plus, l'étude a montré des disparités dans la teneur en TOC, les paramètres Rock-Eval et les glucides neutres entre les deux sites, suggérant une certaine influence des effluents urbains sur les communautés microbiennes et la teneur en glucides. Cependant, l'étude n'a pas définitivement établi l'impact des eaux de ruissellement urbain sur la dynamique de la lignine dans les sources de MO et dans les sols, car ces différences pourraient être influencées par divers facteurs, notamment les communautés microbiennes et la composition initiale. En conclusion, il n'y a pas de preuve concluante d'une influence significative et directe des eaux de ruissellement urbain sur la séquestration et la transformation de la MO dans les sols de mangrove. Néanmoins, les résultats indiquent des impacts discernables sur les communautés microbiennes et les sources de MO, qui, à leur tour, peuvent affecter la dynamique de la MO dans les sols de mangrove.

A. Chapter IV.A: Sources and diagenesis of organic matter in mangrove soils in semi-arid climate

Sarah Louise ROBIN, François BAUDIN, Claude LE MILBEAU, Andrea C ALFARO, Cyril MARCHAND

To be submitted to Geochimica et Cosmochimica Acta

IV.A.1. Abstract

Organic matter (OM) dynamics in mangrove forests have been studied extensively in terms of the capacity of their soils to store organic carbon. While $\delta^{13}C$, $\delta^{15}N$, and C/N values for mangrove soils and sources are well reported, other indicators of OM maturity and composition are lacking. In this study, soil OM sources and decomposition processes were investigated for a semi-arid bay head mangrove forest in New Caledonia. Mangrove tissues and 20-cm soil cores were collected in monospecific stands of *Avicennia marina* and *Rhizophora stylosa*. The isotopic compositions of the samples were assessed, along with their molecular compositions (lignin-derived phenols and neutral carbohydrates). Rock-Eval pyrolysis was also performed on the samples to investigate OM characteristics. Results showed that soil OM was dominated by autochthonous OM, incorporated into the soil as fresh or already highly mineralized. Once in the soil, stable isotope ratios and Rock-Eval parameters followed similar trends beneath both species. However, the more anoxic conditions beneath *R. stylosa* limited OM decomposition as shown by the lower TpS2 values. Surprisingly, neutral carbohydrates and lignin-derived phenols were both lost at higher rates than bulk organic carbon beneath both species. Selective degradation of individual compounds was observed, and species-dependent variations associated with the redox conditions and the OM sources were identified. We suggest that lignin was degraded, even in anoxic environments, because of the amount of labile lignocellulosic components in the soil. The main mechanisms of lignin degradation are loss of $-OCH_3$ groups and ring cleavage, even though side-chain oxidation seemed to occur beneath *R. stylosa*, possibly due to the micro-oxidative environments.

Keywords: mangrove, stable isotopes, Rock-Eval, lignin, neutral carbohydrates

IV.A.2. Introduction

Mangrove forests are intertidal ecosystems developing between the latitudes 30°S and 30°N. While representing less than 0.5% of worldwide forests, mangroves are one of the most efficient carbon sinks in the world. Mangrove forests represent 17% of the total tropical marine organic carbon (OC) stocks, with mean stocks of 739 Mg OC ha^{-1}

compared to 317 Mg OC ha^{-1} for salt marshes and 315 Mg OC ha^{-1} for terrestrial tropical forests (Alongi, 2020). The large carbon stocks of mangrove forests are attributed to the high productivity of the ecosystem with an estimated net primary productivity of 11 Mg C ha^{-1} yr^{-1} (Alongi, 2014), and a mean rate of carbon sequestering efficiency in the soil of 180 g OC m^{-2} yr^{-1} compared to 5.69 g OC m^{-2} yr^{-1} for coral reefs and 62.5 g OC m^{-2} yr^{-1} for terrestrial tropical forests (Alongi, 2020). The sedimentation rates of mangrove forests are usually high, with an average accretion of 5 mm yr^{-1}, due to the high density root systems of mangrove trees, and their low topography (Alongi, 2002; Woodroffe et al., 2016). The anoxic conditions of mangrove soils limit organic matter (OM) aerobic decomposition and therefore, OM sequestration, and preservation is favored (Kristensen et al., 2008). The majority of the OM pool is refractory in mangrove soils, and therefore, once the labile pool has been oxidized, the refractory pool remains rather constant (Alongi et al., 2000). Total OM content can reach up to 40% in mangrove soils (Lallier-Vergès et al., 1998). High net primary productivity, high sedimentation rates, and soil anoxia are the main factors making mangrove soil a favorable reservoir for long-term OC sequestration (Jennerjahn and Ittekkot, 2002; Kristensen et al., 2008; Alongi, 2014).

Sources of OM in mangrove soil can be autochthonous and allochthonous. Autochthonous OM comes from mangrove leaves, roots, decomposed fauna, and the microphytobenthos developing on the soil surface. The autochthonous OM quality and quantity depend on the mangrove species, climate, outwelling, and physico-chemical conditions of the mangrove habitat (Twilley, 1988; Bouillon and Dahdouh-Guebas, 2003). Allochthonous OM is transported to the mangrove forest from the watershed (terrestrial OM) or from the tides (marine OM) (Kristensen et al., 2008). The allochthonous OM in a mangrove forest is controlled by the ecology of adjacent ecosystems, the geomorphology of the mangrove forest, tides, and terrestrial water sources, including river flows or anthropogenic effluents (Sweeney et al., 1980; Cifuentes et al., 1996; Machiwa, 2000; Bouillon and Dahdouh-Guebas, 2003). Studies have shown that up to 80% of suspended sediments can be trapped in mangrove forests during flooding (Furukawa et al., 1997). Multiple parameters are characteristic to each source type and may be used to trace OM origin in mangrove soils (Cifuentes et al., 1996; Gonneea et al., 2004; Regina Hershey et al., 2021).

All the OM that has not been exported by tidal flow is sequestered in mangrove soil and is subject to degradation via leaching with tidal activity, crab activity, and/or decomposition through oxic, suboxic, or anaerobic decay processes (Lallier-Vergès et al., 1998; Kristensen et al., 2000). Degradation by tidal activity is therefore mainly controlled by forest structure, while microbial decomposition is affected by the reactivity of the OM

and the physico-chemical conditions of the soil (Gonneea et al., 2004). The decomposition rates of OM in the soil are determined in part by the nature of the OM, as some molecules (e.g., starch and carbohydrates) are more labile than others (e.g., lignin) (Lallier-Vergès et al., 2008; Chen et al., 2019). OM decomposition starts with the leaching of soluble organic substances, while the more refractory compounds are decayed much less easily, especially in anoxic environments, favoring OM sequestration in mangrove soil (Kristensen et al., 2008). The various parameters characterizing OM must therefore be analyzed carefully as they give information on the sources and the diagenetic processes at the same time.

To determine the OM origin, a combination of proxies must be used, including the quality and the decomposition processes of OM in mangrove soil. Common parameters for tracing OM sources in mangrove forests are stable isotope ratios ($\delta^{13}C$ and $\delta^{15}N$) and C/N ratio, since the stable isotope ratios of OM are preserved during natural transformations (Machiwa, 2000; Dittmar and Lara, 2001; Bouillon et al., 2002; Gonneea et al., 2004; Schwamborn and Giarrizzo, 2015). Rock-Eval analysis, usually used for petroleum applications, allows the tracing of OM sources and OM transformation with the use of indicators such as the hydrogen index (HI), the oxygen index (OI), and the temperature at the maximum of S2 peak (TpS2) (Behar et al., 2001; Disnar et al., 2003; Sebag et al., 2016). The temperature of the furnace is gradually increased during a heating cycle. As the temperature rises, the organic compounds present in the soil begin to decompose and release gases and volatile organic compounds that are collected and analyzed allowing conclusions to be drawn about the quantity and quality of the OM contained in the soil. These indicators have been previously used in determining OC sources in mangrove soils, but have not yet become a permanent proxy of OM in mangrove forest research (Marchand et al., 2008). In addition, molecular proxies such as neutral carbohydrates and lignin-derived phenols indicate OM maturity and diagenesis processes in mangrove soils (Dittmar and Lara, 2001; Marchand et al., 2005, 2008; Duan et al., 2020). After cellulose, lignin is the most abundant biopolymer occurring in the cell walls of vascular plant tissues (Hamilton and Hedges, 1988). Lignin is not easily degraded in the environment, especially in anoxic soils with an estimation of 2% decay loss per year in sediments below *Rhizophora mangle* stands (Benner et al., 1984), probably because of its molecular structure, making lignin hardly accessible by microorganisms (Dittmar and Lara, 2001). Therefore, mangrove soils are expected to have an enrichment of lignin-derived phenols with diagenesis (Dittmar and Lara, 2001; Marchand et al., 2005; Lallier-Vergès et al., 2008). Neutral carbohydrates may also be used to analyze OM diagenesis and sources within mangrove sediments (Benner et al., 1990; Moers et al., 1990; Lacerda

et al., 1995; Marchand et al., 2005; Duan et al., 2020). During OM microbial degradation, storage carbohydrates are more labile and therefore more easily degraded than structural carbohydrates (Jensen et al., 2005). Vascular plant-derived neutral carbohydrates are characterized by a high proportion of pentoses (xylose and arabinose), while microbial-derived neutral carbohydrates have higher hexose (mannose and galactose) content (Chen et al., 2019). Several neutral carbohydrate ratios can therefore be used to assess the dominant origin of carbohydrates in the soil.

In New Caledonia, soil OM quantity and quality in mangrove forests has been investigated for different purposes using multiple proxies. TOC, HI, and C/N ratios have been used to determine the relationship between OM stocks and trace metal cycling (Marchand et al., 2011a). In addition, stable isotope ratios were used to understand the influence of shrimp effluents on mangrove sediments (Molnar et al., 2014; Aschenbroich et al., 2015), to investigate the relationship between vegetation distribution and element distributions (Deborde et al., 2015), and to determine the quantity of OM stored in the soil (Jacotot et al., 2018). However, the use of molecular proxies to examine OM quality in mangrove soils has never been done in semi-arid mangrove forests. Also, there is a lack of investigation on the diagenetic processes and their relation to mangrove conditions. However, a recent study reported the OM litterfall evolution with degradation using isotopic and molecular indicators (Robin et al., submitted). The study suggests that C/N, $\delta^{13}C$ and $\delta^{15}N$ dynamics are species specific, determined by either the chemical structure of the senescent leaves or the position of the stand. In addition, the molecular composition evolution is primarily determined by the initial composition of the leaf litter with a greater loss of the most concentrated lignin-derived phenols and neutral carbohydrates. The aims of this study are therefore 1) to characterize OM sources in a semi-arid bay head mangrove forest without any river inflow, 2) to identify decomposition processes linked to redox conditions, and 3) to determine the labile and refractory molecules by using multiple OM proxies. A typical mangrove forest of the West coast of New Caledonia with the two dominant mangrove species developing in monospecific stands, *Avicennia marina* and *Rhizophora stylosa*, was chosen as a study site. Soil cores of 20-cm deep were analyzed as well as mangrove OM sources. We hypothesize that the soil OM pool is mainly composed of mangrove-derived debris with a possible contribution of marine OM to the most seaward stand, *R. stylosa*. We also hypothesize that the OM accumulates beneath *R. stylosa*, which shows anoxic conditions, and beneath *A. marina* even though it diffuses oxygen in its rhizosphere. Finally, we hypothesize that neutral carbohydrates related to mangrove-derived OM such as pentoses will show labile behavior, while sugars, such as rhamnose and fucose can be produced in the soil by microbial communities. We expect

the lignin-derived phenols to decay at a lower rate than bulk OC and neutral carbohydrates as it has shown refractory behavior in waterlogged anoxic environments.

IV.A.3. Material & methods

IV.A.3.1. Study site

New Caledonia is an archipelago located in the South Pacific. Mangrove forests cover 80% of the west coast of the main island, which has a semi-arid climate. Two mangrove species prevail on the west coast: *Rhizophora spp.*, which develops on the seaside and represent 55% of the mangrove species, and *Avicennia marina*, which develops on the land side at higher elevation, where it represents 15% of the mangrove species (Marchand et al., 2007). The studied mangrove forest is located on the southwest coast (22°12'10.2"S, 166°26'21.9"E) and has a standard vegetation profile with the two distinct *A. marina* and *R. stylosa stands* (*Figure IV.A-1*). The watershed is characterized by a Cretaceous sedimentary formation (sandstone and limestone) that often hosts volcano-clastic fragments (Service de la Géologie de Nouvelle-Calédonie, 2016).

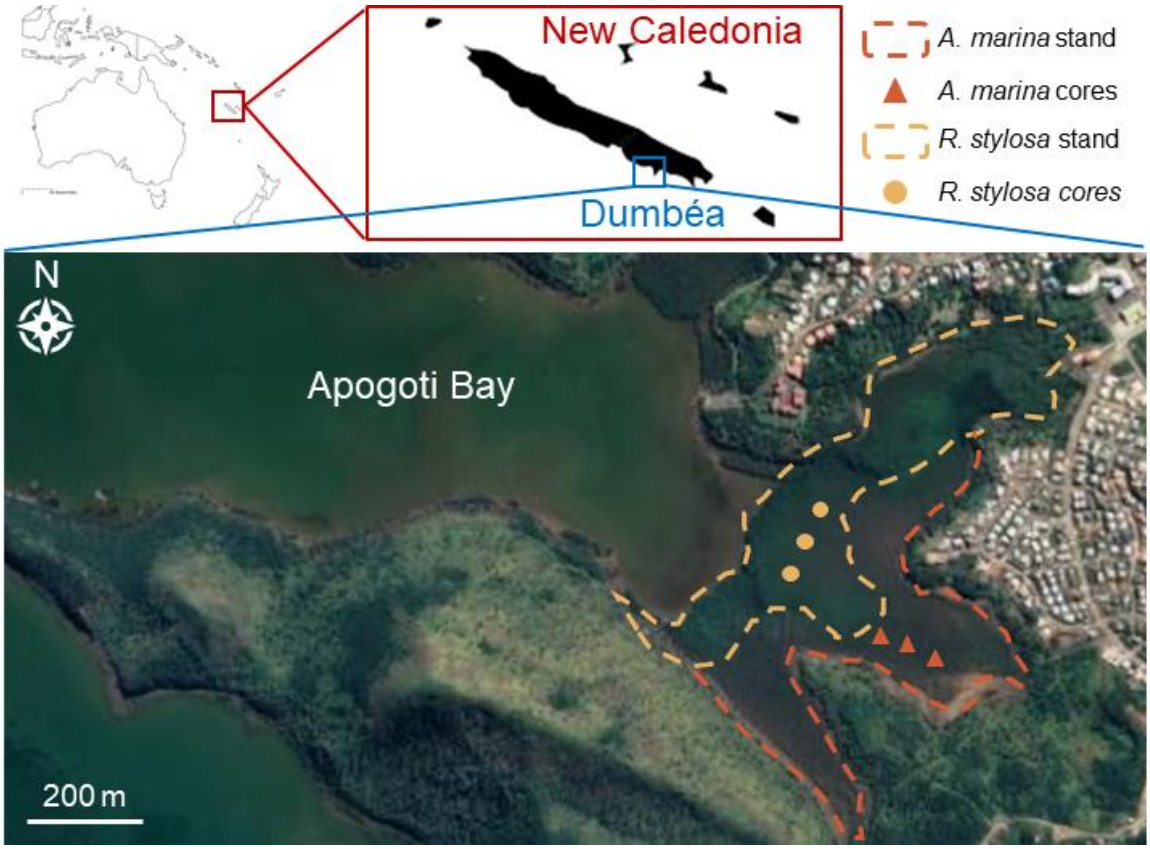

Figure IV.A-1. *R. stylosa* and *A. marina* stands in the mangrove forest of Apogoti Bay in Dumbea, New Caledonia. Satellite image taken in May 2022 (source: Google Earth).

IV.A.3.2. Sampling & sample processing

For both mangrove stands (*A. marina* and *R. stylosa*), soil cores and roots were collected in May 2021. Soil cores of 20-cm depth were collected with an Eijkelkamp gouge auger and cut into 4 depth sections (0-5 cm, 5-10 cm, 10-15 cm, and 15-20 cm). Samples deeper than 20 cm correspond to an older mangrove forest (Robin et al., submitted). Soil samples were transferred into tightly closed plastic bags and frozen upon arrival at the laboratory. Coarse roots from *R. stylosa* trees were cut with a saw. Pneumatophores from *A. marina* trees were gently torn from the main roots and placed into tightly closed plastic bags, and frozen upon arrival at the laboratory. After freeze-drying for 48h, soil samples were sieved through 2-mm mesh sieves and ground with a ball mill. Root samples were ground with a cutting mill. Dried samples were kept at room temperature, in the dark, and away from humidity. The sampling and processing of fresh, senescent, and degraded leaves are communicated in Robin et al. (submitted). Briefly, fresh green leaves and yellow senescent leaves about to fall were collected for both species. The green and senescent leaves were washed, frozen, freeze-dried, and ground with a cutting mill, The degraded leaves were collected after 72 days of litterbag experiment in nylon litterbags (2-mm mesh size), and were processed similarly to the senescent leaves.

IV.A.3.3. Rock-Eval analysis

Rock-Eval pyrolysis was performed on a Rock-Eval 7 (Vinci Technologies) at Sorbonne Université (GEORG platform) using a method adapted for soils and recent sediments (Baudin et al., 2015). Crushed samples desalted with deionized water were first subjected to a 3 min isotherm under a N_2 atmosphere at 200 °C, at which point free hydrocarbons are volatilized (peak S1). Then, heating with a ramp of 30 °C min^{-1} led to the vaporization of products from thermal cracking of OM up to 650 °C (peak S2). Hydrocarbon effluents were continuously detected by a flame ionization detector (FID) and expressed in mg per g of sample, whereas CO and CO_2 were measured online as well as by an infrared cell (peak S3). At the end of the pyrolysis step, samples were automatically transferred into an oxidation oven, where they were subjected to a 1 min isotherm at 300 °C, then a ramp of 20 °C min^{-1} up to 850 °C. Total signals of CO and CO_2 are expressed in mg per g of sample. All those thermograms allow the calculation of the total organic carbon (TOC) by adding pyrolysis carbon and the residual carbon detected during the oxidation phase (Behar et al., 2001). Hydrogen and oxygen indices are calculated as S2/TOC*100 and S3/TOC*100, respectively, and approximate the H/C and O/C atomic ratio of the OM. TpS2 is the temperature of the pyrolysis oven at the maximum yield of S2 peak, and is usually used as a thermal stability parameter of the OM (Behar et al., 2001; Disnar et al., 2003).

IV.A.3.4. Total elements and stable isotope ratios

Total C, total N, and their stable isotopes were measured on an isotope ratio mass spectrometer Sercon Intergra 2 at the LAMA laboratory of the Institute of Research and Development of New Caledonia. About 30 mg of samples were weighed in tin cups and folded into tightly closed spheres. The samples were transported in a combustion column with helium gas where they were heated at 1 000 °C and oxidized with Cu and Cr oxides, while silver wool trapped sulfur and halogens. The samples were then transferred to the reduction column at 600 °C where the Cu interacts with excess oxygen so that the NO_x is reduced to N_2. The water in the samples was trapped with $Mg(ClO_4)_2$ and N_2 and CO_2 of the samples were separated by gas chromatography. The separated molecules were quantified by mass spectrometry in positive ESI mode. The mass spectrometer measures the relative abundances of isotopes in the sample gas. For carbon, it measures the ratio of ^{13}C to ^{12}C (expressed as $\delta^{13}C$), while for nitrogen, it measures the ratio of ^{15}N to ^{14}N (expressed as $\delta^{15}N$). To calculate the δ values, the measured isotopic ratio is compared to a known standard. The standard used is the Vienna Pee Dee Belemnite (VPDB) standard for C, and the atmospheric nitrogen standard for N. For quality control, duplicate of samples were passed through the spectrometer (1 every 10 samples) (*Supplementary Table IV.A-2*).

IV.A.3.5. Neutral carbohydrates

Neutral carbohydrates were analyzed at the Earth Sciences Institute of Orleans (ISTO), France. About 50 mg of each sample were hydrolyzed 4 h at 105 °C in Pyrex tubes with 5 mL of 4M of trifluoroacetic acid (TFA). After cooling in an ice bath, 500 µL of internal standard (2-deoxyglucose at 8 mg L^{-1}) were added and the sample was centrifuged for 30 min at 5 600 rpm. The extract was evaporated, and the dried samples were kept frozen. Prior to analysis, neutral carbohydrates were derived with the addition of 500 µL of ethoxy ammonium chloride solution in pyridine (40 mg m^{-1}) heated for 1 h at 70 °C. A total of 250 µL of BSTFA were added and the sample was once again heated at 70 °C for 1 h. After evaporation, the residue was dissolved in 2 mL of heptane, filtered at 45 µm and injected in the GC-MS. The GC used was a Trace 1300 (Thermo Scientific) coupled to a MS ISQ7000 (Thermo Scientific). The GC was equipped with at Restek Rxi-5Sil MS column (60 m x 0.25 mm, 0.25 µm diameter) with 5 m of pre-column. Helium gas was used as vector and the analysis was carried out at constant 1 mL min^{-1} flow rate. The injector was heated at 280 °C and the transfer line at 300 °C. A 1 µL of sample was injected in splitless mode and passed through the column with a temperature program (*Supplementary Table III.A-2*). For the MS analysis, the source was heated at 240 °C and electronic impact (70 eV) was performed. The spectra were obtained between 50 and 750 Da with a scan time

of 0.4 s $scan^{-1}$. Quality control consisted of duplicate technical samples (≤11% standard deviation) and measurement of the internal standard (*Supplementary Table III.A-3*).

IV.A.3.6. Lignin-derived phenols

A total of 100 mg of each sample was hydrolyzed for 3 h at 170 °C in 8 mL of 2N NaOH with 100 mg of $Fe(NH_4)_2(SO_4)_2$ under N_2. After cooling, the extract was collected once the sample was centrifuged at 3 000 rpm for 10 min. The extract was acidified at pH 1 with HCl and the lignin derived phenols were extracted twice with 3 mL of anhydrous diethyl ether. After complete evaporation, the lignin-derived phenols were diluted in 1 mL of 50:50 methanol: H_2O, filtered at 45 µm and analyzed via UPLC-MS at the University of New Caledonia. Chromatographic separation was achieved using a Vanquish Flex system (Thermo Fisher Scientific, France) consisting in a binary pump, an autosampler and a heated column compartment. Samples were separated on a Hypersil GOLD column (1.9 µm particle size), 50 x 2.1 mm (Thermo Scientific). For elution, a binary gradient program was used (*Supplementary Table III.A-4*), the mobile phase was a mixture of ultrapure water containing 0.1% of formic acid (Carlo Erba; eluent A) and methanol OPTIMA LC/MS (Fisher Scientific) with 0.1% of formic acid (eluent B). The flow rate was set to 0.5 mL min^{-1} and injection (2 µL) was made automatically by the autosampler. UV detection was carried out at 280 nm. MS detection was performed using an Orbitrap Exploris 120 (Thermo Fisher Scientific, France) and operated with the heated electrospray ionization source in negative ion mode with a vaporizer temperature of 300 °C. Scan modes were both full MS – $ddMS^2$ and SRM. The full MS mode had a resolution of 30000 and a scan range of 50 – 250 m/z with HCD Collision energies specified for each molecule. The SRM mode had a resolution of 120 000 at 20% HCD collision energy. The full UPLC-MS optimized parameters are displayed in *Supplementary Table III.A-4*. The quantification was performed with an external calibration curve (*Supplementary Table III.A-5*) and laboratory reference materials spiked with the analytes. For quality control, a blank solution was passed at the beginning and end of every series in the same conditions as the samples and values were all below detection limits (*Supplementary Table IV.A-3*). A quality control solution (QC) consisting of a point of the calibration curve was passed every 10 samples in the same conditions as the samples and the values obtained were all below 15% difference with the expected value (*Supplementary Table IV.A-3*).

IV.A.4. Results

IV.A.4.1. Mangrove-derived organic matter characteristics

The measured root and leaf parameters for both species are displayed in *Table IV.A-1*. Results for senescent and degraded leaves are already published in (Robin et al., submitted). *A. marina* had higher $\delta^{13}C$ and $\delta^{15}N$ values than *R. stylosa* for each tissue (roots and fresh leaves), but lower C/N ratios. The fresh roots of *A. marina* and *R. stylosa* had higher C/N ratios (68 and 100, respectively) and $\delta^{15}N$ values (3.4‰ and 1.2‰, respectively) than fresh leaves (C/N ratios of 21 and 54, respectively, and $\delta^{15}N$ values of 1.1‰ and -1.3‰, respectively).

The TpS2 values of the fresh tissues varied between 332 °C and 394 °C. For both species, the OI values were similar for roots and leaves, varying between 89 and 112 mg CO_2 g^{-1} TOC. The leaf HI values were greater than root HI values and those of *A. marina* (415 and 571 mg HC g^{-1} TOC, respectively) were higher than those of *R. stylosa* (307 and 402 mg HC g^{-1} TOC, respectively) for both tissues.

The leaves of *A. marina* were richer in lignin (4.12 mg g^{-1}) than the leaves of *R. stylosa* (1.33 mg g^{-1}). For both species and the two tissues, the vanillyl phenols were dominant, representing from 41 to 66% of all measured phenols. The cinnamyl phenols were the second most dominant group of phenols in the fresh leaves (27% for *A. marina* and 26% for *R. stylosa*), but were the minor group of phenols in the roots (1.6% for *A. marina* and 3.3% for *R. stylosa*). Therefore, the C/V ratio was an order of magnitude higher in the leaves than in the roots. The acid/aldehyde ratios for the vanillyl and syringyl phenols were higher for *R. stylosa* (1.1-4.7) than *A. marina* (0.82-1.5).

Table IV.A-1. Mean (±SD) roots and leaves characteristics for *A. marina* and *R. stylosa*. Lignin-derived phenols and neutral carbohydrates are in mg g^{-1}. (Some data taken from *Robin et al., submitted*)

Species	***A. marina***				***R. stylosa***			
Tissues	Fresh roots	Fresh leaves	Senescent leaves	Degraded leaves (72 days)	Fresh roots	Fresh leaves	Senescent leaves	Degraded leaves (72 days)
$\delta^{13}C$ (‰vsVPDB)	-26.1±0.2	-25.8±0.3	-27.7±0.03	-27.8±0.5	-26.5±0.3	-27.5±0.1	-28.3±0.3	-28.8±0.4
$\delta^{15}N$ (‰vsAir)	3.4±2.4	1.1±0.6	0.9±0.7	0.4±0.7	1.2±1.0	-1.3±0.5	-0.2±0.2	-0.6±1.0
C/N	68±17	21±4	39±6	37±8	100±16	54±14	166±89	66±43
TpS2 (°C)	332	394	NA	NA	353	349	NA	NA
HI (mg HC g^{-1} TOC)	415	571	NA	NA	307	402	NA	NA
OI (mg CO_2 g^{-1} TOC)	112	91	NA	NA	89	91	NA	NA
Σlignin	1.2±0.4	4.1±0.8	43±11	26±5	1.5±0.2	1.3±0.3	6.6±2.2	8.6±0.4
p-hydroxyl	0.08±0.03	0.62±0.10	0.27±0.03	0.26±0.04	0.38±0.24	0.21±0.02	0.15±0.00	0.13±0.00
Vanillyl	1.0±0.3	2.0±0.6	33±10	14±3	0.74±0.08	0.56±0.27	0.90±0.17	3.4±0.9
Syringyl	0.19±0.42	0.33±0.07	0.22±0.00	0.50±0.05	0.34±0.06	0.22±0.02	0.14±0.06	0.24±0.02
Cinnamyl	0.02±0.00	1.1±0.0	9.2±1.1	12±2	0.05±0.02	0.34±0.06	5.4±2.3	4.9±0.7
C/V	0.02	0.55	0.27	0.86	0.06	0.61	6.0	1.5
S/V	0.19	0.26	0.01	0.04	0.45	0.39	0.15	0.07
P/(V+S)	0.07	0.26	0.03	0.02	0.35	0.27	0.03	0.03
$(Ad/Al)_p$	0.10	0.25	2.6	0.52	0.34	1.0	4.6	1.8
$(Ad/Al)_v$	0.82	0.84	11	1.1	1.1	4.7	21	14
$(Ad/Al)_s$	1.5	1.2	3.0	0.47	3.2	1.9	1.4	1.1
Σneutral carbohydrates	441	383	452±52	380±38	381	228	499±14	250±13
Xylose	180	128	122±23	152±0	128	49	104±7	78±5
Arabinose	123	97	90±14	70±6	71	62	131±6	46±2
Ribose	0.74	1.9	1.0±0.1	0.83±0.22	0.34	0.48	0.76±0.07	0.41±0.05
Rhamnose	36	41	52±6	45±5	39	27	58±0	14±1
Fucose	1.6	1.4	1.9±0.5	2.5±0.9	6.5	3.8	8.0±0.2	8.0±0.9
Mannose	8.1	10	11±2	15±8	17	4.1	11±0	14±4
Galactose	51	38	42±6	25±9	39	34	69±3	34±6
Glucose	41	66	133±1	71±9	80	48	117±3	55±9

P = p-hydroxyl, V = vanillyl, S = syringyl, C = cinnamyl, and Ad/Al = acid over aldehyde ratio.

The roots were richer in neutral carbohydrates (38-44% of dry weight) than the fresh leaves (23-38% of dry weight). Xylose, arabinose, fucose, and galactose were measured in higher concentrations in the roots of both species compared to the leaves, while ribose was more concentrated in the fresh leaves than roots for both species. The fresh tissues of *A. marina* had higher total neutral carbohydrate concentrations than *R. stylosa* with higher xylose, arabinose, ribose and galactose contents. Only fucose was higher for *R. stylosa* compared to that of *A. marina*. Xylose, arabinose, and glucose were the three main neutral carbohydrates representing between 21 and 41%, 19 and 28%, and 9 and 21% of total neutral carbohydrates, respectively. Fucose and ribose were the least

concentrated neutral carbohydrates varying between 1.4 and 6.5 mg g^{-1} and 0.34 and 1.9 mg g^{-1}, respectively.

IV.A.4.2. Soil organic matter characterization

IV.A.4.2.1. Total organic carbon and stable isotope ratios

Soil TOC was higher beneath *R. stylosa* than *A. marina,* with values ranging from 9.9 to 13.1% and from 3.9 to 7.8%, respectively. TOC decreased with depth for both species but starting deeper for *R. stylosa,* from 10-cm depth (*Figure IV.A-2A*). The C/N ratio was also higher in the soil beneath *R. stylosa*, and increased with depth for both species, varying between 13 and 20 for *A. marina* and 23 and 29 for *R. stylosa* (*Figure IV.A-2B*).

The soil of the *A. marina* species was always more enriched in ^{13}C than the soil of *R. stylosa*. For both species, the $\delta^{13}C$ varied only slightly with depth, between -26.6‰ and -25.7‰ for *R. stylosa*, and between -24.7‰ and -24.4‰ for *A. marina* (*Figure IV.A-2C*). The upper soil section was heavier in ^{15}N (1.53‰) under *R. stylosa* than under *A. marina* (0.87‰). From 5 to 20 cm, the $\delta^{15}N$ increased with depth for both species and was higher for *A. marina* than *R. stylosa* up to 2.5‰ and 1.3‰, respectively (*Figure IV.A-2D*).

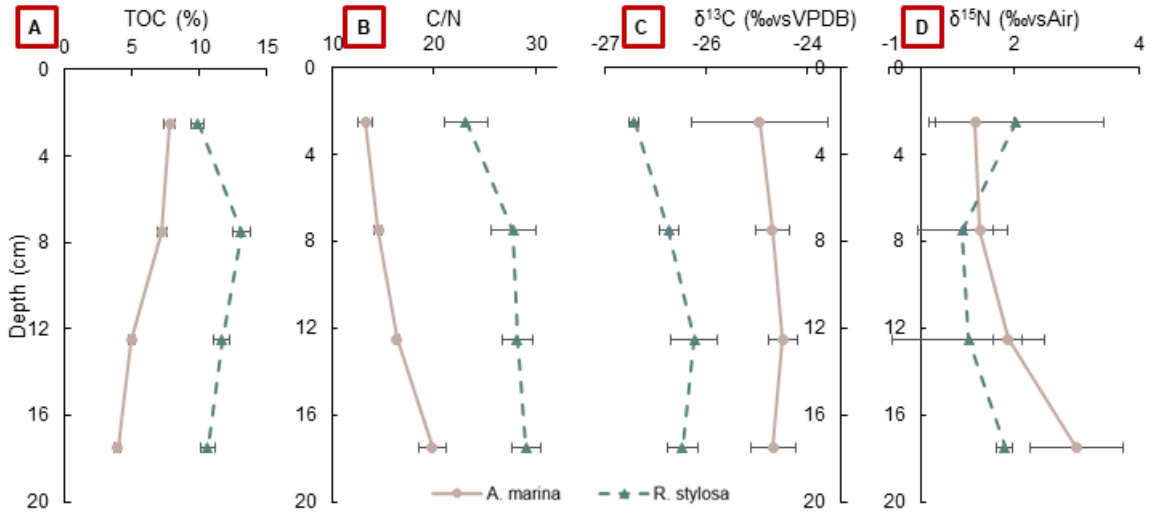

Figure IV.A-2. Mean vertical soil profiles (SD as error bars) beneath *A. marina* and *R. stylosa* for the parameters (A) TOC in %, (B) C/N ratio, (C) $\delta^{13}C$ in ‰ vs VPDB, and (D) $\delta^{15}N$ in ‰ vs Air.

IV.A.4.2.2. Rock-Eval analysis

The variations of TOC versus TpS2 for soil samples are exposed in *Figure IV.A-3A*. The stands of the two species were different in their OM characteristics. The *A. marina* soil had lower TOC, but higher TpS2 values (456 – 471 °C) than *R. stylosa* (329 – 344 °C). However, the TpS2 value decreased slightly with depth for both species. On the HI vs OI diagram, there was a noticeable distinction between the two species (*Figure IV.A-3B*).

For three soil sections out of four, the OM beneath *A. marina* had higher HI values (165 – 366 mg HC g^{-1} TOC) and OI values (95 – 111 mg CO_2 g^{-1} TOC) than the OM beneath *R. stylosa* (198 – 241 mg HC g^{-1} TOC and 82 – 107 mg CO_2 g^{-1} TOC). The HI and OI trends were the same for both species. The HI value increased between the 0-5 and 5-10 cm sections, then decreased with depth, while the OI value decreased between the 0-5 and 10-15 cm sections prior to increasing.

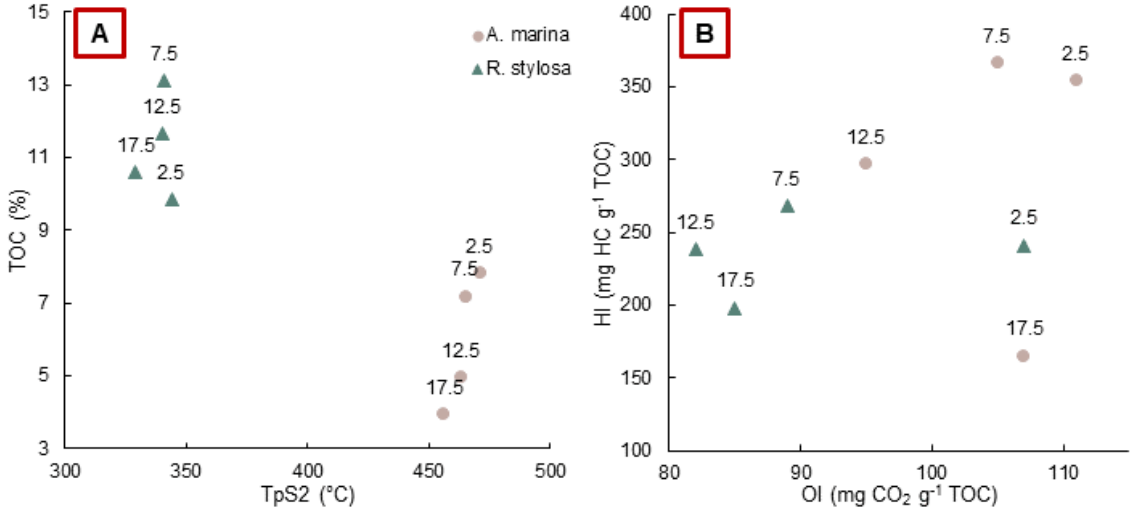

Figure IV.A-3. (A) Total organic carbon (TOC) content versus TpS2 diagram and (B) hydrogen index (HI) versus oxygen index (OI) for the vertical soil profiles beneath both *A. marina* and *R. stylosa*. The data labels represent the soil sections in cm.

IV.A.4.2.3. Neutral carbohydrates

Neutral carbohydrates concentrations relative to TOC for the soil beneath both species are revealed in *Table IV.A-2*. For both species, total carbohydrate content generally decreased with depth from 326 to 161 mg g^{-1} TOC for *A. marina* and from 246 to 127 mg g^{-1} TOC for *R. stylosa*. Arabinose, rhamnose, and glucose were the dominant neutral carbohydrates in the soil beneath *A. marina* in varying orders, while beneath *R. stylosa* the order remained arabinose > xylose > rhamnose. Ribose was the least concentrated neutral carbohydrate in the soil beneath *R. stylosa* varying between 0.85 and 2.33 mg g^{-1} TOC, followed by fucose varying between 3.52 and 8.82 mg g^{-1} TOC. Beneath *A. marina* ribose and fucose were the least concentrated neutral carbohydrates between 0 and 10 cm, but deeper was mannose and galactose, representing between 0.4 and 4.3%.

Beneath *A. marina* xylose, fucose, mannose, galactose, and glucose followed the same trend as the total carbohydrate content, while beneath *R. stylosa* only arabinose and glucose were consistent with the total trend. An important increase in ribose was observed beneath *A. marina* between the 10-15 cm (3.04 mg g^{-1} TOC) and 15-20 cm (14.5 mg g^{-1} TOC) sections. For this latter species, an extensive decrease in mannose, galactose, and

glucose was observed between the 5-10 cm and 10-15 cm sections from 13.4 to 0.61, from 20.5 to 2.63, and from 55.9 to 15 mg g^{-1} TOC, respectively. Consequently, the hexoses/pentoses ratio dropped from 0.43 to 0.04. Beneath *R. stylosa* the maximum hexoses/pentoses (0.29) and xylose/rhamnose (2.26) ratios were observed in the 5-10 cm section. This trend was correlated with the increase in xylose, mannose, and galactose between the 0-5 and 5-10 cm sections.

Table IV.A-2. Neutral carbohydrate concentrations in mg g^{-1} TOC in the soil beneath *A. marina* and *R. stylosa*.

Species	Depth (cm)	Xyl	Ara	Rib	Rha	Fuc	Man	Gal	Glu	Total	Xyl/ Rha	Hex/ Pen
A. marina	0-5	31.0	111	3.33	57.2	13.3	18.7	21.0	70.8	326	0.54	0.28
	5-10	23.1	54.7	2.09	30.8	8.36	13.4	20.5	55.9	209	0.75	0.43
	10-15	11.1	61.7	3.04	27.3	5.87	0.61	2.63	15.0	127	0.41	0.04
	15-20	22.2	59.7	14.5	24.0	7.40	4.34	6.89	21.9	161	0.93	0.14
R. stylosa	0-5	43.0	112	2.33	31.6	8.82	11.9	17.0	19.2	246	1.36	0.19
	5-10	50.0	78.5	1.37	22.1	4.89	14.1	23.4	17.6	212	2.26	0.29
	10-15	38.2	67.5	1.46	19.6	3.52	7.38	12.6	9.18	159	1.95	0.19
	15-20	31.6	53.8	0.85	20.8	3.96	4.43	5.28	5.94	127	1.52	0.11

Xyl = xylose, Ara = arabinose, Rib = ribose, Rha = rhamnose, Fuc = fucose, Man = mannose, Gal = galactose, Glu = glucose, Hex/Pen = hexoses (galactose and mannose) over pentoses (xylose and arabinose) ratio.

IV.A.4.2.4. Lignin-derived phenols content

Lignin-derived phenol concentrations relative to TOC for the soil beneath both species are revealed in *Table IV.A-3*. The soil beneath *R. stylosa* was richer in total lignin-derived phenols than the soil beneath *A. marina*. The most concentrated soil section beneath *A. marina* was the 0-5 cm layer (3.2 mg g^{-1} TOC) and the poorest the 10-15 cm layer (2.4 mg g^{-1} TOC). For *R. stylosa* the richest section was the 5-10 cm layer (7.1 mg g^{-1} TOC), while the poorest was the 15-20 cm layer (3.3 mg g^{-1} TOC). For the entire profile, the order of concentration was vanillyl (40-81%) > syringyl (12-34%) > p-hydroxyl (6-22%) > cinnamyl (3-12%) beneath *A. marina,* and vanillyl (64-80%) > p-hydroxyl (9-19%) > syringyl (5-11%) > cinnamyl (3-6%) beneath *R. stylosa*. Consequently, the C/V ratios were always higher than the S/V ratios, ranging from 0.15 to 0.64, and from 0.03 to 0.28, respectively for *A. marina,* while from 0.07 to 0.17, and from 0.04 to 0.09, respectively, for *R. stylosa*, with no obvious trends.

The trends of phenol groups were opposite between the two species from the upmost section to the 5-10 cm section. Beneath *A. marina*, p-hydroxyl, syringyl, and cinnamyl phenol groups increased from 0.20 to 0.67, from 0.39 to 0.75, and from 0.08 to 0.35 mg g^{-1} TOC, while the vanillyl phenol group decreased by half. Beneath *R. stylosa*, the vanillyl content increased from 4.3 to 5.7 mg g^{-1} TOC, while the three other groups

decreased in concentrations. The p-hydroxyl phenols and cinnamyl phenols followed the same trends with depth for both species.

The acid over aldehyde ratios (Ad/Al) were generally higher for the syringyl groups than the two others with values ranging from 1.26 to 5.93. The Ad/Al ratios were more than three times higher in the 0-5 cm section beneath *A. marina* than beneath *R. stylosa*. For this latter species, the p-hydroxyl and vanillyl Ad/Al ratios increased with depth, while for *A. marina*, the p-hydroxyl and syringyl ratios followed a trend opposite to that of the vanillyl Ad/Al ratio.

Table IV.A-3. Lignin-derived phenols in mg g^{-1} TOC and ratios in the soil beneath *A. marina* and *R. stylosa*.

Species	Depth (cm)	P	V	S	C	Total	C/V	S/V	P/(V+S)	$(Ad/Al)_p$	$(Ad/A)_v$	$(Ad/Al)_s$
A. marina	0-5	0.20	2.6	0.39	0.08	3.2	0.15	0.03	0.07	1.49	1.70	4.50
	5-10	0.67	1.2	0.75	0.35	3.0	0.60	0.28	0.33	0.25	6.94	1.38
	10-15	0.23	1.3	0.67	0.15	2.4	0.50	0.11	0.12	0.59	1.26	5.09
	15-20	0.22	1.5	0.96	0.07	2.8	0.64	0.05	0.09	2.92	1.69	5.33
R. stylosa	0-5	1.3	4.3	0.73	0.38	6.7	0.17	0.09	0.25	0.42	0.30	1.26
	5-10	0.62	5.7	0.38	0.36	7.1	0.07	0.06	0.10	0.77	0.36	5.93
	10-15	0.51	4.3	0.29	0.25	5.4	0.07	0.06	0.11	0.94	1.14	5.12
	15-20	0.40	2.4	0.33	0.10	3.3	0.13	0.04	0.14	2.89	2.52	5.63

P = p-hydroxyl, V = vanillyl, S = syringyl, C = cinnamyl, Ad/Al = acid over aldehyde ratio.

IV.A.5. Discussion

IV.A.5.1. Variations in mangrove tissues characteristics

Regarding the differences between species, the tissues of *A. marina* had higher $\delta^{13}C$ and $\delta^{15}N$ values and lower C/N ratios than *R. stylosa*. A relationship between soil salinity and plant-tissues $\delta^{13}C$ has previously been suggested (Farquhar et al., 1982). *S*alinity stress can cause a reduction in intercellular partial pressure of CO_2, reducing discrimination of ^{13}C over ^{12}C during CO_2 fixation (Lin and Sternberg, 1992; Medina and Francisco, 1997). *A. marina* develops on soils with higher salinity than *R. stylosa* (Robin et al., 2021, 2022), resulting in greater $^{13}C/^{12}C$ ratios in its tissues. Here, the roots of *A. marina* had $\delta^{13}C$ and $\delta^{15}N$ mean values close to terrestrial OM (Middelburg and Nieuwenhuize, 1998). Heavier ^{15}N tissues for the *Avicennia* genus compared to the *Rhizophora* genus has already been expressed in other mangrove forests in Java and in Brazil (Giarrizzo et al., 2011; Herbon and Nordhaus, 2013). During ammonium or nitrate uptake of plants, fractionation against ^{15}N can occur, and the isotope ratio value of the leaf is affected by the isotope ratio of the source and fractionation due to different metabolisms (Fry et al., 2000; Jones et al., 2001). Different mechanisms involved in N reabsorption or remobilization can affect ^{15}N discrimination, and therefore impact $\delta^{15}N$ values (Kolb and

Evans, 2002). Higher C/N ratios in *Rhizophora*'s tissues compared to *Avicennia*'s tissues have also been reported in the literature (Rao et al., 1994; Herbon and Nordhaus, 2013; Vane et al., 2013; Jacotot et al., 2018). In the present study, the ratios obtained for each species are consistent with other measurements recorded in different mangrove forests in the world (Rao et al., 1994; Lallier-Vergès et al., 1998; Smallwood et al., 2003; Regina Hershey et al., 2021). The differences in isotope ratios values between species recorded in this study are likely due to the different ratios of carbohydrates, lipids, lignin, and other biomolecular compounds within the species tissues (Benner et al., 1990; Kristensen et al., 2008). For example, neutral carbohydrates do not contain N atoms, while amino acids are N-rich (Hernes et al., 1996; Kolb and Evans, 2002). Here, the leaves of *A. marina* are richer in lignin-derived phenols than *R. stylosa*. Tissues of both species show a dominance in vanillyl phenols as previously reported (Benner et al., 1990; Lallier-Vergès et al., 2008) and high Ad/Al ratios (>0.8) were obtained, distinguishing the mangrove trees from other angiosperms (Benner et al., 1990). The HI values of the fresh *A. marina* tissues were higher than those of *R. stylosa* as previously observed for the same genera (Marchand et al., 2008). In fact, the *Avicennia*'s tissues had the highest HI values of all species studied (Marchand et al., 2008). This observation may be related to a higher content of hydrocarbons-like compounds, such as neutral carbohydrates (Meyers, 1997; Di-Giovanni et al., 1998) as observed in the present study. The fresh roots of *R. stylosa* had a TpS2 value close to 350 °C, which is characteristic of ligno-cellulose compounds (Disnar et al., 2003). The pneumatophores of *A. marina* had lower total lignin-derived phenol contents explaining the lower TpS2 value than *R. stylosa* roots.

Regarding the differences between tissues, for both species, the proportion of cinnamyl phenols were much lower and the C/N ratios were much higher in roots than leaves, which may be due to higher N-rich lignin in leaves compared to the roots (Vane et al., 2013). The roots also had higher $\delta^{15}N$ values than the leaves for both species, which was previously observed in the literature (Fogel et al., 2008; Jacotot et al., 2018). The difference in $\delta^{15}N$ values between roots and leaves is attributed to the fact that ^{15}N content in roots mostly relies on the soil N sources, while foliar ^{15}N content depends on a multitude of physiological processes involving N (Kolb and Evans, 2002). Higher HI values were obtained for fresh leaves, which was observed for most species in a previous study (Marchand et al., 2008). The wax composition on the leafy tissues may be accountable for these observations (Meyers, 1997; Di-Giovanni et al., 1998). However, for both tissues, the OI values were lower than those measured by Marchand et al., (2008), suggesting less refractory oxygenated functional groups in our samples.

Mangrove tissues vary in their isotopic and molecular compositions. Some parameters were mainly influenced by the species physiology and metabolism, while other parameters were controlled by the mangrove conditions in which the species developed, and therefore may be affected by the position of the trees in the forest.

IV.A.5.2. A soil organic matter pool dominated by autochthonous organic matter

The OM in the soil beneath *A. marina* was characterized by lower C/N and higher $\delta^{13}C$ values than *R. stylosa*. *A. marina* tissues also showed lower C/N and higher $\delta^{13}C$ values than *R. stylosa* tissues. Therefore, we may expect *A. marina* debris to contribute to its soil OM pool. On the one hand, the *A. marina* root system develops close to the surface, horizontally, and promotes oxygen absorption through the development of many pneumatophores (Pi et al., 2009). The total lignin content and lignin ratios cinnamyl over vanillyl phenols (C/V), syringyl over vanillyl phenols (S/V), and p-hydroxyl over the sum of vanillyl and syringyl phenols (P/(V+S)) show the contribution of the root system in the total OM content of the upper soil (0-5 cm) because of comparable values. The upper soil OM is also composed of *A. marina* litterfall as suggested by the high percentage of acetovanillone in the leaf litter (72%) (Robin et al., submitted) and in soil samples (60%) (*Supplementary Table IV.A-1*). However, the decrease in HI values suggests a decrease in the contribution of mangrove-derived debris with depth. The development of a microphytobenthos at the soil surface may also contribute to the OM pool as shown by the relatively enriched $\delta^{13}C$ values and C/N ratios. In the literature, it has been reported that the microphytobenthos contributes to the increase in soil $\delta^{13}C$ and the decrease in C/N, with values ranging from -19 to -25‰ and ratios lower than 10 (Dittmar and Lara, 2001; Marchand et al., 2005; Lamb et al., 2006; Abrantes and Sheaves, 2009; Bala Krishna Prasad and Ramanathan, 2009; Oakes et al., 2010). Compared to *R. stylosa*, the *A. marina* stand in semi-arid climate has a more open canopy, resulting in greater light penetration, necessary for the development of microphytobenthos (Leopold et al., 2013; Jacotot et al., 2018). The TpS2 values were higher than 420 °C for all samples, indicating thermal breakdown of humic substances (Disnar et al., 2003), and therefore highly degraded litterfall may complete the OM pool. The TpS2 value suggests that the most labile OM molecules were lost prior to the introduction of the mangrove debris to the soil. The high rhamnose and fucose percentages in total carbohydrates (18% and 4%) confirm the presence of decomposing microorganisms in the up most soil horizon (Ogier et al., 2001). We suggest that the litterfall penetrating in the soil beneath *A. marina* is already highly degraded through leaching and microbial activity. The ability of *A. marina* to absorb O_2 from the atmosphere and distribute it to its rhizosphere may promote OM degradation and microorganisms' development in the upper soil (Kathiresan and Bingham, 2001).

The *R. stylosa* stand develops on the seaside of the mangrove forest. Its soil OM pool may therefore be influenced by mangrove-derived and marine-derived OM. The soil samples were characterized by $\delta^{13}C$ values lower than -25.7‰ and $\delta^{15}N$ values lower than 1.3‰, which suggests the non-contribution of marine OM to the OM pool as phytoplankton and aquatic plants are described with higher isotopic ratios ($\delta^{13}C$: -24 to -18‰, $\delta^{15}N$: 6 to 12‰) (Cifuentes et al., 1996). The position of the forest in a bay head may limit the contribution of marine sources to the OM pool or the incoming marine-derived OM may quickly be degraded as some show labile behavior such as phytoplankton (Gearing et al., 1984; Bouillon and Dehairs, 2000; Hanamachi et al., 2008). The leaf litter from *R. stylosa* was not dominant in the soil OM pool. The main lignin-derived phenol in *R. stylosa* litter was p-coumaric acid (up to 80%) (Robin et al., submitted) but is negligible in the upper soil (4.8%) (*Supplementary Table IV.A-1*) as previously observed in other mangrove forests (Bala Krishna Prasad and Ramanathan, 2009). Robin et al. (submitted) have shown that for the studied mangrove forest, the litterfall beneath *R. stylosa* decayed more rapidly than the litterfall beneath *A. marina*. Therefore, *R. stylosa* leaf litter may be highly mineralized prior to introduction in the soil. Also, due to the position of the species closer to the sealine, *R. stylosa* leaf litter may be rapidly exported through tidal flushing, limiting incorporation within the soil. The C/N ratio (23), S/V ratio (0.17), and P/(V+S) ratio (0.25) of the upper soil (0-5 cm) suggest a contribution of leaf debris from the *A. marina* stand to the OM pool. With the tides, the litter at the surface of the *A. marina* soil can be transferred to the most seaward stand, on the soil beneath *R. stylosa*. The isotopic ratios and Rock-Eval parameters (TpS2, HI, OI) indicate a contribution of the fresh roots of *R. stylosa* in the soil OM. The C/V ratio of the soil OM is less than 0.1, which also indicates the introduction of OM in the upper soil from the species root system (Marchand et al., 2005). In addition, visible increase in TOC, $\delta^{13}C$, C/N ratio, xylose, mannose, and lignin content due to the increase in vanillyl phenols, were observed between the 0-5 and 5-10 cm sections. These parameters indicate that the root system, which is dominant in the 5-10 cm section, greatly contributes to the soil OM pool. Mannose and xylose are both common constituents of angiosperm hemicelluloses (Benner et al., 1990), and high xylose content (23%) is characteristic of woody tissues (Lallier-Vergès et al., 2008). Similarly, the vanillyl phenols are the dominant lignin phenols in mangrove tissues (Benner et al., 1990). Because of the high OM content at the root system level, there is a decrease in the Eh values (Robin et al., 2022), which is correlated to the decrease in OI values observed. More anoxic conditions limit oxygenation of the OM, resulting in lower OI values. Therefore, we suggest that the leaf debris from *A. marina* and the fresh roots of *R. stylosa* constitute the main OM sources in the soil beneath *R. stylosa.* However, some of the indicators show differences

with the suggested sources, indicating that decay processes have occurred prior to the integration of the OM in the soil.

IV.A.5.3. Organic matter decay is redox-dependent

The vertical variations in the stable isotope ratios and Rock-Eval parameters were similar between the two species. TOC content decreased with increasing depth, indicating OM decomposition, from the upmost section (0-5 cm) beneath *A. marina,* and from the root system section beneath *R. stylosa* (5-10 cm). The soil beneath *A. marina* was characterized by lower TOC content than *R. stylosa*. The higher productivity of *R. stylosa* compared to *A. marina* in semi-arid mangrove forests (Deborde et al., 2015), due to their greater height and canopy density, may account for this result. In addition, the conditions are more favorable for OM decomposition beneath *A. marina* due to its capacity to diffuse oxygen in its rhizosphere (Kathiresan and Bingham, 2001; Marchand et al., 2006). $\delta^{13}C$ for *R. stylosa* and $\delta^{15}N$ for *A. marina* slightly increased with depth, which may result from isotopic fractionation during OM degradation rather than a change in the relative contributions of the sources (Jones et al., 2001; Vinh et al., 2020). The C/N ratio increased for both species with depth because the anaerobic microbial consumption of OM may result in a rise in C/N in the soil (Andrews et al., 1998).

The Rock-Eval parameters showed net differences in OM type in the soil beneath the two mangrove species. *R. stylosa* had lower HI and OI values than *A. marina* partly because of more lignocellulosic compounds contributing to the OM pool (Disnar et al., 2003; Marchand et al., 2008). The much lower TpS2 values beneath *R. stylosa* indicate that the soil OM pool was still greatly composed of thermally labile molecules (Di-Giovanni et al., 1998). The values were closed to those of the fresh mangrove tissues, suggesting less decayed OM in the soil, attributed to the more anoxic conditions beneath this species (Marchand et al., 2008; Deborde et al., 2015). For both species, the HI vs OI diagram indicated that the decomposition occurs through dehydrogenation and slight oxygenation. Previous studies have shown that increase in OI values only occur once the OM has been highly dehydrogenized (Lallier-Vergès et al., 1998; Marchand et al., 2008; Deborde et al., 2015). The highest HI values in the upper soil may be accounted for the higher carbohydrate contents, as neutral carbohydrates are hydrogen-rich compounds (Marchand et al., 2008).

Isotopic and Rock-Eval parameters of the soil OM are source-dependent and therefore species-dependent. These indicators suggest that OM decay occurs in both *A. marina* and *R. stylosa* soils. However, the suboxic conditions in the sub-surface beneath

A. marina account for the thermal stability of the bulk OC, not reported in the *R. stylosa* soil OM pool.

IV.A.5.4. Neutral carbohydrates are selectively degraded in soils

As in the literature, neutral carbohydrates were lost at a higher rate than bulk OC beneath both species (Marchand et al., 2005; Lallier-Vergès et al., 2008). Neutral carbohydrates are expected to be loss during decomposition because they are a large source of C and energy (Chen et al., 2019), and are labile in the litter (Cundell et al., 1979; Mfilinge et al., 2002; Vinh et al., 2020; Robin et al., submitted). In the present study, neutral carbohydrates were lost at a higher rate in the soil of *A. marina* than *R. stylosa*. Litter from *R. stylosa* is richer in tannin than the litter of *A. marina* (Kimura and Wada, 1989). Tannin-rich environments may lower benthic organisms activity (Alongi et al., 1989), which may result in less efficient degradation of carbohydrates (Lacerda et al., 1995). The more anoxic environment beneath *R. stylosa* (Robin et al., 2022) may also limit neutral carbohydrates loss (Lacerda et al., 1995; Marchand et al., 2005). For both species, even though neutral carbohydrate content was lower in soil than in the plants, carbohydrates represented between 13% and 23% of total OC, which is much higher than in the literature for mangrove soils (Marchand et al., 2005; Duan et al., 2020). For exemple, Lallier-Vergès et al. (2008) stated that more than half of the carbohydrates from litterfall were degraded prior to soil incorporation in a tropical mangrove forest of Guadeloupe. Therefore, either more carbohydrates were initially incorporated in the soil than in the other mangrove forests or the microbial production of neutral carbohydrates were favored.

Between plants and soil, there was a relative increase in ribose and fucose for both species, as well as rhamnose and mannose for *A. marina*. These neutral carbohydrates may be produced in the soil by the microbial community (Cowie and Hedges, 1984a), as previously suggested (Lallier-Vergès et al., 2008), or show refractory behavior (Marchand et al., 2005). These neutral carbohydrates showed refractory behavior in the litterfall degradation of the two species at the studied site (Robin et al., submitted). Conversely, xylose and galactose were relatively less concentrated in the soil than in the mangrove tissues. Galactose showed labile behavior in the degrading litterfall of both species (Robin et al., submitted) and xylose also showed labile behavior in mangrove soil in French Guiana (Marchand et al., 2005).

Beneath *R. stylosa*, all neutral carbohydrates, except for the deoxy sugars, continuously decreased with increasing soil depth. In the present study, rhamnose and fucose increased between the 10-15 and 15-20 cm sections. These results, in addition to a decrease in the Xyl/Rha ratio with depth, indicate the increase in relative contributions

of microbial-derived neutral carbohydrates against mangrove-derived carbohydrates with depth (Duan et al., 2017; Chen et al., 2019). Beneath *A. marina*, only rhamnose continuously decreased in relative concentration with depth. Xylose, fucose, glucose, and hexose decreased at first, but increased between the two deepest intervals. Selective degradation was observed within the soil with galactose being the most refractory measured neutral carbohydrate between the 0-5 and 5-10 cm sections (-2.6%), and arabinose the most labile (-50.6%). However, in deeper sections (5-10 and 10-15 cm), galactose was the second most labile carbohydrate after mannose (-87.5%), whereas ribose and arabinose increased relative to TOC. Therefore, we suggest that beneath *A. marina*, two factors may contribute to the variations in the neutral carbohydrates degradation with depth: 1) the suboxic conditions and 2) the reduction of the contribution of the microphytobenthos as an OM source in the soil, which produces neutral carbohydrates.

IV.A.5.5. High loss of lignin relative to bulk organic carbon both in suboxic and anoxic environments

Total lignin-derived phenols relative to bulk OC decreased with increasing depth beneath both species. In the leaf litter, lignin showed labile behavior for the *A. marina* litter during degradation. Conversely, lignin accumulated in the *R. stylosa* leaf litter at the studied site (Robin et al., submitted), as expected from other published results (Fell et al., 1975; Tam et al., 1990; Chale, 1993). In mangrove soils, lignin was lost at a lower rate (Marchand et al., 2005) or similar rate than bulk OC (Dittmar and Lara, 2001; Lallier-Vergès et al., 2008). We suggest that beneath *A. marina*, the suboxic conditions may favor lignin degradation. We suggest that beneath the *R. stylosa* stand developing on the seaside, which has a larger grain size than *A. marina* (*Supplementary Figure IV.A-1*), underground water exchange may favor leaching and/or degradation of lignin in the soil. In addition, the high content of lignin-derived phenols in *R. stylosa* soil may result in a significant fraction of lignin showing labile behavior.

Vanillyl and cinnamyl phenols were the most labile-phenol groups in the soil beneath *A. marina* and *R. stylosa*, respectively, which is similar to the litterfall of the respective species (Robin et al., submitted). However, vanillyl remained the major phenol group for the entire vertical profiles representing between 64 and 80% of lignin-phenols, as previously reported in the literature (Lallier-Vergès et al., 2008). The depletion in cinnamyl phenols with depth for both species may be caused by the association of cinnamyl molecules to labile compounds such as carbohydrates (Hartley, 1973) or to loose ester bounds with lignin (Kirk, 1980) as previously suggested (Dittmar and Lara, 2001). The main mechanisms of lignin decomposition during litterfall degradation and in

waterlogged mangrove soils were ring cleavage and loss of -OCH_3 groups (Robin et al., submitted) (Dittmar and Lara, 2001; Marchand et al., 2005; Bala Krishna Prasad and Ramanathan, 2009). In the present study, the decrease in S/V indicating loss of -OCH_3 was observed with increasing depth for both species, which confirms this mechanism for lignin degradation. Side chain oxidation did not seem to be a mechanism of lignin degradation in the soil of *A. marina*. The Ad/Al ratios did not increase significantly except for $(Ad/Al)_v$ between 5 and 10 cm, which could be attributed to crab activity. Litter can be buried by crabs therefore introducing fresh OM from vascular plants into the soil (Marchand et al., 2005). However, the Ad/Al ratios mainly increased with depth beneath *R. stylosa* suggesting side-chain oxidation of the lignin components (Chen and Chang, 1985; Dittmar and Lara, 2001), which was not observed neither during litterfall degradation at this site (Robin et al., submitted), nor in other anaerobic mangrove soils (Dittmar and Lara, 2001; Marchand et al., 2005; Bala Krishna Prasad and Ramanathan, 2009). We suggest that side-chain oxidation may also be a mechanism of lignin degradation in waterlogged mangrove soils because of oxidative microenvironments not depicted in the redox profiles.

IV.A.6. Conclusion

The OM sources have been characterized in a semi-arid bay head mangrove forest in New Caledonia. Isotopic and molecular analyzes showed that the soil OM pool is dominated by autochthonous OM. Beneath the most landward stand, *A. marina*, the main OM sources were *A. marina* litterfall and roots, and the microphytobenthos, which develop on the soil surface. Beneath the most seaward stand, *R. stylosa*, the main OM sources were the roots of *R. stylosa* and the litter debris from *A. marina*, which most likely was transferred with the tides. *A. marina* and *R. stylosa*-derived OM were distinct in their characteristics due to their position in the mangrove forest and their specific chemical compositions, contributing differently to the soil carbon budget.

Once integrated in the soil, the OM was degraded beneath both species through dehydrogenation, but the anoxic conditions limited oxygenation of the OM during diagenesis. The more anoxic environment beneath *R. stylosa* limits OM decay compared to *A. marina*, which OM pool was composed mostly of mature compounds. The differences in OM sources in the soil beneath both species influenced the values of the isotope ratios and Rock-Eval parameters, but not the trends that were similar for *A. marina* and *R. stylosa*.

Total lignin and neutral carbohydrates showed a general labile behavior in mangrove soil. The order of lability of the phenol groups followed the order in the litterfall

with cinnamyl phenols the most labile in the soil beneath *R. stylosa* and vanillyl phenols beneath *A. marina*. The mechanisms of lignin degradation in mangrove soil disclosed herein are ring cleavage, loss of -OCH_3, and, surprisingly, side chain oxidation in the anoxic soil beneath *R. stylosa*. The individual neutral carbohydrates showed varying behavior with depth and between stands suggesting selective degradation. The increasing carbohydrates in the soil may be caused by the environmental conditions limiting their carbohydrates' lability or their production by the microbial communities such as deoxy sugars.

OM accumulation and sequestration in mangrove soil may be favored through processes involving sulfur. Therefore, perspectives are to investigate the relations between soil OM composition and the sulfur cycle. Rock-Eval pyrolysis is still poorly used as a tool to examine OM in mangrove forests and further studies can be run on the influence of the variations of the neutral carbohydrates and lignin-derived phenols with additional Rock-Eval parameters. The contribution of microbial activities on the neutral carbohydrates pool in mangrove soil can be further investigated. Previous studies in New Caledonia have exposed the presence of an OM-rich layer deeper in the soil of mangrove forests. Future research using the same proxies could be conducted on deeper layers to identify the origin of the OM in depth and characterize it at the molecular level.

IV.A.7. Acknowledgments

The authors acknowledge Kapeliele Gututauava and Pierre Sanlis for the field work. The authors acknowledge Ines Le Mao from NC Bioressources for UPLC-MS optimization and analyzes and Anne Desnues from IRD for the isotopic analyzes.

IV.A.8. Supplementary materials

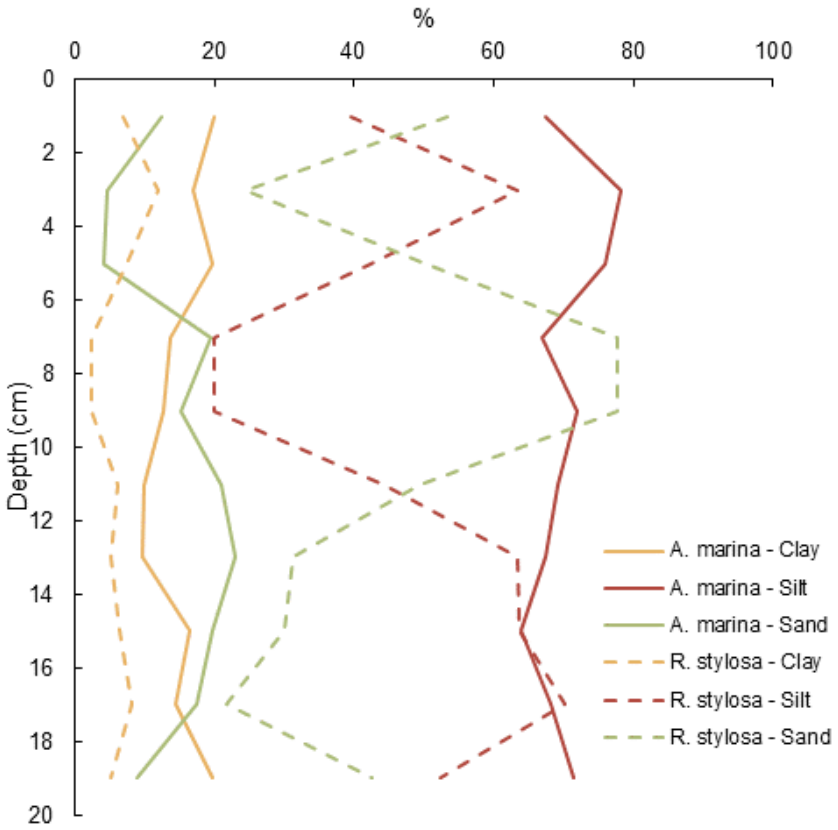

Supplementary Figure IV.A-1. Mean percentage of clay, silt, and sand in the soil samples beneath *A. marina* and *R. stylosa*.

Supplementary Table IV.A-1. Individual lignin-derived phenols in µg g^{-1} for biota and µg g^{-1} of TOC in soil.

A. marina								
	Biota				Soil section (cm)			
	Fresh roots	Fresh leaves	Senescent leaves	Degraded leaves	0-5	5-10	10-15	15-20
PAL	71	425	55	142	70	500	127	40
PON	5	90	75	48	23	43	29	64
PAD	7	106	141	73	104	122	75	117
VAL	474	746	171	300	227	85	347	371
VON	135	662	31 383	12 914	1 939	576	551	499
VAD	388	628	1 879	331	387	588	439	628
SAL	77	150	55	336	70	311	107	150
SON	0.2	0.1	0.4	0.5	6	5	15	12
SAD	116	183	164	158	317	429	544	801
CAD	19	1 123	9 116	11 652	68	303	124	55
FAD	0.9	7	36	15	10	46	26	16
R. stylosa								
	Biota				Soil section (cm)			
	Fresh roots	Fresh leaves	Senescent leaves	Degraded leaves	0-5	5-10	10-15	15-20
PAL	272	97	23	41	817	329	233	87
PON	12	16	17	17	117	37	59	57
PAD	91	97	105	72	340	254	220	252
VAL	304	79	24	57	2 107	1 591	481	499
VON	105	105	375	2 518	1 591	3 578	3 312	674
VAD	333	374	504	781	633	569	550	1 260
SAL	80	75	58	116	317	55	46	48
SON	0.2	0.1	0.4	0.5	9	5	8	10
SAD	257	140	79	127	399	324	238	267
CAD	44	341	5 373	4 838	319	349	185	73
FAD	2	1	38	26	58	8	62	24

Supplementary Table IV.A-2. Quality control of the duplicate samples on an isotope ratio mass spectrometer Sercon Integra 2.

Sample	ΔC (g kg^{-1})	ΔN (g kg^{-1})	$\Delta\delta^{13}C$ (‰vsVPDB)	$\Delta\delta^{15}N$ (‰vsAir)
1	2.93	0.06	0.15	0.90
2	4.14	0.32	0.20	0.18
3	8.71	0.54	0.17	0.20
4	3.32	0.15	0.18	0.40
5	8.00	0.43	0.19	0.24
6	6.54	0.41	0.29	0.40

Supplementary Table IV.A-3. Concentrations in the 11 lignin-derived phenols in the blank and quality control (QC) solutions obtained in mg L^{-1} with the expected value for the QC.

	Blank		Expected QC	QC					
PAL	0.084	0.060	2	2.079	1.930	1.996	2.470	2.137	2.530
PON	0.013	0.0.87	2	1.808	2.164	1.975	1.596	1.818	2.381
PAD	0.004	0.009	2	2.084	2.020	1.913	2.358	1.517	2.332
VAL	0.028	0.071	2	1.888	1.996	1.828	1.852	1.380	1.663
VON	0.256	0.158	20	20.988	19.868	21.320	19.394	20.999	19.637
VAD	0.013	0.149	20	20.915	20.624	21.202	18.977	18.551	19.310
SAL	0.071	0.090	6	6.992	6.615	5.868	6.116	5.012	5.273
SON	0.022	0.058	2	1.845	2.003	1.805	2.040	1.574	1.607
SAD	0.012	0.142	6	6.978	6.122	5.076	5.471	5.476	6.552
CAD	0.101	0.262	20	19.716	21.461	20.556	20.045	19.819	20.475
FAD	0.075	0.077	2	1.879	1.975	1.949	2.529	1.965	2.433

B. Chapter IV.B: Millennial-aged organic matter preservation in anoxic and sulfidic mangrove soils: insights from isotopic and molecular analyzes

Sarah Louise ROBIN, François BAUDIN, Claude LE MILBEAU, Cyril MARCHAND

Submitted to Science of the Total Environment

IV.B.1. Abstract

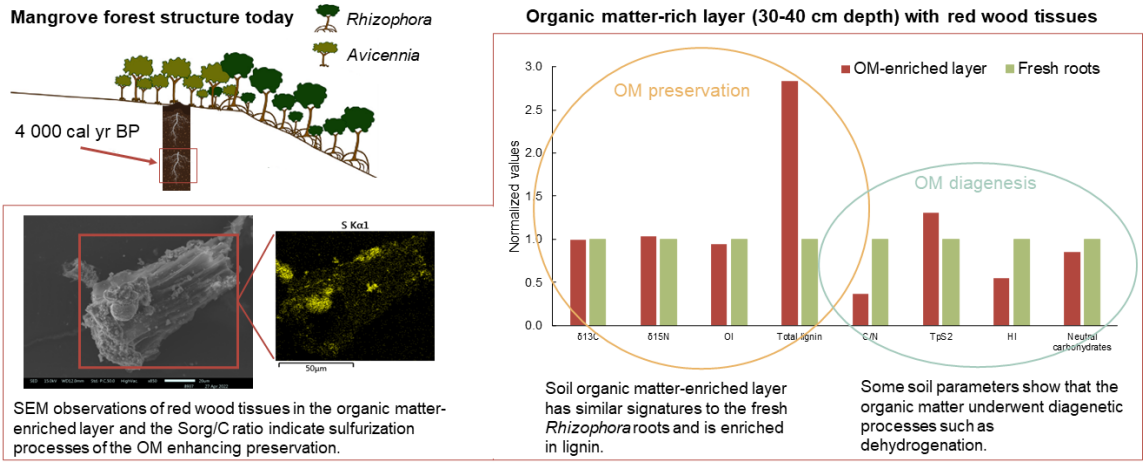

This study focuses on a soil layer enriched in mangrove-derived organic matter (OM) that accumulated during a stable sea-level period of the Holocene in New Caledonia (South Pacific). Radiocarbon dating situates this enriched layer at approximately 4 000 years BP. The aim of this study is to characterize the enriched OM layer employing isotopic, Rock-Eval, and molecular analyzes (lignin and neutral carbohydrates). This OM has undergone diagenetic processes such as dehydrogenation, and the loss of components such as the main neutral carbohydrates: glucose, xylose, and galactose. However, some Rock-Eval parameters, the total lignin content, and isotopic ratios show that this OM is well preserved. In addition, SEM observations highlighted the presence of pyrite associated to preserved root material. Along with high S_{org}/C ratio, these results suggest potential processes of OM sulfurization. Prolonged sea-level stability in addition to anoxic and sulfidic soil conditions enhances OM accumulation and long-term sequestration in mangrove soils.

Keywords: mangrove, stable isotopes, Rock-Eval, carbon dating, neutral carbohydrates, lignin

IV.B.2. Short Communication

Mangrove forests are efficient carbon sinks due to their productivity, estimated at 11 Mg C ha^{-1} yr^{-1}, and their ability to effectively sequester carbon in the soil at an average rate of 180 g organic carbon (OC) m^{-2} yr^{-1} (Alongi, 2020). The OC pool is predominantly refractory, and the presence of anoxic and sulfidic soil conditions, especially at depth, significantly limits OC mineralization, thus facilitating its long-term storage (Kristensen et al., 2008). Nevertheless, mangrove forest migration in response to sea-level changes presents challenges in accurately characterizing the carbon stock of the present mangrove forests (Marchand, 2017).

In the Holocene period, sea-level variations have impacted mangrove distribution (Woodroffe et al., 2016). For about 3 700 years, sea-level on the West Coast of New Caledonia was stable 1.1 m higher than today, before falling around 2 800 cal yr BP (Yamano et al., 2014). The fall of the sea-level resulted in mangrove seaward migration. However, the presence of the former mangrove forest is recorded in soils of the upper current intertidal zone as an organic matter (OM)-rich layer characterized by the presence of red tissues typical of *Rhizophora* trees (Jacotot et al., 2018).

The aim of the present study was to characterize this OM-rich layer using isotopic, molecular, and Rock-Eval analyzes, and to identify decomposition and/or preservation processes related to this millennial-aged OM deriving from mangrove trees.

To reach these goals, triplicate *Rhizophora stylosa* coarse roots were cut with a saw, and green leaves were collected from the trees in a mangrove of the West Coast of New Caledonia to help determine the sources of the OM-rich layer. The study site is a semi-arid mangrove forest typical of the West Coast of New Caledonia with *R. stylosa* present on the seaside of the forest and *Avicennia maria* on the land side. Soil samples in this specific layer, situated between 30 and 40 cm depth, were collected with an Eijkelkamp gouge auger in May 2021. All samples were freeze-dried and ground. Rock-Eval pyrolysis was conducted on a Rock-Eval 7S (Vinci Technologies) and gave multiple parameters on the soil samples including total organic carbon (TOC), total and organic sulfur (S_{tot} and S_{org}), hydrogen index (HI), oxygen index (OI), and the temperature of the oven at the maximum yield of S2 peak (TpS2). Stable isotope ratios ($\delta^{13}C$ and $\delta^{15}N$) and C/N ratios were obtained on an isotope ratio mass spectrometer Sercon Intergra 2. The molecular analysis focused on neutral carbohydrates and lignin-derived phenols. Neutral carbohydrates were extracted through hydrolysis and analyzed via GC-MS after derivatization with BSTFA in pyridine. The GC is a Trace1300 (Thermo Scientific) coupled to a MS ISQ7000 (Thermo Scientific). The GC is equipped with a Restek Rxi-5Sil MS

column (60 m x 0.25 mm, 0.25 µm film thickness). 11 lignin-derived phenols were quantified after hydrolysis and extraction. Chromatographic separation was achieved using a Vanquish Flex system (Thermo Scientific). Samples were separated on a Hypersil GOLD column (1.9 µm particle size), 50 x 2.1 mm (Thermo Scientific). The mobile phase was a mixture of ultrapure water and methanol. MS detection was performed using an Orbitrap Exploris120 (Thermo Scientific). Soil samples were also observed on a scanning electron microscope (SEM) using a JEOL JSM-IT300 LV apparatus coupled with an energy dispersive spectrometer (EDX) Oxford xmax80T device. Radiocarbon dating of the soil samples was performed after hot HCl washing at the radiocarbon dating laboratory of the University of Waikato.

In the enriched soil layer, TOC reached more than 10% while median TOC content in mangrove soils is 2.2% (Kristensen et al., 2008). In *Table IV.B-1*, numerous parameters are presented for both the enriched layer and the fresh roots and leaves of *R. stylosa*. The isotopic values ($\delta^{13}C$ and $\delta^{15}N$) of the layer (-26.4‰ and 1.26‰, respectively) was similar to that of the fresh *R. stylosa* roots (-26.5‰ and 1.22‰, respectively), indicating that the preserved roots contribute significantly to the OM composition. However, the C/N ratio of the soil (36.6) was lower than that of the roots (99.6) or leaves (53.8), highlighting a preference for the degradation of C-rich compounds over N-rich compounds. In fact, the overall neutral carbohydrate (lacking N atoms) content measured in the soil (323 mg g^{-1} TOC) was lower compared to the fresh roots (381 mg g^{-1}), while the lignin (with N atoms) content was higher (4 257 µg g^{-1} TOC and 1 500 µg g^{-1}, respectively). The Rock-Eval parameters suggested that the buried OM is preserved from oxygenation, with a low OI value (81 mg CO_2 g^{-1} TOC), similar to that of the *R. stylosa* tissues, aligning with the anoxic conditions of the soil horizon. However, the buried OM displayed greater thermal stability than the fresh OM and has undergone dehydrogenation, indicated by the lower HI (139 mg HC g^{-1} TOC) and higher TpS2 values (452 °C) compared to the fresh tissues (Marchand et al., 2008). The S_{org} content of the soil horizon was much higher (1.47%) than the S_{org} content in the fresh tissues (<0.3%) and the indicative S_{org}/C ratio was 0.10 for the enriched layer.

Table IV.B-1. Mean values of different parameters in the soil OM-enriched layer and in the fresh roots and leaves of *R. stylosa* at the same site.

Variables	OM-enriched layer	*R. stylosa* fresh roots	*R. stylosa* fresh leaves
Isotopic			
$\delta^{13}C$ (‰vsVPDB)	-26.4±0.2	-26.5±0.3	-27.5±0.1
$\delta^{15}N$ (‰vsAir)	1.26±0.57	1.22±0.95	-1.28±0.45
C/N	36.6±3.2	99.6±16.0	53.8±13.7
Rock-Eval			
TpS2 (°C)	452	347	351
HI (mg HC g^{-1} TOC)	139	252	410
OI (mg CO_2 g^{-1} TOC)	81	86	73
S_{org} (%)	1.47	0.20	0.16
S_{tot} (%)	3.63	0.45	0.63
Carbohydrates (mg g^{-1} for tissues and mg g^{-1} TOC for soil)			
Total	323	381	228
Xylose	8.3	128	49
Arabinose	261	71	62
Ribose	1.0	0.34	0.48
Rhamnose	21	39	27
Fucose	5.2	6.5	3.8
Mannose	7.2	17	4.1
Galactose	5.7	39	34
Glucose	14	80	48
Hexoses	13	56	38
Pentoses	269	199	111
Deoxy sugars	26	49	31
Hex/Pen	0.05	0.28	0.34
Lignin-derived phenols (µg g^{-1} for tissues and µg g^{-1} TOC for soil)			
Total	4 257	1 500	1 325
p-Hydroxyl	633	375	209
Vanillyl	3 072	743	559
Syringyl	457	337	215
Cinnamyl	96	46	342
C/V	0.03	0.06	0.61
S/V	0.15	0.45	0.39
P/(V+S)	0.18	0.35	0.27
PON/P	0.17	0.03	0.08
$(Ad/Al)_p$	0.75	0.34	1.00
$(Ad/Al)_v$	0.13	1.10	4.73
$(Ad/Al)_s$	2.66	3.20	1.88

Hexoses (Hex) = Mannose et Galactose, Pentoses (Pen) = Xylose et Arabinose, Deoxy sugars = Fucose et Rhamnose, P = p-hydroxyl, V = Vanillyl, S = Syringyl, C = Cinnamyl, PON = p-hydroxyacetophenone, and (Ad/Al) = acid over aldehyde ratio.

At the molecular level, the Hex/Pen ratio within the soil's enriched layer (0.05) was nearly an order of magnitude lower than that of the fresh roots (0.28) and leaves (0.34). Polysaccharides originating from plants are notably rich in pentoses content, whereas those arising from microbes primarily consist of hexoses. Consequently, the reduced Hex/Pen ratio underscores the substantial contribution of plant-derived OM to this layer. The smaller ratio was linked to a significant increase in arabinose from the fresh roots (71 mg g^{-1}) to the buried layer (261 mg g^{-1} TOC), alongside the loss of galactose. Previous research has highlighted arabinose's refractory behavior (Marchand et al., 2005), given its presence in hemicellulose, but also pectin, which exhibits higher resistance to decomposition compared to cellulose and hemicellulose (Benner et al., 1990). Additionally, glucose and xylose were measured in lower concentrations within the enriched layer. Among the fresh tissues, xylose, galactose, and glucose were the most abundant sugars. We suggest that, as neutral carbohydrates serve as a significant energy source for soil microbial communities, the major molecules underwent degradation upon OM burial (Opsahl and Benner, 1999). This degradation is particularly pronounced due to the labile nature of glucose and xylose, which are the least stable carbohydrates (Marchand et al., 2005). Conversely, mannose, ribose, and the deoxy sugars remained preserved. Nonetheless, neutral carbohydrates concentrations in the enriched layer indicated low microbial activity in the horizon.

Lignin-derived phenols are exclusively associated with vascular plants. Enrichment of lignin content in this layer, as compared to the fresh roots, was apparent across all four phenol groups, with the most significant increase observed for p-hydroxyl phenols (doubling) and vanillyl phenols (quadrupling). Consequently, the C/V ratio in the soil was halved, while the S/V ratio was reduced to one-third of that found in the fresh roots. Among phenol groups, vanillyl predominates in mangrove debris (Benner et al., 1990) and is similarly prevalent in mangrove soils (Lallier-Vergès et al., 2008). Preservation tendencies favor vanillyl and p-hydroxyl phenols over syringyl and cinnamyl groups (Lallier-Vergès et al., 2008). While the acid/aldehyde ratios were comparable for p-hydroxyl and syringyl groups, they were substantially lower in the soil than in the tissues for the vanillyl group. This variance was primarily attributed to a significant enrichment in vanillin (*Supplementary Table IV.B-1*). Low Ad/Al ratios are commonly encountered in anoxic environments due to the absence of side-chain oxidation processes (Lallier-Vergès et al., 2008). In this context, however, vanillin preservation emerges as the key factor. Additionally, notable enrichment in p-hydroxyacetophenone was evident (*Supplementary Table IV.B-1*), leading to a considerably higher PON/P ratio in the soil compared to the tissues. This may result from the fact that p-hydroxyacetophenone exclusively originates from lignin oxidation, whereas

p-hydroxybenzoic acid and p-hydroxybenzaldehyde may also result from the oxidation of non-lignin precursors within the fresh tissues (Benner et al., 1990). The elevated PON/P ratio thus suggests the predominance of lignin within the buried layer.

SEM-EDX analysis revealed the association between the root material and pyrite (FeS_2) (*Figure IV.B-1*). We suggest that the intricate interaction between OM and pyrite contributed to an enhanced preservation of OM within the waterlogged and anoxic soil conditions. The association of OM with minerals slows decomposition processes, and in environments characterized by high sedimentation rates, facilitates the burial of OM (Wakeham and Canuel, 2006). Furthermore, the S_{org}/C ratio was very high (>0.06), indicative of a high sulfur-OM type according to Orr (1986). We suggest that it is not only the organo-mineral associations that promote preservation, but also the natural sulfurization of OM in sulfidic soils.

The radiocarbon dating (^{14}C-datation) indicated that the soil layer dated back to approximately 4 000 cal yr BP, aligning well with the stable high sea-level period (Yamano et al., 2014). The accumulation of roots and other OM debris during this timeframe can be attributed to the prolonged period of sea-level stability and the limited capacity of microbial communities to decompose mangrove tissues in waterlogged, anoxic conditions. In Belize, a comparable scenario to the one described in this study was identified (McKee and Faulkner, 2000). However, the authors attributed the formation of peat as an adaptation mechanism to rising sea-levels, rather than indicating a period of sea-level stability (McKee et al., 2007).

The results of the present study sheds light on decomposition and preservation processes that occur under specific anoxic and sulfidic conditions in mangrove soils and confirm that these ecosystems can store large amount of carbon notably through sulfurization processes. With the predictions of fast sea level rise worldwide, the capacity of mangrove forests to store carbon in the soils may not be at full efficiency.

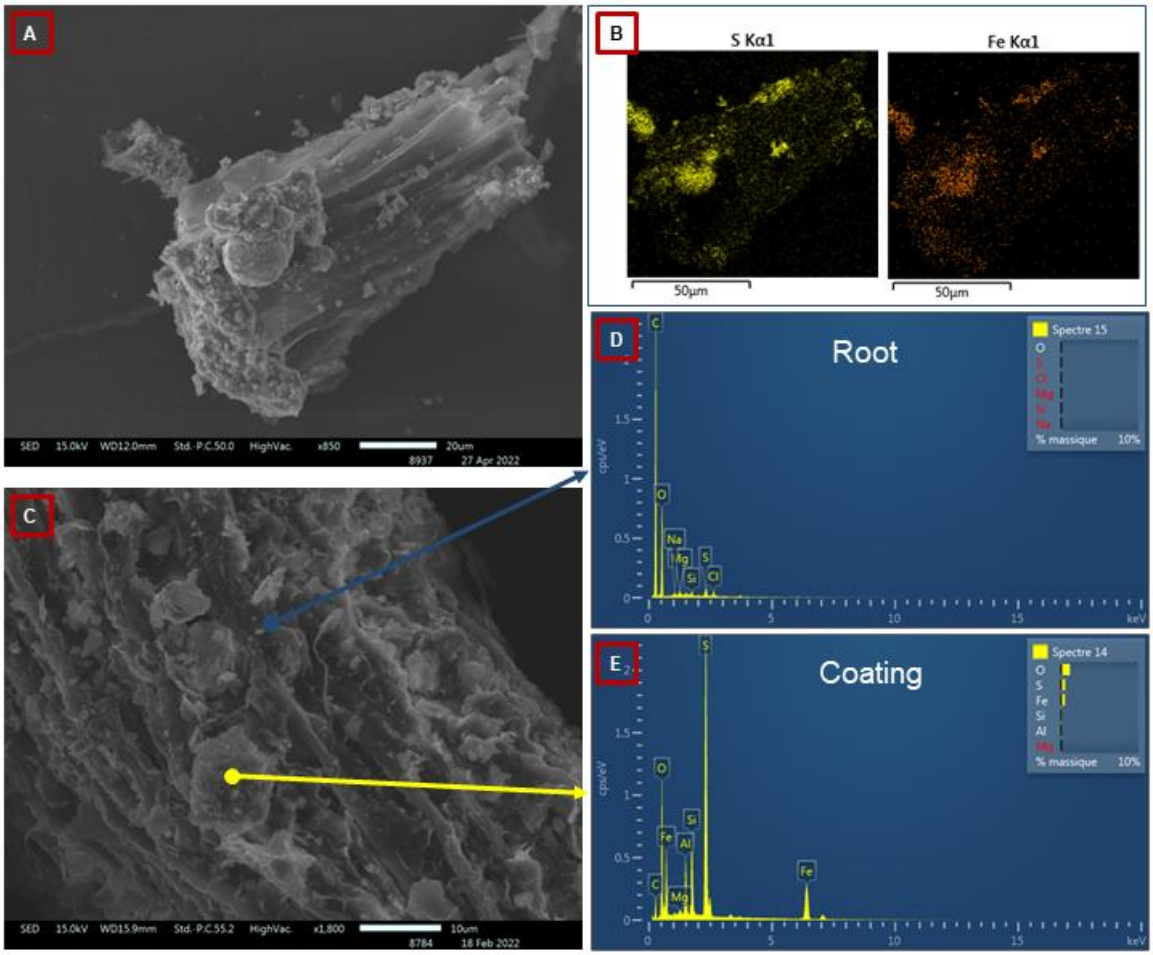

Figure IV.B-1. (A) SEM photo of a preserved root in the soil coated with pyrite crystals as exposed by the (B) EDX associated cartography of S and Fe. (C) SEM photo of preserved root zoomed in with associated EDX spectra of (D) the root and of (E) the coating.

IV.B.3. Acknowledgments

The authors acknowledge Kapeliele Gututauava and Pierre Sanlis for the help with the field work. The authors acknowledge Fiona Petchey from the University of Waikato for ^{14}C-dating. The authors acknowledge Ines Le Mao from NC Bioressources for UPLC-MS optimization and analyzes and Anne Desnues from IRD for the isotopic analyzes.

IV.B.4. Supplementary materials

Supplementary Table IV.B-1. Mean (±SD) individual lignin-derived phenols in the soil enriched layer and roots and leaves of *R. stylosa*.

Lignin-derived phenols (µg g^{-1} for tissues and µg g^{-1} TOC for soil)	**OM-enriched layer**	***R. stylosa* fresh roots**	***R. stylosa* fresh leaves**
p-hydroxybenzaldehyde	302	272±213	97±15
p-hydroxybenzoic acid	106	12±5	16±5
p-hydroxyacetophenone	225	91±22	97±7
Vanillin	2,328	304±89	79±36
Acetovanillone	440	105±14	105±28
Vanillic acid	303	333±157	374±277
Syringaldehyde	121	80±14	75±9
Acetosyringone	13	0.2±0.0	0.1±0.0
Syringic acid	322	257±59	140±7
Coumaric acid	78	44±16	341±60
Ferulic acid	18	1.6±0.4	1.4±0.2

C. Chapter IV.C: Influences of urban runoff on mangrove organic matter sources and transformation in soil

Sarah Louise ROBIN, François BAUDIN, Claude LE MILBEAU, Andrea C ALFARO, Cyril MARCHAND

To be submitted to Geoderma

IV.C.1. Abstract

This study explored the impact of urban runoff in a mangrove forest dominated by *Avicennia marina* and *Rhizophora stylosa* on the compositions of the mangrove-derived organic matter (roots and leaves) and on the diagenesis of the organic matter in the soil. Previous studies showed that the urban rainwater runoff modifies the physico-chemical conditions of the mangrove soil, and the species stand zonation in the intertidal zone. Therefore, we hypothesized that the runoff also impacted the organic matter dynamics within the mangrove forest. The leaves and roots of both species differed in their composition because of environmental factors as shown by stable isotopes, Rock-Eval pyrolysis, and molecular analyzes (lignin and neutral carbohydrates). *R. stylosa* exhibited higher $\delta^{15}N$ values than *A. marina*, potentially linked to urban runoff as a source of ^{15}N-rich molecules. The soil organic matter pool was primarily autochthonous but possibly influenced by runoff-promoted microbial communities. Diagenetic processes involving dehydrogenation and oxygenation were observed in the soil under both mangrove species, resulting in a decline in total organic carbon with depth. Total lignin content increased with depth, but phenol group proportions varied suggesting lignin diagenetic and preservation processes. Neutral carbohydrate content increased beneath *A. marina*, potentially due to microbial activity, while *R. stylosa*'s soil showed a slight neutral carbohydrate decrease with limited microbial activity. Notably, urban runoff did not exert a significant direct influence on organic matter diagenesis in mangrove soils.

Keywords: urban mangrove, stable isotopes, Rock-Eval, neutral carbohydrates, lignin, organic matter

IV.C.2. Introduction

Mangrove forests worldwide face a multitude of anthropogenic pressures, with urbanization being a significant contributor (Alemu I et al., 2021). Urban mangrove forests encompass both newly developing forests in urban coastal areas and established forests that have adapted to anthropogenically developed environments (Reyes et al., 2022). In

urban settings, mangrove forests encounter constraints on their landward expansion due to infrastructure limitations (Gilman et al., 2008). They also become recipients of various types of effluents that can lead to alterations in their physico-chemical and hydrological conditions (Torres et al., 2019), as well as the transfer of nutrients and contaminants from the urban watershed into these ecosystems (Cavalcante et al., 2009; Bastakoti et al., 2019a).

Mangrove ecosystems are renowned for their substantial capacity to sequester atmospheric CO_2 within their biomass and soil (Alongi, 2014). It is estimated that mangrove forests capture approximately 0.9% of the annual anthropogenic atmospheric C accumulation, an impressive amount considering they cover a mere 0.03% of the Earth's total surface area (David, 2017). This C storage is greatly facilitated by soil water saturation and anoxia, conditions that favor C storage levels ten times higher than those observed in temperate forests or other non-inundated tropical forests (Donato et al., 2011). Of the C stored in mangrove forests, 60% to 90% resides within the soil, typically characterized by low oxygen levels that limit the mineralization of organic carbon (OC) (Alongi, 2014). Organic matter (OM) buried in mangrove soils undergoes significant biogeochemical transformations during early diagenesis, marked by a sequence of oxidation reactions driven by bacterial degradation processes. As oxygen becomes depleted, OM undergoes oxidation via various biogeochemical reactions involving alternative electron acceptors such as sulfate (SO_4^{2-}), manganese (Mn^{4+}), nitrate (NO_3^-), and iron (Fe^{3+}). In the context of mangrove soils, continuous tidal sulfate inputs make sulfate reduction the dominant anaerobic process (Kristensen et al., 2008).

In urban mangrove forests, the processes related to C storage and OM transformations in the soil may be subject to alteration due to modified environmental conditions (Robin et al., 2022). These modifications can impact microbial communities (Torres et al., 2019; Fiard et al., 2022) and alter the availability of electron acceptors (Pi et al., 2010), thereby influencing the intricate biogeochemical processes at play. Furthermore, the sequestration and transformation of OM are highly dependent on the composition of the OM itself (Hernes et al., 2001; Bouillon et al., 2008; Kida et al., 2019a). OM can be categorized as either autochthonous (originating from within the mangrove ecosystem, such as mangrove litter and associated fauna) or allochthonous, derived from external sources such as terrestrial watershed runoff and inputs from adjacent marine ecosystems. The influx of urban effluents can also have a significant impact on the sources of OM that are introduced into the mangrove forest either through introduction of allochthonous material or changes in production of autochthonous material (Randhir, 2003; O'Driscoll et al., 2010), and their degradation processes (Robin et al., submitted).

These changes in OM sources can, in turn, influence the OM cycle within the mangrove ecosystem, contributing to a complex interplay of factors that shape the carbon and nutrient dynamics within these unique coastal habitats.

Research on urban mangrove forests is diverse, with a predominant focus on examining the influx and accumulation of urban-derived contaminants within these ecosystems (Cavalcante et al., 2009; Assunção et al., 2017; Bastakoti et al., 2019a; Celis-Hernandez et al., 2020). However, there has been limited exploration regarding the influence of urbanization on OM dynamics within these environments. The objectives of this study are to assess the impact of urban runoff on the chemistry of the mangrove-derived OM sources (mangroves leaves and roots), and to determine the influence of the runoff on the processes governing the sequestration and transformation of OM in the mangrove soil. To this end, a mangrove forest on the West Coast of New Caledonia, receiving urban effluents, was chosen as study site. This forest has a volcano-sedimentary watershed and is constituted of the two dominant mangrove species observed on the West Coast of New Caledonia, *Avicennia marina* and *Rhizophora stylosa*. Urban rainwater runoff from the upper housing allotment flows into this mangrove forest since more than five decades, resulting in a modification of the species zonation in the intertidal zone and modified soil physico-chemical conditions including decreasing soil salinity (Robin et al., 2022).

We hypothesize that the fresh mangrove tissues from this site will have higher modified chemical compositions compared to other semi-arid mangrove forests because the runoff may act as a source of nutriments and the modified soil salinity (0 g L^{-1}) may influence some traits such as $\delta^{13}C$ values. We also hypothesize that the modifications in mangrove tissues will be more visible for the species most impacted by the runoff, *R. stylosa*. To test these hypotheses, fresh leaves and roots of the two species were collected and characterized using stable isotope analysis ($\delta^{13}C$, $\delta^{15}N$, C/N), Rock-Eval pyrolysis, and molecular analyses (lignin and neutral carbohydrate content). Regarding OM transformations in the soil, we hypothesize that the OM is highly degraded in the urban mangrove soil due to the suboxic soil conditions (Robin et al., 2022) and fast leaf litter degradation rates (Robin et al., submitted). To test this hypothesis, soil samples down to 30-cm depth were collected beneath both species and characterized similarly to the biotic samples.

IV.C.3. Material & methods

IV.C.3.1. Study site

The urban mangrove forest under investigation was the same as depicted in Chapter II and Chapter III.A & B. Briefly, this mangrove forest is located in Dumbea, New Caledonia, and it has been receiving urban rainwater runoff from an allotment area for over 50 years. The geological watershed of the mangrove forest is volcano sedimentary. This forest is primarily comprised of two dominant mangrove species found along the West coast of the island: *Avicennia marina* and *Rhizophora stylosa*. These species grow in monospecific stands within the forest. In New Caledonia, *Rhizophora* species typically thrive at the seaside, where soil salinity is close to that of seawater, while *A. marina* tends to grow at higher elevations with soil salinity levels elevated compared to the shoreline (Marchand, 2007). Notably, within this urban site, there is a secondary monospecific stand of *R. stylosa* that forms behind the *A. marina* trees, near the entrance of the runoff (*Figure IV.C-1*), where the surface soil salinity is 0 g L^{-1} (Robin et al., 2022). It's worth mentioning that the *R. stylosa* trees in this landward stand exhibit notably greater height, reaching approximately 8 to 10 meters, which is significantly taller than those observed in other mangrove forests along the West coast of New Caledonia, where they typically attain heights of around 2 meters because of the semi-arid climate.

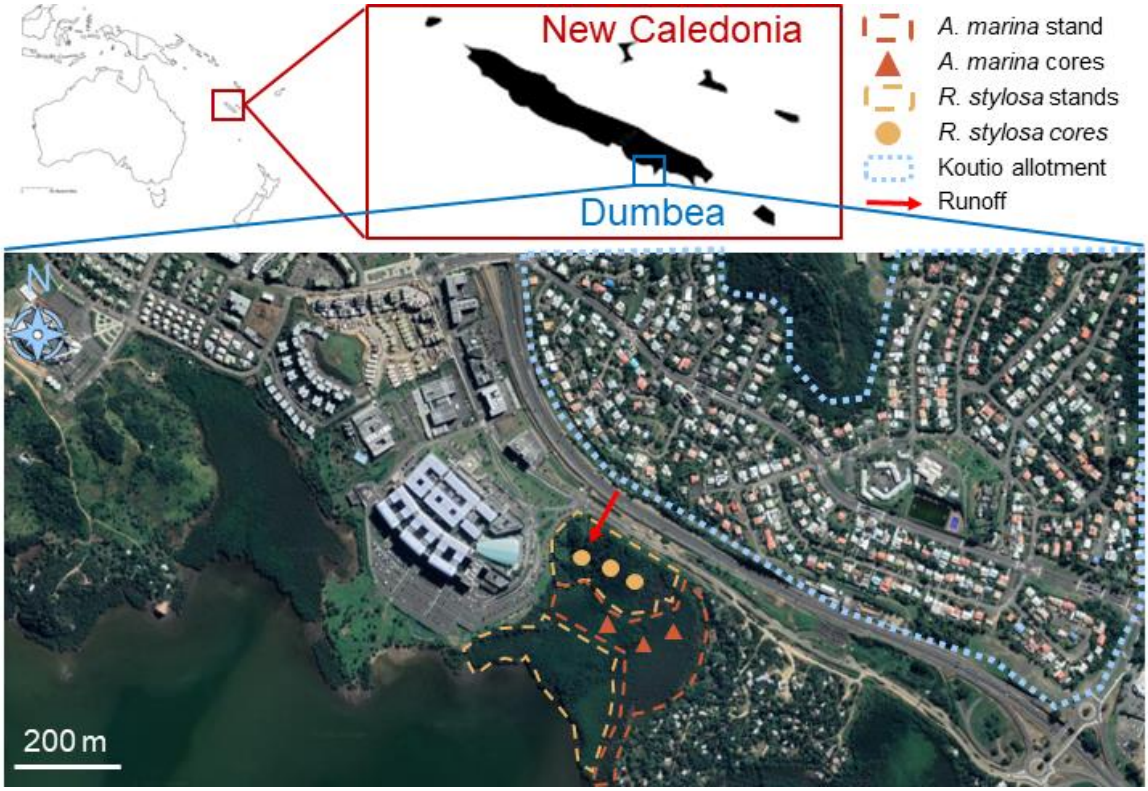

Figure IV.C-1. Mangrove forest studied in Dumbea with delimitations of the species stands and the Koutio allotment, with triplicate cores shown and the entrance of the urban rainwater runoff (satellite image from Google Earth).

IV.C.3.2. Sampling & processing

Soil, fresh leaves, and fresh roots of both mangrove species were collected in May 2021. Green leaves were obtained from the trees, with each sample consisting of 20 leaves collected from five different trees. For *R. stylosa*, the primary underground roots were sawn, while for *A. marina*, pneumatophores were gently detached from the main cable roots. In each stand, triplicate 30-cm soil cores were extracted using an Eijkelkamp gauge auger and subsequently divided into five sections, spanning depths of 0-5, 5-10, 10-15, 15-20, and 20-30 cm. Beneath 30 cm was the bedrock. The leaves, roots, and soil sections were carefully placed into securely sealed plastic bags and transported in a cooler until reaching the laboratory. Upon arrival at the laboratory, the samples were weighed and promptly frozen. Prior to freezing, freeze-drying, and grinding, the biotic samples underwent a thorough washing with MilliQ water.

IV.C.3.3. Sample analyzes

IV.C.3.3.1. Stable isotopes analysis

Total C, total N, and their stable isotopes were measured on an isotope ratio mass spectrometer Sercon Intergra 2 at the LAMA laboratory of the Institute of Research and Development of New Caledonia. About 30 mg of samples were weighed in tin cups and

folded into tightly closed spheres. The samples were transported in a combustion column with helium gas where they were heated at 1 000 °C and oxidized with Cu and Cr oxides, while silver wool trapped sulfur and halogens. The samples were then transferred to the reduction column at 600 °C where the Cu interacts with excess oxygen so that the NO_x is reduced to N_2. The water in the samples was trapped with $Mg(ClO_4)_2$ and N_2 and CO_2 of the samples were separated by gas chromatography. The separated molecules were quantified by mass spectrometry in positive ESI mode. The mass spectrometer measures the relative abundances of isotopes in the sample gas. For carbon, it measures the ratio of ^{13}C to ^{12}C (expressed as $\delta^{13}C$), while for nitrogen, it measures the ratio of ^{15}N to ^{14}N (expressed as $\delta^{15}N$). To calculate the δ values, the measured isotopic ratio is compared to a known standard. The standard used is the Vienna Pee Dee Belemnite (VPDB) standard for C, and the atmospheric nitrogen standard for N. For quality control, duplicate of samples were passed through the spectrometer (1 every 10 samples) (Supplementary Table IV.*A-2*).

IV.C.3.3.2. Rock-Eval analysis

Rock-Eval pyrolysis was conducted using a Rock-Eval 7 instrument (Vinci Technologies) at the GEORG platform of Sorbonne Université, employing a method tailored for soils and recent sediments (Baudin et al., 2015). Initially, desalted crushed samples underwent a 3 min isotherm under N_2 atmosphere at 200 °C, leading to the volatilization of free hydrocarbons (S1). Subsequently, a temperature ramp of 30 °C min^{-1} was applied, causing the vaporization of products resulting from the thermal cracking of OM up to 650 °C (S2). The continuous detection of hydrocarbon effluents was performed using a flame ionization detector (FID) and quantified in mg g^{-1} of the sample. Simultaneously, the levels of CO and CO_2 were monitored online and measured using an infrared cell (S3). Following the pyrolysis step, samples were automatically transferred to an oxidation oven. Here, they were subjected to a 1 min isotherm at 300 °C, followed by a temperature ramp of 20 °C min^{-1} up to 850 °C. The total signals of CO and CO_2 were expressed in mg g^{-1} of the sample. These thermograms enabled the calculation of the total organic carbon (TOC) by combining pyrolysis carbon with the residual carbon detected during the oxidation phase (Behar et al., 2001). Hydrogen and oxygen indices were computed to approximate the H/C and O/C atomic ratios of the OM. Additionally, the TpS2 parameter represented the temperature of the pyrolysis oven at the peak of maximum S2 yield and is typically utilized as a maturity indicator for the OM (Behar et al., 2001; Disnar et al., 2003).

IV.C.3.3.3. Neutral carbohydrates analysis

Neutral carbohydrates were subjected to analysis at the Earth Sciences Institute of Orleans, France. In this process, approximately 50 mg of each sample underwent hydrolysis within Pyrex tubes at 105 °C for a duration of 4 h, utilizing 5 mL of 4M trifluoroacetic acid (TFA). Following this hydrolysis step and subsequent cooling in an ice bath, 500 µL of an internal standard (2-deoxyglucose at 8 mg L^{-1}) were introduced into the sample, which was then centrifuged for 30 minutes at 5 600 rpm. The resulting extract was subjected to evaporation, and the resulting dried samples were preserved in a frozen state. Before the actual analysis, neutral carbohydrates were derivatized by adding 500 µL of an ethoxy ammonium chloride solution in pyridine (40 mg mL^{-1}), which was heated for an hour at 70 °C. Subsequently, 250 µL of BSTFA were incorporated into the sample, followed by another hour of heating at 70 °C. After further evaporation, the residue was dissolved in 2 mL of heptane, filtered with a 45 µm filter, and subsequently injected into the GC-MS system.

The GC instrument employed was a Trace 1300 (Thermo Scientific), coupled with an MS ISQ7000 (Thermo Scientific). It was equipped with a Restek Rxi-5Sil MS column (60 m x 0.25 mm, 0.25 µm diameter) along with a 5 m pre-column. Helium gas served as the carrier, and the analysis was conducted with a constant flow rate of 1 mL min^{-1}. The injector temperature was maintained at 280 °C, and the transfer line was set at 300 °C. A 1 µL aliquot of the sample was injected in splitless mode and passed through the column following a programmed temperature sequence (*Supplementary Table III.A-2*). For the MS analysis, the source temperature was set at 240 °C, and electron impact (70 eV) was applied. Spectra were acquired within a range of 50 to 750 Da, with a scan time of 0.4 s $scan^{-1}$. Quality control consisted of duplicate technical samples (≤11% standard deviation) and measurement of the internal standard (*Supplementary Table III.A-3*).

IV.C.3.3.4. Lignin-derived phenols analysis

Each sample, comprising 100 mg, underwent a hydrolysis process lasting for 3 h at a temperature of 170 °C. This hydrolysis was carried out in the presence of 8 mL of 2N NaOH and 100 mg of $Fe(NH_4)_2(SO_4)_2$ under a N_2 atmosphere. Following cooling, the extract was obtained by centrifuging the sample at 3 000 rpm for 10 minutes. To achieve acidification at pH 1, HCl was added to the extract, and the phenolic compounds derived from lignin were subsequently extracted twice using 3 mL of anhydrous diethyl ether. After complete evaporation, the phenolic compounds were dissolved in 1 mL of a mixture of methanol and water (50:50) and then filtered through a 45 µm filter.

Subsequent analysis was conducted using a UPLC-MS at the University of New Caledonia. Chromatographic separation was achieved employing a Vanquish Flex system (Thermo Fisher Scientific, France). The samples were separated on a Hypersil GOLD column (1.9 µm particle size), measuring 50 x 2.1 mm (Thermo Scientific). For elution, a binary gradient program was employed (*Supplementary Table III.A-4*). The mobile phase consisted of ultrapure water with 0.1% formic acid (eluent A) and methanol OPTIMA LC/MS (Fisher Scientific) with 0.1% formic acid (eluent B). The flow rate was set to 0.5 mL min^{-1}, and automated injection of 2 µL was performed by the autosampler. UV detection occurred at 280 nm. MS detection was carried out using an Orbitrap Exploris 120 (Thermo Fisher Scientific, France) operating with a heated electrospray ionization source in negative ion mode and a vaporizer temperature of 300 °C. Scan modes encompassed full MS – $ddMS^2$ and SRM. The full MS mode featured a resolution of 30 000 and a scan range of 50 – 250 m/z with specified HCD collision energies for each molecule. The SRM mode utilized a resolution of 120 000 at 20% HCD collision energy. Detailed UPLC-MS parameters are presented in *Supplementary Table III.A-4*. The quantification was performed with an external calibration curve (*Supplementary Table III.A-5*) and laboratory reference materials spiked with the analytes. For quality control, a blank solution was passed at the beginning and end of every series in the same conditions as the samples and values were all below detection limits (*Supplementary Table IV.A-3*). A quality control solution (QC) consisting of a point of the calibration curve was passed every 10 samples in the same conditions as the samples and the values obtained were all below 15% difference with the expected value (*Supplementary Table IV.A-3*).

IV.C.4. Results

IV.C.4.1. Fresh sources characteristics

Table IV.C-1 displays various parameters characterizing the fresh leaves and roots of *A. marina* and *R. stylosa* at the studied site. The biota of *R. stylosa* was characterized by lower $\delta^{13}C$ values (-30.7 and -27.0‰) and higher C/N values (28 and 113) than *A. marina*. The tissues also exhibited higher TpS2 values, suggesting greater thermal stability, and lower HI and OI values than *A. marina*. Fresh leaves and roots of *A. marina* had higher total lignin content (1.73 – 4.97 vs 1.07 – 1.40 mg g^{-1}) and neutral carbohydrate contents (322 – 378 vs 272 – 304 mg g^{-1}). The higher lignin content was associated with a higher vanillyl content, and the higher neutral carbohydrate content was associated with a higher glucose content. However, the tissues of *R. stylosa* contained more xylose, fucose, and mannose than the tissues of *A. marina*.

For both species, the roots and leaves can be distinguished by their differences in certain parameters. Fresh roots were characterized by higher $\delta^{13}C$ values and C/N ratios than the fresh leaves. The roots also displayed lower lignin content, associated with lower cinnamyl (0.04 – 0.05 vs. 0.48 – 2.14 mg g^{-1}) and vanillyl contents (0.48 – 1.34 vs. 0.58 – 2.01 mg g^{-1}), whereas the syringyl concentrations were higher (0.30 – 0.35 vs. 0.20 – 0.26 mg g^{-1}) than in the leaves. Regarding neutral carbohydrates, the roots of *A. marina* had higher levels than the leaves, while it was the opposite for *R. stylosa*. Still, for both species, the leaves contained lower xylose content (61 – 66 mg g^{-1}) and higher ribose content (1.4 – 1.6 mg g-1) than the roots (87 – 126 mg g^{-1} and 0.6 – 0.7 mg g^{-1}, respectively).

Table IV.C-1. Fresh leaves and roots characteristics for both *A. marina* and *R. stylosa*.

Species	***A. marina***		***R. stylosa***	
Tissues	**Leaves**	**Roots**	**Leaves**	**Roots**
$\delta^{13}C$ (‰vsVPDB)	-27.7±0.7	-25.6±0.6	-30.7±1.0	-27.0±0.7
$\delta^{15}N$ (‰vsAir)	5.8±1.7	-2.0±0.6	2.6±0.1	3.9±3.0
C/N	17±3	106±50	28±5	113±28
TpS2 (°C)	289	333	351	355
HI (mg HC g^{-1} TOC)	510	460	459	329
OI (mg CO_2 g^{-1} TOC)	172	142	116	120
Σlignin (mg g^{-1})	4.97	1.73	1.40	1.07
p-hydroxyl (mg g^{-1})	0.56	0.06	0.14	0.15
Vanillyl (mg g^{-1})	2.01	1.34	0.58	0.48
Syringyl (mg g^{-1})	0.26	0.30	0.20	0.35
Cinnamyl (mg g^{-1})	2.14	0.04	0.48	0.05
Σneutral carbohydrates (mg g^{-1})	322	378	304	272
Xylose (mg g^{-1})	61	87	66	126
Arabinose (mg g^{-1})	62	125	102	61
Ribose (mg g^{-1})	1.6	0.6	1.4	0.7
Rhamnose (mg g^{-1})	29	28	37	22
Fucose (mg g^{-1})	0.7	1.2	4.5	4.5
Mannose (mg g^{-1})	5.1	4.8	5.6	6.9
Galactose (mg g^{-1})	28	66	61	22
Glucose (mg g^{-1})	135	65	27	29

IV.C.4.2. Stable isotope ratios and Rock-Eval parameters in the soil

In *Figure IV.C-2*, multiple graphs were plotted to depict the evolution of various parameters with depth beneath both *A. marina* and *R. stylosa*. Most parameters exhibited similar trends with depth under both species. The TOC decreased with depth, decreasing from 6.0% to 0.5% beneath *A. marina* and from 10.8% to 1.1% beneath *R. stylosa*. The C/N ratio beneath *R. stylosa* was higher than beneath *A. marina*, but both ratios slightly varied with depth, ranging from 20 to 23 and from 13 to 18, respectively. The upper soils (0-5 cm) beneath both species shared the same $\delta^{15}N$ values of 4.3‰ and decreased below 20 cm to 2.7‰ for *R. stylosa* and 3.8‰ for *A. marina*. The thermal stability of the OM, as indicated by the TpS2 values, was stable with depth for both species, except peak values obtained in the 10-15 cm section beneath *A. marina* (458 °C) and in the 15-20 cm section beneath *R. stylosa* (435 °C). Generally, higher values were obtained beneath *A. marina* (404 – 458 °C) than beneath *R. stylosa* (356 – 435 °C). The HI of the upper soils was higher beneath *A. marina* (384 mg HC g^{-1} TOC) than *R. stylosa* (246 mg HC g^{-1} TOC) and decreased with depth down to 30 cm (75 and 67 mg HC g^{-1} TOC, respectively). The OI clearly increased with depth beneath *A. marina*, ranging from 103 to 202 mg CO_2 g^{-1} TOC, whereas beneath *R. stylosa*, it showed a slight increase, going from 123 to 176 mg CO_2 g^{-1} TOC down to 30 cm. Lastly, the $\delta^{13}C$ and OI values evolved differently with depth beneath both species. The stable isotope ratio of carbon ($\delta^{13}C$) was consistently lower beneath *R. stylosa* (-27.4‰ to -26.1‰), showing a linear increase, while beneath *A. marina* (-26.4‰ to -24.1‰), it exhibited increasing and decreasing phases with depth.

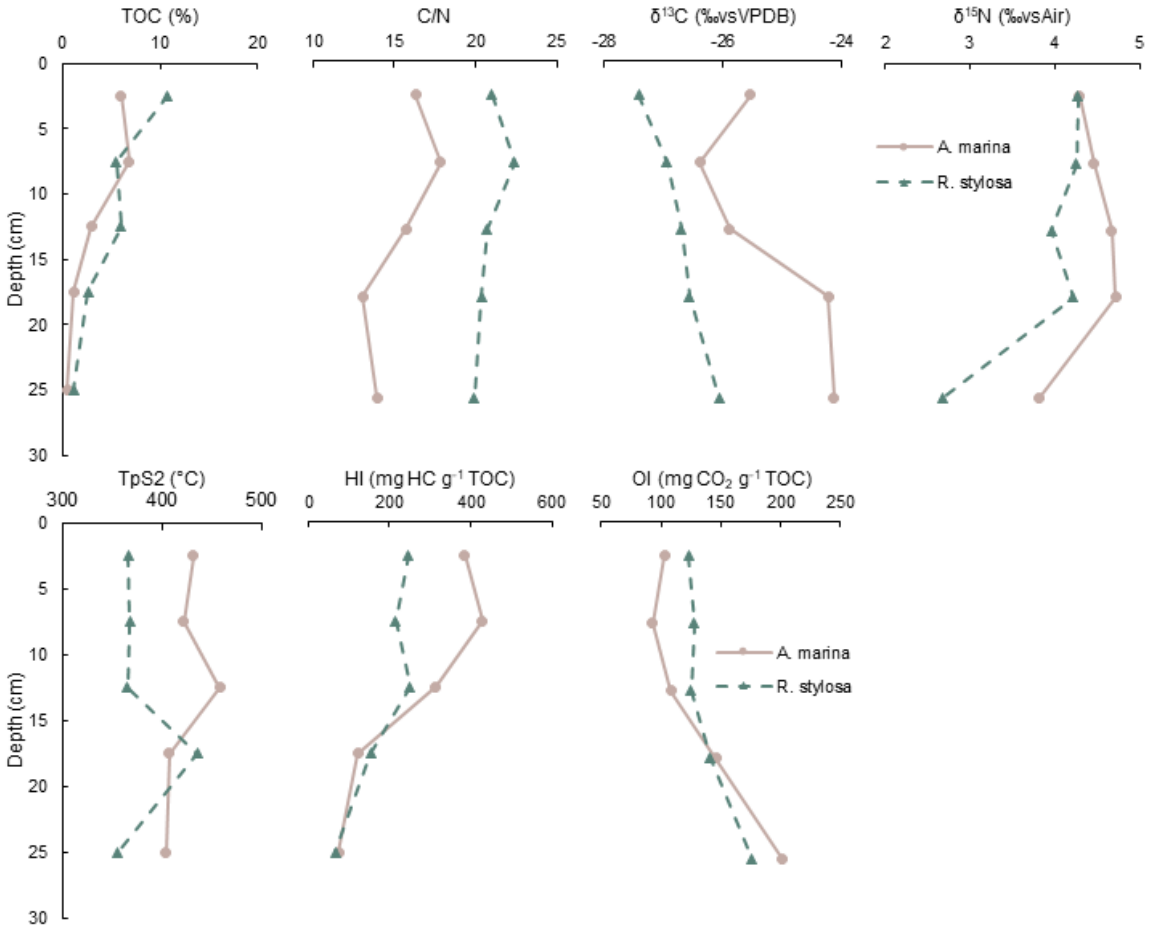

Figure IV.C-2. Changes in parameters with depth beneath both *A. marina* and *R. stylosa*.

IV.C.4.3. Lignin content in the soil

Under *A. marina*, the soil total lignin content decreased from 7 592 µg g^{-1} TOC at 5 cm to 2 334 µg g^{-1} TOC at 10 cm, after which it increased with depth, reaching 11 038 µg g^{-1} TOC (*Figure IV.C-3A*). In the top three sections, the distribution of phenol groups followed this order: vanillyl > syringyl > cinnamyl > p-hydroxyl. In the two deepest sections, the order shifted to syringyl > vanillyl > p-hydroxyl > cinnamyl (*Figure IV.C-3A*). The ratio of p-hydroxyl over the sum of vanillyl and syringyl (P/(V+S)) remained relatively low and stable (0.02 – 0.04), except in the 5-10 cm section (0.09) (*Figure IV.C-3A*).

The soil under *R. stylosa* contained less lignin per TOC compared to the soil under *A. marina*, with the total lignin content varying between 2 708 µg g^{-1} TOC in the 5-10 cm section and 8 481 µg g^{-1} TOC in the 20-30 cm section (*Figure IV.C-3B*). Vanillyl was the dominant phenol group, and cinnamyl was the least dominant throughout the vertical profile (*Figure IV.C-3B*). The P/(V+S) ratio followed a similar trend as under *A. marina* but exhibited larger variations and higher values, ranging from 0.11 to 0.43 (*Figure IV.C-3B*).

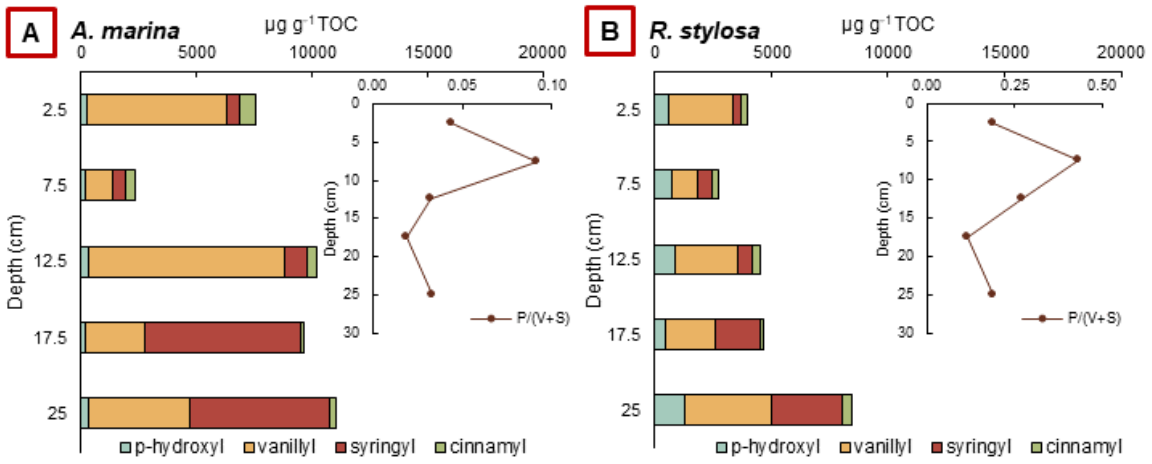

Figure IV.C-3. Mean evolution with depth of the four lignin phenol groups in µg g^{-1} TOC and the P/(V+S) ratio beneath both (A) *A. marina* and (B) *R. stylosa*.

IV.C.4.4. Neutral carbohydrate content in the soil

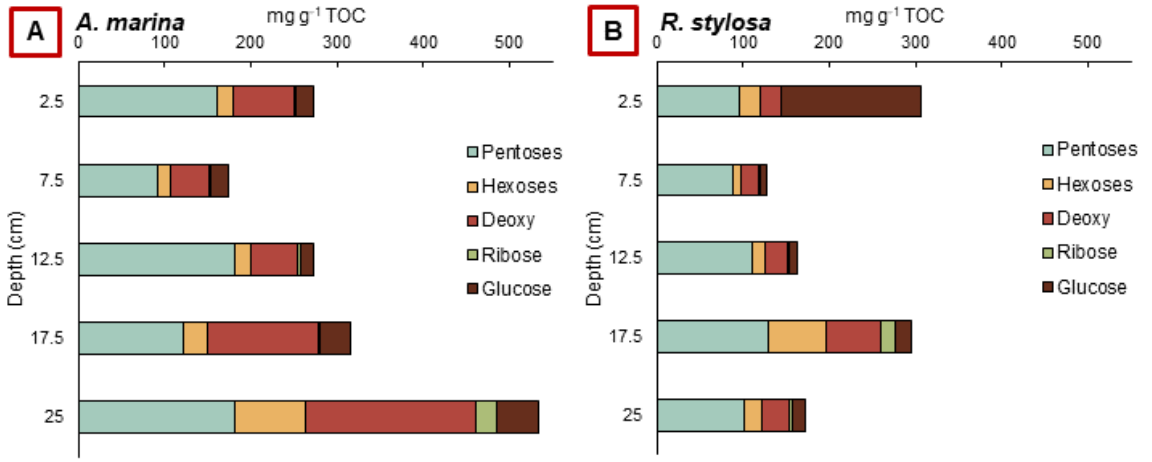

Figure IV.C-4. Mean evolution with depth of the neutral carbohydrates in mg g^{-1} TOC beneath both (A) *A. marina* and (B) *R. stylosa*.

The soil's total neutral carbohydrate content exhibited different trends beneath both species. Under *A. marina*, soil total neutral carbohydrate content increased with depth, rising from 273 mg g^{-1} TOC in the top layer to 533 mg g^{-1} TOC in the deepest layer (*Figure IV.C-4A*). All neutral carbohydrates and groups displayed in *Figure IV.C-4A*, except pentoses had at least doubled their relative concentrations between the top and deepest layers, with the most significant enrichment observed for the deoxy sugars (rhamnose and fucose).

Beneath *R. stylosa*, the soil's total neutral carbohydrate content was highest in the 0-5 cm section (306 mg g^{-1} TOC) and the 15-20 cm section (296 mg g^{-1} TOC), while it was lowest in the 5-10 cm section (128 mg g^{-1} TOC) (*Figure IV.C-4B*). In the top layer (0-5 cm), the amount of glucose constituted 53% of all neutral carbohydrates, significantly higher than in the other sections (6 – 9%) (*Figure IV.C-4B*). The pentoses (xylose and arabinose)

represented the highest fraction of neutral carbohydrates throughout the vertical profile, representing between 32% and 69% (*Figure IV.C-4B*).

IV.C.5. Discussion

IV.C.5.1. Characterization of the fresh mangrove sources and influence of the runoff on the initial compositions

The fresh tissues of *R. stylosa* exhibited lower $\delta^{13}C$ values than *A. marina*, which can be attributed to the lower soil salinity (Robin et al., 2022). Salinity stress can lead to a reduction in the intercellular partial pressure of CO_2, resulting in less discrimination between ^{13}C and ^{12}C during CO_2 fixation (Lin and Sternberg, 1992; Medina and Francisco, 1997). *A. marina* in New Caledonia typically thrives in soils with higher salinity levels than *R. stylosa* (Leopold et al., 2013; Deborde et al., 2015; Robin et al., 2021), leading to higher $^{13}C/^{12}C$ ratios in its tissues. The $\delta^{13}C$ values obtained here are within the range of those obtained in the literature (Abrantes and Sheaves, 2009; Leopold et al., 2013; Jacotot et al., 2018), but lower than those obtained in a mangrove forest sharing the same geological watershed (Chapter IV.A). The lower soil salinity in the urban study site may explain this discrepancy (Robin et al., 2022). Regarding the $\delta^{15}N$ values of the fresh tissues, both species exhibited values in the roots that were lower (-2‰ and 3.9‰ for *A. marina* and *R. stylosa*, respectively) than most values published in the literature (3.9 and 5.3‰ for *Avicennia* and 4.4 and 6.3‰ for *Rhizophora*) (Fry and Smith, 2002; Jacotot et al., 2018). However, the $\delta^{15}N$ values for the roots and leaves of *R. stylosa* in the present study are higher than those depicted for the same species in the mangrove forest sharing the same geological watershed (Chapter IV.A). We suggest that the urban runoff is a source of rich ^{15}N molecules which may be taken up by *R. stylosa*'s tissues as the stand is constantly flooded with it, and it is suggested in the literature that urban runoff may have elevated levels of ^{15}N (Rumolo et al., 2011).

In the present study, higher C/N ratios in *Rhizophora*'s tissues were obtained compared to *Avicennia*'s tissues, as documented in the literature (Rao et al., 1994; Herbon and Nordhaus, 2013; Vane et al., 2013; Jacotot et al., 2018). In this study, the ratios obtained for each species aligned with measurements recorded in various mangrove forests around the world (Rao et al., 1994; Lallier-Vergès et al., 1998; Smallwood et al., 2003; Regina Hershey et al., 2021). The differences in C/N ratios are likely attributable to variations in the ratios of carbohydrates, lipids, lignin, and other biomolecular compounds within the species' tissues (Benner et al., 1990; Kristensen et al., 2008). For instance, neutral carbohydrates do not contain N atoms, whereas amino acids are rich in N (Hernes et al., 1996; Kolb and Evans, 2002). In the present study, the tissues of *A. marina*

contained higher amounts of lignin and neutral carbohydrates than *R. stylosa*, which was already observed for a mangrove forest nearby (Chapter IV.A). Despite having lower neutral carbohydrate content, *R. stylosa* tissues exhibited higher levels of xylose, fucose, and mannose, which confirmed the variations in the initial chemical compositions between species. In fact, previous studies on neutral carbohydrate contents of mangrove tissues have demonstrated variations in relative proportions, ranging between 4% and 31% for xylose, 0.5% and 5% for fucose, and 3% and 10% for mannose among different mangrove species (Marchand et al., 2005; Lallier-Vergès et al., 2008). The two tissues studied for both species are dominated by glucose and the pentoses, while mannose, ribose, and fucose are the three neutral carbohydrates with the lowest concentrations. Those trends are observed but not always true regarding mangrove tissues in the literature, suggesting that environmental conditions can influence the initial composition of mangrove trees in terms of both neutral carbohydrates and lignin (Opsahl and Benner, 1999; Jensen et al., 2005; Keuskamp et al., 2015; Duan et al., 2017).

IV.C.5.2. Organic matter sources and diagenesis beneath *A. marina*

Beneath *A. marina*, the soil OM pool seemed to be primarily composed of *A. marina* litterfall. The soil C/N ratios (13 – 18) and the $\delta^{15}N$ values (3.8 – 4.7‰) were similar to those of fresh leaves (17 and 5.8‰, respectively). The upper soil $\delta^{13}C$ value (-25.5‰) also suggested the contribution of the root system (-25.6‰) to the soil OM pool. Additionally, in the first 15 cm soil layer, the lignin phenol groups were distributed similarly relative to the total lignin content as in the fresh leaves : in the order vanillyl > syringyl > cinnamyl > p-hydroxyl. Similarly, the percentage of pentoses relative to the total neutral carbohydrate content in the upper soil (53 – 67%) suggested that the soil OM pool is mainly mangrove-derived (Marchand et al., 2005). However, the TpS2 (> 400 °C) and HI values (< 460 mg HC g^{-1} TOC) indicated that the OM incorporated has already undergone dehydrogenation and was therefore more thermally stable than the fresh OM (Disnar et al., 2003). We suggest that beneath *A. marina*, the most labile OM molecules from the litterfall were lost before the introduction of mangrove debris into the soil. This is supported by a previous study showed that lignin, especially vanillyl phenols, was lost rapidly (7 days) from the litterfall of *A. marina* at this same site (Robin et al., submitted).

As depth increases, the OM underwent further dehydrogenation, as indicated by a decrease in HI values down to 75 mg HC g^{-1} TOC, and slight oxygenation, with an increase in OI up to 202 mg CO_2 g^{-1} TOC, as expected during the diagenesis of OM (Disnar et al., 2003). The decrease in TOC with depth down to 0.5% also suggests the loss of OM through decomposition or leaching. The $\delta^{13}C$ value increased with depth, indicating that

the decomposition of OM favors ^{12}C consumption over ^{13}C, as previously observed in the literature in mangrove forests (Dittmar and Lara, 2001). Even though indicators showed the decomposition of OM, the total lignin and neutral carbohydrate content increased with depth relative to TOC. We suggest that these increase result from the early decomposition of the litterfall on the soil surface leaving more refractory molecules for soil incorporation. A change in the relative proportion of each phenol group with depth was observed. In the upper layers, vanillyl was the dominant phenol group, and p-hydroxyl was the least dominant, while in the deeper layers (below 15 cm), the syringyl group was dominant, and cinnamyl was the least dominant. This transition shows that syringyl phenols were more refractory than vanillyl phenols, and cinnamyl phenols were more labile than p-hydroxyl phenols under these conditions. Regarding neutral carbohydrates, the enrichment with depth was the highest for the deoxy sugars, suggesting significant production of neutral carbohydrates through microbial activity, enhancing OM decomposition (Hernes et al., 1996). We propose that this enrichment was driven by the increase in Eh at depth (Robin et al., 2022), which promoted microbial activity and the subsequent production of these carbohydrates, in accordance with previous studies (Lacerda et al., 1995; Lallier-Vergès et al., 2008). However, between 5 and 10 cm depth, there was a decrease in both lignin and neutral carbohydrate contents relative to TOC. The lignin-derived ratios indicated that the mechanism of lignin degradation in this horizon was demethylation (P/(V+S) increases), while the neutral carbohydrate content showed that it was a loss of pentoses (mangrove-derived) primarily at this depth. We suggest that the diffusion of O_2 into the rhizosphere, specific to *A. marina* (Scholander et al., 1955), enhances the diagenesis of both carbohydrates and lignin.

Hence, the soil OM pool beneath *A. marina* primarily consisted of litterfall and the root system of this species. It appeared that the OM integrated into the soil had undergone initial stages of degradation, although there was a more substantial reduction in bulk OC compared to lignin and neutral carbohydrates. We propose that the enrichment of neutral carbohydrates relative to TOC is likely attributable to microbial activity. Notably, there was no significant impact of the runoff observed beneath *A. marina* compared to previous study of non-urban site.

IV.C.5.3. Organic matter sources and diagenesis beneath *R. stylosa*

Underneath *R. stylosa*, the soil OM pool appeared to be primarily composed of the root system and soil surface microorganisms but is influenced by the runoff. The $\delta^{13}C$ values of the soil (-25.5 – -27.4‰) are similar to those of the roots of the same species (-27.0‰). The $\delta^{15}N$ value in the upper layer (4.3‰) is a little bit higher than the value for *R.*

stylosa roots (3.9‰), suggesting roots incorporation in the soil and the offset is due to fractionation, or that the urban rainwater runoff may act as a source of ^{15}N-rich molecules to the soil (Sweeney et al., 1980; Tucker et al., 1999; Jones et al., 2001; Rumolo et al., 2011). The decrease in $\delta^{15}N$ with depth indicates the diminution of the runoff's influence on OM isotopic ratios with soil depth. The deepest soil layer may also date from a period prior to urban runoff. Additionally, the glucose content in the 0-5 cm section was significantly higher (53% relative to total neutral carbohydrate) compared to other sections (6 – 9%) or any values recorded for *A. marina* at this site (4 – 11%). We suggest that this elevated glucose content was of microbial origin as a visible whitish layer was observed on the soil surface and it was previously established in the literature that the urban runoff may promote microbial development on the soil surface (Robin et al., submitted). Leaf litter did not appear to be a major component of the soil OM pool, which is consistent with results obtained in the same study site, demonstrating that leaf litter decay rates were highest at the urban site beneath *R. stylosa* (Robin et al., submitted). Furthermore, the constant flooding of the *R. stylosa* stand's floor may promote leaf litter transport further away in the ecosystem or directly to adjacent ecosystems.

In contrast to what was observed beneath *A. marina*, the low TpS2 values (< 360 °C) indicated that the OM incorporated in the soil was rather thermally labile, suggesting that it did not underwent significant diagenetic processes. However, there was an increase in OM thermal stability with depth (> 430 °C) (Disnar et al., 2003). Like *A. marina*, with depth, TOC decreased suggesting the loss of OM through decomposition or leaching, and the $\delta^{13}C$ value increased. The decrease in HI values and the slight increase in OI values indicated a dehydrogenation process and oxygenation process of the OM with depth.

General observation revealed a decrease in neutral carbohydrate content and an increase in lignin content with depth relative to TOC. In the literature, it has been shown that lignin exhibits a rather refractory behavior in mangrove soils, as there are only a few microorganisms capable of decomposing lignin polymers (Benner et al., 1990; Dittmar and Lara, 2001; Marchand et al., 2005). Conversely, neutral carbohydrates are typically easily degraded in mangrove soils because they represent an important energy source for many microorganisms (Lacerda et al., 1995; Lallier-Vergès et al., 2008; Duan et al., 2020). Vanillyl was the dominant phenol group, and cinnamyl was the least dominant in the soil. With depth, the syringyl group showed a more refractory behavior than the p-hydroxyl group. Even though there was an enrichment of lignin relative to bulk OC, degradation of lignin may have occurred through demethylation (indicated by an increase in the P/(V+S) ratio) and ring cleavage, consistent with previous research in anoxic mangrove soils (Marchand et al., 2005; Lallier-Vergès et al., 2008). Surprisingly, the general loss of neutral

carbohydrates was associated with the loss of hexoses, deoxy sugars, and pentoses, with the latter group being the dominant group throughout the depth. There was, therefore, no sign of microbial production of neutral carbohydrates, which contradicts previous observations made in mangrove forests (Hernes et al., 1996; Marchand et al., 2005; Lallier-Vergès et al., 2008). We suggest that the negative redox potential in depth (Robin et al., 2022), revealing anoxic soils beneath *R. stylosa*, limit microbial neutral carbohydrates production.

In contrast to *A. marina*, it appeared that the soil OM pool beneath *R. stylosa* was influenced by the urban runoff, partly due to its role in promoting the development of microbial communities on the soil surface. Furthermore, litterfall did not appear to make a significant contribution to the soil OM pool in this stand, likely because it is readily degraded or transported to the surface. The OM within the soil also underwent processes of dehydrogenation and oxygenation, leading to the depletion of bulk OC and neutral carbohydrates. However, there was no indication of microbial production of neutral carbohydrates observed within the vertical profile of this stand, which may be related to the soil anoxia.

IV.C.6. Conclusion

In conclusion, this study investigated the impact of urban runoff on the initial compositions of mangrove-derived OM sources and processes of OM diagenesis within a mangrove forest in New Caledonia. The mangrove forest has received urban rainwater runoff for more than 50 years modifying the soil physico-chemical parameters. The study centered its investigation on the predominant mangrove species of the territory, *A. marina* and *R. stylosa*. It conducted an extensive analysis of multiple parameters, encompassing stable isotopes, Rock-Eval pyrolysis, and molecular analyses (lignin and neutral carbohydrates).

This study highlighted differences between mangrove species in initial compositions of leaves and roots, which may be partly driven by environmental conditions. *R. stylosa* tissues exhibited higher $\delta^{15}N$ values than the same species in a nearby forest, which may be attributed to the runoff acting as a source of ^{15}N-rich molecules and exposure of this mangrove species to that runoff. The soil OM pool primarily consisted of autochthonous OM with leaf litter the dominant source beneath *A. marina* and the root system the dominant source beneath *R. stylosa*. Beneath *R. stylosa*, it was also suggested that microbial communities developing on the soil surface, promoted by the runoff, may compose the soil OM pool.

Diagenetic processes occurred in the soil beneath both species through dehydrogenation and oxygenation resulting in a general decrease in TOC content. A relative enrichment in total lignin content was observed with depth beneath both species but changes in the phenol groups relative proportions highlighted different individual behaviors. Neutral carbohydrate content relatively increased compared to bulk OC beneath *A. marina* which was attributed to the production by microbial communities during diagenetic processes. Beneath *R. stylosa*, neutral carbohydrate content slightly decreased with depth with no evidence of microbial activity. Therefore, there is no evidence of a significant and direct influence of urban runoff on OM diagenetic processes in mangrove soils.

This research shed light on the complex interplay of factors affecting mangrove ecosystems in the presence of urban runoff. The variations in tissue characteristics and soil OM composition highlighted the need for a comprehensive understanding of these ecosystems' responses to environmental changes.

V. Chapter V: Discussion & Conclusion

V.1. Results synthesis

This thesis has yielded various findings regarding trace metals and organic matter in semi-arid mangrove forests across different matrices, with a specific emphasis on the impact of urbanization on these parameters. The main results are summarized below.

V.1.1. Modified physico-chemical conditions

The comparison of the physico-chemical conditions (salinity, Eh, pH, etc.) of the mangrove soils at the three sites, that is urban, ultrabasic, and control, enabled us to draw conclusions. In Chapter I, the results showed that the **watershed geology influences the physico-chemical conditions** of the mangrove soil, with suboxic conditions at the ultrabasic site due to the constant input of goethite, which facilitates Fe reduction in the soil. The suboxic conditions of the ultrabasic site may enhance mineralization processes and rates in the soil, providing a possible explanation for the lower TOC content observed in soil at the ultrabasic site compared to the anoxic control site.

In Chapter II, the control and urban sites, which share the same geological watershed, also displayed **differences in physico-chemical conditions that may be attributed to urban rainwater runoff**. Particularly, the urban mangrove soils had lower salinity, down to 0 g L^{-1}, and higher pH values (>7). These conditions are unusual for bay-head mangrove forests with no river inputs. The visible effects of these conditions, especially the low salinity, included a change in the zonation of species in the intertidal zone, with an *R. stylosa* stand developing further landward than the *A. marina* stand, at the entrance of the runoff. These *R. stylosa* trees are much taller (>8 m) than those observed on the West Coast of New Caledonia, which are about 2 m tall, due to the semi-arid climate.

V.1.2. The geological and urban watersheds as a source of trace metals

The ultrabasic site, downstream of lateritic soils and an old open-cast Ni mine, exhibited the highest TM concentrations among the three studied sites, with Fe and Ni concentrations well above the global average (Chapter I). Because of the New Caledonian background noise of TM in soil and marine sediments, the control and urban sites, located in a volcano-sedimentary watershed, still showed elevated TM concentrations compared to pristine mangrove forests worldwide. However, **TM concentrations did not reach hazardous levels** and were lower than those found in other urbanized mangrove forests worldwide (Chapter II).

At the urban mangrove site, most TM concentrations in the soil were lower than those at the control site. We propose that urbanization, with the concretization of

the soil, limits TM erosion from the watershed soil. Additionally, the urban mangrove soil exhibited suboxic conditions in the upper layer and anoxic conditions at depth, resulting in potential dissolution of TM. Tidal fluctuations and continuous Fe reduction-oxidation cycles likely contribute to these conditions, making it easier for dissolved TM to be exported to adjacent ecosystems or taken up by plants. Nonetheless, **typical urban activity elements such as Cu, Pb, Ti, and Zn had higher concentrations in the urban mangrove soil**, likely due to urban rainwater runoff (Chapter II).

V.1.3. Trace metal transfer to the fresh mangrove tissues is site/species/tissue/trace metal-dependent

V.1.3.1. Trace metal transfer is site-dependent

The study of the three mangrove forests revealed that the transfer of TM from the soil to the fresh mangrove tissues is site-dependent. Our research emphasized that **TM mobility in the soil was the primary controlling factor for TM transfer to mangrove roots**, as BCF were not correlated with the total TM concentrations in the soil. The availability of TM in the exchangeable fraction of the soil played a crucial role in root uptake, resulting in higher root BCF values at the urban site. Additionally, the presence of pyrite and soil porewater salinity influenced TM availability. Urban mangrove soils exhibited suboxic and non-saline conditions in the upper soil layers, which limited the immobilization of TM by pyrite and the formation of Cl-TM complexes (Chapter II). Consequently, this allowed mangrove roots better access to certain TM.

V.1.3.2. Trace metal transfer is species-dependent

In Chapter I, the results clearly demonstrated **a higher transfer of TM to the roots of *A. marina* compared to *R. stylosa***. While this thesis did not directly measure the factors influencing variations in root BCF between species, it presented multiple suggestions to explain these observations. Existing literature has shown that *R. stylosa* roots exhibit lower permeability than *A. marina* pneumatophores due to lignification of the exodermis cells. Additionally, *A. marina* releases oxygen into its rhizosphere, which mobilizes TM in the soil, facilitating root absorption.

The thesis also investigated the role of the Fe plaque formation on *A. marina* pneumatophores in metal stress adaptation. In Chapter I, it was observed that Fe plaque formation was correlated with Fe concentrations in the soil, with higher plaque concentrations at the ultrabasic site. However, Chapter II highlighted that Fe concentrations in the soil are not the sole factor influencing Fe plaque formation, as higher concentrations were found on pneumatophores collected at the urban site. Therefore, we suggest that **stress represents another factor controlling Fe plaque formation**.

V.1.3.3. Trace metal transfer is tissue-dependent

Although TM concentrations in mangrove roots could be higher than those in the soil (BCF >1), our study revealed **limited TM transfer from roots to leaves** and minimal variations in TF between the urban and control forests (Chapter II). Our research emphasized the regulatory mechanisms employed by mangrove trees to restrict TM transfer to higher organs. SEM observations showed that TM are mainly located in the epidermis of the roots to limit transport to higher tissues. In this thesis, we assessed Fe plaque as a mechanism for TM immobilization. In Chapter I, it was demonstrated that **Fe plaque efficiently captured TM**, retaining more than half of the measured TM concentrations in the roots.

V.1.3.4. Trace metal transfer is trace metal-dependent

The transfer of TM to mangrove tissues exhibited significant variability among different TM. Our results demonstrated that **several factors influenced TM transfer, including TM concentrations in the soil, TM bioavailability in the soil, the TM retention capacity of the Fe plaque, and the role of TM in the metabolic processes of mangrove species**. Although Fe concentrations in mangrove roots were highest at all three sites, their root BCF were relatively low. This suggests that Fe uptake was regulated, but the very high concentrations in the soil still led to elevated concentrations in the roots. Conversely, essential TM such as Cu, Mn, and Zn exhibited the highest root BCF values, reflecting their significant roles in mangrove metabolism.

V.1.4. Trace metal transfer from the soil to the decomposing litterfall is also site, species, and trace metal-dependent

In Chapter III.B, TM content in the degrading litterfall on the mangrove soil surface was also studied. In the urban site, peak TM concentrations relative to bulk leaf litter occurred at different times during litter degradation for *A. marina* (28 days) and *R. stylosa* (56 days). In contrast, at the control site, these peaks occurred later (56-72 days). The urban site exhibited higher TM bioavailability in the soil, potentially leading to enhanced TM transfer from mangrove soil to litterfall. In absolute concentrations, the litterfall of *A. marina* at the urban site had higher TM concentrations than the other areas. This suggests that the leaf litter *A. marina* may have reached its absorption limit. However, the leaf litter of *R. stylosa* exhibited higher total TM concentrations after specific durations of decomposition, **indicating the influence of stand immersion, tidal flooding, and urban rainwater flow on TM accumulation in mangrove litter**.

During litterfall degradation, **most TM, except As and Mn, had higher concentrations in the leaf litter after 72 days of decomposition compared to the**

initial senescent leaves. Still, initial leaching phases were observed for a few TM, including As, Cu, Mn, and Zn. As exhibited initial leaching only in the litterfall of *A. marina*, indicating potential binding with lignin molecules which also exhibited leaching in the first days of litterfall degradation for *A. marina*. Cu and Zn also showed leaching initially at the urban site for *A. marina*, possibly influenced by differences in lignin content between the two species. Mn showed a unique behavior, with relative concentration decreases in the first few weeks of decomposition for both species and sites. Mn is expected to be more leachable than other TM due to its lower ability to bind with refractory molecules. The soluble form of Mn in leaves (Mn^{2+}) may not oxidize to immobilized Mn^{4+} due to anoxic conditions on the mangrove floor (Chapter III.B).

V.1.5. Conceptual model of trace metal dynamics in urban and non-urban mangrove forests

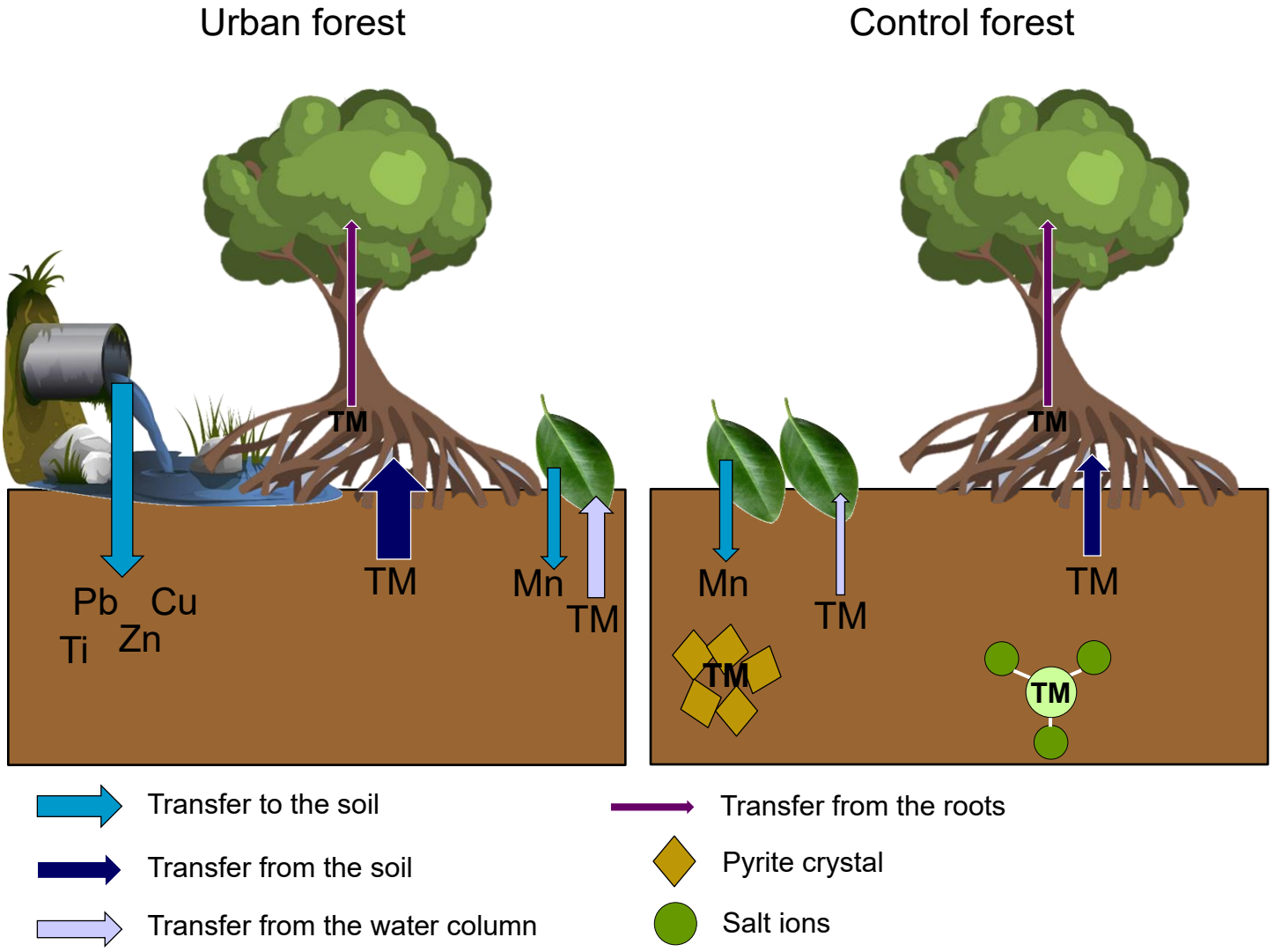

Figure V-1. Conceptual model of trace metal dynamics in the urban mangrove forest (left) and the control mangrove forest (right).

V.1.6. Fresh organic matter from mangrove tissues, organic matter degradation on the soil surface, and evolution of organic matter diagenesis with soil depth is species-dependent in semi-arid mangrove

V.1.6.1. Characterization of the mangrove-derived organic matter (leaves and roots)

At the control site, it was observed that *A. marina* leaves had higher $\delta^{15}N$ and $\delta^{13}C$ values than *R. stylosa* leaves, a phenomenon attributed to species-specific ^{15}N discrimination during N uptake and soil salinity. Previous studies suggested that mangroves growing on saltier soils exhibited lower $^{13}CO_2$ discrimination and higher $\delta^{13}C$ values. Our study also revealed that fresh *A. marina* leaves had higher total N content and lower C/N ratios than *R. stylosa* leaves. These differences were attributed to varying ratios of carbohydrates, lipids, lignin, and other biomolecular compounds within the species' tissues. *A. marina* leaves displayed higher lignin content than *R. stylosa* leaves. *R. stylosa*

tissues exhibited higher levels of specific carbohydrates like xylose, fucose, and mannose, despite having lower overall neutral carbohydrate content (Chapter IV.A).

V.1.6.2. Mangrove litterfall decomposition

In this thesis, the degradation of the litterfall on the soil surface was also studied in Chapter III. The study showed that double exponential models were suitable for describing the decomposition rates of both mangrove species at the control site. This model consists of two phases: an initial rapid decomposition phase followed by a slower phase. When following a single exponential model, 50% of leaf litter mass was lost in 43 days for *A. marina* and 28 days for *R. stylosa*. *R. stylosa* exhibited faster mass loss and lower half-lives than *A. marina*, which contrasts with many previous studies where species with higher initial N content, such as *A. marina* in this study, tended to show faster decomposition rates. The present study suggests that **the position of the species within the intertidal zone plays a key role in litterfall decay rates**, with species closer to the seaside subject to faster decomposition rates due to higher leaching.

Leaf litter from *R. stylosa* exhibited a constant increase in N content with decomposition. This increase may be related to the degradation of hydrolysable components, such as neutral sugars, rather than more refractory, N-rich components like lignin. In fact, with degradation, the neutral carbohydrate content decreased significantly in the leaf litter while the lignin content only slightly decreased. Therefore, a reduction in the C/N ratio was observed with leaf litter degradation for *R. stylosa*. For *A. marina*, an increase in N content was observed in the initial 28 days of decomposition, followed by N loss in the subsequent 28 days, while the C/N ratio remained relatively constant during decomposition. The trends in stable isotope ratios did not follow the C and N trends, respectively. The differences in trends were attributed to the discrimination of ^{13}C or ^{15}N by decomposers as they degraded C-rich and N-rich compounds.

Lignin content increased with decomposition in *R. stylosa* leaf litter, indicating that **bulk leaf material decayed more rapidly than lignin**, as observed in anaerobic environments. In contrast, *A. marina* leaf litter showed a decrease in lignin content during decomposition, likely influenced by less reducing conditions in the upper soil beneath *A. marina* and the higher initial lignin content in senescent leaves. The chemistry of lignin during decomposition varied between the two species. Vanillyl phenols were more labile in *A. marina*, while in *R. stylosa*, vanillyl phenols particularly increased. **The initial lignin chemistry of senescent leaves influenced lignin decay during decomposition**. Both species exhibited similar evolutions in Ad/Al ratios during decomposition. *R. stylosa* consistently had higher Ad/Al ratios than *A. marina*, indicating similar ratios of acids over

aldehydes during decomposition. This suggests that although phenol concentrations differed between leaves, the ratios of acids to aldehydes evolved similarly.

The decomposition of neutral carbohydrates exhibited species-specific behaviors. The order of lability for neutral carbohydrates differed between species suggesting that the initial composition of senescent leaves influences their degradation. Glucose, arabinose, galactose, and rhamnose were among the most labile carbohydrates. Xylose, despite being abundant, increased in concentration during decomposition. This suggests that **initial composition and protective factors, such as lignin, influence carbohydrates stability**.

V.1.6.3. Organic matter decomposition in mangrove soils

The study discussed in Chapter IV.A revealed that the primary OM source in the soil at the control site was autochthonous. Under the landward stand of *A. marina*, the primary contributors to the OM pool were the litterfall of *A. marina*, the roots, and the microphytobenthos thriving on the soil surface as indicated by the C/N ratios, the $\delta^{13}C$ values, and the total lignin content of the upper soil sections. The data obtained in Chapter III.A on the degrading leaf litter confirms that prior to soil incorporation, decomposition processes occurred on the litterfall of *A. marina* with notably a loss in both lignin and neutral carbohydrates. Conversely, beneath the seaward stand of *R. stylosa*, the primary contributors were *R. stylosa* roots and litter debris from *A. marina*, likely transported by tides. These two species yielded distinctive OM characteristics, influenced by their respective positions within the mangrove forest and unique chemical compositions. Once incorporated into the soil, **OM underwent further degradation processes, primarily dehydrogenation, but the presence of anoxic conditions hindered OM oxygenation during diagenesis**. The more anaerobic environment beneath *R. stylosa* resulted in reduced OM decay compared to the landward *A. marina* stand, whose OM pool mainly consisted of mature compounds. While the differences in OM sources beneath the two species influenced isotope ratio values and Rock-Eval parameters, the overall trends were similar for both *A. marina* and *R. stylosa*.

Indicators of diagenesis of the OM in mangrove soils were the **total lignin and neutral carbohydrates general labile behaviors**. The fact that lignin content increases with degradation within *R. stylosa* litter confirms that these leaf debris might not be incorporated into the soil but rather exported. The lignin content in the litterfall of *A. marina* is loss during degradation on the soil surface and keeps being decomposed when incorporated in the mangrove soil. The lability of phenol groups followed the order observed in litterfall, with cinnamyl phenols being the most labile in the soil beneath *R.*

stylosa and vanillyl phenols beneath *A. marina*. The mechanisms involved in lignin degradation in mangrove soils included ring cleavage, loss of -OCH_3, and unexpectedly, side chain oxidation in the anoxic soil beneath *R. stylosa*. Individual neutral carbohydrates displayed varying behavior with depth and between stands, suggesting selective degradation. The increase in neutral carbohydrates in the soil may be due to their refractory nature or production by microbial communities, including deoxy sugars.

V.1.7. Mangrove forests can store and preserve organic matter for millennials in their soils

In Chapter IV.B **a soil OM-enriched layer was observed below 30 cm depth** and described. Isotopic and molecular analyzes revealed that **preserved *R. stylosa* roots contributed significantly** to the OM pool of this layer. However, the low soil's C/N ratio indicated a preference for the degradation of C-rich compounds over N-rich ones. Rock-Eval parameters suggested that the buried OM was preserved from oxygenation due to the anoxic conditions of the soil horizon but exhibited greater thermal stability than fresh OM and had undergone dehydrogenation.

Neutral carbohydrates showed individual behaviors in the soil with a significant increase in arabinose between the fresh sources and the soil, but a loss of galactose, glucose, and xylose reflecting the labile nature of these carbohydrates. Mannose, ribose, and deoxy sugars remained preserved. Lignin-derived phenols showed enrichment in the soil layer, especially p-hydroxyl and vanillyl phenols. Acid/aldehyde ratios were lower in the soil, primarily due to the enrichment in vanillin. A notable increase in p-hydroxyacetophenone contributed to a higher PON/P ratio in the soil, suggesting lignin predominance.

SEM-EDX analyzes revealed an association between root material and pyrite, which likely contributed to enhanced OM preservation in waterlogged, anoxic soil conditions. Furthermore, S_{org}/C ratio indicated **sulfurization of the OM which contributes to OM preservation for millennia**. Radiocarbon dating indicated that the soil layer dated back to approximately 4 000 cal yr BP, coinciding with a stable high sea-level period. During this time, the **accumulation of roots and OM debris occurred due to sea-level stability and limited microbial decomposition in waterlogged, anoxic conditions**.

V.1.8. Conceptual model of organic matter dynamics in semi-arid mangrove forest

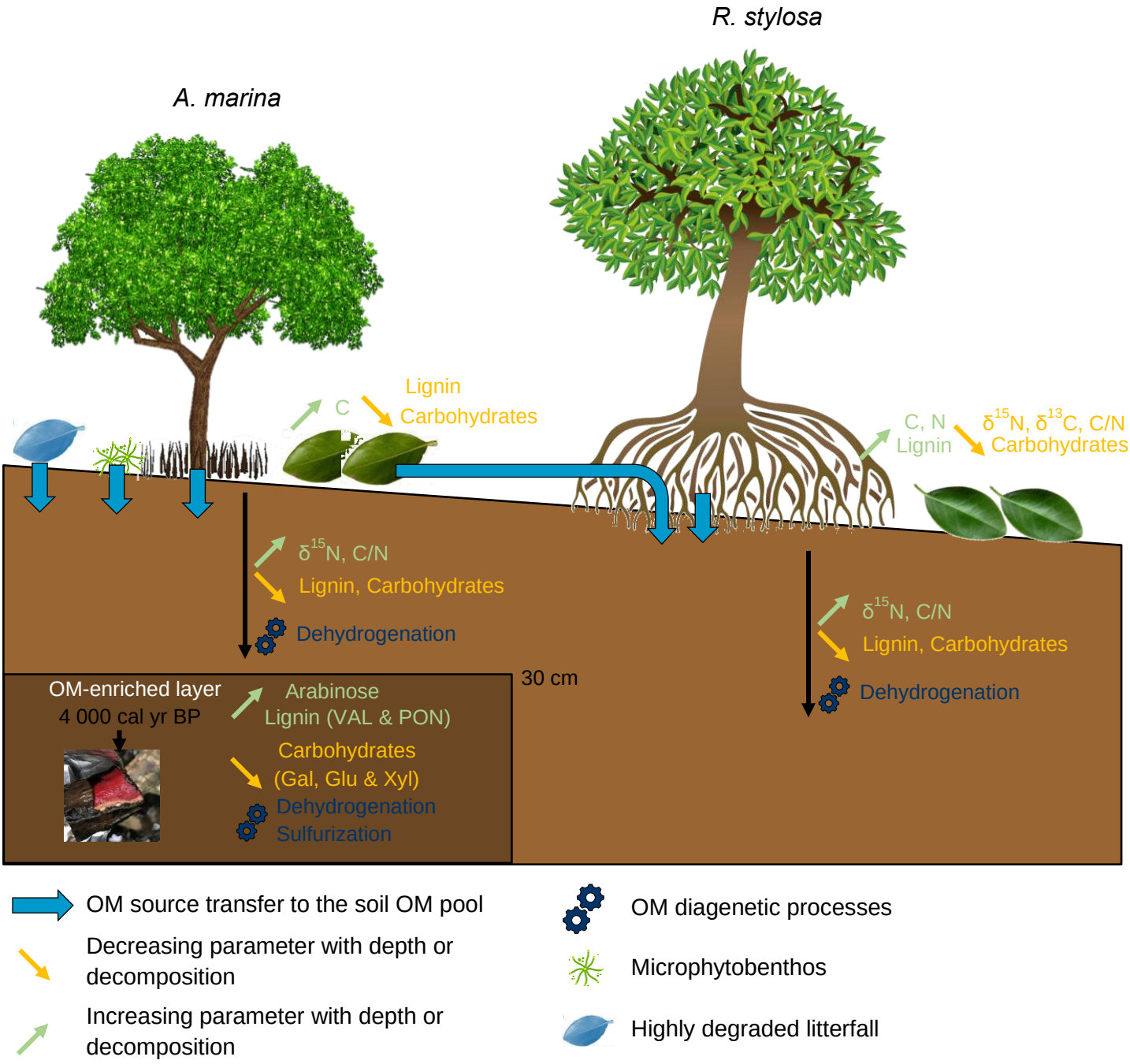

Figure V-2. Conceptual model of organic matter dynamics in the litterfall and soil at the control site for both species and the OM-enriched layer.

V.1.9. Fresh organic matter from mangrove tissues, organic matter degradation on the soil surface, and evolution of organic matter diagenesis with soil depth is influenced by the urban runoff

V.1.9.1. Characterization of the mangrove-derived organic matter (leaves and roots)

In comparison to the control site, both *A. marina* leaves and the roots and leaves of *R. stylosa* exhibited higher $\delta^{15}N$ values in the urban mangrove forest. While the study did not directly measure stable isotopic ratios in urban runoff, it is suggested in the

literature that urban runoff may contain elevated levels of ^{15}N. This is believed to be a contributing factor to the higher $\delta^{15}N$ values observed in the mangrove tissues at the urban site, indicating **an impact of urbanization on the isotopic composition of the mangrove tissues**. Lower $\delta^{13}C$ values were observed in fresh leaves at the urban site compared to the control site. Salinity stress can cause a decrease in the intercellular partial pressure of CO_2, resulting in less discrimination between ^{13}C and ^{12}C during CO_2 fixation. The species at the urban site thrive in soils with lower salinity levels than at the control site, leading to lower $^{13}C/^{12}C$ ratios in the tissues. *A. marina* tissues from the urban site were characterized by higher neutral carbohydrate content, specifically elevated levels of xylose, rhamnose, fucose, and mannose, along with lower lignin content, including reduced cinnamyl content, in comparison to the control site. For *R. stylosa*, the primary differences were lower ribose content and higher glucose content in the tissues (Chapter IV.C). These variations in carbohydrate and lignin composition confirmed that environmental conditions, influenced by urbanization, can impact the initial composition of mangrove trees' tissues.

V.1.9.2. Mangrove litterfall decomposition

At the urban site, both *A. marina* and *R. stylosa* leaf litter decomposed faster compared to the control site with half-lives of 33 and 36 days, respectively. This variation was attributed to the **continuous runoff of urban rainwater, which enhances early leaching processes and microbial development**. However, the difference in decay rates between sites primarily occurs during the later stages of microbial development and the refractory stage. Therefore, we suggest that urbanization, particularly urban runoff, accelerates decomposition rates, possibly by creating a more favorable environment for microbial development at the soil surface. The runoff also enhances the leaching of lignin-derived phenols from the litterfall of *A. marina* in the first 7 days of degradation and enhances the leaching of molecules more labile than lignin such as neutral carbohydrates in the case of *R. stylosa* (Chapter III.A).

V.1.9.3. Organic matter decomposition in mangrove soils

The composition and dynamics of OM in the soil beneath *A. marina* and *R. stylosa* at the urban site were investigated in Chapter IV.C. As for the control site, the primary source of soil OM in the soil beneath *A. marina* appeared to be its litterfall as indicated by the C/N ratios, the $\delta^{15}N$ values and the lignin phenol groups. The soil OM also showed signs of initial degradation with high TpS2 values. Deeper layers showed signs of OM decomposition, with increasing $\delta^{13}C$ values and changes in phenol group proportions. With decomposition, *A. marina* leaf litter's lignin and carbohydrate content decrease but these compounds increase in relative concentrations in the soil. Therefore, we suggest that the

litter undergoes decomposition processes prior to soil incorporation by losing lignin and neutral carbohydrates compounds, leaving mostly refractory molecules in the soil, limiting their loss afterwards.

Underneath *R. stylosa*, the soil OM pool seemed to be influenced by the root system, soil surface microorganisms, and urban runoff. The $\delta^{13}C$ values closely resembled those of *R. stylosa* roots, but a greater $\delta^{15}N$ value suggested urban rainwater influence. Glucose content in the upper layer indicated microbial contributions. Unlike *A. marina*, *R. stylosa* soil OM appeared thermally labile, with minimal diagenetic processes. Therefore, soil-incorporated OM is available for decomposition indicated by the decrease in TOC and carbohydrates with depth, possibly through dehydrogenation and oxygenation processes.

Overall, both sites displayed similar patterns of OM degradation and lignin dynamics in the soil, suggesting that the urban runoff does not have a significant direct influence on OM decomposition in mangrove soil.

V.1.10. Conceptual model of organic matter dynamics in urban mangrove forest

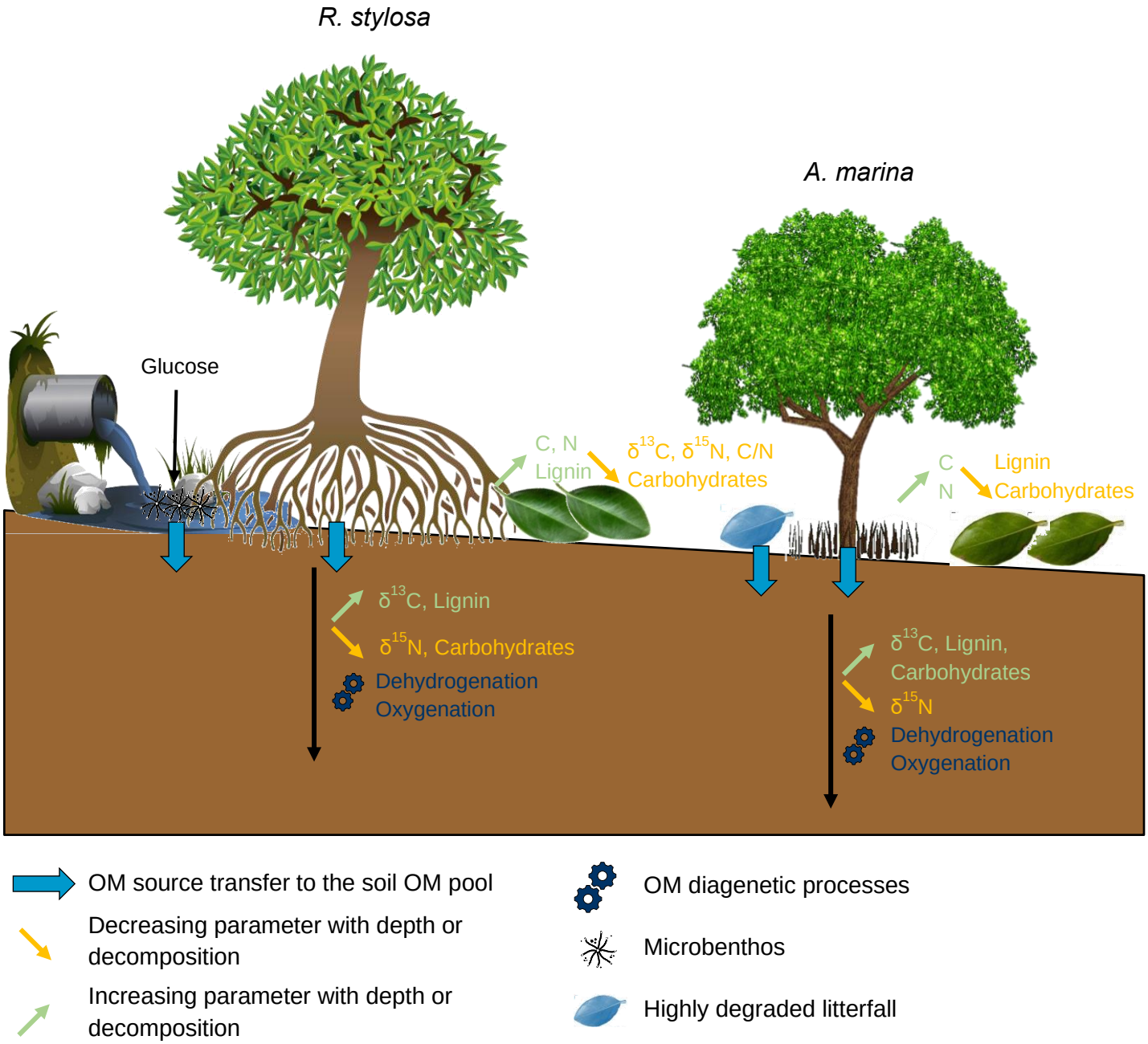

Figure V-3. Conceptual model of organic matter dynamics in the litterfall and soil at the urban site for both species.

V.2. Statistical analyzes

One of the objectives of this thesis was to assess the factors influencing TM dynamics in mangrove soils. The information obtained on the urban and control mangrove forests and the two mangrove species from the four previous chapters were statistically analyzed with correlation matrices and principal component analyzes (PCA) and discussed in this section.

V.2.1. Physico-chemical parameters correlations

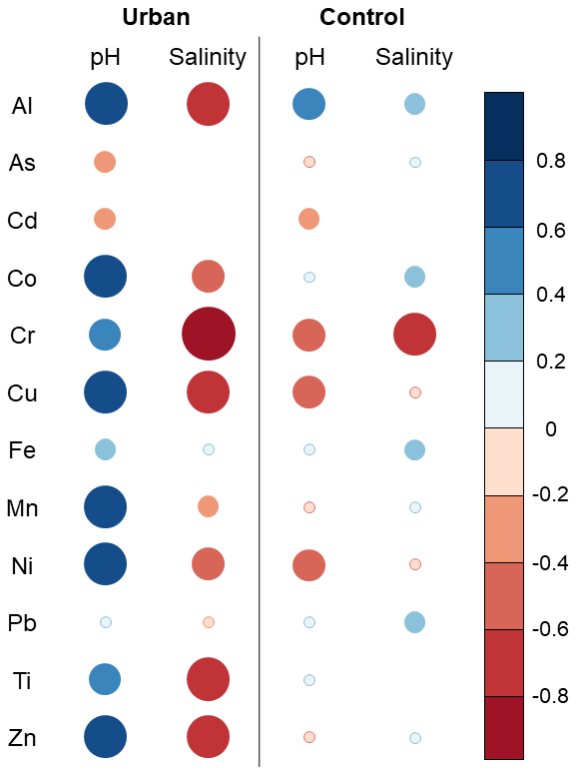

Figure V-4. Correlations between trace metal concentrations in the soil and soil pH or soil salinity at the urban and control sites.

Most TM in the soil at the urban site are highly negatively correlated with salinity and positively correlated with pH (*Figure V-4*). This suggests that as soil salinity decreases and pH increases, the concentrations of TM in the soil also increase. Chapter II demonstrates that urban runoff affects the physico-chemical conditions of the soil by reducing soil salinity and increasing pH. These correlations may indicate that the urban runoff serves as a source of TM, which ultimately accumulates in the mangrove soil, or that these conditions enhance the storage of TM in the soil. When examining the correlations at the control site, we observe the opposite general trends, with TM being negatively correlated with pH but only lightly positively correlated with soil salinity (*Figure V-4*). In the literature, it is noted that higher soil salinity may facilitate TM immobilization in the soil by forming Cl-TM complexes, rendering TM less bioavailable (Cheng et al., 2014). Therefore, we confirm the hypothesis that urban runoff serves as a source of TM in mangrove soils.

V.2.2. Molecular organic matter correlations

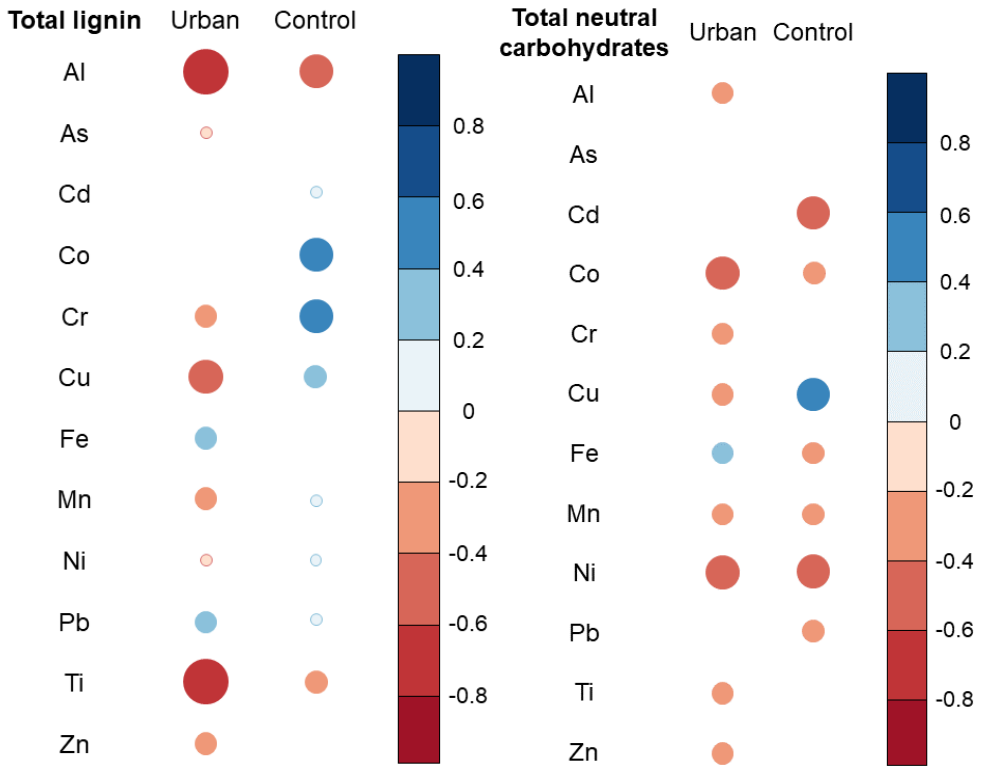

Figure V-5. Correlations at the urban and control sites between trace metal concentrations in the soil and (A) soil total lignin content and (B) soil total neutral carbohydrate content.

V.2.2.1. Lignin

In the literature, it is suggested that lignin promotes the storage of TM in the soil due to its numerous active sites for adsorption, absorption, and sequestration (Thakur et al., 2014). This is one of the reasons why lignin was chosen as a parameter of interest for this thesis. As a result, we expected to find a positive correlation between TM concentrations in the soil and the total lignin content. At the control site, most TM exhibit a slight positive correlation with total lignin (*Figure V-5A*), indicating that lignin is a factor enhancing TM storage in the soil. However, at the urban site, most TM are negatively correlated with lignin content (*Figure V-5A*).

If we examine the different lignin-derived phenol groups, we can observe variations in correlations among species. At the urban site, most TM show negative correlations with p-hydroxyl, vanillyl, and syringyl phenols, but they exhibit positive correlations with cinnamyl phenols beneath *A. marina* (*Figure V-6A*). These correlations indicate that TM may bind to cinnamyl phenols. The cinnamyl group is the only phenol group composed solely of acids (coumaric acid and ferulic acid). Ionic TM can bind to these acids through chelation, where the carboxyl group can donate electrons to the metal cations (Guo et al., 2008). Therefore, we propose that TM primarily bind to the acid molecules of the OM in

the soil beneath *A. marina*. This hypothesis is supported by the positive correlation between most TM and the Ad/Al ratio (*Figure V-6A*). However, beneath *R. stylosa*, it does not seem to be the case. The Ad/Al ratios are negatively correlated with TM concentrations in the soil, as well as with the syringyl group only. TM, on the other hand, show positive correlations with the three other phenol groups (*Figure V-6A*). TM can also bind to the hydroxyl groups of the derived phenols through chelation. With two $-OCH_3$ groups surrounding the hydroxyl group, the syringyl phenols are the most sterically hindered for chelation with the hydroxyl group (*Figure 1-5*). We suggest that beneath *R. stylosa*, TM can bind to all phenol groups, not just the acids, except for the syringyl phenols. The differences between the two stands may be related to OM sources, OM availability, and OM decomposition/preservation processes.

At the control site, variations in correlations are also observed between stands, with no obvious trend (*Figure V-6B*). However, beneath *R. stylosa*, TM are similarly correlated with the four phenol groups. Specifically, Al, Cd, Fe, Mn, Pb, and Ti show negative correlations with the phenol groups, while As, Co, Cr, Cu, Ni, and Zn exhibit positive correlations (*Figure V-6B*). These differences between the two groups may be attributed to the oxidation states of the TM or their distribution in the soil. Most TM in the positively correlated group were measured in higher relative concentrations in the oxidizable fraction of the soil (TM bound to OM) than the TM from the negatively correlated group (*Figure II-4*), which supports the second hypothesis.

In summary, our study reveals complex patterns in the relationship between TM and lignin compounds in soil. While a positive correlation between TM concentrations and total lignin content was expected; results indicate such a correlation at the control site but a negative correlation at the urban site. TM may form complexes with lignin compounds at both sites, but the OM sources and availability may influence the complexations, which also appear to be TM-dependent.

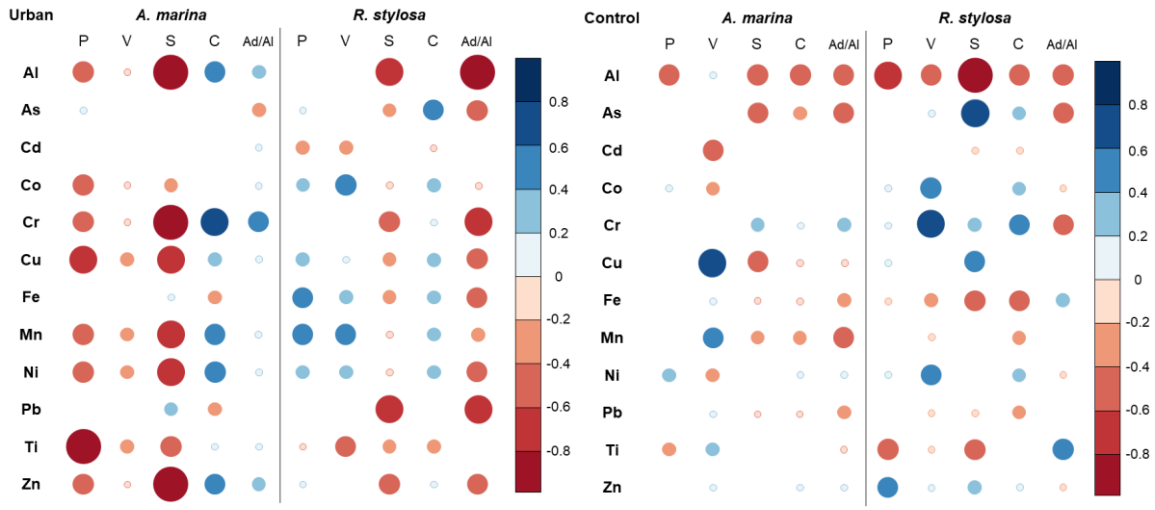

Figure V-6. Correlations between trace metal concentrations in the soil and the lignin-derived phenol groups content (P = p-hydroxyl, V = vanillyl, S = syringyl, C = cinnamyl) as well as the acid/aldehyde ratios (Ad/Al) for both *A. marina* and *R. stylosa* at (A) the urban site and (B) the control site.

V.2.2.2. Neutral carbohydrates

Neutral carbohydrates constitute a substantial portion of the carbon content in mangrove-derived OM. However, they can also originate from allochthonous OM or be generated by microorganisms in the soil. Neutral carbohydrates have the potential to form complexes with TM because they provide a large surface area for TM adsorption. Similar to lignin, neutral carbohydrates contain also hydroxyl and carboxyl groups for chelation with TM (Duan et al., 2020). Nevertheless, neutral carbohydrates typically belong to the labile fraction of OM in mangrove soils, and as a result, they may not significantly contribute to the immobilization of TM (Benner et al., 1990; Marchand et al., 2005). In the context of this thesis, there appears to be a negative correlation between TM concentrations and the total content of neutral carbohydrates in the soil at both research sites (*Figure V-5B*), suggesting that complexation may not be occurring.

The neutral carbohydrates under investigation may originate from various sources and exhibit different affinities for TM in the soil. At the urban site, TM concentrations show negative correlations with all three groups (pentoses, hexoses, and deoxy sugars), and ribose beneath both species (*Figure V-7A*). However, glucose stands apart from the other neutral carbohydrates by exhibiting a positive correlation with almost all TM, but only beneath *R. stylosa* (*Figure V-7A*). In Chapter IV.C, it was demonstrated that beneath *R. stylosa* at the urban site, the glucose content in the upper soil layer was significantly higher than in all other soil layers and in any other stands that were studied. This elevated glucose content was suggested to be a result of microbial activity on the soil surface due to urban runoff. Since the glucose content is negatively correlated with TM beneath *A. marina*, we propose that TM do not form complexes with neutral carbohydrates at the urban site, not

even with glucose. Instead, it is possible that they may bind to other compounds derived from microbial activity as microorganisms produce numerous compounds that can also function as ligands for metal chelation (Hirner et al., 1990).

At the control site, we observed both positive and negative correlations between TM concentrations in the soil and certain neutral carbohydrates beneath both species (*Figure V-7B*). Beneath *R. stylosa*, a few TM show positive correlations with deoxy sugars (fucose and rhamnose). In Chapter IV.A, it was demonstrated that deoxy sugars were the only neutral carbohydrates that exhibited an increase in soil content with depth in this stand. It was suggested that these deoxy sugars were produced by microbial communities during the diagenesis of OM. Therefore, similar to the urban site, it is possible that TM do not bind directly to these carbohydrates but instead form associations with molecules produced by microorganisms in the soil. Underneath *A. marina*, positive correlations are predominantly observed with glucose and the hexoses (mannose and galactose) (*Figure V-7B*). In fact, for all stands except *R. stylosa* at the urban site, the correlations for each TM are similar for glucose and the hexoses (*Figure V-7*). One hypothesis is that these three neutral carbohydrates, given their very similar structures (*Figure 1-6*), may exhibit comparable complexation affinities with the TM. Beneath *A. marina*, these neutral carbohydrates exhibit a decrease in relative concentrations with depth (Chapter IV.A), suggesting a potential complexation with certain TM in these conditions.

In summary, neutral carbohydrates in mangrove soil OM can originate from various sources, including microbial activity in the soil. While they have the potential to form complexes with TM due to their structure, they are typically part of the labile fraction of OM in mangrove soils and may not significantly contribute to TM immobilization. At the urban site, TM concentrations showed negative correlations with certain neutral carbohydrates, suggesting that TM might not form complexes with these carbohydrates but instead bind to other compounds, potentially produced by microorganisms. At the control site, both positive and negative correlations were observed between TM concentrations and specific neutral carbohydrates, which seem to indicate both, complexations with neutral carbohydrates in the soil, but also complexation with microbial-produced compounds other than neutral carbohydrates.

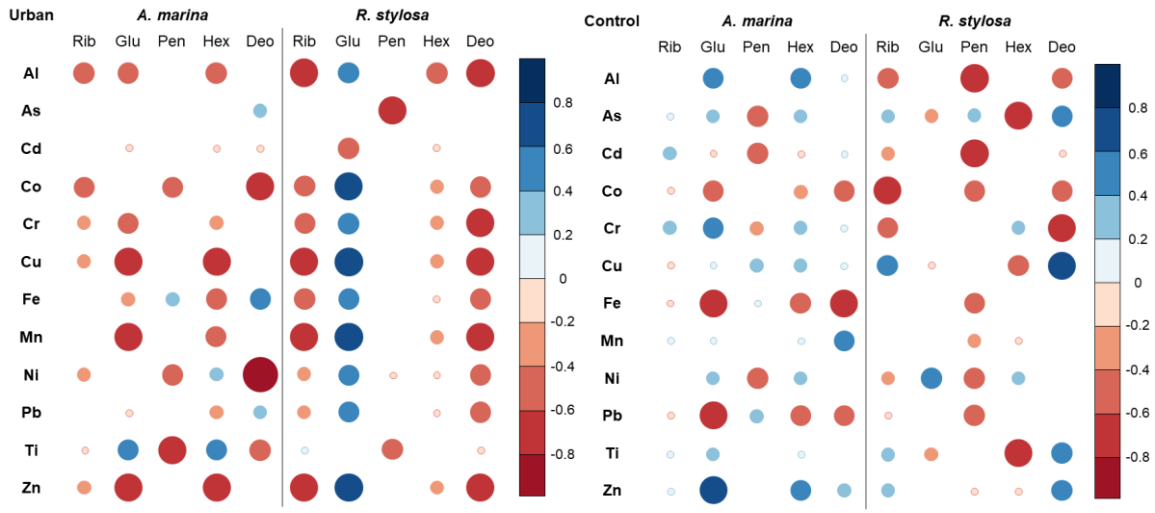

Figure V-7. Correlations between trace metal concentrations in the soil and neutral carbohydrate content (Rib = ribose, Glu = glucose, Pen = pentoses (xylose + arabinose), Hex = hexoses (mannose + galactose), Deo = deoxy sugars (fucose + rhamnose)) for *A. marina* and *R. stylosa* at (A) the urban site and (B) the control site.

V.2.3. Principal component analysis

PCA was used to assess the primary factors influencing the distribution and concentrations of TM in mangrove soils. Across the four stands examined, the first two dimensions explained between 79.4% and 94.6% of the variables (*Figure V-8*). The representations reveal that not all TM were governed by the same variables, particularly evident at the control site beneath *A. marina* (*Figure V-8A*). Notably, As consistently differed from the other TM, with a substantial influence of lignin and neutral carbohydrate components on its soil concentrations *(Figure V-8*).

The key insights derived from the PCA representations are as follows:

1) The C/N ratio emerges as a dominant factor related to most TM concentrations in the soil, specifically at the control site (*Figure V-8A & B & Figure V-9A*). C/N ratios in mangrove soils are influenced by the type of organic material, decomposition stages of OM, and microbial activities. This finding underscores the significant impact of relative C and N concentrations on TM dynamics, surpassing factors such as grain size or redox conditions.

2) pH and $\delta^{15}N$ are the principal factors influencing TM concentrations in the soil, particularly at the urban site (*Figure V-8C & D & Figure V-9 B*). pH and $\delta^{15}N$ levels at the urban site are affected by urban runoff, suggesting that urbanization exerts an influence on TM dynamics and/or TM inputs in mangrove soils.

3) Total organic carbon (TOC) and total sulfur (TS) stand out as major influencing factors for TM concentrations in the soil at both sites (*Figure V-8 & Figure V-9*). This finding

underscores the close relationship between TM dynamics and the carbon and sulfur cycles in mangrove soils.

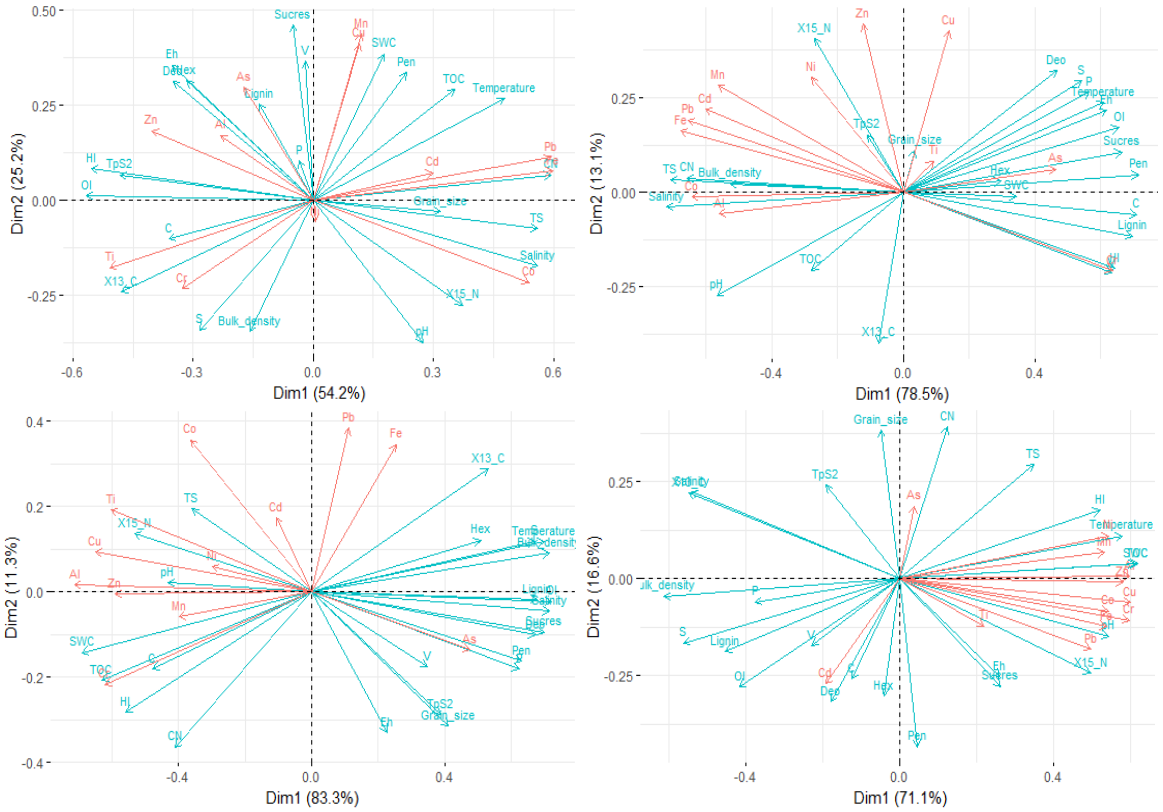

Figure V-8. Principal component analysis of the soil trace metal concentrations (pink) and soil parameters (blue) at the control site beneath (A) *A. marina* and (B) *R. stylosa*, and at the urban site beneath (A) *A. marina* and (B) *R. stylosa*.

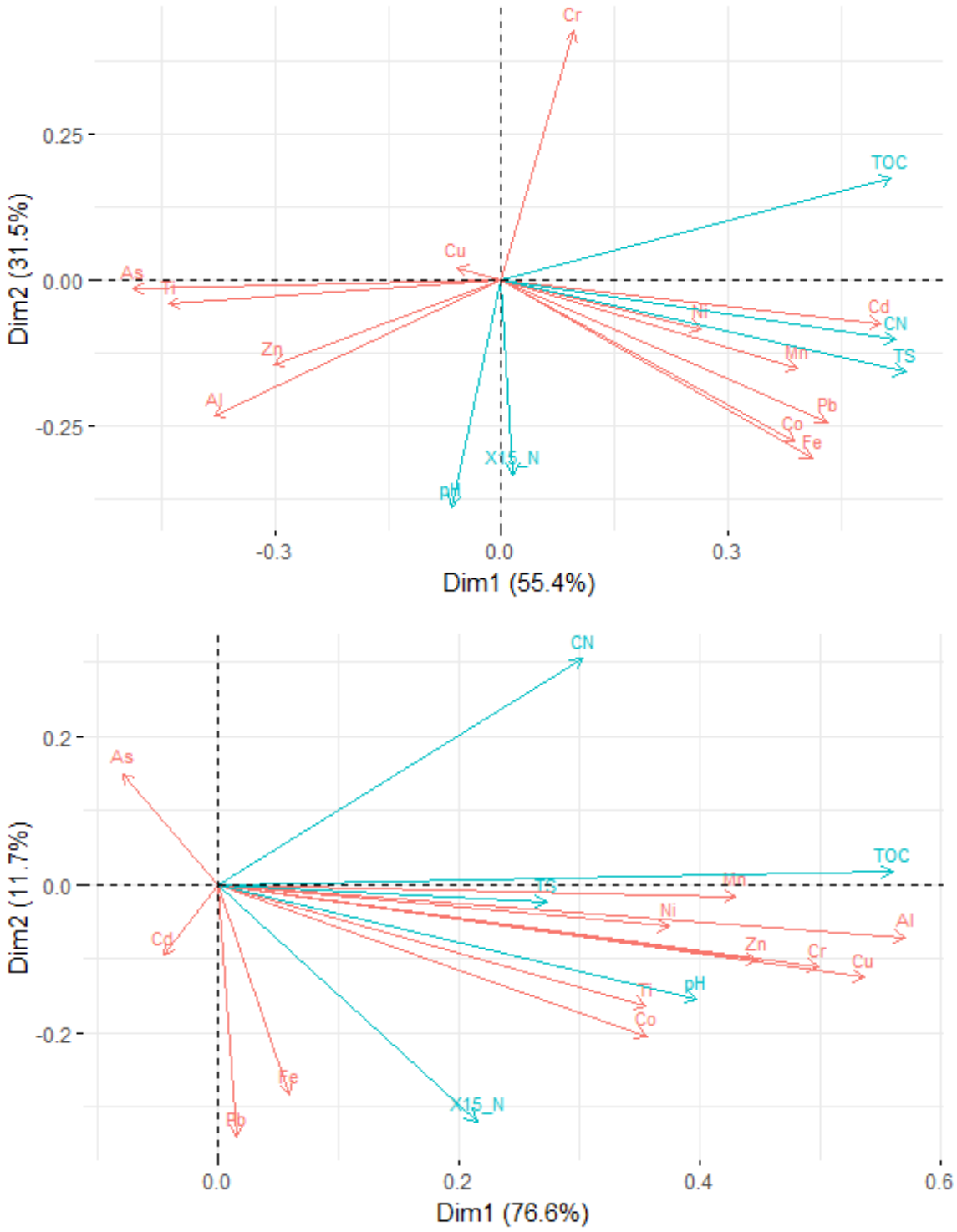

Figure V-9. Principal component analysis of the soil trace metal concentrations (pink) and soil parameters (blue) at the (A) control site and (B) urban site.

V.3. Conclusion

In summary, this thesis has conducted a comprehensive exploration of the intricate dynamics involving trace metals and organic matter within semi-arid mangrove ecosystems, with a particular focus on the impact of urbanization. The study investigated three mangrove forests on the West Coast of New Caledonia, all dominated by the same two mangrove species, *Avicennia marina* and *Rhizophora stylosa*.

Regarding organic matter dynamics, the research identified autochthonous sources of organic matter in mangrove soils, primarily comprising of mangrove litterfall, roots, and potentially microphytobenthos. Organic matter underwent degradation processes, exhibiting variations in degradation rates and chemical characteristics influenced by species and site-specific factors. An intriguing discovery was a buried layer enriched with organic matter and well-preserved roots, dating back approximately 4 000 years. This preservation was attributed to anoxic conditions, pyrite association, and sulfurization under stable sea level. The study also demonstrated that urbanization had a discernible impact on the quality of organic matter derived from mangrove species, as indicated by differences in stable isotopic ratios, lignin content, and neutral carbohydrate composition. Furthermore, the research revealed that urban runoff accelerated litterfall degradation on the mangrove floor, primarily through enhanced microbial activity, while also influencing the composition and dynamics of soil organic matter, especially in the case of the *R. stylosa* stand.

In terms of trace metal dynamics, the thesis showed that urbanization did have an effect on trace metal concentrations in mangrove soils, although they remained within safe limits, not reaching alarming levels observed in other urbanized mangrove forests globally. Urbanization also influenced the bioaccumulation and transfer of trace metals from soil to mangrove tissues by altering the physico-chemical conditions of the mangrove soils. There were variations in root concentrations and bioconcentration factors between species and sites, pointing to different uptake mechanisms and trace metal bioavailability. Leaf concentrations were generally comparable between urban and control sites, indicating adaptive mechanisms against metal stress. The study highlighted distinctions in trace metal uptake among mangrove species, attributed to root structures, metabolic processes, and root adaptations such as iron plaque formation. The research also displayed dynamic changes in trace metal concentrations during leaf litter decomposition, influenced by microbial processes, leaching, and environmental factors. Notably, urban runoff, especially soil immersion, affected trace metal content in litterfall.

Finally, the statistical analysis of all parameters revealed the intricate systems governing trace metal dynamics in mangrove soils. Some key findings included the negative correlations between trace metal concentrations and pH and positive correlations with soil salinity at the control site, suggesting that higher soil salinity might immobilize trace metals. Conversely, at the urban site, trace metal concentrations exhibited strong negative correlations with soil salinity and positive correlations with pH, hinting that urban runoff could be a source of trace metals in these soils. The study also highlighted the complexity of trace metal interactions with lignin compounds and neutral carbohydrates, influenced by organic matter sources and availability. Principle component analysis emphasized the significance of factors such as C/N ratios, TOC, and total sulfur in influencing trace metal distribution, underscoring the intricate relationship between trace metals and carbon, nitrogen, and sulfur cycles. Moreover, at the urban site, trace metal distributions were influenced by pH and the quality of nitrogen compounds, confirming the impact of urbanization on trace metal dynamics.

In conclusion, this thesis has shed light on the multifaceted relationships between trace metals, organic matter, and urbanization within semi-arid mangrove ecosystems. It underscores the importance of considering species-specific responses, microbial influences, and environmental contexts when assessing the effects of urbanization on these vital ecological components. These findings not only advance our scientific knowledge but also offer valuable insights for the conservation and management of these invaluable and vulnerable ecosystems. For example, this thesis showed that soil trace metal concentrations may not be used as the only indicator of trace metal pollutions within mangrove ecosystems.

V.4. Implications

This thesis makes a significant contribution to advancing the scientific knowledge on the relationships between trace metals, organic matter, and urbanization in mangrove ecosystems. The research contributes to a broader understanding of mangrove ecosystems, especially in semi-arid regions, and offers insights that may be applicable to similar ecosystems globally. The findings of this thesis have significant implications for various aspects of environmental science and management:

1) In terms of environmental conservation and management, the study highlights the intricate relationships between urbanization, physico-chemical conditions in mangrove soils, and the dynamics of organic matter and trace metals. The observed impacts on mangrove ecosystems underscore the importance of sustainable urban development practices to minimize detrimental effects on these vital coastal habitats.

2) The research provides valuable insights for urban planning and development. The identification of altered physico-chemical conditions in mangrove soils due to urbanization, including changes in salinity, pH, and trace metal concentrations, emphasizes the need for integrated planning strategies that consider the environmental consequences of urban expansion on adjacent ecosystems.
3) The thesis contributes to ecological health assessment by elucidating the site-dependent transfer of trace metals from soil to mangrove tissues. Understanding these dynamics is crucial for evaluating the health of mangrove ecosystems and developing targeted conservation and restoration measures.
4) The study sheds light on long-term ecosystem dynamics, emphasizing the role of urbanization in altering not only contemporary conditions but also influencing the composition and degradation of organic matter over millennia. This temporal perspective is essential for predicting the long-term consequences of urbanization on mangrove ecosystems.
5) The research has implications for biodiversity conservation, as alterations in physico-chemical conditions impact the zonation of mangrove species and potentially lead to changes in biodiversity patterns. Conservation efforts should consider the diverse responses of mangrove species to urbanization-induced changes in their habitats.
6) The insights into water quality management provided by this thesis highlight the complex interactions between urban runoff and mangrove soil conditions. This knowledge is crucial for developing effective water quality management strategies in urban areas to mitigate the impact on adjacent mangrove ecosystems.
7) The study contributes to climate change adaptation efforts by revealing how urbanization influences the vulnerability of mangrove ecosystems to environmental stressors. This knowledge is important for developing adaptive strategies to ensure the resilience of mangroves in the face of changing climatic conditions.
8) The thesis underscores the importance of educational and outreach programs. By disseminating the findings to various stakeholders, including policymakers, urban planners, and local communities, awareness can be raised about the potential ecological consequences of urbanization on mangrove ecosystems. This information can inform decision-making and promote sustainable practices that balance urban development with the preservation of critical coastal habitats.

V.5. Perspectives

Following this work, many topics can still be explored.

1. Mangrove trees' mechanisms in response to metal stress

During this thesis, mangrove tissues were analyzed as a whole without distinction of compartments (Chapter I & Chapter II). However, several studies have demonstrated the ability of mangrove trees to mitigate the impact of excess TM by storing them in the root epidermis or excreting them through salt-excreting foliar glands (Cheng et al., 2014; Naidoo et al., 2014). In this thesis, it was shown that urbanization increases the bioavailability of TM in the soil and thus their transfer to mangrove roots, but not to the leaves (Chapter II). Consequently, it is possible to investigate the compartmentalization of TM within the root system by studying different types of roots (subterranean, aerial, etc.) and understanding their roles in TM absorption. Different root sections (core, cortex, and bark) can also be analyzed in detail to better understand the mobility of each TM within the mangrove. Greenhouse studies can be implemented to amplify the effect of urbanization or TM concentrations and thus estimate mangrove responses to potentially more significant stresses that could occur in the future. In addition, molecular analyzes (tannins, proteins, sugars, lipids, lignin) can help identify mangrove adaptation mechanisms to metal stress or identify new proxies.

The role of iron oxide plaque in response to metal stress was explored in this thesis (Chapter I & Chapter II). To gain a deeper understanding of the conditions for the formation of this plaque and its ability to immobilize TM, additional studies are necessary. A greenhouse experiment would be beneficial as it would allow for the control of parameters to be studied, such as the iron content in the soil or the level of metal stress. Moreover, an increase in sample size would be preferable to ensure a better representation of the environment, contributing to stronger and more generalizable conclusions. The use of Raman analyzes could also be considered to determine the type of iron oxide present on the surface of pneumatophores. This factor could potentially influence the effectiveness of TM immobilization.

The observation of pyrite within the epidermis of *Avicennia marina* pneumatophores, as presented in Chapter I, requires further investigation. Extensive sampling in pyrite-rich mangroves and meticulous research using scanning electron microscopy coupled with energy-dispersive X-ray spectroscopy is needed to study this phenomenon.

2. Transfer of trace metals to the fauna

The transfer of TM from the soil to mangrove tissues and leaf litter has been studied during this thesis (Chapter II & Chapter III.B). The results have revealed that more TM are transferred from the soil to the root systems at the urban site, but mangrove trees still limit the transfer of TM to the leaves. Furthermore, TM content in the litter increases with degradation, except for Mn. To delve deeper into this topic, it is necessary to study the transfer of TM to the fauna, which plays a role in the human food chain and the lagoon's food web. Some human populations depend heavily on mangrove ecosystems for their protein intake. Initially, analyzes could be conducted on TM in shellfish, crabs, and gobies at the same study sites to maintain continuity in the data. Published studies on this subject are often incomplete and do not examine all relevant matrices. Furthermore, this type of study has never been conducted in the mangrove forests of New Caledonia. To better understand the transfer processes, it is recommended to study multiple organs of individuals and differentiate between stored, assimilated, and bioavailable TM. To identify the origin of TM, the use of complementary isotopic tracers, such as ^{66}Zn, could be beneficial.

3. Exchange of trace metals and organic matter between the mangrove ecosystem and the lagoon with the tidal cycle

After studying the dynamics of TM within the three mangrove sites and the influence of urbanization on these dynamics (Chapter II), it is possible to examine the exchange of TM between the mangrove ecosystem and the lagoon with the tidal cycle. For this purpose, ICP analyzes can be conducted on water and suspended particulate matter (SPM) samples over a 24-hour tidal cycle. The origin of the SPM can be determined through isotopic analyzes (^{13}C, ^{15}N), allowing us to understand the fate of these TM. For this project, the type of exchanged OM can also be explored. In addition to isotopic analyzes, molecular analyzes can confirm the origin of this OM and provide indications on the rate of degradation of this OM and its nutritional value for the food chain.

4. Influence of urbanization on mangrove primary production and respiration of mangrove trees

Visually, the urban forest consists of larger mangrove trees than those in the control forest and are larger than most mangroves on the West coast of New Caledonia. Chapter III of this thesis focuses on the decomposition of leaf litter on the mangrove soil. However, the litter production and primary production of mangrove trees have not yet been assessed. Future work can be considered to measure these values, particularly by quantifying the annual leaf litter production. Research conducted by Leyla Roy during her

thesis (2021-2024) could also be used to estimate primary production from wood and underground biomass (Kristensen et al., 2008). The respiration of mangrove trees at both sites can also be measured for each compartment (leaves, branches, trunk, roots) using a CO_2 analyzer.

5. Influence of urbanization on soil-atmosphere gas-exchange

Soil-atmosphere gas exchanges in mangrove ecosystems are processes that influence both local and global environments. The exchanges of CO_2, CH_4 and N_2O are influenced by various factors, including tidal fluctuations, salinity, temperature, and microbial activity within mangrove soils. In this thesis, results showed how the urban runoff modifies some of these factors such as soil salinity, which is 0 g L^{-1} in surface (Chapter II). Laboratory or *in situ* experiments could be driven to assess the amount of these gases released into the atmosphere.

6. Influence of urbanization on the sulfur cycle

The sulfur cycle is at the core of the elemental cycle in mangrove soil. However, it is highly complex because the oxidation state of sulfur can vary between -2 and +6. Sulfate reduction and its associated chemical reactions are considered key processes that control the chemical environment of mangrove soil (Pan et al., 2019; SamKamaleson and Gonsalves, 2019). Studying the sulfur cycle in the urban mangrove can provide additional insights into the degree of disruption in this ecosystem. Furthermore, it is well-known that the sulfur cycle in mangrove soil is closely linked to the cycling of TM, as discussed in Chapter V of the thesis. Therefore, further research on the origin and chemistry of sulfur in our studied mangrove sites could potentially help understand the relation between the distribution and states of S elements and TM.

7. Influence of urbanization on soil microbial activity

This thesis has demonstrated that leaf litter decomposes more rapidly on the soil of the urban forest, likely due to an increase in soil bacterial activity facilitated by the input of urban water (Chapter III.A). To further explore this perspective, targeted metagenomic analyzes (metabarcoding) could be conducted on the soil of our two study mangrove sites as well as on the decomposing litter. Quantifying and characterizing bacterial communities could confirm or refute the hypotheses presented in this thesis regarding OM degradation. Furthermore, additional analyzes on these bacterial communities can be initiated, particularly on their production of carbohydrates during the degradation of OM in the mangrove soil.

8. Study of the priming effect

In this thesis, different OM diagenesis processes were observed beneath the two species and between sites (Chapter IV). To study the influence of the microbial processes on OM diagenesis, laboratory experiments using mangrove soils from both the urban and control sites could be conducted. Notably, a measurement of the priming effect could give further information on the diagenetic processes occurring in the soil. The priming effect is the difference between the CO_2 released by a soil amended with fresh OM and that of an unamended control soil over a certain period. A negative priming effect indicates preferential utilization of fresh OM by the microorganisms. A positive priming effect indicates three possible mechanisms of OM degradation: 1) "Stoichiometric decomposition" is the acceleration of OM decomposition driven by increased extracellular enzyme production by decomposers, 2) "Nutrient-mining" refers to the energy supply from fresh OM-derived catabolites that assist decomposers in breaking down chemically resistant compounds to recover nutrients, and 3) "Abiotically-mediated process" involves the remobilization of protected organic compounds linked to soil minerals through root exudate-derived organic acids.

9. Microbial processes in the buried layer

In Chapter IV.B, the existence of a buried layer rich in OM in the control mangrove forest was demonstrated. This layer was characterized at the molecular level and using several indicators. However, no studies have yet been conducted on microbial activity and the processes occurring within it. Given that this layer exhibits enhanced OM preservation, it is interesting to explore whether microbial activity processes, such as methane production, persist even at low concentrations. Therefore, it would be relevant to measure CH_4 and CO_2 production in this layer. Furthermore, conducting a microbial community analysis (screening) could provide a better understanding of how this OM preservation is made possible. In Chapter IV.B, it is also suggested that there could be sulfurization of OM. The analysis of microbial communities could potentially confirm this hypothesis by identifying specific microbial communities associated with this process.

References

Abhijith, R., Vennila, A., Purushothaman, C., and Padua, S. (2018). Influence of sediment chemistry on mangrove- phosphobacterial relationship. *Int. J. Chem. Stud.* 6, 1677–1686.

Abrantes, K., and Sheaves, M. (2009). Food web structure in a near-pristine mangrove area of the Australian Wet Tropics. *Estuar. Coast. Shelf Sci.* 82, 597–607. doi: 10.1016/j.ecss.2009.02.021.

Adame, M. F., Connolly, R. M., Turschwell, M. P., Lovelock, C. E., Fatoyinbo, T., Lagomasino, D., et al. (2021). Future carbon emissions from global mangrove forest loss. *Glob. Change Biol.* 27, 2856–2866. doi: 10.1111/gcb.15571.

Alagarsamy, R. (2006). Distribution and seasonal variation of trace metals in surface sediments of the Mandovi estuary, west coast of India. *Estuar. Coast. Shelf Sci.* 67, 333–339. doi: 10.1016/j.ecss.2005.11.023.

Alekseev, Y. E., Garnovskii, A. D., and Zhdanov, Y. A. (1998). Complexes of natural carbohydrates with metal cations. *Russ. Chem. Rev.* 67, 649–669. doi: 10.1070/RC1998v067n08ABEH000343.

Alemu I, J. B., Richards, D. R., Gaw, L. Y.-F., Masoudi, M., Nathan, Y., and Friess, D. A. (2021). Identifying spatial patterns and interactions among multiple ecosystem services in an urban mangrove landscape. *Ecol. Indic.* 121, 107042. doi: 10.1016/j.ecolind.2020.107042.

Alongi, D. M. (1988). Bacterial productivity and microbial biomass in tropical mangrove sediments. *Microb. Ecol.* 15, 59–79. doi: 10.1007/BF02012952.

Alongi, D. M. (2002). Present state and future of the world's mangrove forests. *Environ. Conserv.* 29, 331–349. doi: 10.1017/S0376892902000231.

Alongi, D. M. (2014). Carbon cycling and storage in mangrove forests. *Ann. Rev. Mar. Sci.* 6, 195–219. doi: 10.1146/annurev-marine-010213-135020.

Alongi, D. M. (2015). The impact of climate change on mangrove forests. *Curr. Clim. Change Rep.* 1, 30–39. doi: 10.1007/s40641-015-0002-x.

Alongi, D. M. (2020). Global significance of mangrove blue carbon in climate change mitigation. *Sci* 2, 67. doi: 10.3390/sci2030067.

Alongi, D. M. (2021). Macro- and micronutrient cycling and crucial linkages to geochemical processes in mangrove ecosystems. *J. Mar. Sci. Eng.* 9, 456. doi: 10.3390/jmse9050456.

Alongi, D. M., Christoffersen, P., and Tirendi, F. (1993). The influence of forest type on microbial-nutrient relationships in tropical mangrove sediments. *J. Exp. Mar. Biol. Ecol.* 171, 201–223. doi: 10.1016/0022-0981(93)90004-8.

Alongi, D. M., Tirendi, F., and Clough, B. F. (2000). Below-ground decomposition of organic matter in forests of the mangroves Rhizophora stylosa and Avicennia marina along the arid coast of Western Australia. *Aquat. Bot.* 68, 97–122. doi: 10.1016/S0304-3770(00)00110-8.

Altschuler, Z. S., Schnepfe, M. M., Silber, C. C., and Simon, F. O. (1983). Sulfur diagenesis in everglades peat and origin of pyrite in coal. *Science* 221, 221–227. doi: 10.1126/science.221.4607.221.

Andrews, J. E., Greenaway, A. M., and Dennis, P. F. (1998). Combined carbon isotope and C/N ratios as indicators of source and fate of organic matter in a poorly flushed, tropical estuary: Hunts Bay, Kingston Harbour, Jamaica. *Estuar. Coast. Shelf Sci.* 46, 743–756. doi: 10.1006/ecss.1997.0305.

Angyal, S. J. (1989). "Complexes of metal cations with carbohydrates in solution," in *Advances in Carbohydrate Chemistry and Biochemistry* (Elsevier), 1–43. doi: 10.1016/S0065-2318(08)60411-4.

Appenroth, K.-J. (2010). What are "heavy metals" in Plant Sciences? *Acta Physiol. Plant.* 32, 615–619. doi: 10.1007/s11738-009-0455-4.

Arfi, Y., Chevret, D., Henrissat, B., Berrin, J.-G., Levasseur, A., and Record, E. (2013). Characterization of salt-adapted secreted lignocellulolytic enzymes from the mangrove fungus Pestalotiopsis sp. *Nat. Commun.* 4, 1810. doi: 10.1038/ncomms2850.

Argyropoulos, D. S., and Ben Menachem, S. (1997). "Lignin," in *Biotechnology in the pulp and paper pndustry* (Berlin, Heidelberg: Springer), 127–158.

Armstrong, J., and Armstrong, W. (1988). Phragmites australis - A preliminary study of soil-oxidizing sites and internal gas transport pathways. *New Phytol.* 108, 373–382. doi: 10.1111/j.1469-8137.1988.tb04177.x.

Aschenbroich, A., Marchand, C., Molnar, N., Deborde, J., Hubas, C., Rybarczyk, H., et al. (2015). Spatio-temporal variations in the composition of organic matter in surface sediments of a mangrove receiving shrimp farm effluents (New Caledonia). *Sci. Total Environ.* 512–513, 296–307. doi: 10.1016/j.scitotenv.2014.12.082.

Ashton, E. C., Hogarth, P. J., and Ormond, R. (1999). "Breakdown of mangrove leaf litter in a managed mangrove forest in Peninsular Malaysia," in *Diversity and Function in Mangrove Ecosystems*, ed. R. S. Dodd (Dordrecht: Springer Netherlands), 77–88. doi: 10.1007/978-94-011-4078-2_8.

Aspinall, G. O. (1970). "Pectins, plant gums, and other plant polysaccharides," in *The carbohydrates chemistry and biochemistry* (Cambridge, USA: Academic Press), 515–536.

Assunção, M. A., Frena, M., Santos, A. P. S., and dos Santos Madureira, L. A. (2017). Aliphatic and polycyclic aromatic hydrocarbons in surface sediments collected from mangroves with different levels of urbanization in southern Brazil. *Mar. Pollut. Bull.* 119, 439–445. doi: 10.1016/j.marpolbul.2017.03.071.

Bala Krishna Prasad, M., and Ramanathan, A. L. (2009). Organic matter characterization in a tropical estuarine-mangrove ecosystem of India: Preliminary assessment by using stable isotopes and lignin phenols. *Estuar. Coast. Shelf Sci.* 84, 617–624. doi: 10.1016/j.ecss.2009.07.029.

Ball, M. C. (1998). Mangrove species richness in relation to salinity and waterlogging: A case study along the Adelaide River floodplain, Northern Australia. *Glob. Ecol. Biogeogr. Lett.* 7, 73. doi: 10.2307/2997699.

Baltzer, F. (1981). La sédimentation et la diagenèse précoce sur les côtes à mangrove en aval des massifs ultrabasiques en Nouvelle-Calédonie. *ORSTOM* 12, 175–189.

Barik, J., Mukhopadhyay, A., Ghosh, T., Mukhopadhyay, S. K., Chowdhury, S. M., and Hazra, S. (2018). Mangrove species distribution and water salinity: an indicator species approach to Sundarban. *J. Coast. Conserv.* 22, 361–368. doi: 10.1007/s11852-017-0584-7.

Barker, S. A., and Somers, P. J. (1970). “Bacterial and fungal polysaccharides,” in *The carbohydrates chemistry and biochemistry* (Cambridge, USA: Academic Press), 569–587.

Bastakoti, U., Bourgeois, C., Marchand, C., and Alfaro, A. C. (2019a). Urban-rural gradients in the distribution of trace metals in sediments within temperate mangroves (New Zealand). *Mar. Pollut. Bull.* 149, 110614. doi: 10.1016/j.marpolbul.2019.110614.

Bastakoti, U., Robertson, J., Marchand, C., and Alfaro, A. C. (2019b). Mangrove removal: Effects on trace metal concentrations in temperate estuarine sediments. *Mar. Chem.* 216, 103688. doi: 10.1016/j.marchem.2019.103688.

Batty, L. (2000). The effect of pH and plaque on the uptake of Cu and Mn in Phragmites australis(Cav.) Trin ex. Steudel. *Ann. Bot.* 86, 647–653. doi: 10.1006/anbo.2000.1191.

Baudin, F., Disnar, J.-R., Aboussou, A., and Savignac, F. (2015). Guidelines for Rock–Eval analysis of recent marine sediments. *Org. Geochem.* 86, 71–80. doi: 10.1016/j.orggeochem.2015.06.009.

Bayen, S. (2012). Occurrence, bioavailability and toxic effects of trace metals and organic contaminants in mangrove ecosystems: A review. *Environ. Int.* 48, 84–101. doi: 10.1016/j.envint.2012.07.008.

Behar, F., Beaumont, V., and De B. Penteado, H. L. (2001). Rock-Eval 6 technology: Performances and developments. *Oil Gas Sci. Technol.* 56, 111–134. doi: 10.2516/ogst:2001013.

Beliaeff, B., Bouvet, G., Fernandez, J.-M., David, C., and Laugier, T. (2011). Guide pour le suivi de la qualité du milieu marin en Nouvelle-Calédonie.

Benner, R., Fogel, M. L., and Sprague, E. K. (1991). Diagenesis of belowground biomass of Spartina alterniflora in salt-marsh sediments. *Limnol. Oceanogr.* 36, 1358–1374. doi: 10.4319/lo.1991.36.7.1358.

Benner, R., Maccubbin, A. E., and Hodson, R. E. (1984). Anaerobic biodegradation of the lignin and polysaccharide components of lignocellulose and synthetic lignin by sediment microflora. *Appl. Environ. Microbiol.* 47, 998–1004. doi: 10.1128/aem.47.5.998-1004.1984.

Benner, R., Weliky, K., and Hedges, J. I. (1990). Early diagenesis of mangrove leaves in a tropical estuary: Molecular-level analyses of neutral sugars and lignin-derived phenols. *Geochim. Cosmochim. Acta* 54, 1991–2001. doi: 10.1016/0016-7037(90)90267-O.

Bird, E. C. F., Dubois, J.-P., and Iltis, J. A. (1984). *The impacts of opencast mining on the rivers and coasts of New Caledonia*. Tokyo, Japan : [New York, NY, USA: United Nations University ; Unipub, distributor].

Bonanomi, G., Incerti, G., Antignani, V., Capodilupo, M., and Mazzoleni, S. (2010). Decomposition and nutrient dynamics in mixed litter of Mediterranean species. *Plant Soil* 331, 481–496. doi: 10.1007/s11104-009-0269-6.

Bosire, J. O., Dahdouh-Guebas, F., Kairo, J. G., Kazungu, J., Dehairs, F., and Koedam, N. (2005). Litter degradation and CN dynamics in reforested mangrove plantations at Gazi Bay, Kenya. *Biol. Conserv.* 126, 287–295. doi: 10.1016/j.biocon.2005.06.007.

Bouillon, S., Connolly, R. M., and Lee, S. Y. (2008). Organic matter exchange and cycling in mangrove ecosystems: Recent insights from stable isotope studies. *J. Sea Res.* 59, 44–58. doi: 10.1016/j.seares.2007.05.001.

Bouillon, S., and Dahdouh-Guebas, F. (2003). Sources of organic carbon in mangrove sediments: variability and possible ecological implications. *Hydrobiologia* 495, 33–39. doi: 10.1023/A:1025411506526.

Bouillon, S., and Dehairs, F. (2000). Estimating spatial and seasonal phytoplankton $\delta^{13}C$ variations in an estuarine mangrove ecosystem. *Isot. Environ. Health Stud.* 36, 273–284. doi: 10.1080/10256010008036387.

Bouillon, S., Raman, A. V., Dauby, P., and Dehairs, F. (2002). Carbon and nitrogen stable isotope ratios of subtidal benthic invertebrates in an estuarine mangrove ecosystem (Andhra Pradesh, India). *Estuar. Coast. Shelf Sci.* 54, 901–913. doi: 10.1006/ecss.2001.0864.

Bourgeois, C., Alfaro, A. C., Bisson, E., Alcius, S., and Marchand, C. (2020). Trace metal dynamics in soils and plants along intertidal gradients in semi-arid mangroves (New Caledonia). *Mar. Pollut. Bull.* 156, 111274. doi: 10.1016/j.marpolbul.2020.111274.

Bourgeois, C., Alfaro, A. C., Dencer-Brown, A., Duprey, J. L., Desnues, A., and Marchand, C. (2019a). Stocks and soil-plant transfer of macro-nutrients and trace metals in temperate New Zealand estuarine mangroves. *Plant Soil* 436, 565–586. doi: 10.1007/s11104-019-03945-x.

Bourgeois, C., Alfaro, A. C., Leopold, A., Andréoli, R., Bisson, E., Desnues, A., et al. (2019b). Sedimentary and elemental dynamics as a function of the elevation profile in a semi-arid mangrove toposequence. *CATENA* 173, 289–301. doi: 10.1016/j.catena.2018.10.025.

Bragazza, L., Iacumin, P., Siffi, C., and Gerdol, R. (2010). Seasonal variation in nitrogen isotopic composition of bog plant litter during 3 years of field decomposition. *Biol. Fertil. Soils* 46, 877–881. doi: 10.1007/s00374-010-0483-7.

Branoff, B. L. (2017). Quantifying the influence of urban land use on mangrove biology and ecology: A meta-analysis. *Global Ecol. Biogeogr.* 26, 1339–1356. doi: 10.1111/geb.12638.

Broadley, M. R., White, P. J., Hammond, J. P., Zelko, I., and Lux, A. (2007). Zinc in plants. *New Phytol.* 173, 677–702. doi: 10.1111/j.1469-8137.2007.01996.x.

Brown, G. E., and Parks, G. A. (2001). Sorption of trace elements on mineral surfaces: Modern perspectives from spectroscopic studies, and comments on sorption in the marine environment. *Int. Geol. Rev.* 43, 963–1073. doi: 10.1080/00206810109465060.

Buchman, M. F. (1999). NOAA Screening Quick Reference Tables. Seattle WA: Coastal Protection and Restoration Division, National Oceanic and Atmospheric Administration.

Bunt, J. (1996). Mangrove zonation: An examination of data from seventeen riverine estuaries in tropical Australia. *Ann. Bot.* 78, 333–341. doi: 10.1006/anbo.1996.0128.

Cao, C., Wang, L., Li, H., Wei, B., and Yang, L. (2018). Temporal variation and ecological risk assessment of metals in soil nearby a Pb–Zn mine in Southern China. *Int. J. Environ. Res. Public Health* 15, 940. doi: 10.3390/ijerph15050940.

Cavalcante, R. M., Sousa, F. W., Nascimento, R. F., Silveira, E. R., and Freire, G. S. S. (2009). The impact of urbanization on tropical mangroves (Fortaleza, Brazil): Evidence from PAH distribution in sediments. *J. Environ. Manage.* 91, 328–335. doi: 10.1016/j.jenvman.2009.08.020.

Celis-Hernandez, O., Giron-Garcia, M. P., Ontiveros-Cuadras, J. F., Canales-Delgadillo, J. C., Pérez-Ceballos, R. Y., Ward, R. D., et al. (2020). Environmental risk of trace elements in mangrove ecosystems: An assessment of natural vs oil and urban inputs. *Sci. Total Environ.* 730, 138643. doi: 10.1016/j.scitotenv.2020.138643.

Cennerazzo, J. (2017). Dynamique des HAP et des composés organiques issus de leur transformation dans les compartiments du sol et de la rhizosphère.

Center for International Earth Science Information Network (2012). Population, landscape, and climate estimates (PLACE), v3 (1990, 2000, 2010). *NASA Socioeconomic Data and Applications Center*. Available at: https://sedac.ciesin.columbia.edu/data/set/nagdc-population-landscape-climate-estimates-v3 [Accessed April 18, 2022].

Chakraborty, P., Chakraborty, S., Vudamala, K., Sarkar, A., and Nath, B. N. (2016). Partitioning of metals in different binding phases of tropical estuarine sediments: importance of metal chemistry. *Environ. Sci. Pollut. Res.* 23, 3450–3462. doi: 10.1007/s11356-015-5475-6.

Chakraborty, P., Sarkar, A., Vudamala, K., Naik, R., and Nath, B. N. (2015). Organic matter — A key factor in controlling mercury distribution in estuarine sediment. *Mar. Chem.* 173, 302–309. doi: 10.1016/j.marchem.2014.10.005.

Chale, F. M. M. (1993). Degradation of mangrove leaf litter under aerobic conditions. *Hydrobiologia* 257, 177–183. doi: 10.1007/BF00765010.

Chatterjee, M., Silva Filho, E. V., Sarkar, S. K., Sella, S. M., Bhattacharya, A., Satpathy, K. K., et al. (2007). Distribution and possible source of trace elements in the sediment cores of a tropical macrotidal estuary and their ecotoxicological significance. *Environ. Int.* 33, 346–356. doi: 10.1016/j.envint.2006.11.013.

Chaudhuri, P., Nath, B., and Birch, G. (2014). Accumulation of trace metals in grey mangrove Avicennia marina fine nutritive roots: The role of rhizosphere processes. *Mar. Pollut. Bull.* 79, 284–292. doi: 10.1016/j.marpolbul.2013.11.024.

Chen, C.-L., and Chang, H.-M. (1985). "Chemistry of lignin biodegradation," in *Biosynthesis and biodegradation of wood components* (Orlando, Florida, USA: Academic Press), 535–556.

Chen, X., Zhao, X., Ge, J., Zhao, Y., Wei, Z., Yao, C., et al. (2019). Recognition of the neutral sugars conversion induced by bacterial community during lignocellulose wastes composting. *Bioresour. Technol.* 294, 122153. doi: 10.1016/j.biortech.2019.122153.

Cheng, H., Chen, D.-T., Tam, N. F.-Y., Chen, G.-Z., Li, S.-Y., and Ye, Z.-H. (2012). Interactions among Fe2+, S2–, and Zn2+ tolerance, root anatomy, and radial oxygen loss in mangrove plants. *J. Exp. Bot.* 63, 2619–2630. doi: 10.1093/jxb/err440.

Cheng, H., Jiang, Z.-Y., Liu, Y., Ye, Z.-H., Wu, M.-L., Sun, C.-C., et al. (2014). Metal (Pb, Zn and Cu) uptake and tolerance by mangroves in relation to root anatomy and lignification/suberization. *Tree Physiol.* 34, 646–656. doi: 10.1093/treephys/tpu042.

Chowdhury, R., Favas, P. J. C., Jonathan, M. P., Venkatachalam, P., Raja, P., and Sarkar, S. K. (2017). Bioremoval of trace metals from rhizosediment by mangrove plants in Indian Sundarban Wetland. *Mar. Pollut. Bull.* 124, 1078–1088. doi: 10.1016/j.marpolbul.2017.01.047.

Chowdhury, R., Favas, P. J. C., Pratas, J., Jonathan, M. P., Ganesh, P. S., and Sarkar, S. K. (2015). Accumulation of trace metals by mangrove plants in Indian Sundarban wetland: prospects for phytoremediation. *Int. J. Phyto.* 17, 885–894. doi: 10.1080/15226514.2014.981244.

Christensen, K. K., and Wigand, C. (1998). Formation of root plaques and their influence on tissue phosphorus content in Lobelia dortmanna. *Aquat. Bot.* 61, 111–122. doi: 10.1016/S0304-3770(98)00067-9.

Cifuentes, L. A., Coffin, R. B., Solorzano, L., Cardenas, W., Espinoza, J., and Twilley, R. R. (1996). Isotopic and elemental variations of carbon and nitrogen in a mangrove estuary. *Estuar. Coast. Shelf Sci.* 43, 781–800. doi: 10.1006/ecss.1996.0103.

Clark, M. W., McConchie, D., Lewis, D. W., and Saenger, P. (1998). Redox stratification and heavy metal partitioning in Avicennia-dominated mangrove sediments: a geochemical model. *Chem. Geol.* 149, 147–171. doi: 10.1016/S0009-2541(98)00034-5.

Clough, B. (1984). Growth and salt balance of the mangroves Avicennia marina (Forsk.) Vierh. and Rhizophora stylosa Griff. in relation to salinity. *Funct. Plant Biol.* 11, 419. doi: 10.1071/PP9840419.

Clough, B. F. (1992). "Primary productivity and growth of mangrove forests," in *Coastal and Estuarine Studies*, eds. A. I. Robertson and D. M. Alongi (Washington, D. C.: American Geophysical Union), 225–249. doi: 10.1029/CE041p0225.

Cluzel, D., Aitchison, J. C., and Picard, C. (2001). Tectonic accretion and underplating of mafic terranes in the Late Eocene intraoceanic fore-arc of New Caledonia (Southwest Pacific): geodynamic implications. *Tectonophysics* 340, 23–59. doi: 10.1016/S0040-1951(01)00148-2.

Cordova, M. R., Ulumuddin, Y. I., Purbonegoro, T., and Shiomoto, A. (2021). Characterization of microplastics in mangrove sediment of Muara Angke Wildlife Reserve, Indonesia. *Mar. Pollut. Bull.* 163, 112012. doi: 10.1016/j.marpolbul.2021.112012.

Costanza, R., Grasso, M., Hannon, B., Limburg, K., Naeem, S., O'Neill, R. V., et al. (1998). The value of the world's ecosystem services and natural capital. *Ecol. Econ.* 25, 3–15. doi: 10.1038/387253a0.

Cowie, G. L., and Hedges, J. I. (1984a). Carbohydrate sources in a coastal marine environment. *Geochim. Cosmochim. Acta* 48, 2075–2087. doi: 10.1016/0016-7037(84)90388-0.

Cowie, G. L., and Hedges, J. I. (1984b). Determination of neutral sugars in plankton, sediments, and wood by capillary gas chromatography of equilibrated isomeric mixtures. *Anal. Chem.* 56, 497–504. doi: 10.1021/ac00267a046.

Crémière, A., Strauss, H., Sebilo, M., Hong, W.-L., Gros, O., Schmidt, S., et al. (2017). Sulfur diagenesis under rapid accumulation of organic-rich sediments in a marine mangrove from Guadeloupe (French West Indies). *Chem. Geol.* 454, 67–79. doi: 10.1016/j.chemgeo.2017.02.017.

Cundell, A. M., Brown, M. S., Stanford, R., and Mitchell, R. (1979). Microbial degradation of Rhizophora mangle leaves immersed in the sea. *Estuar. Coast. Mar. Sci.* 9, 281–286. doi: 10.1016/0302-3524(79)90041-0.

Dalvi, A. D., Bacon, W. G., and Osborne, R. C. (2004). The past and the future of nickel laterites. in (Toronto), 27.

David, F. (2017). Dynamique du carbone et relations trophiques dans un estuaire à mangrove sous pression anthropique (Can Gio, Vietnam).

Davis, A. P., Shokouhian, M., and Ni, S. (2001). Loading estimates of lead, copper, cadmium, and zinc in urban runoff from specific sources. *Chemosphere* 44, 997–1009. doi: 10.1016/S0045-6535(00)00561-0.

Day, J. W., Conner, W. H., Ley-Lou, F., Day, R. H., and Navarro, A. (1987). The productivity and composition of mangrove forests, Laguna de Términos, Mexico. *Aquat. Bot.* 27, 267–284. doi: 10.1016/0304-3770(87)90046-5.

De Granville, J. J. (1974). Aperçu sur la structure des pneumatophores de deux espèces des sols hydromorphes en Guyane. *Cahier ORSTOM*, 3–22.

Deborde, J., Marchand, C., Molnar, N., Patrona, L., and Meziane, T. (2015). Concentrations and fractionation of carbon, iron, sulfur, nitrogen and phosphorus in mangrove sediments along an intertidal gradient (semi-arid climate, New Caledonia). *J. Mar. Sci. Eng.* 3, 52–72. doi: 10.3390/jmse3010052.

Demirevska-Kepova, K., Simova-Stoilova, L., Stoyanova, Z., Hölzer, R., and Feller, U. (2004). Biochemical changes in barley plants after excessive supply of copper and

manganese. *Environ. Exp. Bot.* 52, 253–266. doi: 10.1016/j.envexpbot.2004.02.004.

Deng, J., Guo, P., Zhang, X., Shen, X., Su, H., Zhang, Y., et al. (2019). An evaluation on the bioavailability of heavy metals in the sediments from a restored mangrove forest in the Jinjiang Estuary, Fujian, China. *Ecotoxicol. Environ. Saf.* 180, 501–508. doi: 10.1016/j.ecoenv.2019.05.044.

Di-Giovanni, C., Disnar, J. R., Bichet, V., Campy, M., and Guillet, B. (1998). Geochemical characterization of soil organic matter and variability of a postglacial detrital organic supply (chaillexon lake, france). *Earth Surf. Process. Landforms* 23, 1057–1069. doi: 10.1002/(SICI)1096-9837(199812)23:12<1057::AID-ESP921>3.0.CO;2-H.

Disnar, J. R., Guillet, B., Kéravis, D., Di-Giovanni, C., and Sebag, D. (2003). Soil organic matter (SOM) characterization by Rock-Eval pyrolysis: scope and limitations. *Org. Geochem.* 34, 327–343. doi: 10.1016/S0146-6380(02)00239-5.

Dittmar, T., Hertkorn, N., Kattner, G., and Lara, R. J. (2006). Mangroves, a major source of dissolved organic carbon to the oceans. *Global Biogeochem. Cycles* 20. doi: 10.1029/2005GB002570.

Dittmar, T., and Lara, R. J. (2001). Molecular evidence for lignin degradation in sulfate-reducing mangrove sediments (Amazonia, Brazil). *Geochim. Cosmochim. Acta* 65, 1417–1428. doi: 10.1016/S0016-7037(00)00619-0.

Dittmar, T., Lara, R. J., and Kattner, G. (2001). River or mangrove? Tracing major organic matter sources in tropical Brazilian coastal waters. *Mar. Chem.* 73, 253–271. doi: 10.1016/S0304-4203(00)00110-9.

Donato, D. C., Kauffman, J. B., Murdiyarso, D., Kurnianto, S., Stidham, M., and Kanninen, M. (2011). Mangroves among the most carbon-rich forests in the tropics. *Nat. Geosci.* 4, 293–297. doi: 10.1038/ngeo1123.

Douillet, P. (2001). Atlas hydrodynamique du lagon sud-ouest de Nouvelle-Calédonie. Institut de recherche pour le développement.

Douillet, P., Ouillon, S., and Cordier, E. (2001). A numerical model for fine suspended sediment transport in the southwest lagoon of New Caledonia. *Coral Reefs* 20, 361–372. doi: 10.1007/s00338-001-0193-6.

D'Souza, J. (2016). "Arbuscular mycorrhizal diversity from mangroves: A review," in *Recent Advances on Mycorrhizal Fungi* Fungal Biology., ed. M. C. Pagano (Cham: Springer International Publishing), 109–116. doi: 10.1007/978-3-319-24355-9_10.

Duan, D., Lan, W., Chen, F., Lei, P., Zhang, H., Ma, J., et al. (2020). Neutral monosaccharides and their relationship to metal contamination in mangrove sediments. *Chemosphere* 251, 126368. doi: 10.1016/j.chemosphere.2020.126368.

Duan, D., Lei, P., Lan, W., Li, T., Zhang, H., Zhong, H., et al. (2021). Litterfall-derived organic matter enhances mercury methylation in mangrove sediments of South China. *Sci. Total Environ.* 765, 142763. doi: 10.1016/j.scitotenv.2020.142763.

Duan, D., Zhang, D., Yang, Y., Wang, J., Chen, J., and Ran, Y. (2017). Source, composition, and environmental implication of neutral carbohydrates in sediment

cores of subtropical reservoirs, South China. *Biogeosciences* 14, 4009–4022. doi: 10.5194/bg-14-4009-2017.

Duke, N. C. (2007). Biodiversité des mangroves de Nouvelle-Calédonie. Australia: Centre for Marine studies, University of Queensland.

Duke, N. C., Ball, M. C., and Ellison, J. C. (1998). Factors influencing biodiversity and distributional gradients in mangroves. *Global Ecol. Biogeogr. Lett.* 7, 27. doi: 10.2307/2997695.

Duke, N. C., Meyneck, J.-O., Dittmann, S., Ellison, A. M., Anger, K., Berger, U., et al. (2007). A world without mangroves? 317, 41–42. doi: 10.1126/science.317.5834.41b.

Ellison, A. M. (2008). Managing mangroves with benthic biodiversity in mind: Moving beyond roving banditry. *J. Sea Res.* 59, 2–15. doi: 10.1016/j.seares.2007.05.003.

Eric, T. P. K. (2003). Heavy metals contents in sediments, mangroves and bivalves from Ting Kok, Hong Kong. *China Environ. Sci.* 23, 480–484.

Ezcurra, P., Ezcurra, E., Garcillán, P. P., Costa, M. T., and Aburto-Oropeza, O. (2016). Coastal landforms and accumulation of mangrove peat increase carbon sequestration and storage. *Proc. Natl. Acad. Sci. U.S.A.* 113, 4404–4409. doi: 10.1073/pnas.1519774113.

Fandeur, D., Juillot, F., Morin, G., Olivi, L., Cognigni, A., Webb, S. M., et al. (2009). XANES Evidence for oxidation of Cr(III) to Cr(VI) by Mn-oxides in a lateritic regolith developed on serpentinized ultramafic rocks of New Caledonia. *Environ. Sci. Technol.* 43, 7384–7390. doi: 10.1021/es900498r.

FAO (2007). The world's mangroves 1980-2005. Rome, Italy: FAO Forestry Paper.

Farquhar, G. D., Ball, M. C., Von Caemmerer, S., and Roksandic, Z. (1982). Effect of salinity and humidity on 13C value of halophytes - Evidence for diffusional isotope fractionation determined by the ratio of intercellular/atmospheric partial pressure of CO2 under different environmental conditions. *Oecologia* 52, 121–124. doi: 10.1007/BF00349020.

Fell, J. W., Cefalu, R. C., Master, I. M., and Tallman, A. S. (1975). Microbial activities in the mangrove (Rhizophora mangle) leaf detrital system. *Proc. Int. Sym. Biol. Manage. Mangroves* 2, 661–679.

Fell, J. W., and Master, I. M. (1980). The association and potential role of fungi in mangrove detrital systems. *Bot. Mar.* 23, 257–263.

Fernandez, J.-M., Ouillon, S., Chevillon, C., Douillet, P., Fichez, R., and Gendre, R. L. (2006). A combined modelling and geochemical study of the fate of terrigenous inputs from mixed natural and mining sources in a coral reef lagoon (New Caledonia). *Mar. Pollut. Bull.* 52, 320–331. doi: 10.1016/j.marpolbul.2005.09.010.

Ferreira, T. O., Otero, X. L., Vidal-Torrado, P., and Macías, F. (2007). Effects of bioturbation by root and crab activity on iron and sulfur biogeochemistry in mangrove substrate. *Geoderma* 142, 36–46. doi: 10.1016/j.geoderma.2007.07.010.

Fiard, M., Cuny, P., Sylvi, L., Hubas, C., Jézéquel, R., Lamy, D., et al. (2022). Mangrove microbiota along the urban-to-rural gradient of the Cayenne estuary (French Guiana, South America): Drivers and potential bioindicators. *Sci. Total Environ.* 807, 150667. doi: 10.1016/j.scitotenv.2021.150667.

Field, C. D. (1995). Impact of expected climate change on mangroves. *Hydrobiologia* 295, 75–81. doi: 10.1007/BF00029113.

Fleming, M., and Lin, G. (1990). Influence of mangrove detritus in an estuarine ecosystem. *BULLETIN OF MARINE SCIENCE* 47, 8.

Flores-Verdugo, F., Day, J., and Briseno-Duenas, R. (1987). Structure, litter fall, decomposition, and detritus dynamics of mangroves in a Mexican coastal lagoon with an ephemeral inlet. *Mar. Ecol. Prog. Ser.* 35, 83–90. doi: 10.3354/meps035083.

Fogel, M. L., Wooller, M. J., Cheeseman, J., Smallwood, B. J., Roberts, Q., Romero, I., et al. (2008). Unusually negative nitrogen isotopic compositions (δ15N) of mangroves and lichens in an oligotrophic, microbially-influenced ecosystem. *Biogeosciences* 5, 1693–1704. doi: 10.5194/bg-5-1693-2008.

Fonseca, K. T. (1994). Biogeoquímica de metais pesados na rizosfera de plantas de um manguezal do Rio de Janeiro.

Fourqurean, J. W., and Schrlau, J. E. (2003). Changes in nutrient content and stable isotope ratios of C and N during decomposition of seagrasses and mangrove leaves along a nutrient availability gradient in Florida Bay, USA. *Chem. Ecol.* 19, 373–390. doi: 10.1080/02757540310001609370.

Friess, D. A., Rogers, K., Lovelock, C. E., Krauss, K. W., Hamilton, S. E., Lee, S. Y., et al. (2019). The state of the world's mangrove forests: past, present, and future. *Annu. Rev. Environ. Resour.* 44, 89–115. doi: 10.1146/annurev-environ-101718-033302.

Fritioff, Å., Kautsky, L., and Greger, M. (2005). Influence of temperature and salinity on heavy metal uptake by submersed plants. *Environ. Pollut.* 133, 265–274. doi: 10.1016/j.envpol.2004.05.036.

Froelich, P. N., Klinkhammer, G. P., Bender, M. L., Luedtke, N. A., Heath, G. R., Cullen, D., et al. (1979). Early oxidation of organic matter in pelagic sediments of the eastern equatorial Atlantic: suhoxic diagenesis. *Geochim. Cosmochim. Acta* 43, 1075–1090. doi: 10.1016/0016-7037(79)90095-4.

Fromard, F., Michaud, E., and Hossaert-McKey, M. (2018). *Mangrove une forêt dans la mer*. 1st ed. Paris: Le Cherche Midi.

Fry, B., Bern, A. L., Ross, M. S., and Meeder, J. F. (2000). δ15N studies of nitrogen use by the red mangrove, Rhizophora mangle L. in South Florida. *Estuar. Coast. Shelf Sci.* 50, 291–296. doi: 10.1006/ecss.1999.0558.

Fry, B., and Smith, T. J. (2002). Stable isotope studies of red mangroves and filter feeders from the Shark River estuary, Florida. *Bull. Mar. Sci.* 70, 871–890.

Furukawa, K., Wolanski, E., and Mueller, H. (1997). Currents and sediment transport in mangrove forests. *Estuar. Coast. Shelf Sci.* 44, 301–310. doi: 10.1006/ecss.1996.0120.

Garg, N., and Chandel, S. (2011). “Arbuscular mycorrhizal networks: process and functions,” in *Sustainable Agriculture Volume 2*, eds. E. Lichtfouse, M. Hamelin, M. Navarrete, and P. Debaeke (Dordrecht: Springer Netherlands), 907–930. doi: 10.1007/978-94-007-0394-0_40.

Garten, C. T., and Taylor, G. E. (1992). Foliar 13C within a temperate deciduous forest: spatial, temporal, and species sources of variation. *Oecologia* 90, 1–7. doi: 10.1007/bf00317801.

Gautam, M. K., Lee, K.-S., Song, B.-Y., Lee, D., and Bong, Y.-S. (2016). Early-stage changes in natural 13C and 15N abundance and nutrient dynamics during different litter decomposition. *J. Plant Res.* 129, 463–476. doi: 10.1007/s10265-016-0798-z.

Ge, Y., and Li, Z. (2018). Application of lignin and its derivatives in adsorption of heavy metal ions in water: a review. *ACS Sustain. Chem. Eng.* 6, 7181–7192. doi: 10.1021/acssuschemeng.8b01345.

Gearing, J. N., Gearing, P. J., Rudnick, D. T., Requejo, A. G., and Hutchins, M. J. (1984). Isotopic variability of organic carbon in a phytoplankton-based, temperate estuary. *Geochim. Cosmochim. Acta* 48, 1089–1098. doi: 10.1016/0016-7037(84)90199-6.

Ghosh, S., Bakshi, M., Mahanty, S., and Chaudhuri, P. (2021). Understanding potentially toxic metal (PTM) induced biotic response in two riparian mangrove species Sonneratia caseolaris and Avicennia officinalis along river Hooghly, India: Implications for sustainable sediment quality management. *Mar. Environ. Res.* 172, 105486. doi: 10.1016/j.marenvres.2021.105486.

Giarrizzo, T., Schwamborn, R., and Saint-Paul, U. (2011). Utilization of carbon sources in a northern Brazilian mangrove ecosystem. *Estuar. Coast. Shelf Sci.* 95, 447–457. doi: 10.1016/j.ecss.2011.10.018.

Giblin, A. E. (1988). Pyrite formation in marshes during early diagenesis. *Geomicrobiol. J.* 6, 77–97. doi: 10.1080/01490458809377827.

Gilman, E. L., Ellison, J., Duke, N. C., and Field, C. (2008). Threats to mangroves from climate change and adaptation options: A review. *Aquat. Bot.* 89, 237–250. doi: 10.1016/j.aquabot.2007.12.009.

Gonneea, M. E., Paytan, A., and Herrera-Silveira, J. A. (2004). Tracing organic matter sources and carbon burial in mangrove sediments over the past 160 years. *Estuar. Coast. Shelf Sci.* 61, 211–227. doi: 10.1016/j.ecss.2004.04.015.

Gontard, T., and de Coudenhove, G. (2010). Etude de veille économique: la filière pêche en Nouvelle-Calédonie. Nouméa, New Caledonia: Etablissement de régulation des prix agricoles.

Gunina, A., and Kuzyakov, Y. (2015). Sugars in soil and sweets for microorganisms: Review of origin, content, composition and fate. *Soil Biol. Biochem.* 90, 87–100. doi: 10.1016/j.soilbio.2015.07.021.

Guo, X., Zhang, S., and Shan, X. (2008). Adsorption of metal ions on lignin. *J. Hazard. Mater.* 151, 134–142. doi: 10.1016/j.jhazmat.2007.05.065.

Gwenzi, W. (2020). Occurrence, behaviour, and human exposure pathways and health risks of toxic geogenic contaminants in serpentinitic ultramafic geological environments (SUGEs): A medical geology perspective. *Sci. Total Environ.* 700, 134622. doi: 10.1016/j.scitotenv.2019.134622.

Halder, S., and Walther, J. V. (2011). Far from equilibrium enstatite dissolution rates in alkaline solutions at earth surface conditions. *Geochim. Cosmochim. Acta* 75, 7486–7493. doi: 10.1016/j.gca.2011.09.013.

Hamilton, S. E., and Casey, D. (2016). Creation of a high spatio-temporal resolution global database of continuous mangrove forest cover for the 21st century (CGMFC-21): CGMFC-21. *Glob. Ecol. Biogeogr.* 25, 729–738. doi: 10.1111/geb.12449.

Hamilton, S. E., and Hedges, J. I. (1988). The comparative geochemistries of lignins and carbohydrates in an anoxic fjord. *Geochim. Cosmochim. Acta* 52, 129–142. doi: 10.1016/0016-7037(88)90062-2.

Hanamachi, Y., Hama, T., and Yanai, T. (2008). Decomposition process of organic matter derived from freshwater phytoplankton. *Limnology* 9, 57–69. doi: 10.1007/s10201-007-0232-2.

Harbison, P. (1986). Mangrove muds—A sink and a source for trace metals. *Mar. Pollut. Bull.* 17, 246–250. doi: 10.1016/0025-326X(86)90057-3.

Hartley, R. D. (1973). Carbohydrate esters of ferulic acid as components of cell-walls of Lolium multiflorum. *Phytochemistry* 12, 661–665. doi: 10.1016/S0031-9422(00)84460-X.

Hassan, S. E., Hijri, M., and St-Arnaud, M. (2013). Effect of arbuscular mycorrhizal fungi on trace metal uptake by sunflower plants grown on cadmium contaminated soil. *New Biotechnol.* 30, 780–787. doi: 10.1016/j.nbt.2013.07.002.

He, B., Li, R., Chai, M., and Qiu, G. (2014). Threat of heavy metal contamination in eight mangrove plants from the Futian mangrove forest, China. *Environ. Geochem. Health* 36, 467–476. doi: 10.1007/s10653-013-9574-3.

Hedges, J. I., and Ertel, J. R. (1982). Characterization of lignin by gas capillary chromatography of cupric oxide oxidation products. *Anal. Chem.* 54, 174–178. doi: 10.1021/ac00239a007.

Hedges, J. I., and Mann, D. C. (1979). The characterization of plant tissues by their lignin oxidation products. *Geochim. Cosmochim. Acta* 43, 1803–1807. doi: 10.1016/0016-7037(79)90028-0.

Hensel, P., Proffitt, E., Delgado, P., Shigenaka, G., Yender, R., Michel, J., et al. (2014). *Oil spills in mangroves: planning & response considerations*. US Department of Commerce. National Oceanic and Atmospheric Administration.

Herbon, C., and Nordhaus, I. (2013). Experimental determination of stable carbon and nitrogen isotope fractionation between mangrove leaves and crabs. *Mar. Ecol. Prog. Ser.* 490, 91–105. doi: 10.3354/meps10421.

Hernes, P. J., Benner, R., Cowie, G. L., Goñi, M. A., Bergamaschi, B. A., and Hedges, J. I. (2001). Tannin diagenesis in mangrove leaves from a tropical estuary: a novel

molecular approach. *Geochim. Cosmochim. Acta* 65, 3109–3122. doi: 10.1016/S0016-7037(01)00641-X.

Hernes, P. J., Hedges, J. I., Peterson, M. L., Wakeham, S. G., and Lee, C. (1996). Neutral carbohydrate geochemistry of particulate material in the central equatorial Pacific. *Deep Sea Res. Part II: Trop. Stud. in Oceanogr.* 43, 1181–1204. doi: 10.1016/0967-0645(96)00012-4.

Hirner, A. V., Kritsotakis, K., and Tobschall, H. J. (1990). Metal-organic associations in sediments - I. Comparison of unpolluted recent and ancient sediments and sediments affected by anthropogenic pollution. *Appl. Geochem.* 5, 491–505. doi: 10.1016/0883-2927(90)90023-X.

Holloway, C. J., Santos, I. R., and Rose, A. L. (2018). Porewater inputs drive Fe redox cycling in the water column of a temperate mangrove wetland. *Estuar. Coast. Shelf Sci.* 207, 259–268. doi: 10.1016/j.ecss.2018.04.016.

Holloway, C. J., Santos, I. R., Tait, D. R., Sanders, C. J., Rose, A. L., Schnetger, B., et al. (2016). Manganese and iron release from mangrove porewaters: A significant component of oceanic budgets? *Mar. Chem.* 184, 43–52. doi: 10.1016/j.marchem.2016.05.013.

Holmer, M., Kristensen, E., Banta, G., Hansen, K., Jensen, M. H., and Bussawarit, N. (1994). Biogeochemical cycling of sulfur and iron in sediments of a South-East Asian mangrove, Phuket island, Thailand. *Biogeochemistry* 26, 145–161. doi: 10.1007/BF00002904.

Hossain, M. D., and Nuruddin, A. A. (2016). Soil and mangrove: A review. *J. Environ. Sci. Technol.* 9, 198–207. doi: 10.3923/jest.2016.198.207.

Hossain, M., Siddique, M. R. H., Abdullah, S. M. R., Saha, S., Ghosh, D. C., Rahman, Md. S., et al. (2014). Nutrient dynamics associated with leaching and microbial decomposition of four abundant mangrove species leaf litter of the Sundarbans, Bangladesh. *Wetlands* 34, 439–448. doi: 10.1007/s13157-013-0510-1.

Hu, Y., Huang, Y. Z., and Liu, Y. X. (2014). Influence of iron plaque on chromium accumulation and translocation in three rice (*Oryza sativa* L.) cultivars grown in solution culture. *Chem. Ecol.* 30, 29–38. doi: 10.1080/02757540.2013.829050.

Huang, G.-Y., and Wang, Y.-S. (2010). Physiological and biochemical responses in the leaves of two mangrove plant seedlings (Kandelia candel and Bruguiera gymnorrhiza) exposed to multiple heavy metals. *J. Hazard. Mater.* 182, 848–854. doi: 10.1016/j.jhazmat.2010.06.121.

Huang, S., Jiang, R., Song, Q., Zhang, Y., Huang, Q., Su, B., et al. (2020a). Study of mercury transport and transformation in mangrove forests using stable mercury isotopes. *Sci. Total Environ.* 704, 135928. doi: 10.1016/j.scitotenv.2019.135928.

Huang, X., Wang, X., Li, X., Yan, Z., and Sun, Y. (2020b). Occurrence and transfer of heavy metals in sediments and plants of Aegiceras corniculatum community in the Qinzhou Bay, southwestern China. *Acta Oceanol. Sin.* 39, 79–88. doi: 10.1007/s13131-020-1555-7.

Huerta-Diaz, M. A., and Morse, J. W. (1992). Pyritization of trace metals in anoxic marine sediments. *Geochim. Cosmochim. Acta* 56, 2681–2702. doi: 10.1016/0016-7037(92)90353-K.

Imgraben, S., and Dittmann, S. (2008). Leaf litter dynamics and litter consumption in two temperate South Australian mangrove forests. *J. Sea Res.* 59, 83–93. doi: 10.1016/j.seares.2007.06.004.

Insee (2020). Population légale de la Nouvelle-Calédonie en 2019. Institut de la statistique et des études économiques.

International Monetary Fund (2022). Financial development index database. Available at: https://data.imf.org/?sk=F8032E80-B36C-43B1-AC26-493C5B1CD33B&sId=1485894037365 [Accessed April 18, 2022].

Isee (2023). Composantes de l'évolution de la population de la Nouvelle-Calédonie depuis 1965.

Ivaldi, C., Daou, M., Vallon, L., Bisotto, A., Haon, M., Garajova, S., et al. (2021). Screening new xylanase biocatalysts from the mangrove soil diversity. *Microorganisms* 9, 1484. doi: 10.3390/microorganisms9071484.

Jacotot, A., Marchand, C., and Allenbach, M. (2019). Biofilm and temperature controls on greenhouse gas (CO2 and CH4) emissions from a Rhizophora mangrove soil (New Caledonia). *Sci. Total Environ.* 650, 1019–1028. doi: 10.1016/j.scitotenv.2018.09.093.

Jacotot, A., Marchand, C., Rosenheim, B. E., Domack, E. W., and Allenbach, M. (2018). Mangrove sediment carbon stocks along an elevation gradient: Influence of the late Holocene marine regression (New Caledonia). *Mar. Geol.* 404, 60–70. doi: 10.1016/j.margeo.2018.07.005.

Jayachandran, S., Chakraborty, P., Ramteke, D., Chennuri, K., and Chakraborty, S. (2018). Effect of pH on transport and transformation of Cu-sediment complexes in mangrove systems. *Mar. Pollut. Bull.* 133, 920–929. doi: 10.1016/j.marpolbul.2018.03.054.

Jennerjahn, T. C., and Ittekkot, V. (2002). Relevance of mangroves for the production and deposition of organic matter along tropical continental margins. *Naturwissenschaften* 89, 23–30. doi: 10.1007/s00114-001-0283-x.

Jensen, M. M., Holmer, M., and Thamdrup, B. (2005). Composition and diagenesis of neutral carbohydrates in sediments of the Baltic-North Sea transition. *Geochim. Cosmochim. Acta* 69, 4085–4099. doi: 10.1016/j.gca.2005.01.021.

Jian, L., Junyi, Y., Jingchun, L., Chongling, Y., Haoliang, L., and Spencer, K. L. (2017). The effects of sulfur amendments on the geochemistry of sulfur, phosphorus and iron in the mangrove plant (Kandelia obovata (S. L.)) rhizosphere. *Mar. Pollut. Bull.* 114, 733–741. doi: 10.1016/j.marpolbul.2016.10.070.

Joardar Mukhopadhyay, M., and Sharma, A. (1991). Manganese in cell metabolism of higher plants. *Bot. Rev* 57, 117–149. doi: 10.1007/BF02858767.

Johnston, S. G., Morgan, B., and Burton, E. D. (2016). Legacy impacts of acid sulfate soil runoff on mangrove sediments: Reactive iron accumulation, altered sulfur cycling

and trace metal enrichment. *Chem. Geol.* 427, 43–53. doi: 10.1016/j.chemgeo.2016.02.013.

Jones, A. B., O'Donohue, M. J., Udy, J., and Dennison, W. C. (2001). Assessing ecological impacts of shrimp and sewage effluent: biological indicators with standard water quality analyses. *Estuar. Coast. Shelf Sci.* 52, 91–109. doi: 10.1006/ecss.2000.0729.

Kathiresan, K., and Bingham, B. L. (2001). "Biology of mangroves and mangrove ecosystems," in *Advances in Marine Biology* (Elsevier), 81–251. doi: 10.1016/S0065-2881(01)40003-4.

Kehrig, H. A., Pinto, F. N., Moreira, I., and Malm, O. (2003). Heavy metals and methylmercury in a tropical coastal estuary and a mangrove in Brazil. *Org. Geochem.* 34, 661–669. doi: 10.1016/S0146-6380(03)00021-4.

Keuskamp, J. A., Hefting, M. M., Dingemans, B. J. J., Verhoeven, J. T. A., and Feller, I. C. (2015). Effects of nutrient enrichment on mangrove leaf litter decomposition. *Sci. Total Environ.* 508, 402–410. doi: 10.1016/j.scitotenv.2014.11.092.

Khan, M. A., Mahmood-ur-Rahman, Ramzani, P. M. A., Zubair, M., Rasool, B., Khan, M. K., et al. (2020). Associative effects of lignin-derived biochar and arbuscular mycorrhizal fungi applied to soil polluted from Pb-acid batteries effluents on barley grain safety. *Sci. Total Environ.* 710, 136294. doi: 10.1016/j.scitotenv.2019.136294.

Kida, M., Kondo, M., Tomotsune, M., Kinjo, K., Ohtsuka, T., and Fujitake, N. (2019a). Molecular composition and decomposition stages of organic matter in a mangrove mineral soil with time. *Estuar. Coast. Shelf Sci.* 231, 106478. doi: 10.1016/j.ecss.2019.106478.

Kida, M., Tanabe, M., Tomotsune, M., Yoshitake, S., Kinjo, K., Ohtsuka, T., et al. (2019b). Changes in dissolved organic matter composition and dynamics in a subtropical mangrove river driven by rainfall. *Estuar. Coast. Shelf Sci.* 223, 6–17. doi: 10.1016/j.ecss.2019.04.029.

Kimura, M., and Wada, H. (1989). Tannins in mangrove tree roots and their role in the root environment. *Soil Sci. Plant Nutr.* 35, 101–108. doi: 10.1080/00380768.1989.10434741.

Kirk, K. T. (1980). *Lignin biodegradation: Microbiology, chemistry, and potential applications*. 1st ed. Boca Raton, Florida, USA: CRC Press.

Kolb, K. J., and Evans, R. D. (2002). Implications of leaf nitrogen recycling on the nitrogen isotope composition of deciduous plant tissues. *New Phytol.* 156, 57–64. doi: 10.1046/j.1469-8137.2002.00490.x.

Kowasch, M. (2018). Nickel mining in northern New Caledonia - a path to sustainable development? *J. Geochem. Expl.* 194, 280–290. doi: 10.1016/j.gexplo.2018.09.006.

Kristensen, E., Andersen, F., Holmboe, N., Holmer, M., and Thongtham, N. (2000). Carbon and nitrogen mineralization in sediments of the Bangrong mangrove area, Phuket, Thailand. *Aquat. Microb. Ecol.* 22, 199–213. doi: 10.3354/ame022199.

Kristensen, E., Bouillon, S., Dittmar, T., and Marchand, C. (2008). Organic carbon dynamics in mangrove ecosystems: A review. *Aquat. Bot.* 89, 201–219. doi: 10.1016/j.aquabot.2007.12.005.

Kristensen, E., Connolly, R. M., Otero, X. L., Marchand, C., Ferreira, T. O., and Rivera-Monroy, V. H. (2017). "Biogeochemical cycles: Global approaches and perspectives," in *Mangrove Ecosystems: A Global Biogeographic Perspective*, eds. V. H. Rivera-Monroy, S. Y. Lee, E. Kristensen, and R. R. Twilley (Cham: Springer International Publishing), 163–209. doi: 10.1007/978-3-319-62206-4_6.

Kruitwagen, G., Pratap, H. B., Covaci, A., and Wendelaar Bonga, S. E. (2008). Status of pollution in mangrove ecosystems along the coast of Tanzania. *Mar. Pollut. Bull.* 56, 1022–1031. doi: 10.1016/j.marpolbul.2008.02.018.

Lacerda, L. D., Ittekkot, V., and Patchineelam, S. R. (1995). Biogeochemistry of mangrove soil organic matter: a comparison between Rhizophora and Avicennia soils in South-eastern Brazil. *Estuar. Coast. Shelf Sci.* 40, 713–720. doi: 10.1006/ecss.1995.0048.

Lacerda, L. D., Martinelli, L. A., Rezende, C. E., Mozeto, A. A., Ovalle, A. R. C., Victoria, R. L., et al. (1988). The fate of trace metals in suspended matter in a mangrove creek during a tidal cycle. *Sci. Total Environ.* 75, 169–180. doi: 10.1016/0048-9697(88)90030-7.

Laegdsgaard, P., and Johnson, C. (1995). Mangrove habitats as nurseries: unique assemblages of juvenile fish in subtropical mangroves in eastern Australia. *Mar. Ecol. Prog. Ser.* 126, 67–81. doi: 10.3354/meps126067.

Lallier-Vergès, E., Marchand, C., Disnar, J.-R., and Lottier, N. (2008). Origin and diagenesis of lignin and carbohydrates in mangrove sediments of Guadeloupe (French West Indies): Evidence for a two-step evolution of organic deposits. *Chem. Geol.* 255, 388–398. doi: 10.1016/j.chemgeo.2008.07.009.

Lallier-Vergès, E., Perrussel, B. P., Disnar, J.-R., and Baltzer, F. (1998). Relationships between environmental conditions and the diagenetic evolution of organic matter derived from higher plants in a modern mangrove swamp system (Guadeloupe, French West Indies). *Org. Geochem.* 29, 1663–1686. doi: 10.1016/S0146-6380(98)00179-X.

Lamb, A. L., Wilson, G. P., and Leng, M. J. (2006). A review of coastal palaeoclimate and relative sea-level reconstructions using δ13C and C/N ratios in organic material. *Earth-Sci. Rev.* 75, 29–57. doi: 10.1016/j.earscirev.2005.10.003.

Leal, M., and Spalding, M. D. (2022). The state of the world's mangroves 2022. Global Mangrove Alliance.

Lebo, S. E. (2002). "Lignin," in *Encyclopedia of Polymer Science and Technology* (New York, USA: John Wiley & Sons, Inc.), 23.

Lee, S. Y. (1995). Mangrove outwelling: a review. *Hydrobiologia* 295, 203–212. doi: 10.1007/BF00029127.

Lee, S. Y., Primavera, J. H., Dahdouh-Guebas, F., McKee, K., Bosire, J. O., Cannicci, S., et al. (2014). Ecological role and services of tropical mangrove ecosystems: a

reassessment: Reassessment of mangrove ecosystem services. *Glob. Ecol. Biogeogr.* 23, 726–743. doi: 10.1111/geb.12155.

Lei, P., Zhong, H., Duan, D., and Pan, K. (2019). A review on mercury biogeochemistry in mangrove sediments: Hotspots of methylmercury production? *Sci. Total Environ.* 680, 140–150. doi: 10.1016/j.scitotenv.2019.04.451.

Leopold, A., Marchand, C., Deborde, J., and Allenbach, M. (2017). Water biogeochemistry of a mangrove-dominated estuary under a semi-arid climate (New Caledonia). *Estuar. Coast.* 40, 773–791. doi: 10.1007/s12237-016-0179-9.

Leopold, A., Marchand, C., Deborde, J., Chaduteau, C., and Allenbach, M. (2013). Influence of mangrove zonation on CO2 fluxes at the sediment–air interface (New Caledonia). *Geoderma* 202–203, 62–70. doi: 10.1016/j.geoderma.2013.03.008.

Leopold, A., Marchand, C., Renchon, A., Deborde, J., Quiniou, T., and Allenbach, M. (2016). Net ecosystem CO2 exchange in the “Coeur de Voh” mangrove, New Caledonia: Effects of water stress on mangrove productivity in a semi-arid climate. *Agric. For. Meteorol.* 223, 217–232. doi: 10.1016/j.agrformet.2016.04.006.

Letourneau, D. R., and Volmer, D. A. (2021). Mass spectrometry-based methods for the advanced characterization and structural analysis of lignin: A review. *Mass Spectrom. Rev.* 42, 144–188. doi: 10.1002/mas.21716.

Lewis, M., Pryor, R., and Wilking, L. (2011). Fate and effects of anthropogenic chemicals in mangrove ecosystems: A review. *Environ. Pollut.* 159, 2328–2346. doi: 10.1016/j.envpol.2011.04.027.

Li, J., Yu, J., Yan, C., Du, D., Liu, J., and Lu, H. (2018). Distribution correlations of cadmium to calcium, phosphorus, sodium and chloridion in mangrove Aegiceras corniculatum root tissues. *Mar. Pollut. Bull.* 126, 179–183. doi: 10.1016/j.marpolbul.2017.10.074.

Li, T., and Ye, Y. (2014). Dynamics of decomposition and nutrient release of leaf litter in Kandelia obovata mangrove forests with different ages in Jiulongjiang Estuary, China. *Ecol. Engin.* 73, 454–460. doi: 10.1016/j.ecoleng.2014.09.102.

Lin, G., and Sternberg, L. (1992). Effect of growth form, salinity, nutrient and sulfide on photosynthesis, carbon isotope discrimination and growth of red mangrove (Rhizophora mangle L.). *Funct. Plant Biol.* 19, 509–517. doi: 10.1071/PP9920509.

Lin, Y., Fan, J., Yu, J., Jiang, S., Yan, C., and Liu, J. (2018). Root activities and arsenic translocation of Avicennia marina (Forsk.) Vierh seedlings influenced by sulfur and iron amendments. *Mar. Pollut. Bull.* 135, 1174–1182. doi: 10.1016/j.marpolbul.2018.08.040.

Lindahl, B. D., Ihrmark, K., Boberg, J., Trumbore, S. E., Högberg, P., Stenlid, J., et al. (2007). Spatial separation of litter decomposition and mycorrhizal nitrogen uptake in a boreal forest. *New Phytol.* 173, 611–620. doi: 10.1111/j.1469-8137.2006.01936.x.

Liu, H., Zhang, J., Christie, P., and Zhang, F. (2008). Influence of iron plaque on uptake and accumulation of Cd by rice (Oryza sativa L.) seedlings grown in soil. *Sci. Total Environ.* 394, 361–368. doi: 10.1016/j.scitotenv.2008.02.004.

Lovelock, C. E., Ball, M. C., Martin, K. C., and C. Feller, I. (2009). Nutrient enrichment increases mortality of mangroves. *PLoS ONE* 4, e5600. doi: 10.1371/journal.pone.0005600.

Lugo, A. E., and Snedaker, S. C. (1974). The ecology of mangroves. *Annu. Rev. Ecol. Evol. Syst.* 5, 39–64. doi: 10.1146/annurev.es.05.110174.000351.

MacFarlane, G. R. (2003). Chlorophyll a fluorescence as a potential biomarker of zinc stress in the grey Mangrove, Avicennia marina (Forsk.) Vierh. *Bull. Environ. Contam. Toxicol.* 70, 90–96. doi: 10.1007/s00128-002-0160-0.

MacFarlane, G. R., and Burchett, M. D. (2000). Cellular distribution of copper, lead and zinc in the grey mangrove, Avicennia marina (Forsk.) Vierh. *Aquat. Bot.* 68, 45–59. doi: 10.1016/S0304-3770(00)00105-4.

MacFarlane, G. R., and Burchett, M. D. (2001). Photosynthetic pigments and peroxidase activity as indicators of heavy metal stress in the grey mangrove, Avicennia marina (Forsk.) Vierh. *Mar. Pollut. Bull.* 42, 233–240. doi: 10.1016/s0025-326x(00)00147-8.

MacFarlane, G. R., and Burchett, M. D. (2002). Toxicity, growth and accumulation relationships of copper, lead and zinc in the grey mangrove Avicennia marina (Forsk.) Vierh. *Mar. Environ. Res.* 54, 65–84. doi: 10.1016/S0141-1136(02)00095-8.

MacFarlane, G. R., Koller, C. E., and Blomberg, S. P. (2007). Accumulation and partitioning of heavy metals in mangroves: A synthesis of field-based studies. *Chemosphere* 69, 1454–1464. doi: 10.1016/j.chemosphere.2007.04.059.

Machado, W., Gueiros, B. B., Lisboa-Filho, S. D., and Lacerda, L. D. (2005). Trace metals in mangrove seedlings: role of iron plaque formation. *Wetlands Ecol Manage* 13, 199–206. doi: 10.1007/s11273-004-9568-0.

Machiwa, J. (2000). d13C signatures of flora, macrofauna and sediment of a mangrove forest partly affected by sewage wastes. *Tanz. J. Sci.* 26, 15–28. doi: 10.4314/tjs.v26i1.18325.

Macintosh, D. J., and Ashton, E. C. (2002). A review of mangrove biodiversity conservation and management. Denmark: Centre of Tropical Ecosystems Research.

MacKenzie, R. A., Foulk, P. B., Klump, J. V., Weckerly, K., Purbospito, J., Murdiyarso, D., et al. (2016). Sedimentation and belowground carbon accumulation rates in mangrove forests that differ in diversity and land use: a tale of two mangroves. *Wetlands Ecol. Manage.* 24, 245–261. doi: 10.1007/s11273-016-9481-3.

Mackey, A. P., and Smail, G. (1996). The decomposition of mangrove litter in a subtropical mangrove forest. *Hydrobiologia* 332, 93–98. doi: 10.1007/BF00016688.

Maisch, M., Lueder, U., Kappler, A., and Schmidt, C. (2019). Iron lung: how rice roots induce iron redox changes in the rhizosphere and create niches for microaerophilic Fe(II)-oxidizing bacteria. *Environ. Sci. Technol. Lett.* 6, 600–605. doi: 10.1021/acs.estlett.9b00403.

Maitrepierre, L. (2012). “Types de temps et cyclones,” in *Atlas de la Nouvelle-Calédonie et dépendances* (Marseille, France: IRD), 4.

Marchand, C. (2007). Relations entre les caractéristiques physico-chimiques du substrat et la nature des palétuviers - Implications sur la répartition spatiale des espèces -. Institut de Recherche pour le Développement.

Marchand, C. (2008). Structuration écologique et bilan des processus biogéochimiques au sein d'une mangrove "atelier" (Baie de Téremba, Nouvelle Calédonie).

Marchand, C. (2017). Soil carbon stocks and burial rates along a mangrove forest chronosequence (French Guiana). *For. Ecol. Manag.* 384, 92–99. doi: 10.1016/j.foreco.2016.10.030.

Marchand, C., Albéric, P., Lallier-Vergès, E., and Baltzer, F. (2006). Distribution and characteristics of dissolved organic matter in mangrove sediment pore waters along the coastline of French Guiana. *Biogeochemistry* 81, 59–75. doi: 10.1007/s10533-006-9030-x.

Marchand, C., Allenbach, M., and Lallier-Vergès, E. (2011a). Relationship between heavy metals distribution and organic matter cycling in mangrove sediments (Conception Bay, New Caledonia). *Geoderma* 160, 444–456. doi: 10.1016/j.geoderma.2010.10.015.

Marchand, C., Baltzer, F., Lallier-Vergès, E., and Albéric, P. (2004). Pore-water chemistry in mangrove sediments: relationship with species composition and developmental stages (French Guiana). *Mar. Geol.* 208, 361–381. doi: 10.1016/j.margeo.2004.04.015.

Marchand, C., Disnar, J. R., Lallier-Vergès, E., and Lottier, N. (2005). Early diagenesis of carbohydrates and lignin in mangrove sediments subject to variable redox conditions (French Guiana). *Geochim. Cosmochim. Acta* 69, 131–142. doi: 10.1016/j.gca.2004.06.016.

Marchand, C., Fernandez, J.-M., and Moreton, B. (2016). Trace metal geochemistry in mangrove sediments and their transfer to mangrove plants (New Caledonia). *Sci. Total Environ.* 562, 216–227. doi: 10.1016/j.scitotenv.2016.03.206.

Marchand, C., Fernandez, J.-M., Moreton, B., Landi, L., Lallier-Vergès, E., and Baltzer, F. (2012). The partitioning of transitional metals (Fe, Mn, Ni, Cr) in mangrove sediments downstream of a ferralitized ultramafic watershed (New Caledonia). *Chem. Geol.* 300–301, 70–80. doi: 10.1016/j.chemgeo.2012.01.018.

Marchand, C., Lallier-Vergès, E., and Allenbach, M. (2011b). Redox conditions and heavy metals distribution in mangrove forests receiving effluents from shrimp farms (Teremba Bay, New Caledonia). *J. Soils Sediments* 11, 529–541. doi: 10.1007/s11368-010-0330-3.

Marchand, C., Lallier-Vergès, E., Disnar, J.-R., and Kéravis, D. (2008). Organic carbon sources and transformations in mangrove sediments: A Rock-Eval pyrolysis approach. *Org. Geochem.* 39, 408–421. doi: 10.1016/j.orggeochem.2008.01.018.

Marchand, C., Virly, S., Buisson, D., and Duke, N. (2007). Typologies et biodiversité des mangroves de Nouvelle-Calédonie. 213.

Marx, S. K., and McGowan, H. A. (2010). "Long-distance transport of urban and industrial metals and their incorporation into the environment: sources, transport pathways and historical trends," in *Urban Airborne Particulate Matter* Environmental Science

and Engineering., eds. F. Zereini and C. L. S. Wiseman (Berlin, Heidelberg: Springer Berlin Heidelberg), 103–124. doi: 10.1007/978-3-642-12278-1_6.

Massel, S. R., Furukawa, K., and Brinkman, R. M. (1999). Surface wave propagation in mangrove forests. *Fluid Dyn. Res.* 24, 219–249. doi: 10.1016/S0169-5983(98)00024-0.

Maurizot, P., Robineau, B., Vendé-Leclerc, M., and Cluzel, D. (2020a). Introduction to New Caledonia: geology, geodynamic evolution and mineral resources. *Geological Society, London, Memoirs* 51, 1–12. doi: 10.1144/M51-2019-33.

Maurizot, P., Sevin, B., Lesimple, S., Bailly, L., Iseppi, M., and Robineau, B. (2020b). Mineral resources and prospectivity of the ultramafic rocks of New Caledonia. *Memoirs* 51, 247–277. doi: 10.1144/M51-2016-17.

McIvor, A., Möller, I., Spencer, T., and Spalding, M. (2012). Reduction of wind and swell waves by mangroves. The Nature Conservancy and Wetlands International.

McKee, K. L., Cahoon, D. R., and Feller, I. C. (2007). Caribbean mangroves adjust to rising sea level through biotic controls on change in soil elevation. *Glob. Ecol. Biogeogr.* 16, 545–556. doi: 10.1111/j.1466-8238.2007.00317.x.

McKee, K. L., and Faulkner, P. L. (2000). Mangrove peat analysis and reconstruction of vegetation history at the Pelican Cays, Belize. *Atoll Res. Bull.* 468, 47–58. doi: 10.5479/si.00775630.468.47.

Mcleod, E., Chmura, G. L., Bouillon, S., Salm, R., Björk, M., Duarte, C. M., et al. (2011). A blueprint for blue carbon: toward an improved understanding of the role of vegetated coastal habitats in sequestering CO_2. *Front. Ecol. Environ.* 9, 552–560. doi: 10.1890/110004.

Medina, E., and Francisco, M. (1997). Osmolality and 13C of leaf tissues of mangrove species from environments of contrasting rainfall and salinity. *Estuar. Coast. Shelf Sci.* 45, 337–344. doi: 10.1006/ecss.1996.0188.

Mendelssohn, I. A., Kleiss, B. A., and Wakeley, J. S. (1995). Factors controlling the formation of oxidized root channels: A review. *Wetlands* 15, 37–46. doi: 10.1007/BF03160678.

Metian, M., Warnau, M., Chouvelon, T., Pedraza, F., Rodriguez y Baena, A. M., and Bustamante, P. (2013). Trace element bioaccumulation in reef fish from New Caledonia: Influence of trophic groups and risk assessment for consumers. *Mar. Environ. Res.* 87–88, 26–36. doi: 10.1016/j.marenvres.2013.03.001.

Meyers, P. A. (1997). Organic geochemical proxies of paleoceanographic, paleolimnologic, and paleoclimatic processes. *Org. Geochem.* 27, 213–250. doi: 10.1016/S0146-6380(97)00049-1.

Mfilinge, P., Atta, N., and Tsuchiya, M. (2002). Nutrient dynamics and leaf litter decomposition in a subtropical mangrove forest at Oura Bay, Okinawa, Japan. *Trees* 16, 172–180. doi: 10.1007/s00468-001-0156-0.

Middelburg, J. J., and Nieuwenhuize, J. (1998). Carbon and nitrogen stable isotopes in suspended matter and sediments from the Schelde Estuary. *Mar. Chem.* 60, 217–225. doi: 10.1016/S0304-4203(97)00104-7.

Miththapala, S. (2008). *Mangroves*. Colombo, Sri Lanka: Ecosystems and Livelihoods Group Asia, IUCN.

Mitrovica, J. X., and Peltier, W. R. (1991). On postglacial geoid subsidence over the equatorial oceans. *J. Geophys. Res.* 96, 20053–20071. doi: 10.1029/91JB01284.

Moers, M. E. C., Baas, M., De Leeuw, J. W., Boon, J. J., and Schenck, P. A. (1990). Occurrence and origin of carbohydrates in peat samples from a red mangrove environment as reflected by abundances of neutral monosaccharides. *Geochim. Cosmochim. Acta* 54, 2463–2472. doi: 10.1016/0016-7037(90)90233-B.

Moers, M. E. C., Jones, D. M., Eakin, P. A., Fallick, A. E., Griffiths, H., and Larterj, S. R. (1993). Carbohydrate diagenesis in hypersaline environments: application of GC-IRMS to the stable isotope analysis of derivatized saccharides from surticial and buried sediments. *Org. Geochem.* 20, 927–933. doi: 10.1016/0146-6380(93)90104-J.

Molnar, N., Marchand, C., Deborde, J., Della patrona, L., and Meziane, T. (2014). Seasonal pattern of the biogeochemical properties of mangrove sediments receiving shrimp farm effluents (New Caledonia). *J. Aquac. Res. Dev.* 5, 262. doi: 10.4172/2155-9546.1000262.

Molnar, N., Welsh, D. T., Marchand, C., Deborde, J., and Meziane, T. (2013). Impacts of shrimp farm effluent on water quality, benthic metabolism and N-dynamics in a mangrove forest (New Caledonia). *Estuar. Coast. Shelf Sci.* 117, 12–21. doi: 10.1016/j.ecss.2012.07.012.

Morrissey, J., and Guerinot, M. L. (2009). Iron uptake and transport in plants: the good, the bad, and the ionome. *Chem. Rev.* 109, 4553–4567. doi: 10.1021/cr900112r.

Morse, J. W., and Luther, G. W. (1999). Chemical influences on trace metal-sulfide interactions in anoxic sediments. *Geochim. Cosmochim. Acta* 63, 3373–3378. doi: 10.1016/S0016-7037(99)00258-6.

Mukherjee, D., Mukherjee, A., and Kumar, B. (2009). Chemical fractionation of metals in freshly deposited marine estuarine sediments of sundarban ecosystem, India. *Environ. Geol.* 58, 1757–1767. doi: 10.1007/s00254-008-1675-4.

Murdiyarso, D., Purbopuspito, J., Kauffman, J. B., Warren, M. W., Sasmito, S. D., Donato, D. C., et al. (2015). The potential of Indonesian mangrove forests for global climate change mitigation. *Nat. Clim. Change* 5, 1089–1092. doi: 10.1038/nclimate2734.

Nagajyoti, P. C., Lee, K. D., and Sreekanth, T. V. M. (2010). Heavy metals, occurrence and toxicity for plants: a review. *Environ Chem Lett* 8, 199–216. doi: 10.1007/s10311-010-0297-8.

Nagelkerken, I., Blaber, S. J. M., Bouillon, S., Green, P., Haywood, M., Kirton, L. G., et al. (2008). The habitat function of mangroves for terrestrial and marine fauna: A review. *Aquat. Bot.* 89, 155–185. doi: 10.1016/j.aquabot.2007.12.007.

Naidoo, G., Hiralal, T., and Naidoo, Y. (2014). Ecophysiological responses of the mangrove Avicennia marina to trace metal contamination. *Flora: Morphol. Distrib. Funct. Ecol. Plants* 209, 63–72. doi: 10.1016/j.flora.2013.10.003.

Nath, B., Birch, G., and Chaudhuri, P. (2013). Trace metal biogeochemistry in mangrove ecosystems: A comparative assessment of acidified (by acid sulfate soils) and non-acidified sites. *Sci. Total Environ.* 463–464, 667–674. doi: 10.1016/j.scitotenv.2013.06.024.

Nath, B., Chaudhuri, P., and Birch, G. (2014). Assessment of biotic response to heavy metal contamination in Avicennia marina mangrove ecosystems in Sydney Estuary, Australia. *Ecotoxicol. Environ. Saf.* 107, 284–290. doi: 10.1016/j.ecoenv.2014.06.019.

Nations Unies (2022). Perspectives d'urbanisation du monde.

Neal, C., Jarvie, H., Rowland, P., Lawler, A., Sleep, D., and Scholefield, P. (2011). Titanium in UK rural, agricultural and urban/industrial rivers: Geogenic and anthropogenic colloidal/sub-colloidal sources and the significance of within-river retention. *Sci. Total Environ.* 409, 1843–1853. doi: 10.1016/j.scitotenv.2010.12.021.

Nguyen, T.-N., Marchand, C., Strady, E., Huu-Phat, N., and Nhu-Trang, T.-T. (2019). Bioaccumulation of some trace elements in tropical mangrove plants and snails (Can Gio, Vietnam). *Environ. Pollut.* 248, 635–645. doi: 10.1016/j.envpol.2019.02.041.

Nicholson, K. N., Maurizot, P., Black, P. M., Picard, C., Simonetti, A., Stewart, A., et al. (2011). Geochemistry and age of the Nouméa Basin lavas, New Caledonia: Evidence for Cretaceous subduction beneath the eastern Gondwana margin. *Lithos* 125, 659–674. doi: 10.1016/j.lithos.2011.03.018.

Nizam, A., Meera, S. P., and Kumar, A. (2022). Genetic and molecular mechanisms underlying mangrove adaptations to intertidal environments. *iScience* 25, 103547. doi: 10.1016/j.isci.2021.103547.

Noël, V., Juillot, F., Morin, G., Marchand, C., Ona-Nguema, G., Viollier, E., et al. (2017). Oxidation of Ni-rich mangrove sediments after isolation from the sea (Dumbea Bay, New Caledonia): Fe and Ni behavior and environmental implications. *ACS Earth Space Chem.* 1, 455–464. doi: 10.1021/acsearthspacechem.7b00005.

Noël, V., Marchand, C., Juillot, F., Ona-Nguema, G., Viollier, E., Marakovic, G., et al. (2014). EXAFS analysis of iron cycling in mangrove sediments downstream a lateritized ultramafic watershed (Vavouto Bay, New Caledonia). *Geochim. Cosmochim. Acta* 136, 211–228. doi: 10.1016/j.gca.2014.03.019.

Noël, V., Morin, G., Juillot, F., Marchand, C., Brest, J., Bargar, J. R., et al. (2015). Ni cycling in mangrove sediments from New Caledonia. *Geochim. Cosmochim. Acta* 169, 82–98. doi: 10.1016/j.gca.2015.07.024.

Nordhaus, I., Salewski, T., and Jennerjahn, T. C. (2011). Food preferences of mangrove crabs related to leaf nitrogen compounds in the Segara Anakan Lagoon, Java, Indonesia. *Journal of Sea Research* 65, 414–426. doi: 10.1016/j.seares.2011.03.006.

Nordhaus, I., Salewski, T., and Jennerjahn, T. C. (2017). Interspecific variations in mangrove leaf litter decomposition are related to labile nitrogenous compounds. *Estuar. Coast. Shelf Sci.* 192, 137–148. doi: 10.1016/j.ecss.2017.04.029.

Noske, R. (1996). Abundance, zonation and foraging ecology of birds in mangroves of Darwin Harbour, Northern Territory. *Wildl. Res.* 23, 443. doi: 10.1071/WR9960443.

Nunn, P. D., and Carson, M. T. (2015). Sea-level fall implicated in profound societal change about 2570 cal yr BP (620 BC) in western Pacific island groups: Sea-level fall implicated in profound societal change in western Pacific island groups. *Geogr. Environ.* 2, 17–32. doi: 10.1002/geo2.3.

Oakes, J. M., Connolly, R. M., and Revill, A. T. (2010). Isotope enrichment in mangrove forests separates microphytobenthos and detritus as carbon sources for animals. *Limnol. Oceanogr.* 55, 393–402. doi: 10.4319/lo.2010.55.1.0393.

O'Driscoll, M., Clinton, S., Jefferson, A., Manda, A., and McMillan, S. (2010). Urbanization effects on watershed hydrology and in-stream processes in the southern United States. *Water* 2, 605–648. doi: 10.3390/w2030605.

Oelkers, E. H., and Schott, J. (2001). An experimental study of enstatite dissolution rates as a function of pH, temperature, and aqueous Mg and Si concentration, and the mechanism of pyroxene/pyroxenoid dissolution. *Geochim. Cosmochim. Acta* 65, 1219–1231. doi: 10.1016/S0016-7037(00)00564-0.

Ogier, S., Disnar, J.-R., Albéric, P., and Bourdier, G. (2001). Neutral carbohydrate geochemistry of particulate material (trap and core sediments) in an eutrophic lake (Aydat, France). *Org. Geochem.* 32, 151–162. doi: 10.1016/S0146-6380(00)00138-8.

O'Leary, M. H. (1981). Carbon isotope fractionation in plants. *Phytochemistry* 20, 553–567. doi: 10.1016/0031-9422(81)85134-5.

Opsahl, S., and Benner, R. (1995). Early diagenesis of vascular plant tissues: Lignin and cutin decomposition and biogeochemical implications. *Geochim. Cosmochim. Acta* 59, 4889–4904. doi: 10.1016/0016-7037(95)00348-7.

Opsahl, S., and Benner, R. (1999). Characterization of carbohydrates during early diagenesis of five vascular plant tissues. *Org. Geochem.* 30, 83–94. doi: 10.1016/s0146-6380(98)00195-8.

Orr, W. L. (1986). Kerogen/asphaltene/sulfur relationships in sulfur-rich Monterey oils. *Org. Geochem.* 10, 499–516. doi: 10.1016/0146-6380(86)90049-5.

Otte, M. L., Rozema, J., Koster, L., Haarsma, M. S., and Broekman, R. A. (1989). Iron plaque on roots of *Aster tripolium* L.: interaction with zinc uptake. *New Phytol.* 111, 309–317. doi: 10.1111/j.1469-8137.1989.tb00694.x.

Pan, F., Liu, H., Guo, Z., Li, Z., Wang, B., Cai, Y., et al. (2019). Effects of tide and season changes on the iron-sulfur-phosphorus biogeochemistry in sediment porewater of a mangrove coast. *J. Hydro.* 568, 686–702. doi: 10.1016/j.jhydrol.2018.11.002.

Panagos, P., Ballabio, C., Lugato, E., Jones, A., Borrelli, P., Scarpa, S., et al. (2018). Potential sources of anthropogenic copper inputs to european agricultural soils. *Sustainability* 10, 2380. doi: 10.3390/su10072380.

Parida, A. K., and Jha, B. (2010). Salt tolerance mechanisms in mangroves: a review. *Trees* 24, 199–217. doi: 10.1007/s00468-010-0417-x.

Peters, E. C., Gassman, N. J., Firman, J. C., Richmond, R. H., and Power, E. A. (1997). Ecotoxicology of tropical marine ecosystems. *Environ. Toxicol. Chem.* 16, 12–40. doi: 10.1002/etc.5620160103.

Pi, N., Tam, N. F. Y., and Wong, M. H. (2010). Effects of wastewater discharge on formation of Fe plaque on root surface and radial oxygen loss of mangrove roots. *Environ. Pollut.* 158, 381–387. doi: 10.1016/j.envpol.2009.09.004.

Pi, N., Tam, N. F. Y., and Wong, M. H. (2011). Formation of iron plaque on mangrove roots receiving wastewater and its role in immobilization of wastewater-borne pollutants. *Mar. Pollut. Bull.* 63, 402–411. doi: 10.1016/j.marpolbul.2011.05.036.

Pi, N., Tam, N. F. Y., Wu, Y., and Wong, M. H. (2009). Root anatomy and spatial pattern of radial oxygen loss of eight true mangrove species. *Aquat. Bot.* 90, 222–230. doi: 10.1016/j.aquabot.2008.10.002.

Polidoro, B. A., Carpenter, K. E., Collins, L., Duke, N. C., Ellison, A. M., Ellison, J. C., et al. (2010). The loss of species: mangrove extinction risk and geographic areas of global concern. *PLoS ONE* 5, e10095. doi: 10.1371/journal.pone.0010095.

Prasad, M. B. K., Ramanathan, A. L., Shrivastav, S. Kr., Anshumali, and Saxena, R. (2006). Metal fractionation studies in surfacial and core sediments in the Achankovil River basin in India. *Environ. Monit. Assess.* 121, 77–102. doi: 10.1007/s10661-005-9108-2.

Purnobasuki, H., Purnama, P. R., and Kobayashi, K. (2017). Morphology of four root types and anatomy of root-root junction in relation gas pathway of *Avicennia Marina* (Forsk) Vierh roots. *Vegetos- An Inter. Jour. of Plnt. Rese.* 30, 100. doi: 10.5958/2229-4473.2017.00143.4.

Purnobasuki, H., and Suzuki, M. (2005). Functional anatomy of air conducting network on the pneumatophores of a mangrove plant, Avicennia marina (Forsk.) Vierh. *Asian J. Plant Sci.* 4, 334–347.

Ram, N., and Verloo, M. (1985). Effect of various organic materials on the mobility of heavy metals in soil. *Environ. Pollut. Series B Chemical Physical* 10, 241–248. doi: 10.1016/0143-148X(85)90017-5.

Ramos e Silva, C. A., da Silva, A. P., and de Oliveira, S. R. (2006). Concentration, stock and transport rate of heavy metals in a tropical red mangrove, Natal, Brazil. *Mar. Chem.* 99, 2–11. doi: 10.1016/j.marchem.2005.09.010.

Randhir, T. (2003). Watershed-scale effects of urbanization on sediment export: Assessment and policy. *Water Resour. Res.* 39. doi: 10.1029/2002WR001913.

Rao, R. G., Woitchik, A. F., Goeyens, L., van Riet, A., Kazungu, J., and Dehairs, F. (1994). Carbon, nitrogen contents and stable carbon isotope abundance in mangrove leaves from an east African coastal lagoon (Kenya). *Aquat. Bot.* 47, 175–183. doi: 10.1016/0304-3770(94)90012-4.

Rauret, G., López-Sánchez, J. F., Sahuquillo, A., Rubio, R., Davidson, C., Ure, A., et al. (1999). Improvement of the BCR three step sequential extraction procedure prior to the certification of new sediment and soil reference materials. *J. Environ. Monitor.* 1, 57–61. doi: 10.1039/a807854h.

Ray, A. K., Tripathy, S. C., Patra, S., and Sarma, V. V. (2006). Assessment of Godavari estuarine mangrove ecosystem through trace metal studies. *Environ. Int.* 32, 219–223. doi: 10.1016/j.envint.2005.08.014.

Ray, R., Baum, A., Rixen, T., Gleixner, G., and Jana, T. K. (2018). Exportation of dissolved (inorganic and organic) and particulate carbon from mangroves and its implication to the carbon budget in the Indian Sundarbans. *Sci. Total Environ.* 621, 535–547. doi: 10.1016/j.scitotenv.2017.11.225.

Ray, R., Mandal, S. K., González, A. G., Pokrovsky, O. S., and Jana, T. K. (2021). Storage and recycling of major and trace element in mangroves. *Sci. Total Environ.* 780, 146379. doi: 10.1016/j.scitotenv.2021.146379.

Reece, J. B., Urry, L. A., Cain, M. L., Wasserman, S. A., Minorsky, P. V., and Jackson, R. B. (2014). “Plant structure, growth, and development,” in *Campbell Biology* (Pearson), 752–774.

Regina Hershey, N., Bijoy Nandan, S., Schwing, P. T., and Neelima Vasu, K. (2021). Carbon and nitrogen dynamics in a tropical mangrove along the southwestern coast of India. *Mar. Ecol.* 42, 13. doi: 10.1111/maec.12676.

Reid, I. D. (1995). Biodegradation of lignin. *Canadian J. Bot.* 73, 1011–1018. doi: 10.1139/b95-351.

Reyes, G., Smyth, A., and Reynolds, L. (2022). What are urban mangroves? *EDIS* 2022. doi: 10.32473/edis-ss706-2022.

Rezaei, M., Kafaei, R., Mahmoodi, M., Sanati, A. M., Vakilabadi, D. R., Arfaeinia, H., et al. (2021). Heavy metals concentration in mangrove tissues and associated sediments and seawater from the north coast of Persian Gulf, Iran: Ecological and health risk assessment. *Environ. Nanotechnol. Monit. Manage.* 15, 100456. doi: 10.1016/j.enmm.2021.100456.

Rezende, C. E., Lacerda, L. D., Ovall, A. R. C., Silva, C. A. R., and Martinelli, L. A. (1990). Nature of POC transport in a mangrove ecosystem: A carbon stable isotopic study. *Estuar. Coast. Shelf Sci.* 30, 641–645. doi: 10.1016/0272-7714(90)90099-D.

Rice, D. L., and Windom, H. L. (1982). Trace metal transfer associated with the decomposition of detritus derived from estuarine macrophytes. *Bot. Mar.* 25, 213–223.

Robertson, A. I. (1986). Leaf-burying crabs: Their influence on energy flow and export from mixed mangrove forests (Rhizophora spp.) in northeastern Australia. *J. Exp. Mar. Biol. Ecol.* 102, 237–248. doi: 10.1016/0022-0981(86)90179-6.

Robertson, A. I. (1988). Decomposition of mangrove leaf litter in tropical Australia. *J. Exp. Mar. Biol. Ecol.* 116, 235–247. doi: 10.1016/0022-0981(88)90029-9.

Robertson, A. I., Alongi, D. M., and Boto, K. G. (1992). “Food chains and carbon fluxes,” in *Coastal and Estuarine Studies*, eds. A. I. Robertson and D. M. Alongi (Washington, D. C.: American Geophysical Union), 293–326. doi: 10.1029/CE041p0293.

Robin, S. L., Le Milbeau, C., Gututauava, K., and Marchand, C. (submitted). Influence of species and stand position on the evolution of isotopic and molecular signatures of

leaf litter during degradation in urban mangrove forest. *Geochim. Cosmochim. Acta*.

Robin, S. L., and Marchand, C. (2022). Polycyclic aromatic hydrocarbons (PAHs) in mangrove ecosystems: A review. *Environ. Pollut.* 311, 119959. doi: 10.1016/j.envpol.2022.119959.

Robin, S. L., Marchand, C., Ham, B., Pattier, F., Laporte-Magoni, C., and Serres, A. (2021). Influences of species and watersheds inputs on trace metal accumulation in mangrove roots. *Sci. Total Environ.* 787, 147438. doi: 10.1016/j.scitotenv.2021.147438.

Robin, S. L., Marchand, C., Mathian, M., Baudin, F., and Alfaro, A. C. (2022). Distribution and bioaccumulation of trace metals in urban semi-arid mangrove ecosystems. *Front. Environ. Sci.*, 17. doi: 10.3389/fenvs.2022.1054554.

Ruiz, J.-L., Ravary, F., and Debar, L. (2020). Suivi environnemental des milieux: ZAC PANDA et DSM-Année 2019. SECAL.

Rumolo, P., Barra, M., Gherardi, S., Marsella, E., and Sprovieri, M. (2011). Stable isotopes and C/N ratios in marine sediments as a tool for discriminating anthropogenic impact. *J. Environ. Monit.* 13, 3399. doi: 10.1039/c1em10568j.

Sadat-Noori, M., and Glamore, W. (2019). Porewater exchange drives trace metal, dissolved organic carbon and total dissolved nitrogen export from a temperate mangrove wetland. *J. Environ. Manage.* 248, 109264. doi: 10.1016/j.jenvman.2019.109264.

Sahoo, K., and Dhal, N. K. (2009). Potential microbial diversity in mangrove ecosystems: A review. *Indian J. Mar. Sci.* 38, 249–256.

SamKamaleson, A., and Gonsalves, M.-J. (2019). Role of sulfur-oxidizing bacteria on the ecology in tropical mangrove sediments. *Reg. Stud. Mar. Sci.* 28, 100574. doi: 10.1016/j.rsma.2019.100574.

Sánchez-Andrés, R., Sánchez-Carrillo, S., Alatorre, L. C., Cirujano, S., and Álvarez-Cobelas, M. (2010). Litterfall dynamics and nutrient decomposition of arid mangroves in the Gulf of California: Their role sustaining ecosystem heterotrophy. *Estuar. Coast. Shelf Sci.* 89, 191–199. doi: 10.1016/j.ecss.2010.07.005.

Sanders, C. J., Maher, D. T., Tait, D. R., Williams, D., Holloway, C., Sippo, J. Z., et al. (2016). Are global mangrove carbon stocks driven by rainfall?: Mangrove Carbon Stocks. *J. Geophys. Res. Biogeosci.* 121, 2600–2609. doi: 10.1002/2016JG003510.

Scholander, P. F., van Dam, L., and Scholander, S. I. (1955). Gas exchange in the roots of mangroves. *American J. Bot.* 42, 92–98. doi: 10.1002/j.1537-2197.1955.tb11097.x.

Schwamborn, R., and Giarrizzo, T. (2015). Stable isotope discrimination by consumers in a tropical mangrove food web: How important are variations in C/N ratio? *Estuar. Coast.* 38, 813–825. doi: 10.1007/s12237-014-9871-9.

Sebag, D., Verrecchia, E. P., Cécillon, L., Adatte, T., Albrecht, R., Aubert, M., et al. (2016). Dynamics of soil organic matter based on new Rock-Eval indices. *Geoderma* 284, 185–203. doi: 10.1016/j.geoderma.2016.08.025.

Service de la Géologie de Nouvelle-Calédonie (2016). Carte de la géologie de la Nouvelle-Calédonie. Available at: https://dtsi-sgt.maps.arcgis.com/apps/webappviewer/index.html?id=da224a6ff1c24c029de4024d7ae8af26 [Accessed December 12, 2021].

Shtiza, A., Swennen, R., and Tashko, A. (2005). Chromium and nickel distribution in soils, active river, overbank sediments and dust around the Burrel chromium smelter (Albania). *J. Geochem. Expl.* 87, 92–108. doi: 10.1016/j.gexplo.2005.07.005.

Silva, C. A. R., Lacerda, L. D., Ovalle, A. R., and Rezende, C. E. (1998). The dynamics of heavy metals through litterfall and decomposition in a red mangrove forest. *Mangroves Salt Marshes* 2, 149–157. doi: 10.1023/A:1009923223882.

Singh, G., Ranjan, R. K., Chauhan, R., and Ramanathan, A. L. (2010). "Dissolved metal distribution in Indian mangrove ecosystem: Case studies from East Coast of India," in *Management and Sustainable Development of Coastal Zone Environments*, eds. A. L. Ramanathan, P. Bhattacharya, T. Dittmar, M. B. K. Prasad, and B. R. Neupane (Dordrecht: Springer Netherlands), 212–224. doi: 10.1007/978-90-481-3068-9_14.

Sippo, J. Z., Maher, D. T., Tait, D. R., Ruiz-Halpern, S., Sanders, C. J., and Santos, I. R. (2017). Mangrove outwelling is a significant source of oceanic exchangeable organic carbon. *Limnol. Oceanogr.* 2, 1–8. doi: 10.1002/lol2.10031.

Smallwood, B. J., Wooller, M. J., Jacobson, M. E., and Fogel, M. L. (2003). Isotopic and molecular distributions of biochemicals from fresh and buried Rhizophora mangle leaves. *Geochem. Trans.* 4, 38–46. doi: 10.1186/1467-4866-4-38.

Spalding, M. D., Blasco, F., and Field, C. D. (1997). *World Mangrove Atlas*. Okinawa, Japan: The International Society for Mangrove Ecosystems.

Spalding, M. D., Ruffo, S., Lacambra, C., Meliane, I., Hale, L. Z., Shepard, C. C., et al. (2014). The role of ecosystems in coastal protection: Adapting to climate change and coastal hazards. *Ocean Coast. Manage.* 90, 50–57. doi: 10.1016/j.ocecoaman.2013.09.007.

St-Cyr, L., and Crowder, A. A. (1988). Iron oxide deposits oh the roots of *phragmites australis* related to the iron bound to carbonates in the soil. *J. Plant Nutri.* 11, 1253–1261. doi: 10.1080/01904168809363883.

St-Cyr, L., Fortin, D., and Campbell, P. G. C. (1993). Microscopic observations of the iron plaque of a submerged aquatic plant (Vallisneria americana Michx). *Aquat. Bot.* 46, 155–167. doi: 10.1016/0304-3770(93)90043-V.

Steinke, T. D., and Ward, C. J. (1987). Degradation of mangrove leaf litter in the St Lucia Estuary as influenced by season and exposure. *S. Afr. J. Bot.* 53, 323–328. doi: 10.1016/S0254-6299(16)31392-8.

Suárez-Abelenda, M., Ferreira, T. O., Camps-Arbestain, M., Rivera-Monroy, V. H., Macías, F., Nóbrega, G. N., et al. (2014). The effect of nutrient-rich effluents from shrimp farming on mangrove soil carbon storage and geochemistry under semi-

arid climate conditions in northern Brazil. *Geoderma* 213, 551–559. doi: 10.1016/j.geoderma.2013.08.007.

Sweeney, R. E., Kalil, E. K., and Kaplan, I. R. (1980). Characterisation of domestic and industrial sewage in Southern California coastal sediments using nitrogen, carbon, sulphur and uranium tracers. *Mar. Environ. Res.* 3, 225–243. doi: 10.1016/0141-1136(80)90029-X.

Taillardat, P., Ziegler, A. D., Friess, D. A., Widory, D., Truong Van, V., David, F., et al. (2018). Carbon dynamics and inconstant porewater input in a mangrove tidal creek over contrasting seasons and tidal amplitudes. *Geochim. Cosmochim. Acta* 237, 32–48. doi: 10.1016/j.gca.2018.06.012.

Talbot, J. M., Yelle, D. J., Nowick, J., and Treseder, K. K. (2012). Litter decay rates are determined by lignin chemistry. *Biogeochemistry* 108, 279–295. doi: 10.1007/s10533-011-9599-6.

Tam, N. F. Y., Vrijmoed, L. L. P., and Wong, Y. S. (1990). Nutrient dynamics associated with leaf decomposition in a small subtropical mangrove community in Hong Kong. *Bull. Mar. Sci.* 47, 68–78.

Tam, N. F. Y., Wong, Y. S., Lan, C. Y., and Wang, L. N. (1998). Litter production and decomposition in a subtropical mangrove swamp receiving wastewater. *J. Exp. Mar. Biol. Ecol.* 226, 1–18. doi: 10.1016/S0022-0981(97)00233-5.

Tardy, Y., and Roquin, C. (1992). “Geochemistry and evolution of lateritic landscapes,” in *Weathering soils and paleosols* (Amsterdam: Elsevier), 407–443.

Taylor, G. J., and Crowder, A. A. (1983). Use of the DCB technique for extraction of hydrous Iron oxides from roots of wetland plants. *American J. Bot.* 70, 1254–1257. doi: 10.2307/2443295.

Thakur, S., Singh, L., Wahid, Z. A., Siddiqui, M. F., Atnaw, S. M., and Din, M. F. M. (2016). Plant-driven removal of heavy metals from soil: uptake, translocation, tolerance mechanism, challenges, and future perspectives. *Environ Monit Assess* 188, 206. doi: 10.1007/s10661-016-5211-9.

Thakur, V. K., Thakur, M. K., Raghavan, P., and Kessler, M. R. (2014). Progress in green polymer composites from lignin for multifunctional applications: a review. *ACS Sustain. Chem. Eng.* 2, 1072–1092. doi: 10.1021/sc500087z.

Thatoi, H., Behera, B. C., Mishra, R. R., and Dutta, S. K. (2013). Biodiversity and biotechnological potential of microorganisms from mangrove ecosystems: a review. *Ann. Microbiol.* 63, 1–19. doi: 10.1007/s13213-012-0442-7.

Thollot, P. (1996). *Les poissons de mangrove du lagon sud-ouest de Nouvelle-Calédonie*. Paris: ORSTOM.

Thomas, N., Lucas, R., Bunting, P., Hardy, A., Rosenqvist, A., and Simard, M. (2017). Distribution and drivers of global mangrove forest change, 1996–2010. *PLoS ONE* 12, e0179302. doi: 10.1371/journal.pone.0179302.

Thornton, I. (2012). “Geochemical aspects of the distribution and forms of heavy metals in soils,” in *Effect of heavy metal pollution on plants: Metals in the environment* Pollution monitoring series. (Springer Science & Business Media), 258.

Torres, G. G., Figueroa-Galvis, I., Muñoz-García, A., Polanía, J., and Vanegas, J. (2019). Potential bacterial bioindicators of urban pollution in mangroves. *Environ. Pollut.* 255, 113293. doi: 10.1016/j.envpol.2019.113293.

Tremel-Schaub, A., and Feix, I. (2005). *Contamination des sols : Transferts des sols vers les plantes*. ADEME Editions.

Trescases, J.-J. (1975). *L'évolution géochimique supergène des roches ultrabasiques en zone tropicale: formation des gisements nickélifères de Nouvelle-Calédonie*. Paris: O.R.S.T.O.M.

Tripathi, R. D., Tripathi, P., Dwivedi, S., Kumar, A., Mishra, A., Chauhan, P. S., et al. (2014). Roles for root iron plaque in sequestration and uptake of heavy metals and metalloids in aquatic and wetland plants. *Metallomics* 6, 1789–1800. doi: 10.1039/c4mt00111g.

Tucker, J., Sheats, N., Giblin, A. E., Hopkinson, C. S., and Montoya, J. P. (1999). Using stable isotopes to trace sewage-derived material through Boston Harbor and Massachusetts Bay. *Mar. Environ. Res.* 48, 353–375. doi: 10.1016/S0141-1136(99)00069-0.

Tuholske, C., Tane, Z., López-Carr, D., Roberts, D., and Cassels, S. (2017). Thirty years of land use/cover change in the Caribbean: Assessing the relationship between urbanization and mangrove loss in Roatán, Honduras. *Appl. Geogr.* 88, 84–93. doi: 10.1016/j.apgeog.2017.08.018.

Turekian, K. K., and Wedepohl, K. H. (1961). Distribution of the elements in some major units of the Earth's crust. *Geol. Soc. America Bull.* 72, 175. doi: 10.1130/0016-7606(1961)72[175:DOTEIS]2.0.CO;2.

Turner, R. G., and Marshall, C. (1972). The accumulation of zinc by subcellular fractions of roots of Agrostis tenuis sibth. in relation to zinc tolerance. *New Phytol.* 71, 671–676.

Twilley, R. R. (1988). "Coupling of mangroves to the productivity of estuarine and coastal waters," in *Coastal-Offshore Ecosystem Interactions* Lecture Notes on Coastal and Estuarine Studies., ed. B.-O. Jansson (Berlin, Heidelberg: Springer Berlin Heidelberg), 155–180. doi: 10.1007/978-3-642-52452-3_7.

Twilley, R. W., Lugo, A. E., and Patterson-Zucca, C. (1986). Litter production and turnover in basin mangrove forests in Southwest Florida. *Ecology* 67, 670–683. doi: 10.2307/1937691.

UNESCO (2020). Lagoons of New Caledonia: Reef diversity and associated ecosystems. *UNESCO World Heritage Centre*. Available at: https://whc.unesco.org/en/list/1115/ [Accessed October 12, 2020].

Valiela, I., Bowen, J. L., and York, J. K. (2001). Mangrove forests: one of the world's threatened major tropical environments. *BioScience* 51, 807. doi: 10.1641/0006-3568(2001)051[0807:MFOOTW]2.0.CO;2.

Valiela, I., Wilson, J., Buchsbaum, R., Rietsma, C., Bryant, D., Foreman, K., et al. (1984). Importance of chemical composition of salt marsh litter on decay rates and feeding by detritivores. *Bull. Mar. Sci.* 35, 261–269.

Vallentyne, J. R. (1963). Isolation of pyrite spherules from recent sediments. *Limnol. Oceanogr.* 8, 16–30. doi: 10.4319/lo.1963.8.1.0016.

van Bijsterveldt, C. E. J., van Wesenbeeck, B. K., Ramadhani, S., Raven, O. V., van Gool, F. E., Pribadi, R., et al. (2021). Does plastic waste kill mangroves? A field experiment to assess the impact of macro plastics on mangrove growth, stress response and survival. *Sci. Total Environ.* 756, 143826. doi: 10.1016/j.scitotenv.2020.143826.

Van Der Valk, A. G., and Attiwill, P. M. (1984). Decomposition of leaf and root litter of Avicennia marina at Westernport Bay, Victoria, Australia. *Aquat. Bot.* 18, 205–221. doi: 10.1016/0304-3770(84)90062-7.

Vane, C. H., Kim, A. W., Moss-Hayes, V., Snape, C. E., Diaz, M. C., Khan, N. S., et al. (2013). Degradation of mangrove tissues by arboreal termites (*Nasutitermes acajutlae*) and their role in the mangrove C cycle (Puerto Rico): Chemical characterization and organic matter provenance using bulk δ ^{13} C, C/N, alkaline CuO oxidation-GC/MS, and solid-state ^{13} C NMR. *Geochem. Geophys. Geosyst.* 14, 3176–3191. doi: 10.1002/ggge.20194.

Verkleij, J. A. C., and Schat, H. (1990). “Mechanisms of metal tolerance in higher plants,” in *Heavy metal tolerance in plants - evolutionary aspects* (Boca Raton, Florida, USA: CRC Press), 179–193.

Vinh, T. V., Allenbach, M., Linh, K. T. V., and Marchand, C. (2020). Changes in leaf litter quality during its decomposition in a tropical planted mangrove forest (Can Gio, Vietnam). *Front. Environ. Sci.* 8, 10. doi: 10.3389/fenvs.2020.00010.

Vithanage, M., Kumarathilaka, P., Oze, C., Karunatilake, S., Seneviratne, M., Hseu, Z.-Y., et al. (2019). Occurrence and cycling of trace elements in ultramafic soils and their impacts on human health: A critical review. *Environ. Int.* 131, 104974. doi: 10.1016/j.envint.2019.104974.

Vracko, P., Tuomisto, J., Grad, J., and Kunseler, E. (2007). Exposure of children to chemical hazards in food.

Wafar, S., Untawale, A. G., and Wafar, M. (1997). Litter fall and energy flux in a mangrove ecosystem. *Estuar. Coast. Shelf Sci.* 44, 111–124. doi: 10.1006/ecss.1996.0152.

Wakeham, S. G., and Canuel, E. A. (2006). “Degradation and preservation of organic matter in marine sediments,” in *Marine Organic Matter: Biomarkers, Isotopes and DNA* The Handbook of Environmental Chemistry., ed. J. K. Volkman (Berlin/Heidelberg: Springer-Verlag), 295–321. doi: 10.1007/698_2_009.

Wang, Y., Zhu, H., and Tam, N. F. Y. (2014a). Polyphenols, tannins and antioxidant activities of eight true mangrove plant species in South China. *Plant Soil* 374, 549–563. doi: 10.1007/s11104-013-1912-9.

Williams, P. N., Santner, J., Larsen, M., Lehto, N. J., Oburger, E., Wenzel, W., et al. (2014). Localized flux maxima of arsenic, lead, and iron around root apices in flooded lowland rice. *Environ. Sci. Technol.* 48, 8498–8506. doi: 10.1021/es501127k.

Wilson, J., Buchsbaum, R., Valiela, I., and Swain, T. (1986). Decomposition in salt marsh ecosystems: phenolic dynamics during decay of litter of Spartina alterniflora. *Mar. Ecol. Prog. Ser.* 29, 177–187. doi: 10.3354/meps029177.

Wingler, A., Purdy, S., MacLean, J. A., and Pourtau, N. (2006). The role of sugars in integrating environmental signals during the regulation of leaf senescence. *J. Exp. Bot.* 57, 391–399. doi: 10.1093/jxb/eri279.

Woodroffe, C. D., Rogers, K., McKee, K. L., Lovelock, C. E., Mendelssohn, I. A., and Saintilan, N. (2016). Mangrove sedimentation and response to relative sea-level rise. *Annu. Rev. Mar. Sci.* 8, 243–266. doi: 10.1146/annurev-marine-122414-034025.

Wu, Q., Leung, J. Y. S., Tam, N. F. Y., Chen, S., Mai, B., Zhou, X., et al. (2014). Biological risk and pollution history of polycyclic aromatic hydrocarbons (PAHs) in Nansha mangrove, South China. *Mar. Pollut. Bull.* 85, 92–98. doi: 10.1016/j.marpolbul.2014.06.014.

Xie, T., Lu, S., Zeng, J., Rao, L., Wang, X., Win, M. S., et al. (2020). Soluble Fe release from iron-bearing clay mineral particles in acid environment and their oxidative potential. *Sci. Total Environ.* 726, 138650. doi: 10.1016/j.scitotenv.2020.138650.

Yadav, A., Ram, A., Majithiya, D., Salvi, S., Sonavane, S., Kamble, A., et al. (2015). Effect of heavy metals on the carbon and nitrogen ratio in Avicennia marina from polluted and unpolluted regions. *Mar. Pollut. Bull.* 101, 359–365. doi: 10.1016/j.marpolbul.2015.10.020.

Yamaguchi, N., Ohkura, T., Takahashi, Y., Maejima, Y., and Arao, T. (2014). Arsenic distribution and speciation near rice roots influenced by Iron plaques and redox conditions of the soil matrix. *Environ. Sci. Technol.* 48, 1549–1556. doi: 10.1021/es402739a.

Yamano, H., Cabioch, G., Chevillon, C., and Join, J.-L. (2014). Late Holocene sea-level change and reef-island evolution in New Caledonia. *Geomorphology* 222, 39–45. doi: 10.1016/j.geomorph.2014.03.002.

Yan, Z., Sun, X., Xu, Y., Zhang, Q., and Li, X. (2017). Accumulation and tolerance of mangroves to heavy metals: a review. *Curr. Pollut. Rep.* 3, 302–317. doi: 10.1007/s40726-017-0066-4.

Yang, Z., Song, W., Zhao, Y., Zhou, J., Wang, Z., Luo, Y., et al. (2018). Differential responses of litter decomposition to regional excessive nitrogen input and global warming between two mangrove species. *Estuar. Coast. Shelf Sci.* 214, 141–148. doi: 10.1016/j.ecss.2018.09.018.

Youssef, T., and Saenger, P. (1996). Anatomical adaptive strategies to flooding and rhizosphere oxidation in mangrove seedlings. *Aust. J. Bot.* 44, 297–313. doi: 10.1071/BT9960297.

Zabel, R. A., and Morrell, J. J. (2020). “Chemical changes in wood caused by decay fungi,” in *Wood Microbiology* (Elsevier), 215–244. doi: 10.1016/B978-0-12-819465-2.00008-5.

Zawislanski, P. T., Chau, S., Mountford, H., Wong, H. C., and Sears, T. C. (2001). Accumulation of Selenium and trace metals on plant litter in a tidal marsh. *Estuar. Coast. Shelf Sci.* 52, 589–603. doi: 10.1006/ecss.2001.0772.

Zhang, M., Ahmad, M., Lee, S. S., Xu, L. H., and Ok, Y. S. (2014). Sorption of Polycyclic Aromatic Hydrocarbons (PAHs) to lignin: effects of hydrophobicity and

temperature. *Bull. Environ. Contam. Toxicol.* 93, 84–88. doi: 10.1007/s00128-014-1290-x.

Zheng, W., Chen, X., and Lin, P. (1997). Accumulation and biological cycling of heavy metal elements in Rhizophora stylosa mangroves in Yingluo Bay, China. *Mar. Ecol. Prog. Ser.* 159, 293–301. doi: 10.3354/meps159293.

Zhou, Y., Peng, Y., Li, X., and Chen, G. (2011). Accumulation and partitioning of heavy metals in mangrove rhizosphere sediments. *Environ. Earth Sci.* 64, 799–807. doi: 10.1007/s12665-011-0904-4.

Zhou, Y., Zhao, B., Peng, Y., and Chen, G. (2010). Influence of mangrove reforestation on heavy metal accumulation and speciation in intertidal sediments. *Mar. Pollut. Bull.* 60, 1319–1324. doi: 10.1016/j.marpolbul.2010.03.010.

Zhu, X., Yang, F., and Wei, C. (2015). Factors influencing the heavy metal bioaccessibility in soils were site dependent from different geographical locations. *Environ. Sci. Pollut. Res.* 22, 13939–13949. doi: 10.1007/s11356-015-4617-1.

Annexes

Annexe 1: Robin, S. L., and Marchand, C. (2022). Polycyclic aromatic hydrocarbons (PAHs) in mangrove ecosystems: A review. Environ. Pollut. 311, 119959. doi: 10.1016/j.envpol.2022.119959.

Annexe 2: Jacotot, A., Gayral, I., Robin, S. L., and Marchand, C. (2023). Soil concentrations and atmospheric emissions of biogenic hydrogen sulphide (H2S) in a Rhizophora mangrove forest. Estuar. Coast. Shelf Sci. 291, 108439. doi: 10.1016/j.ecss.2023.108439.

Annexe 1

Polycyclic aromatic hydrocarbons (PAHs) in mangrove ecosystems: a review

Sarah Louise ROBIN, Cyril MARCHAND

Published in Environmental Pollution

DOI: 10.1016/j.envpol.2022.119959

Abstract

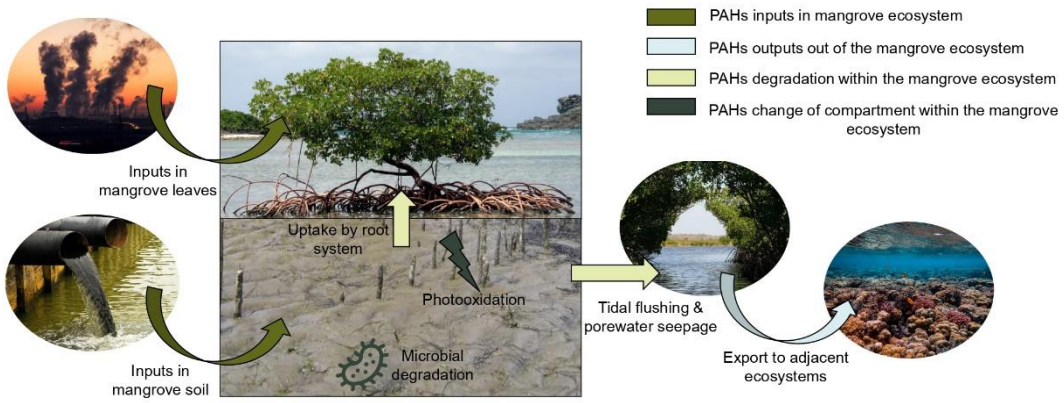

Polycyclic aromatic hydrocarbons (PAHs) are organic pollutants of increasing concern in the different fields of the environment and human health. There are 16 of them that are recognized as priority pollutants by the US environmental protection agency due to their mutagenic and carcinogenic potentials. Due to their hydrophobicity and stability, they are persistent in the environment and can be transported over long distances. Their toxicological effects on multiple species, including humans, as well as their bioaccumulation in the food web became major topics in organic pollutants research this last decade. In the environment, multiple studies have been conducted on their accumulation in the soil and their degradation processes resulting in numerous review papers. However, the dynamics of PAHs in mangrove ecosystems is not yet completely understood. In this review paper, an exhaustive presentation of what is known about PAHs and their transfer, accumulation, and degradation in mangrove ecosystems is offered. This article brings to light the knowledge already acquired on the subject and the perspective research necessary to fully comprehend PAHs dynamics in mangrove ecosystems.

Keywords: organic pollutants, mangrove forests, anthropogenic contaminants, oil pollution

1. Introduction

Polycyclic aromatic hydrocarbons (PAHs) are neutral, non-polar organic molecules composed of hydrogen and carbon atoms only, with at least two fused aromatic rings (Lee and Vu, 2010). 130 PAHs have been identified but 16 of them are qualified as priority pollutants by the US Environmental Protection Agency. Those organic molecules are particularly dangerous for human health and the environment as they present toxic effects such as mutagenesis and carcinogenesis (Table 1) (Brimo, 2017).

Table 1. List of the 16 priority polycyclic aromatic hydrocarbons, their toxicity levels, and their carcinogenic and mutagenic potentials from the Environmental Protection Agency and the International Center for Cancer Research.

PAH	Toxicity	Carcinogenic	Mutagenic
Naphthalene	Moderate	Not confirmed	Not observed
Acenaphthene	Moderate	Not confirmed	Observed
Acenaphthylene	Moderate	Not confirmed	Observed
Fluorene	Low	Not confirmed	Observed
Phenanthrene	Moderate	Not confirmed	Observed
Anthracene	Moderate	Not confirmed	Observed
Fluoranthene	Moderate	Not confirmed	Observed
Pyrene	Moderate	Not confirmed	Observed
Benzo[a]anthracene	High	Confirmed	Observed
Chrysene	Moderate	Confirmed	Observed
Benzo[b]fluoranthene	High	Confirmed	Observed
Benzo[k]fluoranthene	Moderate	Confirmed	Observed
Benzo[a]pyrene	High	Confirmed	Observed
Indeno[1,2,3-cd]pyrene	High	Confirmed	Observed
Benzo[ghi]perylene	Moderate	Not confirmed	Observed
Dibenzo[a,h]anthracene	High	Confirmed	Observed

Sources of PAHs are either natural or anthropogenic, and either pyrolytic, petrogenic, or biogenic (Abdel-Shafy and Mansour, 2016). Primary natural sources are wildfires, geological formation of fossil fuels, and volcanic activity. Primary anthropogenic sources are heating and electricity for households (gas, wood, and coal burning), transports' exhaust, and industrial emissions (Rengarajan et al., 2015). The emissions' percentage of each source varies widely between seasons, rural and urban areas, and between countries (Shen et al., 2013). PAHs can be transported by volatilization or leaching, and be degraded by microbial activity, chemical oxidation, or photo oxidation

(Haritash and Kaushik, 2009). Microbial degradation is considered the least aggressive remediation technique for the environment (de Almeida et al., 2021) and is the main focus for fast and effective restoration of contaminated sediments (Ahmad et al., 2019). Chemical, physical, and thermal treatments are also considered for PAHs degradation such as photocatalytic degradation, electrokinetic remediation, and microwave heating (Benamar et al., 2019; Dong et al., 2019; Sivagami et al., 2019).

Mangrove forests are intertidal ecosystems developing along tropical and sub-tropical coastlines (Alongi, 2002). They cover the coastline of more than 100 countries on 5 different continents (Hamilton and Casey, 2016) (Figure 1). Mangrove forests provide many ecosystem services such as littoral protection, species habitat, and contaminant and sediment filtering (Lee et al., 2014). They represent only 0.5% of the global forest area, and have a relatively simple forest structure, but are of the most productive ecosystems on Earth with a global productivity of 26±6 Tg of organic carbon (OC) per year (Breithaupt et al., 2012). More than 50 species of mangrove trees are identified across the globe, representing 22 genera and 16 families (Kathiresan and Bingham, 2001). These species develop on soil with more or less high porewater salinity, up to 90 g L^{-1}, and depend on the tidal cycle and river inputs for elements and nutrients exchange (Kathiresan and Bingham, 2001; Kristensen et al., 2008). Almost 50% of mangrove forests' total area is located in the top 4 countries with the largest mangroves' superficies: Indonesia (28.4%), Brazil (9.4%), Malaysia (5.8%), and Papua New Guinea (5.1%) (Hamilton and Casey, 2016). On average, a third of the population of these countries live on the coastline, where mangrove forests can develop (CIESIN, 2012). Consequently, there is competition for space between mangrove ecosystems and economic and urban development. Development also leads to an increase in contaminants release such as PAHs via multiple routes (e.g., atmospheric, aquatic) towards the coast, and consequently, to mangrove forests (Figure 2). The high sedimentation rate, organic matter (OM) richness, and biogeochemical reactivity of the substrate are three factors making mangrove forests regions of potential contaminants accumulation such as PAHs (Harbison, 1986; Bouillon et al., 2008; Kristensen et al., 2008, 2017; Alongi, 2014; Marchand, 2017). The fate of PAHs in mangrove forests depends on multiple variables such as the biodiversity and the hydrodynamics conditions, and vary with seasons and tides (Figure 2).

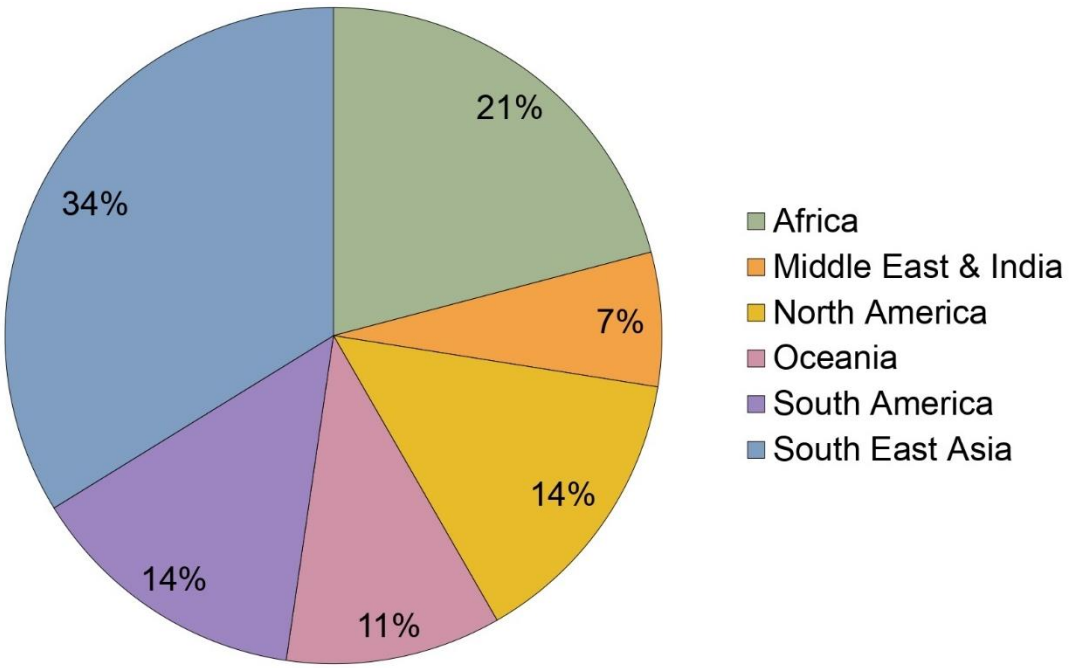

Figure 1. Global area percentages of mangrove forests by region in 2010 (From CIESIN, 2012).

Many reviews have been published on PAHs sources and toxicity in the environment (Baek et al., 1991; Lima et al., 2005; Tsibart and Gennadiev, 2013; Gauthier et al., 2014; Abdel-Shafy and Mansour, 2016; Alegbeleye et al., 2017; Mojiri et al., 2019; Patel et al., 2020), as well as natural or anthropogenic degradation processes (Haritash and Kaushik, 2009; Wick et al., 2011; Gupta et al., 2015; Sakshi and Haritash, 2020; Bianco et al., 2021; Imam et al., 2022). However, only one review looked at PAHs biodegradation in mangrove ecosystems specifically (de Almeida et al., 2021), and one paragraph was dedicated to PAHs dynamic in mangrove ecosystems in another review on contaminants in mangrove forests (Bayen, 2012). There is therefore a lack of data collection and analysis on PAHs sources, distributions, and dynamics in mangrove ecosystems despite their potential proximity to PAHs sources, and PAHs negative effects on human health and the environment. The important urban development, especially in tropical coastal areas, is correlated to an increase in PAHs concentrations in the environment, which represents a real contamination threat to mangrove forests. Many coastal human populations depend on mangrove forests and their resources such as fisheries for personal and economic use (Lee et al., 2014). PAHs potential toxicity in mangrove ecosystems is an environmental concern and a public health concern. The dynamic conditions of geochemical parameters in mangrove ecosystems induce different dynamics in PAHs inputs, outputs, and fate in the multiple compartments of mangrove forests. This paper is the first to review the knowledge on factors affecting PAHs dynamic in mangrove sediments, their transfer to mangrove trees, as well as their ecotoxicological

effects. A critical review is made between the parameters affecting PAHs dynamics and their variability within mangrove ecosystems. An exhaustive list of PAHs concentrations in mangrove sediments and other related compartments around the world is presented in relation with current contamination indexes. The processes of PAHs transfer to mangrove trees and their ecotoxicological effects are also reviewed. A brief section is dedicated to PAHs microbial biodegradation and the current used bioindicators of PAHs sediments contamination are reviewed. To conclude, perspectives on future work that could be done to improve the understanding of this subject are suggested and scientific gaps are identified.

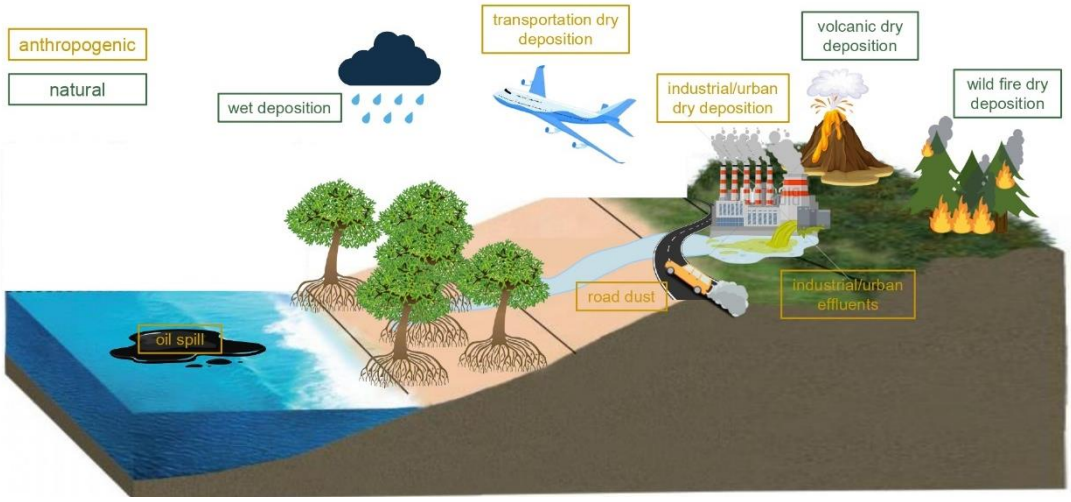

Figure 2. Sources and inputs of polycyclic aromatic hydrocarbons in mangrove ecosystems.

2. Polycyclic aromatic hydrocarbons contamination levels of mangrove ecosystems worldwide

2.1. Indexes of polycyclic aromatic hydrocarbons in marine and coastal sediments

A classification of sediment contamination by the 16 priority PAHs has been offered in literature (Baumard et al., 1998a, 1998b). Coastal sediments can have a low (< 100 ng g^{-1}), moderate (100 – 1 000 ng g^{-1}), high (1 000 – 5 000 ng g^{-1}), or very high (> 5 000 ng g^{-1}) contamination level. Another guideline used worldwide developed by the National Oceanic and Atmospheric Administration (NOAA) assesses the biological toxicity level of marine sediments via two values: the effects range median (ERM) and the effects range low (ERL) (Table 2) (Buchman, 1999). Below the ERL, it is assumed that biological toxicity effects are very scarce, while above the ERM biological toxicity effects are common. The ERL-ERM guideline is the most commonly used sediment quality guideline for mangrove sediments but others exist such as the effect level approach (Macdonald et al., 1996) and the consensus-based approach (Swartz, 1999). The effect level approach is similar to the

ERL-ERM guideline as there are two values for each PAH, the threshold effect level (TEL) and the probable effect level (PEL) (Table 2) (Macdonald et al., 1996). Using a database of PAHs concentrations in estuarine or marine sediments and observed biological effects on benthic communities across North America, they've reported three ranges of PAHs concentrations. Below the TEL the adverse biological effects are rare, between the TEL and the PEL the adverse biological effects are occasional, and above the PEL they are recurrent (Macdonald et al., 1996). The consensus-based approach aimed to take into account the cocktail effects of PAHs mixtures on benthic ecosystems. Three values for total PAHs concentrations were calculated: the threshold effect concentration (TEC) at 290 µg g^{-1} of OC, the median effect concentration (MEC) at 1 800 µg g^{-1} of OC, and the extreme effect concentration (EEC) at 10 000 µg g^{-1} of OC (Swartz, 1999). The consensus-based approach is less protective of the ecosystem than the two other approaches mentioned (Binelli et al., 2008). However, authors tend to agree that no sediment quality guideline is ideal for mangrove sediments, which differ in many ways. Further ecotoxicological studies must therefore be driven.

Table 2. Sediment quality guidelines with the threshold effect level (TEL)/probable effect level (PEL) values and effect range low (ERL)/effect range mean (ERM) values in ng g^{-1} with % incidence of effects.

	Guidelines				% incidence of effects		
	TEL	PEL	ERL	ERM	<ERL	ERL-ERM	>ERM
Naphthalene	34.6	391	160	2 100	16.0	41.0	88.9
Acenaphthene	6.71	88.9	16	500	20	32.4	84.2
Acenaphthylene	5.87	128	44	640	14.3	17.9	100
Fluorene	21.2	144	19	540	27.3	36.5	86.7
Phenanthrene	86.7	544	240	1 500	18.5	46.2	90.3
Anthracene	46.9	245	85.3	1 100	25.0	44.2	85.2
Fluoranthene	113	1 494	600	5 100	20.6	63.6	92.3
Pyrene	153	1 398	665	2 600	17.2	53.1	87.5
Benzo[a]anthracene	74.8	693	261	1 600	21.1	43.8	92.6
Chrysene	108	846	384	2 800	19.0	45.0	88.5
Benzo[a]pyrene	88.8	763	430	1 600	10.3	63.0	80.0
Dibenzo[a,h]anthracene	6.22	135	63.4	260	11.5	54.4	66.7
Sum of 16 PAHs	1 684	16 770	4 022	44 792	14.3	36.1	85.0

2.2. Polycyclic aromatic hydrocarbons concentrations in mangrove ecosystems

Regarding mangrove sediments, different levels of sediments contamination were reported worldwide. In Brazil, moderate to high contamination levels of sediment in mangrove forests near urban centers (Rio de Janeiro and Fortaleza) were measured (Cavalcante et al., 2009; Araújo et al., 2020), but the total PAHs concentrations (max 2

235 ng g^{-1}) were all under the ERL (4 022 ng g^{-1}), even near Rio de Janeiro, where an important oil spill occurred in 2000 (Tables 2 & 3). High to very high sediment contamination levels, and PAHs concentrations (2 150 – 10 400 ng g^{-1}) greater than the ERL, were measured in a mangrove forest in the Sundarbans (Balu et al., 2020), granting boating activity on the multiple rivers across the Sundarbans for these contaminations (Tables 2 & 3). The sediments of multiple mangrove stations in Hong-Kong have very high contamination levels with values (356 – 11 098 ng g^{-1}) between the ERL and ERM (44 792 ng g^{-1}) (Tables 2 & 3) (Tam et al., 2001). The most contaminated measured mangrove stations are located in one of the most polluted bay of Hong Kong and receive livestock, industrial, and urban discharges (Table 3) (Tam et al., 2001). To our knowledge, concentrations of PAHs greater than the ERM have only been measured in a highly contaminated mangrove site after the 2000 oil spill in Guanabara Bay with concentrations as high as 240 394 ng g^{-1} for the sum of the 16 priority PAHs (Farias et al., 2008). In 4 years, the total PAHs concentration in the same mangrove surface sediments has dropped by 70%, favored by oil vertical migration and weathering due to the large grain size of the sediment (Farias et al., 2008). The decay rates varied between single PAHs. In the first 4 years after the oil spill, the ratio chrysene/(naphthalene + phenanthrene) increased from 4% to 30%, showing a greater loss of naphthalene plus phenanthrene than chrysene (Farias et al., 2008). Chrysene did not follow any particular decay pattern, while naphthalene, less persistent in the environment, followed a linear decay rate (Farias et al., 2008). Other than this situation, the highest total concentrations of 16 PAHs measured in mangrove surface sediments were reported i) in the Indian part of the Sundarbans with a concentration of 12 993 ng g^{-1} (Zuloaga et al., 2013), ii) in the Niger Delta with concentrations of 16 000 (Oyo-Ita et al., 2013) and 35 270 ng g^{-1} (Essien et al., 2011), and iii) in the Guanabara Bay, Brazil with a concentration of 28 278 ng g^{-1} (Maciel-Souza et al., 2006) (Table 3). Those concentrations represent very high contamination level of sediments above the ERL (Table 2). Sources of PAHs are mix but the major one in the latest studies are the incomplete combustion of fossil fuel (car exhaust and coal combustion) in Hong Kong, agricultural and domestic waste/sewage in Nigeria, and an oil spill that occurred only 7 months prior to sample collection in Brazil (Maciel-Souza et al., 2006; Essien et al., 2011; Oyo-Ita et al., 2013; Zuloaga et al., 2013).

Table 3. Concentrations of polycyclic aromatic hydrocarbons in mangrove ecosystems.

Compartment	Location	N° of PAH	Sum of PAH (ng g^{-1})	Baumard's classification	Reference
Surface mangrove sediments	Arabian Gulf	16	4 - 533	Low to Moderate	Orif & El-Maradny, 2018
		16	64 – 1 219	Low to High	Mohebbi-Nozar et al., 2016
	Brazil	16	6 – 129	Low to Moderate	Araújo et al., 2020
		16	6 – 434	Low to Moderate	Assunção et al., 2017
		16	100 – 2 235	Moderate to High	Cavalcante et al., 2009
		16	3 – 273	Low to Moderate	Garcia & Martins, 2021
		16	1 232 – 28 278	High to Very high	Maciel-Souza et al., 2006
		16	8 - 25	Low	Souza et al., 2018
	Cameroon	16	83 – 544	Moderate	Mbusnum et al., 2020
	China	16	80 – 853	Low to Moderate	Cai et al., 2019
		16	102 – 1 019	Moderate	Huang et al., 2021
		16	108 - 213	Moderate	Huang et al., 2022
		16	170 – 350	Moderate	Kaiser et al., 2016
		16	148 – 1 123	Moderate to High	Qiu et al., 2018
		15	24 – 238	Low to Moderate	Vane et al., 2009
		16	150 – 610	Moderate	Wu et al., 2014
		16	387 - 726	Moderate	Zhang et al., 2004
	Colombia	16	27 – 565	Low to Moderate	Angulo-Cuero et al., 2021
	Guadeloupe	11	103 – 1 657	Moderate to High	Bernard et al., 1996
		16	47 – 978	Low to Moderate	Ramdine et al., 2012
	Hong Kong	16	169 – 1 058	Moderate	Guo et al., 2005
		16	56 – 3 758	Low to High	Ke et al., 2005
		15	356 – 11 098	Moderate to Very high	Tam et al., 2001
		15	666 – 1 042	Moderate	Zheng et al., 2000
	Indonesia	16	45 – 200	Low to Moderate	Dsikowitzky et al., 2011
	Malaysia	16	151 – 4 973	Moderate to High	Vaezzadeh et al., 2019
		17	20 - 112	Low to Moderate	Raza et al., 2013
	Nigeria	16	6 100 – 35 270	Very high	Essien et al., 2011
		16	1 670 – 16 000	High to Very high	Oyo-Ita et al., 2013
	Saudi Arabia	18	1 - 7	Low	Bashir et al., 2017
		13	18 - 230	Low to Moderate	El-Maradny et al., 2021
	Sundarbans	16	2 150 – 10 400	High to Very high	Balu et al., 2020
		16	241 – 1 376	Moderate to High	Sarkar, 2016
		17	222	Moderate	Zanardi-Lamardo et al., 2019
		16	122 – 534	Moderate	Zuloaga et al., 2009
		19	208 – 12 993	Moderate to Very high	Zuloaga et al., 2013
	USA	16	1 – 23	Low	Lewis and Russell, 2015
	Zanzibar	11	20 - 82	Low	Mahugija et al., 2017
Core mangrove sediments	Brazil	16	10 – 1 001	Low to Moderate	Nudi et al., 2007
	China	16	313 – 5 168	Moderate to Very high	Li et al., 2014
	Hong Kong	16	939 – 5 856	Moderate to Very high	Li et al., 2009
	Sundarbans	19	9 – 4 250	Low to High	Binelli et al., 2008
		16	132 – 2 938	Moderate to High	Domínguez et al., 2010
		19	20 – 2 204	Low to High	Sarkar et al., 2012
		16	132 – 2 938	Moderate to High	Sarkar, 2016
Leaves	Arabian Gulf	16	7 – 1 033		Orif & El-Maradny, 2018
	China	16	1 389 – 7 925		Li et al., 2014
		16	410 – 722		Qiu et al., 2018
		16	86 - 181		Wang et al., 2012
	Saudi Arabia	18	3 - 90		Bashir et al., 2017
		13	111 - 795		El-Maradny et al., 2021
Roots	Arabian Gulf	16	23 – 2 096		Orif & El-Maradny, 2018

	China	16	440 – 6 882	Li et al., 2014
		16	124 – 504	Qiu et al., 2018
		16	79 - 90	Wang et al., 2012
	Saudi Arabia	18	1 - 31	Bashir et al., 2017
		13	33 - 410	El-Maradny et al., 2021
Crabs	Brazil	16	26 – 2 290	Nudi et al., 2007
	Nigeria	15	19 - 134	Benson et al., 2022
	Zanzibar	11	2 – 29	Mahugija et al., 2017
Bivalves	Colombia	16	24 – 169	Angulo-Cuero et al., 2021
	Sundarbans	16	21 – 5 919	Zuloaga et al., 2009
Oysters	Malaysia	16	309 – 2 225	Vaezzadeh et al., 2019
Fish tissues	Zanzibar	6	0.028 – 0.037	Juma et al., 2018

Various concentrations of the 16 priority PAHs have been measured in mangrove sediments worldwide. High to very high sediment contaminations levels have been exposed in different mangrove sites, but the high concentrations are always explained by the proximity of the mangrove forests with anthropogenic activities such as urbanization and industrial effluents. Since the concentrations of PAHs in mangrove sediments do not always reflect PAHs bioavailability and toxicity, no universal quality guidelines for mangrove sediments have been offered. PAHs measurements in other compartments than sediments, such as mangrove trees and fauna, are scarce. Decrease of PAHs concentrations in sediments can also be due to the transfer of PAHs from sediments to the biota. An evaluation of PAHs concentrations in mangrove biotic matrices is essential as litter represents an important source of nutrients for species such as fishes and crustaceans, that can be consumed by the human populations.

3. Factors enhancing polycyclic aromatic hydrocarbons accumulation in mangrove sediments

3.1. Sedimentation rate and sediments texture

Mangrove ecosystems are transit and depository environments at the interface between land and sea. Mangrove forests sedimentation rate is high, mainly due to the mangrove trees root systems, varying between 0.1 and 10 mm yr^{-1}, with an average accretion of 5 mm yr^{-1} (Alongi, 2012; Woodroffe et al., 2016). The high sedimentation rate implies higher potential PAHs accumulation from the watershed. PAHs are mainly stored in soils and sediments due to their lipophilicity and their affinity with particles (Sarkar et al., 2012). PAHs concentrations are larger in the particular phase than in the dissolved phase (Cao et al., 2015). Smaller particles tend to have higher concentrations of contaminants because smaller particles imply greater surface area per volume of sorption and lower density particles (Zhao et al., 2010). In addition, clays have good fixing capacities and tend to form aggregates (Chen et al., 2009; Liu et al., 2011). Mangrove soil texture is variable between regions and depends on multiple parameters. Sandy loam, silt loam, sandy clay

loam, and clay loam have been reported for mangrove sediments in literature (Furukawa et al., 1997; Hossain and Nuruddin, 2016). Because of the low-energy water entering mangrove forests and the dense root systems of mangrove trees, clay particles easily flocculate and are trapped in the mangrove ecosystem (Furukawa et al., 1997; Hossain and Nuruddin, 2016). In most studies, no trend is observed between depth and PAHs concentration due to the heterogeneity in mangrove sediment texture within a sedimentary core (Domínguez et al., 2010; Sarkar et al., 2012; Sarkar, 2016). The size of the molecule also has an influence on PAHs distribution. High molecular weight (HMW) PAHs are less easily degraded and, being more hydrophobic than low molecular weight (LMW) PAHs, they have a greater affinity for particles (Yu et al., 2005). Consequently, HMW PAHs have a greater tendency for adsorption on particle surfaces, which is why they are less concentrated in porewaters but more concentrated in mangrove sediments (Sarkar et al., 2012; Balu et al., 2020).

3.2. Organic matter quality and quantity

Mangrove ecosystems are of the most productive ecosystem on the planet with an estimated net primary production of mangrove plants of 11.1 Mg of C ha^{-1} yr^{-1} (Alongi, 2014). In comparison, phytoplankton have a net primary production estimated at 1.7 Mg of C ha^{-1} yr^{-1} and coral reefs at 10 Mg of C ha^{-1} yr^{-1} (Alongi, 2014). About 10% of the produced OM is sequestered in the mangrove soil, while 40% is decomposed, 30% exported, and 9% consumed (Duarte and Cebrián, 1996; Breithaupt et al., 2012; Alongi, 2020). The global OM burial rate in mangrove soil is estimated at 1.35 Mg of OC ha-1 yr^{-1} (Bouillon et al., 2008). The total organic carbon (TOC) content in mangrove sediments varies between 0.5% and more than 40% of dry weight (Kristensen et al., 2008). TOC content is larger in mangrove sediments with a majority of autochthonous OM sources, low litterfall exports, and low OM mineralization rate (Bouillon and Dahdouh-Guebas, 2003; Marchand et al., 2005; Lallier-Vergès et al., 2008). In the sediment, the combination of OM and organic pollutants has been widely demonstrated (Means et al., 1980; Gustafsson et al., 1997). In the Sundarbans mangroves, OM content and grain size control petrogenic PAHs distribution (Domínguez et al., 2010). Other studies observed positive correlations between TOC and PAHs concentrations in mangrove sediments (Zhang et al., 2004; Ke et al., 2005; Liang et al., 2007; Garcia and Martins, 2021). The OM has a high adsorption ability for various organic and inorganic contaminants including PAHs (Brimo, 2017). However, studies do not always show a positive correlation between OM and PAHs concentrations in sediments (Sojinu et al., 2010; Raza et al., 2013; Cai et al., 2019; Balu et al., 2020; Mbusnum et al., 2020; Huang et al., 2021). A suggestion is that the linear relationship between OM and PAHs concentrations is observed only if the

concentrations of PAHs are >2 000 ng g^{-1} (Simpson et al., 1996). Multiple hypotheses are raised for these observations. First, if the flux of hydrocarbon is continuous, then they are not fully integrated into the OM (Sojinu et al., 2010). Some studies suggested that the relationship between OM and PAHs concentrations in the sediment depends on the nature of the OM (Johnson et al., 2001; Doick et al., 2005). For example, PAHs have a stronger affinity for humic acids than for fulvic acids (Johnson et al., 2001; Doick et al., 2005). The difference between the two fractions is OM maturity. The humic fraction is more mature with a lignin percentage higher than the fulvic fraction, whereas neutral sugars are in higher concentrations in the fulvic fraction. Lignin is a robust co-polymer integrated in the secondary cell walls of vascular plants and offers structural support as well as limited water loss from roots (Thakur et al., 2014). Lignin has various active sites to trap PAHs via absorption, adsorption, and sequestration (Thakur et al., 2014). In mangrove sediments, lignin-derived carbon mainly comes from mangrove trees litter (Kristensen et al., 2008). The carbon content derived from lignin is actually higher in mangrove sediments than in mangrove plants (Marchand et al., 2005) as lignin is a rather refractory compound in anoxic conditions, with a half-life estimated at 150 years in mangrove sediments (Dittmar et al., 2001). Mangrove detritus in sediments become enriched in lignin with time because lignin lost is slower than bulk OC and neutral sugars (Marchand et al., 2005; Lallier-Vergès et al., 2008). A positive correlation between PAH hydrophobicity and lignin sorption has been shown in literature (Zhang et al., 2014). The two main mechanisms involved in PAH sorption on lignin are i) pi-pi electron-donor-acceptor interactions between the electron donor aromatic rings of the PAH and the electron acceptor aromatic rings of lignin, and ii) partitioning of PAH on the amorphous sites of lignin (Zhang et al., 2014). The sorption of PAH to lignin is a spontaneous reaction (Zhang et al., 2014). Other authors showed that black carbon, considered as a super-sorbent, can be a better parameter of correlation with PAHs distribution than TOC in mangrove sediments (Nam et al., 2008; Luz et al., 2010; Sánchez-García et al., 2010; Huang et al., 2021).

3.3. Soil anoxia and canopy density

Once deposited in mangrove sediments, PAHs are less subject to degradation. On the one hand, PAHs are less exposed to photodegradation (Brimo, 2017) because mangrove forests' canopy is dense, and mangrove leaves have chemical compounds for UV-protection, limiting UV rays penetration under the canopy (Kathiresan and Bingham, 2001). On the other hand, PAHs are less subject to oxidation (Brimo, 2017), especially in anoxic zones. Due to waterlogging, sediment OM richness, and rapid use of O_2 for OM mineralization in the surface layer, O_2 can rarely penetrate below the surface resulting in suboxic or anoxic mangrove sediments in the sub-surface and deep layers (Kristensen et

al., 2008). In mangrove sediments, sulphate-reduction in anoxic conditions is the dominant OM mineralization pathway, accounting for about 50% of C oxidation (Kristensen et al., 2017). In Fe rich sediments, Fe respiration can also be a main anaerobic pathway, similar to sulphate-reduction (Kristensen et al., 2017).

PAHs accumulation in mangrove sediments is driven by multiple factors including sedimentation rate, sediments texture, and OM. Their concentrations can decrease over time or within an area via degradation or via export outside the mangrove forest after remobilization.

4. Factors reducing polycyclic aromatic hydrocarbons concentrations in mangrove sediments

4.1. Export towards adjacent ecosystems and vertical migration

PAHs concentrations in mangrove sediments can decrease over time through multiple processes. PAHs in porewater, or adsorbed onto particulate OM, can also migrate down the sedimentary core or be exported to adjacent ecosystems (Cao et al., 2015). Vertical and horizontal migrations depend on i) tidal flushing, which is more or less important daily depending on the horizontal location in the forest, ii) seasons, which affect rainwater inputs in the mangrove forest and evapotranspiration of the soil, limiting the exchange of dissolved PAHs in the dry season, and iii) porewater percolation and seepage, enhanced by crabs holes and anchor roots holes, which can contribute significantly to water circulation from the mangrove floor to the nearshore (Marchand et al., 2004; Stieglitz et al., 2013). Crab bioturbation has a mechanistic effect on PAHs desorption from sediments, increasing PAHs concentrations in the dissolved phase, more subject to export (Qin et al., 2010). Higher PAHs concentrations in porewater were measured in sites with higher tidal ranges compared to sites with low tidal ranges as the stronger tidal movement favors PAHs dispersion and transfer (Cai et al., 2019; Garcia and Martins, 2021). A higher depositional rate of contaminated sediments increases PAHs accumulation, while a greater resuspension of sediments through stronger wave or tide actions enhances PAHs degradation, uptake, or export (Boonyatumanond et al., 2006). Mangrove sediments closer to the shoreline are more subject to daily tidal flushing, and therefore export of PAHs, than on the landside of the mangrove forest. Some mangrove sites have an input of freshwater from a riverine branch increasing the hydrodynamic energy near the branch. A suggestion is that, for the surface sediments, the hydrodynamic condition of the mangrove forest is the main parameter regulating PAHs distribution (Domínguez et al., 2010).

4.2. Abiotic degradation

Abiotic processes are photochemical degradation, vertical migration, and tidal action (Farias et al., 2008). Even though PAHs are less exposed to photodegradation once deposited in mangrove sediments, the process can occur when the UV rays from the sunlight pass through the canopy, and takes place only in the sediment surface layer due to the limited light penetration capacity in mangrove sediments (Marquès et al., 2016). The photodegradation varies depending on many parameters such as sediments texture and temperature, and PAHs light absorption spectrum of individual PAH (Zhang et al., 2010). Oxidation of PAHs in mangrove sediments also occurs mainly at the surface, where O_2 is available. At a micro-scale, oxic conditions, and therefore PAHs oxidation, can occur below the surface level due to crab burrows or some root systems, which allow for O_2 to travel down the sedimentary core (Kristensen et al., 2008, 2017).

4.3. Microbial PAH-biodegradation

Microbial degradation is the main process degrading PAHs in mangrove sediments (Farias et al., 2008). The biodegradation of PAHs by microorganisms is limited by two factors, the toxic effects of PAHs on the microorganism and the low water solubility of PAHs (Semboung Lang, 2017). For example, the mangrove fungi *Aspergillus sydowii* showed efficient PAH-degradation characteristics but at low concentrations only (Bankole et al., 2020). At high PAHs concentrations, toxicity of PAHs inhibits enzymes induction and fungi proliferation. PAHs biodegradation has been granted to diverse bacteria, fungi, and archaea. Common microbial taxa associated with PAHs degradation in mangrove sediments are the bacteria *Mycobacterium*, *Pseudomonas*, *Bacillus*, *Rhodococcus*, *Sphingomonas*, *Paracoccus*, *Acinetobacter*, the archaea *Halobacteriaceae*, and the fungi *Fusarium solani*, and *Aspergillus* (Guo et al., 2005; Yu et al., 2005; Bhattacharyya et al., 2015; Cabral et al., 2018; Ahmad et al., 2019; Jia et al., 2020; de Almeida et al., 2021). Some strains are mono-degrading microorganisms, they are only able to degrade one PAH, and others are multi-degrading microorganisms, capable of degrading multiple PAHs in mangrove sediments. Mono-degrading strains are more common than multi-degrading strains (Liu et al., 2010; HuiJie et al., 2011). Multiple studies showed that PAHs polluted mangrove forests have higher microorganisms species richness in their sediments (Guo et al., 2011; Ghizelini et al., 2019), and that the microbial community evolves with the contamination within a same area (de Almeida et al., 2021). It seems that gram-negative bacteria are more involved in PAHs degradation in mangrove sediments, and nitrogen-fixing bacteria growth is restricted in PAHs contaminated sites (Ahmad et al., 2019). Since the degradation rates of PAHs depend on the microbial community and the number of

PAH-degrading microorganisms, sites that have had PAHs contamination in the past, such as oil spills, are more subject to high degradation rates because the microbial community has been acclimatized (Bauer and Capone, 1988; Guo et al., 2005). Some microorganisms involved in PAH-degradation have specific degrading genes such as the bacteria *Mycobacterium*, while other microorganisms (e.g., *Bacillus* spp.) favor PAH degradation via PAH mobility, or production of important intermediates, which is the case for the bacteria *Novosphingobium pentaromativorans* (Wanapaisan et al., 2018). Some microorganisms use hydrocarbons as a source of carbon to induce enzymes for the degradation of other hydrocarbons. It is the case of the bacteria *Sphingomonas paucimobilis*, which metabolizes 4, 5, and 6-rings PAHs via ring cleavage, with the use of fluoranthene as a carbon source (Ye et al., 1996). *Mycobacterium* spp. also have pyrene-induced enzymes capable of metabolizing other PAHs (Heitkamp et al., 1988). PAHs degradation is therefore a synergistic process including multiple microorganisms.

Microbial communities in mangrove sediments seem controlled by abiotic variables such as the season, physico-chemical parameters, the texture of the sediment, and the percentage of OM (Kathiresan and Bingham, 2001; Sahoo and Dhal, 2009; Colares and Melo, 2013; D'Souza, 2016; Ben Ayed et al., 2021). Mangrove sediments temperature varies between 25 and 35 °C, which is usually ideal for microbial development (Semboung Lang, 2017). pH values of mangrove sediments vary between sites and depend mainly on water inputs, OM decomposition, and sulfide oxidation (Kristensen et al., 2017). Mangrove trees can grow on sediments with pH ranging from ~5 to 8, with the optimum pH between 6.7 and 7.3 (Kathiresan and Bingham, 2001). The most efficient conditions for PAHs degradation in mangrove sediments by microorganisms are neutral pH and 27 °C (Song et al., 1990; Baker, 1994). The anoxic and sulfidic conditions of most mangrove sediments do not limit microbial growth since anaerobic bacteria and fungi are able to proliferate in the absence of oxygen (Li et al., 2009; Arfi et al., 2012a).

In a microcosm study, bacterial degradation of phenanthrene was higher during the wet season of a tropical region, probably due to a higher input of nutrients and a diversification in the PAH-degrading bacteria community (Tiralerdpanich et al., 2021). Other studies showed the higher diversity in microorganisms in mangrove sediments during the wet season due to lower soil salinity and higher soil temperature, which favors microbial development (Basak et al., 2016; Ben Ayed et al., 2021). Salinity is another important factor influencing PAHs biodegradation. A positive relationship between salinity and total PAHs concentrations in mangrove sediments was observed as salinity can decrease microbial activity, and therefore microbial PAHs degradation, resulting in higher PAHs concentrations (Raza et al., 2013). Multiple authors even suggest that salinity is the

main factor influencing PAHs biodegradation processes (Chen et al., 2008; Tam and Yao, 2002). In mangrove ecosystems, salinity varies with topography, season, climate, hydrology, tidal flooding, and specificities of the mangrove forest such as freshwater inputs (Kathiresan and Bingham, 2001; Kristensen et al., 2017). Soil salinity is one of the main drivers of mangrove species distribution (Kathiresan and Bingham, 2001). Some species such as *Rhizophora apiculata* grows better at low salinity values, lower than 20 g L^{-1}, while others like *Avicennia marina* tolerates salinities up to 92 g L^{-1} (Kathiresan and Bingham, 2001). Salinity is greater at higher elevation due to less daily immersion by the tides, resulting in more evapotranspiration (Marchand et al., 2004, 2011). During dry seasons, salinity increases also due to more evapotranspiration and less rainwater dilution (Marchand et al., 2004). With the percolation process, salinity tends to increase with depth along the sedimentary profile (Marchand et al., 2004). Other contaminants, such as trace metals, can also limit PAHs biodegradation in mangrove sediments. It has been shown that Mn(II) inhibits PAHs-biodegradation in anaerobic conditions because of its toxicity on PAH-degrading bacteria (Li et al., 2011). Toxicity of Mn(II) on microorganisms is attributed to adverse effects on PC12 cells and dehydrogenase activity (Reaney and Smith, 2005). In mangrove forests, anaerobic conditions are obtained in sub-surface and deep sediments layers as the O_2 is rapidly consumed for OM mineralization in upper layers (Kristensen et al., 2008). Trace metals such as Mn are immobilized in mangrove sediments because of high sedimentation rate, OM richness, and biogeochemical reactivity (Harbison, 1986). High trace metal concentrations in mangrove sediments have been widely reported in literature (Lewis et al., 2011; Bayen, 2012; Marchand et al., 2012; Yan et al., 2017; Kulkarni et al., 2018; Robin et al., 2021).

5. Polycyclic aromatic hydrocarbons transfer to mangrove tissues and their effects on mangrove trees

5.1. Transfer of polycyclic aromatic hydrocarbons to mangrove tissues

PAHs can be accumulated in the roots and leaves of mangrove trees (Li et al., 2014; Bashir et al., 2017; Orif and El-Maradny, 2018). Higher PAHs concentrations in the leaves of mangrove trees were measured compared to in their roots and the mangrove sediments in multiple sites (Li et al., 2014; Bashir et al., 2017; El-Maradny et al., 2021). Leaf BCF up to 5.41 and 5.57 for phenanthrene and anthracene, respectively, were registered for the species *Avicennia marina* (Bashir et al., 2017), while in a mangrove forest of the Red Sea, total PAHs concentrations in *A. marina* of 795 ng g-1 in leaves were measured, for 409 ng g^{-1} in roots and 230 ng g^{-1} in sediments (El-Maradny et al., 2021). However, in laboratory settings and in situ experiments, transfer of PAHs from roots to shoots seemed limited (Lu et al., 2011; Orif and El-Maradny, 2018; Jia et al., 2016b). The

transfer of PAHs from sediments to roots occurs via adsorption and absorption at the root system level (Wang et al., 2010). The sorption of PAHs to roots is regulated mainly by lipids, but also by carbohydrates (Zhang and Zhu, 2009). Roots exudates such as citric acid, oxalic acid, and malic acid enhance PAHs mobility and bioavailability in the sediment increasing their uptake by the plants (Jia et al., 2016b). However, roots exudates also promote microorganisms growth in the rhizosphere, which contributes to PAHs degradation (Lu et al., 2011; Verâne et al., 2020; Jia et al., 2016b). In the roots, the polarity of the epidermal tissue, different for each mangrove species, appears to influence PAHs sorption as well (Li et al., 2017). The microbial community associated to mangrove roots differs between species, which can therefore impact PAHs sorption within the root system (Arfi et al., 2012b).

Uptake of PAHs in the leaves occurs via roots transfer through the vascular bundle, or absorption and adsorption through the atmosphere (Wang et al., 2010). The stomata on mangrove leaves are usually covered with a hydrophilic waxy layer enhancing atmospheric PAHs sorption (Wang et al., 2008; Orif and El-Maradny, 2018). The distribution of PAHs in mangrove leaves varies between species and within the leaf. Under foliar PAHs stress, the mangrove species Avicennia marina has shown irregular stomatal behavior, which can result from out-venting of excessive LMW PAHs (Youssef, 2002). An uneven distribution of B[a]P on mangrove leaves was observed with a negative correlation between the polarity of the leaf cuticle and the amount of B[a]P retained (Guo et al., 2021). It seems that B[a]P is more concentrated on the salt glands' edge of the leaf due to its high wax concentrations, for the mangrove species *Avicennia marina* and *Aegiceras corniculatum* (Guo et al., 2021).

Mangrove trees have different mechanisms that can be used to prevent diffusion of PAHs in the tissues up to the foliage (Wang et al., 2012; Tansel et al., 2013; Naidoo and Naidoo, 2017; Guo et al., 2021). Some mangrove species such as *Avicennia* spp. have an iron plaque at the surface of their roots. The iron plaque results from the oxidation of free Fe^{2+} in the rhizosphere to Fe^{3+} when O_2 is available (Taylor and Crowder, 1983). The *Avicennia* spp. diffuse O_2 in the rhizosphere, and therefore an FeOOH plaque forms at the surface of their roots and pneumatophores (Taylor and Crowder, 1983). Multiple authors showed the ability of the iron plaque to immobilize inorganic pollutants such as trace metals, and therefore limit metal stress for mangrove plants and other species (Otte et al., 1989; Batty, 2000; Machado et al., 2005; Liu and Li, 2008; Pi et al., 2010; Hu et al., 2014; Robin et al., 2021). The role of the iron plaque against organic pollutants (PAHs and PBDEs) on two mangrove species has been studied (Pi et al., 2017). The microcosm study showed that the plaque is able to immobilize up to 20% of total PAHs while only 0.1% of

total PAHs were measured in the mangrove tissues (Pi et al., 2017). The percentage of immobilization of PAHs in the iron plaque was dependent of tidal flushing, with more immobilization observed when longer and more frequent flooding was applied (Pi et al., 2017). An explanation is that a more frequent tidal flushing regime leads to more anaerobic sediments condition (Pi et al., 2009), which enhances PAHs accumulation (Juhasz and Naidu, 2000). This study also showed a positive correlation between iron plaque formation and PAHs trapping (Pi et al., 2017).

Petrogenic PAHs, characterized by LMW PAHs, are more bioavailable to organisms than the pyrolytic ones dominated by HMW PAHs. In the marine environment, pyrolytic PAHs are rather associated to particles, whereas petrogenic PAHs are introduced as less associated to suspended particles, or even as dissolved (Zuloaga et al., 2013). Therefore, higher bioconcentration factors (concentration in a tissue divided by concentration in sediments) for LMW PAHs are observed in mangrove ecosystems (Wang et al., 2012; Li et al., 2014). Older PAHs, that have been in the sediment for a longer time, show lower bioavailability to plants and microorganisms (Liu et al., 2011; Jia et al., 2016a).

5.2. Toxicity of polycyclic aromatic hydrocarbons on mangrove trees

Oil pollution affects mangrove trees by inhibiting growth, reducing photosynthesis, inducing leaf necrosis, and to a point, death (Suprayogi and Murray, 1999; Naidoo, 2016). PAHs penetrate the tissues through slow diffusion from the root surface via plasmodesmata (Orcutt and Nilsen, 2000; Alkio et al., 2005). Once in the tissues, PAHs being hydrophobic will bound to the lipid fractions of the organelles and the cell membranes (Zaalishvili et al., 2002). PAHs cause damages to the cell membrane by increasing the permeability of lipidic molecules. These organic pollutants also disrupt and fragment cell components such as chloroplasts, mitochondria, and nuclei, which can cause cell's death (Zaalishvili et al., 2002). By damaging the cell membrane, PAHs alter the regulation of the trans membrane electrical potential, which regulates metal uptake and bioavailability (Gauthier et al., 2014). PAHs seem to also inhibit metallothioneins, which play a key role in the detoxification of metals (Gauthier et al., 2014; Kumar et al., 2021). PAHs contamination in mangrove sediments can also favor negative genetic mutations in mangrove trees (Klekowski et al., 1994). Phenols and polyphenols in mangrove roots can potentially limit PAHs toxicity via adsorption of PAHs (phenols) and antioxidant activity (polyphenols) (Zhang et al., 2014; Wang et al., 2014a, 2014b).

PAHs contamination of mangrove sediments can result in a toxic uptake by the mangrove trees, affecting their vital processes. The uptake of organic contaminants such as PAHs is species dependent. Each mangrove species has different roots and leaves

compositions, such as wax content and epidermal polarity, which more or less inhibit PAHs uptake (Misra et al., 1984; Dodd et al., 1995; Purnobasuki et al., 2017). Some species also developed mechanisms that limit PAHs toxicity such as the formation of iron plaque able to immobilize PAHs and prevent PAHs uptake in the tissues. Other than mangrove trees, the studies of PAHs contaminations of mangrove fauna are scarce. Few papers address the potential of mangrove fauna as PAHs bioindicators for mangrove sediments contamination (Nudi et al., 2007; Mahugija et al., 2017; Juma et al., 2018; Vaezzadeh et al., 2019).

6. Bioindicators of polycyclic aromatic hydrocarbons contamination in mangrove sediments

Mangrove forests are the habitat of numerous species of fish and crustaceans that are directly or indirectly in contact with the PAHs present in the ecosystem, and that are consumed by human populations. The fauna can be exposed to PAHs via direct exposure in sediments or water, or via ingestion of contaminated bivalves, litterfall, and other OM (Zuloaga et al., 2009). Multiple studies have looked at potential species for the role of bioindicators of PAHs contamination in mangrove ecosystem (Nudi et al., 2007; Mahugija et al., 2017; Juma et al., 2018; Vaezzadeh et al., 2019). In order to be a good bioindicator, the chosen species must fulfill many requirements: i) as a clear taxonomy, ii) is spread over a wide geographical area, iii) represents the response of other species to the pressure, iv) has enough individuals to be collected, and v) can be rather easily collected. PAHs being hydrophilic, their bioaccumulation in different tissues depends on the lipid content of the tissue and on the PAH octanol-water partition coefficient (Kow) (Nudi et al., 2007; Vaezzadeh et al., 2019). Depending on the species habitat and feeding strategy, PAHs will not be assimilated similarly. The mangrove oyster *Crassostrea belcheri* fulfills most of the requirements to be a suitable bioindicator, but as a filter-feeder, it assimilates most of the PAHs from the water and not from the sediment (Vaezzadeh et al., 2019). Similarly, no correlation between PAHs concentrations in the sediment and in crabs (with the exact species not being reported) were obtained by other authors (Mahugija et al., 2017). They explain the lack of correlation by the fact that crabs feed from other resources than mangrove sediments, such as litterfall and organic matter in water (Mahugija et al., 2017). The crab *Ucides cordatus* is suggested to be an appropriate bioindicator because the total PAHs concentrations measured in the crab's hepatopancreas are strongly correlated to the concentrations in the sediment surface layer, plus, they have been found alive in highly contaminated sites (Nudi et al., 2007). However, results show that the petrogenic PAHs predominate in the crab's hepatopancreas, which is not the case in sediments, suggesting that care must be taken if choosing this species as a bioindicator.

Fishes are already used in the marine environment as bioindicators of PAHs contamination (Juma et al., 2018). The International Council of the Exploration of the Sea suggests to use the bile of the fish as the analyzing organ for PAHs assimilation because it is where they are concentrated before excretion (Juma et al., 2018). The biomarker potential of the Gobi fish *Periophtalmus sobrinus*, which buries in mangrove sediments and feeds on organisms in the sediment, was also studied (Juma et al., 2018). The study concluded on the good potential of the Gobi fish bile as a PAHs bioindicator, but they have looked at 3-4 rings PAHs only and have not looked at the correlation with sediment PAHs concentrations (Juma et al., 2018). Another study exposed the bioaccumulation of HMW carcinogenic PAHs such as benzo(a)phenanthrene, benzo(k)fluoranthene, and benzo(a)anthracene in the visceral mass of the bivalve *Sanguinolaria acuminata* (Zuloaga et al., 2009). In mangrove sediments, where the bivalve was collected, the LMW PAHs were predominant. The bivalve can be a suitable bioindicator of PAHs contamination but cannot be used alone as it does not reflect PAHs distribution and bioavailability in the sediment.

7. Perspectives and future research directions

The understanding of organic pollutants dynamics, such as PAHs, in coastal sediments has been reinforced this last decade, as organic pollutants became an environmental and health concern, especially in urban and industrial areas. Many research focused on remediation processes in different environmental compartments. The alarming urbanization rate of tropical coastlines is a real threat to mangrove forests and can largely participate in PAHs inputs in these key ecosystems. The daily fluctuation of physico-chemical parameters with tides, the heterogeneity of the sediment, and the biogeochemical reactivity, render very difficult to figure out and predict PAHs distribution in mangrove sediments and porewaters, which are dynamic compartments. To better understand the factors influencing PAHs dynamic in mangrove ecosystems, especially near anthropogenic areas, more research must be focused on:

- The correlation between PAHs sequestration in sediments and the nature and structure of OM. Positive and negative correlations between PAHs and specific components of OM such as lignin-derived phenols or neutral sugars may be sought. This will help forecast the zones in which PAHs accumulation could be favored.

- The influence of other organic contaminants on the accumulation or degradation of PAHs in mangrove forests. Other organic contaminants may induce competition for microbial degradation decreasing PAHs accumulation but may also induce competition for

sorption on lignin or clay, decreasing PAHs sequestration. Information on the most dangerous cocktails of contaminants could be collected.

- The influence of inorganic contaminants on the accumulation or degradation of PAHs in mangrove forests. Mn(II) may not be the only toxic element for PAH-degrading bacteria and further correlations must be pursued. Other elements, which may be used to induce microbial growth in order to decrease PAHs degradation could actually inhibit degradation.

- The hydrological modelling of mangrove sites and the transport of PAHs outside the mangrove forest via tidal flushing and/or porewater seepage. If enough data are gathered, modelling on the transport of PAHs in the adjacent ecosystems could be obtained if the hydrological context of the site is given.

- The establishment of a specific sediment quality guideline for intertidal ecosystems such as mangrove forests, considering the bioavailability and export probabilities of the PAHs. Multiple guidelines could be offered depending on the region, the hydrodynamics context, or plant biodiversity. This will help scientists and collectivities to get comparable results.

- The uptake of PAHs by mangrove trees, fauna, and adjacent ecosystems' biota. Better knowledge must be obtained on more biotic compartments as mangrove crustaceans and fish represent a large source of proteins for many communities. A larger database can be useful for policy decisions, such as areas to protect or limitations in contaminants release. Massive data collection can also help making comparisons in PAHs concentrations in space and in time.

- A proper (or multiple) bioindicator of PAHs contamination. Mangrove species specificities should also be considered and examined in the uptake, transfer, and excretion of PAHs from their organs. A proper bioindicator is necessary to allow universal and rapid identification of PAHs contaminated sites.

- The impact of PAHs on vital biotic components such as metallothioneins via UPLC-MS. The effect of PAHs contamination on metallothioneins in mangrove trees has not yet been proven. This knowledge would help better understand the level of toxicity of PAHs on mangrove trees.

References

Abdel-Shafy, H. I., and Mansour, M. S. M. (2016). A review on polycyclic aromatic hydrocarbons: Source, environmental impact, effect on human health and remediation. Egypt. J. Pet. 25, 107–123. doi: 10.1016/j.ejpe.2015.03.011.

Ahmad, M., Yang, Q., Zhang, Y., Ling, J., Sajjad, W., Qi, S., et al. (2019). The distinct response of phenanthrene enriched bacterial consortia to different PAHs and their degradation potential: a mangrove sediment microcosm study. J. Hazard. Mater. 380, 120863. doi: 10.1016/j.jhazmat.2019.120863.

Alegbeleye, O. O., Opeolu, B. O., and Jackson, V. A. (2017). Polycyclic aromatic hydrocarbons: A critical review of environmental occurrence and bioremediation. J. Environ. Manage. 60, 758–783. doi: 10.1007/s00267-017-0896-2.

Alkio, M., Tabuchi, T. M., Wang, X., and Colón-Carmona, A. (2005). Stress responses to polycyclic aromatic hydrocarbons in Arabidopsis include growth inhibition and hypersensitive response-like symptoms. J. Exp. Bot. 56, 2983–2994. doi: 10.1093/jxb/eri295.

Alongi, D. M. (2002). Present state and future of the world's mangrove forests. Environ. Conserv. 29, 331–349. doi: 10.1017/S0376892902000231.

Alongi, D. M. (2012). Carbon sequestration in mangrove forests. Carbon Manage. 3, 313–322. doi: 10.4155/cmt.12.20.

Alongi, D. M. (2014). Carbon cycling and storage in mangrove forests. Ann. Rev. Mar. Sci. 6, 195–219. doi: 10.1146/annurev-marine-010213-135020.

Alongi, D. M. (2020). Global significance of mangrove blue carbon in climate change mitigation. Sci 2, 67. doi: 10.3390/sci2030067.

Angulo-Cuero, J., Grassi, M. T., Dolatto, R. G., Palacio-Cortés, A. M., Rosero-Moreano, M., and Aristizábal, B. H. (2021). Impact of polycyclic aromatic hydrocarbons in mangroves from the Colombian pacific coast: Evaluation in sediments and bivalves. Mar. Pollut. Bull. 172, 112828. doi: 10.1016/j.marpolbul.2021.112828.

Araújo, M. P., Hamacher, C., de Oliveira Farias, C., Martinho, P., de Oliveira Chaves, F., and Gomes Soares, M. L. (2020). Assessment of brazilian mangroves hydrocarbon contamination from a latitudinal perspective. Mar. Pollut. Bull. 150, 110673. doi: 10.1016/j.marpolbul.2019.110673.

Arfi, Y., Buée, M., Marchand, C., Levasseur, A., and Record, E. (2012b). Multiple markers pyrosequencing reveals highly diverse and host-specific fungal communities on the mangrove trees Avicennia marina and Rhizophora stylosa. Microb. Ecol. 79, 433–444. doi: 10.1111/j.1574-6941.2011.01236.x.

Arfi, Y., Marchand, C., Wartel, M., and Record, E. (2012a). Fungal diversity in anoxic-sulfidic sediments in a mangrove soil. Fungal Ecol. 5, 282–285. doi: 10.1016/j.funeco.2011.09.004.

Assunção, M. A., Frena, M., Santos, A. P. S., and dos Santos Madureira, L. A. (2017). Aliphatic and polycyclic aromatic hydrocarbons in surface sediments collected from mangroves with different levels of urbanization in southern Brazil. Mar. Pollut. Bull. 119, 439–445. doi: 10.1016/j.marpolbul.2017.03.071.

Baek, S. O., Field, R. A., Goldstone, M. E., Kirk, P. W., Lester, J. N., and Perry, R. (1991). A review of atmospheric polycyclic aromatic hydrocarbons: Sources, fate and behavior. Water Air Soil Pollut. 60, 279–300. doi: 10.1007/BF00282628.

Baker, K. H. (1994). “Bioremediation of surface and subsurface soils,” in Bioremediation (New York (USA): McGraw-Hill, Inc.), 203–259.

Balu, S., Bhunia, S., Gachhui, R., and Mukherjee, J. (2020). Assessment of polycyclic aromatic hydrocarbon contamination in the Sundarbans, the world’s largest tidal mangrove forest and indigenous microbial mixed biofilm-based removal of the contaminants. Environ. Pollut. 266, 115270. doi: 10.1016/j.envpol.2020.115270.

Bankole, P. O., Semple, K. T., Jeon, B.-H., and Govindwar, S. P. (2020). Enhanced enzymatic removal of anthracene by the mangrove soil-derived fungus, Aspergillus sydowii BPOI. Front. Environ. Sci. Eng. 14, 113. doi: 10.1007/s11783-020-1292-3.

Basak, P., Pramanik, A., Sengupta, S., Nag, S., Bhattacharyya, A., Roy, D., et al. (2016). Bacterial diversity assessment of pristine mangrove microbial community from Dhulibhashani, Sundarbans using 16S rRNA gene tag sequencing. Genom. Data 7, 76–78. doi: 10.1016/j.gdata.2015.11.030.

Bashir, M. E.-A., El-Maradny, A., and El-Sherbiny, M. (2017). Bio-concentration of Polycyclic Aromatic Hydrocarbons in the grey Mangrove (Avicennia marina) along eastern coast of the Red Sea. Open Chem. 15, 344–351. doi: 10.1515/chem-2017-0038.

Batty, L. (2000). The effect of pH and plaque on the uptake of Cu and Mn in Phragmites australis(Cav.) Trin ex. Steudel. Ann. Bot. 86, 647–653. doi: 10.1006/anbo.2000.1191.

Bauer, J. E., and Capone, D. G. (1988). Effects of co-occuring aromatic hydrocarbons on degradation of individual polycyclic aromatic hydrocarbons in marine sediment slurries. Appl. Environ. Microbiol. 54, 1649–1655. doi: 10.1128/aem.54.7.1649-1655.1988.

Baumard, P., Budzinski, H., and Garrigues, P. (1998b). PAHs in Arcachon Bay, France: Origin and biomonitoring with caged organisms. Mar. Pollut. Bull. 36, 577–586. doi: 10.1016/S0025-326X(98)00014-9.

Baumard, P., Budzinski, H., Michon, Q., Garrigues, P., Burgeot, T., and Bellocq, J. (1998a). Origin and bioavailability of PAHs in the Mediterranean Sea from mussel and sediment records. Estuar. Coast. Shelf Sci. 47, 77–90. doi: 10.1006/ecss.1998.0337.

Bayen, S. (2012). Occurrence, bioavailability and toxic effects of trace metals and organic contaminants in mangrove ecosystems: A review. Environ. Int. 48, 84–101. doi: 10.1016/j.envint.2012.07.008.

Ben Ayed, A., Saint-Genis, G., Vallon, L., Linde, D., Turbé-Doan, A., Haon, M., et al. (2021). Exploring the diversity of fungal DyPs in mangrove soils to produce and characterize novel biocatalysts. J. Fungi 7, 321. doi: 10.3390/jof7050321.

Benamar, A., Tian, Y., Portet-Koltalo, F., Ammami, M. T., Giusti-Petrucciani, N., Song, Y., et al. (2019). Enhanced electrokinetic remediation of multi-contaminated dredged sediments and induced effect on their toxicity. Chemosphere 228, 744–755. doi: 10.1016/j.chemosphere.2019.04.063.

Benson, T. A., Hart, A. I., and Daniel, U. I. (2022). Polycyclic aromatic hydrocarbons (PAHs) profile in the tissues of mangrove crab in Idema Creek Basin, Bayelsa state Nigeria. Int. J. Contemp. Res. Rev. 13, 20221–20230.

Bernard, D., Pascaline, H., and Jeremie, J.-J. (1996). Distribution and origin of hydrocarbons in sediments from lagoons with fringing mangrove communities. Mar. Pollut. Bull. 32, 734–739. doi: 10.1016/0025-326X(96)00034-3.

Bhattacharyya, A., Majumder, N. S., Basak, P., Mukherji, S., Roy, D., Nag, S., et al. (2015). Diversity and distribution of Archaea in the mangrove sediment of Sundarbans. Archaea 2015, 1–14. doi: 10.1155/2015/968582.

Bianco, F., Race, M., Papirio, S., Oleszczuk, P., and Esposito, G. (2021). The addition of biochar as a sustainable strategy for the remediation of PAH–contaminated sediments. Chemosphere 263, 128274. doi: 10.1016/j.chemosphere.2020.128274.

Binelli, A., Sarkar, S. K., Chatterjee, M., Riva, C., Parolini, M., Bhattacharya, B. deb, et al. (2008). A comparison of sediment quality guidelines for toxicity assessment in the Sunderban wetlands (Bay of Bengal, India). Chemosphere 73, 1129–1137. doi: 10.1016/j.chemosphere.2008.07.019.

Boonyatumanond, R., Wattayakorn, G., Togo, A., and Takada, H. (2006). Distribution and origins of polycyclic aromatic hydrocarbons (PAHs) in riverine, estuarine, and marine sediments in Thailand. Mar. Pollut. Bull. 52, 942–956. doi: 10.1016/j.marpolbul.2005.12.015.

Bouillon, S., Connolly, R. M., and Lee, S. Y. (2008). Organic matter exchange and cycling in mangrove ecosystems: Recent insights from stable isotope studies. J. Sea Res. 59, 44–58. doi: 10.1016/j.seares.2007.05.001.

Bouillon, S., and Dahdouh-Guebas, F. (2003). Sources of organic carbon in mangrove sediments: variability and possible ecological implications. Hydrobiologia 495, 33–39. doi: 10.1023/A:1025411506526.

Breithaupt, J. L., Smoak, J. M., Smith, T. J., Sanders, C. J., and Hoare, A. (2012). Organic carbon burial rates in mangrove sediments: Strengthening the global budget. Global Biogeochem. Cycles 26, 2012GB004375. doi: 10.1029/2012GB004375.

Brimo, K. (2017). Modélisation de la dynamique des hydrocarbures aromatiques polycycliques (HAP) dans des sols soumis à un gradient de contamination allant d'un contexte agricole à un contexte industriel. 222.

Buchman, M. F. (1999). NOAA Screening Quick Reference Tables. Seattle WA: Coastal Protection and Restoration Division, National Oceanic and Atmospheric Administration.

Cabral, L., Pereira de Sousa, S. T., Júnior, G. V. L., Hawley, E., Andreote, F. D., Hess, M., et al. (2018). Microbial functional responses to long-term anthropogenic impact in mangrove soils. Ecotoxicol. Environ. Saf. 160, 231–239. doi: 10.1016/j.ecoenv.2018.04.050.

Cai, Y., Wu, J., Zhang, Y., Lin, Z., and Peng, Y. (2019). Polycyclic aromatic hydrocarbons in surface sediments of mangrove wetlands in Shantou, South China. J. Geochem. Expl. 205, 106332. doi: 10.1016/j.gexplo.2019.106332.

Cao, Q. min, Wang, H., Qin, J. qiao, Chen, G. zhu, and Zhang, Y. bei (2015). Partitioning of PAHs in pore water from mangrove wetlands in Shantou, China. Ecotoxicol. Environ. Saf. 111, 42–47. doi: 10.1016/j.ecoenv.2014.09.023.

Cavalcante, R. M., Sousa, F. W., Nascimento, R. F., Silveira, E. R., and Freire, G. S. S. (2009). The impact of urbanization on tropical mangroves (Fortaleza, Brazil): Evidence from PAH distribution in sediments. J. Environ. Manage. 91, 328–335. doi: 10.1016/j.jenvman.2009.08.020.

Center for International Earth Science Information Network (2012). Population, landscape, and climate estimates (PLACE), v3 (1990, 2000, 2010). NASA Socioeconomic Data and Applications Center. Available at: https://sedac.ciesin.columbia.edu/data/set/nagdc-population-landscape-climate-estimates-v3 [Accessed April 18, 2022].

Chen, J. L., Wong, Y. S., and Tam, N. F. Y. (2009). Static and dynamic sorption of phenanthrene in mangrove sediment slurry. J. Hazard. Mater. 168, 1422–1429. doi: 10.1016/j.jhazmat.2009.03.043.

Chen, J., Wong, M. H., Wong, Y. S., and Tam, N. F. Y. (2008). Multi-factors on biodegradation kinetics of polycyclic aromatic hydrocarbons (PAHs) by Sphingomonas sp. a bacterial strain isolated from mangrove sediment. Mar. Pollut. Bull. 57, 695–702. doi: 10.1016/j.marpolbul.2008.03.013.

Colares, G. B., and Melo, V. M. M. (2013). Relating microbial community structure and environmental variables in mangrove sediments inside Rhizophora mangle L. habitats. Appl. Soil Ecol. 64, 171–177. doi: 10.1016/j.apsoil.2012.12.004.

de Almeida, F. F., Freitas, D., Motteran, F., Fernandes, B. S., and Gavazza, S. (2021). Bioremediation of polycyclic aromatic hydrocarbons in contaminated mangroves: Understanding the historical and key parameter profiles. Mar. Pollut. Bull. 169, 112553. doi: 10.1016/j.marpolbul.2021.112553.

Dittmar, T., Lara, R. J., and Kattner, G. (2001). River or mangrove? Tracing major organic matter sources in tropical Brazilian coastal waters. Mar. Chem. 73, 253–271. doi: 10.1016/S0304-4203(00)00110-9.

Dodd, R. S., Fromard, F., Rafii, Z. A., and Blasco, F. (1995). Biodiversity among West African Rhizophora: Foliar wax chemistry. Biochem. Systemat. Ecol. 23, 859–868. doi: 10.1016/0305-1978(95)00083-6.

Doick, K. J., Burauel, P., Jones, K. C., and Semple, K. T. (2005). Distribution of aged 14 C−PCB and 14 C−PAH residues in particle-size and humic fractions of an agricultural soil. Environ. Sci. Technol. 39, 6575–6583. doi: 10.1021/es050523c.

Domínguez, C., Sarkar, S. K., Bhattacharya, A., Chatterjee, M., Bhattacharya, B. D., Jover, E., et al. (2010). Quantification and source identification of polycyclic aromatic hydrocarbons in core sediments from Sundarban mangrove wetland, India. Arch. Environ. Contam. Toxicol. 59, 49–61. doi: 10.1007/s00244-009-9444-2.

Dong, C.-D., Lu, Y.-C., Chang, J.-H., Wang, T.-H., Chen, C.-W., and Hung, C.-M. (2019). Enhanced persulfate degradation of PAH-contaminated sediments using magnetic carbon microspheres as the catalyst substrate. Proc. Saf. Environ. Protec. 125, 219–227. doi: 10.1016/j.psep.2019.03.011.

Dsikowitzky, L., Nordhaus, I., Jennerjahn, T. C., Khrycheva, P., Sivatharshan, Y., Yuwono, E., et al. (2011). Anthropogenic organic contaminants in water, sediments and benthic organisms of the mangrove-fringed Segara Anakan Lagoon, Java, Indonesia. Mar. Pollut. Bull. 62, 851–862. doi: 10.1016/j.marpolbul.2011.02.023.

D'Souza, J. (2016). "Arbuscular mycorrhizal diversity from mangroves: A review," in Recent Advances on Mycorrhizal Fungi Fungal Biology., ed. M. C. Pagano (Cham: Springer International Publishing), 109–116. doi: 10.1007/978-3-319-24355-9_10.

Duarte, C. M., and Cebrián, J. (1996). The fate of marine autotrophic production. Limnol. Oceanogr. 41, 1758–1766. doi: 10.4319/lo.1996.41.8.1758.

El-Maradny, A., El-Sherbiny, M. M., Ghandourah, M., El-Amin Bashir, M., and Orif, M. (2021). PAH bioaccumulation in two polluted sites along the eastern coast of the Red Sea, Saudi Arabia. Int. J. Environ. Sci. Technol. 18, 1335–1348. doi: 10.1007/s13762-020-02929-0.

Essien, J. P., Eduok, S. I., and Olajire, A. A. (2011). Distribution and ecotoxicological significance of polycyclic aromatic hydrocarbons in sediments from Iko River estuary mangrove ecosystem. Environ. Monit. Assess. 176, 99–107. doi: 10.1007/s10661-010-1569-2.

Farias, C. O., Hamacher, C., Wagener, A. de L. R., and Scofield, A. de L. (2008). Origin and degradation of hydrocarbons in mangrove sediments (Rio de Janeiro, Brazil) contaminated by an oil spill. Org. Geochem. 39, 289–307. doi: 10.1016/j.orggeochem.2007.12.008.

Furukawa, K., Wolanski, E., and Mueller, H. (1997). Currents and sediment transport in mangrove forests. Estuar. Coast. Shelf Sci. 44, 301–310. doi: 10.1006/ecss.1996.0120.

Garcia, M. R., and Martins, C. C. (2021). A systematic evaluation of polycyclic aromatic hydrocarbons in South Atlantic subtropical mangrove wetlands under a coastal zone development scenario. J. Environ. Manage. 277, 111421. doi: 10.1016/j.jenvman.2020.111421.

Gauthier, P. T., Norwood, W. P., Prepas, E. E., and Pyle, G. G. (2014). Metal–PAH mixtures in the aquatic environment: A review of co-toxic mechanisms leading to more-than-additive outcomes. Aquat. Toxicol. 154, 253–269. doi: 10.1016/j.aquatox.2014.05.026.

Ghizelini, A. M., Martins, K. G., Gießelmann, U. C., Santoro, E., Pasqualette, L., Mendonça-Hagler, L. C. S., et al. (2019). Fungal communities in oil contaminated mangrove sediments – Who is in the mud? Mar. Pollut. Bull. 139, 181–188. doi: 10.1016/j.marpolbul.2018.12.040.

Guo, C., Ke, L., Dang, Z., and Tam, N. F. (2011). Temporal changes in Sphingomonas and Mycobacterium populations in mangrove sediments contaminated with different concentrations of polycyclic aromatic hydrocarbons (PAHs). Mar. Pollut. Bull. 62, 133–139. doi: 10.1016/j.marpolbul.2010.08.022.

Guo, C. L., Zhou, H. W., Wong, Y. S., and Tam, N. F. Y. (2005). Isolation of PAH-degrading bacteria from mangrove sediments and their biodegradation potential. Mar. Pollut. Bull. 51, 1054–1061. doi: 10.1016/j.marpolbul.2005.02.012.

Guo, S., Wei, C., Zhu, Y., and Zhang, Y. (2021). The distribution and retained amount of benzo[a]pyrene at the micro-zones of mangrove leaf cuticles: Results from a novel analytical method. Environ. Pollut. 287, 117589. doi: 10.1016/j.envpol.2021.117589.

Gupta, S., Pathak, B., and Fulekar, M. H. (2015). Molecular approaches for biodegradation of polycyclic aromatic hydrocarbon compounds: a review. Rev. Environ. Sci. Biotechnol. 14, 241–269. doi: 10.1007/s11157-014-9353-3.

Gustafsson, Ö., Haghseta, F., Chan, C., MacFarlane, J., and Gschwend, P. M. (1997). Quantification of the dilute sedimentary soot phase: implications for PAH speciation and bioavailability. Environ. Sci. Technol. 31, 203–209. doi: 10.1021/es960317s.

Hamilton, S. E., and Casey, D. (2016). Creation of a high spatio-temporal resolution global database of continuous mangrove forest cover for the 21st century (CGMFC-21): CGMFC-21. Global Ecol. Biogeogr. 25, 729–738. doi: 10.1111/geb.12449.

Harbison, P. (1986). Mangrove muds—A sink and a source for trace metals. Mar. Pollut. Bull. 17, 246–250. doi: 10.1016/0025-326X(86)90057-3.

Haritash, A. K., and Kaushik, C. P. (2009). Biodegradation aspects of Polycyclic Aromatic Hydrocarbons (PAHs): A review. J. Hazard. Mater. 169, 1–15. doi: 10.1016/j.jhazmat.2009.03.137.

Heitkamp, M. A., Franklin, W., and Cerniglia, C. E. (1988). Microbial metabolism of polycyclic aromatic hydrocarbons: Isolation and characterization of a Pyrene-degrading bacterium. Appl. Environ. Microbiol. 54, 2549–2555. doi: 10.1128/aem.54.10.2549-2555.1988.

Hossain, M. D., and Nuruddin, A. A. (2016). Soil and mangrove: A review. J. Environ. Sci. Technol. 9, 198–207. doi: 10.3923/jest.2016.198.207.

Hu, Y., Huang, Y. Z., and Liu, Y. X. (2014). Influence of iron plaque on chromium accumulation and translocation in three rice (Oryza sativa L.) cultivars grown in solution culture. Chemistry and Ecology 30, 29–38. doi: 10.1080/02757540.2013.829050.

Huang, Q., Zhu, Y., Wu, F., and Zhang, Y. (2021). Parent and alkylated polycyclic aromatic hydrocarbons in surface sediments of mangrove wetlands across Taiwan Strait, China: Characteristics, sources and ecological risk assessment. Chemosphere 265, 129168. doi: 10.1016/j.chemosphere.2020.129168.

Huang, R., Zhang, C., Xu, X., Jin, R., Li, D., Christakos, G., et al. (2022). Underestimated PAH accumulation potential of blue carbon vegetation: Evidence from sedimentary records of saltmarsh and mangrove in Yueqing Bay, China. Sci. Total Environ. 817, 152887. doi: 10.1016/j.scitotenv.2021.152887.

HuiJie, L., CaiYun, Y., Yun, T., GuangHui, L., and TianLing, Z. (2011). Using population dynamics analysis by DGGE to design the bacterial consortium isolated from mangrove sediments for biodegradation of PAHs. Int. Biodeter. Biodegr. 65, 269–275. doi: 10.1016/j.ibiod.2010.11.010.

Imam, A., Kumar Suman, S., Kanaujia, P. K., and Ray, A. (2022). Biological machinery for polycyclic aromatic hydrocarbons degradation: A review. Bioresour. Technol. 343, 126121. doi: 10.1016/j.biortech.2021.126121.

Jia, H., Li, J., Li, Y., Lu, H., Liu, J., and Yan, C. (2020). The remediation of PAH contaminated sediment with mangrove plant and its derived biochars. J. Environ. Manage. 268, 110410. doi: 10.1016/j.jenvman.2020.110410.

Jia, H., Lu, H., Liu, J., Li, J., Dai, M., and Yan, C. (2016a). Effects of root exudates on the leachability, distribution, and bioavailability of phenanthrene and pyrene from mangrove sediments. Environ. Sci. Pollut. Res. 23, 5566–5576. doi: 10.1007/s11356-015-5772-0.

Jia, H., Wang, H., Lu, H., Jiang, S., Dai, M., Liu, J., et al. (2016b). Rhizodegradation potential and tolerance of Avicennia marina (Forsk.) Vierh in phenanthrene and pyrene contaminated sediments. Mar. Pollut. Bull. 110, 112–118. doi: 10.1016/j.marpolbul.2016.06.075.

Johnson, M. D., Keinath, T. M., and Weber, W. J. (2001). A distributed reactivity model for sorption by soils and sediments. 14. characterization and modeling of Phenanthrene desorption rates. Environ. Sci. Technol. 35, 1688–1695. doi: 10.1021/es001391k.

Juhasz, A. L., and Naidu, R. (2000). Bioremediation of high molecular weight polycyclic aromatic hydrocarbons: a review of the microbial degradation of benzo[a]pyrene. Int. Biodeter. Biodegr. 45, 57–88. doi: 10.1016/S0964-8305(00)00052-4.

Juma, R. R., Salum, N. S., Tairova, Z., Strand, J., Bakari, S. S., and Sheikh, M. A. (2018). Potential of Periophthalmus sobrinus and Siganus sutor as bioindicator fish species for PAH pollution in tropical waters. Reg. Stud. Mar. Sci. 18, 170–176. doi: 10.1016/j.rsma.2017.09.016.

Kaiser, D., Schulz-Bull, D. E., and Waniek, J. J. (2016). Profiles and inventories of organic pollutants in sediments from the central Beibu Gulf and its coastal mangroves. Chemosphere 153, 39–47. doi: 10.1016/j.chemosphere.2016.03.041.

Kathiresan, K., and Bingham, B. L. (2001). “Biology of mangroves and mangrove ecosystems,” in Advances in Marine Biology (Elsevier), 81–251. doi: 10.1016/S0065-2881(01)40003-4.

Ke, L., Yu, K., Wong, Y., and Tam, N. (2005). Spatial and vertical distribution of polycyclic aromatic hydrocarbons in mangrove sediments. Sci. Total Environ. 340, 177–187. doi: 10.1016/j.scitotenv.2004.08.015.

Klekowski, E. J., Corredor, J. E., Morell, J. M., and Del Castillo, C. A. (1994). Petroleum pollution and mutation in mangroves. Mar. Pollut. Bull. 28, 166–169. doi: 10.1016/0025-326X(94)90393-X.

Kristensen, E., Bouillon, S., Dittmar, T., and Marchand, C. (2008). Organic carbon dynamics in mangrove ecosystems: A review. Aquat. Bot. 89, 201–219. doi: 10.1016/j.aquabot.2007.12.005.

Kristensen, E., Connolly, R. M., Otero, X. L., Marchand, C., Ferreira, T. O., and Rivera-Monroy, V. H. (2017). “Biogeochemical cycles: Global approaches and perspectives,” in Mangrove Ecosystems: A Global Biogeographic Perspective, eds. V. H. Rivera-Monroy, S. Y. Lee, E. Kristensen, and R. R. Twilley (Cham: Springer International Publishing), 163–209. doi: 10.1007/978-3-319-62206-4_6.

Kulkarni, R., Deobagkar, D., and Zinjarde, S. (2018). Metals in mangrove ecosystems and associated biota: A global perspective. Ecotoxicol. Environ. Saf. 153, 215–228. doi: 10.1016/j.ecoenv.2018.02.021.

Kumar, S., Yadav, A., Kumar, A., Verma, R., Lal, S., Srivastava, S., et al. (2021). Plant metallothioneins as regulators of environmental stress responses. Int. J. Plant Environ. 7, 27–38. doi: 10.18811/ijpen.v7i01.3.

Lallier-Vergès, E., Marchand, C., Disnar, J.-R., and Lottier, N. (2008). Origin and diagenesis of lignin and carbohydrates in mangrove sediments of Guadeloupe (French West Indies): Evidence for a two-step evolution of organic deposits. Chem. Geol. 255, 388–398. doi: 10.1016/j.chemgeo.2008.07.009.

Lee, B.-K., and Vu, V. T. (2010). “Sources, distribution and toxicity of polycyclic aromatic hydrocarbons (PAHs) in particulate matter,” in Air Pollution (IntechOpen), 101–127.

Lee, S. Y., Primavera, J. H., Dahdouh-Guebas, F., McKee, K., Bosire, J. O., Cannicci, S., et al. (2014). Ecological role and services of tropical mangrove ecosystems: a reassessment: Reassessment of mangrove ecosystem services. Glob. Ecol. Biogeogr. 23, 726–743. doi: 10.1111/geb.12155.

Lewis, M. A., and Russell, M. J. (2015). Contaminant profiles for surface water, sediment, flora and fauna associated with the mangrove fringe along middle and lower eastern Tampa Bay. Mar. Pollut. Bull. 95, 273–282. doi: 10.1016/j.marpolbul.2015.04.001.

Lewis, M., Pryor, R., and Wilking, L. (2011). Fate and effects of anthropogenic chemicals in mangrove ecosystems: A review. Environ. Pollut. 159, 2328–2346. doi: 10.1016/j.envpol.2011.04.027.

Li, C.-H., Ye, C., Wong, Y.-S., and Tam, N. F.-Y. (2011). Effect of Mn(IV) on the biodegradation of polycyclic aromatic hydrocarbons under low-oxygen condition in mangrove sediment slurry. J. Hazard. Mater. 190, 786–793. doi: 10.1016/j.jhazmat.2011.03.121.

Li, C.-H., Zhou, H.-W., Wong, Y.-S., and Tam, N. F.-Y. (2009). Vertical distribution and anaerobic biodegradation of polycyclic aromatic hydrocarbons in mangrove sediments in Hong Kong, South China. Sci. Total Environ. 407, 5772–5779. doi: 10.1016/j.scitotenv.2009.07.034.

Li, F., Zeng, X., Yang, J., Zhou, K., Zan, Q., Lei, A., et al. (2014). Contamination of polycyclic aromatic hydrocarbons (PAHs) in surface sediments and plants of mangrove

swamps in Shenzhen, China. Mar. Pollut. Bull. 85, 590–596. doi: 10.1016/j.marpolbul.2014.02.025.

Li, R., Tan, H., Zhu, Y., and Zhang, Y. (2017). The retention and distribution of parent, alkylated, and N/O/S-containing polycyclic aromatic hydrocarbons on the epidermal tissue of mangrove seedlings. Environ. Pollut. 226, 135–142. doi: 10.1016/j.envpol.2017.04.025.

Liang, Y., Tse, M. F., Young, L., and Wong, M. H. (2007). Distribution patterns of polycyclic aromatic hydrocarbons (PAHs) in the sediments and fish at Mai Po Marshes Nature Reserve, Hong Kong. Water Res. 41, 1303–1311. doi: 10.1016/j.watres.2006.11.048.

Lima, A. L. C., Farrington, J. W., and Reddy, C. M. (2005). Combustion-derived polycyclic aromatic hydrocarbons in the environment—A review. Environ. Forensics 6, 109–131. doi: 10.1080/15275920590952739.

Liu, B., Wang, P., Chen, L., and Zhang, Y. (2011). Effects of aging and flooding on sorption of PAHs in mangrove sediment. Fresenius Environ. Bull. 20, 623–630.

Liu, H., Yang, C., Tian, Y., Lin, G., and Zheng, T. (2010). Screening of PAH-degrading bacteria in a mangrove swamp using PCR–RFLP. Mar. Pollut. Bull. 60, 2056–2061. doi: 10.1016/j.marpolbul.2010.07.013.

Liu, J., and Li, X. (2008). Sulfur cycle in the typical meadow Calamagrostis angustifolia wetland ecosystem in the Sanjiang Plain, Northeast China. J. Environ. Sci. 20, 470–475. doi: 10.1016/S1001-0742(08)62081-1.

Lu, H., Zhang, Y., Liu, B., Liu, J., Ye, J., and Yan, C. (2011). Rhizodegradation gradients of phenanthrene and pyrene in sediment of mangrove (Kandelia candel (L.) Druce). J. Hazard. Mater. 196, 263–269. doi: 10.1016/j.jhazmat.2011.09.031.

Luz, L. G., Carreira, R. S., Farias, C. O., Scofield, A. de L., Nudi, A. H., and Wagener, A. de L. R. (2010). Trends in PAH and black carbon source and abundance in a tropical mangrove system and possible association with bioavailability. Org. Geochem. 41, 1146–1155. doi: 10.1016/j.orggeochem.2010.06.003.

Macdonald, D. D., Carr, R. S., Calder, F. D., Long, E. R., and Ingersoll, C. G. (1996). Development and evaluation of sediment quality guidelines for Florida coastal waters. Ecotoxicology 5, 253–278. doi: 10.1007/BF00118995.

Machado, W., Gueiros, B. B., Lisboa-Filho, S. D., and Lacerda, L. D. (2005). Trace metals in mangrove seedlings: role of iron plaque formation. Wetlands Ecol. Manage. 13, 199–206. doi: 10.1007/s11273-004-9568-0.

Maciel-Souza, M. do C., Macrae, A., Volpon, A. G. T., Ferreira, P. S., and Mendonça-Hagler, L. C. (2006). Chemical and microbiological characterization of mangrove sediments after a large oil-spill in Guanabara Bay - RJ - Brazil. Braz. J. Microbiol. 37. doi: 10.1590/S1517-83822006000300013.

Mahugija, J. A., Ahmed, K. N., and Makame, Y. M. (2017). Polycyclic aromatic hydrocarbons (PAHs) contamination in coastal mangrove ecosystems of the Zanzibar archipelago. West. Indian Ocean J. Mar. Sci. 16, 25–34.

Marchand, C. (2017). Soil carbon stocks and burial rates along a mangrove forest chronosequence (French Guiana). For. Ecol. Manag. 384, 92–99. doi: 10.1016/j.foreco.2016.10.030.

Marchand, C., Baltzer, F., Lallier-Vergès, E., and Albéric, P. (2004). Pore-water chemistry in mangrove sediments: relationship with species composition and developmental stages (French Guiana). Mar. Geol. 208, 361–381. doi: 10.1016/j.margeo.2004.04.015.

Marchand, C., Disnar, J. R., Lallier-Vergès, E., and Lottier, N. (2005). Early diagenesis of carbohydrates and lignin in mangrove sediments subject to variable redox conditions (French Guiana). Geochim. Cosmochim. Acta 69, 131–142. doi: 10.1016/j.gca.2004.06.016.

Marchand, C., Fernandez, J.-M., Moreton, B., Landi, L., Lallier-Vergès, E., and Baltzer, F. (2012). The partitioning of transitional metals (Fe, Mn, Ni, Cr) in mangrove sediments downstream of a ferralitized ultramafic watershed (New Caledonia). Chem. Geol. 300–301, 70–80. doi: 10.1016/j.chemgeo.2012.01.018.

Marchand, C., Lallier-Vergès, E., and Allenbach, M. (2011). Redox conditions and heavy metals distribution in mangrove forests receiving effluents from shrimp farms (Teremba Bay, New Caledonia). J. Soils Sediments 11, 529–541. doi: 10.1007/s11368-010-0330-3.

Marquès, M., Mari, M., Audí-Miró, C., Sierra, J., Soler, A., Nadal, M., et al. (2016). Photodegradation of polycyclic aromatic hydrocarbons in soils under a climate change base scenario. Chemosphere 148, 495–503. doi: 10.1016/j.chemosphere.2016.01.069.

Mbusnum, K. G., Malleret, L., Deschamps, P., Khabouchi, I., Asia, L., Lebarillier, S., et al. (2020). Persistent organic pollutants in sediments of the Wouri Estuary Mangrove, Cameroon: Levels, patterns and ecotoxicological significance. Mar. Pollut. Bull. 160, 111542. doi: 10.1016/j.marpolbul.2020.111542.

Means, J. C., Wood, S. G., Hassett, J. J., and Banwart, W. L. (1980). Sorption of polynuclear aromatic hydrocarbons by sediments and soils. Environ. Sci. Technol. 14, 1524–1528. doi: 10.1021/es60172a005.

Misra, S., Choudhury, A., Ghosh, A., and Dutta, J. (1984). The role of hydrophobic substances in leaves in adaptation of plants to periodic submersion by tidal water in a mangrove ecosystem. J. Ecol. 72, 621. doi: 10.2307/2260071.

Mohebbi-Nozar, S. L., Zakaria, M. P., Mortazavi, M. S., Ismail, W. R., and Kodadadi Jokar, K. (2016). Concentrations and source identification of Polycyclic Aromatic Hydrocarbons (PAHs) in mangrove sediments from north of Persian Gulf. Polycycl. Aromat. Compd. 36, 601–612. doi: 10.1080/10406638.2015.1037004.

Mojiri, A., Zhou, J. L., Ohashi, A., Ozaki, N., and Kindaichi, T. (2019). Comprehensive review of polycyclic aromatic hydrocarbons in water sources, their effects and treatments. Sci. Total Environ. 696, 133971. doi: 10.1016/j.scitotenv.2019.133971.

Naidoo, G. (2016). Mangrove propagule size and oil contamination effects: Does size matter? Mar. Pollut. Bull. 110, 362–370. doi: 10.1016/j.marpolbul.2016.06.040.

Naidoo, G., and Naidoo, K. (2017). Ultrastructural effects of polycyclic aromatic hydrocarbons in the mangroves Avicennia marina and Rhizophora mucronata. Flora 235, 1–9. doi: 10.1016/j.flora.2017.08.006.

Nam, J. J., Gustafsson, O., Kurt-Karakus, P., Breivik, K., Steinnes, E., and Jones, K. C. (2008). Relationships between organic matter, black carbon and persistent organic pollutants in European background soils: Implications for sources and environmental fate. Environ. Pollut. 156, 809–817. doi: 10.1016/j.envpol.2008.05.027.

Nudi, A. H., de Luca Rebello Wagener, A., Francioni, E., de Lemos Scofield, A., Sette, C. B., and Veiga, A. (2007). Validation of Ucides cordatus as a bioindicator of oil contamination and bioavailability in mangroves by evaluating sediment and crab PAH records. Environ. Int. 33, 315–327. doi: 10.1016/j.envint.2006.11.001.

Orcutt, D. M., and Nilsen, E. T. (2000). The physiology of plants under stress: Soil and biotic factors. Toronto, Ontario, Canada: John Wiley & Sons, Inc.

Orif, M., and El-Maradny, A. (2018). Bio-accumulation of Polycyclic Aromatic Hydrocarbons in the grey mangrove (Avicennia marina) along Arabian Gulf Saudi coast. Open Chem. 16, 340–348. doi: 10.1515/chem-2018-0038.

Otte, M. L., Rozema, J., Koster, L., Haarsma, M. S., and Broekman, R. A. (1989). Iron plaque on roots of Aster tripolium L.: interaction with zinc uptake. New Phytol 111, 309–317. doi: 10.1111/j.1469-8137.1989.tb00694.x.

Oyo-Ita, O. E., Offem, J. O., Ekpo, B. O., and Adie, P. A. (2013). Anthropogenic PAHs in mangrove sediments of the Calabar River, SE Niger Delta, Nigeria. Appl. Geochem. 28, 212–219. doi: 10.1016/j.apgeochem.2012.09.011.

Patel, A. B., Shaikh, S., Jain, K. R., Desai, C., and Madamwar, D. (2020). Polycyclic Aromatic Hydrocarbons: sources, toxicity, and remediation approaches. Front. Microbiol. 11, 562813. doi: 10.3389/fmicb.2020.562813.

Pi, N., Tam, N. F. Y., and Wong, M. H. (2010). Effects of wastewater discharge on formation of Fe plaque on root surface and radial oxygen loss of mangrove roots. Environ. Pollut. 158, 381–387. doi: 10.1016/j.envpol.2009.09.004.

Pi, N., Tam, N. F. Y., Wu, Y., and Wong, M. H. (2009). Root anatomy and spatial pattern of radial oxygen loss of eight true mangrove species. Aquat. Bot. 90, 222–230. doi: 10.1016/j.aquabot.2008.10.002.

Pi, N., Wu, Y., Zhu, H. W., Wong, Y. S., and Tam, N. F. Y. (2017). The uptake of mixed PAHs and PBDEs in wastewater by mangrove plants under different tidal flushing regimes. Environ. Pollut. 231, 104–114. doi: 10.1016/j.envpol.2017.07.085.

Purnobasuki, H., Purnama, P. R., and Kobayashi, K. (2017). Morphology of four root types and anatomy of root-root junction in relation gas pathway of Avicennia Marina (Forsk) Vierh roots. Vegetos- An Inter. Jour. of Plnt. Rese. 30, 100. doi: 10.5958/2229-4473.2017.00143.4.

Qin, X., Sun, H., Wang, C., Yu, Y., and Sun, T. (2010). Impacts of crab bioturbation on the fate of polycyclic aromatic hydrocarbons in sediment from the Beitang estuary of Tianjin, China. Environ. Toxicol. Chem. doi: 10.1002/etc.154.

Qiu, Y.-W., Qiu, H.-L., Li, J., and Zhang, G. (2018). Bioaccumulation and cycling of Polycyclic Aromatic Hydrocarbons (PAHs) in typical mangrove wetlands of Hainan Island, South China. Arch. Environ. Contam. Toxicol. 75, 464–475. doi: 10.1007/s00244-018-0548-4.

Ramdine, G., Fichet, D., Louis, M., and Lemoine, S. (2012). Polycyclic aromatic hydrocarbons (PAHs) in surface sediment and oysters (Crassostrea rhizophorae) from mangrove of Guadeloupe: Levels, bioavailability, and effects. Ecotoxicol. Environ. Saf. 79, 80–89. doi: 10.1016/j.ecoenv.2011.12.005.

Raza, M., Zakaria, M. P., Hashim, N. R., Yim, U. H., Kannan, N., and Ha, S. Y. (2013). Composition and source identification of polycyclic aromatic hydrocarbons in mangrove sediments of Peninsular Malaysia: indication of anthropogenic input. Environ. Earth Sci. 70, 2425–2436. doi: 10.1007/s12665-013-2279-1.

Reaney, S. H., and Smith, D. R. (2005). Manganese oxidation state mediates toxicity in PC12 cells. Tox. Appl. Pharmacol. 205, 271–281. doi: 10.1016/j.taap.2004.10.013.

Rengarajan, T., Rajendran, P., Nandakumar, N., Lokeshkumar, B., Rajendran, P., and Nishigaki, I. (2015). Exposure to polycyclic aromatic hydrocarbons with special focus on cancer. Asian Pacific J. Tropical Biomed. 5, 182–189. doi: 10.1016/S2221-1691(15)30003-4.

Robin, S. L., Marchand, C., Ham, B., Pattier, F., Laporte-Magoni, C., and Serres, A. (2021). Influences of species and watersheds inputs on trace metal accumulation in mangrove roots. Sci. Total Environ. 787, 147438. doi: 10.1016/j.scitotenv.2021.147438.

Sahoo, K., and Dhal, N. K. (2009). Potential microbial diversity in mangrove ecosystems: A review. Indian J. Mar. Sci. 38, 249–256.

Sakshi, and Haritash, A. K. (2020). A comprehensive review of metabolic and genomic aspects of PAH-degradation. Arch. Microbiol. 202, 2033–2058. doi: 10.1007/s00203-020-01929-5.

Sánchez-García, L., Cato, I., and Gustafsson, Ö. (2010). Evaluation of the influence of black carbon on the distribution of PAHs in sediments from along the entire Swedish continental shelf. Mar. Chem. 119, 44–51. doi: 10.1016/j.marchem.2009.12.005.

Sarkar, S. K. (2016). “Polycyclic Aromatic Hydrocarbons (PAHs) in sediment cores from Sundarban Wetland,” in Marine Organic Micropollutants SpringerBriefs in Environmental Science. (Cham: Springer International Publishing), 49–68. doi: 10.1007/978-3-319-43301-1_4.

Sarkar, S. K., Binelli, A., Chatterjee, M., Bhattacharya, B. D., Parolini, M., Riva, C., et al. (2012). Distribution and ecosystem risk assessment of Polycyclic Aromatic Hydrocarbons (PAHs) in core sediments of Sundarban mangrove wetland, India. Polycycl. Aromat. Compd. 32, 1–26. doi: 10.1080/10406638.2011.633592.

Semboung Lang, F. (2017). Dépollution des sédiments d’une mangrove de l’estuaire du Wouri : évaluation du potentiel de microflores.

Shen, H., Huang, Y., Wang, R., Zhu, D., Li, W., Shen, G., et al. (2013). Global atmospheric emissions of Polycyclic Aromatic Hydrocarbons from 1960 to 2008 and future predictions. Environ. Sci. Technol. 47, 6415–6424. doi: 10.1021/es400857z.

Simpson, C. D., Mosi, A. A., Cullen, W. R., and Reimer, K. J. (1996). Composition and distribution of polycyclic aromatic hydrocarbon contamination in surficial marine sediments from Kitimat Harbor, Canada. Sci. Total Environ. 181, 265–278. doi: 10.1016/0048-9697(95)05026-4.

Sivagami, K., Padmanabhan, K., Joy, A. C., and Nambi, I. M. (2019). Microwave (MW) remediation of hydrocarbon contaminated soil using spent graphite – An approach for waste as a resource. J. Environ. Manage. 230, 151–158. doi: 10.1016/j.jenvman.2018.08.071.

Sojinu, O. S. S., Wang, J.-Z., Sonibare, O. O., and Zeng, E. Y. (2010). Polycyclic aromatic hydrocarbons in sediments and soils from oil exploration areas of the Niger Delta, Nigeria. J. Hazard. Mater. 174, 641–647. doi: 10.1016/j.jhazmat.2009.09.099.

Song, H.-G., Wang, X., and Bartha, R. (1990). Bioremediation potential of terrestrial fuel spills. Appl. Environ. Microbiol. 56, 652–656. doi: 10.1128/aem.56.3.652-656.1990.

Souza, M. R. R., Santos, E., Suzarte, J. S., Carmo, L. O., Frena, M., Damasceno, F. C., et al. (2018). Concentration, distribution and source apportionment of polycyclic aromatic hydrocarbons (PAH) in Poxim River sediments, Brazil. Mar. Pollut. Bull. 127, 478–483. doi: 10.1016/j.marpolbul.2017.12.045.

Stieglitz, T. C., Clark, J. F., and Hancock, G. J. (2013). The mangrove pump: The tidal flushing of animal burrows in a tropical mangrove forest determined from radionuclide budgets. Geochim. Cosmochim. Acta 102, 12–22. doi: 10.1016/j.gca.2012.10.033.

Suprayogi, B., and Murray, F. (1999). A field experiment of the physical and chemical effects of two oils on mangroves. Environ. Exp. Bot. 42, 221–229. doi: 10.1016/S0098-8472(99)00037-4.

Swartz, R. C. (1999). Consensus sediment quality guidelines for polycyclic aromatic hydrocarbon mixtures. Environ. Toxicol. Chem. 18, 780–787. doi: 10.1002/etc.5620180426.

Tam, N. F. Y., Ke, L., Wang, X. H., and Wong, Y. S. (2001). Contamination of polycyclic aromatic hydrocarbons in surface sediments of mangrove swamps. Environ. Pollut. 114, 255–263. doi: 10.1016/S0269-7491(00)00212-8.

Tam, N. F. Y., and Yao, M. W. Y. (2002). Concentrations of PCBs in coastal mangrove sediments of Hong Kong. Mar. Pollut. Bull. 44, 642–651. doi: 10.1016/S0025-326X(01)00306-X.

Tansel, B., Lee, M., and Tansel, D. Z. (2013). Comparison of fate profiles of PAHs in soil, sediments and mangrove leaves after oil spills by QSAR and QSPR. Mar. Pollut. Bull. 73, 258–262. doi: 10.1016/j.marpolbul.2013.05.011.

Taylor, G. J., and Crowder, A. A. (1983). Use of the DCB technique for extraction of hydrous Iron oxides from roots of wetland plants. American J. Bot. 70, 1254–1257. doi: 10.2307/2443295.

Thakur, V. K., Thakur, M. K., Raghavan, P., and Kessler, M. R. (2014). Progress in green polymer composites from lignin for multifunctional applications: a review. ACS Sustain. Chem. Eng. 2, 1072–1092. doi: 10.1021/sc500087z.

Tiralerdpanich, P., Nasaree, S., Pinyakong, O., and Sonthiphand, P. (2021). Variation of the mangrove sediment microbiomes and their phenanthrene biodegradation rates during the dry and wet seasons. Environ. Pollut. 289, 117849. doi: 10.1016/j.envpol.2021.117849.

Tsibart, A. S., and Gennadiev, A. N. (2013). Polycyclic aromatic hydrocarbons in soils: Sources, behavior, and indication significance (a review). Eurasian Soil Sc. 46, 728–741. doi: 10.1134/S1064229313070090.

Vaezzadeh, V., Zakaria, M. P., Bong, C. W., Masood, N., Mohsen Magam, S., and Alkhadher, S. (2019). Mangrove oyster (Crassostrea belcheri) as a biomonitor species for bioavailability of Polycyclic Aromatic Hydrocarbons (PAHs) from sediment of the west coast of Peninsular Malaysia. Polycycl. Aromat. Compd. 39, 470–485. doi: 10.1080/10406638.2017.1348366.

Vane, C. H., Harrison, I., Kim, A. W., Moss-Hayes, V., Vickers, B. P., and Hong, K. (2009). Organic and metal contamination in surface mangrove sediments of South China. Mar. Pollut. Bull. 58, 134–144. doi: 10.1016/j.marpolbul.2008.09.024.

Verâne, J., dos Santos, N. C. P., da Silva, V. L., de Almeida, M., de Oliveira, O. M. C., and Moreira, Í. T. A. (2020). Phytoremediation of polycyclic aromatic hydrocarbons (PAHs) in mangrove sediments using Rhizophora mangle. Mar. Pollut. Bull. 160, 111687. doi: 10.1016/j.marpolbul.2020.111687.

Wanapaisan, P., Laothamteep, N., Vejarano, F., Chakraborty, J., Shintani, M., Muangchinda, C., et al. (2018). Synergistic degradation of pyrene by five culturable bacteria in a mangrove sediment-derived bacterial consortium. J. Hazard. Mater. 342, 561–570. doi: 10.1016/j.jhazmat.2017.08.062.

Wang, P., Du, K.-Z., Zhu, Y.-X., and Zhang, Y. (2008). A novel analytical approach for investigation of anthracene adsorption onto mangrove leaves. Talanta 76, 1177–1182. doi: 10.1016/j.talanta.2008.05.021.

Wang, P., Zhang, Y., and Wu, T.-H. (2010). Novel method for in situ visualization of polycyclic aromatic hydrocarbons in mangrove plants. Tox. Environ. Chem. 92, 1825–1829. doi: 10.1080/02772248.2010.482833.

Wang, Y., Zhu, H., and Tam, N. F. Y. (2014b). Effect of a polybrominated diphenyl ether congener (BDE-47) on growth and antioxidative enzymes of two mangrove plant species, Kandelia obovata and Avicennia marina, in South China. Mar. Pollut. Bull. 85, 376–384. doi: 10.1016/j.marpolbul.2014.02.012.

Wang, Y., Zhu, H., and Tam, N. F. Y. (2014a). Polyphenols, tannins and antioxidant activities of eight true mangrove plant species in South China. Plant Soil 374, 549–563. doi: 10.1007/s11104-013-1912-9.

Wang, Z., Liu, Z., Yang, Y., Li, T., and Liu, M. (2012). Distribution of PAHs in tissues of wetland plants and the surrounding sediments in the Chongming wetland, Shanghai, China. Chemosphere 89, 221–227. doi: 10.1016/j.chemosphere.2012.04.019.

Wick, A. F., Haus, N. W., Sukkariyah, B. F., Haering, K. C., and Daniels, W. L. (2011). Remediation of PAH-contaminated soils and sediments: A literature review. Virginia Polytechnic Institute and State University.

Woodroffe, C. D., Rogers, K., McKee, K. L., Lovelock, C. E., Mendelssohn, I. A., and Saintilan, N. (2016). Mangrove sedimentation and response to relative sea-level rise. Annu. Rev. Mar. Sci. 8, 243–266. doi: 10.1146/annurev-marine-122414-034025.

Wu, Q., Leung, J. Y. S., Tam, N. F. Y., Chen, S., Mai, B., Zhou, X., et al. (2014). Biological risk and pollution history of polycyclic aromatic hydrocarbons (PAHs) in Nansha mangrove, South China. Mar. Pollut. Bull. 85, 92–98. doi: 10.1016/j.marpolbul.2014.06.014.

Yan, Z., Sun, X., Xu, Y., Zhang, Q., and Li, X. (2017). Accumulation and tolerance of mangroves to heavy metals: a review. Curr. Pollut. Rep. 3, 302–317. doi: 10.1007/s40726-017-0066-4.

Ye, D., Siddiqi, M. A., Maccubbin, A. E., Kumar, S., and Sikka, H. C. (1996). Degradation of polynuclear aromatic hydrocarbons by Sphingomonas paucimobilis. Environ. Sci. Technol. 30, 136–142. doi: 10.1021/es9501878.

Youssef, T. (2002). Physiological responses of Avicennia marina seedlings to the phytotoxic effects of the water-soluble fraction of light Arabian crude oil. The Environmentalist 22, 149–159. doi: 10.1023/A:1015385700669.

Yu, S. H., Ke, L., Wong, Y. S., and Tam, N. F. Y. (2005). Degradation of polycyclic aromatic hydrocarbons by a bacterial consortium enriched from mangrove sediments. Environ. Int. 31, 149–154. doi: 10.1016/j.envint.2004.09.008.

Zaalishvili, G., Sadunishvili, T., Scalla, R., Laurent, F., and Kvesitadze, G. (2002). Electron microscopic investigation of nitrobenzene distribution and effect on plant root tip cells ultrastructure. Ecotoxicol. Environ. Saf. 52, 190–197. doi: 10.1006/eesa.2002.2181.

Zanardi-Lamardo, E., Mitra, S., Vieira-Campos, A. A., Cabral, C. B., Yogui, G. T., Sarkar, S. K., et al. (2019). Distribution and sources of organic contaminants in surface sediments of Hooghly river estuary and Sundarban mangrove, eastern coast of India. Mar. Pollut. Bull. 146, 39–49. doi: 10.1016/j.marpolbul.2019.05.043.

Zhang, J., Cai, L., Yuan, D., and Chen, M. (2004). Distribution and sources of polynuclear aromatic hydrocarbons in Mangrove surficial sediments of Deep Bay, China. Mar. Pollut. Bull. 49, 479–486. doi: 10.1016/j.marpolbul.2004.02.030.

Zhang, L., Xu, C., Chen, Z., Li, X., and Li, P. (2010). Photodegradation of pyrene on soil surfaces under UV light irradiation. J. Hazard. Mater. 173, 168–172. doi: 10.1016/j.jhazmat.2009.08.059.

Zhang, M., Ahmad, M., Lee, S. S., Xu, L. H., and Ok, Y. S. (2014). Sorption of Polycyclic Aromatic Hydrocarbons (PAHs) to lignin: effects of hydrophobicity and temperature. Bull. Environ. Contam. Toxicol. 93, 84–88. doi: 10.1007/s00128-014-1290-x.

Zhang, M., and Zhu, L. (2009). Sorption of Polycyclic Aromatic Hydrocarbons to carbohydrates and lipids of ryegrass root and implications for a sorption prediction model. Environ. Sci. Technol. 43, 2740–2745. doi: 10.1021/es802808q.

Zhao, H., Li, X., Wang, X., and Tian, D. (2010). Grain size distribution of road-deposited sediment and its contribution to heavy metal pollution in urban runoff in Beijing, China. J. Hazard. Mater. 183, 203–210. doi: 10.1016/j.jhazmat.2010.07.012.

Zheng, G. J., Lam, M. H. W., Lam, P. K. S., Richardson, B. J., Man, B. K. W., and Li, A. M. Y. (2000). Concentrations of persistent organic pollutants in surface sediments of the mudflat and mangroves at Mai Po Marshes Nature Reserve, Hong Kong. Mar. Pollut. Bull. 40, 5. doi: 10.1016/S0025-326X(00)00190-9.

Zuloaga, O., Prieto, A., Ahmed, K., Sarkar, S. K., Bhattacharya, A., Chatterjee, M., et al. (2013). Distribution of polycyclic aromatic hydrocarbons in recent sediments of Sundarban mangrove wetland of India and Bangladesh: a comparative approach. Environ. Earth Sci. 68, 355–367. doi: 10.1007/s12665-012-1743-7.

Zuloaga, O., Prieto, A., Usobiaga, A., Sarkar, S. K., Chatterjee, M., Bhattacharya, B. D., et al. (2009). Polycyclic Aromatic Hydrocarbons in intertidal marine bivalves of Sunderban mangrove wetland, India: An approach to bioindicator species. Water Air Soil Pollut. 201, 305–318. doi: 10.1007/s11270-008-9946-y.

Annexe 2

Soil concentrations and atmospheric emissions of biogenic hydrogen sulphide (H_2S) in a Rhizophora mangrove forest

Adrien Jacotot, Inès Gayral, Sarah Louise ROBIN, Cyril MARCHAND

Published in Estuarine, Coastal and Shelf Science

DOI: 10.1016/j.ecss.2023.108439

Abstract

Mangrove forests are potentially large biogenic sources of atmospheric hydrogen sulphide (H_2S), featuring among the carbon-richest ecosystems in the world associated with strong soil anoxia and large quantities of sulphates brought by tides. H_2S is highly toxic and acts as a precursor for atmospheric sulphur compounds and sulphate aerosols, which contribute to acid deposition and have implications for global climate change. Therefore, understanding H_2S emissions in mangroves holds great importance. Yet, its range of emissions remains uncertain. In this exploratory study, soil H_2S concentrations were measured during tide stall at both high and low tide in a semi-arid mangrove, which has never been done before. Then, potential H_2S fluxes to the atmosphere were estimated at low tide. Soil concentrations were greater at high tide than low tide, probably due to larger soil anoxia (average of 377 vs 179 mV), with average values of 1.40 ± 0.55 and 0.73 ± 0.32 mmol L^{-1}, respectively. Temperature was a key factor controlling soil concentrations, with higher values in the warm season than in the cold season. Average H2S emissions ranged from 5.81 ± 2.58 to 28.74 ± 6.98 µg S m^{-2} h^{-1} with a mean value of 14.90 ± 7.90 µg S m^{-2} h^{-1}. This study contributes to reducing the uncertainty in the variation range of H_2S fluxes from mangroves, which may be significant for the global sulphur cycle.

Keywords: mangrove, H_2S fluxes, soil-gas concentration, diffusion gradient, Fick's law, New Caledonia

1. Introduction

Mangrove forests are ecosystems composed of C3 halophytic trees growing on the land-sea intertidal continuum on most (sub)tropical coasts of the world. Mangrove forests are renowned for their long-term carbon (C) sequestration potential, which has earned them a place on the "Blue Carbon" ecosystems list (Donato et al., 2011). Their large C sequestration capacity stems from both i) large primary productivity of the trees and ii)

oxygen-limited decomposition of soil organic matter (SOM) due to the almost permanently waterlogged conditions, in turn controlled by the local tidal regime. Aerobic oxidation of SOM, the energetically prevailing thermodynamic process, is mostly restricted to the topmost few centimetres of the soil and to micro-aerobic zones of the rhizosphere due to crab burrows and oxygen transfers from the atmosphere down to the soil (Kristensen et al., 2017). Dissimilatory sulphate reduction (DSR), a strictly anaerobic process, is the second dominant SOM decomposition pathway in mangrove soils, accounting for up to 50% of total C mineralization (Kristensen et al., 2008). Hydrogen sulphide (H_2S), produced by DSR (Bartonet al., 2014), is the main biogenic sulphur gas emitted from mangroves, contributing up to 70% of total S emissions (Ganguly et al., 2018). H2S is best known for its strong rotten egg odour and its high toxicity for animal and plant life (Barton et al., 2014), but is also a precursor of atmospheric sulphur dioxide (SO_2), sulphuric acid (H_2SO_4) and sulphate (SO_4) aerosols, which contribute to acid deposition. Additionally, sulphate aerosols impact global climate change, with a potential cooling effect of 0.75 W m^{-2} (Ganguly et al., 2018). According to Watts (2000), H_2S emissions from natural sources are larger than anthropogenic emissions (4.42 vs 3.30 Tg yr^{-1}). However, the contribution of coastal wetlands remains very uncertain, in particular that of mangrove forests due to a great scarcity of measurement data.

2. Material and methods

In this context, the objectives of this work were to measure soil H2S concentrations and to estimate potential emissions to the atmosphere from a Rhizophora spp. mangrove forest in New Caledonia (Southern hemisphere; 22◦16′49.3″S, 166 ◦28′15.3″E). This mangrove ecosystem experiences a semi-diurnal tidal regime (range of 1.10–1.70 m), and a tropical wet and dry climate classified as category Aw according to the Köppen-Geiger classification. The region has two distinct seasons: a wet and warm season spanning from November to April, and a dry and cold one from May to October. To measure porewater H_2S concentrations in the soil, core samples were collected once per month between January and August 2017, during low and high tide. Triplicate porewater samples were extracted from six depths (0.05 to 0.55 m with a 0.10 m interval) using Rhizon micro-samplers and transferred to gas-sealed vials with a nitrogen headspace (1:1 vol). Each vial was then shaken to achieve gas equilibrium between the dissolved sulphides in the porewater and the gas phase. Subsequently, a subsample of the vial headspace was taken for further analysis. Lastly, a supplementary gas sample was collected 5 cm above the soil during low tide to measure atmospheric H_2S concentration. H_2S concentrations were analysed using gas chromatography equipped with a pulsed flame photometric detector (PFPD, OI Analytical) for H_2S detection (Shimadzu, GC-17A, Japan) and a GS-

GasPro capillary column (30 m × 0.32 mm, Agilent Technologies, USA). Analytical conditions were set as follows: injector, oven, and detector temperatures were fixed at 200, 65 and 250 °C, respectively. Injection volume was 1 ml with a 1:20 split. Retention time for H_2S was ~3.6 min. The peak areas were integrated and reported to a 7-points calibration curve created with pure nitrogen as zero and from dilutions of a 25 ppm H_2S gas standard. The conversion from partial pressure of H_2S in the headspace (ppm) to concentration in the water samples (mmol L^{-1}) were done following Bastviken et al. (2004), using Henry 's law and a Henry's law constant of 0.1 M atm^{-1} (Sander, 1999). In addition, an extra core was collected during six campaigns (January to June 2017) to measure redox potential, soil water content, pH, soil density, salinity and soil organic carbon content, both during low and high tide (Jacotot et al., 2019). H_2S fluxes to the atmosphere were estimated for low-tide periods, when the soil is exposed to the atmosphere, using a soil-atmosphere gradient method (SAGM). The SAGM is based on Fick's first law that relates the gas concentration gradient between two depths with the gas diffusion coefficient in the soil (Ds). The entire calculation procedure and the equations used are detailed in Supplementary Material. The use of SAGM is constrained by the determination of a proper value of the tortuosity factor (ε) that influences Ds. This determination can be done in-situ using gas tracers, but also estimated using empirical models. Herein, five values of ε were first determined with empirical models, all based on soil porosity and water content (Step 1 in Supplementary Material). To determine the optimal ε value, we used a dataset from Jacotot et al. (2019) consisting of soil CH_4 concentrations, and surface to atmosphere CH_4 fluxes measured using incubation chambers. These measurements were obtained at the same site and on the same date as the H_2S concentrations presented in this study. For detailed information regarding the measurement methodologies employed, please refer to Jacotot et al. (2019). Subsequently, the SAGM was applied to calculate five sets of CH_4 fluxes to the atmosphere using the five potentials values of ε (Step 1). To assess the differences between the SAGM-derived CH_4 fluxes and the ones obtainedfrom static chambers, the Normalized Root Mean Square Error (NRMSE) was calculated (Step 2 in Supplementary Material). Finally, the ε value that yielded the lowest NRMSE was selected for the subsequent calculation of H_2S fluxes by SAGM using measurements taken 0.05 m below and 0.05 m above the soil surface.

3. Results and discussion

Table 1. Soil H_2S concentrations (nmol L^{-1}) at low tide (mean±SD) measured between January and August 2017.

Months (2017)	January	February	March	April	May	June	July	August
Depth (cm)	*High tide*							
5	168 ± 41	141 ± 27	119 ± 37	51 ± 21	108 ± 10	87 ± 54	53 ± 36	24 ± 21
15	164 ± 40	167 ± 50	142 ± 66	39 ± 06	83 ± 10	123 ± 34	81 ± 75	41 ± 36
25	141 ± 46	117 ± 22	138 ± 45	54 ± 11	52 ± 41	98 ± 05	99 ± 19	51 ± 33
35	147 ± 23	147 ± 47	88 ± 50	63 ± 10	61 ± 20	97 ± 07	112 ± 29	76 ± 35
45	124 ± 35	159 ± 80	115 ± 64	58 ± 12	58 ± 20	107 ± 05	94 ± 40	69 ± 64
55	154 ± 15	121 ± 41	103 ± 26	66 ± 02	71 ± 19	107 ± 10	110 ± 21	56 ± 35
Depth (cm)	*Low tide*							
5	85 ± 10	101 ± 52	51 ± 09	31 ± 03	61 ± 15	36 ± 06	21 ± 07	11 ± 05
15	85 ± 23	100 ± 24	54 ± 11	33 ± 05	50 ± 19	38 ± 08	33 ± 14	20 ± 09
25	66 ± 08	82 ± 08	58 ± 20	33 ± 02	64 ± 13	38 ± 03	41 ± 07	19 ± 05
35	79 ± 13	86 ± 09	51 ± 29	35 ± 03	70 ± 14	41 ± 05	44 ± 02	33 ± 05
45	66 ± 21	89 ± 34	47 ± 18	35 ± 04	40 ± 06	41 ± 07	43 ± 06	26 ± 06
55	70 ± 06	81 ± 13	63 ± 09	38 ± 04	52 ± 14	41 ± 07	54 ± 02	26 ± 08

Our results demonstrated that soil H_2S concentrations varied over an order of magnitude and were driven by both tidal regime and seasonal temperature oscillations (Table 1 and Fig. 1A). Larger concentrations were observed at high tide (1.40± 0.55 mmol L^{-1}, 0.34–2.40 mmol L^{-1}) than at low tide (0.73 ± 0.32 mmol L^{-1}, 0.16 –1.44 mmol L^{-1}). A possible hypothesis to explain the difference in concentrations between high and low tides is that during high tide, the waters from the lagoon circulating in the soil 's interstitial pores may facilitate the renewal of electron acceptors by introducing sulphates. This, along with the strong anoxia of the sediment (redox values between 250 and 400 mV; Fig. 2A in Supplementary Material), could potentially support a high rate of DSR and accumulation of H_2S. However, measurements of sulphate concentrations are necessary to support or reject this hypothesis. Conversely, at low tide the absence of a water column above the soil and a lower soil water content (Fig. 2E in Supplementary Material) allow i) emission of the H_2S produced during high tide at the surface, and ii) oxygen diffusion within the soil, thus favouring aerobic SOM decom position and H_2S oxidation. In addition, whatever the tidal regime, seasonal differences in soil H_2S concentrations were evidenced, with larger values during the warm season (Fig. 1A). While many factors can influence gas production, considering that all measurements were done during tide stall and that no significant variations in the physical and chemical drivers were observed between the warm and cool seasons except of temperature changes (see in Jacotot et al., 2019), we suggest that H_2S soil concentrations were mainly driven by the seasonal temperature variability. Indeed, the temperature sensitivity of SOM decomposition is a phenomenon

widely described in the literatures (e.g. Conant et al., 2011; Davidson and Janssens, 2006). Eventually, no clear vertical stratification of H_2S concentrations was observed, at either high or low tide, suggesting a relative homogeneity of the physical and chemical properties of the soil column that drive gas production and oxidation; which is supported by the low variability in depth of the physico-chemical parameters measured (Fig. 2 in Supplementary Material). Lastly, the concentrations measured in our study are comparable to those measured in the mangroves of Belize by Lee et al. (2008) . However, these authors observed a large increase in H_2S concentrations below 15 cm depth, which was not the case in our study. This difference may be attributed to the relative homogeneity of the soil column, as discussed above. At low tide, the estimated average soil-atmosphere H2S emission during the study period was 14.90 ± 7.90 µg S m^{-2} h^{-1} (Fig. 1B). The largest emissions were measured in February with 28.74 ± 6.98 µg S m^{-2} h^{-1} and the smallest in August with 5.81 ± 2.58 µg S m^{-2} h^{-1}, consistent with the seasonal variation in soil H_2S concentrations and temperature (Fig. 1A). However, it is possible that these fluxes are overestimated.

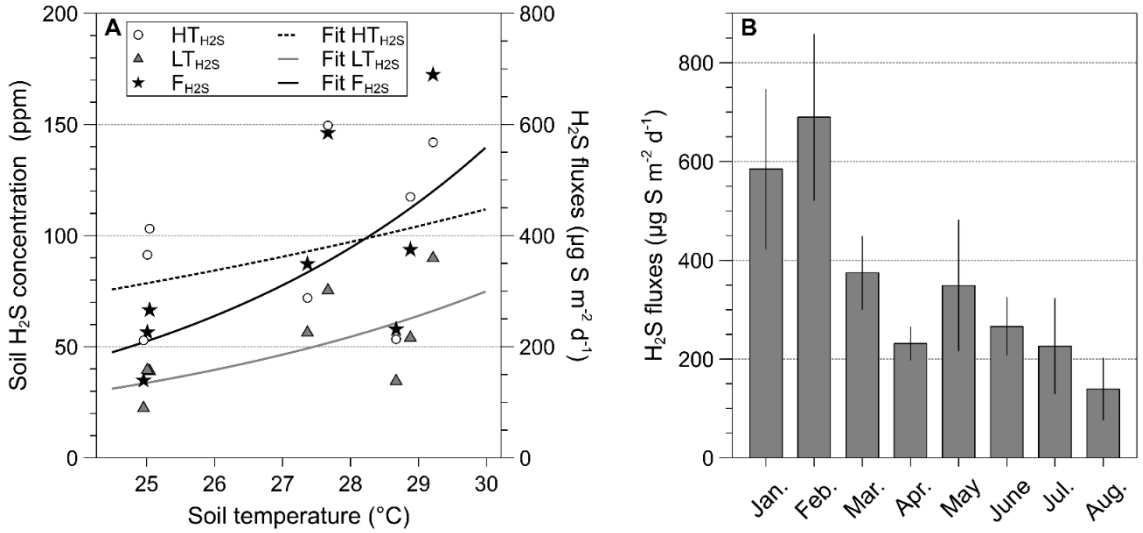

Figure 1. Relationships between A) Monthly averages of soil H_2S concentrations ans soil temperature (°C) and B) Soil-atmosphere H2S fluxes (µg S m^{-2} h^{-1}) at low tide between January and August 2017. In the left panel, circles and triangles indicate high tide (HT) and low tide (LT) soil concentrations, respectively, while stars represent fluxes and lines are the best fit regressions with soil temperature.

At low tide, mangrove soils are covered with a biological membrane composed of an assemblage of heterotrophic bacteria and autotrophic eukaryotes (Decho, 2000). This biofilm has been shown to act as a physical barrier, reducing gas transfer at the soil-air interface (see e.g. Jacotot et al., 2019; Leopold et al., 2013). In this study, theoretical fluxes were calculated with the SAGM method, which does not account for a biofilm. As an indication, Jacotot et al. (2019) noted an average increase of ~17% in CH_4 fluxes after

removing the biofilm. To put these numbers into perspective, we only found two studies of in-situ H_2S fluxes in mangrove forests, and they both reported similar emissions to the present study, ranging from 3 to 31µg S m^{-2} h^{-1} in Florida (Castro and Dierberg, 1987), and from 19 ± 5 to 51 ± 12 µg S m^{-2} h^{-1} in the Sundarbans (Ganguly et al. 2018). By comparing these values to mangroves-associated ecosystems, such as saltmarshes, Delaune et al. (2002) reported H_2S fluxes ranging from 5 to 79 µg S m^{-2} h^{-1}, which falls within the range of values observed in mangroves and supports this range of emission values. Nevertheless, the available literature is currently insufficient to establish a plausible range of variation in H_2S emissions from mangroves, as these may strongly differ in their physiographic characteristics. In addition, based on our study, extrapolating to an average H_2S flux of the ecosystem is challenging because only low-tide fluxes were estimated. However, to estimate average fluxes, emissions based on the tidal cycle should be taken into account, as these ecosystems are submerged part of the time. Therefore, the presence of an oxygenated water column can potentially offset surface fluxes, as H_2S can be oxidized during its diffusion. Regardless, based on an average from the available data for mangroves, the annual emissions would vary between 0.02 and 0.44 g S m^{-2}, which, compared with the 0.035 g S m^{-2} reported by Yu et al. (2019) for coastal wetlands, would make mangroves potential hotspots of H_2S emissions among coastal ecosystems.

In conclusion, this scoping study allowed for the determination of H_2S fluxes in a semi-arid mangrove forest. The main important drivers of H_2S emissions identified herein were the soil H_2S concentrations as well as seasonal temperature variability. The fluxes presented here were similar to those reported by other studies, allowing furthering refining the global range of variation of H_2S emissions from mangrove soils. A research effort should be performed to extend these measures to other mangrove sites that differ in their physiographical conditions, but also to understand the impact of local physicochemical parameters on H_2S emissions.

References

Barton, L.L., Fardeau, M.-L., Fauque, G.D., 2014. Hydrogen sulfide: a toxic gas produced by dissimilatory sulfate and sulfur reduction and consumed by microbial oxidation. In: Kroneck, P.M.H., Torres, M.E.S. (Eds.), The Metal-Driven Biogeochemistry of Gaseous Compounds in the Environment, Metal Ions in Life Sciences. Springer Netherlands, Dordrecht, pp. 237–277. https://doi.org/10.1007/978-94-017-9269-1_ 10.

Bastviken, D., Cole, J., Pace, M., Tranvik, L., 2004. Methane emissions from lakes: dependence of lake characteristics, two regional assessments, and a global estimate: lake methane emissions. Global Biogeochem. Cycles 18. https://doi.org/10.1029/2004GB002238.

Castro, M.S., Dierberg, F.E., 1987. Biogenic hydrogen sulfide emissions from selected Florida wetlands. Water, Air, Soil Pollut. 33, 1–13.

Conant, R.T., Ryan, M.G., Ågren, G.I., Birge, H.E., Davidson, E.A., Eliasson, P.E., Evans, S.E., Frey, S.D., Giardina,C.P., Hopkins, F.M., Hyv¨ onen, R., Kirschbaum, M.U. F., Lavallee, J.M., Leifeld, J., Parton, W.J., Megan Steinweg, J., Wallenstein, M.D., Martin Wetterstedt, J.å., Bradford, M.A., 2011. Temperature and soil organic matter decomposition rates - synthesis of current knowledge and a way forward. Global Change Biol. 17, 3392–3404. https://doi.org/10.1111/j.1365-2486.2011.02496.x.

Davidson, E.A., Janssens, I.A., 2006. Temperature sensitivity of soil carbon decomposition and feedbacks to climate change. Nature 440, 165–173. https://doi.org/10.1038/nature04514.

Decho, A.W., 2000. Microbial biofilms in intertidal systems: an overview. Continent. Shelf Res. 17.

Delaune, R.D., Devai, I., Lindau, C.W., 2002. Flux of reduced sulfur gases along a salinity gradient in Louisiana coastal marshes. Estuar. Coast Shelf Sci. 54, 1003–1011. https://doi.org/10.1006/ecss.2001.0871.

Donato, D.C., Kauffman, J.B., Murdiyarso, D., Kurnianto, S., Stidham, M., Kanninen, M., 2011. Mangroves among the most carbon-rich forests in the tropics. Nat. Geosci. 4, 293–297. https://doi.org/10.1038/ngeo1123.

Ganguly, D., Ray, R., Majumdar, N., Chowdhury, C., Jana, T.K., 2018. Biogenichydrogen sulphide emissions and non-sea sulfate aerosols over the Indian Sundarban mangrove forest. J. Atmos. Chem. 75, 319–333. https://doi.org/10.1007/s10874018-9382-3.

Jacotot, A., Marchand, C., Allenbach, M., 2019. Biofilm and temperature controls on greenhouse gas (CO2 and CH4) emissions from a Rhizophora mangrove soil (New Caledonia). Sci. Total Environ. 650, 1019–1028. https://doi.org/10.1016/j.scitotenv.2018.09.093.

Kristensen, E., Bouillon, S., Dittmar, T., Marchand, C., 2008. Organic carbon dynamics in mangrove ecosystems: a review. Aquat. Bot. 89, 201–219. https://doi.org/10.1016/j.aquabot.2007.12.005.

Kristensen, E., Connolly, R.M., Otero, X.L., Marchand, C., Ferreira, T.O., RiveraMonroy, V.H., 2017. Biogeochemical cycles: global approaches and perspectives. In: Rivera-Monroy, V.H., Lee, S.Y., Kristensen, E., Twilley, R.R. (Eds.), Mangrove Ecosystems: A Global Biogeographic Perspective. Springer International Publishing, Cham, pp. 163–209. https://doi.org/10.1007/978-3-319-62206-4_6.

Lee, R.Y., Porubsky, W.P., Feller, I.C., McKee, K.L., Joye, S.B., 2008. Porewater biogeochemistry and soil metabolism in dwarf red mangrove habitats (Twin Cays, Belize). Biogeochemistry 87, 181–198. https://doi.org/10.1007/s10533-008-91769.

Leopold, A., Marchand, C., Deborde, J., Chaduteau, C., Allenbach, M., 2013. Influence of mangrove zonation on CO2 fluxes at the sediment–air interface (New Caledonia). Geoderma 202– 203, 62–70. https://doi.org/10.1016/j.geoderma.2013.03.008.

Sander, R., 1999. Compilation of Henry's Law Constants for Inorganic and Organic Species of Potential Importance in Environmental Chemistry, Version 3.

Watts, S.F., 2000. The mass budgets of carbonyl sulfide, dimethyl sulfide, carbon disulfide and hydrogen sulfide. Atmos. Environ. 34, 761–779. https://doi.org/ 10.1016/S1352-2310(99)00342-8.

Yu, Q., Si, G., Zong, T., Mulder,J., Duan, L., 2019. High hydrogen sulfide emissions from subtropical forest soils based on field measurements in south China. Sci. Total Environ. 651, 1302–1309. https://doi.org/10.1016/j.scitotenv.2018.09.301.